INTERNATIONAL LAND RECLAMATION AND MINE DRAINAGE CONFERENCE

AND

THIRD INTERNATIONAL CONFERENCE ON THE ABATEMENT OF ACIDIC DRAINAGE

Volume 1 of 4: Mine Drainage

Proceedings of a conference held in Pittsburgh, PA on April 24-29, 1994.
This conference served as the annual meeting for both the American Society for Surface Mining and Reclamation and the Canadian Land Reclamation Association.

These conference proceedings were made possible through contributions provided by:

- United States Department of the Interior
  - *Bureau of Mines
  - *Office of Surface Mining Reclamation and Enforcement
  - *Bureau of Land Management
  - *Geological Survey
- United States Environmental Protection Agency
- Pennsylvania Department of Environmental Resources
- Tennessee Valley Authority
- USDA Soil Conservation Service
- Canada's MEND Program

UNITED STATES DEPARTMENT OF THE INTERIOR
Bureau of Mines Special Publication SP 06A-94

UNITED STATES DEPARTMENT OF THE INTERIOR
Bureau of Mines Special Publication SP 06A-94

INTERNATIONAL LAND RECLAMATION AND MINE DRAINAGE CONFERENCE

AND

THIRD INTERNATIONAL CONFERENCE ON THE ABATEMENT OF ACIDIC DRAINAGE

Volume 1 of 4: Mine Drainage

Proceedings of a conference held in Pittsburgh, PA on April 24-29, 1994.
This conference served as the annual meeting for both the American Society for Surface Mining and Reclamation and the Canadian Land Reclamation Association.

Copies of this and the three companion volumes can be obtained by through NTIS.

Volume 1: Mine Drainage - SP 06A-94
Volume 2: Mine Drainage - SP 06B-94
Volume 3: Reclamation and Revegetation - SP 06C-94
Volume 4: Abandoned Mine Lands and Topical Issues - SP 06D-94

TABLE OF CONTENTS

MODELING MINE WATER QUALITY

ASSESSING THE RISK OF ARD
Ferguson K. D. and Robertson, J. D. 2

AN EMPIRICAL TECHNIQUE FOR PREDICTING THE CHEMISTRY OF WATER SEEPING FROM MINE-ROCK PILES
Morin, K. A. and Hutt, N. M. 12

ASSESSMENT OF CONTAMINANT LOAD CHANGES CAUSED BY REMINING ABANDONED COAL MINES
Hawkins, J. W. 20

MATHEMATICAL SIMULATION OF A WASTE ROCK HEAP
Scharer, J. M., Pettit, C. M., Chambers, D. B., and Kwong, E. C. 30

MODELING RECHARGE AND RUNOFF TO PREDICT COPPER AND ZINC TRANSPORT FROM LIME-AMENDED TAILINGS AT THE SILVER BOW CREEK CERLCA SITE
Schafer, W. M., Goering, J. G., Grady, T. R., Spotts, E., and Neuman, D. R. 40

MODELING FIELD-SCALE TRANSPORT OF WEATHERING PRODUCTS IN MINING WASTE ROCK DUMPS
Eriksson, N. and Destouni, G. 50

WATER TREATMENT WITH WETLANDS

BEST PROFESSIONAL JUDGEMENT ANALYSIS FOR CONSTRUCTED WETLANDS AS A BEST AVAILABLE TECHNOLOGY FOR THE TREATMENT OF POST-MINING GROUNDWATER SEEPS
Hellier, W. W., Giovannitti, E. F., and Slack, P. T. 60

EVALUATION OF ACIDIC MINE DRAINAGE TREATMENT IN CONSTRUCTED WETLAND SYSTEMS
Dietz, J. M., Watts, R. G., and Stidinger, D. M. 70

METAL REMOVAL IN WETLAND TREATMENT SYSTEMS
Eger, P., Wagner, J. R., Kassa, Z., and Melchert, G. D. 80

IRON RETENTION AND VEGETATIVE COVER AT THE SIMCO CONSTRUCTED WETLAND: AN APPRAISAL THROUGH YEAR EIGHT OF OPERATION
Stark, L. R., Williams, F. M., Stevens, Jr., S. E., and Eddy, D. P. 89

MANGANESE AND IRON REMOVAL FROM COAL MINE DRAINAGE BY USE OF A GREEN ALGAE-MICROBIAL MAT CONSORTIUM
Phillips, P., Bender, J., Simms, R., Rodriguez-Eaton, S., and Britt, C. 99

ARSENIC AND NICKEL REMOVAL BY WETLAND SEDIMENTS
Fyson, A., Kalin, M., and Adrian, L. W.. 109

PREDICTING MINE WATER QUALITY

EARLY WEATHERING BEHAVIOR OF PYRITIC COAL SPOIL PILES INTERSTRATIFIED WITH CHEMICAL AMENDMENTS
Donovan, J. J. and Ziemkiewicz, P. F. 119

EVALUATION OF NEUTRALIZATION POTENTIAL DETERMINATIONS FOR METAL MINE WASTE AND A PROPOSED ALTERNATIVE
Lapakko, K. A. 129

EVALUATION OF ACID-BASE ACCOUNTING TO PREDICT THE QUALITY OF DRAINAGE AT SURFACE COAL MINES IN PENNSYLVANIA, U.S.A.
Brady, K. B. C., Perry, E. F., Beam, R. L., Bisko, D. C., Gardner, M. D., and Tarantino, J. M. 138

OBSERVED PREFERENTIAL DEPLETION OF NEUTRALIZATION POTENTIAL OVER SULFIDE MINERALS IN KINETIC TESTS: SITE-SPECIFIC CRITERIA FOR SAFE NP/AP RATIOS
Morin, K. A. and Hutt, N. M. 148

CHEMICAL PREDICTIVE MODELING OF ACID MINE DRAINAGE FROM WASTE ROCK: MODEL DEVELOPMENT AND COMPARISON OF MODELED OUTPUT TO EXPERIMENTAL DATA
White, III, W. W., Trujillo, E. M., and Lin, C. 157

WEATHERING BEHAVIOUR OF MINE TAILINGS AND WASTE ROCK: A SURFACE INVESTIGATION
Domvile, S. J., Li, M. G., Sollner, D. D., and Nesbitt, W. 167

DEVELOPMENTS IN PREDICTION AND MANAGEMENT OF ACID FORMING MINE WASTES IN AUSTRALIA AND SOUTHEAST ASIA
Miller, S. D., Jeffery, J. J., and Donohue, T. A. 177

WATER TREATMENT - CHEMICAL

THE EFFECTS OF ANOXIC LIMESTONE DRAINS ON MINE WATER CHEMISTRY
Hedin, R. S. and Watzlaf, G. R. 185

SUCCESSIVE ALKALINITY-PRODUCING SYSTEMS (SAPS) FOR THE TREATMENT OF ACIDIC MINE DRAINAGE
Kepler, D. A. and McCleary, E. C. 195

THE BIOSULFIDE PROCESS: INTEGRATED BIOLOGICAL/CHEMICAL ACID MINE DRAINAGE TREATMENT - RESULTS OF LABORATORY PILOTING
Rowley, M. V., Warkentin, D. D., Yan, V. T., and Piroshco, B. M. 205

BENCH-SCALE TEST TO SELECTIVELY RECOVER METALS FROM METAL MINE DRAINAGE USING BIOGENIC H_2S
Hammack, R. W., Dvorak, D. H., and Edenborn, H. M. 214

PROSPECT OF METAL RECOVERY/RECYCLE FROM ACID MINE DRAINAGE
Rao, S. R., Kuyucak, N., Sheremata, T., Leroux, M., Finch, J. A., and Wheeland, K. G. 223

PIPELINE TREATMENT OF A METAL MINE DRAINAGE CONTAINING COPPER AND ZINC
Hustwit, C. C. and Sykes, R. G. 233

TREATMENT OF ACID MINE DRAINAGE BY THE HIGH DENSITY SLUDGE PROCESS
Murdock, D. J., Fox, J. R. W., and Bensley, J. G. 241

CONTROL OF AMD - WET COVERS

SUBAQUEOUS DISPOSAL OF REACTIVE MINE WASTE: AN OVERVIEW AND UPDATE OF CASE STUDIES - MEND/CANADA
Fraser, W. W. and Robertson, J. D. 250

THE LABORATORY QUALITY ASSURANCE COMPONENT OF ENVIRONMENTAL MONITORING: A CASE STUDY INVOLVING SUBAQUEOUS TAILINGS RESEARCH
Maynard, A. W. and Thomas, K. B. 260

SUBAQUEOUS DISPOSAL OF MINE WASTE: LABORATORY INVESTIGATION
Lapakko, K. A. 270

WATER COVERS FOR THE DECOMMISSIONING OF SULFIDIC MINE TAILINGS IMPOUNDMENTS
St-Arnaud, L. 279

GEOCHEMISTRY OF SUBMERGED TAILINGS IN ANDERSON LAKE, MANITOBA: RECENT RESULTS
Pedersen, T. F., McNee, J. J., Mueller, B., Flather, D. H., and Pelletier, C. A. 288

WATER COVER ON ACID GENERATING URANIUM TAILINGS - LABORATORY AND FIELD STUDIES
Davé, N. K. and Vivyurka, A. J. 297

SITE CHARACTERIZATION MONITORING

SEDIMENT QUALITY ASSESSMENT NEAR TWO ONTARIO MINE SITES: HOW RELEVANT ARE THE PROVINCIAL GUIDELINES?
Prairie, R. and McKee, P. 307

APPLICATIONS OF GEOPHYSICAL METHODS FOR MONITORING ACID MINE DRAINAGE
King, A. R. and Hynes, T. 317

METHODOLOGY FOR LOCATING AND QUANTIFYING ACID MINE DRAINAGE IN GROUND WATERS ENTERING SURFACE WATERS
Lee, D. R. and Dal Bianco, R. 327

EFFECTS OF INCREASED IRON CONCENTRATIONS ON THE MOBILITY OF CADMIUM, COPPER AND ZINC IN LEACHATES AFTER REMEDIAL ACTIONS AT AN OLD SULPHIDIC MINE WASTE SITE
Håkansson K., Karlsson, S., and Allard, B. 336

HIGH-FREQUENCY GEOCHEMICAL MONITORING OF TOE SEEPAGE FROM MINE-ROCK DUMPS, BHP MINERALS' ISLAND COPPER MINE, BRITISH COLUMBIA
Morin, K. A., Horne, I. A., and Riehm, D. 346

INTERNAL HYDROGEOLOGIC MONITORING OF AN ACIDIC WASTE ROCK DUMP AT WESTMIN RESOURCES' MYRA FALLS OPERATIONS, BRITISH COLUMBIA
Morin, K. A., Jones, C. E., and van Dyk, R. P. 355

CONTROL OF AMD - ALKALINE ADDITION

EFFECTS OF SELECTIVE HANDLING OF PYRITIC, ACID-FORMING MATERIALS ON THE CHEMISTRY OF PORE GAS AND GROUND WATER AT A RECLAIMED SURFACE COAL MINE, CLARION COUNTY, PA, USA
Cravotta III, C. A., Dugas, D. L., Brady, K. B. C., and Kovalchuk, T. E. 365

ALKALINE OVERBURDEN ADDITION TO ACID-PRODUCING MATERIALS TO PREVENT ACID MINE DRAINAGE
Skousen, J. and Larew, G. 375

CONCENTRATED ALKALINE RECHARGE POOLS FOR ACID SEEP ABATEMENT: PRINCIPLES, DESIGN, CONSTRUCTION, AND PERFORMANCE
Nawrot, J. R., Conley, P. S., and Sandusky, J. E. 382

COAL REFUSE DISPOSAL USING ENGINEERING DESIGN AND LIME CHEMISTRY
Rich D. H. and Hutchinson, K. R. 392

MINE WATER GEOCHEMISTRY

OXIDATION RATES AND POLLUTION LOADS IN DRAINAGE; CORRELATION OF MEASUREMENTS IN A PYRITIC WASTE ROCK DUMP
Bennett, J. W., Gibson, D. K., Ritchie, A. I. M., Tan, Y., Broman, P. G., and Jönsson, H. 400

MONITORING GASEOUS AND LIQUID FLUX IN SULFIDE WASTE ROCK
Schafer, W. M., Smith, S., Luckay, C., and Smith, T. 410

COMPARISON OF DULUTH COMPLEX ROCK DISSOLUTION IN THE LABORATORY AND FIELD
Lapakko, K. A. 419

ACID-NEUTRALIZATION REACTIONS IN INACTIVE MINE TAILINGS IMPOUNDMENTS AND THEIR EFFECT ON THE TRANSPORT OF DISSOLVED METALS
Blowes, D. W., Ptacek, C. J., Frind, E. O., Johnson, R. H., Robertson, W. D., and Molson, J. W. 429

AUTHOR INDEX 439-440

UNIT OF MEASURE ABBREVIATIONS USED IN THESE PROCEEDINGS

Å	angstrom
ac	acre
Bq	becquerel
bu	bushel
cal	calorie
cm	centimeter
cmol	centimole
cps	count per second
°C	degree Celsius
d	day
dS	decisiemen
ft	foot
g	gram
gal	gallon
gpd	gallon per day
gpm	gallon per minute
h	hour
ha	hectare
hL	hectoliter
hp	horse power
Hz	hertz
in	inch
J	joule
K	kelvin
kcal	kilocalorie
kg	kilogram
kHz	kilohertz
km	kilometer
kmt	kilo metric ton
kN	kilonewton
kPa	kilopascal
kV	kilovolt
L	liter
lb	pound
m	meter
M	molar
mA	milliampere
meq	milliequivalent
mg	milligram
Mg	megagram
min	minute
mL	milliliter
mm	millimeter
mmho	millimho
mol	mole
mmol	millimole
MPa	megapascal
mS	millisiemen
mt	metric ton
mV	millivolt
MW	megawatt
μg	microgram
μL	microliter
μm	micrometer
μmho	micromho
μmol	micromole
N	normal
N	newton
nm	nanometer
Pa	pascal
pCi	picocurie
ppb	part per billion
ppm	part per million
ppt	part per thousand
psi	pound per square inch
psig	pound per square inch gauge
r	revolution
rad	radian
rpm	revolutions per minute
s	second
st	short ton
vol %	volume percent
wt %	weight percent
yd	yard
yr	year

INTERNATIONAL LAND RECLAMATION AND MINE DRAINAGE CONFERENCE AND THIRD INTERNATIONAL CONFERENCE ON THE ABATEMENT OF ACIDIC DRAINAGE

Proceedings of a conference serving as the annual meetings of the American Society for Surface Mining and Reclamation, the Canadian Land Reclamation Association, and the West Virginia Surface Mine Drainage Task Force, in conjunction with the Third International Conference on the Abatement of Acidic Drainage.

ABSTRACT

Mine drainage and mine reclamation are topics of major interest to the mining industry, federal and local governments, and the general public. This publication and its companion three volumes are the proceedings of a conference held in Pittsburgh, Pennsylvania, April 24-29, 1994. There were twelve sessions (69 papers) that dealt with mine drainage, including modeling, geochemistry, prediction, treatment, control strategies, characterization, hydrology, and case studies. These sessions comprise volumes 1 and 2. The six sessions (34 papers) that dealt with reclamation and revegetation of disturbed lands are included in volume 3. Volume 4 includes the six sessions (34 papers) that dealt with such topical issues as fires at abandoned mine sites, subsidence, hydrology, mine wastes, and policy. Poster session presentations are represented by 49 papers and 92 abstracts that have been placed in the back of volumes 2, 3, and 4, consistent with the subject of that volume.

Reference to companies and specific products in these papers does not imply endorsement by the Bureau of Mines.

ASSESSING THE RISK OF ARD[1]

Keith D. Ferguson[2] and James D. Robertson[3]

Abstract: Predictions of the potential for acid rock drainage (ARD) usually focus on assessing the probability that samples and waste units will generate contaminated leachate. The rate of ARD generation, its quantity, and the possible consequences of release are usually considered in far less detail. Such analyses are deficient and do not fully assess the risk of ARD. Risk can be quantified as the product of probability of an event occurring times consequences. The result is modified by the mitigative measures or contingency plans proposed to prevent or control the undesirable event. Several methods of risk assessment are available and might be applicable to assessing the risk of ARD. These include, qualitative assessments, "what if" analysis, point-scoring systems, failure mode and effect analysis (FMEA), and quantitative probabilistic analysis. The first three simple approaches are more appropriate for advanced exploration and mine projects, while the last two more detailed techniques could be used for existing minesites. Simple qualitative risk assessments have been used by regulatory agencies, either intentionally or unintentionally, in reviewing virtually all recent projects. The more sophisticated approaches have been applied relatively infrequently in mine assessments. Placer Dome Inc. is applying and developing several schemes for ARD analysis for all phases of mining development from exploration through closure. Risk assessments need to be applied more consistently to ensure that rational decisions are made in mine project development and that over conservative criteria are not used in project assessment.

Introduction

Evaluating and accepting risk is a necessary part of deciding to proceed with any new mining project. Risk can be defined as a triplite of three questions:

- What can go wrong?
- How probable is it to go wrong?
- If it does go wrong, what are the consequences?

Mathematically, risk is often defined as the product of probability on an event occurring times consequences. The result may be modified by developing contingency plans.

In the context of Acid Rock Drainage (ARD) asessments, the above three questions could be restated as

- How could ARD be formed?
- How probable is it?
- What are the consequences of ARD generation?

The first question relates to possible sources of ARD, including ore and low grade stockpiles, underground and pit walls, waste rock dumps, leach dumps, road cuts, and borrow pits. If a prevention strategy has been defined for the project, the possible failure modes of the strategy may be examined in detail in a risk assessment.

The probability of ARD is usually examined in a geochemical testing program, e.g. acid/base accounting (ABA) and kinetic testing. The ABA results are often compared with criteria, or the researcher may use his or her experience to estimate a probability of ARD generation.

---

[1]Paper presented at the International Land Reclamation and Mine Drainage Conference and the Third International Conference on the Abatement of Acidic Drainage, Pittsburgh, PA, April 24-29, 1994.

[2]Keith D. Ferguson, Manager Environmental Affairs, Placer Dome Canada, Ltd., Vancouver, B.C., Canada.

[3]James D. Robertson, Manager Environmental Engineering, Placer Dome Inc., Vancouver, B.C., Canada

ARD is not a concern if it does not migrate from the wastes. This is relevant in very arid climates or when rocks with significant acid neutralization capacity are down gradient of the seepage. Therefore, the probability of ARD generation needs to consider both the capacity of the rocks to generate acidic or metal contaminated leachate and the potential of contaminated drainage to migrate beyond the waste boundary.

The consequences of ARD release depend upon the nature of the ARD (strength and volume), the assimilative capacity of the receiving environment, and the proximity and value of aquatic resources. In short, not all impacts are equal.

To date, assessments of the potential for ARD often focus primarily on the probability that the waste will generate contaminated drainage. The migration potential is not usually considered in detail, and the possible consequences of ARD release are examined only in broad terms. Such assessments do not fully consider the risk of ARD.

Several methods of risk assessment are available that may be applicable to more completely assess the risk of ARD. These include ranking schemes, point scoring schemes, failure mode and effect analysis (FMEA), fault and event trees, consequence evaluations, modelling, and quantitative probabilistic analysis.

Simple qualitative risk assessments have been used by mining companies and regulatory agencies, either intentionally or unintentionally, in assessing mining plans. The more sophisticated techniques have been used infrequently. FMEA was used for the assessment of two mining projects in British Columbia (Pelletier and Dushnisky 1993, and Van Zyl and Bamberg 1992). Some techniques being developed by Placer Dome Inc. (PDI) and their applications are discussed in the remainder of this paper.

Some Risk Assessment Techniques and Applications

Issue Ranking Matrix

When evaluating new projects for possible acquisition, relatively little information is usually available to assess the risk of ARD. A simple approach is therefore required. A ranking matrix used by PDI is shown in figure 1. The probability of ARD and parameter migration potential are ranked according to subjective low, medium, and high ratings. The risk is categorized from 1 to 4 and can be modified by one level depending upon the degree of environmental sensitivity (consequences).

The probability may be defined by: observation of ARD from existing facilities or outcrop seeps, the presence of massive sulfides or carbonates in core, or the availability of mineralogical and

Migration Potential	Probability of ARD: Low	Medium	High
Low	1	2	2
Medium	2	3	3
High	2	3 Waste dumps	4 Tailings/Underground Workings

- Add one level for high environmental sensitivity.
- Deduct one level for low environmental sensitivity.

Explanation:

- ARD Produced from historic underground workings
- massive sulphide orebody so ARD from tailings virtually assured
- mine adjacent to river with significant fishery (salmon) resource
- high snowfall/rainfall area (>1m)
- existing workings relatively small but will be expanded significantly in future mining
- limited space available for waste storage but potential for water cover given net precipitation area

Figure 1: Issue Raking Matrix for ARD

geochemical data. The parameter migration potential reflects climatic conditions, possible isolation of sources (e.g., dry minewalls), or limited quantities of wastes (eg., small waste rock dumps in underground operations).

Because the analysis is entirely subjective, the information and assumptions used should be fully explained in supporting documentation.

ARD Category Visualization

Acid/base accounting is often used to predict whether ARD is likely to occur. Unfortunately there is much debate as to interpretation of results for single samples and especially for mixed waste rock dumps composed of partly mixed acid and non-acid producing materials. Graphical techniques to visualize the data and to compare them to literature-reported criteria are important tools for the researcher to assess the probability of ARD.

Table 1: Categories Used by PDI in Screening ABA Data

Category	NP/AP Range	Description
Likely	NP/AP < 1	likely to generate ARD unless sulfide minerals are relatively unreactive
Possibly	1 < NP/AP < 2	possibly acid generating if neutralizing minerals preferentially depleted, coated, or unreactive.
Non-Acid Generating	NP/AP > 2	not expected to generate ARD

Criteria used to interpret the results of ABA were summarized by Ferguson and Morin (1991). Smith and Barton-Bridges (1991) proposed a neutralizing potential to acid production potential (NP/AP) criterion of 3 to 1 (3:1), and that samples below this ratio value should be subjected to kinetic testing. The authors noted that static tests assume the NP is instantly available, all sulfur converts to acid, and all sulfides are reactive. Since these assumptions are not valid for many samples, a safety factor is required for interpretations. However, the authors presented very little data in their paper to justify the chosen NP/AP ratio.

Ferguson and Morin (1991) and Cravotta et. al (1990) both presented theoretical arguments suggesting that the NP/AP criterion to separate potentially acid and non-acid generating samples could be about 2:1. However, in the database presented by the Ferguson and Morin, no sample with an NP/AP greater than 1 produced acidic leachate in 166 laboratory leaching tests. Moreover, there is no clear documented evidence of rock with a NP/AP greater than 1 producing ARD under field conditions.

The NP/AP ratio may be considered as a "safety factor" as used in other engineering analyses. Higher safety factors are probably required for mines in wet climates where carbonate minerals may be preferentially leached from the mine wastes relative to sulfide minerals. The criteria in table 1 have been used by PDI as an initial screen of waste rock ABA data.

An example application is shown in figure 2. The ore clearly has a higher probability of generating ARD compared to the waste rock and rip-rap material.

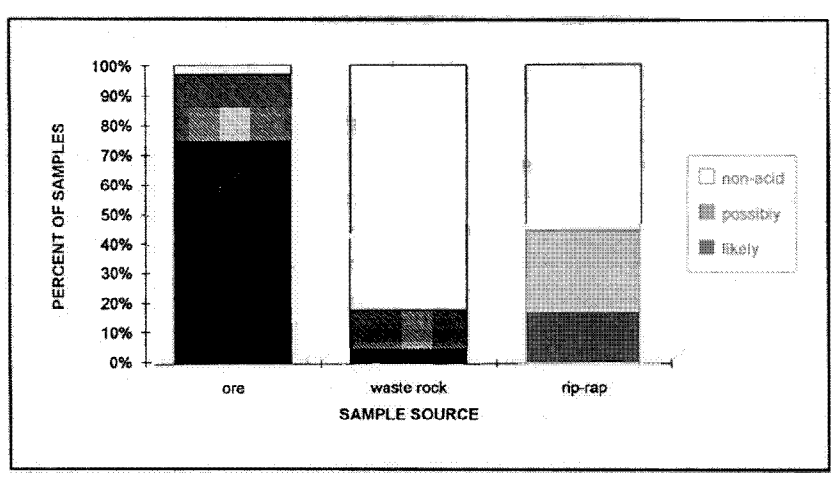

Figure 2: ARD Potential by Category

Tailings are finer grained and more homogeneous than waste rock. Ferguson and Morin (1991) combined data from 35 mines in Canada and Sweden and found a critical NP/AP of 1:1 was probably adequate to identify potentially acid generating tailings. A graphical presentation of AP and NP for tailings, adapted from Miller et. al. (1991), is shown in figure 3. The tailings are predicted to be potentially acid generating.

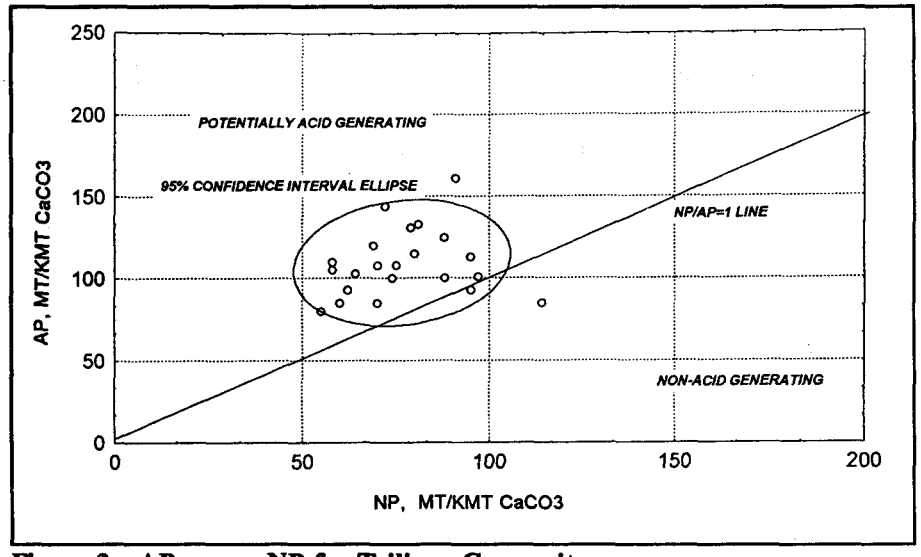

Figure 3: AP versus NP for Tailings Composites

Fault Trees and Event Trees

The concept of examining possible "faults" and resulting "events" are integral parts of designing a mine but have rarely been applied in a rigorous manner to ARD assessments.

Fault trees are typically used to identify all the mechanisms by which an undesirable event could occur. The undesirable event is identified at the top of the tree, and all the subordinate events occur in the lower tree structure. The technique is well suited to examining the probable success of an ARD prevention plan. Figure 4 shows a fault tree for a plan to flood a tailings impoundment to prevent ARD formation. Probabilities can be assigned to each event, the total probability of failure calculated, and the most likely failure mode identified.

Event trees are used to examine the consequences of an initiating event in detail. For example, the effect of an excessive storm causing release from a tailings impoundment could be examined (fig. 4). The loading of contaminants could be estimated and possible impacts on the environment determined based on the presence or absence of aquatic resources.

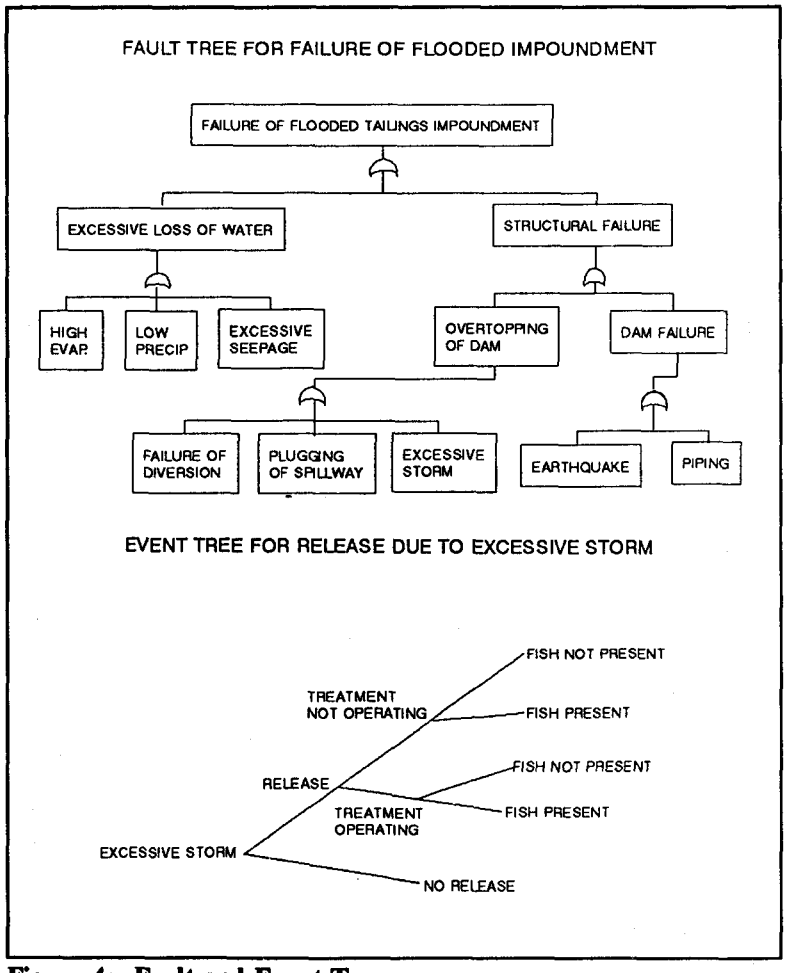

Figure 4: Fault and Event Trees

Consequence Evaluation

Simple models can also be constructed to examine the consequences of ARD release. For example, in some cases, the natural environment may have a significant capacity to assimilate ARD. While this should not be relied on to control ARD, an evaluation of the possible consequences does help to focus effort. This is illustrated in the following example.

An open pit mine was proposed in an area of very high rainfall (greater than 4 m)

with large streams containing high alkalinity (both as dissolved bicarbonate and as calcite in sediments). The question posed was "Could ARD from the waste rock dump and open pit cause a pH depression or problems with heavy metals in the adjacent river?"

The question was answered with the following assumptions:

- The pH in the river may fall if the total alkalinity reaches zero
- The total alkalinity is zero when the acidity load equals the alkalinity load
- Acidity and alkalinity behave as conservative pollutants
- The open pit and waste rock dump would not generate ARD concurrently

The critical acidity in the seepage from the waste rock dump and open pit was back-calculated using a simple mass balance equation and average monthly flows.

$$A_s = \frac{F_d * A_d - F_u * A_u}{F_s}$$

where A_s = acidity (negative alkalinity) of acid water
F_d = flow in river downstream of source
A_d = alkalinity in river downstream of source (assumed 0)
F_u = flow in river upstream of source
A_u = alkalinity in river upstream of source
F_s = flow of acid water from source

Results indicated the maximum acidity in the waste rock dump seepage that could be assimilated by the receiving streams without a pH depression ranged from 1,600 to 6,500 mg/L (as $CaCO_3$). Since seepage from other acid generating waste rock dumps of equivalent size has reached these acidity levels, ARD from the dump could be of concern. The dilution of seepage by the river ranged from 18:1 to 73:1 relatively low values, so the river could be sensitive to significant metal concentrations in any acidic drainage.

The maximum acidity tolerated from the open pit ranged from 5,500 to 22,000 mg/L (as $CaCO_3$); relatively high values and unlikely to be realized in the field unless the rock is extremely reactive. The dilution of pitwater by the river ranged from 63:1 to 251:1. Therefore, ARD from the pit is not as likely to cause a metal contamination problem as in the waste rock dump; less care is required for assessment and prevention of ARD from the pit.

Probability Analysis

In quantitative analysis, a single discrete number in most instances does not adequately describe risk because input numbers in the assessment are uncertain. Probability analysis may assist in more fully describing risk. Probability analysis has been applied by Annandale and Chantler (1992) to a mine site water and contaminant balance in order to estimate the probability of achieving water quality parameters. The following case illustrates an application to estimate only the probability of ARD.

For one mine, PDI assessed the probability that mass-weighted and surface-area-weighted net acid production potential (NAPP)[4] for a waste rock dump would achieve criteria. The analysis was done in three steps. First, probability distribution functions were fitted to the NP and AP datasets for each of five rock types; lognormal distributions were found to provide the best fit. Second, a spreadsheet model was constructed to combine synthesized NAPP distributions according to the mass and the surface area of each rock type into single distributions for the entire waste rock dump. One rock type was extremely friable and slaked to a much finer grain size than the other four types

[4] The NAPP is used in South Pacific countries for prediction of ARD and is defined as AP minus NP expressed as kg H_2SO_4/t. The NAPP therefore has an opposite sign to the net neutralizing potential (NNP).

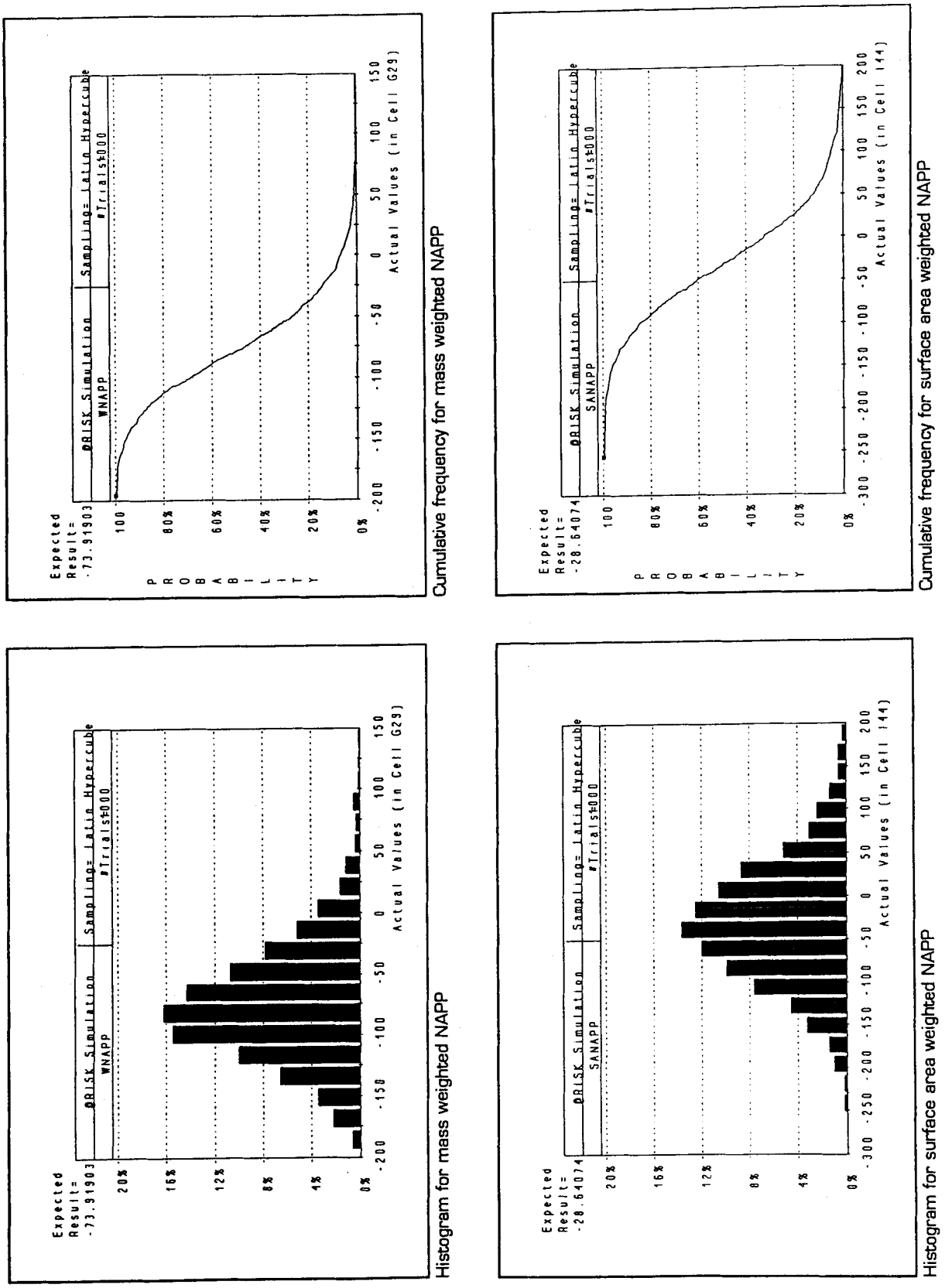

Figure 5: Frequency Plots for Mass and Surface Weighted NAPP

and therefore had a greater contribution to the surface area weighted NAPP. Third, the distributions were sampled using a latin hypercube stratified sampling method to construct the weighted NAPP distributions (fig. 5). The probability of the entire dump achieving selected criteria could then be determined directly from the plots. For example, the probability of the mixed waste rock dump achieving a mass and surface area weighted NAPP value of greater than zero were about 7% and 30% respectively. Criteria should not be the sole basis on which predictions are made. The shape of the probability density functions also show the range, central tendency, and moments of the data. In the case described here, the analysis showed that the friable rock type caused a disproportionate increase in the acid production potential. Special material handling plans (underwater disposal) were developed to address the higher potential for ARD from that material.

Modelling of Consequences of ARD

Even where waste has an intrinsic capacity to generate ARD, contaminated drainage may not exit from the waste deposit if sufficient neutralizing minerals are present in the flow path. This may be particularly relevant in a tailings deposit where carbonate minerals will be present below a water table. An example is discussed below.

The tailings contained on average of about 3.5% sulfur as pyrrhotite and pyrite and about 7% carbonate as calcite. Leaching tests indicated the sulfide minerals were amenable to oxidation and that in the long term, net acid would be produced if sufficient oxygen were present to support oxidation. However, the water table was relatively high in the deposit and may limit the depth of oxidation.

The model WATAIL (Scharer, et al., 1993) was used to study the effects of various depths of tailings below the water table on net acid production. The model was applied to four separate areas (nodes) of the deposit. For node 1 the depth to the water table was taken as 4 m, for node 2 as 2 m, and for nodes 3 and 4 as 1 m. Essentially the model examined the possible drawdown of a water table near a pervious dyke. The total depth of the tailings deposit was 5 m for all nodes. The model simulated 100 years of oxidation and seepage. Acidic leachate breakthrough did not occur for nodes 2 to 4, while breakthrough occurred from node 1 in 55 years (fig. 6). Even though acid breakthrough is not predicted for some nodes, migration of those metals mobile at alkaline pH, such as zinc and cadmium, may still occur. Based on this analysis, a decision was made to increase the depth of tailings in the lower portion of the impoundment and to raise the water table by constructing a water-retaining dam.

In a second example, a simple model was constructed to predict the sulfate and metal concentrations in drainage from a waste rock dump where potentially acid generating rock was to be placed on top of a dump because of the mining sequence. A geochemical rather than oxidation-limited model was used since the quantity of potentially acid generating rock was small and exhibited a low intrinsic oxidation rate from kinetic tests; calculations also indicated oxygen was not limited, given the depth and reactivity of the material.

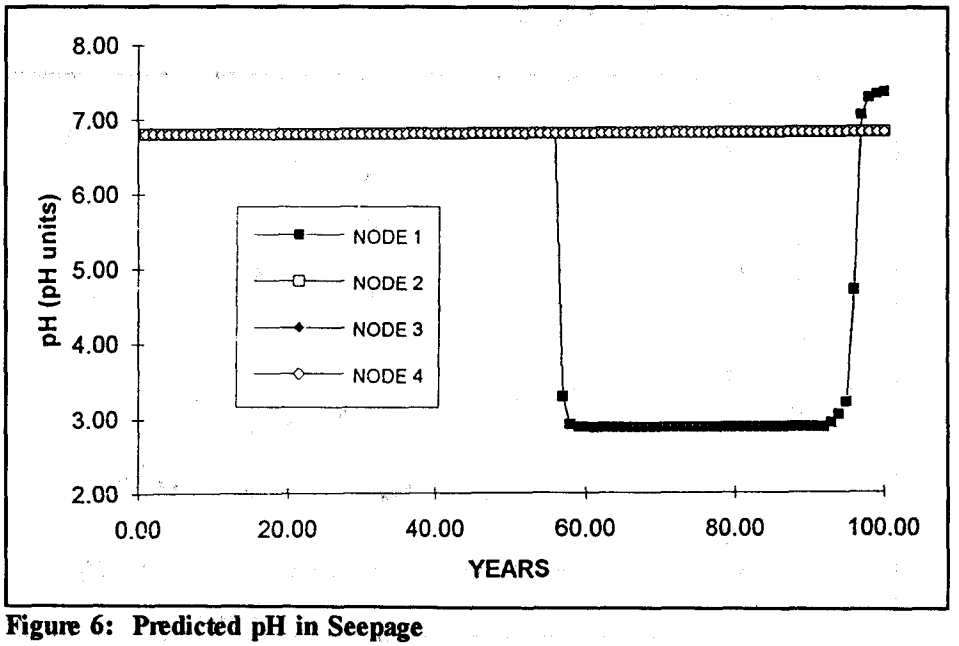

Figure 6: Predicted pH in Seepage

Results from a series of seven field barrel tests were used to determine oxidation rates (sulfate and metal production rates). A mean sulfate production rate was normalized to the percent sulfur in the sample and the number of days prior to leachate sampling. The normalized rate was found to vary by only two to three times. A decay rate was applied(time$^{-0.5}$) to account for the build up of coatings during long dry periods and the resulting decrease in sulfate production. To estimate metal concentrations, zinc, copper, and cadmium were correlated with sulfate for the barrel data. Correlations were not strong but were adequate for this level of modelling. For zinc, relationships were established for three ranges: high, medium, and low reactivity (sulfate production) (fig. 7).

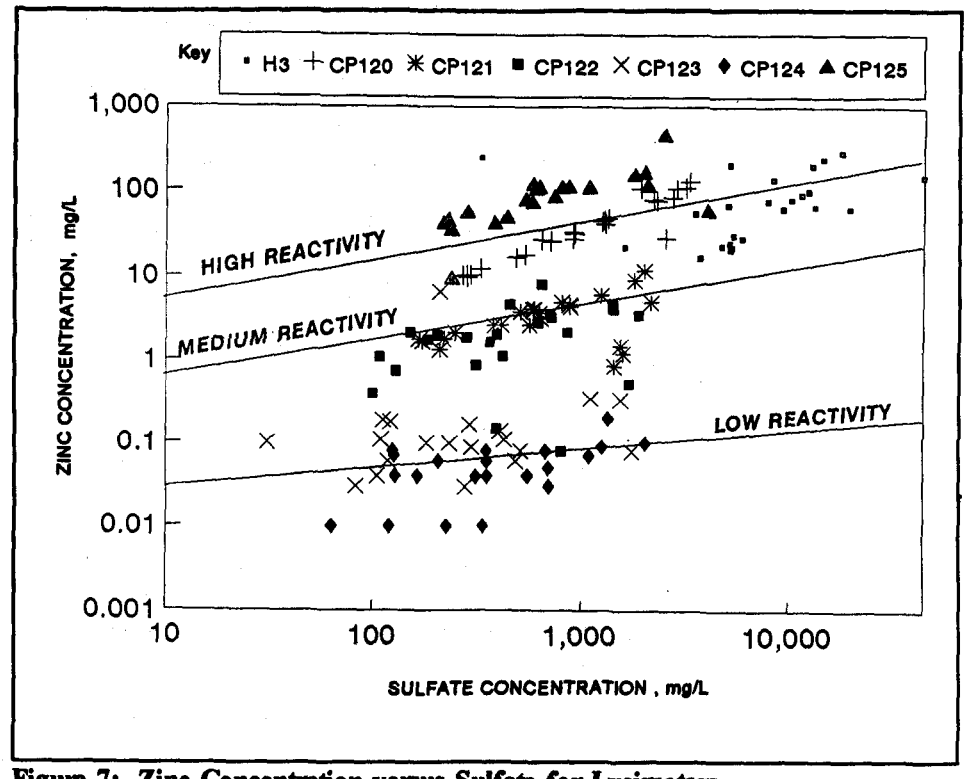

Figure 7: Zinc Concentration versus Sulfate for Lysimeters

The model was run to calculate sulfur and metal concentrations from the waste rock dump based on recorded precipitation and dry periods from July 1992 to October 1993 (duration of barrel experiments). The seepage from each class of waste (high, medium, and low reactivity and no acid generation) was weighted according to the possible tonnage and surface area of the dump. The seepage was diluted by the "uncontaminated" receiving water according to simple ratios of catchment areas.

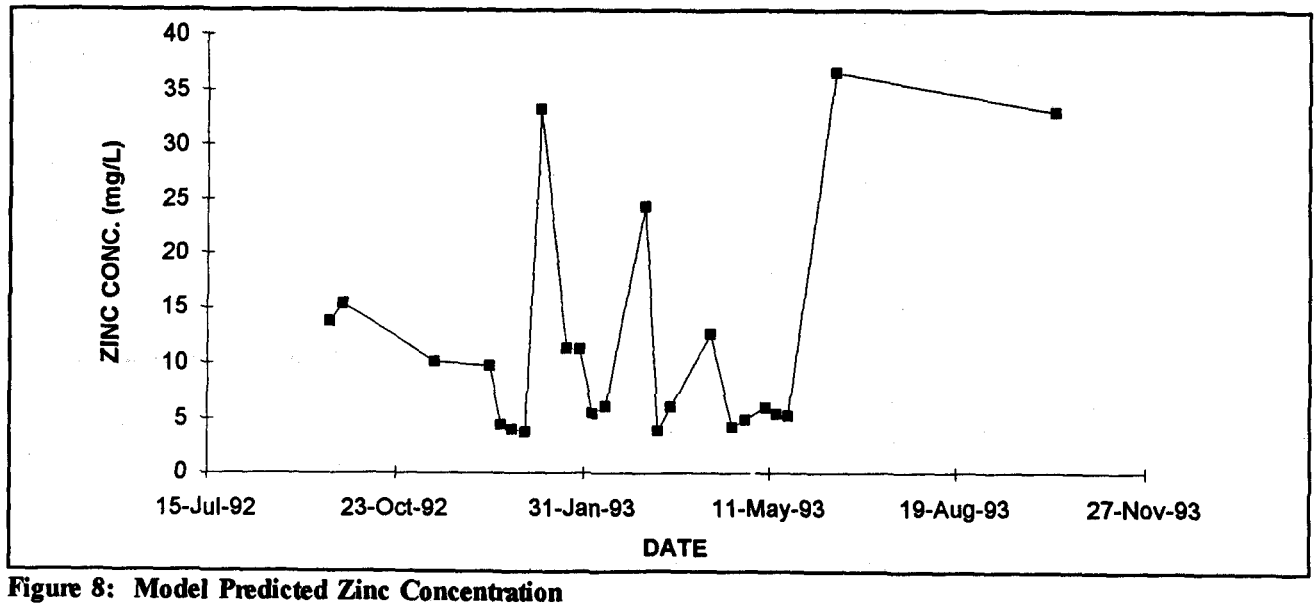

Figure 8: Model Predicted Zinc Concentration

Results for zinc are shown in figure 8. The model was very simple; results may not be highly accurate but are adequate to make management decisions. The results indicated that zinc concentrations could be significant in the receiving environment, and therefore mitigative measures including covers would be required.

Conclusion

The formal application of risk assessment to environmental analysis in mining is rather new. The analysis need not be complex to provide a useful insight into the probability and consequences of ARD and the need or level of mitigative measures. Risk assessment techniques such as those discussed above show much promise for analysis of ARD problems, particularly since the assessment of ARD is still an inexact science.

Some possible applications of risk assessment techniques to the various phases of mine development are shown in table 2. These tools are applicable to both operators and regulators of mines. With the growing use of these techniques, more rational decisions in mine design, approval, and operation should be possible.

Table 2: Possible Application of Some Risk Assessment Techniques to ARD

RISK ASSESSMENT TECHNIQUE	PROJECT PHASES				
	Operators		Operators/Regulators		
	Acquisition	Pre-feasibility	Feasibility/Design	Operation	Closure
Ranking Matrix	•••	••	••	-	-
Category Visualization	••	•••	•••	••	•
Fault/Event Trees	-	••	•••	•••	•••
Consequence Evaluation	•	•••	•••	••	••
Probability Analysis	-	-	•••	••	•
Modelling	-	-	•••	•••	•••

probably not applicable
possibly applicable but may not have sufficient resolution
• possibly applicable
••• very applicable

References

Annandale, G.W. and A.G. Chantler, 1992. "Uncertainty in Planning ARD Control Measures: Risk Modelling and and Intepretation" In: Risk Assessment/Management Issues in the Environmental Planning of Mines, Society for Mining, Metallurgy, and Exploration, Inc., Littleton, Colorado.

Cravotta III, C.A., Brady, K.B.C., Smith, M.W., and R.L. Beam, 1990. "Effectiveness of the Addition of Alkaline Materials at Surface Coal Mines in Preventing or Abating Acid Mine Drainage: Part 1. Geochemical Considerations". In: 1990 Mining and Reclamation Conference and Exhibition, April 23-26, Charleston, West Virginia.

Ferguson, K.D. and K.A. Morin, 1991. "The Prediction of Acid Rock Drainage - Lessons from the Database". Proceedings: Second International Conference on the Abatement of Acidic Drainage" Sept. 16 to 18, 1991, Montreal, Quebec.

Miller, S.D., Jeffrey, J.J., and J.W.C. Wong, 1991. "In-pit Identification and Management of Acid Forming Waste Rock at the Golden Cross Gold Mine, New Zealand". Proceedings: Second International Conference on the Abatement of Acidic Drainage" Sept. 16 to 18, 1991, Montreal, Quebec.

Pelletier,C.A., and K. Dushnisky, 1993. "Qualitative Environmental Risk Assessment Applied to the Proposed Windy Craggy Project" In: Proceedings of the Seventeenth Annual British Columbia Mine Reclamation Symposium, May 4 to 7, 1993, Port Hardy, B.C..

Scharer, J.M., Annable, W.K., and R.V. Nicholson, 1993. "WATAIL 1.0 User's Manual A Tailings Basin Model to Evaluate Transient Water Quality of Acid Mine Drainage" for Falconbridge Ltd. and MEND Ontario, Institute of Groundwater Research, University of Waterloo, Waterloo, Ontario.

Smith, A. and J.B. Barton-Bridges, 1991. "Some Considerations in the Prediction and Control of Acid Mine Drainage Impact on Groundwater from Mining in North America". In: Proceedings of the EPPIC Water Symposium, May 16-17, 1991. Johannesburg, South Africa.

Van Zyl, D. and S. Bamberg, 1992. "Qualitative Environmental Risk Assessment for Mine Development" In: Risk Assessment/Management Issues in the Environmental Planning of Mines, Society for Mining, Metallurgy, and Exploration, Inc., Littleton, Colorado.

AN EMPIRICAL TECHNIQUE FOR PREDICTING THE CHEMISTRY OF WATER SEEPING FROM MINE-ROCK PILES[1]

Kevin A. Morin[2] and Nora M. Hutt[3]

Abstract: Mine-rock piles are complex hydrogeologic systems. As a result, the current knowledge of their physical and chemical hydrogeology is too limited to permit accurate predictions of water chemistry through time based on detailed simulations of their internal processes. However, a simplistic empirical model based on general knowledge and available data can be used to obtain rough estimates of seepage chemistry through time. This empirical model is based on five factors: (1) the production rates of metals, nonmetals, acidity, and alkalinity under acid and pH-neutral conditions, (2) the volume rate of flow through the rock pile based on infiltration of precipitation, (3) the elapsed time between infiltration events, (4) the residence time of the water within the rock pile, and (5) the percentage of mine rock in the pile flushed by the flowing water. The last factor is most difficult to define at many minesites, but can be assumed due to its apparently frequent narrow range of 5 to 20%. A hypothetical example illustrates how to use the model and highlights other complications like secondary-mineral precipitation that may also have to be considered. A field example based on data from an actual minesite demonstrates the accuracy of the model as compared to measured concentrations. Again, this model ignores many complexities of mine-rock piles and is thus only useful for rough estimates of future chemistry.

Additional Keywords: acidic drainage, mine-rock piles, waste rock, geochemical predictions, hydrogeology

Background and Objectives

A mining operation can consist of several primary and secondary components such as an open pit or underground workings, tailings, waste-rock dumps and ore stockpiles, and various dams, roads, and construction pads made of mine rock (e.g., Morin 1988). An integrated program for the prediction of future movement of water and its associated chemistry is obviously of great value to any mining operation about to begin, currently operating, or about to close. Predictive geochemical techniques for tailings have received preferential attention over the last 10 yr, as demonstrated in Canada by the numerous reports generated under contracts for the now defunct National Uranium Tailings Program and the current federal Mine Environment Neutral Drainage (MEND) Program (e.g., Senes 1991). Predictive procedures for pits and underground workings have also been developed under MEND and the British Columbia AMD Task Force to an initial level (Morin 1991) and are now being expanded (Morin and Hutt 1994, Morin 1994). However, predictive geochemical techniques for mine-rock dumps, dams, piles, and roads (hereafter simply called "piles") are still tentative due to their complexity.

Mine-rock piles are complex hydrogeologic systems, and current hydrogeologic theory is not able to characterize them accurately (e.g., Morin et al., 1991). As a result, this limited knowledge of the physical and geochemical aspects of piles precludes accurate predictions of future water chemistry through impressive mathematical equations without empirical "fitting" factors. Instead, a simpler model for rough estimates of future

---

[1]Paper presented at the International Land Reclamation and Mine Drainage Conference and the Third International Conference on the Abatement of Acidic Drainage, Pittsburgh, PA, USA, April 24-29, 1994.

[2]Kevin A Morin, Morwijk Enterprises Ltd, 47-115 Kamehameha Highway, Kaneohe, Hawaii, USA 96744 (address until 2/28/94).

[3]Nora M. Hutt, Normar Enterprises, Box 357, Wildwood, Alberta, Canada T0E 2M0

chemistry can be based on an empirical approach.

The first objective of this paper is to present the five factors that form an empirical model for the prediction of aqueous chemistry issuing from a mine-rock pile. These factors are (1) the production rates of metals, nonmetals, acidity, and alkalinity under acid and pH-neutral conditions from a unit weight of rock, (2) the volume rate of flow through a rock pile based on infiltration of precipitation, (3) the elapsed time between infiltration events, (4) the residence time of the water within the rock pile, and (5) the percentage of mine rock in the pile flushed by the flowing water. The second objective of this paper is to present a hypothetical example followed by an actual field example. In the field example, the empirical model is calibrated to one mine-rock pile at a minesite and then used in predictive mode for the other piles in various stages of acid generation.

Factor 1: Geochemical Production Rates

The primary reason for concern over some mine-rock piles is that they contain reactive minerals that can release metals and nonmetals, such as copper, sulfate, acidity, and alkalinity. These reaction products can then be swept away by any water flowing over the rock surfaces or can accumulate on unflushed surfaces. The unflushed surfaces do not immediately influence water chemistry, but can affect chemistry during irregular events such as the shifting of the pile or plugging of preferential flow channels (see factor 5) so that previously unflushed surfaces become regularly flushed. In any case, it is the prediction of the regular removal rate of the reaction products that is the purpose of this paper. For simplicity, only the regularly flushed surfaces are considered here.

The most common method for obtaining production rates is often labelled "kinetic tests" (e.g., fig. 1). Such tests involve repetitive monitoring of water passing over a mass of rock for several months to years. Under laboratory conditions, a common kinetic test involves "humidity cells" in which effluent concentrations often asymptotically approach long-term production rates after 30 to 40 weeks of weekly rinsing and analysis. Because sulfide oxidation and metal leaching can often be treated as kinetic (time-dependent) processes, the production rates can be expressed in units of milligrams of metal or non-metal per unit weight (kilograms) or surface area (square meters) of rock per unit time, such as 10 mg zinc/kg of rock/wk.

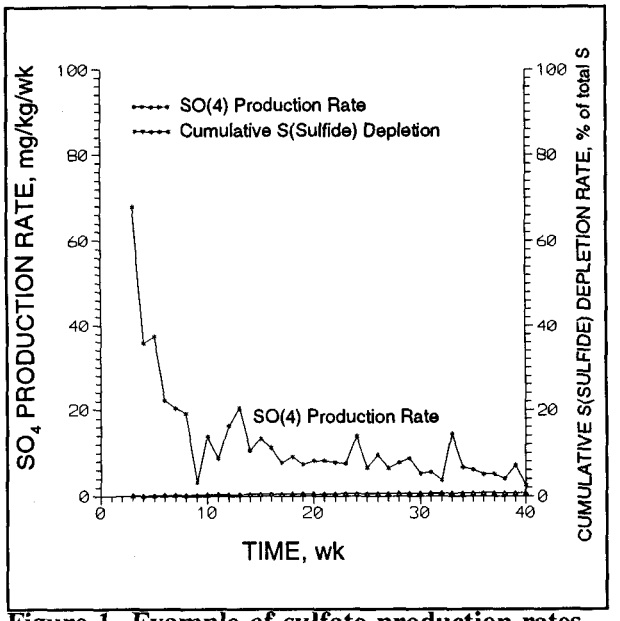

Figure 1. Example of sulfate production rates from a mine-rock kinetic test.

One area of confusion in published literature lies in distinguishing between unit-surface-area and unit-weight rates, which implicitly includes the issues of (1) whether the rock occurs as coarse boulders or fine rock and (2) whether fine rock or boulders should be used in kinetic testing. For practical purposes, there is often little reason for this confusion or for considering the grain size. Laboratory-based kinetic tests often use rock ground to finer than 1/4 inch. This is generally representative of most of the reactive particle surface area in a pile, as shown numerically in the next paragraph.

With the assumptions that rock particles resemble cubes (other shapes can also be considered) with a length of 0.2 m and that the bulk density of a rock mass is 1.8 metric tonnes (mt) a cubic meter, then 1 mt of rock will have a volume of 0.555 m^3 and contain an average of 69.4 rock particles with a total particle surface area of 16.6 m^3/mt. This would seem relevant to literature reports of coarse rock accumulating at the base of end-dumped piles.

In reality, this preferential accumulation is not particularly important because there is often some finer rock located between the coarse rock. If 1 mt of rock consisted 80% of rock particles with a length of 0.2 m (as above) and 20% with a length of 0.0032m (average of minus 1/4 inch used in laboratory kinetic tests), which would not even completely fill the coarser porespace, then the particle surface area of this 1 mt would be 221 m^3, with only 6% coming from the coarse fraction (table 1). Consequently, the assumption that all the rock is coarse can result in errors of more than a factor of 10 on the reactive surface area per unit weight, whereas the assumption that all the rock is fine will often result in errors of less than a factor of 5. In light of the complexities of a pile, the general nature of this empirical model, and the desire for a safety factor in the calculations, the coarse fraction is ignored with no unwarranted effect on the predictions. As a result, the production rates from laboratory-based kinetic tests as mg/kg/wk can often be used for an entire pile directly with no great concern for grain-size effects.

Table 1. Effect of grain size on reactive surface area per unit weight (see assumptions in text)

COARSE FRACTION (0.2 m)		FINE FRACTION (0.0032 m)		TOTAL SURFACE AREA (m^2)	% OF TOTAL FROM COARSE FRACTION
% TOTAL WEIGHT	SURFACE AREA(m^2)	% TOTAL WEIGHT	SURFACE AREA(m^2)		
0	0	100	1040	1040	0
10	1.66	90	936	938	0.18
20	3.32	80	832	835	0.40
30	4.98	70	728	733	0.68
40	6.64	60	624	631	1.05
50	8.30	50	520	528	1.57
60	9.96	40	416	426	2.34
70	11.6	30	312	324	3.58
80	13.3	20	208	221	6.01
90	14.9	10	104	119	12.5
95	15.8	5	52	67.8	23.3
100	16.6	0	0	16.6	100

Factor 2: Infiltration of Water

If rock has significant geochemical production rates (factor 1), but no water moves through the pile, then none of the reaction products will leave the pile. In effect, a lack of infiltration results in containment of the products, but in reality there will be infiltration events even in arid climates. Both the volume of infiltrating water (this factor) and the elapsed time between infiltration events (factor 3) affect the concentrations and loadings seen in the basal seepage. For example, arid climates can sometimes generate high concentrations (as mg/L) because there may be little regular infiltration to dilute the reaction products that accumulate between infiltration events.

Water movement into and through a pile can be initiated by a relatively small precipitation event, which would not lead to infiltration in finer-grained soils (ElBoushi 1975). Thus, even minor rainfall must be considered in the empirical model. However, precipitation events are relatively easy to define based on climatic monitoring regularly conducted at most mines (e.g., fig. 2). As the precipitation falls, some water is lost to evaporation and to runoff if the top of the pile is relatively fine-grained. A general rule of thumb may be that perhaps 40 to 60% of precipitation will infiltrate into the rock, but the actual value at a site should be determined from local monitoring and modelling. In any case, daily precipitation (e.g., fig. 2) is mathematically converted into infiltration based on the minimum amount to initiate infiltration and the infiltration factor.

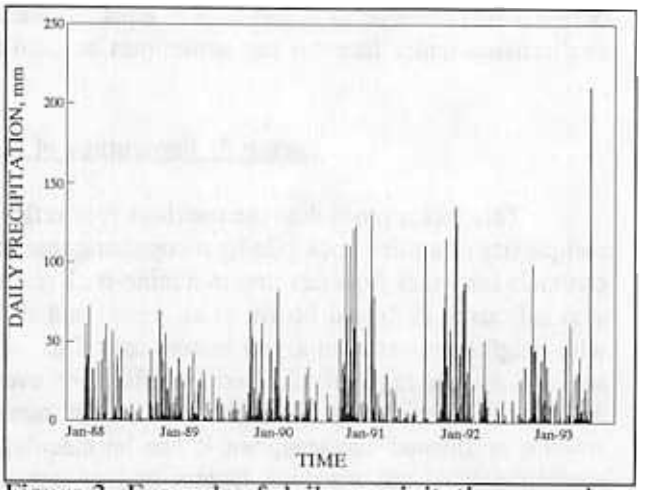

Figure 2. Example of daily-precipitation records at a mine.

Factor 3: Elapsed Time Between Infiltration Events

The importance of this factor comes from the realization that infiltration does not occur every day and that, on days when there is no precipitation, reaction products (factor 1) are accumulating in the flow channels (factor 5). As a result, when infiltration finally appears after a delay, concentrations are notably higher than during regular daily rainfall. This behavior has been noted in various mine-rock dumps and in small-scale in-field rock piles (e.g., Rescan 1992, Norecol, Dames, and Moore 1993).

The elapsed time between infiltration events is easily obtained from climatic data at a minesite (e.g., fig. 1) with the realization that there is a minor threshold below which no infiltration will occur (ElBoushi, 1975). However, due to movement of gas and humidity within piles and the anticipated effects of condensation during daily and seasonal cycles, there may be some flushing of rock surfaces in the absence of infiltration (Morin et al. 1991). Although there is no field evidence for cyclic condensation in piles, its importance has been documented in underground mines (Morth et al. 1972). Additionally, the field example later in this paper shows that average annual precipitation, distributed on a daily basis and assuming flushing of rock surfaces occurred daily, was sufficient to obtain reasonable results. Consequently, the actual importance of infiltration events relative to other processes capable of generating water movement within a pile remains unclear.

Factor 4: Residence Time of Water Within a Pile

This factor is actually a refinement to the previous one. The previous factor addressed the elapsed time between infiltration events, but this factor considers the field studies which show that infiltrating water can require hours to days to pass through a pile and can actually be delayed for greater lengths of time at locations where perched water tables exist (Morin et al. 1991 and 1994). For example, if two infiltration events occur within 48 h in the upper portion of a pile, but the water from both events is caught in a perched groundwater zone at intermediate depths, then the underlying rock surfaces continue to generate reaction products until the water passes through the perched zone. For example, the water from various infiltration events may pass through the upper half of a pile 7 days apart (factor 3), but may pass through the lower half at almost the same time as one event.

This is an interesting factor in that it touches on some complexities in mine-rock hydrogeologic systems, but the delineation of the irregularities is beyond the current ability to accurately detect and monitor them. So, while this factor may become more important in the future, this current empirical model assumes that the elapsed time

between seepage events at the base is equal to the elapsed time between infiltration events. Toe-ditch monitoring as discussed under factor 5 can sometimes be used to evaluate the validity of this assumption

Factor 5: Percentage of Rock Surfaces Flushed by Water Flow

This factor more than the previous four reflects the true complexity of a mine-rock pile by recognizing that preferential channels for water flow develop in a mine-rock pile (fig.3; see also ElBoushi 1975 and Morin et al. 1991) and that for piles with heights greater than a few meters only 5 to 20% of rock surfaces may be regularly flushed by infiltration events (factor 3). There is currently no direct method for measuring the amount of flushed surfaces, but it can be calculated from a combination of the previous factors and on-site monitoring data of toe-drainage ditches or groundwater monitor wells. The calculation of this factor from the other information highlights both the empirical model's weakness, in that all factors cannot be measured, and its value and simplicity in that (1) a complex factor beyond current capability to measure can be empirically determined as explained below, (2) this complex factor is often in the range of 5 to 20% in full-size rock piles so that its measurement is not required for rough estimates, and (3), once the factor is calculated, the model can be used in a predictive mode as shown in the field example below.

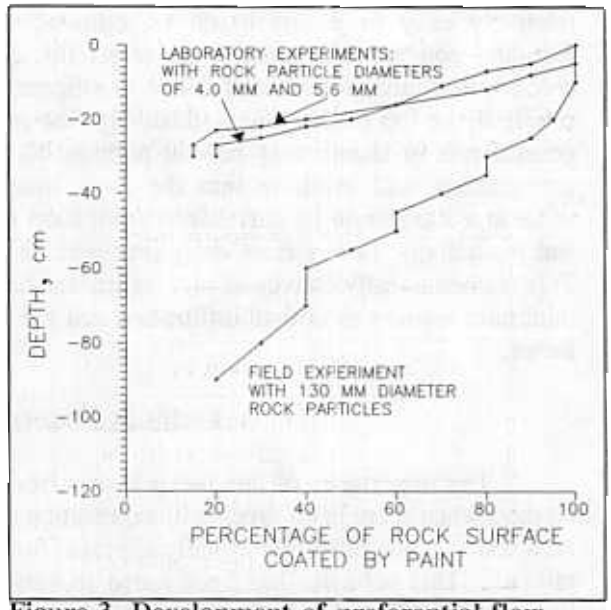

Figure 3. Development of preferential flow channels in rock piles (from ElBoushi, 1975).

Where toe ditches are monitored for flow and chemistry, the average residence time of water in the pile (factor 4) will become apparent when the time of precipitation is compared with the time of maximum flow in the ditch. Additionally, the flow multiplied by concentration will provide a loading, which will in turn reveal the amount of rock flushed to obtain the loading, when the loading is divided by the production rates (factor 1). When this amount of rock is divided by the total weight of rock in the pile, the percentage of flushed rock surface (factor 5) is obtained. In effect, factor 5 is back-calculated from factors 1 through 4 and the predictive targets of the model: the seepage flows and chemistry. This calculation of factor 5 represents calibration of the model to current conditions and no doubt includes effects of other factors not explicitly considered in the model. In any case, the few case studies for which factor 5 has been back-calculated and the direct measurements by ElBoushi (1975) indicated the percentage of rock regularly flushed often lies in the range of 5 to 20%.

It is worthwhile to briefly consider here the remaining 80 to 95% of rock surfaces that can accumulate reaction products year after year. Some of these surfaces would be flushed when extreme infiltration events occur. The regular flow channels would thus be overwhelmed, and the excess water would spill over onto adjacent rock surfaces (see the field example below). Other surfaces may not be flushed until other events occur, such as the shifting of the pile to form new flow channels or the plugging of old flow channels by fine rock or mineral precipitants. These events should be considered in long-term predictions, but are not considered here for simplicity and brevity.

Hypothetical Example

With all of the five empirical factors defined above, a hypothetical example is timely to demonstrate the operation of the model. The hypothetical pile is 600 m long, 300 m wide, and 20 m high. It contains 6.5 million

mt of rock. The long-term production rate (factor 1) of zinc was measured in a humidity cell at 5 mg/kg/wk. Precipitation events generate 1 mm of infiltration (factor 2) and occur every 2 days (factor 3). The elapsed time between flushing events throughout the pile is set equal to the infiltration events of every 2 days (factor 4). The percentage of total rock surface flushed is assumed to be 10%. As a result, the concentration of zinc predicted in the toe seepage is 506 mg/L (table 2). Such a high concentration is possible in acidic waters, but is unexpected in pH-neutral waters due to the solubility of secondary zinc minerals such as sulfates and carbonates. Consequently, not all of the zinc may report to toe seepage. If observed zinc concentrations in the toe seepage were 250 mg/L, or if predicted solubility levels based on geochemical models such as MINTEQ (Allison et al. 1990) were 250 mg/L, then approximately 50% of the produced zinc would be retained in the pile as relatively soluble zinc minerals. These minerals would then be capable of dissolving at a later time to maintain or raise concentrations in toe seepage should one or more other parameters such as pH change.

Table 2. Summary of the hypothetical example for mine-rock flushing.

Factor	Hypothetical Value
1	Geochemical production rate of zinc = 5 mg/kg/wk
2	Precipitation event is 1 mm or 180,000 L over the surface of the pile
3	Infiltration event occurs every 2 days so that the rock accumulates 1.4 mg Zn/kg between events [(5 mg kg^{-1} wk^{-1} / 7 d wk^{-1}) * 2 d]
4	Simplified in this example: seepage events occur every 2 days like infiltration
5	10% of the rock or 650 million kg is flushed by the infiltration
RESULT	PREDICTED CONCENTRATION: (1.4 mg Zn/kg) • (650,000,000 kg) / 180,000 L = 506 mg Zn/L

Field Example

This example is based on geochemical work performed at a mine in Canada that has several mine-rock piles. The model was first applied to one of the piles for which some data on flow and chemistry were available, in order to calculate the percentage of rock surfaces flushed and ensure reasonable values were obtained. The model was then used in predictive mode to estimate water chemistry in toe seepages at other piles under acidic and pH-neutral conditions.

At this site, daily climatic data were not available. Instead monthly averages were available for a nearby location and, for the purposes of average annual predictions, average annual precipitation was used and was assumed to infiltrate on a daily basis. Production rates were obtained from a series of humidity cells operated for a minimum of 40 weeks. Back-calculations for one pile (fig. 4) showed that on average approximately 5% of the rock surfaces (based on zinc) were flushed by most infiltration events, but the flow channels were apparently overwhelmed at ditch flows above 400 m^3/d. The lower rock-surface flushing based on copper reflects the loss of aqueous copper within the dump to secondary mineral precipitation, as indicated by visual observations and MINTEQ calculations.

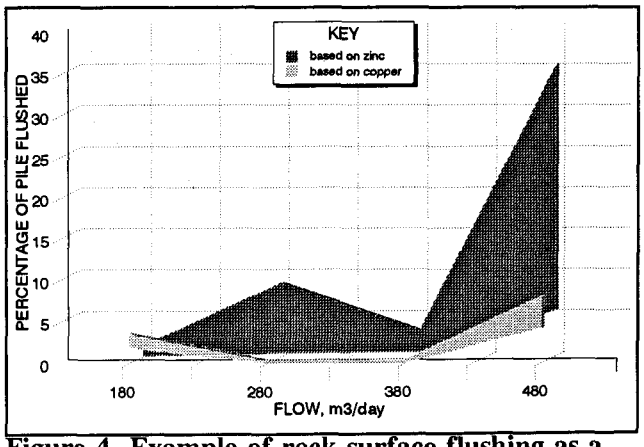

Figure 4. Example of rock-surface flushing as a percentage of total surface area versus toe-ditch flow rate.

With a value of 5% used for factor 5, concentrations for other piles were predicted under acidic and pH-neutral conditions. These values were often in general agreement with observed concentrations around the site at pH 2.5 and pH 7.0 (table 3), except for parameters whose concentrations are regulated within the piles by secondary-mineral precipitation and thus should not be found at the predicted concentrations. Based on these results, the empirical model was taken as a general predictor for the minesite with assistance from MINTEQ, and was used to predict changes in concentrations when a particular pile was expected to exhaust all neutralization potential and become acidic.

Table 3. Comparison of predicted and observed values for the field example.

Parameter (mg/L)	ACIDIC (pH 2.5)			pH-NEUTRAL (pH 7.0)		
	Predicted	Average Observed	Highest Observed	Predicted	Average Observed	Highest Observed
Acidity mg/L	4300	3420	8230	~0	22	290
Sulfate mg/L	4100[1]	2000	9230	1700[1]	2000	3300
Cadmiummg/L	0.40[1]	0.07	0.07	0.99[1]	<0.015	<0.015
Copper mg/L	310[1]	600	600	2.0[1]	0.20	5.0
Nickel mg/L	1.6	0.84	2.1	0.01	0.02	0.2
Lead . mg/L	4.4[1]	<0.05	<0.05	10[1]	<0.05	<0.05
Zinc . mg/L	4.0	5.4	28	1.1	0.056	20

[1] These parameters should not appear at predicted levels because secondary-mineral precipitation is limiting their concentrations according to MINTEQ evaluations.

The relatively good agreement of predicted and observed values not affected by mineral precipitation in table 3 is notable because of the assumption that average precipitation was distributed evenly on a daily basis in the calculations. In other words, chemistry was well predicted, whereas transient flow rates were not. This may indicate that water-flow-generating processes such as condensation are resulting in near-daily flushing of rock surfaces within flow channels. There is insufficient information at this site to further evaluate and resolve such issues.

Conclusion

This paper has presented an empirical model for general predictions of chemical concentrations in seepage from mine-rock piles. This model is based on five factors that account for, but simplify, geochemical production rates, water movement, and rock-surface flushing. The hypothetical example demonstrated the model, but indicated that other processes like secondary-mineral precipitation may also have to be considered. The field example based on an actual minesite showed that relatively good agreement was found between model predictions and observed concentrations under acidic and neutral pH conditions, except for parameters affected by mineral precipitation.

Acknowledgements

We would like to thank an anonymous reviewer and Dr. Bill Price (B.C. Ministry of Energy, Mines, and Petroleum Resources) who helped to improve the quality and clarity of this paper and the conference organizers, particularly Ms. Lowanse, who coordinated manuscript preparation and submission.

'Ua mau ke ea ō ka 'āina i ka aloha 'āina

References

Allison, J.D., D.S. Brown, and K.J. Novo-Gradac. 1990. MINTEQA2/PRODEFA2, a geochemical model for environmental systems: Version 3.0 User's Manual. U.S. Environmental Protection Agency, Environmental Research Laboratory, Athens, Georgia, USA.

ElBoushi, I.M. 1975. Amount of water needed to initiate flow in rubbly rock particles. Hydrology 27: 275-284.

Morin, K.A. 1994. Prediction of water chemistry in open pits during operation and after closure. In 18th Annual Mine Reclamation Symposium, Technical and Research Committee on Reclamation. (Vernon, British Columbia, April).

Morin, K.A. 1991. Acid drainage from mine walls: The Main Zone Pit at Equity Silver Mines. Report for the British Columbia Acid Mine Drainage Task Force and the Mine Environment Neutral Drainage (MEND) Program.

Morin, K.A. 1988. Groundwater contamination from precious-metal, base-metal, uranium, phosphate, and potash (KCl) mining operations. p.175-187. In C.L. Lin ed., Proceedings of the International Groundwater Symposium, International Association of Hydrogeologists. (Halifax, Nova Scotia, May 1-5).

Morin, K.A., and N.M. Hutt. 1994. MINEWALL Version 2.0: expansion, improvement, and verification of existing code. Draft report for Canadian MEND Program.

Morin, K.A., C.E. Jones, and R.P. van Dyk. 1994. Internal hydrogeologic monitoring of an acidic waste-rock dump at Westmin Resources' Myra Falls Operations, British Columbia. In Third International Conference on the Abatement of Acidic Drainage (these proceedings).

Morin, K.A., E. Gerencher, C.E. Jones, and D.E. Konasewich. 1991. Critical literature review of acid drainage from waste rock. Report for the Mine Environment Neutral Drainage (MEND) Program.

Morth, A.H., E.E. Smith, and K.S. Shumate. 1972. Pyrite systems: a mathematical model. Contract Report for the U.S. Environmental Protection Agency, EPA-R2-72-002.

Norecol, Dames, and Moore. 1993. Long term kinetic acid generation studies Cinola Project, Queen Charlotte Islands British Columbia [sic]. Report for the British Columbia Acid Mine Drainage Task Force.

Rescan Consultants Inc. 1992. Hydrological and metal loadings study, Phase report. Mine Report for Island Copper Mine, BHP Minerals Canada Limited.

Senes Consultants Limited. 1991 The Reactive Acid Tailings Assessment Program (RATAP.BMT3). MEND Program project.

ASSESSMENT OF CONTAMINANT LOAD CHANGES CAUSED BY REMINING ABANDONED COAL MINES[1]

Jay W. Hawkins[2]

Abstract: Determination of contaminant loading changes caused by remining of abandoned coal mines requires knowledge of the characteristics of the hydrologic data before and after remining. Under an approved remining program, a coal mine operator can remine abandoned coal mines without assuming treatment responsibilities of the previously degraded water, as long as these discharging waters are not further degraded. Normality tests performed on the hydrologic data from 57 mine discharges from 24 remining operations indicate generally nonnormal distributions and extreme right-skewness (toward the smaller values). Analysis of the differences among medians indicates that the water quality of underground mines was more highly degraded than that of surface mines. Analyses of pre- and post-remining mine discharge water quality and flow rates of the 57 discharges illustrate that most the sites exhibited either no change or a significant decrease in contaminant rate because of remining. The discharge flow rate was the dominant controlling factor when the post-remining pollution load was observed to be significantly better or worse than the pre-remining load, as was shown with the correlation and other analyses. Generally, when the mine discharges were degraded as a result of remining, this was caused by short-term changes in flow and/or concentration that occurred shortly after reclamation. Reduction of recharge from the surface and adjacent unmined strata should decrease the mine discharge flow rate and in turn the contaminant load.

Additional Key Words: remining, contaminant load, alternate effluent standards

Introduction

Remining, as it is used in this paper, is the surface mining of abandoned surface and/or underground mines that originally created and continue to possess discharges that fail to meet the applicable effluent standards. Under a regulated remining program, an operator can mine these sites without assuming legal responsibility for treatment of the previously degraded water, as long as the water is not further degraded. If the water is further degraded, the treatment level is based on site-specific pre-remining contaminant load levels and not legislatively promulgated effluent standards. To establish pre-remining pollution load levels, a mine operator must collect a consecutive series of pre-remining water samples and measure the flow rate. Remining contaminant loading rate effluent standards (baseline loading rate) are based on these data. However, the baseline loading rate is also dependent on the strength of the pollution abatement plan and the cost of conventional treatment. If, after remining, the contaminant loading rates are no worse than the pre-remining levels and all other physical and temporal reclamation requirements are satisfied, discharge monitoring ceases and the reclamation bonds are released.

This paper presents the results of univariate and bivariate statistical analyses of data from 57 mine discharges emanating from remining operations in the bituminous coalfields in Pennsylvania. The data were obtained from 24 remining permits of the Pennsylvania Department of Environmental Resources (PADER) that were selected from a larger group of 105 potential sites (fig. 1). The selected permits possessed sufficient post-remining hydrologic data (at least 1 yr, dating from rough backfilling) to allow comparison with the pre-remining data.

Acidity, total iron, sulfate, and flow rate are analyzed in this report. Under present Pennsylvania remining regulations, acidity and iron baseline loading effluent standards are required for all permits, regardless of the concentration. Sulfate is analyzed because it serves as a conservative indicator of acid mine drainage (AMD) production and can be used to evaluate changes in discharge quality. Increased sulfate levels, in the Appalachian basin, are generally indicative of AMD production. Discharge flow rate is needed along with concentration to calculate contaminant loads.

AMD is created when sulfide minerals (usually pyrite) oxidize and the oxidation products are subsequently mobilized. Ground water serves as the transport medium of these products.

---

[1]Paper presented at the International Land Reclamation and Mine Drainage Conference and the Third International Conference on the Abatement of Acidic Drainage, Pittsburgh, PA, April 24-29, 1994.

[1]Jay W. Hawkins, Hydrologist, U.S. Bureau of Mines, Pittsburgh, PA, USA.

Recharge events tend to "flush out" the oxidation products as the wetting front moves through the unsaturated portion of the spoil. During surface mining, overburden material is broken into clay (<0.002 mm) to boulder (>256 mm) sized particles, exposing pyritic minerals to oxidation from atmospheric oxygen and iron-oxidizing bacteria. This promotes a state of geochemical flux during and after mining. Subsidence observations and aquifer testing indicate that mine spoil continues to undergo physical changes caused by compaction, shifting, and piping by ground water for at least 30 months after reclamation (Aljoe and Hawkins, 1992). Spoil continues to physically change well beyond 30 months after reclamation, but at a reduced rate.

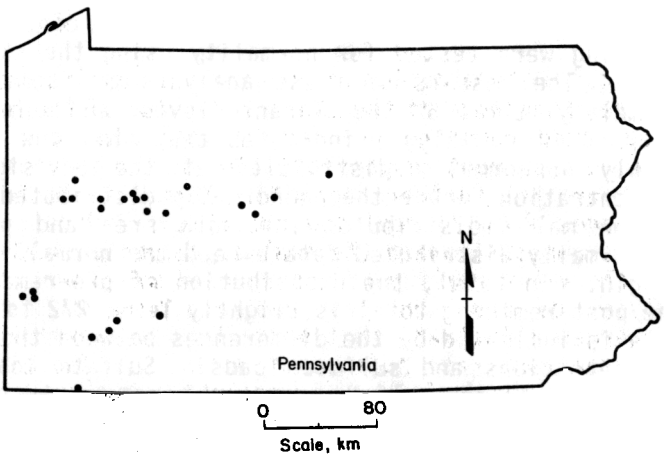

Figure 1. Location of the study sites.

The number of mine discharges at each site ranged from one to five. Mine operators report contaminant concentrations in milligrams per liter (mg/L) and flow in gallons per minute (gpm). The data are then transformed into loads of pounds of contaminant per day (lb/d), which is the effluent baseline pollution load unit used in Pennsylvania, as well as other States, for remining permits. The flows and loads were converted to liters per minute (L/min) and kilograms per day (kg/d), respectively. Table 1 summarizes these data. For portions of the statistical analyses, the data were further separated into underground and surface mine discharges.

Table 1. Summary of remining data. All data are median flow or concentration values, except n which is the number of samples.

	PRE-REMINING					POST-REMINING				
Site	n	flow	acid	Fe	SO_4	n	flow	acid.	Fe	SO_4
1	17	8	19	0.2	339	13	4	30	0.2	420
2	21	1181	321	24.1	814	41	1283	261	20.5	852
3	22	23	511	62.0	1132	14	4	512	36.0	1089
4	10	144	43	2.9	92	45	155	162	21.9	602
5	38	193	18	0.1	151	19	182	11	0.1	118
6	21	110	143	2.7	732	16	140	128	2.3	722
7	31	469	1020	11.3	1077	11	466	850	12.8	1087
8	10	204	777	99.3	1695	40	117	294	37.6	2189
9	4	261	1447	58.1	2671	16	95	742	54.7	2230
10	9	250	4	0.6	53	33	144	3	0.5	51
11	6	280	302	10.9	991	17	38	262	6.7	882
12	12	462	58	0.2	NA	63	140	23	0.4	326
13	11	53	5	0.2	NA	56	30	10	0.2	649
14	28	11	9	1.2	159	46	15	9	0.8	204
15	9	19	136	3.5	236	24	8	299	1.6	876
16	3	189	456	295.0	1430	71	148	541	218.5	1202
17	26	64	80	1.0	515	43	45	2	1.7	690
18	24	265	2	0.4	153	33	348	10	0.3	270
19	18	34	16	0.2	74	36	42	83	1.1	446
20	8	140	208	3.3	740	7	4	19	0.5	749
21	16	42	90	2.5	231	21	61	90	2.6	379
22	28	238	231	4.8	931	10	428	151	5.9	779
23	8	344	89	4.6	253	25	220	127	9.8	374
24	18	11	566	64.1	673	12	0	677	176.8	1816

Tests for Normality

Discharge flow rate, contaminant concentration, and loading rate data before and after remining were tested for normality using the skewness test and the chi-square goodness-of-fit test. The results of these analyses are summarized in table 2. The data were tested for normality at the 5% significance level, and form of skewness (left or right) was determined.

The analysis indicates that the flow rate, concentration, and loading rate data are mainly nonnormally distributed at the 5% significance level. One exception is sulfate concentration, where the nonnormally distributed data for concentration nearly equal those that are normally distributed for both pre- and post-remining periods. For other parameters, nonnormally distributed data exceed the normally distributed data sets by at least a two-to-one margin. In total, the distribution of pre-remining variables is 277 nonnormal to 112 normal. The post-remining total is slightly less, 272 to 117. A strong influence of flow on the loading rate is indicated by the differences between the pre- and post-remining distribution of sulfate concentrations and sulfate loads. Sulfate loads are similar to the corresponding flow and dissimilar to the sulfate concentrations. This indicates that the flow influence on sulfate load is stronger than the concentration influence.

Table 2. Summary of normality testing results. A P value greater than 0.05 indicates the data were not normally distributed at the 5% significance level; a P value less than 0.05 indicates that the assumption of normality cannot be rejected with greater than 95% confidence. NA signifies that there were insufficient degrees of freedom to adequately conduct the chi-square test.

	Skewness test		Skewness		Chi-square test		
Pre-Remining	P<0.05	P>0.05	Left	Right	P<0.05	P>0.05	NA
Flow rate	45	12	12	45	12	1	44
Acid conc.	35	22	22	35	4	7	46
Acid load	42	15	8	49	9	2	46
Fe conc.	40	17	11	46	6	4	47
Fe load	45	12	10	47	10	4	43
SO_4 conc.	28	24	22	30	4	8	40
SO_4 load	42	10	12	40	11	1	40
Post-Remining							
Flow rate	41	16	7	50	21	7	29
Acid conc.	35	22	13	43	21	6	30
Acid load	40	17	3	54	24	5	28
Fe conc.	52	5	6	51	17	8	31
Fe load	42	15	5	52	25	4	28
SO_4 conc.	27	25	15	37	12	12	28
SO_4 load	35	17	2	50	15	8	29

Table 2 illustrates that the data are mainly skewed right (toward lower values). The ratio of right-to-left skewed data ranges from a low of about 1.4 to 1 for pre-remining sulfate concentration to a high of 25 to 1 for post-remining sulfate load. In general, the number of concentration data sets skewed right in the post-remining period exceeds that for the pre-remining period. This may be caused by the state of flux of the post-remining spoil aquifer, which yields periodic extreme concentration and flow values. Loading data skewness is more often to the right than either flow or concentration. This increase appears to be caused by the interdependence of

concentration to flow (e.g., concentration increases caused by "flushing" or concentration decreases caused by dilution). The majority (629 of 777) of the pre- and post-remining data tend to be skewed right. Table 2 shows that the chi-square and the skewness tests produce similar results. However, because of the nonapplicability of the chi-square test in many cases, a direct comparison cannot be made. The chi-square test results illustrate that the majority of the data are nonnormally distributed at the 5% significance level. However, there are some inconsistencies within the concentration data sets before and after remining.

Chi-square testing of the pre-remining concentration data indicates that they are more often normally than nonnormally distributed. Conversely, the post-remining data tend to be more often nonnormally distributed than the pre-remining data. However, pre-remining iron concentration tends to be nonnormally distributed. The post-remining data are mainly nonnormal for acidity and iron concentrations. Post-remining sulfate concentration is equally likely to be normally or nonnormally distributed. The differences between pre- and post-remining concentration may be related to the lower number of tests that could be performed compared with the skewness tests. The chi-square testing indicates that the contaminant loads exhibit distributions similar to those of the corresponding flow data. This suggests that flow rate is the dominant influence on loading rates, as also observed by Smith (1988). This is especially evident with chi-square tests for the pre-remining acidity and sulfate.

Exploratory Data Analysis

One tool of exploratory data analysis is the "notched box-and-whisker" plot. These plots are used to graphically display basic statistical parameters to compare subsets of data. For more information on notched box-and-whisker plots, the reader is directed to McGill et al. (1978).

Figure 2 is a notched box-and-whisker plot representing the sum of the median flow rate measurements for each site classified by mine type (underground and surface) before and after remining. A comparison of surface and underground mine discharge flow rate characteristics before and after remining indicates that there is no significant difference at the 95% confidence level.

Figure 3 exhibits the mine average acidity concentration determined from the individual discharge medians. This figure shows that the pre- and post-remining median acidity concentration for underground mines is significantly higher than that for surface mines. The elevated acidity exhibited by the underground mines occurs because ground water flows almost exclusively through parts of the mine where AMD forms (relatively high sulfur coal, seat, and roof rock). Conversely, Hawkins and Aljoe (1991) observed that in surface mines, ground water flows through discrete paths in the spoil. Parts of the spoil may consist mainly of acid-forming materials (e.g., high-sulfur shales, sandstones, and spoiled coal), while other parts may be mostly alkaline-forming materials (e.g., limestones and carbonate-rich shales). Underground mine discharges generally exhibit a wider range of values than those from surface mines. Post-remining acidity concentration is similar to pre-remining, indicating little change occurred relative to mine type.

Figure 4 is a plot of the average iron concentration determined from the individual discharge medians. The shape is similar to the acidity, although more subdued. The underground mine concentration median is above that for surface mines, although the differences are not significant at the 95% level. The post-remining plot is not significantly different from the pre-remining data.

Figure 5 represents a plot of the average of the pre- and post-remining discharge sulfate concentration medians for each site. The underground mine median value is higher than that of surface mines. The difference between the pre-remining medians is not significant. The data range is likewise wide for the underground mines. Post-remining sulfate, on the other hand, shows a significant difference at the 95% level. This is caused by a rise in the underground mine median and a narrowing of the approximate 95% confidence interval about the median (notches) of the underground mine data. Daylighting of the abandoned underground mines may increase AMD production, but greatly reduces the variability of sulfate concentration.

Notched box-and-whisker plots (not shown) created for pre- and post-remining of the contaminant loads for underground and surface mines are similar to the corresponding concentration plot. The loadings did not show a difference at the 95% confidence level between mine types. The plots for flow pre- and post-remining also did not exhibit significant differences in the medians at the 95% confidence level. This indicates that flow rate may have a stronger influence on loading than concentration does, which mirrors trends exhibited by the normality tests.

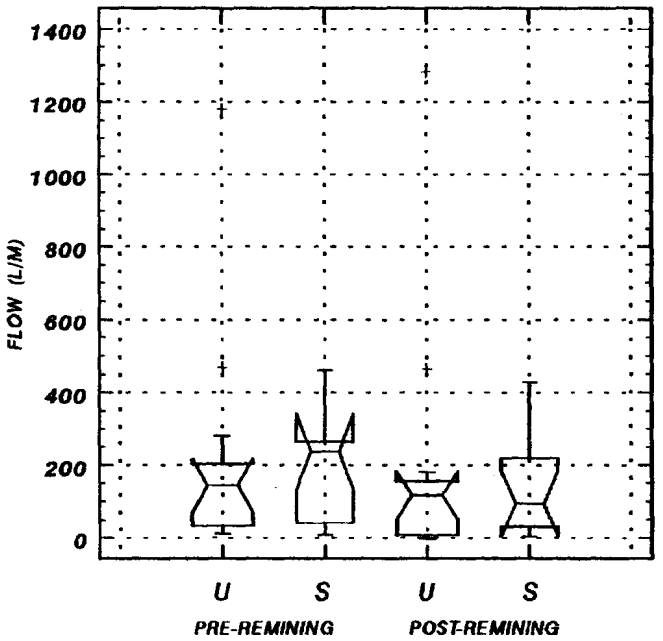

Figure 2. Median flow rate measurements of underground (U) and surface (S) mines before and after remining.

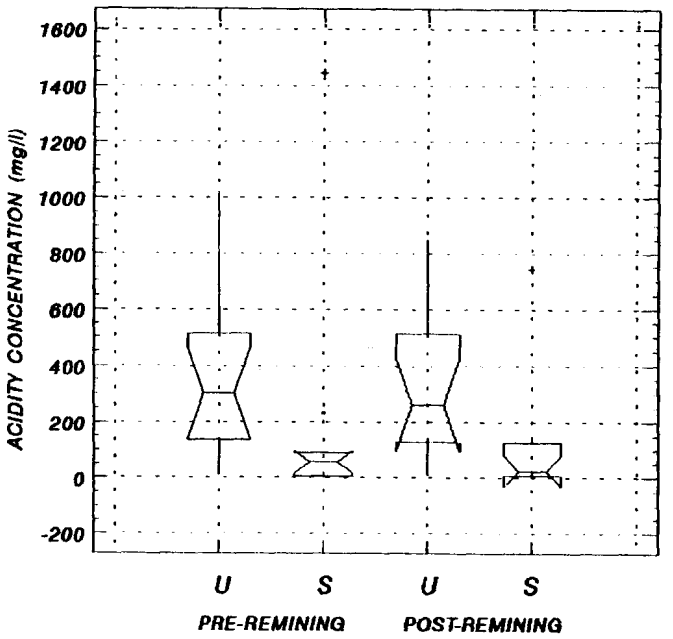

Figure 3. Acidity concentration medians of underground (U) and surface (S) mines before and after remining.

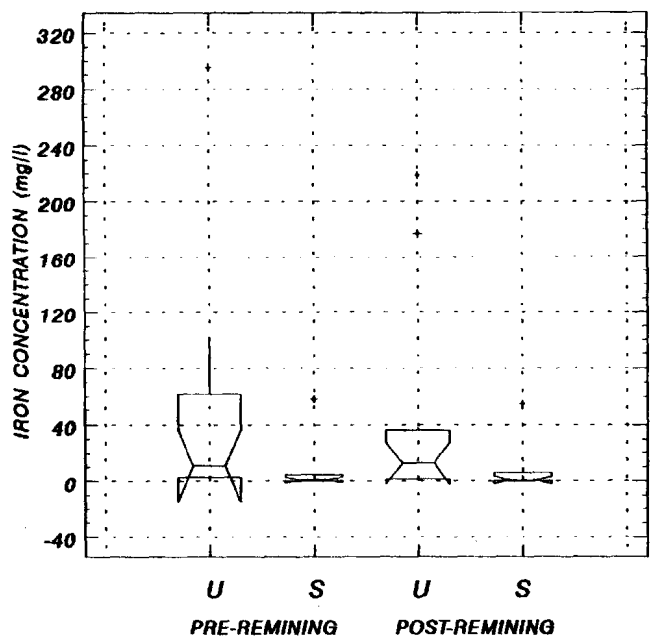

Figure 4. Iron concentration medians of underground (U) and surface (S) mines before and after remining.

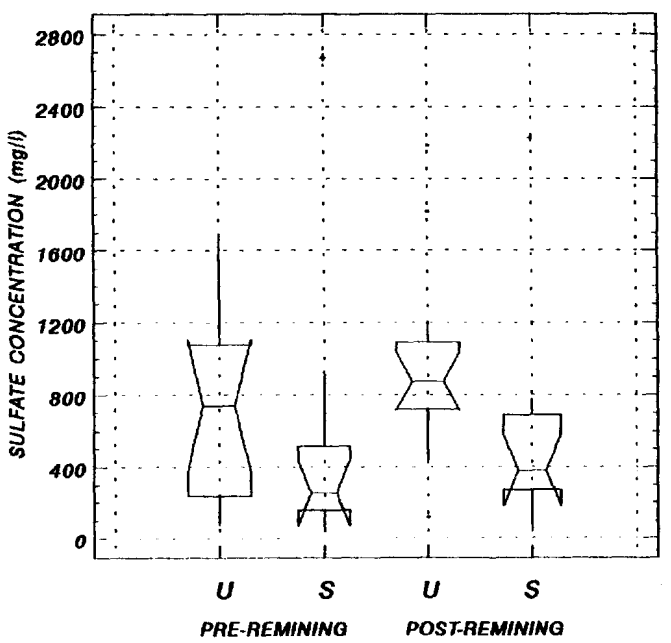

Figure 5. Sulfate concentration medians of underground (U) and surface (S) mines before and after remining.

Data Correlation

Correlation coefficient is a measure of the interrelationship between two variables from which the degree of statistical significance can be determined. Correlation coefficient is generally determined using parametric testing procedures (Davis 1986). Spearman's rank correlation is a nonparametric test used to calculate the correlation coefficient. For this study, the coefficient significance level was set at P = 0.05. Correlation coefficient values were calculated to show the effect that flow and concentration have on load. As summarized in table 3, flow is more often strongly correlated to the contaminant load than concentration.

Table 3.–Summary of significant correlations. The values are the number of data sets exhibiting a significant positive and negative correlation at the P=0.05 level.

	Pre-Remining			Post-Remining		
Flow vs Load	Acidity	Fe	SO_4	Acidity	Fe	SO_4
Positive	42	29	37	51	42	51
Negative	0	0	0	0	0	0
Concentration vs Load						
Positive	10	14	8	30	30	12
Negative	5	5	4	7	2	6

About 82% (93 of 114) of the total acidity loads are strongly correlated to flow, while the concentration exhibits a significant correlation to load in about half (52 of 114) the cases (table 3). Flow correlations are in all cases positive, indicating flow increases cause load increases. Strong correlations of flow to acidity load are increased moderately by remining. Pre-remining acidity concentration exhibits a positive correlation to contaminant load about 25% as often as flow. Post-remining acidity concentration was correlated positively to load three times more often than pre-remining, which may be caused by the state of flux that exists shortly after reclamation. In five cases, pre-remining acidity concentration exhibited a negative correlation to load. This may be caused by dilution from high-flow events. Negative acidity concentrations to load correlations for the post-remining data were not substantially different from those for pre-remining data.

Iron exhibited the lowest flow-to-contaminant-load correlation of the three contaminants. About 51% (29 of 57) of the pre-remining flow was strongly correlated to iron load, compared with 25% (14 of 57) of the cases in which concentration showed a significant positive correlation to load (table 3). Strong correlations of post-remining flow to iron load increased to 74% (42 of 57). The instances of positive correlation of iron concentration to load doubled after remining. The number of negative correlations of iron concentration to load was low and did not change significantly after remining.

Almost 89% (88 of 99) of both pre- and post-remining flow-to-sulfate-load correlations were positive. No negative flow-to-load correlations were noted (table 3). Flow-to-sulfate-load strong correlations increased after remining. Of all the contaminants, combined pre- and post-remining sulfate concentration to load showed the least number of strongly correlated data. Concentration to load correlation, both positive and negative, changed very little because of remining.

Significant positive correlations of flow to load exceeded concentration-to-load correlations by 252 to 104. The increase of the post-remining positive correlation of flow and concentration to load may be related to the previously discussed state of flux of mine spoil after remining.

All negative correlations were exhibited by concentration to load. This may be caused by contaminant dilution by increased flow or geochemical changes in ground water quality that can reduce concentrations through chemical reactions. During high-flow events, the sources and flow paths of the ground water can change, thus causing water quality changes. Chemical reactions, because of water quality changes, can reduce the acidity and iron content, but usually will not affect the sulfate content at the noted levels. Negative sulfate concentration to load

correlations were similar to those for iron and acidity, indicating that dilution may be the main cause of most of the negative correlations.

Determination of Contaminant Load Reduction

To determine the effectiveness of remining to reduce contaminant load, the remining operation discharges were analyzed. The pre- and post-remining data were analyzed using an exploratory data analysis system (schematic summary), which is presently used by the PADER, and the Mann-Whitney U test.

PADER System

Initially, under the PADER system, a minimum of 6 monthly samples were required, although 12 consecutive monthly samples were strongly recommended. The PADER now requires 12 consecutive months of data. In theory, 12 monthly samples will include both low- and high-flow periods in the background data, which will more accurately characterize the preexisting discharges. For the analysis using the PADER system, all discharges from each site were combined into a single hydrologic unit to determine the effectiveness of remining on a site-by-site basis. Pre-remining water quality data are analyzed using some basic exploratory data analyses and nonparametric statistics (PADER 1988). Results for each discharge or hydrologic unit are presented in a table containing the loading data range, the median, the first and third quartiles, the approximate 95% tolerance limits, and the 95% confidence interval about the median for each of the regulated contaminants. Table 4 is an example of these results. Tukey (1976) and Velleman and Hoaglin (1981) present explanations of these values and how they are calculated. Under the PADER system, there are four mechanisms by which treatment of a discharge can be initiated (triggered) using the data in this table.

Table 4.–Example of PADER baseline contaminant load summary table. Units used in this table are as used for permitting by the PADER.

Mine ID:	Mine Name:			Hydrologic Unit ID:	
		Loading in Pounds Per Day			
Parameter:		Flow(gpm)	Acidity	Iron	Sulfate
Number of Samples (N):		43	43	43	43
1. Range	Low:	3.00	0.07	0.00	28.27
	High:	42.00	1.01	1.41	214.56
2. Median		12.00	0.29	0.21	99.53
3. Quartiles	Low:	9.00	0.22	0.15	70.98
	High:	17.00	0.41	0.60	132.63
4. Approximate 95% Tolerance Limits	Low:	3.00	0.07	0.02	31.01
	High:	34.00	0.82	1.29	210.47
5. 95% Confidence Int. about Median	Low:	10.22	0.25	0.11	85.77
	High:	13.78	0.33	0.31	113.28

The first triggering method requires a series of 6 consecutive samples to exceed the upper bound of the approximate 95% tolerance limit (item 4 in table 4). If two consecutive samples exceed the upper bound of the approximate 95% tolerance limits, during and after mining, this triggers weekly sampling. If 4 consecutive weekly samples exceed the approximate 95% tolerance limits, the operator initiates treatment within 30 days. If two consecutive weekly samples drop below the 95% tolerance limits at any time during the weekly sampling, monthly monitoring resumes and treatment is not required. If treatment is incurred, it is suspended if two consecutive weekly samples drop below the 95% tolerance limits.

Second, treatment is initiated when the statistical analysis indicates the during- or post-remining median contaminant load has increased in comparison to the pre-remining median at the 5% significance level. This is determined by comparison of the 95% confidence interval about the

median (item 5 in table 4) of the pre- and post-remining data. The median is calculated on a complete water year (October 1 through September 30) basis.

The third triggering method uses the same method. However, the median is determined for water-year periods 1 (October 1 through April 30) or 2 (May 1 through September 30). Finally, treatment can be triggered if analyses, including but not limited to the means and variances of the data, indicate that the difference between water years or water-year periods is significant at the 1% level. The third and fourth triggering methods are seldom used.

Table 5.—Summary of weekly sampling and discharge treatment triggering from remining. "Yes" indicates that triggering occurred at least once to one or more discharges and/or hydrologic units for that site. "No" indicates triggering never occurred.

	Acidity		Iron		Sulfate	
	Yes	No	Yes	No	Yes	No
Weekly sampling	10	14	5	19	11	11
Treatment	3	21	3	21	5	17

Weekly sampling was initiated at least once after remining by acidity for 10 of 24 sites (table 5). Three of these sites subsequently triggered treatment. Iron triggered weekly sampling in 5 out of 24 sites. Of these 5 sites, 3 triggered discharge treatment. Of the 3 discharge treatment incidences, for acidity and iron, 2 occurred concurrently; therefore treatment was initiated at least once on 4 sites. The high load events that triggered treatment were in all cases transient. High-loads usually occurred shortly after reclamation (<1 yr) and usually declined to below tolerance limits within a short period (<6 months) after initiation. Site 8 was the only mine to initiate treatment more than 13 months after reclamation.

Sulfate would have triggered weekly sampling, if it was an effluent contaminant, for 50% of the sites. Almost half of the weekly sampling events would initiate treatment. The high number of sites where sulfate loads would initiate weekly sampling and then treatment may be caused by hydrologic and geochemical changes that occur in the spoil following remining. Pyritic material surface area exposed to oxidation is greatly increased by mining. This promotes AMD production, which is indicated by elevated sulfate levels. The increased rock surface area also increases the exposure of alkaline strata, when present, to weathering and dissolution, thus adding alkalinity to the ground water. This alkalinity reduces acidity levels and raises the pH, which increases the potential for dissolved iron to oxidize and precipitate out of solution. However, sulfate concentrations are little affected by increases in alkalinity and pH at the given sulfate and calcium levels.

For the second triggering method, the reason for using a water year is to ensure that the data used in the comparison are not biased by most of the sampling occurring during a protracted low- or high-flow period. The large number of possible water year periods for the 57 discharges precluded strict adherence to this part of the PADER system. Instead, the data for the entire post-remining period were compared with the pre-remining data. Any sampling bias of the data was minimized because each of the post-remining data sets included from 2 to over 10 of each low- and high-flow periods. The potential bias is also reduced by the use of the data median, which is less sensitive than the mean to extreme values (Snedecor and Cochran 1971).

The results using the second PADER system indicate that remining at most of the sites did not cause additional degradation. The median acidity and iron loads for 21 out of 24 sites were within or below the pre-remining 5% significance level. The one site where acidity was above pre-remining levels coincided with one of the iron excursions. Median loads for acidity from 7 of 24 sites and for iron from 4 of 24 sites were below the pre-remining 5% significance level. Three of the excursions coincided, making a total of 8 sites with significant decrease in load. Of these 11 excursions, 7 also exhibited a significant flow reduction at the 5% level. However, a 2-fold or greater increase in concentration coincided with 6 of the excursions.

Of the four excursions of the median acidity and/or iron loads above the 5% significance level, none exhibited a significant increase in flow. However, 3 of the 4 exhibited substantial increases in concentration (a factor of 5 or more).

Sulfate load comparison exhibits similar results to acidity and iron: 3 above, 15 within, and 4 below the pre-remining 5% significance level. Flow was a significant factor in 3 of 4 excursions below the 5% significance level, although concentration did not vary by more than 11%. However, flow was not a significant factor for the 3 excursions above the 5% level, while concentration increased by a factor of 6 or more in 2 out of the 3 cases.

Flow played a critical role in load rate excursions outside the 5% significance level, especially for decreases in load. The results indicate that concentration is a weaker factor than flow in causing excursions outside the 5% significance level. However, concentration changes were more often associated with excursions above (71%) rather than below (40%) the 5% level.

Table 6.—Summary of the results from the second PADER triggering method.

	Above	Within	Below
Acidity Load	1	16	7
Iron Load	3	17	4
Sulfate Load	3	15	4

Mann-Whitney U Test

The Mann-Whitney U (MW) test is a nonparametric version of the Student's t test that determines if the median (or mean) of two data sets come from different populations at the 5% significance level (Davis 1986). Mine water quality and flow can vary widely within a site. Therefore, the MW test was applied to individual discharges, rather than the entire mine, to provide a clearer determination of the effect of remining on flow and water quality.

The MW test results (table 7) indicate that acidity and iron concentration and load were unchanged or improved (decreased) at the 5% significance level for most of the discharges. The number of discharges above the 5% level (indicating degradation) is lower for acidity and iron loads than for concentrations. This may be related to the strong influence that flow has on the contaminant load. The test results for acidity and iron loading are similar to those for flow and dissimilar for concentration.

The number of discharges exhibiting increased sulfate concentration and load is higher than the number of discharges exhibiting increased acidity or iron values. Over 34% of the discharges show increased sulfate concentration and almost 20% have an increased sulfate load at the 5% significance level. This higher "failure" rate exhibited by sulfate is likely due to changes in ground water flow paths and material contacted after remining, as previously discussed.

Table 7.—Summary of the Mann-Whitney U test results. Below means the post-remining median was below pre-remining at the 5% significance level. Above means the median was above at the 5% level and within indicates that the data did not exceed the upper or lower 5% significance levels.

	Below	Above	Within
Acidity concentration	24	7	26
Acidity load	17	4	36
Iron concentration	18	9	30
Iron load	17	5	35
Sulfate concentration	9	18	25
Sulfate load	14	10	28
Flow rate	16	4	37

Summary and Conclusions

To accurately assess the success of remining in reducing discharge contaminant loads, a basic understanding of the hydrologic characteristics is required. Testing indicates that water quality and flow data are nonnormally distributed. Remining appears to increase the nonnormality of the data. The data are mainly skewed toward lower values. Trends exhibited by the test results indicate that flow is the dominant factor for determining the contaminant load rate.

Water discharging from underground mines is more degraded by AMD than that from surface mines. This may be caused by differences in the ground water flow regime of the two mine types.

Remining is generally successful in preventing additional ground and surface water degradation in terms of contaminant concentrations, load, and flow of mine discharges. Most discharges have post-remining contaminant loads that are equal to or below the pre-remining levels. Short-term transient changes (< 6 months) in flow and/or concentration are the main reasons that degradation appears to have occurred at some of the discharges.

When the analyses indicate that a significant change in terms of contaminant load occurred, a change in the discharge rate is the most common reason. If flow can be reduced through mining and/or reclamation practices, the probability that the operation will not incur permanent treatment liability is greatly increased. Concentration is a secondary factor in some cases.

Concentration may play a somewhat stronger role in load determination when a significant increase in load is indicated than when a significant decrease is indicated.

Discharge flow-reduction practices can be incorporated into the permit-application abatement plan. Flow reduction can be achieved by exclusion or diversion of ground and surface water away from the reclaimed site. Methods that decrease infiltrating surface water include installation of diversion ditches, capping the site with a low-permeability material, spoil regrading, and revegetation. Abandoned sites, prior to remining, commonly have unreclaimed pits and closed-contour depressions that serve as infiltration zones for surface water. For abandoned surface mines, regrading and revegetating spoil often will reduce surface water infiltration and increase runoff by eliminating these recharge zones.

Methods for decreasing ground water recharge to the spoil include drains and/or grout curtains installed near the final highwall, pit floor drains, horizontal free-draining dewatering wells, and sealing of adjacent underground mine entries.

Although this study was conducted exclusively in Pennsylvania, the geologic and hydrologic conditions in other Appalachian States are similar enough to those of the western Pennsylvania coalfields to expect similar levels of contaminant-load reduction.

Literature Cited

Aljoe, W. W. and J. W. Hawkins. 1992. Application of aquifer testing in surface and underground mines. p. 541-555. In Proceedings of the NGWA - FOCUS Conference on Eastern Region Ground Water Issues (Newton, MA, Natl Ground Water Assoc.).

Davis, J. C. 1986. Statistics and data analysis in geology. Wiley, New York. 646 p

Hawkins, J. W. and W. W. Aljoe. 1991. Hydrologic characteristics of a surface mine spoil aquifer. p. 47-68. In Proceedings of the Second International Conference on the Abatement of Acidic Drainage (Montreal, Quebec, Canada).

McGill, R., J. W. Tukey, and W A. Larsen 1978. Variations of box plots Am. Statistician 32(1):12-16.

Pennsylvania Department of Environmental Resources, The Pennsylvania State University, and Kohlmann Ruggiero Engineers. 1988. REMINE.

Smith, M. W. 1988. Establishing baseline pollution load from preexisting pollutional discharges for remining in Pennsylvania. p. 311-318. In Mine Drainage and Surface Mine Reclamation. Proceedings Vol. II: Mine Reclamation, Abandoned Mine Lands and Policy Issues. Bur. Mines IC 9184.

Snedecor, G. W. and W. G Cochran. 1971 Statistical methods. The IA State Univ Press, Ames, IA. 593 p.

Tukey, J. W. 1976. Exploratory data analysis. Addison-Wesley Publishing Co., Reading, MA. 688 p.

Velleman, P. F. and D. C. Hoaglin. 1981. Applications, basics, and computing of exploratory data analysis. Duxbury Press, Wadsworth, Inc., Belmont, CA. 354 p.

MATHEMATICAL SIMULATION OF A WASTE ROCK HEAP[1]

Jeno M. Scharer[2,3], Carol M. Pettit[2], Doug B. Chambers[2] and Edmund C. Kwong[3]

Abstract: A computer model has been developed to simulate the generation of acidic drainage in waste rock piles. The model considers the kinetic rates of biological and chemical oxidation of sulfide minerals (pyrite, pyrrhotite) present as fines and rock particles, as well as chemical processes such as dissolution (kinetic or equilibrium controlled), complexation (from equilibrium and stoichiometry of several complexes), and precipitation (formation of complexes and secondary minerals). Through mass balance equations and solubility constraints (e.g., pH, phase equilibria) the model keeps track of the movement of chemical species through the waste pile and provides estimates of the quality of seepage (pH, sulfate, iron, acidity, etc.) leaving the heap. The model has been expanded to include the dissolution (thermodynamic and sorption equilibrium), adsorption and coprecipitation of uranium and radium. The model was applied to simulate waste rock heaps in British Columbia, Canada and in Thüringia, Germany. To improve the accuracy and confidence of long-term predictions of seepage quality, the entire history of the heaps was simulated. Cumulative acidity loads and water treatment considerations were used as a basis for evaluation of various decommissioning alternatives. Simulation of the technical leaching history of a heap in Germany showed it will generate contaminated leachate requiring treatment for acidity and radioactivity for several hundred years; cover installation was shown to provide a significant reduction of potential burdens, although chemical treatment would still be required beyond 100 years.

Additional Key Words: computer model, waste rock model, technical leaching, prediction, uranium.

Introduction

Acidic drainage from waste rock containing sulfide minerals is a serious environmental problem. The accurate prediction of the potential magnitude and duration of the contaminant loading is of concern to both mine operators and regulatory agencies. Mathematical modeling is a recommended tool for evaluating the extent of the problem and for providing direction for assessing management and decommissioning strategies.

A computer model has been developed to simulate the generation of acidic drainage in waste rock piles (SENES 1993). The model simulates the waste rock pile as an equivalent rectangle of specified depth and surface area. The depth is then subdivided into 20 horizontal layers, forming a series of interconnected modeling units. Water infiltrating the waste rock is assumed to flow downwards and exit as seepage at the base of the waste rock pile. The void space within the unsaturated waste rock pile is assumed to contain a small amount of pore water associated with the surface of the rock particles. The waste rock particles are characterized as being either fines or rocks (figure 1).

---

[1]Paper presented at the International Land Reclamation and Mine Drainage Conference and the Third International Conference on Abatement of Acidic Drainage, Pittsburgh, PA. April 24-29, 1994.

[2]Jeno M. Scharer, Biochemical Engineering Consultant, Carol M. Pettit, Environmental Engineer, and Douglas B. Chambers, Vice President and Director of Radioactivity and Risks Studies, SENES Consultants Limited, Richmond Hill, ON, Canada.

[3]Jeno M. Scharer, Associate Professor, and Edmund C. Kwong, Graduate Student, Dept. Chem. Eng., University of Waterloo, Waterloo, ON, Canada.

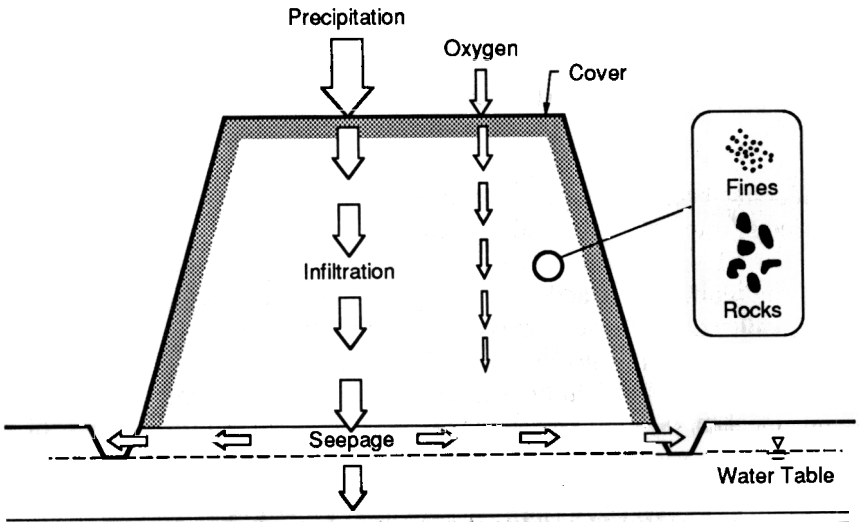

Figure 1. Concepts adopted for modelling of waste rock piles.

Model Structure

The computer model is comprised of seven main modules as shown in figure 2. The **Initial Inventory Module** assigns the initial concentrations and calculates the internal geochemical, kinetic, and physical parameters used in the subsequent modules. The theoretical basis for the model and the equations describing sulfide oxidation, oxygen transport, enthalpy (temperature) transport, pH calculation and aqueous speciation, and dissolution-precipitation reactions were previously described by Scharer et al. (1992).

The **Case-Specific Module** contains the instructions for simulation of timed events and specific scenarios, such as construction of the waste pile (i.e., placement of lifts, reprofiling, installation of a cover) and changes in the nature of the infiltration flow (i.e., infiltration rate, recirculation of leach solution). These activities are simulated by making changes to the corresponding model parameters (e.g., infiltration flows, mineralogy, oxygen diffusion coefficient, moisture content).

The **Kinetics Module** contains all of the equations for evaluating sulfide oxidation, oxygen transport, and temperature. The stoichiometric equations for the oxidation of iron sulfides, pyrite and pyrrhotite into their reaction products have been reviewed (Lowson 1982, Nordstrom 1982). The abiotic oxidation of sulfide minerals is modeled by the following relationship (Moses and Herman 1991, McKibben and Barnes 1986):

$$k_c = A\ (0.33\ pH)^{0.7}\ e^{-\frac{E_a}{RT}}\ [O_2] \tag{1}$$

where:

k_c	=	chemical surficial reaction rate constant (mol m^{-2} s^{-1}),
E_a	=	Arrhenius activation energy (J/mol),
$[O_2]$	=	oxygen concentration (mol/m^3),
A	=	Arrhenius pre-exponential factor,
R	=	molar gas constant (J mol^{-1} K^{-1}),
T	=	temperature (K).

The preexponential factor (A) for the chemical rate constants is dependent on the pyrite/pyrrhotite content. The chemical reaction rate has been shown to be a weak function of the pH (McKibben and Barnes 1986). The

biological oxidation rate, however,includes both temperature and pH dependence in the following manner (Scharer et al. 1991):

$$k_B = B\left[\frac{1}{1+10^{2.5-pH}+10^{pH-4}}\right]e^{-\frac{E_a}{RT}} \qquad (2)$$

where: B = biological scaling factor, and

k_B = biological surficial reaction rate constant (mol m^{-2} s^{-1})

The constant "B" in equation 2 is the biological scaling factor (SENES and Beak 1988) used to fit site specific data and is, in turn, a function of moisture content, nutrient levels, and the partial pressure of oxygen and carbon dioxide. Bacterial oxidation becomes significant at pH values below 4; at pH 2 to 3, the biological oxidation rate is approximately 16 to 35 fold greater than the abiological rate. The waste rock is assumed to consist of fine grained and coarse rock particles. The specific reaction rate (mol kg^{-1} s^{-1}) for fine particles is calculated from the abiological and biological oxidation rates as follows:

$$R_{s,p} = (k_c + k_B)a/\rho \qquad (3)$$

where: $R_{s,p}$ = overall specific reaction rate (mol kg^{-1} s^{-1}) - fine particles,

a = specific surface area of sulfide minerals (m^2/m^3), and

ρ = density of the sulfide mineral (kg/m^3).

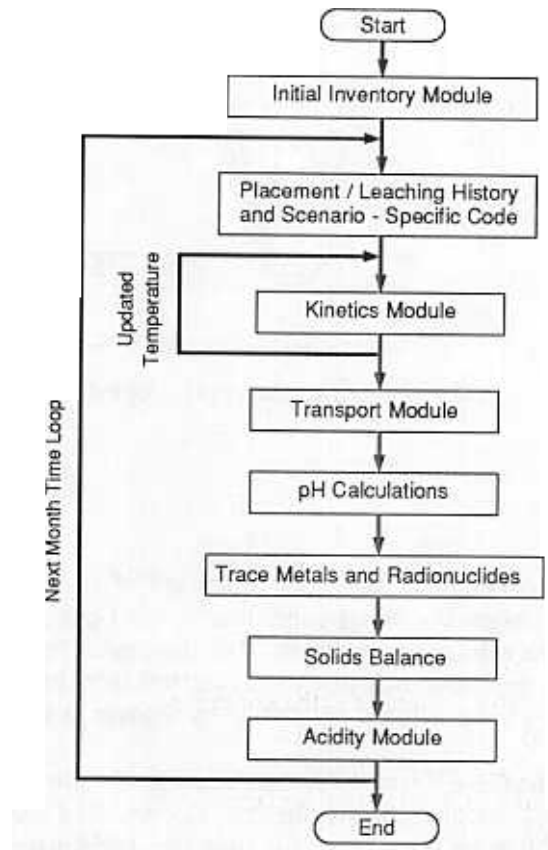

Figure 2. Structure of model of waste rock pile

The specific surface area of fine particles is evaluated by employing a Pareto-type distribution function (Scharer et al. 1992). The fine particles are modeled on the basis of shrinking particle kinetics. A shrinking reactive front concept is used to model oxidation of larger sulfide particles (larger than 2 mm particle size) or sulfide embedded in a rock matrix. The physical model consists of two phenomena: (1) the transport of oxygen through a liquid film and a layer of reaction products (primarily ferric hydroxide) and (2) the temporal shrinking of the reactive front as the sulfide is being oxidized. It can be shown that the overall oxidation rate per unit surface area is given by the combination of the two phenomena:

$$k_r = \frac{C}{\gamma}\left(\frac{1}{\frac{C}{\gamma(k_c+k_B)}+\frac{\Delta x}{D}}\right. \qquad (4)$$

where:

k_r	=	overall specific reaction rate of rock surfaces (mol m^{-2} s^{-1}),
γ	=	stoichiometric constant relating oxygen uptake to mineral oxidation,
Δx	=	thickness of layer surrounding the particle (m),
C	=	local concentration of the oxygen in the pore space (mol/m^3), and
D	=	diffusion coefficient of oxygen through the liquid film and layer of reaction products (m^2/s).

The transport of oxygen through the pore space is widely regarded as a rate controlling process (Cathles and Schlitt 1980, Davis and Ritchie 1986, Scharer et al. 1991). The principal mode of oxygen transport is molecular diffusion in open (i.e. non water filled) zones. The advective transport of oxygen in the percolating pore water is considered to be less significant (Scharer et al. 1991). The differential equation describing the transport process is the following:

$$\frac{\partial C}{\partial t} + D_e \frac{\partial^2 C}{\partial z^2} + vK_H \frac{\partial C}{\partial z} - \gamma \bar{R}_s = 0 \tag{5}$$

where:

$\bar{R}_s$	=	volume average sulfate oxidation rate (mol m^{-3} s^{-1}),
C	=	concentration of oxygen in the pore space (mol/m^3),
D_e	=	effective diffusion coefficient of oxygen through the waste rock (m^2/s),
z	=	depth into matrix (m),
t	=	time (s),
v	=	water infiltration rate (m/s), and
K_H	=	modified Henry's law constant (mol/m^3 oxygen in liquid per mol/m^3 oxygen in the gas phase).

In some situations, the convective transport of gaseous oxygen may be important. Since gas flow rates are usually not known, an effective dispersion coefficient is estimated and employed instead of diffusion in equation 5. The volume average sulfide oxidation rate is a function of the local oxygen concentration. Equation 5 possesses highly variable, both spatial and temporal, coefficients. For this reason, the equation is solved numerically using finite difference methods.

The temperature has a profound effect on both the chemical and the biological oxidation rates. To calculate the temperature, a simple enthalpy balance is employed. Since it is difficult to construct a global enthalpy model, the monthly temperature at various depths is evaluated as a temperature increment (ΔT) resulting from enthalpies of sulfide oxidation reactions:

$$\rho_B C_P \frac{\partial \Delta T}{\partial t} + k \frac{\partial^2 \Delta T}{\partial z^2} + F_W C_W \frac{\partial \Delta T}{\partial z} = Q_{RX} - \Delta H_V E_W \tag{6}$$

where:

ΔT	=	temperature rise in the material (K),
C_p	=	heat capacity of the solids (J kg^{-1} K^{-1}),
ρ_B	=	bulk density (kg/m^3),
k	=	thermal conductivity (J m^{-1} K^{-1} s^{-1}),
F_W	=	vertical water flux (mol m^{-2} s^{-1}),
C_W	=	molar heat capacity of water (J mol^{-1} K^{-1}),
Q_{RX}	=	sulfide reaction enthalpy generation (J m^{-3} s^{-1}),
ΔH_V	=	enthalpy of evaporation (J/mol), and
E_W	=	evaporative water loss (mol m^{-3} s^{-1}).

The monthly baseline temperatures are used as the first estimate for the monthly temperatures in the Kinetics Module. The temperature rises are calculated and the entire Kinetics Module is then repeated using the updated temperatures.

The **Transport Module** estimates the movement of aqueous species through each of the 20 simulated layers using material balances. The reaction stoichiometry and the overall sulfide oxidation rate determined in the kinetics module are used to calculate the sulfate and iron concentrations. The iron is partitioned into ferrous and ferric forms according to the pH and oxygen conditions. Other major aqueous species (e.g., uranium, calcium, radium, potassium, aluminum) are determined, and the model checks for the formation of secondary minerals (e.g., jarosite) and performs an inventory of minerals in each layer (e.g., calcite, gypsum, siderite, aluminum hydroxide, iron hydroxide).

The **pH Module** performs the complexation-speciation of numerous dissolved constituents and calculates the pH using published thermodynamic data and algebraic algorithms (Parkhurst et al. 1980, Motekaitis and Martell 1988). The pore water pH is estimated by solving for electroneutrality.

The **Trace Metals and Radionuclides Module** determines the concentrations of dissolved radionuclides (uranium and radium). The uranyl ion concentration is first estimated from thermodynamic data considering equilibrium with respect to uranite and uranyl carbonate (Mocker 1992). After calculating the various complexed species, the total uranium in solution is obtained. The sorption equilibrium on solid ferric hydroxide, aluminum hydroxide, and organic surfaces is estimated simultaneously, and the lower of the two concentrations (solubility versus sorption equilibrium) is used as the representative concentration. As time progresses the predominance of solubility equilibrium may "switch" to sorption equilibrium. At low pH values, neither solution nor sorption equilibrium is anticipated (SENES 1985, Byerley et al. 1987). Unlike uranium, radium-226 is not expected to form a pure solid phase. Rather, the coprecipitation of radium-226 sulfate with gypsum is modeled as a nonideal solid solution (SENES 1988). The sorption of dissolved radium-226 on solid surfaces is calculated simultaneously and compared with predictions from coprecipitation theory. The estimation of radium concentration also includes radioactive decay.

The **Solids Balance Module** evaluates the extent of secondary mineral formation and dissolution. Solid-liquid material balances are utilized with thermodynamic data to establish the concentrations of aluminum hydroxide, calcite, dolomite, ferric hydroxide, gypsum, jarosite, siderite, and metal sulfides in each layer.

The **Acidity Module** estimates the acidity of the seepage from the waste rock pile. Acidity of an aqueous solution may be defined as the capacity to accept hydroxyl (OH^-) ions in a basic titration from an ambient pH to pH of 8.5. In the simulated pore water, the dissolved complexes of iron, aluminum, copper, and zinc are the principal OH^--accepting species. The acidity can be conveniently expressed as the difference in equivalents between nonaccepting anions and cations (Stumm 1992):

$$\begin{aligned} Acidity = {} & [Cl^-] + 2[SO_4^{2-}] + [NO_3^-] - [Na^+] - [K^+] \\ & - 2\,[Ca^{2+}] - 2[Mg^{2+}] \end{aligned} \tag{7}$$

The total acid production for the entire waste rock pile is calculated from the acid production flux in the bottom layer which is assumed to exit as seepage flow. The total acidity is evaluated as a "running average" annual acidity, expressed as kilograms $CaCO_3$ equivalent acidity per annum.

Model Development and Calibration

In a previous application (Knapp et al. 1992, SENES 1991b), the model was adapted to simulate the continuous deposition of fresh waste rock onto existing waste rock piles at a silver mine in British Columbia, Canada.

The model was used to evaluate several possible cover scenarios: compacted clay, semicompacted clay, noncompacted clay, and pervious till. The various covers were characterized in the model by specifying (1) corresponding infiltration rates and (2) the apparent oxygen diffusion coefficients (determined experimentally at University of Waterloo by Chao et al. 1991). Figure 3A shows the agreement between model predictions and field data. Figure 3B illustrates the benefits achieved through use of the various cover types.

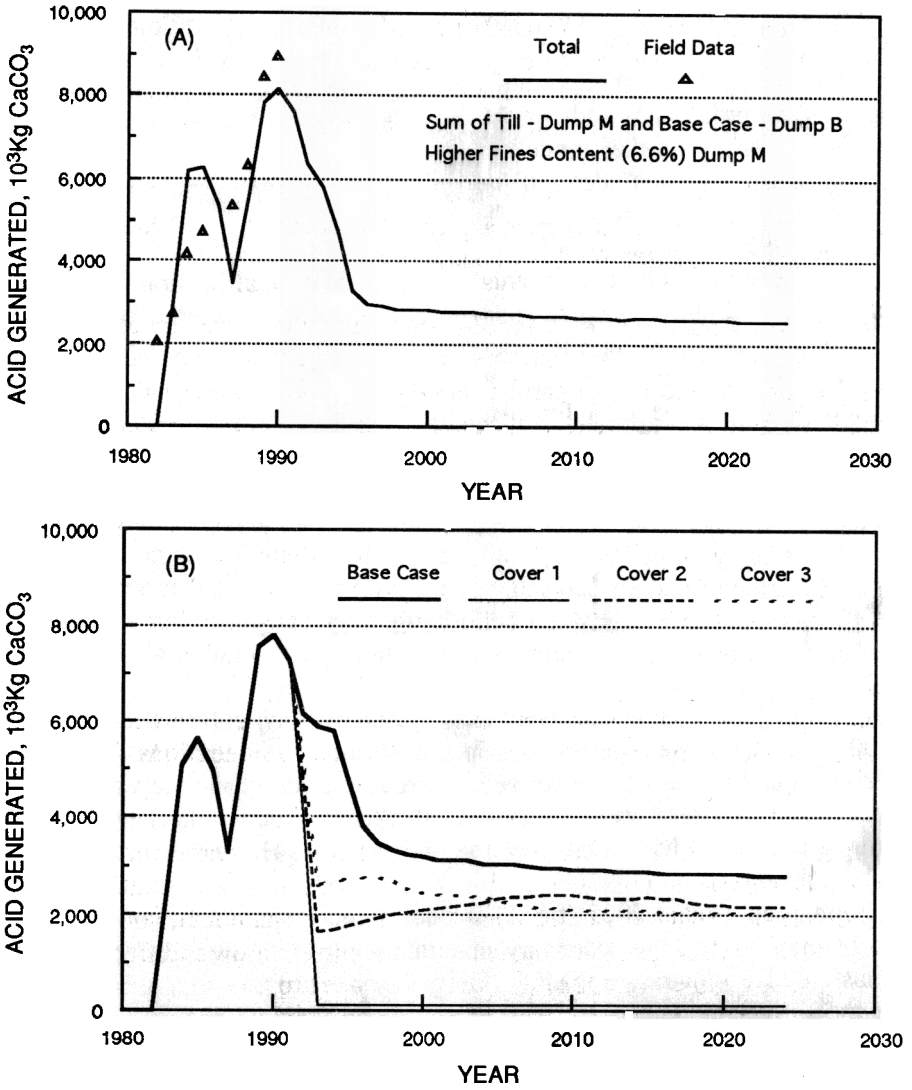

Figure 3. Acid generated, (A) and comparison of cover effectiveness (B) at dumps M and B, British Columbia, Canada.

For the most recent application, the model was adapted to simulate the simultaneous construction and leaching of a waste rock pile at a uranium mine in Thüringia, Germany. Simulating the entire history of the waste rock pile allowed for better characterization of the current conditions which improved the confidence level for long-term predictions of seepage quality. Leaching of the waste rock pile was simulated by specifying the aqueous concentrations of the chemical species present in the infiltration flow to correspond with the assumed quality of the leach solution. The infiltration flow was then reassigned to simulate natural precipitation, as the waste rock pile currently receives infiltration from natural precipitation only. The apparent oxygen diffusion coefficient was also reassigned to correctly simulate different oxygen conditions during active leaching, following reprofiling activities which result in compacted surface layers, and the future placement of a cover.

Calibration entails "tuning" the model to simulate the behavior of the waste rock pile over the period of time for which operating data are available. The usual calibration data includes measured temperature and oxygen profiles, recorded flow measurements, pH and chemical analyses of seepage reporting to the collection ditches. Certain key parameters and scaling factors are assumed to be distributed and are systematically sampled until reasonable agreement between predictions and current field data is obtained. Some of the modeling parameters are based on "best estimates" derived by previous calibration of several tailings sites (SENES 1985, 1991a, Scharer et al. 1992) and waste rock heaps (SENES 1991b). Numerical estimates of rate constants are usually based on laboratory and field experiments performed at different temperatures, pH's, and with bacteria (SENES 1985). In the current case, the primary calibration data were seepage data for pH, sulfate, iron, and uranium. The simulated calibration curves show good agreement with the available field data (fig. 4).

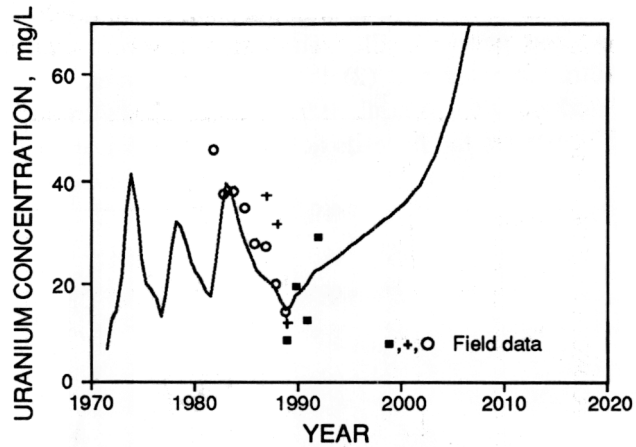

Figure 4. Calibration: predicted uranium for heap leach outflow.

Results of Modeling Scenarios

The simulation of the base case scenario (no remedial measures) shows the current pH of 2 to 3 will be maintained for next 100 years due to the buffering provided by secondary minerals (e.g., jarosite and iron hydroxide). Around 2100, the pH rises quickly to neutral, as jarosite and iron hydroxide have been depleted; the profiles of sulfate and iron also decrease to lower long-term values around 2100. Acidity calculations begin at the cessation of technical leaching, and the acidity shows a gradual overall decline until neutral pH conditions are achieved around 2100.

The broad uranium peak around 2025 (fig. 5) is due to continued release of uranium through oxidation of pyrite and dissolution of uranium-bearing secondary minerals while the flow through the heap is greatly reduced. The uranium predictions are also shown as a loading (kilograms/year) to take into account the difference in seepage rates during and after the active leaching phase (fig. 6); the broad uranium peak is actually much less in terms of uranium load than uranium removed during active leaching. The simulation shows that there may be considerable uranium remaining which has been made more susceptible to oxidative dissolution through the leaching activity; this uranium would be expected to be released from the waste heap in the future.

The radium profile (fig. 7) shows three plateaus which indicate radium levels are being controlled by a solid phase (e.g., adsorption onto a secondary mineral and/or coprecipitation with gypsum). Radium is quickly mobilized as these solid phases dissolve. The first plateau of 6 Bq/L is due to adsorption of radium onto gypsum. The second plateau is due to adsorption onto iron hydroxide. While the third long-term plateau of 8 Bq/L is controlled by adsorption onto the organic carbon. Only a small fraction of the total radium is leached from the heap.

The simulation of the various decommissioning alternatives (reprofiling plus cover) showed that there was very little observed difference between these decommissioning alternatives. The major effect was due to the installation of a cover in each case, as the cover greatly reduces the infiltration of water and transport of oxygen. A long-term pH plateau of 5 is predicted, although high sulfate levels will be maintained over the long term (fig. 8). Presumably this results from the buffering provided by dissolution of mica (sericite), which gives rise to dissolved potassium and

aluminum sulfates. The uranium peak is one third of that for the uncovered scenario and occurs 200 years later. The predicted radium levels are not significantly reduced.

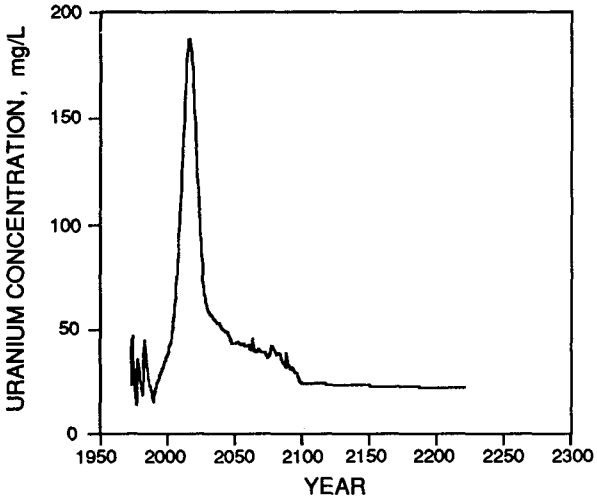

Figure 5. Base case scenario: predicted uranium for heap leach outflow.

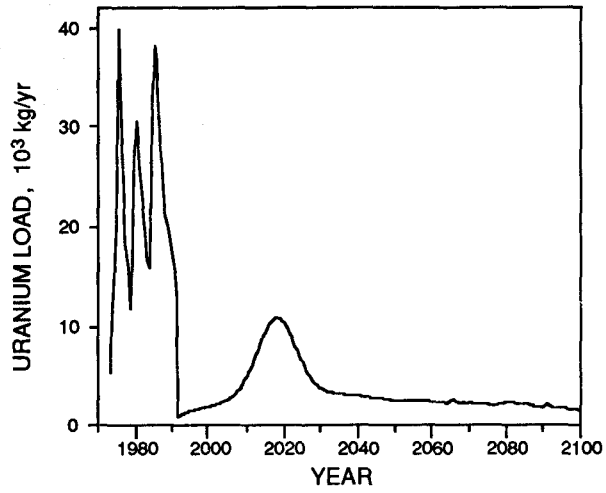

Figure 6. Base case scenario: predicted uranium load for heap leach outflow.

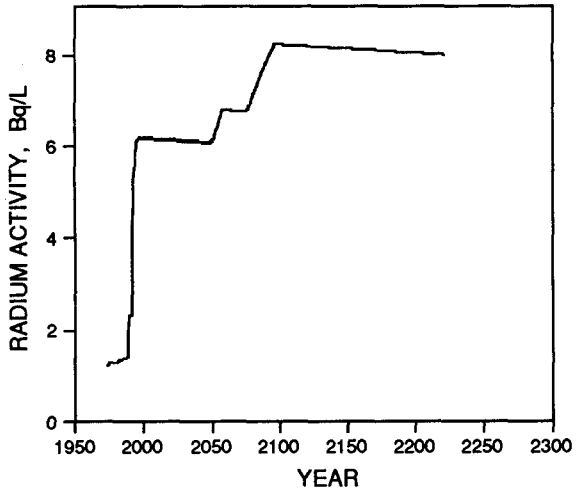

Figure 7. Base case scenario: predicted radium for heap leach outflow.

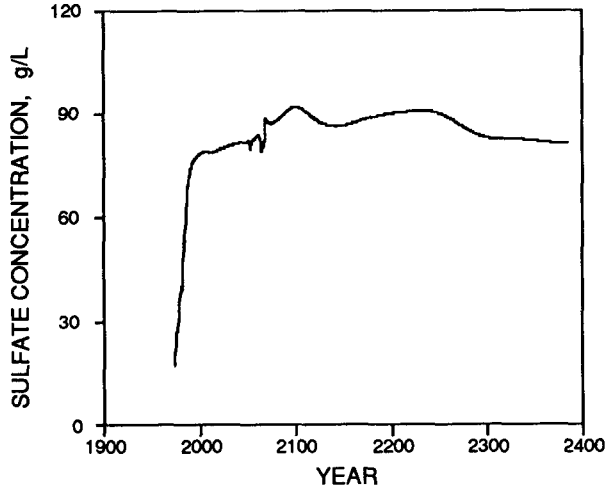

Figure 8. Cover scenario A: predicted sulfate for heap leach outflow.

The cover reduces the loadings; however, long-term treatment of the seepage will still be necessary. Sludge production is a major concern with long-term treatment and will vary depending upon the efficiency of the solids removal process and the chemical addition rate. Experience has shown these levels may range from 1 to 3 metric tons (mt) sludge per mt of acidity. The simulation of the base case (no remedial measures) predicts large lime demands; upwards of 500,000 mt of lime are required to treat 366,000 mt of acidity released over the next 100 years. By 2100, sulfides are depleted; however levels of uranium, iron and radium-226 are still elevated and treatment for these elements will be needed well into the future. The predicted cumulative sludge volume for the base-case scenario (no cover) is shown in figure 9 and the covered case is shown in figure 10. With cover application, the rates of acid release are predicted to decline dramatically due to greatly reduced flows. For the next 400 years, this acid production is approximately 16% of the acid produced in the uncovered case over a much shorter period (i.e. 100 years). However, contaminants are still elevated in 2400 and will continue to require treatment. Due to the much lower seepage flow, less than 100,000 mt of lime would be required over the next 400 years.

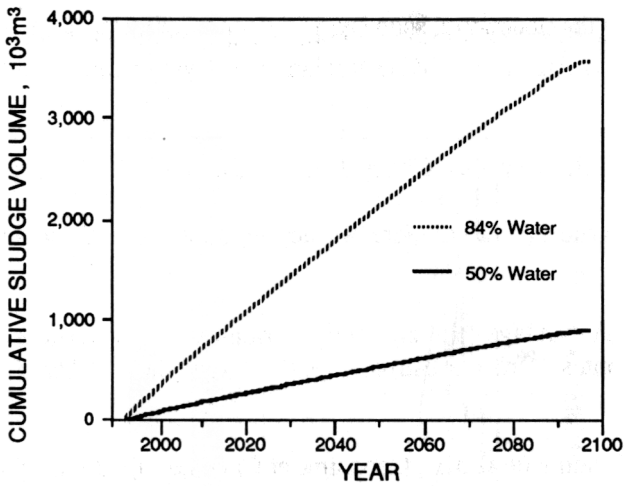

Figure 9. Base case scenario: predicted cumulative sludge volume.

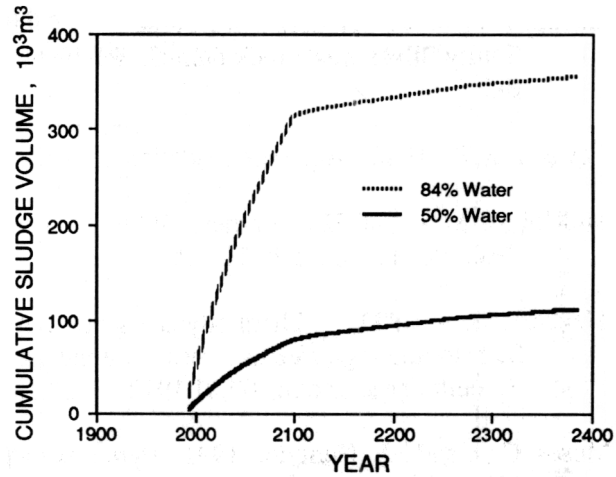

Figure 10. Cover scenario A: predicted cumulative sludge volume.

Conclusions

1) A model has been developed to simulate the placement and leaching history of a waste rock pile.
2) The model confirms that the existing waste rock pile will generate contaminated leachate requiring treatment for acidity and radioactivity for long periods of time.
3) Cover installation provides a significant reduction of potential contaminant burdens.
4) The cover would require care and maintenance into perpetuity, and chemical treatment would be required for a long time (beyond 100 years).
5) Treatment requirements for the uncovered pile would result in the generation of significant sludge volumes requiring future storage. Covering the waste pile would reduce this storage requirement.

The authors gratefully acknowledge the provision of data from Wismut GmbH, Chemnitz, Germany and commentary from Brenk Systemplanung, Aachen, Germany.

References

Byerley, J.J., J.M. Scharer, and A.M. Charles. 1987 Uranium biosorption from process solutions. Chem. Eng. 36:B49-B59.

Cathles, L.M. and W.J. Schlitt. 1980. A model of the dump leaching process that incorporates oxygen balance, heat balance and two dimensional air convection. P. 9-15. In W.J. Schlitt (ed.), Proceedings of the Symposium on Leaching and Recovering Copper from As-Mined Materials. Las Vegas, NV.

Chao, S.B., R. Roostaazad, J.M. Scharer, M. Moo-Young, and R.V. Nicholson. 1991. A study of the gaseous and hydraulic mass transfer characteristics of waste rock till cover. Prepared for Equity Silver Mines Ltd., by Dept. of Chem. Eng. and Dept. of Earth Sciences, Univ. Waterloo.

Davis, G.B. and A.I.M. Ritchie. 1986. A model of oxidation in pyritic mine wastes: part 1, equations and approximate solutions. Applied Math. Modeling 10:314-322.

Knapp, R.A., J.M. Scharer, C.M. Pettit, R.J. Patterson, and R.V. Nicholson. 1992. Acid generation modeling - Equity Silver waste rock dumps. Presented at the 16th Annual BC Mine Reclamation Symposium, Smithers, BC.

Lowson, R.T. 1982. Aqueous oxidation of pyrite by molecular oxygen. Chem. Rev. 82(5):461-497.

McKibben, M.A. and H.L. Barnes. 1986. Oxidation of pyrite in low temperature acidic, solutions. Geochim. et Cosmochim. Acta 50:1509-1520.

Mocker, D. 1992. Thermodynamische Berechnungen Anlage 2. zu den Berichten. Bewertung des Selbstreinigungseffektes des Grundwasserhorizontes im Abstrom der Lagerstätte Königstein. Berbeitungszeitraum: 02.01.1992 bis 30.10.1992.

Moses, C.O. and J.S. Herman. 1991. Pyrite oxidation at circumneutral pH. Geochim. et Cosmochim. Acta 55:471-482.

Motekaitis, R.J. and A.E. Martell. 1988. The determination and use of stability constants. VCH Publishers, New York.

Nordstrom D.K. 1982. Aqueous pyrite oxidation and the consequent formation of secondary iron minerals P. 37-56. In J.A. Kittrick, D.S. Fenning, and L.R. Hossner, (eds.). Acid Sulphate Weathering. Soils Sci. Soc. Am. Spec. Pub. No. 10.

Parkhurst, D.L., D.C. Thorstenson, and L.N. Plummer. 1980. P. 80-96, PHREEQE - a computer program for geochemical calculations. U.S. Geol. Surv., Water Res. Inv.

Scharer, J.M., R.V. Nicholson, B.E. Halbert, and W.J. Snodgrass. 1992. A computer program to assess acid generation in pyritic tailings. ACS Symposium Series, The Environmental Geochemistry of Sulfide Oxidation. Washington, DC.

Scharer, J.M., V. Garga, R. Smith, and B.E. Halbert. 1991. Use of steady state models for assessing acid generation in pyrite mine tailings. P. 211-230. In Proceedings of the 2nd International Conference on the Abatement of Acidic Drainage, V.2. Montreal, PQ.

SENES Consultants Limited (SENES). 1993. Development of a computer model for simulating the in-situ technical leaching history of a waste rock heap. Internal Draft.

SENES Consultants Limited (SENES). 1991a. Reactive acid tailings assessment program (RATAP.BMT3). Prepared for CANMET.

SENES Consultants Limited (SENES). 1991b. Acid generation modeling Equity Silver waste rock dump. Report to Equity Silver Mines Limited.

SENES Consultants Limited and Beak Consultants Ltd. 1988. Adaptation of the reactive acid tailings assessment program to base metal tailings. CANMET DSS #15SW-2344-7-9208.

SENES Consultants Limited (SENES). 1985. Evaluation of biomass for uranium recovery from process streams. Final report. Prepared in association with the Institute for Biotechnology Research, Dept. of Chem. Eng., Univ. Waterloo, for CANMET. DSS File No. 26SQ.23440-4-9172.

Stumm, W. 1992. Chemistry of the solid-water interface: processes at the mineral-water and particle-water interface in natural systems. Wiley, New York, 428 p.

MODELING RECHARGE AND RUNOFF TO PREDICT COPPER AND ZINC TRANSPORT FROM LIME-AMENDED TAILINGS AT THE SILVER BOW CREEK CERLCA SITE[1]

William M. Schafer[2], John G. Goering[3], Tom R. Grady[2], Edward Spotts[2], and Dennis R. Neuman

Abstract: Remediation of mining waste deposited along the margins of Silver Bow Creek as a result of historic mining was evaluated in a multi-year research project funded cooperatively by the State of Montana, EPA, and ARCO Coal. The objective of the Streambank Tailings and Revegetation Study (STARS) was to evaluate the environmental performance of base addition, deep mixing techniques, and revegetation relative to the fate and transport of key metals of concern at the site. This paper summarizes the effect of lime amendments and revegetation on potential leaching of metals into groundwater, and runoff and erosion from streambank areas contaminated with tailings. Water flux in the unreclaimed and revegetated tailings was simulated using UNSAT2. Results of modeling water flux in the vadose zone indicated that 3 to 8 cm of groundwater recharge occurs in an average year in untreated tailings. Revegetation alters the site water balance so that groundwater recharge is unlikely. The amount of metals that migrate into surface water during high-intensity summer thunderstorms was predicted for existing conditions and for lime-treated and revegetated tailings. The US Department of Agriculture GLEAMS model was used to predict long-term runoff and erosion from the site. A three-year GLEAMS simulation indicated that STARS treatments would decrease runoff by 2 to 3-fold, and would change the timing of runoff. On the existing tailings, runoff was predicted intermittently from March through September. On reclaimed areas, runoff was predicted only in March and April when Silver Bow Creek provides more dilution. Substantial reductions in metal loading could be achieved due to reduction in runoff from mid-summer thunderstorms which are historically associated with fish kills.

Introduction

The Silver Bow Creek site located downstream from the Butte mining complex in Montana is one of the largest Superfund (Comprehensive Environmental Response, Liability and Compensation Act) mining waste sites in the United States. Large volumes of metallic sulfide tailings were fluvially transported by Silver Bow Creek and the upper Clark Fork River in the early 1900's. As a consequence, the floodplain system is widely contaminated with metal-enriched, low pH, acid-forming materials which have contributed to degradation of surface water quality.

Streambank tailings at the Silver Bow site may pose a significant environmental risk to both surface water and groundwater. Fish mortality has been a common occurrence in the Clark Fork River downstream of Silver Bow Creek during high-intensity convective thunderstorm events. Dissolution of metals in runoff from tailings areas probably causes short term increases in metal loads. Addition of alkaline amendments to increase soil pH and decrease metal solubility in conjunction with revegetation may reduce metal transport during runoff events.

Although widespread alluvial groundwater contamination is absent along Silver Bow Creek, recharge to groundwater by metal-enriched tailings pore water has the potential to degrade water quality. Tailings are generally located 30 to 100 cm above groundwater and overlie natural floodplain soils. Potential evaporation exceeds

---

[1]Paper presented at the International Land Reclamation and Mine Drainage Conference and the Third International Conference on the Abatement of Acidic Drainage, Pittsburgh, PA, April 24-29, 1994.

[2]William M. Schafer, Principal, Tom Grady, Senior Project Manager, and Ed Spotts, Project Manager, Schafer and Associates, Bozeman, MT, USA.

[3]John G. Goering, Research Scientist, and Dennis R. Neuman, Research Scientist, Reclamation Research Unit, Montana State University, Bozeman, MT, USA.

precipitation in this semi-arid area. As a result, three conditions must exist for appreciable migration of metals to occur. The tailings pore water must contain elevated metal levels, downward flow of water must occur through the tailings, and metals must not be attenuated by underlying natural soils in the vadose zone. Direct sampling of tailings pore water using lysimeters indicated that elevated levels of iron, aluminum, manganese, copper, cadmium, zinc, and arsenic are common.

The STARS investigation was initiated to develop methods for remediating streambank tailings areas. A series of small plots was amended with lime and seeded with metal-tolerant plants in 1989. Various amendment incorporation methods were evaluated in the field investigation. Environmental performance monitoring of the STARS treatments was conducted from 1989 through mid-1992 (Schafer & Associates et al. 1993). The purpose of this investigation is to report on the effectiveness of selected STARS treatments in reducing the transport of metals into surface water and groundwater.

Methods

Field Site Description

Fluvially-deposited tailings and mine waste along 35 km of Silver Box Creek have generally denuded the floodplain in a 15 to 300 m wide corridor. The tailings have pore waters with pH from 3.0 to 4.5 and elevated concentrations of total or soluble copper, zinc, arsenic, cadmium, iron, aluminum, manganese, and lead. Two field study sites were selected on tailings with differing physical characteristics. The "Rocker" field site, which is typical of high-gradient stream reaches, consists of coarse sands and gravels with thin inter-stratified silt layers. Groundwater is located at a depth of 135 cm. The "Ramsay" field site is typical of low-gradient stream reaches. Tailings deposits are 30 to 60 cm thick and extend laterally 200 m from the channel. Mine waste and natural sediments at Ramsay are silt and clay-textured and groundwater was located at 190 cm.

Unsaturated Flow Modeling Using UNSAT2

A number of public domain models are available for simulating variably saturated flow in porous media. A saturated-unsaturated flow model, UNSAT2, was used to simulate differences in the rate and direction of convective water flux in untreated and revegetated tailings. UNSAT2 (Davis and Neuman 1983) has been widely applied to predict water flux in agricultural soils, in waste management facilities, and in earthen dams. UNSAT2, which was used as a 1-D model for this simulation, contains a number of options for simulating the capillary influence of groundwater, evaporation from bare soil surfaces, and withdrawal of water for transpiration by plants.

The numerical basis for unsaturated flow simulation in partially saturated soils is derived from the Buckingham-Darcy flux law [1], (Jury et al. 1991). The first hydraulic head term refers to the soil matric or suction potential. The second term in the hydraulic head expression is the unity downward gradient for vertical flow. In a soil at equilibrium with a shallow water table h is equal to -z so that the matric potential gradient is -1 and the total head (H) is zero, hence no flux occurs. By measuring the matric potential at a given distance above the water table, the direction of flow in unsaturated soil can be inferred. The soil matric potential always has a negative sign while the suction potential is equal in value to matric potential but is expressed as a positive number. The negative sign in [1] is used so that downward flux will be negative while upward flow is positive. When the matric potential gradient is less than -1 then upward flux occurs. Conversely, when the matric potential gradient is greater than -1, downward flux will occur.

$$J_w = -K_u \left(\frac{\partial h}{\partial z} + 1 \right)$$

where J_w is the rate of water flux (cm),
K_u is the unsaturated hydraulic conductivity (cm/s),
and h and z are components of total head (cm) such that ($h+z=H$) [1]

The Richards equation [2] which is the fundamental numerical expression governing transient water movement in unsaturated soil is derived by combining [1] with the continuity equation. UNSAT2 like other transient flow models was developed on the basis of the Richards equation with additional source and sink terms for plant water extraction.

$$\frac{\partial \theta}{\partial t} \quad \frac{\partial}{\partial z} \left[K_u \left(\frac{\partial h}{\partial z} + 1 \right) \right] \qquad [2]$$

UNSAT2 version 2.1, written in Fortran-77 is a two-dimensional finite element model. In addition to conventional fixed head, fixed flux, and impermeable boundary conditions, UNSAT2 also provides a number of special boundary conditions controlled by atmospheric variables. Examples include seepage faces, infiltration, and evaporation surfaces. The type of boundary as well as the value of the boundary data can be changed using a simulation restart feature. The relationship between hydraulic conductivity, suction, and water content can be described using the vanGenuchten equation [3] in version 2.1.

$$S_e = \frac{}{[1+(\alpha h)^N]^{(1-\frac{1}{N})}}$$

$$\text{where } S_e = \frac{(\theta - \theta_r)}{(\theta_s - \theta_r)} \qquad [3]$$

θ = volumetric water content (cm^3/cm^3), θ_r = residual water content
θ_s = saturated water content, and N and α are vanGenuchten parameters

GLEAMS Model Theory and Structure

The USDA-ARS GLEAMS model (Knisel 1980) was used to simulate runoff and erosion from STARS treatments compared to untreated streambank tailings. The USDA GLEAMS model was used to evaluate qualitative changes in runoff from untreated and revegetated streambank tailings areas. Rainfall-runoff tests were also conducted to identify effects of treatment on metal concentration in runoff. The GLEAMS model consists of several component submodels for calculation of root zone hydrology, erosion, nutrient flux, and pesticide flux. Separate parameter input files are developed to run each component. Pass files are created by each component run for use in subsequent batch routines. Only the hydrology and erosion components of the GLEAMS model were used for this simulation.

The first component, hydrology, uses daily rainfall data, monthly temperature and solar radiation data, and various soil parameters for computation of the daily water balance. The amount and timing of runoff as well as other components of the water balance are computed, and pertinent information on storm size and runoff are passed to the erosion model component.

The technique used for estimation of runoff from daily rainfall data is the Soil Conservation Service (SCS) curve number approach which has been widely adopted throughout North America. The curve number approach

(Mockus 1985) relates the depth of runoff for a given depth of rainfall to the antecedent soil water content and to the "curve number" (CN). Curve numbers vary from 0 to 100, and are related to the infiltration capacity of the soil. Detailed guides have been developed for estimating curve numbers (Mockus, 1985). High curve numbers are typical of impermeable soils and disturbed areas while low curve numbers are found on well-vegetated permeable natural soils.

Rainfuall runoff is numerically related to runoff by the curve number. During a rainfall event, no runoff is presumed to occur until the rainfall depth exceeds 20% of the remaining soil water storage capacity. Soil storage is the difference between saturation and the antecedent moisture content (which is influenced by historical rainfall and evaporation). While the SCS curve number approach relies on a generalized assessment of the antecedent moisture condition, the GLEAMS model maintains a daily water balance so that s can be computed. In addition, the water balance module tracks cumulative runoff, evaporation, transpiration, percolation, and changes in soil water content.

The erosion component of the GLEAMS model utilizes the Yalin equation to compute the sediment transport capacity of runoff. Estimated soil loss can be either "detachment-limited" or "transport-limited". Detachment can occur due either to rain-drop splash or to the energy of overland flow. Overland flow from hillslopes can be routed in a number of ways. The simplest simulation is for overland flow to be routed directly to a channel at the edge of the domain. In addition, overland flow can be concentrated into a channel within the field boundary. Additionally, the hillslope profile can be segmented into various shapes (*eg.* uniform, convex, concave, or complex). Overland flow and sediment are routed through each segment. Deposition or flow-induced detachment can occur within any hillslope of channel element within the model domain. The hydrology and erosion components of the GLEAMS model have been validated at experimental research watersheds in Montana, Texas, Oklahoma, Ohio, Georgia, Nebraska, West Virginia, Mississippi, Iowa, Arizona, and New Mexico (Knisel 1980). In general, the long-term trend in runoff and erosion rates were accurately predicted by GLEAMS although model performance on individual storms was less reliable.

MODEL CALIBRATION

UNSAT2 Domain and Boundary Conditions

To simulate unsaturated flow at the STARS field sites, the hydraulic properties of typical samples were characterized using a variety of field and laboratory tests. Simulation was performed at the Rocker and Ramsay Flats sites in because these sites were most representative of the variety of streambank tailings conditions along Silver Bow Creek.

All soil samples characterized by desorption analysis (relationship between measured water content and suction) were grouped into 5 "type" textures (Fig. 1). The relationship between water content and water potential was fit to the soil hydraulic relationship developed by vanGenuchten [3]. Desorption and unsaturated hydraulic conductivity (K_u) curves for each "type" soil are presented in Figs. 1 and 2.

The domain modeled for each site was a 240 cm deep profile. Elements were thinner at the soil surface to avoid numerical instability associated with the steep water potential gradients that develop at the soil surface in response to evaporation. The type textures selected and the depth to the water table were based on field logs of lysimeter, piezometer, and neutron probe installations at each site.

The domain was initially modeled with a constant head boundary at the groundwater table to simulate the free water surface. The nodes at the soil surface were a special type called evaporation/infiltration (EI) nodes within UNSAT2. During simulation, a potential evaporation or infiltration flux can be set. In an EI node, the actual evaporation or infiltration can be equal or less than the potential rate depending on the ability of the soil system to transmit water to satisfy the potential flux at the surface.

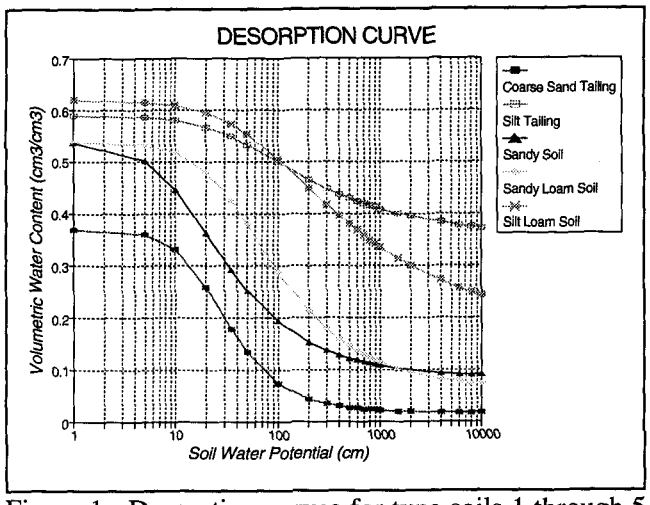

Figure 1. Desorption curves for type soils 1 through 5 for the STARS investigation.

In order to simulate the fully-drained soil profile (*eg.* field capacity), the domain was initialized as a nearly-saturated condition (a suction of -20 cm). A fixed head boundary of 0 cm of suction was set at the groundwater table at each site (Rocker at 135 cm, and Ramsay at 190 cm). The profiles were allowed to freely drain with no imposed surface flux for 90 days at Rocker and 180 days at the less permeable Ramsay site to reach fully-drained conditions.

For the simulation, the year was partitioned into three time periods beginning on June 1. The net water balance for each portion of the year was inferred from climatological observations (Fig. 3). The first 90 days was assumed to have a net water deficit (precipitation minus 70% of potential evaporation) of 25 cm which was applied equally throughout the 90 day "summer". The next 180 days consisted of a slow rate of surface infiltration amounting to 5 cm over the fall and winter. The final 90 days of the simulated year was the "spring" when precipitation greatly exceeded evaporation. A total of 10 cm of infiltration was assumed to occur over the 90 day period. These values for potential surface flux were imposed equally for each day of the 0 to 90, 91 to 270, and 271 to 360 day simulation period. The head conditions existing at the end of the initial draindown period were used as input representing day 0 conditions.

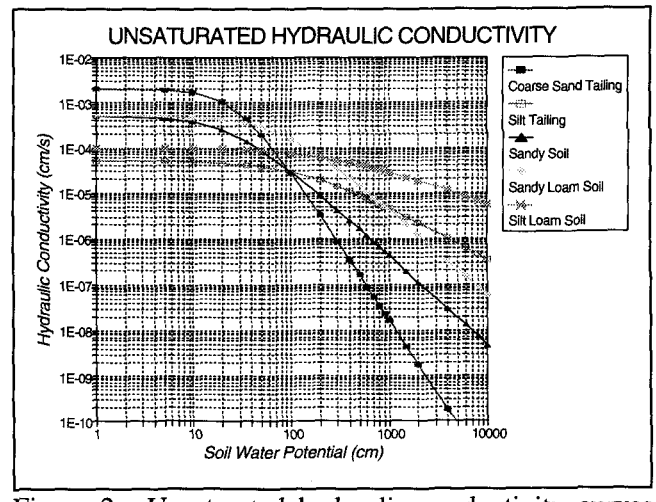

Figure 2. Unsaturated hydraulic conductivity curves for type soils 1 through 5 for the STARS investigation.

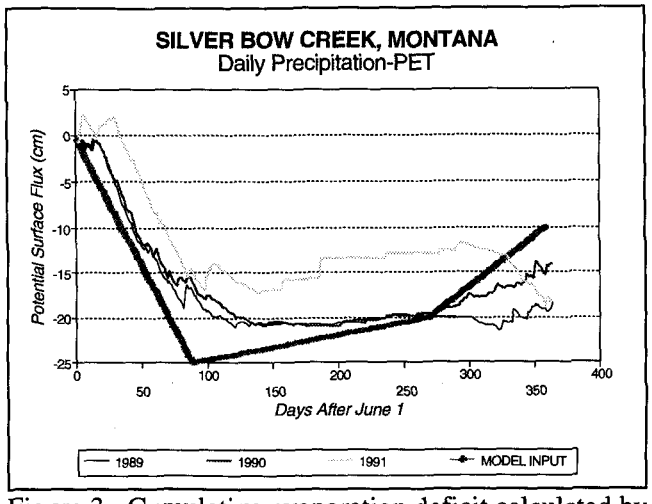

Figure 3. Cumulative evaporation deficit calculated by subtracting 70% of potential evaporation from precipitation is plotted for 1989 through 1991.

At each site, two individual soil surface conditions were simulated. A bare soil condition was used to simulate existing tailings. A vegetated plot representative of the deep plow plot was also simulated. The model domain was changed from a fixed head boundary below the water table to a zero flux boundary during the year simulated. This head change was necessary to construct a mass water balance of the water lost to evaporation. The climate modeled was conservative in that slightly wetter-than-average conditions were used. Hence these simulations would tend to slightly overestimate the tendency for streamside tailings to generate groundwater recharge in an average year.

GLEAMS Model Parameter Estimation. The GLEAMS model requires extensive parameter estimation and input before it can be used to simulate runoff and erosion from unknown areas. Due to the complexity of the GLEAMS model, only the control and the most successful amendment/revegetation treatment at each location were simulated using GLEAMS.

Precipitation input for GLEAMS runs was from the Anaconda, Montana National Oceanographic and Atmospheric Administration (NOAA) weather station (average precipitation 32.5 cm). A comparison of rain gauge measurements from each of the STARS field sites indicated that the Anaconda site correlated well with other stations in the basin and tended to have somewhat higher cumulative precipitation. Three full years of input data (1989 through 1991) were used in the GLEAMS simulations. Mean monthly average temperature and solar radiation values were calculated for a climate station located at Ramsay for the entire period of record. GLEAMS results are not highly sensitive to small variations in daily temperature and solar radiation, hence monthly inputs were used.

Input parameters for the hydrology and erosion simulation are listed in Table 1. The most sensitive parameter in the GLEAMS model is the runoff curve number (CN). Due to the sensitivity of this parameter, great care was taken in estimating CN values. Rainfall simulation test data were used to calculate CN values. The control plots at Ramsay had an unusually high curve number (95) presumably because of the rainfall-induced compaction on the exposed tailings. The coarse texture of tailings at Rocker resulted in a control curve number estimated to be 55. Due to the extremely high infiltration rate, no runoff occurred at Rocker during the rainfall simulation tests. The revegetated plots at Ramsay had much lower measured CN values than the control (59) due to the effects of tillage and revegetation. The curve numbers selected for the GLEAMS simulation (78 at Ramsay Flats) were conservatively set higher than the measured CN values due to potential bias in site selection for the rainfall simulation tests.

In general, a relatively thin root zone depth was input to simulate the control plots because observed changes in soil water content due to evaporation were confined to the upper 30 cm of soil. Values for hydraulic conductivity and soil water-holding capacity were based on measurements taken at each site.

The leaf area index (LAI) values and the crop type are important variables in simulating the on-site water balance. For the control plots, a LAI value of near zero was input so that GLEAMS would default to soil evaporation. For the vegetated plots, numerous preliminary GLEAMS runs were performed to try to simulate the observed changes in soil water content from the site. Very high values of LAI had to be input for simulated plant evapotranspiration to approach simulated soil evaporation in magnitude. Despite the fact that actual LAI values on the deep-till plots are near 1 or less, higher LAI values were input to improve model results. The beginning and end of the growing season and relative seasonal LAI values were input to simulate actual conditions.

Table 1. Input parameters used for the GLEAMS model - Silver Bow Creek, Montana.

GLEAMS MODEL DOMAIN	
HYDROLOGIC PARAMETERS	**EROSION PARAMETERS**
Area = 1,000 by 1,000 trapezoidal watershed Saturated Hydraulic Conductivity = measured at each site Soil Profile Percent Full = Initial water content 85% of field capacity Evaporation Coefficient = varies by site SCS Curve Number = varies by site, based on rainfall simulation Root Zone Depth = varies by site, generally 6 inches for control and 36 inches for vegetated Soil Characteristics = porosity, field capacity, wilting point, organic matter percent, clay, and silt content varies by site, based on observed soil morphology Monthly Mean Daily Maximum and Minimum Temperature = Based on Ramsay Flats climate station Monthly Mean Daily Solar Radiation = Based on Ramsay Flats climate station Vegetation Characteristics = varies by site, growing season duration and LAI based on calibration results	Slope = Overall 1.5 %, 1,440 feet at 1.5 % then steepening to 30% for last 30 feet Watershed shape = length to width ratio 2:1 Soil Erodibility K Factor = varies by site, based on USLE nomograph Cropping Practice P Factor = set to 1.0 for all simulations Cover Factor = varies by site, generally 1.0 for control and 0.2 for vegetated

Simulation Model Runs

Groundwater Recharge Estimation Using UNSAT2

Rocker. Changes in stored water under the bare soil and revegetated modeling scenarios are presented in Fig. 4. In the bare soil evaporation case, a measurable quantity of water was withdrawn from the coarse-textured tailings in the upper 60 cm of the soil profile (Fig. 4). The matric potential decreased to -15,000 cm (the imposed value for minimum permissible head at the surface node) at the soil surface in response to summer evaporation. This decline in matric potential created a very steep upward gradient causing water to move to the surface from a depth of about 30 to 60 cm in depth. The rate of water movement in the surface layer became so slow, however, that only 4.2 cm of actual evaporation occurred, a small fraction of the potential evaporation of 25 cm. Bare soil has been found to serve as an effective evaporation barrier by other investigators (Hillel 1980). During the subsequent fall and winter period, the imposed infiltration of 5 cm more than replenished the water withdrawn by evaporation so that water moved downward through the profile (Day 270). Additional percolation occurred during the rapid infiltration "spring" period (Day 360). Overall, the bare soil at Rocker had a net groundwater recharge of 8.4 cm or about 25 percent of the average annual precipitation.

Simulation of a revegetated plot at Rocker suggested that plant roots would remove water to a much greater depth than surface evaporation. A significant decrease in water content occurred throughout the domain, but the decline in matric potential was most pronounced within the root zone (upper 90 cm). The revegetated plot had 5.2 cm less water at the end of the year than at the beginning and therefore was not expected to generate recharge. Vegetation at the Rocker site was expected to be sub-irrigated as evidenced by the gradual decline in the water table during the summer. Overall, the bare streambank tailings areas would be expected to have 8.4 cm of percolation over the year while the revegetated plot was not expected to generate any percolation.

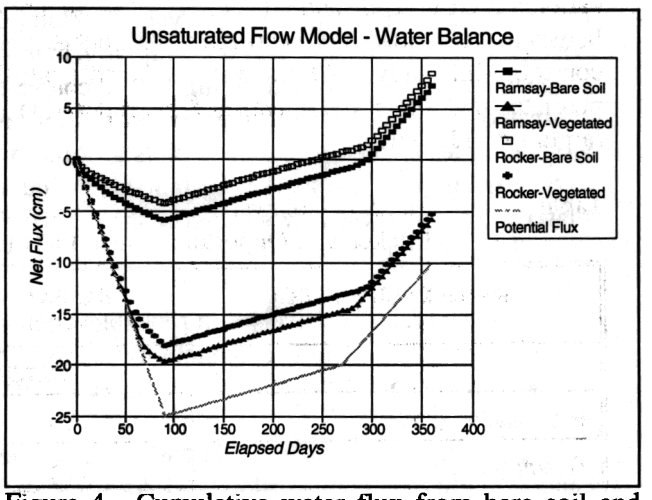

Figure 4. Cumulative water flux from bare soil and vegetated tailings at Rocker and Ramsay. A net annual increase in soil water indicates the potential for groundwater recharge.

Ramsay. Patterns of water use and changes in stored soil water simulated at the Ramsay Flats site were similar in many regards to Rocker despite significant differences between the sites. Ramsay soil had a slower hydraulic conductivity and greater depth to groundwater than at Rocker.

Despite the low permeability of the tailings at Ramsay, an appreciable amount of groundwater recharge is expected where bare tailings are exposed. In the bare soil case, a total of 6 cm was removed by evaporation during the summer period. As expected surface evaporation did not extract water content much below the top 30 cm of soil. Overall for the year the bare soil site gained 7.2 cm of water, only slightly less than at the coarser-textured Rocker site.

The simulation of the vegetated plot suggested that water would be removed by plants to 105 cm in depth. Plants withdrew 19.7 cm of water during the summer period. The matric potential of the vegetated Ramsay plot dropped to -15 bars at the soil surface and from -2 to -6 bars in the remainder of the root zone. Recharge the following winter created an obvious wetting front as water was replenished in the upper 45 cm of tailings. After the spring recharge period, the vegetated case at Ramsay was 5.8 cm drier than at the beginning of the year indicating that groundwater recharge is not likely to occur after vegetation becomes established.

Runoff and Erosion Modeling

Rocker. Simulation of the control and vegetated areas at Rocker were conducted using GLEAMS (Table 2). The soil material at Rocker was coarser in texture than at Ramsay Flats and so had a lower water-holding capacity, a much higher infiltration rate, and had less erosive soils than at Ramsay Flats. The water balance results for three years of simulated rainfall at Rocker indicated that 4.29 cm inches of percolation (*eg.* groundwater recharge) would occur on the control plot, while the higher evaporative use of water by established vegetation would prevent percolation. Runoff averaged 1.68 cm and 1.55 cm on the control and vegetated areas respectively. Predicted runoff was less at Rocker than at Ramsay due to the lower runoff curve number of both the control and vegetated treatments at Rocker. Runoff was only predicted in March and April, presumably in response to snowmelt events. Less difference in runoff was noted between the control and deep plow plots because reclamation had less overall effect on the curve number due to the already rapid infiltration on the control plot. Predicted soil loss at the Rocker site was 0.7 tons/acre for the control and 0.14 tons/acre for the deep plow plot. These low rates of soil loss were due to the coarse texture and rapid infiltration rates of soil at Rocker.

Ramsay. Runoff and erosion were simulated for the Ramsay control and vegetated treatments Ramsay using the calibrated GLEAMS model (Table 2). Significant differences in the amount of runoff and erosion were predicted between the control and deep plow treatments. For the 3-year simulation, 3.71 cm of runoff occurred from the control, while only 1.70 cm was predicted from the deep plow plot. No percolation below the root zone was predicted for either treatment, hence evaporation and transpiration accounted for the remaining average annual rainfall of 32.5 cm.

Table 2. Summary of water balance results and soil loss from the USDA CREAMS runoff model for the Rocker and Opportunity sites Flats (1989 to 1991).

WATER BALANCE TERM	RAMSAY CONTROL	RAMSAY DEEP PLOW	ROCKER CONTROL	ROCKER DEEP-TILL
WATER BALANCE SUMMARY				
Precipitation (cm/yr)	32.5	32.5	32.5	32.5
Runoff (cm/yr)	3.71	1.70	1.68	1.55
ET (cm/yr)	30.0	35.8	26.9	32.8
Percolation (cm/yr)	0.0	0.0	4.29	0.0
Soil Loss (t/acre/yr)	13.7	1.2	0.7	0.14

The timing of runoff also differed between the control and vegetated treatments. Peak monthly runoff for both treatments occurred in April or May, depending on the year. Measurable amounts of runoff occurred throughout the summer from the control plot, while no runoff occurred after the end of May from the vegetated plot. This difference in the timing of runoff is thought to be significant in that most fish kills on the Clark Fork have been observed in July and August after convective thunderstorms. Runoff during midsummer may contain higher concentrations of dissolved metals due to the formation of metal-enriched salt crusts in the soil surface during warm weather. In addition, the higher spring instream flow means that runoff from streambank areas is more diluted when it mixes with the channel in spring than in summer.

Significant differences in erosion rates were also noted between the control and deep-plow treatments. For the control site, an average annual soil loss of 13.7 tons/acre was predicted while only 1.2 tons/acre was predicted for the deep plow site. The ten-fold reduction in erosion was due to the reduction in runoff as well as the protection provided by the vegetative cover established on the deep plow plots.

Discussion

Flux of Metals to Groundwater

Transport of metals from streambank tailings to groundwater would require three distinct conditions including increased solubility of metals in tailings pore water, downward flow of water, and limited attenuation of metals in the underlying buried soil layers. While direct measurement indicates that tailings pore water has elevated concentrations of soluble metals, modeling indicates that a substantial quantity of downward convective flow occurs from untreated tailings. The lack of widespread groundwater contamination along Silver Bow Creek therefore indicates that natural soils serve as an effective geochemical barrier to metal transport. Revegetation will further reduce the risk of groundwater contamination by reducing the net groundwater recharge.

Assessment of Surface Water Impacts

Runoff rates predicted by the GLEAMS simulation were compared with US Geological Survey (USGS) streamflow records on lower Silver Bow Creek to determine the mass loading of runoff from streambank areas compared with instream flows. In addition, chemical characteristics of water collected during rainfall-runoff trials were used to calculate mass loading of metals into Silver Bow Creek during typical high-intensity thunderstorms. The purpose of this transport analysis was to;

- determine if modeling results identify surface runoff of metals as a critical transport mechanism;
- evaluate the effectiveness of STARS treatments as a means of reducing potential impacts to surface water;
- and to determine the relative importance of dissolved versus total metals delivered to Silver Bow Creek.

Hydrograph Mass Loading. To compute the mass loading of metals in surface runoff from streambank areas, it was first necessary to estimate the contribution of runoff water from streambank areas. For this analysis, the contributing area was assumed to be the lower 10 miles of the Silver Bow Creek floodplain. Only the lower portion of the floodplain was used because most convective storms are rather localized, and it was implausible to assume that the entire watershed would be affected by a convective storm cell. The streambank tailings contributing area was assumed to consist of a 100 foot wide corridor (120.8 acres) along Silver Bow Creek. Rainfall-runoff characteristics from the untreated tailings control plot were used to simulate the response of the streambank tailings area. Runoff from the streambank tailings area was assumed to have zero time of concentration due to its close proximity to the channel. Duration of each daily runoff event was assumed to be 6 hours.

Actual flows from the USGS gaging station (#1232600) near Opportunity, MT were used to determine the amount of dilution that would occur when streambank tailings runoff reached Silver Bow Creek. The entire 3-year period of record used in the GLEAMS simulation run was reviewed, and three time periods were selected representing the single largest runoff event from each year. In 1989 (Fig. 5), a 0.80 inch rainstorm on August 23 resulted in 0.11 inches of runoff. This event over a 6-hour duration resulted in 2.23 cfs of flow from the streambank area which would have made up 8.9% of the instream flow of 25 cfs reported for August 23. As expected, the tailings area runoff peak from the August 23 event occurred on the rising limb of the basin-wide hydrograph. This response would be expected due to the size of the Silver Bow Creek watershed at Opportunity (284 mi^2). Similar analysis of stream hydrograph records and computed runoff in May, 1991, and in September, 1991, resulted in streambank runoff computed to be 15.1 % and 9.2 % of baseflow.

Metal Mass Loads. Runoff from simulated rainfall tests from untreated and lime-amended plots at Opportunity were analyzed for a suite of dissolved and total metals. Table 3 lists the levels of dissolved and total copper and zinc in runoff samples representing the "first flush" of runoff (0.05 inch) as well as the long-term runoff. During an intense thunderstorm, the calculated concentration of total copper and zinc in Silver Bow Creek may range from 1.4 to 9.0 mg/l and 1.1 to 6.9 mg/l respectively. Dissolved copper and zinc may range from 0.4 to 4.5

CONSTITUENT	CONTROL PLOT		LIME-TREATED PLOT	
	INITIAL RUNOFF (mg/l)	LONG-TERM RUNOFF (mg/l)	INITIAL RUNOFF (mg/l)	LONG-TERM RUNOFF (mg/l)
Copper - Total	60	14.3	1.31	0.60
Copper - dissolved	30	4.0	0.45	0.093
Zinc - Total	46.2	11.4	1.66	0.41
Zinc - dissolved	35	9.3	0.55	0.033

Table 3. Total and dissolved Cu and Zn in simulated rainfall-induced runoff from control and lime-treated plots.

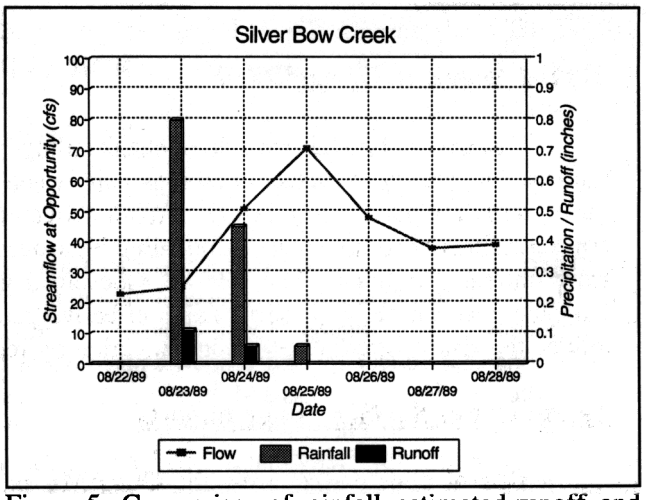

Figure 5. Comparison of rainfall, estimated runoff, and streamflow in August, 1989.

mg/l and 0.93 to 5.25 mg/l respectively. These levels of copper and zinc exceed the acute criteria for protection of freshwater life by several orders of magnitude. The hardness-corrected copper and zinc standards at a hardness of 100 mg/l are 0.018 and 0.117 mg/l.

The runoff contribution of metals to Silver Bow Creek from revegetated plots was also calculated. On each of the dates when runoff was simulated from bare tailings, no runoff was predicted from any of the lime-amended and vegetated plots. As a consequence, predicted metal loading was decreased to zero by the STARS treatments. It should be noted that while no runoff was predicted for convective thunderstorms during the summer months, runoff was expected to occur during snowmelt. The maximum contribution of streambank runoff to Silver Bow Creek for revegetated plots occurred in March or April of the year and was equal to less than 2 percent of the instream flow. Coupled with the 25-fold or greater reduction in total metal concentration in runoff from revegetated plots, the overall contribution to Silver Bow Creek from the streambank areas would be expected to decline by 100 to 200-fold due to basin-wide implementation of the STARS technology.

Literature Cited

Davis, L.A., and S.P. Neuman. 1983. Documentation and User's Guide; UNSAT2 - Variably Saturated Flow Model. Final Report for the U.S. Nuclear Regulatory Commission. NUREG/CR-3390.

Hillel, D. 1980. Applications of Soil Physics. Academic Press. New York. 385 pgs.

Jury, W.A., W.R. Gardner and W.H. Gardner. 1991. Soil Physics. John Wiley and Sons. New York. 328 pgs.

Knisel, W.G. (Editor) 1980. CREAMS: A field Scale Model for Chemicals, Runoff and Erosion from Agricultural Management Systems. USDA Conservation Research Report 26.

Knisel, W.G., F.M. Davis, and R.A. Leonard. 1992. GLEAMS Version 2.0 User's Manual. USDA Southeast Watershed Research Laboratory. Tifton, GA.

Mockus, V. 1985 (Revision) National Engineering Handbook Section 4: Hydrology. USDA-SCS.

Schafer and Associates, and Reclamation Research Unit. 1993. Silver Bow Creek RI/FS. Streambank Tailings and Revegetation Studies. Phase III Final Report. Submitted to Montana Department of Health and Environmental Sciences.

MODELING FIELD-SCALE TRANSPORT OF WEATHERING PRODUCTS IN MINING WASTE ROCK DUMPS[1]

N. Eriksson and G. Destouni[2]

Abstract: A stochastic-advective approach to modeling field-scale transport of weathering products in mining waste rock dumps is presented for irreversible dissolution of primary minerals in the waste rock. The effect of flow heterogeneity is investigated for a classical unimodal distribution of water residence time and for bimodal distributions that reflect the existence of preferential flow paths. The relationship between the characteristic time scale of the dissolution process and the characteristic hydrological time scales expressed by the water residence times in the dump plays an important role for the effect of flow heterogeneity on the field-scale solute transport. In particular, flow heterogeneity manifested by the existence of preferential flow paths will reduce the maximum value of the field-scale solute flux and increase the temporal spreading of the solute breakthrough curve at the lower boundary of the dump.

Additional Key Words: mining waste, flow heterogeneity, solute flux, water residence time distribution, stochastic modeling, preferential flow paths.

Introduction

When uncovering the ore body in an open pit, large quantities of waste rock are produced and deposited on the ground surface. Oxidative weathering of sulfide minerals produces free acidity, sulfate and dissolved metal species. Heavy metals may then leach through the deposit into surrounding drainage ditches or underlying aquifers. To evaluate the need for protective measures and to optimize such measures, the transport of environmentally disturbing weathering products through waste rock dumps needs to be quantified. The required output of such modeling is the field-scale mass arrival of solute to and through the lower boundary of the waste rock dump, to be used as input for predicting the subsequent solute movement in the drainage ditches or the aquifer (Destouni and Eriksson 1994).

Because waste rock dumps constitute highly heterogeneous formations with regard to their texture and structure, realistic models of field-scale solute transport in mining waste rock should be able to handle large and irregular variability in their model parameters. A stochastic-advective approach to modeling reactive solute transport in heterogeneous porous media (Shapiro and Cvetkovic 1988, Cvetkovic and Shapiro 1990, Destouni and Cvetkovic 1991, Dagan et al 1992) will be extended to include irreversible dissolution of primary minerals in this paper. For weathering products that are soluble in water, the weathering process will be considered as a spatially and temporally distributed source of solute. Weathering of chalcopyrite will thereby be used as an illustrative study case, based on field data and simulation results that were reported by Strömberg and Banwart (1994).

For the considered study case, the effects of spatial variability in hydraulic properties of the waste rock and of the temporal variation of the weathering rate on the field-scale solute transport through the dump will be investigated. A

---

[1]Paper presented at the International Land Reclamation and Mine Drainage Conference and the Third International Conference on the Abatement of Acidic Drainage, Pittsburg, PA, April 24-29, 1994.

[2]N. Eriksson, -Ph.D. student-, G. Destouni, -Associate Professor-, Department of Water Resources Engineering, Royal Institute of Technology, Stockholm, Sweden.

mathematical model for handling the concept of preferential flow paths in the stochastic-advective framework will be discussed (Destouni 1993; Destouni et al. 1993, Sassner et al 1994). In particular, the importance of the relationship between the characteristic time scale of the dissolution reaction and the characteristic water residence times in the dump will be elucidated. Preferential flow paths, channeling, or piping has been observed in mining waste rock (Harries and Ritchie 1983), however, the existence and influence of such preferential flow paths has not been quantified. At the Aitik site in northern Sweden, which is the site investigated by Strömberg and Banwart (1994), field observations and modeling results indicate that only 20% of the waste material contributes to the observed release of sulfate and copper (Gibson et al 1992), which may be a preferential flow path effect.

Solute Transport in Weathering Waste Rock

In waste rock dumps, interacting physical, chemical, and biochemical processes weather (dissolve) the waste rock continuously. In this paper, weathering of primary mineral is considered as an irreversible, heterogeneous reaction. Under oxic conditions, the weathering process will take place throughout the total height of the dump and the source of solute will be distributed along the streamlines that define the mean flow direction. When water infiltrates the waste rock, weathering products that are soluble in water will be transported through the dump into the underlying aquifer or into surrounding drainage ditches. To quantify the long-term release of solute at the lower boundary of the waste rock dump we consider advection-dominated transport where the flow of water is steady and the mean flow direction is downward.

The advective approach is based on the assumption that field-scale spreading of solute is primarily an effect of variability in solute advection between different stream tubes such that local dispersive mechanisms can be neglected (Dagan1989). Under these conditions the mass balance equation for an arbitrary stream tube can be formulated as:

$$\theta\frac{\partial c}{\partial t}+\frac{\partial(qc)}{\partial z}=\theta\left[\frac{\partial c}{\partial t}\right]_{chem} \qquad (1)$$

where c is the solute concentration, t is time , θ is the volumetric water content, z is the vertical space coordinate with origin at the dump surface and positive downward, and q is the flow of water per unit cross-sectional area normal to z.

The right-hand side of the equation expresses the change in concentration due to the prevailing weathering processes such that

$$\left[\frac{\partial c}{\partial t}\right]_{chem}=\frac{1}{\theta}r\alpha=-\frac{1}{\theta}\frac{\partial c^{*}}{\partial t} \qquad (2)$$

where r is the reaction rate defined as the produced amount of the considered aqueous phase species per unit time and unit area of reacting interface, and α is the specific reactive surface area of the primary mineral defined per unit bulk volume. Furthermore, $\partial c^{*}/\partial t$ expresses the rate of dissolution of the solid phase species with $c^{*}\equiv\rho_m\eta$, in which ρ_m is the considered mineral content per unit bulk volume and η is the amount of produced aqueous phase species per unit amount of dissolved mineral.

Combining equations 1 and 2, inserting the mean porewater velocity $v = q / \theta$, and introducing the new variable $d\tau \equiv dz / v(z)$, equation 1 can be rewritten as:

$$\theta \frac{\partial c}{\partial t} + \theta \frac{\partial c}{\partial \tau} = -\frac{\partial c^*}{\partial t} \qquad 3)$$

In equation 3, $\tau(z) = \int_0^z d\zeta / v(\zeta)$ expresses the water residence time in the steam tube, or the travel time for an ideal tracer from the surface of the dump to the depth z (Shapiro and Cvetkovic 1988).

The specific surface area α in equation 2 will be a function of the primary mineral content of the deposit and may thus vary with time due to the weathering process. The reaction rate, r, is dependent on the rate determining step of the reaction and may also be time-dependent, for instance, due to changes in pH or temperature. For chalcopyrite oxidation $(CuFeS_{2(s)} + 4O_{2(aq)} \rightarrow Cu^{2+} + Fe^{2+} + 2SO_4^{2-})$ of relatively fresh waste rock (deposited 5 years on the average) Strömberg and Banwart (1994) reported an r value in the order of 10^{-11} moles/(m^{2}s); this value was the result of initial geochemical modeling of an oxic waste rock dump with the mineral content, ρ_m, approximately equal to 10 moles/m^3. The specific surface area of chalcopyrite was estimated to about 2,000 m^2/m^3, however, comparison with field data indicated that only a fraction of the area is reactive. Because neither field data nor the geochemical modeling of Strömberg and Banwart (1994) provide information on the long-term dynamics of the dissolution rate, different functions $c^*(t)$ are conceivable for the dissolution process, two of which will be presented here for illustrative purposes.

The first dissolution process, in the following referred to as case 1, is obtained by assuming a constant rate of dissolution until all the primary mineral has been dissolved, and can be expressed as:

$$c^* = c_0^*(1 - kt) \ , \qquad (4)$$

in which k is a constant rate coefficient and c_0^* is defined from the initial mineral content ρ_{m0}. Assuming initial conditions consistent with those reported by Strömberg and Banwart (1994), a relevant k value for chalcopyrite dissolution can be estimated by differentiating equation 4 and inserting in equation 2, which results in $k = \alpha r / c_0^*$. With a reactive surface area of 10% of the specific surface area, $k = 0.1 \cdot 2000 \cdot 10^{-11}/10 = 2 \cdot 10^{-10}$ s^{-1}, which corresponds to a turnover time $t_s = 1/k$ of approximately 150 years.

Inserting equation 4 in equation 3 and solving for the solute mass flux $s(t,Z) = c(t,Z)q(Z)$, where Z is the total height of the waste rock dump, yields:

$$\frac{s(t,Z)}{c_0^* Z} = \begin{cases} \dfrac{t}{Tt_s} & \text{for } t < \mathrm{T} \\ \dfrac{1}{t_s} & \text{for } \mathrm{T} \le t < t_s \\ \dfrac{1}{t_s} - \dfrac{t - t_s}{\mathrm{T}t_s} & \text{for } t_s \le t \le t_s + \mathrm{T} \\ 0 & \text{for } t > t_s + \mathrm{T} \end{cases} \qquad \mathrm{T} \le t_s$$

$$\frac{s(t,Z)}{c_0^* Z} = \begin{cases} \dfrac{t}{\mathrm{T}t_s} & \text{for } t < t_s \\ \dfrac{1}{\mathrm{T}} & \text{for } t_s \le t < \mathrm{T} \\ \dfrac{1}{\mathrm{T}} - \dfrac{t - \mathrm{T}}{\mathrm{T}t_s} & \text{for } \mathrm{T} \le t \le t_s + \mathrm{T} \\ 0 & \text{for } t > t_s + \mathrm{T} \end{cases} \qquad \mathrm{T} > t_s \tag{5}$$

The solute flux $s(t,Z)$ quantifies the mass flow rate produced in a stream tube per unit cross-sectional area of the dump. In equation 5, $\mathrm{T} = \tau(Z)$ is the water residence time in an arbitrary stream tube spanning the vertical extent of the dump. For Swedish hydrological conditions (average annual rainfall: 0.7m/yr), an average infiltration rate of 0.5 m/yr can be expected, implying an average water residence time of 4 yr for a 20-m-high waste rock dump with an average volumetric water content of 10%.

The second dissolution process, in the following referred to as case 2, describes an exponentially decreasing mineral content and can be expressed as:

$$c^* = c_0^* \, e^{-kt} \tag{6}$$

Inserting equation 6 in equation 3 and solving for $s(t,Z)$, yields:

$$\frac{s(t,Z)}{c_0^* Z} = \frac{1}{\mathrm{T}}(1 - e^{-kt}) \qquad \text{for } t < \mathrm{T}$$

$$\frac{s(t,Z)}{c_0^* Z} = \frac{1}{\mathrm{T}}(e^{k\mathrm{T}} - 1)\, e^{-kt} \qquad \text{for } t \ge \mathrm{T} \tag{7}$$

In figure 1, the solutions 5 and 7 for case 1 (linearly decreasing mineral content, solid line) and case 2 (exponentially decreasing mineral content, dashed line), respectively, are illustrated; these solutions are relevant for an individual stream tube or for a homogeneous dump. The maximal solute flux is reached when water that has traveled in the considered stream tube throughout the total height of the dump reaches the lower boundary of the dump at $z = Z$. For case 1 dissolution, the solute flux will remain constant at its maximum value until all mineral has been dissolved, after which the solute mass flux will drop linearly to zero during the time period of one water residence time T. For case 2 dissolution, the solute flux will decrease exponentially in time after reaching its maximum value at $t = \mathrm{T}$. The maximum level of the solute flux will be the same in both cases for equal water residence time, T. The case 2 dissolution will continue over a longer period of time, but at a lower solute flux than case 1.

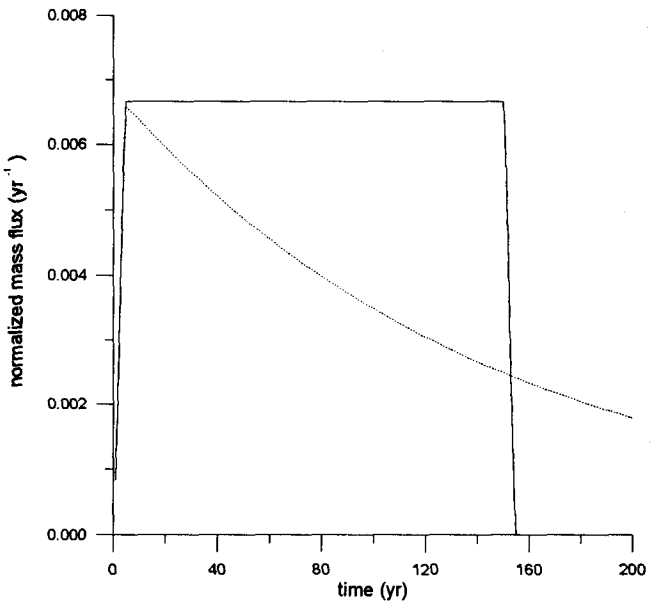

Figure 1. The normalized solute flux $s(t,Z)/c_0^*Z$ for Z=20m and T=4yr and k=1/150 yr^{-1} is illustrated for case 1 (linearly decreasing mineral content, solid line) and case 2 (exponentially decreasing mineral content, dashed line) dissolution. The solute flux peak is reached at the same time (t = T) for both dissolution processes. For case 2 dissolution, however, the solute flux is distributed over a longer period of time and continues at a lower level than for the case 1 dissolution.

The two illustrated dissolution cases (figure 1) represent two examples of possible dissolution dynamics. Because for our study case, i.e. the Aitik site, neither field nor laboratory data have yet been obtained for evaluating any potential changes in the dissolution rate, we will in the following illustrate the modeling methodology by use of case 1. This particular case, i.e. constant dissolution rate, was also used by Gibson et al (1992) to predict copper leaching at the Aitik site. Wherever applicable, however, the case 2 dissolution, or other dissolution dynamics, can readily be incorporated in the modeling approach that will be discussed in the following.

Transport Through a Heterogeneous Waste Rock Dump

Because waste rock dumps are large and heterogeneous porous formations, large and irregular variability in flow and transport parameters is conceivable. Such heterogeneity implies an unevenly distributed waterflow within the dump, such that both q and θ vary between different stream tubes. Because of the significant size of a typical waste rock dump, it is not likely that field measurments will provide sufficient data for deterministic knowledge of the fluctuations in v throughout the dump. A rational way to deal with this uncertainty is to regard v as a random variable (Dagan 1989). In the following, we will therefore regard the water residence time $\mathrm{T} = Z/v$ as a random variable, quantified by a probability density function (pdf), $f(\mathrm{T})$.

We regard each stream tube in the actual dump as a realization of an ensemble of all possible stream tubes according to $f(\mathrm{T})$, which are statistically equivalent on the field scale but locally different. As a consequence, the solute mass flux becomes a random function of the random variable T, depending deterministically on k, c_0^*, Z, and t. The pdf $f(\mathrm{T})$ is assumed stationary, i.e., the moments of $f(\mathrm{T})$ do not depend on spatial position. Under ergodic conditions, i.e., if the considered waste rock dump is sufficiently large relative to the correlation scale of T, ensemble averaging and space averaging at the lower boundary of the dump are equivalent (Cvetkovic et al. 1992; Destouni 1992). The expected solute flux can then be expressed as:

$$\bar{s}(t,Z) = \int_0^\infty s(t,Z;\mathrm{T}) f(\mathrm{T}) d\mathrm{T} \tag{8}$$

The choice of $f(\mathrm{T})$ in equation 8 will in each field situation depend on the available field data and the sensitivity of the solution to the chosen pdf. The function $f(\mathrm{T})$ may thus be an ordinary unimodal pdf, or a bi- or multimodal distribution to reflect potential preferential flow paths. An often used unimodal pdf of T is the lognormal distribution (e.g., Simmons 1982; Cvetkovic et al. 1992)

$$f(\mathrm{T}) = \frac{1}{\mathrm{T}\sqrt{2\pi\sigma^2}} \exp\left[-\frac{1}{2} \frac{\left(\ln \mathrm{T} - \ln \mathrm{T}^{\mathrm{G}}\right)^2}{\sigma^2} \right]. \tag{9}$$

In equation 9, T^{G} is the geometric mean of the water residence time and σ^2 is the variance of $\ln \mathrm{T}$.
Figure 2 illustrates the effect of flow heterogeneity on the expected solute flux for case 1 dissolution (linearly decreasing mineral content), by comparison of solution 8 for a lognormally distributed water residence time, T, to the homogeneous solution 5. The comparison shows that for realistic parameter values and for the considered unimodal distribution of T, flow heterogeneity within the waste rock dump does not have a significant effect on the expected solute flux through the dump. The reason for this insensitivity is that the characteristic hydrological time scale, i.e., the average water residence time of 4 years, is much smaller than the characteristic chemical time scale of 150 years. As a consequence, the transport process becomes chemically dominated.

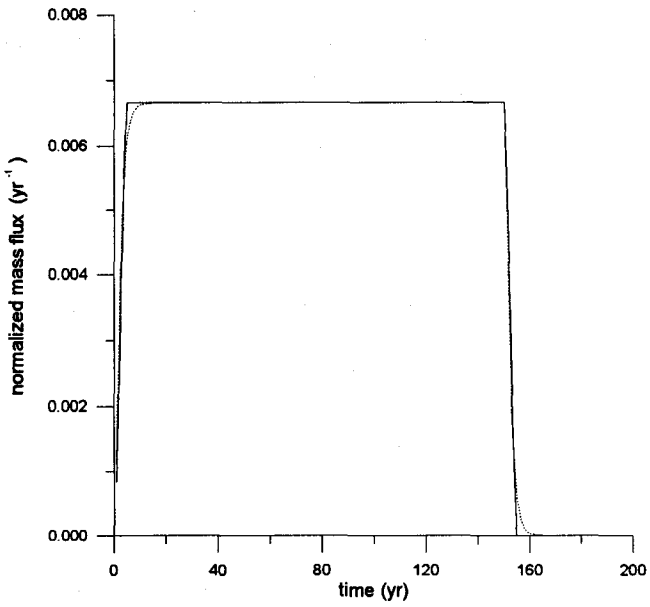

Figure 2. The normalized expected solute flux, $\bar{s}(t,Z)/c_0^* Z$ for a lognormally distributed water residence time with T^G=3.44 yr and σ^2=0.3 ($\bar{\mathrm{T}}$=4yr; dashed line,) compared with the homogeneous solution 5 with T=4yr (solid line). The comparison shows that for realistic variance in the water residence time, flow heterogeneity does not have significant effect on the expected solute flux.

Transport Through a Waste Rock Dump With Preferential Flow Paths

In many cases, high-permeability channels or preferential flow paths may be the primary controls of water movement through the dump. Although confirmation through field observations is lacking (Morin et al. 1991),

double- or multipeaked solute plumes or breakthrough curves have been reported for field soils (Jury et al. 1986, Butters et al. 1989, Roth et al. 1991, Sassner et al. 1994). The concept of preferential flow paths implies that a large part of the waterflow takes place in a small part of the cross-sectional area of the dump. This concept does not exclude flow in the regions of less mobile water; it only implies water residence times that are significantly greater than in the preferential flow paths. The concept of preferential flow paths can therefore be appropriately described by a bi- or multimodal distribution of the water residence time (Destouni 1993, Sassner et al 1994, Destouni et al. 1994).

A bimodal distribution quantifies the existence of two populations of water residence times, which are related to each other by use of water flow continuity formulated as

$$\bar{q} = \upsilon\overline{q_1} + (1-\upsilon)\overline{q_2} \ . \tag{10}$$

In equation 10, $\bar{q}$ is the mean water flow per unit cross-sectional area of the dump, and $\overline{q_1}$ and $\overline{q_2}$ are the mean water fluxes in the relatively slow flow paths (SFP) and in the preferential, or fast flow paths (FFP), respectively. Furthermore, $\upsilon\overline{q_1}/\bar{q}$ quantifies the volumetric flow fraction through the SFP, and υ is the probability for the local water flux being dominated by SFP. For illustrative purposes, we will in the following assume that the water flux through 20% of the cross-sectional area of the dump is influenced by FFP, and that the water flux through the remaining 80% is dominated by SFP, i.e., $\upsilon = 0.8$.

For bimodally distributed q, a relevant bimodal pdf of the water residence time T can be expressed as (Destouni et al. 1994)

$$f(\mathrm{T}) = \frac{\upsilon}{\mathrm{T}\sqrt{2\pi\sigma_1^2}} \exp\left[-\frac{1}{2}\frac{\left(\ln \mathrm{T} - \ln \mathrm{T}_1^{\mathrm{G}}\right)^2}{\sigma_1^2}\right] + \frac{1-\upsilon}{\mathrm{T}\sqrt{2\pi\sigma_2^2}} \exp\left[-\frac{1}{2}\frac{\left(\ln \mathrm{T} - \ln \mathrm{T}_2^{\mathrm{G}}\right)^2}{\sigma_2^2}\right], \tag{11}$$

which is a combination of two lognormal distributions. In equation 11, $\mathrm{T}_i^{\mathrm{G}}$ is the geometric mean of the water residence time and σ_i^2 is the variance of $\ln \mathrm{T}$, in which i =1 refers to the SFP and i =2 to the FFP. The geometric mean of the water residence time is related to the geometric mean of the water flux through $\mathrm{T}_i^{\mathrm{G}} = Z\theta / q_i^{\mathrm{G}}$, in which $q_i^G = \exp(\ln \overline{q_i} - \sigma_i^2/2)$.

Equation 11 quanitifies the residence time distribution of an ideal tracer (non-reactive, non-diffusive). This distribution is combined with the prevailing local (bio)chemical reactions and diffusive mechanisms through equation 8. In this paper, we have only considered irreversible chemical dissolution, which is quantified by the term $s(t, Z; \mathrm{T})$ in equation 8; this term is in turn quantified by equation 5 for case 1 dissolution, and by equation 7 for case 2 dissolution. Other types of local mass transfer mechanisms, such as equilibrium and/or non-equilibrium adsorption-desorption (Destouni and Cvetkovic 1991), degradation (van der Zee and Destouni 1992), or diffusive mass transfer between mobile and immobile water zones (Destouni 1993, Destouni et al. 1994) can also be incorporated in this modeling approach. For the case of preferential flow paths, incorporation of diffusive mass transfer between mobile and immobile water could be relevant. However, the studies of Destouni (1993) and Destouni et al. (1994) showed that the influence of this mechanism on field-scale solute transport is small; for simplicity, we shall therefore neglect diffusive mass transfer in the following.

In figure 3, the effect of the existence of preferential flow paths on the solution 8 is illustrated for case 1 dissolution and for two different bimodal pdfs (equation 11) by comparison with the homogeneous solution 5. For both bimodal pdfs the mean water flux $\overline{q}$=0.5m/yr; the parameters T_i^G, however, differ between the two pdfs. The comparison shows that the expected solute flux is sensitive to even small changes in the mean water residence time in the preferential flow paths. The effect of preferential flow paths is that the peak value of the solute flux decreases and a tail develops in the expected breakthrough curve. When $\overline{T_2}$=1.09yr (T_2^G=0.94yr), equation 10 implies that $\overline{T_1}$=1,000yr (T_1^G=600yr), which leads to a significant decrease in the peak value of the solute flux and a considerable tailing effect. The reason for these effects is that the characteristic hydrological time scale in the SFP is greater than the characteristic time scale of the weathering process. This indicates that preferential flow paths may affect the field scale solute transport of weathering products significantly. Moreover, the existence of preferential flow paths may also be the reason for the field observations of solute concentration being considerably lower than expected from geochemical modeling with reaction rates based on literature values (Strömberg and Banwart 1994).

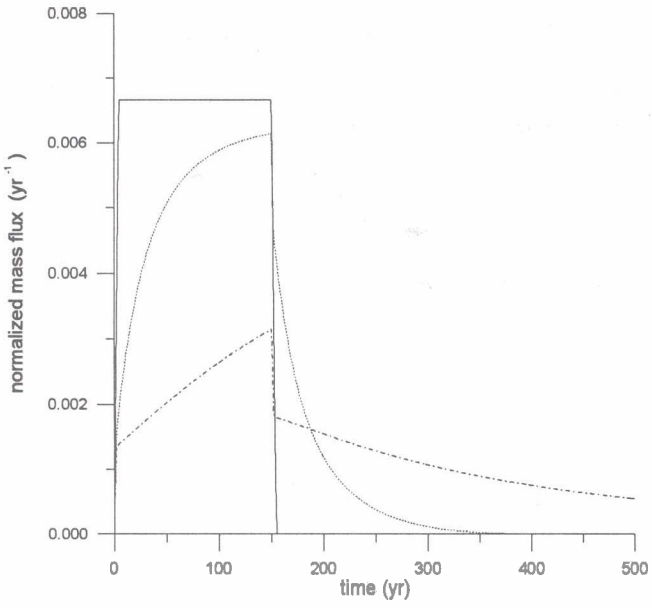

Figure 3. The homogeneous solution 5 with T=4yr (q=0.5m/yr) (solid line) and the normalized heterogeneous solutions 8 for υ= 0.8 and for two bimodal pdfs: T_1^G=60yr, T_2^G=1.02yr, σ_1^2=0.3, σ_2^2=1.0 (dashed line) and T_1^G=600yr, T_2^G =0.94yr, σ_1^2=0.3, σ_2^2=1.0 (dash-dotted line). The comparison shows that the existence of preferential flow paths may considerably affect both the maximum value and the temporal distribution of the solute flux.

Conclusions

The effect of flow heterogeneity on the field scale mass flux of dissolved weathering products from a waste rock dump has been investigated for a classical unimodal distribution of water residence time and for bimodal distributions that reflect the existence of preferential flow paths. Results indicate that for realistic parameter values, flow heterogeneity reflected by a unimodal distribution of water residence time does not affect the solute flux significantly. The reason for this insensitivity is the difference in characteristic time scales between the water residence time in the dump and the dissolution process. Flow heterogeneity in the form of preferential flow paths, however, is better described by bi- or multimodal distributions and may have a considerable impact on field-scale solute flux in terms of both the peak value and the temporal spreading of solute. Hence, flow heterogeneity should be taken into account when estimating field-scale solute transport in mining waste rock dumps by coupling spatially distributed hydrological modeling with local or average geochemical conditions.

For simplicity, we have in this paper only regarded the water residence time as a random variable. The stochastic-advective modeling approach that was presented here, however, can readily be extended to include randomness also in the rate coefficient, k, or any other parameter of interest. Furthermore, additional chemical reactions and mass transfer mechanisms, such as equilibrium and/or non-equilibrium adsorption-desorption (Destouni and Cvetkovic

1991), degradation (van der Zee and Destouni 1992), or diffusive mass transfer between mobile and immobile water zones (Destouni 1993, Destouni et al. 1994) or precipitation/dissolution of secondary minerals (Eriksson and Destouni 1994, paper in preparation) can also be incorporated in the stochastic-advective modeling approach. In addition, the transport process in the underlying aquifer, can be coupled with the solute flux from the waste rock dump(Destouni and Eriksson 1994).

Acknowledgements.

Financial support for this work has been provided by the Swedish Waste Research Council (AFR) and the Swedish Natural Science Research Council (NFR; second author).

References

Butters, G. L., W. A. Jury, and F. F. Ernst, 1989. Field scale transport of bromide in an unsaturated soil, Experimental methodology and results, Water Resour. Res., 25: 1575-1581.

Cvetkovic, V. D., G. Dagan, and A. Shapiro, 1992. A solute flux approach to transport in heterogeneous formations 1. Uncertainty analysis, Water Resour. Res., 28: 1377-1388.

Cvetkovic, V. D., and A. M. Shapiro, 1990. Mass arrival of sorptive solute into the groundwater, Water Resour. Res.,26, 2057-2068.

Dagan, G., 1989. Flow and transport in porous formations, Springer-Verlag, Heidelberg, 465 pp

Dagan, G., V. D. Cvetkovic, and A. M. Shapiro, 1992. A solute flux approach to transport in heterogeneous formations 1. The general framework, Water Resour. Res., 28: 1369-1376.

Destouni, G., 1992 The effect of vertical soil heterogeneity on field scale solute flux. Water Resour. Res., 28: 1303-1309.

Destouni, G., 1993. Field-scale solute flux through macroporous soils, in Water Flows and Solute Transport in Soils (eds. Russo, D., and Dagan,G.), Springer-Verlag, Heidelberg, 33-44.

Destouni, G., and V. D. Cvetkovic, 1991. Field scale mass arrival of sorptive solute into the groundwater, Water Resour. Res., 27: 1315-1325.

Destouni, G. and N. Eriksson, 1994. Field scale transport of weathering products from mining waste. In Proceedings of The International Symposium on Transport and Reactive Processes in Aquifers. (Organized by IAHR, ETH, Zurich, Switzerland, April 11-15, 1994).

Destouni, G., M. Sassner, and K. H. Jensen, 1994. Chloride migration in heterogeneous soil, 2. Stochastic modelling, Water Resour. Res. (in press)

Eriksson N. and G. Destouni, 1994. Flow heterogeneity and precipitation/dissolution of secondary minerals affecting field-scale transport of weathering products. Prepared for the Nordic Hydrological Conference. (Faroe Islands, Denmark, August 2-4, 1994 (in preparation)).

Gibson D. K., G. Pantteis and A. I. M. Ritchie, 1992. An estimate of present and future pollution loads from the waste rock heaps at the Aitik mine site; assassment after first ten months monitoring. ANSTO/C266, commercial report for Boliden Mineral AB.

Harries, J. R. and A. I. M. Ritchie, 1983. Runoff fraction and pollution levels in runoff from a waste rock dump undergiong pyritic oxidation. Water Air Soil Pollut 19, 155-170.

Jury, W. A., H. Elabd, and M. Resketo, 1986. Field studie of napropamide movement through unsaturated soil. Water Resour. Res., 22: 749-755.

Morin, K. A., E. Gerencher, C. E. Jones, and D. E. Konasewich, 1991. Critical literature review of acid drainage from waste rock. Canadian Mine Environmental Neutral Drainage (MEND) Program, MEND Project 1.11.1, Canada Centre for Mineral and Energy Technology (CANMET), 175 pp.

Roth, K., W. A. Jury, H. Fluhler, and W. Attinger, 1991. Transport of chloride through an unsaturated field soil. Water Resour. Res., 27: 2533-2541.

Sassner, M., K. H. Jensen, and G. Destouni, 1994. Chloride migration in heterogeneous soil, 1. Experimental methodology and results. Water Resuor. Res. (in press).

Shapiro, A. M. and V. D. Cvetkovic, 1988. Stochastic analysis of solute arrival in heterogeneous porous media. Water Resour. Res., 24: 1711-1718.

Simmons, C. S., 1982. A stochastic-convective transport representation of dispersion in one-dimentional porous media systems. Water Resour. Res., 18: 1193-1214.

Strömberg, B. and S. Banwart, 1994. Kinetic modeling of geochemical processes at Aitik mining waste rock site in northern Sweden. Applied Geochemistry (accepted).

Van der Zee S. E. A. T. M. and G. Destouni, 1992. Transport of inorganic solutes in soil. In Advances in Soil Science, Interacting Processes in Soil Science (eds. Wagenet R. J., P. Baveye and B. A. Stewart), Lewis Publishers, Boca Raton, Florida, 95-145.

BEST PROFESSIONAL JUDGMENT ANALYSIS FOR CONSTRUCTED WETLANDS AS A BEST AVAILABLE TECHNOLOGY FOR THE TREATMENT OF POST-MINING GROUNDWATER SEEPS[1]

William W. Hellier, Ernest F. Giovannitti and Peter T. Slack[2]

Abstract: The Pennsylvania Department of Environmental Resources (Department) performed a best professional judgment (BPJ) analysis to determine the best available technology economically achievable (BAT) for the treatment of postmining ground water seeps from surface coal mining operations. Acidity, Fe, and Mn were selected as the pollutants of primary interest to be removed. Data from 73 constructed wetlands, subcategorized according to the wetlands' influent net acidity or alkalinity, were analyzed. The sizing guidelines obtained from the data compare favorably with previous sizing guidelines presented by the U.S. Bureau of Mines. The sizing guidelines were applied to data from 794 postmining ground water seeps from the bituminous coal mining counties of Pennsylvania based on the median quantity and quality data for the seeps in five subcategories of net acidity or alkalinity. Costs to treat the seeps for 25 yr were determined for conventional treatment and for constructed wetlands treatment, both with and without anoxic limestone drain pretreatment, and both considering and not considering Mn removal. Based on the analysis, constructed wetlands treatment was found to be BAT for treatment of postmining ground water seeps, particularly for mildly acidic and alkaline seeps.

Additional Key Words: Best professional judgment, ground water seeps, constructed wetlands.

Introduction

When the U.S. Environmental Protection Agency (EPA 1982) developed its coal mining technology-based effluent limitations (40CFR434), it considered only discharges that occur during active mining. It did not establish limitations for ground water seeps that could occur after mining had been completed. Passive treatment systems were not in routine use when the effluent guidelines were evaluated. Since that time, constructed wetlands and anoxic limestone drains (ALD's) have emerged as potential alternative technologies. In the absence of federally promulgated guidelines, best available technology economically achievable (BAT) may be developed by means of a best professional judgment (BPJ) analysis. Section 304 of the Federal Clean Water Act specifies that the following factors are to be used to identify the BAT: (1) age of equipment and facilities involved, (2) the process employed, (3) process changes, (4) engineering aspects of the application to various types of control technology, (5) non-water quality impacts, (6) total cost of the application of technology in relation to the pollutant reduction benefits to be achieved, (7) the cost of achieving such effluent reduction, and (8) other factors deemed appropriate.

---

1 Paper presented at the International Land Reclamation and Mine Drainage Conference and the Third International Conference on the Abatement of Acidic Drainage, Pittsburgh, PA, April 24-29, 1994.

2 William W. Hellier, Wetlands Coordinator, Ernest F. Giovannitti, Director, and Peter T. Slack, Chief, Permits Division, Commonwealth of Pennsylvania, Department of Environmental Resources, Bureau of Mining and Reclamation, Harrisburg, PA, USA.

The Department performed a BPJ analysis for postmining ground water seeps (hereinafter "seeps") as described above (Hellier 1993). Based on the analysis, the Department finds that for some categories of seeps, treatment with constructed wetlands (hereinafter "wetlands") is a cost-effective, environmentally sound alternative to more conventional treatment.

Performance data from 73 wetlands were used in this BPJ analysis. Cost information from several sources, including consultants, coal operators, and government agencies, was used to determine the capital, operation and maintenance, and amortization costs for wetlands sized according to guidelines developed below. The cost information was applied to actual seeps to determine the overall costs of using wetlands treatment. Costs for conventional and wetlands treatment were compared, and the BAT was determined.

Postmining ground water seeps may occasionally develop after reclamation. They are not caused or affected by the type, age, or condition of the mining equipment. The methods of mining do not affect the choice of treatment technology that would be used should a seep occur. Finally, there is no processing of material at a coal mine that will cause a seep. Seeps occur because of the hydrology and geology of the reclaimed mine site. The technology employed in treating seeps is independent of these factors.

Wastewater Characteristics and Performance of Wetlands

The Department characterized seeps on the basis of data taken from 794 postmining seeps arising from 406 different surface mine permitted areas in the bituminous coal mining counties of Pennsylvania. These seeps can be subcategorized according to their net acidity or alkalinity: (1) very acid seeps - net acidity >300 mg/L (as $CaCO_3$), (2) moderately acid seeps - 100 ≤ net acidity ≤ 300 mg/L, (3) weakly acid seeps - 0 ≤ net acidity < 100 mg/L, (4) weakly alkaline seeps net alkalinity < 80 mg/L, and (5) strongly alkaline seeps - net alkalinity ≥ 80 mg/L. Figure 1 summarizes the water quality of seeps in the five subcategories (Tukey 1977, Helsel 1987).

Conventional treatment was considered as a candidate technology for the treatment of seeps. The conventional treatment process described in the EPA development documents for the Coal Mining Point Source Category is a proven technology. Treatment consist of using alkaline compounds such as CaO, $Ca(OH)_2$, Na_2CO_3, $NaHCO_3$, NaOH, or NH_3 to neutralize any acid in the discharge, to give it a positive net alkalinity, and to raise its pH to a value in the range 6.0 ≤ pH ≤ 9.0. In the process, Fe and Mn compounds are converted to less soluble oxides or hydroxides. The treated discharge is then detained in one or more settling basins for 24 h or more. The metal oxides and hydroxides are removed in the settling basins by sedimentation, sometimes assisted by application of a coagulant. Typically at least two settling basins are built in series to minimize solids carryover at the outfall. BAT regulations, 40CFR34, describe the effluent quality achievable using conventional treatment. These requirements are summarized in Table 1.

Table 1. Pennsylvania's BAT limitations.

Pollutant parameter	30-Day average	Daily (24 hr.) average
Iron (Fe).....	3.5	7
Manganese (Mn) mg/L.	2	4
Suspended solids mg/L.	35	70
pH*.....	6-9	6-9

*Between 6 and 9 at all times.

These BAT limitations apply to discharges in existence as of October 1985. "New source" discharges occurring after that time must also comply with these limits, except for Fe limits, which are 3 mg/L (30-day average) and

6 mg/L (daily average). For all practical purposes, BAT and "new source" effluent requirements are equivalent in terms of the technology needed to achieve compliance. Although not part of EPA's BAT requirements, the Department's regulations require that alkalinity > acidity at all times.

A commonly used passive treatment system is the constructed wetland. Both aerobic and anaerobic processes occur in wetlands. Aerobic processes remove Fe and Mn by oxidation, hydrolysis, and settling of the resulting oxides and hydroxides. Al is removed by hydrolysis and settling. Hydrolysis of metals consumes OH- and liberates H+. To prevent this additional acid contributing to pollution of the receiving waters, one relies on (1) alkalinity originally present in the seep, (2) pretreatment by an anoxic limestone drain, or (3) a rock and organic substrate that generates alkalinity under anoxic conditions.

Anaerobic conditions develop in the substrate. Bacteria, using the substrate as a carbon source, reduce SO_4^{-2} to S^{-2}, thereby removing acidity. Part of the S^{-2} escapes to the atmosphere as H_2S, while part precipitates metals in such forms as FeS. The bacteria incorporate C into HCO_3^-, thereby generating alkalinity. Because HCO_3^- from limestone also contributes alkalinity, the rock incorporated into the substrate is often limestone (Anderson and Schiff 1987).

Alkalinity may also be added by means of an anoxic limestone drain (ALD). The limestone is buried in a trench, forming a drain through which the water to be treated is passed in the absence of O_2. Anoxic conditions are supposed to prevent coating of the limestone by $Fe(OH)_3$. The limestone dissolves, imparting alkalinity and neutralizing part or all of the acidity. The treated water is directed into a settling basin or constructed wetland, where the cations are removed by oxidation, hydrolysis, and settling, as above.

The Department examined wetlands that were used in the treatment of 73 of the 794 postmining ground water seeps, subcategorizing the wetlands in the same manner as it subcategorized the 794 seeps. Figs. 2-4 show the performance of the five subcategories of wetlands as grams per day of pollutant removed per square meter of wetland area. A mass flow per unit time per unit area is called a flux. The removal is therefore the difference between the influent and effluent fluxes of pollutant. Figure 2 shows that when the influent was originally acid, the effluent net acidity has been significantly reduced relative to the influent net acidity; however, when the influent net acidity > 100 mg/L wetlands with acid influents have acid effluents. Wetlands whose influent net acidity < 100 mg/L tend to have alkaline effluents. Wetlands tend to have effluent [Fe] that is substantially lower than their influent [Fe] (Fig. 3). Wetlands are not as effective in terms of Mn removal (Fig. 4).

The U.S. Bureau of Mines has initially made an empirical estimate for minimum sizes for wetlands (Hedin and Nairn 1992). For a net alkaline water the minimum size based on Fe loading is

$$A(m^2) = Fe\ (g/d)/(20\ gd^{-1}m^{-2})$$

and for Mn loading

$$A(m^2) = Mn\ (g/d)/(0.5\ gd^{-1}m^{-2})$$

The Bureau also suggests that an anaerobic wetland could be designed on the basis of

$$A\ (m^2) = [\text{net acidity}]\ (g/d)/(5\ gd^{-1}m^{-2})$$

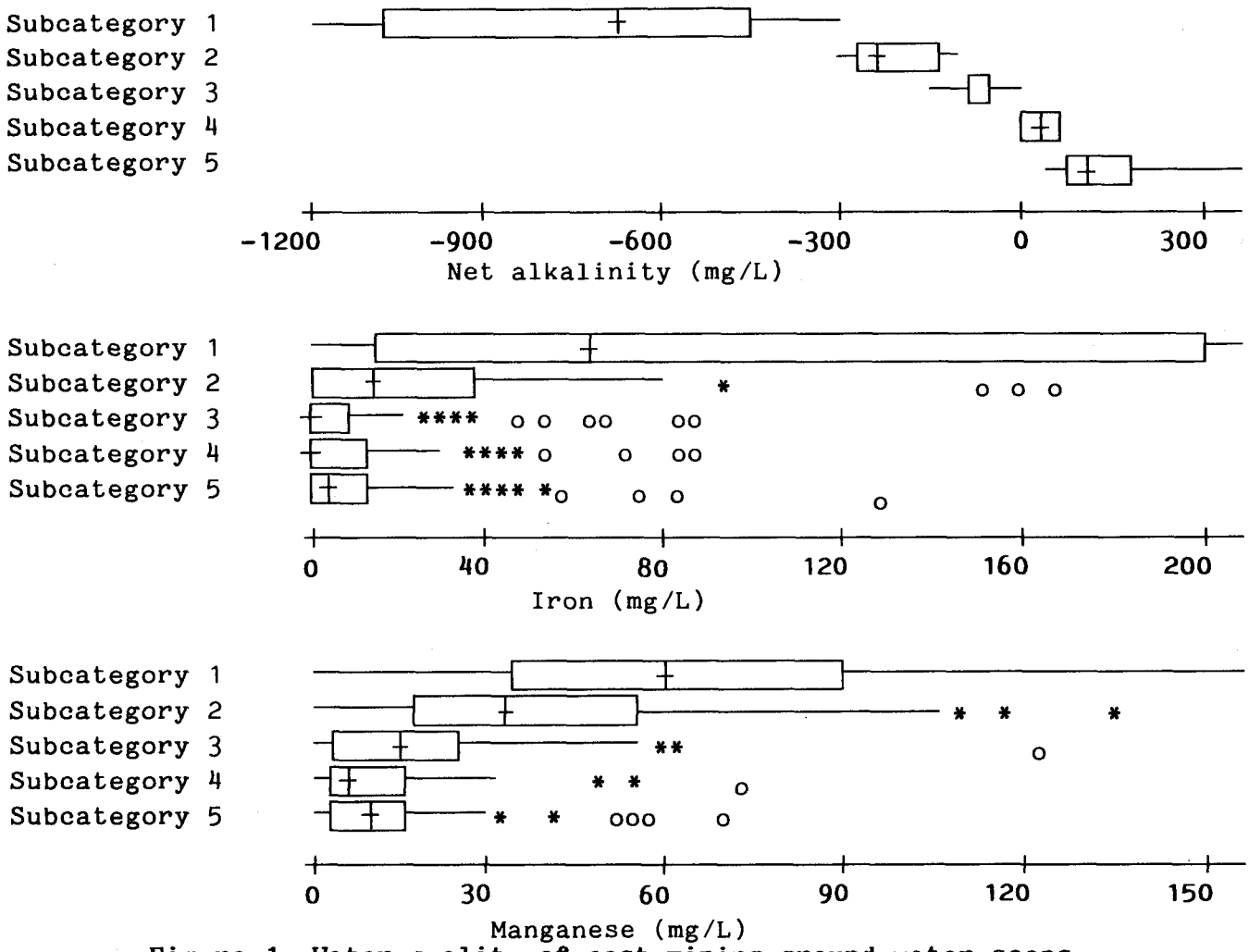

Figure 1. Water quality of post mining ground water seeps.

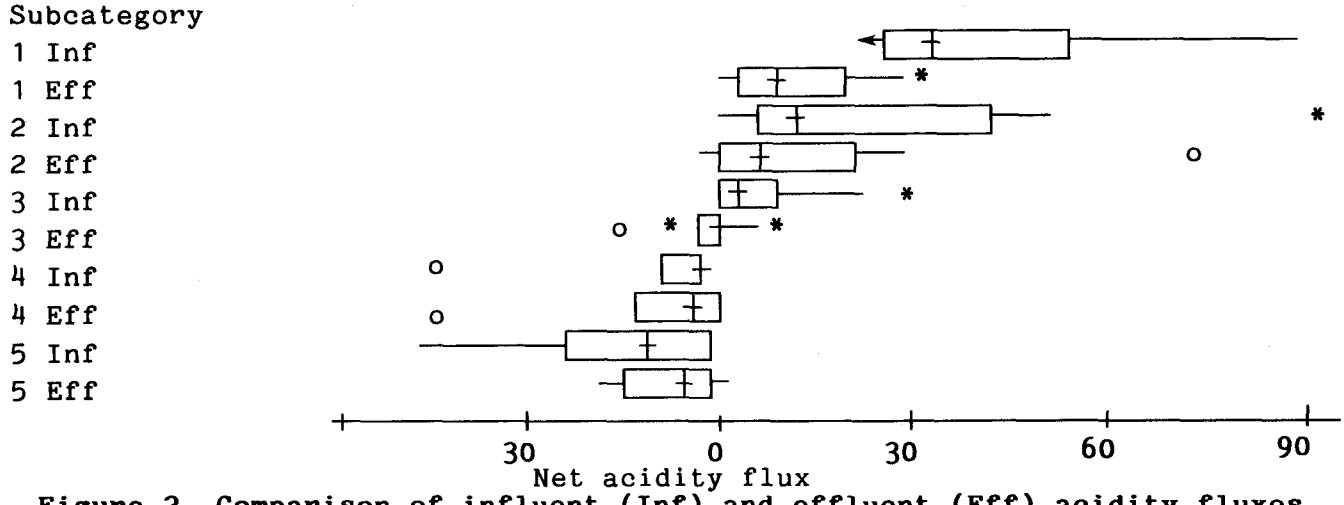

Figure 2. Comparison of influent (Inf) and effluent (Eff) acidity fluxes for the five subcategories of constructed wetlands.

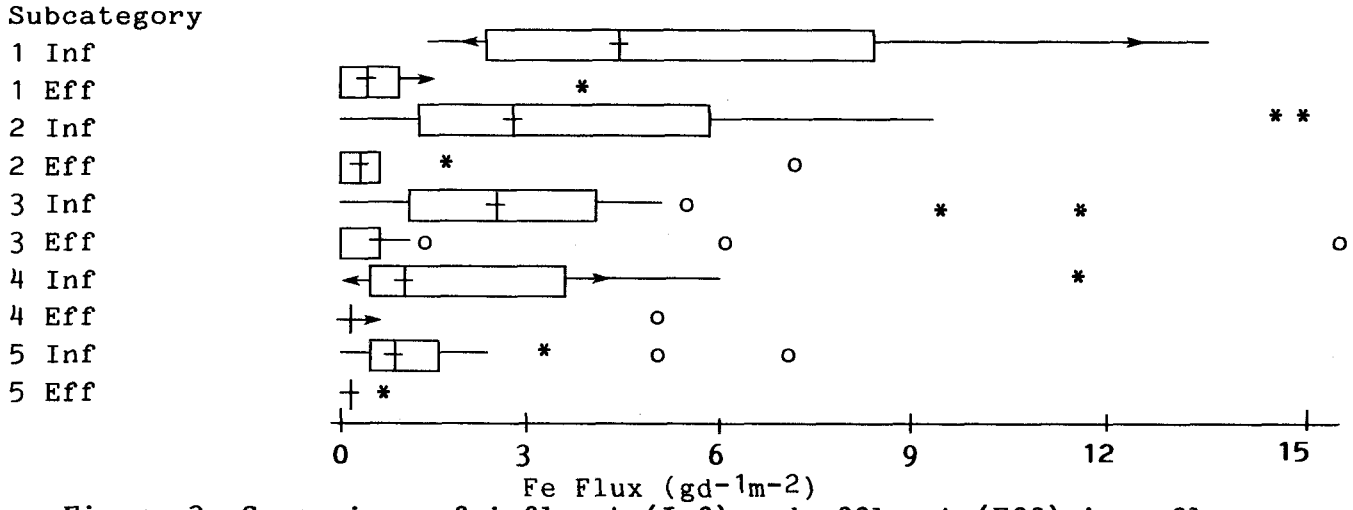

Figure 3. Comparison of influent (Inf) and effluent (Eff) iron fluxes for the five subcategories of constructed wetlands.

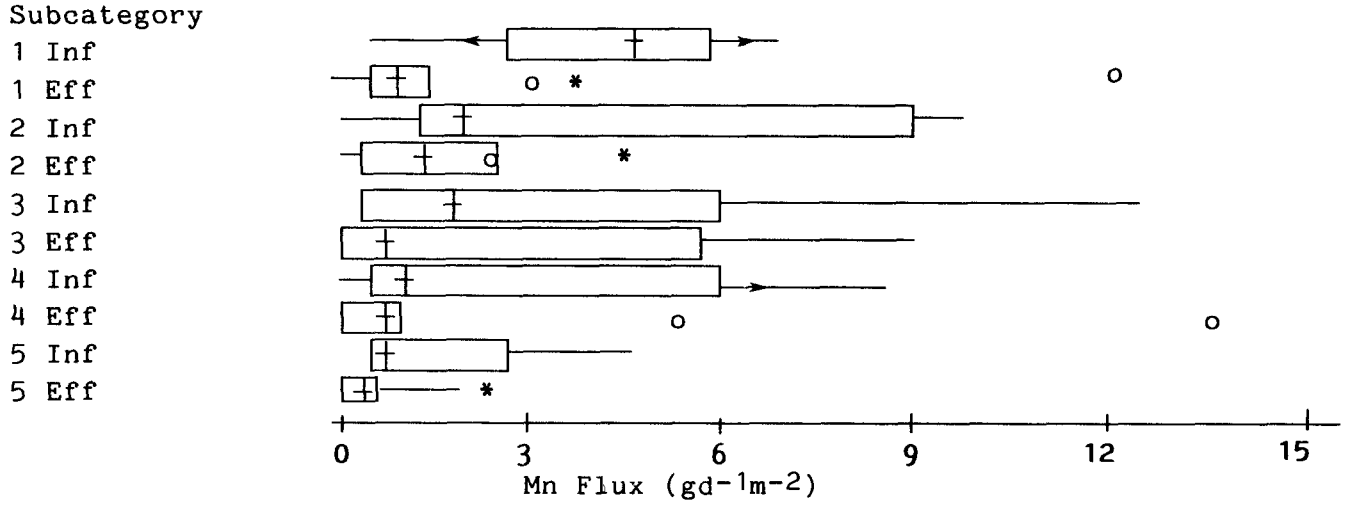

Figure 4. Comparison of influent (Inf) and effluent (Eff) manganese fluxes for the five subcategories of constructed wetlands.

to remove excess acidity. Because acidity is neutralized by alkalinity produced under anaerobic conditions, whereas Fe and Mn are primarily removed by oxidation under aerobic conditions, the area necessary for Fe and Mn removal cannot necessarily be considered a part of the area needed for acidity removal. One design suggested by the Bureau of Mines is removal of Fe and Mn in a wetland designed to take advantage of aerobic conditions, following in series a wetland that has been designed to take advantage of anaerobic conditions, generate alkalinity, and remove acidity. Because the wetlands are in series, the required area is the sum of the area of the acidity removal wetland and the Fe and Mn removal wetland.

The Department's data for subcategory 1 discharges show a substantially higher median acidity removal of 29.16 $gd^{-1}m^{-2}$. Long-term removal of such high amounts of acidity may not occur, and the data may be indicative of a transient condition based on high initial rates of alkalinity generation in the substrate. The median removal rate falls to 10.59 $gd^{-1}m^{-2}$ for

subcategory 2. Wieder et al. (1993) initially found high acidity removal rates for subcategory 1 wetlands, but the rates of acidity consumption declined over time.

For subcategory 3, the median acidity removal rate of 6.01 $gd^{-1}m^{-2}$ is close to the threshold value of 5 $gd^{-1}m^{-2}$ suggested by the U.S. Bureau of Mines. The influent net acidity flux for this subcategory is low; the wetland removes substantially all of the acidity. The Bureau of Mines data are based on wetlands with higher influent net acidity loadings, whereas the wetlands examined by the Department were sized based on perceived ''worst-case'' conditions, i.e., high acidity, [Fe], and [Mn]. The Department's data suggest that the Bureau of Mines 5 $gd^{-1}m^{-2}$ is an acceptable conservative design guideline.

The data for Fe removal suffer from the same limitations: influent Fe loadings in $gd^{-1}m^{-2}$ are low, and the wetlands have relatively large areas. The U.S. Bureau of Mines gathered data from wetlands that had high [Fe] in both influent and effluent. From these wetlands' data, the Bureau (Hedin and Nairn 1993) found a design removal rate of 20 $gd^{-1}m^{-2}$. Most of the wetlands in the Department's study had influent loadings substantially < 20 $gd^{-1}m^{-2}$, as a consequence, the Department cannot determine empirically whether 20 $gd^{-1}m^{-2}$ of Fe would have been removed had it been present. The median removal rate was 4.24 $gd^{-1}m^{-2}$ for very acid influent. While the Department's data cannot be used to corroborate the Bureau of Mines' 20 $gd^{-1}m^{-2}$, the Department accepts the Bureau of Mines' conclusions but recommends design based on an iron removal rate of 5 $gd^{-1}m^{-2}$ for influent pH <6.5. For influent pH >6.5, 20 $gd^{-1}m^{-2}$ may be used.

The Department's data agree closely with the Bureau of Mines' suggested design criterion for Mn removal. Hence, a removal rate of 0.5 $gd^{-1}m^{-2}$ is suggested for all net acidity and alkalinity ranges.

Sizing Recommendations

It would appear reasonable that wetlands should be designed on the basis of summing the areas from equations 1, 2, and 3 for conditions of influent pH>6.5:

$$A(m^2) = (\text{net acidity loading g/d})/(5\ gd^{-1}\ m^{-2}) + \text{loading g/d})/(20\ gd^{-1}m^{-2}) + (\text{Mn loading g/d})/(0.5\ gd^{-1}m^{-2}). \quad (4)$$

For less alkaline conditions or for acid conditions, the sizing could be based on

$$A(m^2) = (\text{net acidity loading g/d})/(5\ gd^{-1}\ m^{-2}) + \text{loading g/d})/(5\ gd^{-1}m^{-2}) + (\text{Mn loading g/d})/(0.5\ gd^{-1}m^{-2}). \quad 5)$$

Removal of up to 85% of the Fe present in the influent is achievable, as is removal of up to 50% of the Mn when the influent is alkaline (but only about 25% if the influent is acid). Wetlands designed to take advantage of anaerobic processes should produce alkaline discharges for subcategory 3, 4, and 5 influents. Wetlands designed to take advantage of anaerobic processes should remove most of the acidity for subcategory 2 influents. Wetlands remove much acidity for subcategory 1 influents, but the effluent remains acid.

Potential Merit of ALD's

ALD's can be considered as ancillary treatment to either diminish the influent net acidity to <100 mg/L or make the influent alkaline, so that

the wetlands can take advantage of the more favorable net acidity or alkalinity ranges for Mn removal and for the discharge of an alkaline effluent. At present, because the technology is relatively new, the Department does not possess sufficient data to assess the effectiveness of ALD's. Pretreatment with an ALD reduces the design size of the wetlands, but the operator bears the responsibility for any needed wetland expansion should the ALD provide unsuccessful. ALD's are thought to be self-supporting pretreatment units for subcategory 2 and 3 seeps. For acidity in subcategory 2, they may be the treatment of choice owing to economic considerations. For subcategory 3, wetlands tend to remove the acidity without the need for pretreatment by an ALD. ALD's may be installed as precautionary measures for subcategory 3 and 4 influents. For subcategory 4, it is reasoned that the hydrolysis reactions that remove the cations may remove most or all of the alkalinity if it was initially too low. For subcategory 5 influents, an ALD is unnecessary.

Selection of Pollutant Parameters

Under current regulations, Pennsylvania technology-based effluent requirements currently apply to the parameters pH, net acidity, Fe, and Mn for discharges that occur during active mining. The same parameters were considered for seeps. Acidity has several adverse effects on the environment, including but not limited to damage to aquatic life, damage to bridges and other structures, and potential damage to drinking water treatment and distribution facilities. Therefore, the Department finds that seeps must be treated such that the final discharge has a residual alkalinity; i.e., acidity <0. This will generally mean pH > 6.0.

The oxides and hydroxides of Fe, especially FeO(OH), precipitate from solution and form a sediment that settles out on the bottoms of receiving streams. The sediment produces an unsightly condition and smothers benthic life, usually making the stream unsuitable as a fishery. In addition, dissolved iron in the receiving stream can generate added treatment costs should the stream be used as a drinking water supply source. For this reason, Fe in seeps should be removed.

Under alkaline conditions Mn is present primarily as MnO_2. This compound causes black staining on rocks. In drinking water, Mn can cause taste problems in some food and beverages, as well as laundry stains. It has not been shown to be present in biologically harmful amounts in alkaline discharges. Because of the historic technology-based effluent limits currently applied to Mn for discharges from active sites, Mn is also considered as a pollutant parameter for seeps.

In considering discharges occurring during active operations, EPA 1982 determined that technology-based effluent requirements for 114 organic pollutants and for the inorganic pollutants CN-, Sb, Be, Cd, Ag, Tl, As, Cr, Cu, Pb, Hg, Ni, Se, and Zn were unnecessary. The Department has determined from analysis of several seeps that these pollutants are not present at levels of concern. Furthermore, the Department finds that Al limits are unnecessary, because Al is not present in appreciable concentrations in wetland effluents with pH > 6.0. In summary, the pollutant parameters selected for consideration are pH, net acidity, Fe, and Mn.

Cost Considerations

The capital costs of a wetland are directly dependent on the required area, based on equations 4 or 5. To arrive at a construction cost per unit area, the Department interviewed several persons who have built wetlands to determine a cost per unit area. The median cost is $32.29 per square meter

in 1992 dollars. Wetlands bear a small monthly operation and maintenance cost (about $100) for such tasks as minor repairs and fertilization. The Department considered the 25 yr operation and maintenance costs as constant from site to site. The amortized annual capital replacement costs are determined by the formula

$$\text{Cost}=(\text{capital cost})\ i\ 1=i)^{n}/[(1=i)^{n-1}] \qquad 6)$$

This figure is multiplied by 25 to arrive at the 25 yr cumulative amortization costs. The total 25-yr cost is the sum of the initial capital costs, the 25-yr operation and maintenance cost, and the cumulative amortization costs. Twenty-five years is an estimate of the operational lifespan of the wetlands before replacement is needed. Conventional treatment costs were also calculated on the basis of 25 yr of operation.

Once the total costs have been determined, the unit costs (i.e., costs per kilogram of pollutant removed) can be obtained by dividing the total costs by the total amount of pollution removed in 25 yr (kg net acidity+kg Fe+kg Mn). The choice of equation 4 or equation 5 has only about a $0.20 per kilogram effect on the unit cost. With the exception of subcategory 5, the cost per kilogram of pollution removed increases progressively as one procedure from strongly acid water to less acid water to alkaline water. This is due to the division by the quantity of pollutants removed, which becomes less as the water becomes more alkaline. This trend applies whether a wetland or conventional treatment is used.

The costs for conventional treatment were determined by adding the capital cost of the treatment facilities to 25 times the sum of the annual operation and maintenance cost and the annual cost to amortize the capital cost for the treatment facilities (DER et al. 1988). A value of 8% is assumed to be the "true" interest rate for both wetlands and conventional treatment. The costs for conventional treatment are compared with the costs for wetlands treatment in table 2. The figures in the table are used in the conclusions below. The table shows that as the influent becomes less acid, or more alkaline, passive treatment becomes increasingly cost effective.

Table 2. Median Comparative Unit Costs of Several Modes of Treatment.

Subcategory	Conventional treatment removing acid, Fe, and Mn	Wetland removing Fe, and Mn	ALD/wetland Fe, and Mn	Wetland removing acid and Fe but not Mn	ALD/wetland removing acid and Fe but not Mn
1	$1.24	$4.18	$3.43	$2.36	$1.82
2	5.56	6.64	5.21	2.65	1.42
3	23.06	11.31	11.23	4.37	6.18
4	114.34	28.38	33.96	10.20	81.00
5	95.99	25.01	does not apply	9.09	does not apply

The BPJ analysis can now be conducted as follows:

1. Age of equipment and facilities involved, the process employed, and proaess changes. These factors are primarily associated with the manufacturing sector of industry and relate to the difficulty which some manufacturers may have in retrofitting BAT technology. The relative merits of conventional treatment and wetlands with or without an ALD are independent of these factors.

2. Engineering aspects of the application to various types of control technology: Conventional treatment and treatment by wetlands, either with or without an ALD, are technologically feasible. Conventional treatment requires less space but much more operational supervision than passive treatment systems. On the other hand, passive treatment systems can achieve substantial reductions in net acidity, iron, and manganese when subjected to a variable influent loading, while for optimum performance, conventional treatment feed rates must be continually adjusted.

3. Consideration of non-water-quality impacts: Wetlands at least partly replace a valuable natural resource that has been significantly damaged by past practice. Wetlands are anesthetically pleasing features of reclamation, and they provide wildlife habitat. They help conserve energy and mitigate the greenhouse effect. They are safer than conventional facilities and cause less of a sludge disposal problem. Conventional treatment, on the other hand, often occupies less land space.

4. Total cost of the application technology in relation to the pollution reduction benefits to be achieved and the cost of achieving such pollutant reduction: These are summarized in table 2. As influents become less acid or more alkaline, passive treatment becomes increasingly cost effective compared to conventional treatment.

Conclusions and Recommendations

The use of passive treatment technology is a cost-effective, environmentally sound alternative to the use of conventional mine drainage treatment for many postmining seep situations. The technology offers the added advantage of operational reliability while requiring minimal operational control.

Data on the 73 better-designed constructed wetlands systems (figs. 2-4) indicate that this technology can produce an effluent quality that is similar to, and in some cases better than, EPA's BAT effluent requirements (40CFR 434) for active mining. The data do not support, however, that a standardized set of BAT effluent limitations can be developed for such technology.

Section 122.44(k) of EPA's National Pollutant Discharge Elimination System (NPDES) regulations allows for "best management practices" to be specified in lieu of technology-based effluent requirements when numerical effluent limits are infeasible or when such practices are reasonably necessary to carry out the purposes and the intent of the Federal Clean Water Act. Passive treatment technology seems to fit in well with the "best management practices" concept.

With this concept in mind, and based upon the results of this BPJ analysis, the following recommendations are made:

1. BAT for post mining seeps from surface mining activities should be achieved through the use of passive treatment technology as a "best management practice" in lieu of numeric effluent limitations.

2. Where the use of passive treatment technology is not feasible (due to the size and poor quality of the seep), then conventional treatment should be considered BAT. This would generally be the case when the net acidity of a seep exceed 300 mg/L as $CaCO_3$.

3. Because of the significantly higher costs to remove manganese in post mining seeps, it is recommended that the design and sizing of passive

treatment for manganese removal be required only when needed to achieve the water quality standards for [Mn] in the receiving stream.

4. The Department should continue investigating the mechanisms of pollutant removal using passive treatment technology in order to refine the design and operational requirements for this technology.

At the time this paper was prepared and submitted, the Department had not yet begun regulatory changes to implement the recommendations. The final outcome may not totally reflect the results of this BPJ analysis.

Literature Cited

Anderson, R.F., and S.L. Schiff. 1987. Alkalinity generation and the fate of sulfur in lake sediments. Can. J. Fish and Aquatic Science 44 188-193.

Commonwealth of Pennsylvania Department of Environmental Resource (DER), The Pennsylvania State University, and Kohlman Ruggiero Engineers. 1988 REMINE software.

Hedin, R.S., and R.W. Nairn. 1992. Designing and sizing passive mine drainage treatment systems. p. 111-121. In proceedings, 13th Annual West Virginia Surface Mine Drainage Task Force Symposium, (Morgantown, WV).

Hedin, R.S. and R.W. Nairn. 1993. Contaminant removal capabilities of constructed wetlands to treat coal mine drainage. p. 187-195. In G.A. Moshiri (ed.). Constructed Wetlands for Water Quality Improvement. Lewis Publishers, Inc. Boca Raton, FL.

Hellier, W.W. 1993. Best Professional Judgment Analysis for the Treatment of Postmining Ground Water Seeps. PA Department of Environmental Resources, Harrisburg, PA. 147 p.

Helsel, D.R. 1987. Advantages of Nonparaetric Procedures for Analysis of Water Quality Data. Hydrological Sciences, J. des Sciences Hydrologiques 32: 179-190.

Tukey, J.W. 1977. Exploratory Data Analysis. Addison-Wesley Publishing Co., Reading, MA. p. 35-54.

U.S. Environmental Protection Agency. 1982. Development document for effluent limitation guidelines and standards for the coal mining point source category. EPA 440/1-82/057. 407 p.

Wieder, R.,K. 1993. Ion input/output budgets for five wetlands constructed for acid mine drainage treatment. Water, Air, and Soil Pollution Aug. 93-127, 000-000 (in press).

EVALUATION OF ACIDIC MINE DRAINAGE TREATMENT IN CONSTRUCTED WETLAND SYSTEMS[1]

Jonathan M. Dietz[2], Robert G. Watts[3], Dennis M. Stidinger[4]

Abstract: The Pennsylvania Department of Environmental Resources, Bureau of Abandoned Mine Reclamation, Division of Mine Hazards (DER) has identified wetland treatment as an appropriate technology to reduce impacts of AMD on surface waters. DER constructed six surface flow wetland treatment systems (WTSs) with a variety of designs at three sites; Canoe Creek, Jennings Environmental Education Center, and Cucumber Run. The WTSs were constructed to reduce AMD impacts on receiving streams, to evaluate treatment effectiveness, to evaluate biological and chemical processes, and to develop design criteria for future WTS construction. The majority of constructed WTSs did not achieve the treatment goals for iron (3.0 mg/L), aluminum (5.0 mg/L), and manganese (7.0 mg/L) established by DER. The WTSs did significantly lower metal concentrations (on average) in the AMD for iron by 35% to 95%, aluminum by 0% to 50%, and manganese by 0% to 30%. In addition to metals, the wetland treatment systems also decreased acidity concentrations by 40% to 90%, which should reduce the pH and metal impacts of the AMD on the receiving stream. This project also provided data indicating WTS performance did not substantially diminish for the duration (2 yr) of this study, and observed fluctuations in effluent quality were due to variable influent quality. The results from the WTSs suggest that a number of physical (e.g., settling and absorption), chemical (e.g., hydrolysis), and biological processes (e.g., dissimilatory sulfate reduction) are important for improving water quality. Finally, the project provided invaluable data that indicate acidity removal is the most appropriate parameter for future surface flow WTS design. The study found acidity removal (in grams per day), unlike iron, aluminum and manganese, to correlate with WTS size. In addition, acidity removal was not affected by changes in influent AMD chemistry. Based on the data from this study, a surface flow WTS design criteria of 6 $g/d/m^2$ (1.25×10^{-3} $lb/d/ft^2$) for acidity removal is recommended to predict sizing requirements for future WTS construction.

Introduction

In Pennsylvania, thousands of miles of streams are impacted by acidic mine drainage (AMD), causing degradation of surface water quality and impacts on receiving stream aquatic biota. In many areas of Pennsylvania, AMD originates from the continued oxidation of pyritic minerals primarily associated with abandoned and unreclaimed coal mine (surface and deep) sites. Typically, this AMD is extremely acidic and contains high concentrations of metals (e.g., iron, aluminum, and manganese).

The Department of Environmental Resources, Bureau of Abandoned Mine Reclamation, Division of Mine Hazards (DER) has undertaken reclamation of abandoned mine sites across Pennsylvania to reduce and/or eliminate safety hazards and impacts of abandoned sites on the environment. Owing to long term treatment, low cost, and low maintenance, DER has identified

---

[1]Paper presented at the International Land reclamation and Mine Drainage Conference and the Third International Conference on the Abatement of Acidic Drainage, Pittsburgh, PA, April 24-29, 1994.

[2]Jonathan M. Dietz, Environmental Scientist, Gannett Fleming, Inc., Harrisburg, PA, USA.

[3]Robert G. Watts, Bureau of Mine Hazards, PA Department of Environmental Resources, Harrisburg, PA, USA.

[4]Dennis M. Stidinger, P.E., President, General Engineering Division, The EADS Group, Clarion, PA, USA.

wetland treatment as an appropriate technology to reduce the impacts of AMD on surface waters. At the time of this project, information on wetland systems constructed for treatment of AMD was limited. The majority of studies focused on biological and chemical treatment processes (e.g., iron oxidation). Little or no information was available on wetland design and sizing criteria.

This study was a multipurpose project initiated by DER to achieve a number of goals. For the purpose of this project the goals, as defined by DER, include: to evaluate the reduction of iron, aluminum, and manganese concentrations as well as improvements to other AMD pollutants by the constructed WTSs; to evaluate long term operation and maintenance of constructed wetlands; to evaluate chemical and biological processes in wetland systems that may have beneficial impacts on water quality; to establish design criteria from constructed wetlands for use in designing wetlands at future abatement locations.

Three sites, Canoe Creek, Jennings Environmental Education Center, and Cucumber Run, were selected by DER to construct experimental wetland treatment systems (WTS). The results from each site are discussed below.

Site Selection

The Canoe Creek, Jennings Environmental Education Center, and Cucumber Run sites were selected based upon the protection of surface waters and recreational waters, public awareness, and proximity to important recreational resources. Descriptions of each location follow.

Canoe Creek is located in Clarion County and is a tributary to the Clarion River. This stream has been classified by DER as a high quality cold water fishery. A number of AMD discharges from historical surface mining in the upper watershed of Canoe Creek degraded water quality in a first order tributary to Canoe Creek and also threatened water quality in the mainstem. WTSs were constructed on two of the larger discharges (K2 and K3) to reduce pollutant loading to the receiving stream.

Jennings Environmental Education Center (JEEC) in Moraine State Park is located in Butler County along Big Run, which is a tributary to Slippery Rock Creek. Moraine State Park is an important recreational resource to the area, and the JEEC is a public environmental information center. AMD from an abandoned deep coal mine, located on the hillside east of JEEC and Route 8, had discharged across Route 8 and onto an area adjacent to JEEC for a number of years. The AMD had degraded the aesthetic quality of the area adjacent to JEEC and water quality in Big Run (pH depression and increased metals). An attempt was made in the 1970's by the DER to seal the mine; however, the efforts were unsuccessful, and AMD continued to discharge near the JEEC. A WTS was constructed at JEEC to reduce visual impacts of the AMD at the JEEC and improve water quality in Big Run. In addition, DER felt the project could be used as an instructional tool at JEEC for AMD, wetland treatment, and wetland function and values.

Cucumber Run, located in Ohiopyle State Park, is a small cold water fishery that flows over Cucumber Falls, a point of interest in the park, before entering the Youghiogheny River. Historical mining in the Cucumber Run watershed has resulted in the input of AMD to Cucumber Run. The AMD has impacted the cold water fishery and the appearance of Cucumber Falls, and the Youghiogheny River. WTSs were constructed on three discharges (CUC1, CUC2, CUC3) emanating from collapsed deep mine on the North Branch of Cucumber Run. The WTSs were intended to reduce water quality impacts of AMD on Cucumber Run and decrease the aesthetic impacts on the Cucumber Falls and Youghiogheny River.

WTS Design

WTS design involves the integration of biological (e.g., wlfate reduction), physical (e.g., available space), and chemical (e.g., iron concentration) factors. At the time this project was conceived, little was known about design or biological processes involved in the remediation of AMD. As a result, the majority of wetlands were designed with similar features. The basic design utilized in this project was a multicell design with each unit comprised of 1 to 1½ ft (0.3 to 0.5 m) deep of "spent" mushroom compost, a water depth of 0 to ½ ft (0 to 0.1 m) over the compost, and locally transplanted cattails (*Typha lattifolia*) and other plant species. "Spent" mushroom compost

was chosen as the substrate material because of local availability and potential advantages as a planting and treatment medium. Cattails were selected because of the specie's colonizing ability in AMD sites. Several WTS designs incorporated slightly different features. Two of the WTSs (K2 and CUC1) included an initial open water basin, because high influent ferrous iron or suspended solids were present. In addition, the K2 WTS incorporated limestone below the compost substrate (fifth pond), which was added to evaluate the effects of this substrate material on WTS effectiveness. Finally, the first and fourth units of the JEEC WTS were modified after construction utilizing a drain line surrounded by limestone in an attempt to direct flow through the compost.

The size of each WTS was based primarily on available area for construction, and multicell designs were incorporated to reduce possible short circuiting. The K2 WTS contained a pretreatment unit and four compost units (approximately 190 m^2 each) for a total treatment area of 952 m^2. The K3 WTS contained three compost units with sizes of approximately 115 m^2 (Cell1), 72 m^2 (Cell 2), and 37 m^2 (Cell 3) for a total treatment area of 224 m^2. The JEEC WTS contained four treatment units with sizes of approximately 224 m^2 (Cell 1), 259 m^2 (Cell 2), 344 m^2 (Cell 3), and 334 m^2 (Cell 4) for a total treatment area of 1,161 m^2. The CUC1 WTS contained one treatment unit with a total area of 1,340 m^2, but contained an open water area that reduced the compost area to 1,140 m^2. The CUC2 WTS was the smallest WTS and contained only two compost units with sizes of 44 m^2 (Cell 1) and 48 m^2 (Cell 2). The CUC3 WTS contained four compost units with sizes of 155 m^2 (Cell 1), 96 m^2 (Cell 2), 86 m^2 (Cell 3), and 123 m^2 (Cell 4) each) for a total treatment area of 460 m^2.

WTS Monitoring Program

Sampling was initiated on the wetlands shortly after construction was completed. Sampling stations were located in WTSs to collect influent, effluent from the WTSs, and intermediate points between individual treatment units. Biweekly and monthly sampling at each WTS was conducted by DER personnel. The duration of sampling at WTSs follows: August 1988 to May 1991 at the K2 WTS; August 1988 to May 1991 at the K2 WTS; July 1988 to May 1991 at the K3 WTS; April 1989 to February 1991 at the JEEC WTS; and June 1990 to December 1991 at the CUC1, CUC2, and CUC3 WTS.

The sampling program monitored parameters to provide data regarding WTS treatment effectiveness and treatment processes within the wetlands. Collected water samples were analyzed for pH, alkalinity, acidity, sulfate, total iron, ferrous iron, total manganese, total aluminum, and hardness. In addition, water flow was measured at several sampling locations within each WTS to evaluate loadings and removal rates.

Results and Discussion

The following sections discuss the results of the six WTSs with respect to the goals described in the introduction. For a complete evaluation of results, the document "Evaluation of Wetlands Constructed For The Treatment of Acidic Mine Drainage" (Dietz and Stidinger 1993) is available upon request from DER, Bureau of Abandoned Mined Land Reclamation (Robert G. Watts).

Treatment Effectiveness

WTSs were evaluated with respect to treatment effectiveness for a number of different parameters (i.e., pH, iron, aluminum, manganese, and acidity). The average influent and effluent concentrations from the systems are summarized in table 1. Reduction in iron concentration varied considerably in the WTSs, ranging from greater than 90% (K2) to less than 30% (CUC1) of influent concentrations. The K2 and K3 WTSs decreased iron concentrations on average by more than 90%, the majority of the decreases occurred in the first units and appeared to be the result of ferrous iron oxidation, which accounted for 85% of the decreases in total iron. Similar to the Canoe Creek WTSs, total iron decreases across the CUC2 WTS were related to ferrous iron decreases. The CUC1 WTS received influent iron similar to the K2 WTS (85.6 mg/L), but this WTS only decreased the iron by approximately 28%. Similar to the Canoe Creek

Table 1. Influent and Effluent Averages For Monitored Parameters at WTSs.

WTS	Station	Total Fe (mg/L)	Total Al (mg/L)	Total Mn (mg/L)	Lab[1] pH	Acidity (mg/L as $CaCO_3$)	Sulfate (mg/L)
K2	Influent[2]	98.3	0.80	12.2	4.64	126.5	594
	Effluent	6.7	0.42	8.5	4.90	6.0	462
K3	Influent	41.0	2.4	30.7	5.20	114.3	1,388
	Effluent	2.7	3.4	28.0	4.41	40.6	1,202
JEEC	Influent	22.4	18.5	6.2	2.90	258.4	516
	Effluent	14.5	14.3	6.0	3.33	153.6	519
CUC1	Influent	85.6	15.0	3.9	2.60	392.0	303
	Effluent	61.9	12.0	4.1	2.70	272.0	312
CUC2	Influent[2]	36.3	1.2	4.2	3.27	108.3	718
	Effluent	12.9	1.0	4.8	3.51	56.2	754
CUC3	Influent	10.6	4.2	4.8	3.12	106.5	332
	Effluent	5.5	3.0	4.3	4.01	26.8	313

[1] pH values in table are -LOG transformation of hydrogen ion statistical results.
[2] Influent values are based on flow adjusted averages of multiple influent data.

WTSs, a large fraction of the influent total iron in the CUC1 was comprised of ferrous iron, which decreased from an influent average of 50 mg/L to an effluent average of 14 mg/L; however, unlike the Canoe Creek WTSs, the total iron concentration did not decrease in proportion to the decrease in ferrous iron. The CUC3 and JEEC WTSs received influent iron concentrations lower than the amounts received by all the other WTSs, and decreased total iron concentrations by approximately 50% and 35%, respectively; however, different from the other WTSs, ferrous iron increased from less than 1 mg/L to above 3 mg/L in both WTSs.

Average influent aluminum concentrations ranged from less than 1 mg/L (K2) to a high of 18.5 mg/L (JEEC). Aluminum concentrations decreased slightly across all the WTSs except the K3 WTS, which increased aluminum by 1 mg/L. The maximum decrease in aluminum occurred across the JEEC, which decreased on average by 4.2 mg/L; however, this was only about a 23% decrease. Average manganese received by the WTSs ranged from a low of 3.9 mg/L (CUC1) to a high of 30.7 mg/L. As was observed with aluminum, manganese was slightly lowered across most WTSs except CUC1 and CUC2, which increased manganese on average by 0.2 mg/L and 0.6 mg/L, respectively. The effect that the WTSs had on pH was minimal, ranging from -0.6 in the K3 WTS to 0.9 in the CUC3 WTS. The pH decrease across the K3 WTS may have been related to ferrous iron oxidation and precipitation and may have caused of the aluminum increase, which has a pH dependent sowbility.

The WTSs had a much greater effect on acidity; average acidity decreased across all the systems. The K2 WTS decreased average acidity by more than 120 mg/L (as $CaCO_3$), an almost complete removal of acidity. Acidity would have been removed completely except for a known AMD seep that entered the third compost unit. Three other WTSs (JEEC, CUC1, CUC2) decreased average acidity by more than 100 mg/L with percent decreases ranging from 30% to 65%. The remaining WTSs, K3 and CUC3, decreased average acidity by slightly more than 70 mg/L, which were decreases of 65% and 75%, respectively.

DER established average discharge criteria for iron (3 mg/L), aluminum (5.0 mg/L), and

manganese (7.0 mg/L) for the WTSs. Only the K3 WTS achieved iron concentrations below the 3.0 mg/L criteria. Two other WTSs, CUC3 and K2, discharged average iron levels that were reasonably close (a factor of 2) to the effluent criteria. Effluent aluminum concentrations were, for the majority of WTSs, less than the established level of 5.0; however, average influent concentrations at the same systems were also below the established treatment goals. The only WTS that had influent concentrations well above the aluminum treatment goal was the JEEC system with an average influent of 18.5 mg/L, and this system did not lower aluminum concentrations below the effluent goal of 5.0 mg/L. Similar to aluminum, only one WTS (K3) received manganese well above the criteria and the K3 WTS did not substantially reduce manganese.

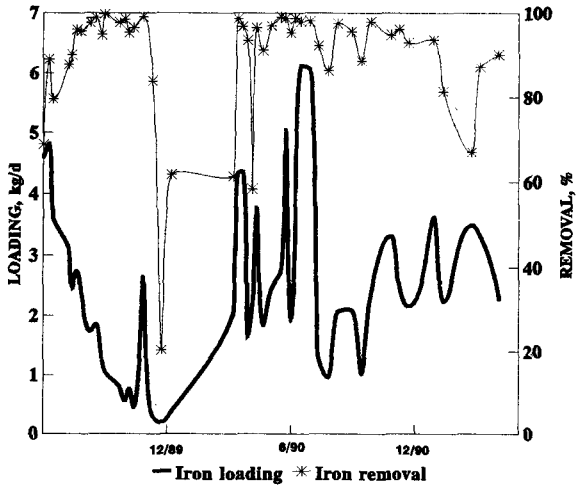

Figure 1. Iron loading and percent iron removal in the K2 wetland treatment system.

Although the treatment goals, in many cases, were not met by the wetland systems, the monitoring data indicate that the WTSs vastly improved AMD water quality. Iron levels were significantly reduced by all WTSs, with removal ranging between 50% and 90% of influent concentrations, and the wetland systems reduced average acidity of the AMD by greater than 40%. The inability of the WTS to achieve the treatment goals is not likely a result of inadequacy of wetland treatment, but due to the general lack of specific knowledge regarding sizing design criteria at the time of this project.

Long-term Operation

Owing to the variability of influent concentrations and flows, effluent concentration data could not be used for evaluation of seasonal and long-term treatment effectiveness. To address seasonal and long-term effluent water quality from the WTSs, influent loading and percent removal for two selected parameters (iron and acidity) were examined for the K2 and K3 WTSs, which were sampled for the longest period of time (over 2½ yr).

Iron loading and removal for the K2 and K3 WTSs are presented in figures 1 and 2. Iron removal remained above 80% in both WTSs throughout much of the monitoring, except for

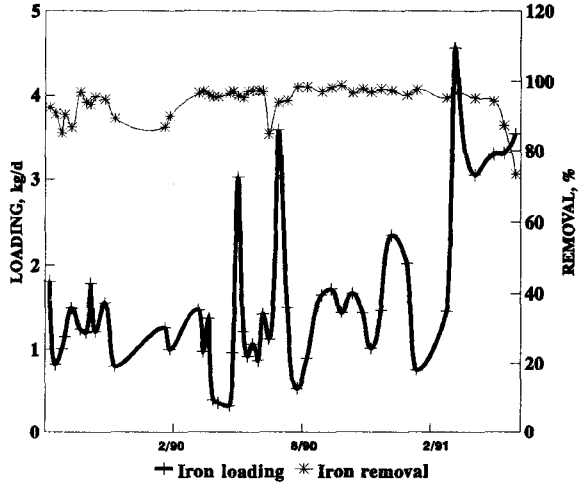

Figure 2. Iron loading and percent iron removal in the K3 wetland treatment system.

several short periods. One period of reduced removal in the K2 WTS corresponded with low iron loading at the end of 1989, which suggests removal may be dependent on loading. A slight decrease in removal at the end of monitoring occurred in both WTSs. The decline in removal in the K3 WTS corresponded with elevated iron loadings well above iron loadings during the previous 2 yr. It is difficult to determine if this is a result of lowered treatment effectiveness of the system or a result of loading.

Acidity loading and removal for the K2 and K3 WTSs, presented in figures 3 and 4, varied considerably over the monitoring period. A period of high removal, greater than 100% (greater than 100% removals are the result of including alkalinity

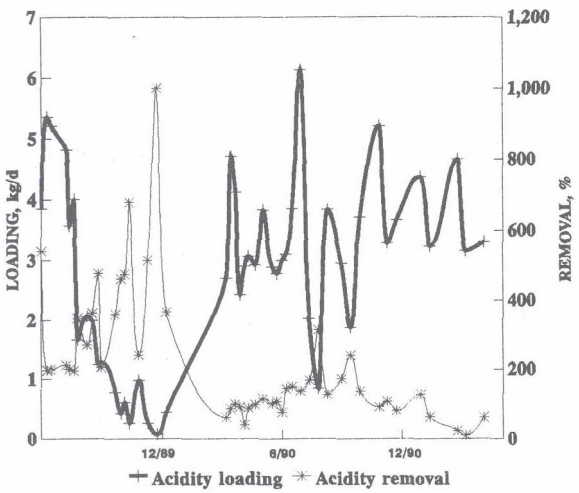

Figure 3. Acidity loading and percent acidity removal in the K2 wetland treatment system.

production), occurred in the K2 WTS around the end of the 1989 monitoring year and was associated with a period of low acidity loading (similar to iron loading in figure 1). Possible seasonal effects on removal may have occurred in both WTSs during the 1990 monitoring year, with higher removal occurring during the warmer growing seasons; however, the variability of loading on the systems, as occurred during 1989 in the K2 WTS, may mask or have caused this observable effect.

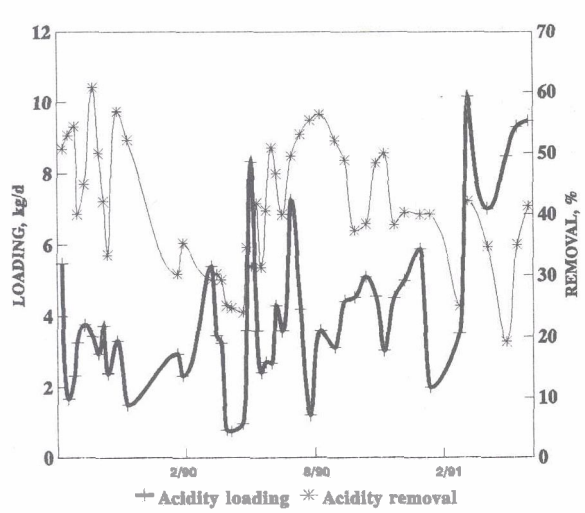

Figure 4. Acidity loading and percent acidity removal in the K3 wetland treatment system.

This long term evaluation of the WTSs is qualitative and somewhat inconclusive. The acidity and iron loading variability received by the WTSs tends to mask or contribute to observed removal trends. Greater controls on flow and concentration of AMD received by the WTSs would be required, which may not be practical or feasible under field conditions. In addition, WTS monitoring for periods longer than 2½ yr may provide a better evaluation of long-term effectiveness.

Wetland Processes

Research has identified a number of biological, chemical, and physical processes (e.g., sulfate reduction and cation exchange) that may be involved in the remediation of AMD in wetland treatment systems. WTS receiving high ferrous iron (i.e., K2, K3, CUC1, and CUC2), a highly soluble form, decreased across the wetland systems (based on monitoring data), suggesting that oxidation processes are involved in lowering ferrous iron and total iron in these wetlands. The low pH conditions (3 to 4) in the Cucumber Run wetlands indicate that chemical oxidation of ferrous iron would have been slow and that oxidation was most likely due to biological oxidation, which has been found to occur in wetland type environments (Gerber et al. 1985, Dietz 1989). The Canoe Creek wetlands had higher influent pH (5 to 6), which suggests, at least in the first units, that chemical oxidation occurred.

Sulfate reduction, an anaerobic process that produces alkalinity, has been found to occur, even at low pH (< 4), in wetland environments affected with AMD (Dietz 1989). Monitoring data from several WTSs (i.e., K2, K3, CUC3) indicate that sulfate concentrations significantly decreased by between 20 and 180 mg/L. Sulfate increased slightly in the other WTSs, which may have been the result of high influent sulfate variability or AMD inflows at intermediate locations in the WTSs. An additional source of acidity removal and alkalinity production may have occurred from carbonate mineral (limestone) solubilization, either from material placed in the wetland (Canoe Creek K2 WTS and JEEC WTS) or from crushed limestone, which is a common additive to mushroom compost. Although no dissolution measurements were made, dissolution of $CaCO_3$ should increase hardness, from the release of calcium, however, no observed

Table 2. Average Flow (L/min) and Loading (GPD) For Parameters For The WTSs.

WTS	Flow (L/min)	Iron GPD	Aluminum GPD	Manganese GPD	Acidity GPD
K2	22.7	2,340	18.4	302	2,670
K3	50.7	1,540	120	1,270	4,530
JEEC	129	3,740	3,284	1,120	45,470
CUC1	66.6	2620	234	94.3	7,520
CUC2	7.9	327	4.3	20.8	964
CUC3	13.6	191	78.2	88.6	2,010

increases in hardness were observed across any WTS. The absence of hardness increases may have been due to interferences of divalent and trivalent metals (e.g., iron and aluminum) that are well documented on the colorimetric hardness test used in this study (APHA 1991).

Loading and Removal Rates

The monitoring program was designed to evaluate parameters loadings and removals of each WTS and intermediate cells. WTS loadings, in grams per day (g/d), were determined by multiplying sampling date flow, in liters per minute (L/min), by influent concentration. Sampling date loadings were used to determine an average loading over the sampling program. Removal rates, also in g/d, were determined by subtracting sampling date effluent loading from influent loading, and were then used to determine the average removal rates. Unit area removal rates, in grams per day per square meter ($g/d/m^2$), were determined by dividing removal rate (g/d) by the surveyed WTS and cell sizes. Acidity removal and alkalinity production rates were combined to provide the acidity removal rate.

The average influent flows for the WTSs and the loading for selected parameters received by each WTS are summarized in table 2. Flows received by the WTSs were variable ranging from 7.9 L/min (2.1 gal/min) at the CUC2 to 129.1 L/min (34.1 gal/min) at the JEEC. Average acidity loading tended to correlate well with the flow received by each WTS. The JEEC received the highest acidity loading of 45,470 g/d and the CUC2 received the lowest acidity loading of 964 g/d. Average iron loading did not correlate as well with flow as did acidity. The JEEC WTS, which received the highest AMD flow, also received the highest iron loading of 3,740 g/d, but several iron loadings received by the WTSs (K2 and CUC3) were influenced by concentration. Aluminum and manganese loadings did not correlate with flow as was observed for iron.

Table 3 summarizes average removal rates and unit area removal rates for each parameter in each WTS. Removal rates for iron ranged from 102.5 g/d at the CUC3 to 2,260 g/d at the K2. The average influent iron concentration for each of these wetlands (table 1), which were 10.6 and 98.3 mg/L, suggest that iron removal may be influenced by influent iron concentrations. This is further supported by examination of removal results from duplicate sequential units within the K2 WTS. The iron loading to cell 1 averaged 1,170 g/d and cell 2 averaged 330 g/d, with corresponding removal rates of 840 g/d and 170 g/d, respectively. Further, iron removal at two WTSs (K3 and CUC2), which had similar average influent iron (41.0 and 35.2 mg/L), differed by almost an order of magnitude (table 3). Examination of average influent pH (5.20 and 3.27, respectively) and influent ferrous iron (37.5 and 17.3 mg/L, respectively) suggest that iron removal may be related to other influent water quality conditions.

Unit area removal rates for iron ranged from 0.22 to 6.47 $g/d/m^2$ at the WTSs. The two wetlands with the highest unit area removal rates, Canoe Creek K2 (2.37 $g/d/m^2$) and K3 (6.47 $g/d/m^2$), also had the highest influent pH values of 4.64 and 5.20, respectively. The highest iron removal rate was from K3, which also had one of the highest influent concentrations (41 mg/L); the lowest removal rate

Table 3. Average Removal Rates in GPD and GDM For Parameters For The WTSs.

WTS	Iron		Aluminum		Manganese		Acidity	
	GPD	GDM	GPD	GDM	GPD	GDM	GPD	GDM
K2	2,260	2.37	2.21	0.002	-12.9	-0.01	4,400	4.62
K3	1,450	6.47	-73.0	-0.33	58.6	0.26	2110	9.45
JEEC	1,540	1.33	952.	0.82	74.5	0.06	20,600	17.7
CUC1	1,280	0.95	45.7	0.03	-0.81	-0.001	2,626	1.95
CUC2	188	2.05	0.09	0.001	1.47	0.02	367	3.99
CUC3	102	0.22	33.4	0.07	16.2	0.01	2,880	6.27

was from CUC3, which had the lowest influent concentration (10.6 mg/L). Therefore, the unit area removal rates for iron also suggest that iron removal is dependent on influent water quality.

Average removal rates for aluminum and manganese were more variable than iron removal rates. Aluminum removal rates ranged from -73.0 g/d at the K3, which indicates aluminum was added by the WTS, to 952 g/d at the JEEC. Unit area removal rates for aluminum ranged from -0.33 g/d/m^2 at the K3 to 0.83 g/d/m^2 at the JEEC. The remaining area rates were approximately zero. Manganese also had negative removal rates at several WTS including -12.9 g/d at the K2 and -0.81 g/d at the CUC1. The highest removal rate for manganese of 74.3 g/d occurred across the JEEC. The majority of unit area manganese removal rates were approximately zero, except for a rate of 0.26 g/d/m^2 measured at the K3 WTS.

Average acidity removal rates ranged from a low of 367 g/d in the CUC2, the smallest WTS, to a high of 20,600 g/d in the JEEC, the second largest WTS. This suggests that removal rates may be dependent upon WTS size. The largest WTS (CUC1) did not have the largest removal rate; however, this WTS had a large open water area at the beginning and no barriers to prevent short circuiting of the WTS. This size-dependent relationship of acidity removal is further supported by acidity removal rates from two different size, sequential cells from the JEEC WTS and two similar-size, sequential cells in the K2 WTS. Cell 2 (259 m^2) in the JEEC WTS had a removal rate of 2,972 g/d and Cell 3 (344 m^2) had a correspondingly greater removal rate 3,628 g/d. Cell 2 and 3 in the K2 WTS had comparable treatment areas of 187 m^2 and 181 m^2 with similar removal rates of 1,316 g/d and 1,119 g/d.

Unit area removal rates were fairly consistent in the WTSs, ranging from a low of 1.95 g/d/m^2 at the CUC1 to 17.7 g/d/m^2 at the JEEC. The low rate at the CUC1 may have been due to poor use of the treatment area as previously mentioned. This poor acidity removal in deep open water areas is further substantiated by the low acidity removal rate of 0.1 g/d/m^2 from the open water sediment pond at the K2 WTS. The high rate for the JEEC may have been due to modifications (see WTS Design section) at the JEEC that were made in an attempt to improve treatment effectiveness, and suggests that modifications were, in part, beneficial. Without these two WTS unit area removal rates, the range decreases to a low of 3.99 g/d/m^2 and a high of 9.45 g/d/m^2. In addition, cell 2 and cell 3 from the JEEC, which had different treatment areas, had very similar unit area removal rates of 11.5 g/d/m^2 and 10.6 g/d/m^2, respectively. The similar sized cells (cell 1 and 2) from the K2 WTS also had similar unit area removal rates of 7.0 g/d/m^2 and 6.2 g/d/m^2, respectively. These results from the JEEC and K2 WTSs also suggest that there is no effect of influent acidity concentration or any other water quality parameter on acidity removal.

Design Criteria

The remaining goal of the DER project was to develop design guidelines for future WTS

projects. Removal efficiencies in the WTSs varied owing to differences in design, flow, and AMD loading of parameters. Total iron removal rates for the systems were inconsistent and appear to be affected by influent water quality (e.g., influent iron concentration, fraction of ferrous, and pH). In addition, the removal rates from the WTSs suggest iron removal rates (g/d) are not a function of size; therefore, no size independent unit area removal rate (g/d/m^2) can be determined. As was found for iron removal rates, both aluminum and manganese removal rates were inconsistent, contained negative rates, and varied by greater than two orders of magnitude; therefore, these two parameters would not produce adequate estimates on which to base WTS design criteria.

Although no treatment goals were established for acidity, this water quality parameter was included in the design analysis, due to the relationship between this parameter and hydrolyzable metals. Total acidity is defined as the sum of hydrolyzable metals (e.g., ferric iron and aluminum), mineral acidity (e.g., sulfuric acid), hydrogen ions (i.e., pH), and carbonate acidity (Stumm and Morgan 1981). Effluent acidity and total iron data for the CUC1 (r^2=68%), CUC2 (r^2=28%), JEEC (r^2=81%), and K2 (r^2=20%) were found to be significantly correlated. This suggests that iron and acidity removal are dependent, and acidity removal should have a corresponding reduction of metals (e.g., iron and aluminum).

WTS removal rates for acidity ranged from 367 to 20,600 g/d and appear to correlate with the size of the WTS. Further, the results from the individual cells in K2 (cell 1 and cell 2) and the JEEC (cell 2 and cell 3) WTS suggest removal rates, based on unit area (i.e., g/d/m^2), are independent of WTS size and influent quality. Finally, unit area acidity removal rate differences may be attributed to WTS design, as found at the CUC1 (1.95 g/d/m^2) and JEEC WTS (17.7 g/d/m^2).

Due to water quality independence, size independence, and its relationship to WTS design, the acidity unit area removal rate (g/d/m^2) was selected as the parameter for sizing WTSs. Further, complete removal of acidity would likely decrease the majority of iron (ferric) and aluminum, which both have pH dependent solubility. In addition, 100% removal of acidity would have the added benefit of increasing effluent pH. Only manganese would not be addressed by acidity removal due to the presence of reduced manganese (Mn^{+2}), which is not subject to hydrolysis. The oxidized form of manganese (Mn^{+4}) is subject to hydrolysis; however, manganese oxidation is not likely at the low redox conditions that normally occur within a compost WTS.

A mean acidity unit area removal rate of 8.2 g/d/m^2 was estimated from WTS (K3, CUC2 and CUC3 WTS) and individual treatment cell (K2 and JEEC WTS) removal rates. Rates not used in the average included the CUC1 WTS and the K2 sediment pond (because of the large amount of open water), cell 3 of the K2 WTS (because of the seep), and cell 1 and 4 of the JEEC WTS (because of the unique modifications made to the two cells). The 95% confidence limit of this mean is 6 g/d/m^2 to 9.4 g/d/m^2. The lower limit of 6 g/d/m^2 is a conservative value that should incorporate variability in site conditions, vegetation, and mushroom compost composition and is recommended as the design criterion for future WTSs that incorporate a surface flow design that utilizes only compost as a substrate material.

Higher acidity removal rate design criteria may be warranted if the WTS incorporates unique design features other than the standard design used in this project. A single unit in the K2 WTS (cell 4) contained limestone underneath the mushroom compost and was found to have a slightly higher removal rate of 10 g/d/m^2. WTS design that incorporates limestone troughs, as was attempted in two cells of the JEEC WTS, may warrant higher design criteria in the 15 to 20 g/d/m^2 range. A recent initial investigation of a small-scale WTS that incorporated a subsurface flow design, based on the JEEC attempts, yielded acidity removal rates in the 25 to 50 g/d/m^2 range (Dietz et al. 1993)

Recommendations

WTS size (compost wetland) should be based on a conservative acidity loading that considers variability of influent flow and acidity (e.g., 95% upper confidence limit of mean acidity loading data) and uses a conservative removal rate (e.g., 6 g/d/m2). In addition, WTS sizing should be based on complete removal of acidity plus the production of 20 to 40 mg/L (as $CaCO_3$) of alkalinity (Dietz and Stidinger 1993). (Examples of WTS design

calculations are contained in appendix D of the "Evaluation of Wetlands Constructed for the Treatment of Acidic Mine Drainage")

Once the total WTS size has been determined, the total area should be divided between two and four treatment units to prevent hydraulic short circuiting. In addition, when possible, the units should be rectangular with open channels for the influent and effluent. Channels should be located at opposite ends of the unit to provide additional protection against short circuiting of the system. The wetlands should contain a minimum of 0.3 m (1 ft) of compost planted with cattails (*Typha lattifolia*) or some other indigenous wetland vegetation. As previously discussed, limestone placed beneath the compost or some type of limestone-subsurface flow system (e.g., JEEC WTS) may be warranted in future designs to improve treatment effectiveness and/or reduce overall WTS surface area. Additional benefit may be gained by placement of a detention and/or open-water basin prior to the WTS, providing more consistent treatment by reducing loading and flow variability and reducing high ferrous iron (>10 mg/L) when in combination with a high pH (>5).

Literature Cited

American Public Health Assoc. (APHA). 1989. Standard methods for the examination of water and wastewater, 17th edition. APHA. New York.

Dietz, J.M. 1989. Biogeochemistry of iron and sulfur in laboratory sphagnum microcosms treated with a synthetic acidic mine water. M.S. Thesis. PA State Univ. University Park, PA.

Dietz, J.M. and D.M. Stidinger. 1993. Evaluation of wetlands constructed for the treatment of acidic mine drainage. Prepared by The EADS Group, General Engineering Division, for the PA Dept. of Environmental Resources, Division of Mine Hazards, Harrisburg, PA. SL 1015-101.2

Dietz, J.M., J. Gruver, and D.M. Stidinger. 1993. Technical investigation of the abatement of acid mine drainage in a sub-surface wetland environment. Prepared by The EADS Group, General Engineering Division, for the U.S. Bureau of Mines. Contract J0209007

Gerber, D.W., J.E. Burris, and R.W. Stone. 1985. Removal of dissolved iron and manganese ions by a Sphagnum moss. p.#365-373. In Wetlands and water management on mined lands. The PA State Univ., University Park, PA.

Stumm, W. and J.J. Morgan. 1981. Aquatic chemistry: An introduction emphasizing chemical equilibria in natural waters, 2d ed., New York. 766#p.

Wieder, R.K., G.E. Lang, and A.E. Whitehouse. 1984. Destruction of a wetland ecosystem by inputs of circumneutral, treated coal mine drainage. p.#433-441. In The 1984 Symposium on Surface Mine Hydrology, Sedimentology, and Reclamation. Univ. of KY, Lexington, KY.

METAL REMOVAL IN WETLAND TREATMENT SYSTEMS[1]

Paul Eger, Jon R. Wagner, Zena Kassa, and Glenn D. Melchert[2]

Abstract: Wetland treatment has successfully removed nickel, copper, cobalt, and zinc from neutral mine drainage in northeastern Minnesota. Pilot and full-scale overland flow wetlands have removed up to 90% of the incoming nickel and 50% to 90% of the other metals. Nickel is the major contaminant in the mine drainage, with average concentrations from 2 to 5 mg/L. The other metals were generally present at concentrations less than 0.1 mg/L. In short-term tests, using drainage that contained around 1 mg/L zinc and 0.4 mg/L of copper and cobalt, concentrations were reduced about 90%. Input and output flow and water quality measurements were collected, and a mass balance was calculated. To determine the fate of the metals and the removal mechanisms, samples of vegetation and peat were collected to examine the distribution, form, and depth of metal removal. Although the overall metal concentrations in the predominant vegetation types (cattail, grass, and sedge) had increased by factors ranging from 3 for above ground vegetation to around 14 for cattail roots, the mass of metal removed by the vegetation was less than 1% of the total mass removed. The remaining metals were associated with the peat substrate. Core samples of the peat were collected and divided into 2 to 4 cm sections. Each section underwent a sequential extraction procedure and was analyzed for total concentration and metal forms. Nickel removal occurred to a depth of 20 cm, with about 60% of the nickel being organically bound.

Additional Key Words: metal sulfides, peat, adsorption, complexation, nickel, copper, cobalt, zinc.

Introduction

Acid mine drainage is a serious environmental problem. Thousands of miles of streams have been affected by acid drainage from both coal and metal mines (U.S. Bureau of Mines 1985). Acid drainage associated with metal mines usually contains elevated concentrations of the metals associated with the ore body. These metals, in addition to the acid, can pose dangers to downstream human and aquatic communities. Although this type of drainage can be chemically treated in an active treatment plant, this is an expensive and long-term commitment, particularly since drainage problems can persist for over a hundred years.

An alternative approach to chemical treatment is the use of wetlands to remove metals from mine drainage. In wetlands, a variety of processes are responsible for metal removal. These include a mixture of chemical, biological, and microbiological reactions that occur in the aerobic and anaerobic zones of wetlands.

Treatment effectiveness in most studies has been measured as the difference between input and output concentrations, and as a result there are often insufficient data to complete an overall mass balance for the system, or to determine the fate of the removed metals. These type of data are important not only because they allow better estimations of performance, but also better prediction of system lifetimes and future availability of the removed metals. In 1989, a joint project between the Minnesota Department of Natural Resources and LTV Steel Mining Company was begun to evaluate the effectiveness of wetland treatment systems to remove metals from mine drainage. Previous reports have described the background of the project, the mine and construction of the wetland cells (Eger et al. 1989, 1991).

---

[1]Paper presented at the International Land Reclamation and Mine Drainage Conference and the Third International Conference on the Abatement of Acidic Drainage, Pittsburgh, PA, April 24-29, 1994.

[2]Paul Eger, Principal Engineer, Jon R. Wagner, Research Analyst, Zena Kassa, Research Analyst, and Glenn D. Melchert, Hydrologist, Minnesota Department of Natural Resources, Division of Minerals, St. Paul, Minnesota.

Methods

Cell Description

Four test cells, 6 m wide by 30.5 m long, were constructed in northeastern Minnesota. Since design and operating conditions varied between the cells, this paper will focus on the results from only one of the cells (cell 1). This cell contained an undisturbed portion of the original wetland, which contained primarily grasses (*Carex sp.*) and sedges (*Calamograstis sp.*), and to a lesser degree, cattails (*Typha latifolia*). The cell was hydrologically isolated from the surrounding area by a perimeter peat berm which contained a sand-bentonite cut-off wall. The cut-off wall extended from the top of the berm into the silty clay underlying the wetland. Input flow was distributed across one end of the cell with a 5 cm perforated PVC pipe, while the outflow was collected at the other end in a collection trough set to maintain the water in the cell at an average depth of 5 cm. Data for the other cells will be discussed in a future publication which is presently being prepared.

Input and output flows from each cell were measured continuously with Data Industrial electronic flow meters. The flow meters were calibrated in the laboratory prior to initiation of the study, and were periodically checked during the field season.

Water quality samples of the input and output were collected at least once per week and analyzed for pH, specific conductance, alkalinity, calcium, magnesium, sodium, potassium, sulfate, iron, manganese, copper, nickel, cobalt, and zinc. Results reported in this paper are for total metal values; the difference between total and filtered metals was generally less than 5%.

Vegetation

Preoperational vegetation samples were collected in July 1989. Sedge and grass leaves were collected randomly at five sites within the cell. Duckweed samples were collected from approximately 12 open-water sites, and entire cattail plants were collected from the surrounding area.

Cattail samples were rinsed, separated into leaves, roots, and rhizomes, and air dried. Any visible soil was removed from the roots and rhizomes. All samples were oven dried, ground and screened to minus 20 mesh, ashed, digested with concentrated nitric acid, and analyzed for metal content by atomic absorption.

In July 1991, additional vegetation samples were collected. Cattails, grasses and sedges were collected at sites that were 6, 12, 18, and 24 m from the inlet end of the cell (at 1.5 m intervals across the cell) and then composited for each distance from the inlet end of the cell. Duckweed samples were collected randomly from open water sites within the cell and composited. These vegetation samples were handled, processed, and analyzed in a manner similar to that used for the 1989 samples.

In August 1991, percent cover was estimated by inspecting random 0.5-m^2 subplots at ten foot intervals down the length of the cell. Above ground biomass was collected from within a 0.1 -m^2 frame placed within the larger 0.5-m^2 frame. The above ground biomass was then separated into cattails, grasses and sedges, and duckweed, oven dried at 24°C for 24 h, and then weighed. Total above ground biomass was calculated by multiplying the total area of the cell (186 m^2) by the average of the biomass values determined for each vegetation type.

Below ground biomass was not directly measured. Literature values (Zhang et al. 1991, Hill 1987) indicate that the ratio for Typha roots-rhizomes-leaves biomass is approximately 1:18:14. Mass calculations for metal uptake by the underground portion of cattails were based on this ratio.

Peat samples

Baseline peat samples were collected in September 1988. Six core samples were collected using a Macauley sampler. Triplicate samples were collected in the center of the cell at distances of 4.5 and 14 m from the inlet (fig. 1). Samples were collected at depths of 0 to 20 cm, 20 to 50 cm, and then at 50 cm intervals until mineral soil was encountered.

The peat samples were oven dried at 105° C for 24 h, processed with a blender to break up clumps, and sieved to minus 80 mesh. Greater than 70% of all the processed samples were less than 80 mesh. All samples were digested using a total digestion procedure, in which 0.5 g of sample was digested with a concentrated acid solution containing 1 mL HCl, 2 mL HNO_3, and 0.5 mL HF at 90°C for 2 h.

In late May 1991, after 2 yr of operation, additional peat samples were collected from the 0 to 20 cm segment and from the 20 to 50 cm segment, at the sites shown in figure 1. Triplicate samples were collected at several of the sites (for both surface and deep segments) to determine the variability between samples. The deep samples were collected with a Macauley sampler, while the shallow samples were collected with a power soil auger that had been modified to accept a 10-cm-ID stainless steel tube with serrated cutting teeth. Shallow samples that were at first collected with a Macauley sampler were small in volume and difficult to collect due to the loose consistency of the surface peat; in contrast, the power auger samples were larger in volume (and therefore less apt to be influenced by local concentration variations within the peat, and more likely to accurately represent the actual conditions within the cell).

After 3 yr of operation, another set of samples were collected to determine the depth and form of metal removal. These samples were collected with the power soil auger in March 1992 when the wetland was frozen. Three cores were collected at each site, and each core was 20 to 40 cm long. The cores were extracted from the core tube, wrapped in freezer paper, and stored in the freezer. Each core was cut into 2 to 4-cm segments while the core was still frozen. These sections were stored in the freezer until the sequential extraction procedure was performed.

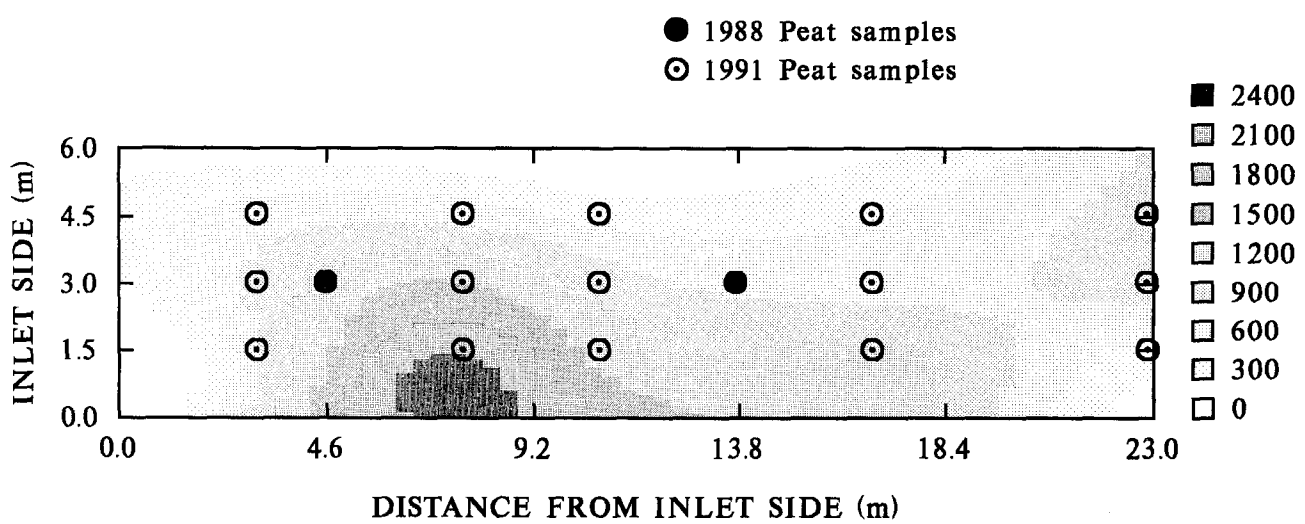

Figure 1. Plan view of cell 1, showing locations of 1988 and 1991 peat samples, and mean nickel concentrations in the surface peat (0 to 20 cm) as of May 25, 1991. (The nickel concentration contour lines were generated by a computer model that performs weighted quadratic multiple regressions of all data points.)

A series of steps was used to differentiate the form of the metal in the core (fig. 2). In general, the procedure was the same as the one developed by Weider (1991, Miller et al. 1983), except that the peat was not rinsed and centrifuged between each step. A comparison of samples run with and without rinsing showed little difference between the results. The only major difference in our extraction procedure was the inclusion of additional pyrophosphate extraction tests. Initial results indicated that a large fraction of metal removal occurred in the carbonate form (EDTA extraction). Since EDTA can also extract metals that are bound to organics, a total of six pyrophosphate extractions were performed to determine if additional metal would be extracted. Based on these results, it was determined that four extraction steps were needed to extract the majority (>90% extraction) of the metals associated with the organics. A 10 g subsample of the substrate was analyzed using a total digestion with HNO_3, HF, and HCl.

Results

Water Quality

The input drainage can be characterized as a high hardness, neutral mine drainage with elevated concentrations of sulfate, nickel, copper, zinc, and cobalt. The major contaminant is nickel, which is typically about 1 to 2 mg/L. Flow rates into the cell were usually around 3.8 L/min (1 gpm) but ranged from around 2 to 8 L/min. Residence time, measured with Rhodamine dye and a potassium iodide tracer, was on the order of 48 hr.

The cell was generally effective in removing nickel from the drainage (table 1), and was effective in removing copper, cobalt, and zinc after concentrations in the input were increased in the fall of 1990. During the first 2 yr of the study, the input concentrations of copper, cobalt, and zinc were all less than 0.03 mg/L, and although there was a statistical difference between the input and output zinc concentrations, there was no difference for cobalt and copper (Eger et al. 1991). Beginning in the fall of 1990, the source of input water was changed, resulting in an increase in influent metal concentrations. In 1991, mass removal ranged from 73% for nickel to 26% for cobalt (table 1). Over the entire 3 yr of the study, nickel removal was 79%.

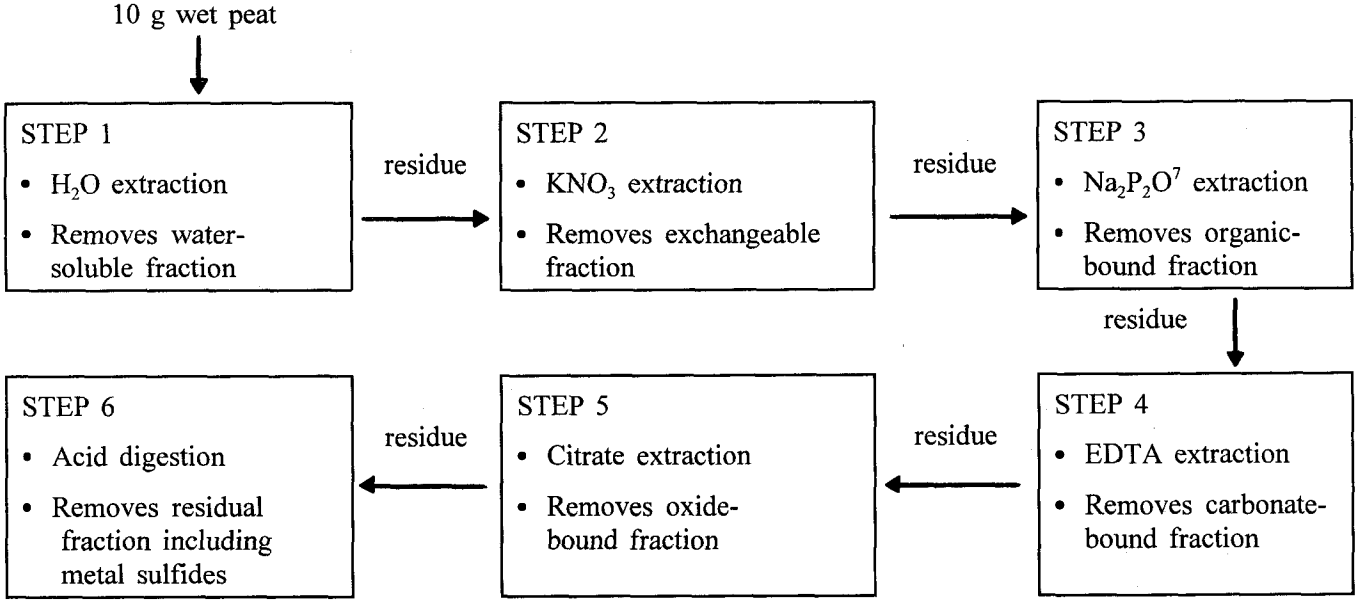

Figure 2. Sequential extraction procedure used to differentiate the metal forms present in 1992 peat samples.

Metal Removal

Metal mass input and output for the cell was determined by multiplying the total daily flow by the measured or the calculated average concentration for the site. Mass balance calculations based on the difference between the inflow and outflow mass indicated that about 3 kg of nickel was retained in the cell over the 3 yr course of the study. Since the input concentrations of other metals were generally lower than nickel, the total removal was also lower. From September 1990 through 1991, the cell removed less than 0.1 kg of copper and cobalt and about 0.3 kg of zinc (table 1). If the overall mass removed is divided by the area of the cell and the total number of days of operation, a daily rate of removal per unit area ($g/m^2/d$) can be determined (table 1). The nickel removal rate in our system was about 0.04 to 0.05 $g/m^2/d$, while removal rates for the other metals were generally about an order of magnitude lower. During the fall of 1990, the zinc removal rate was similar to the nickel rate due to the elevated zinc content of the drainage. The lower rates in 1991 for copper, cobalt, and zinc are the result of the lower input concentrations.

Metal removal was assumed to have occurred in two compartments within the system; the vegetation (i.e., cattails, grasses and sedges, duckweed), and the peat. Over 99% of the metal that was removed was associated with the peat. The mass removal calculated from the peat and vegetation data was in the same general range as that calculated from the input and output water chemistry and flow data.

Over the course of the study, nickel concentrations increased in all parts of the cattails. Average nickel concentration in the roots, rhizomes, and leaves increased from 28.0, 9.8, and 5.5 mg/kg to 72.0, 16.8, and 12.0 mg/kg, respectively. In this cell, mean nickel concentrations in the grasses and sedges did not significantly change during the same time period, while concentrations in the duckweed increased from 175 to 735 mg/kg (though the small biomass of duckweed in the cell makes it a relatively minor agent of nickel removal).

Table 1. Overall mass removal in wetland treatment cell 1.

	Time periods	Average conc. (mg/L)		Mass retained	Percent removal	Areal Rate of removal
		Input	Output	(g)		($g/m^2/day$)
Nickel	1989-1991	1.65	0.39	2920	80	0.04
	1991	1.98	0.92	1290	73	0.04
Copper	Fall 1990[1]	0.19	0.02	39	83	0.005
	1991	0.04	0.01	50	91	0.002
Cobalt	Fall 1990[1]	0.31	0.02	66	89	0.009
	1991	0.02	0.01	4.4	26	0.0001
Zinc	Fall 1990[1]	1.13	0.01	271	94	0.04
	1991	0.06	0.02	20	51	0.0006
Sulfate	Fall 1990[1]	2020	2050	---	---	---
	1991	2430	2400	---	---	---
pH	Fall 1990[1]	6.89	6.76	---	---	---
	1991	7.12	6.84	---	---	---

[1] From short term tests conducted with elevated input metal concentrations (Eger et al. 1991).

Preoperational peat samples contained an average nickel content of 174 mg/kg dry peat in the 0 to 20 cm segment, and 134 mg/kg dry peat in the 20 to 50 cm segment. In general, there was less than 20% variation in the preoperational values. Assuming a bulk density of 0.1 g dry peat per cubic centimeter of wet peat (Minnesota Department of Natural Resources 1987), the total nickel mass present in each portion of the cell was calculated. By late May 1991, the mean nickel concentration of the 0-20 cm samples collected from the cell had increased to 1020 mg/kg. Nickel concentrations in the surface peat were generally highest in the samples collected from sites 25 ft from the inlet side of the cell, and the distribution of concentrations suggest that a preferential flow path exists in the cell (fig. 1). Nickel concentrations in the 20-50 cm samples were similar to the baseline values, indicating little nickel removal in the deeper layers of peat.

Metal Forms; Depth of Removal

Since nickel was the main contaminant in the drainage, this paper concentrates on the results for this metal. Additional data on the other metals (copper, cobalt, and zinc) will be discussed in a report presently in preparation. Nickel concentrations in the upper portion of the peat increased during the study by more than an order of magnitude. Concentrations generally decreased with depth, reaching background concentrations at 20 to 30 cm (fig. 3).

Most of the nickel removal during the sequential extraction procedures occurred in the pyrophosphate step, indicating that most (60%) of the nickel was associated with the organic fraction (fig. 3). The next largest fraction was in the nitric acid extraction, which generally removes metals that are associated with sulfides and primary or secondary mineral forms. In the deeper peat (20 to 30 cm), where little increase in nickel concentration had occurred during the study, the largest amount of nickel was in the precipitated form.

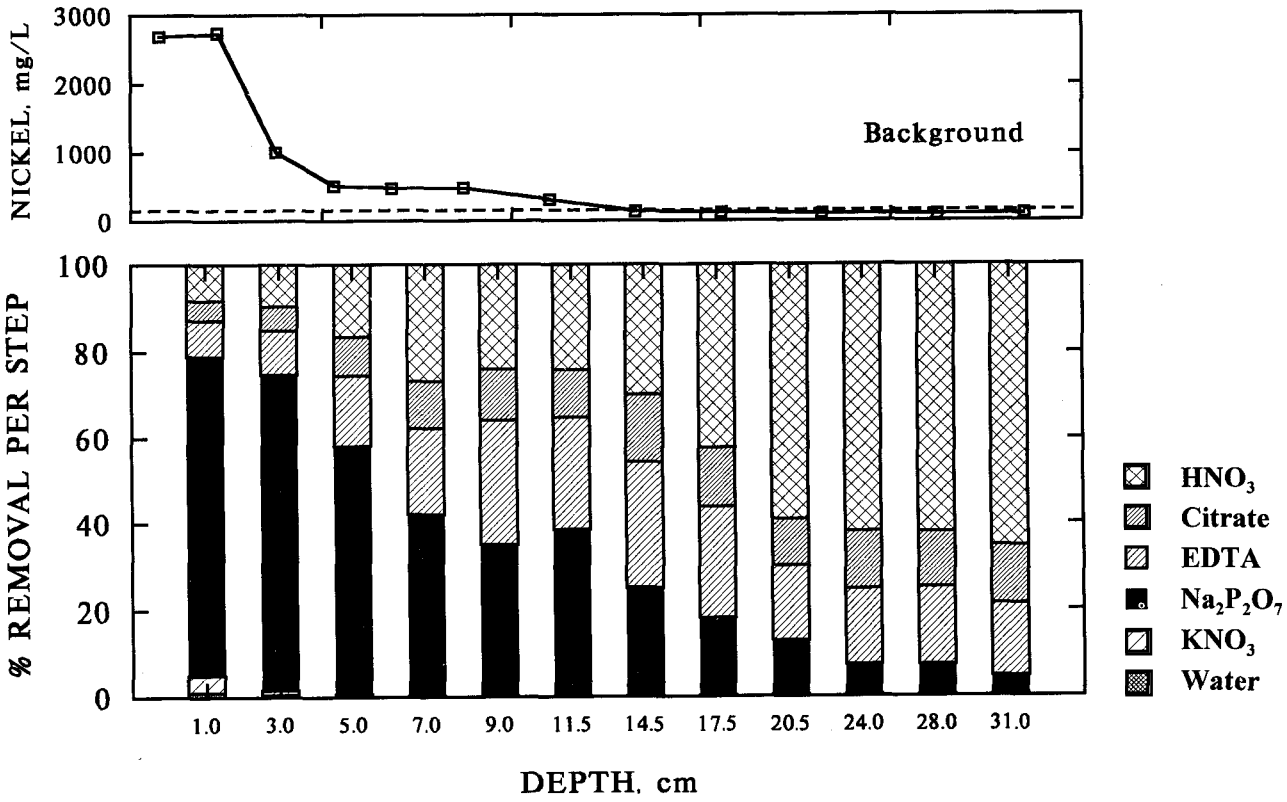

Figure 3. Nickel concentration vs. peat depth (top), and percent nickel removal by each extraction step vs. peat depth (bottom). Data is from 1992 cell 1 peat samples (after 3 yr of operation).

Discussion

In this study, significant amounts of metals were removed from neutral mine drainage in an overland flow wetland. Although metal concentrations increased in the vegetation in the wetland, greater than 99% of the metal removal was associated with the peat substrate. This finding is consistent with our initial work on removal in a white cedar wetland (Eger and Lapakko 1988) and with data reported by others (Skousen 1992, Wildeman et al. 1991).

Vegetation naturally accumulates metals in areas where mineralization occurs. Nickel concentrations in black spruce (*Picea mariana*) and Labrador tea (*Ledum groenlandicum*) overlying a mineralized area in northeastern Minnesota were 5 to 6 times higher than background values (Agrawal 1964). These higher concentrations were in the same general range as those found in the plants in the treatment cell.

The primary removal mechanism in this wetland was the removal of metals by association with the organic fraction of the peat. Peat contains a complex mixture of organic compounds with a series of functional groups. These groups provide a variety of sites for metals to bind. Sulfide precipitation was much less important in the overall removal of nickel. These results are consistent with the changes in water quality observed in the treatment cell. The pH of the drainage decreased as it passed through the cell; the result of the exchange of metal ions in the water for hydrogen ions on the peat. In contrast, there was no statistically significant difference between the input and output sulfate concentration, which implies that the overall rate of sulfate reduction was small (table 1).

The minor amount of removal associated with sulfide precipitation is similar to that reported in studies by Wieder for peat wetlands, in which minimal accumulation of sulfur was found (Wieder and Lang 1986). Wieder suggests that although metal sulfides may form, they are later oxidized and converted to other forms. The oxidation of sulfide precipitates may not be a major concern in a constructed wetland if the water level is maintained so that the substrate remains saturated. In compost based wetlands, however, significant amounts of reduced and elemental sulfur have been measured (Hedin et al. 1989). Compost provides a readily decomposable organic substrate, and sulfate reduction rates up to 1,200 $mmol/m^3/d$ have been measured (Reynolds et al. 1991). More typical rates are on the order of several hundred millimoles per cubic meter per day (Eger 1992).

The specific mechanisms of metal removal are important because they affect the overall lifetime of the wetland. Long term treatment of mine drainage is an important regulatory issue, and the ability of wetlands to provide continued treatment has not been demonstrated. As a result, the Office of Surface Mining has required back-up chemical treatment for wetlands built to control coal mine drainage (O.S.M. 1988). If the removal is primarily due to removal by organics, then the system lifetime is limited by the total amount of removal sites that are available in the top portion of the wetland. If the primary removal mechanism was sulfate reduction, the process would continue as long as there was an organic food source and an input of sulfate. Sulfate reduction would be more likely to offer long-term treatment. Although additional adsorption sites will be generated annually as plants die and decompose, the formation of new sites is minimal. To provide a balance between the input of metals and the formation of new removal sites in our test cell, input flow would need to be reduced by about an order of magnitude (table 2).

Another method to increase the treatment life of the wetland is to construct the system so that the surface peat can be replaced. This approach has been used by LTV Steel Mining Company at their Dunka Mine in northeastern Minnesota, where a peat mixture was placed on top of an existing wetland (Frostman et al. 1993). New material can be added when the removal capacity of the mixture is exhausted.

Another factor that limits the removal in natural wetlands is the transport of metals to reaction sites. Although peat depth in our wetland was about 1 m, only the upper 20 cm was effective in removing metals. In natural wetlands, flow occurs primarily across the surface, generally within the upper 30 cm (Romanov 1968).

This occurs as a result of a minimal vertical hydraulic gradient and a decrease in hydraulic conductivity with depth. However, wetlands can be constructed to encourage vertical flow and provide more contact with the substrate. This type of wetland requires additional engineering design, but the increase in treatment per unit area can be significant (Eger and Melchert 1992).

Conclusion

Wetlands can effectively remove metals from neutral mine drainage. Over 99% of the removal in our system was associated with the peat substrate. Although metal concentrations increased in the vegetation, the levels were comparable to levels in areas of natural mineralization. Wetland vegetation is important since it disperses flow, stabilizes the substrate, provides additional organic material, and improves the aesthetics of the wetland. The primary removal mechanism in this system was associated with the organic fraction of the peat, and the bulk of removal occurred in the upper 20 cm of the wetland. As a result, the removal capacity of this wetland is limited, and although new adsorption sites are produced by decomposing vegetation, the metal load into the system would have to be reduced by an order of magnitude to remain in balance. Wetlands can be successful in providing long-term treatment of mine drainage, provided that input flows into the wetland are reduced or that periodic maintenance of the wetland is performed.

Table 2. Comparison of annual production of metal removal sites with current annual metal input.

Annual input of removal sites:	
• Peat accumulation rate	1 mm/yr[1]
• Bulk density	0.1 g/cm^3
• Removal capacity	10 g Ni/kg dry peat[2]
• Area of cell	186 m^2
• Annual removal capacity	0.2 kg Ni/yr
Present loading rate to cell	
• Flow	3.8 L/min
• Concentration	2.0 mg/L
• Average days of flow	225
• Annual metal input	2.5 kg Ni/yr
Flow reduction needed to balance input with annual generation of sites	92%

[1] Craft and Richardson 1993
[2] Eger and Lapakko 1988

Literature Cited

Agrawal, M. U. 1964. Biogeochemical investigation in a swamp environment. M.S. Thesis, University of Minnesota, Minneapolis, MN. 128 p.

Craft, C.B. and C. Richardson. 1993. Peat accretion and N, P, and organic C accumulation in nutrient-enriched and unenriched Everglades peatlands. Ecological Applications 3 (3):446-458.

Eger, P. 1992. The use of sulfate reduction to remove metals from acid mine drainage. Paper presented at 1992 American Society for Surface Mining and Reclamation Meeting. (Duluth, MN, June 14-18, 1992).

Eger, P., and K. Lapakko. 1988. Nickel and copper removal from mine drainage by a natural wetland. In Mine Drainage and Surface Mine Reclamation. Vol. 1. Mine water and mine waste. BuMines IC 9183.

Eger, P., and K. Lapakko. 1989. Use of wetlands to remove nickel and copper from mine drainage. In Constructed Wetlands for Wastewater Treatment. (Lewis Publishers, Chelsea, MI).

Eger, P. and G. Melchert. 1992. The design of a wetland treatment system to remove trace metals from mine drainage. Paper presented at 1992 American Society for Surface Mining and Reclamation Meeting. (Duluth, MN, June 14-18, 1992).

Eger, P., G. Melchert, D. Antonson, and J. Wagner. 1991. The use of wetland treatment to remove trace metals from mine drainage. Presented at the International Symposium on Constructed Wetland for Water Quality Improvement. (Pensacola, FL, 1991).

Frostman T., S. Gale, and D. Koschak. 1993. Base metal removal from mine drainage. Presented at 1993 10th National Meeting. (Spokane, WA, May 16-19, 1993).

Hedin, R. S., R. Hammack, and D. Hyman. 1989. Potential importance of sulfate reduction processes in wetlands constructed to treat mine drainage. In Constructed Wetlands for Wastewater Treatment. (Lewis Publishers, Chelsea, MI).

Hill, B. B. 1987. Typha productivity in a Texas pond: implications for energy and nutrient dynamics in freshwater wetlands. Aquatic Botany 27. p. 385-394.

Miller, W. P., W. W. McFee, and J. M. Kelly. 1983. Mobility and retention of heavy metals in sandy soils. J. Environ. Qual. 12:579-584.

Minnesota Dept. Natural Resources. 1987. Planning of milled peat production systems at two sites in northern Minnesota. (Division of Minerals, St. Paul, MN).

Office of Surface Mining. 1988. Use of wetland treatment systems for coal mine drainage. OSMRE Dir. TSR-10. U.S. OSMRE, Washington, DC.

Reynolds, J. S., T. Wildeman. 1991. Determination of the rate of sulfide production in a constructed wetland receiving acid mine drainage. In Proceedings of the National Conference of the American Society of Surface Mining and Reclamation. (Durango, CO, May 14-17, 1991).

Romanov, V. V. 1968. Hydrophysics of bogs. Israel Program for Scientific Translations.

Skousen, J., A. Sexstone, K. Garbutt, and J. Sencindiver 1992. Wetlands for treating acid mine drainage. Green Lands 22(4):31-39

U.S. Bureau of Mines. 1985. Control of acid mine drainage. Proceedings of a Technology Transfer Seminar, BuMines IC 9027. p. 2.

Wieder, R. K. 1991. Laboratory procedure manual. Villanova University.

Wieder, R. K. and G. E. Lang. 1986. Fe, Al, Mn and S chemistry of sphagnum in four peatlands with different metal and sulfur input. Water, Air, Soil Pollution 29:309-320.

Wildeman, T., J. Gusek, and G. Brodie. 1991. Wetland design for mining operations. Draft handbook presented at the American Society of Surface Mining and Reclamation Conference. (Durango, CO, May 14-17, 1991).

Zhang, T., J. B. Ellis, D. M. Revitt, and R. B. E. Shutes. 1991. Metal uptake and associated pollution control by *Typha latifolia* in urban wetlands. Urban Pollution Research Center, Middlesex Polytechnic, Queensway, Enfield, EN3 4SF, UK.

IRON RETENTION AND VEGETATIVE COVER AT THE SIMCO CONSTRUCTED WETLAND: AN APPRAISAL THROUGH YEAR EIGHT OF OPERATION[1]

Lloyd R. Stark,[2] Frederick M. Williams,[2] S. Edward Stevens, Jr.,[3] and David P. Eddy[2]

Abstract: The Simco constructed wetland near Coshocton, OH, has received mine water containing an average of 89 mg/L at a loading of approximately 15 g Fe/m^2/d since 1985. Its capacity to remove iron is evaluated by analyses of (1) inlet and outlet water chemistry, (2) concentration treatment efficiency over time, and (3) area-adjusted iron retention over time. Since 1990, the wetland system outlet has not required any chemical treatment, meeting Federal compliance levels for iron and pH. Source water iron concentrations have exhibited a gradual tendency to decline over the years. Treatment efficiency has improved over time, exceeding 90% as the wetland aged. Area-adjusted iron retention (g/m^2/d) is a strong positive correlate to iron load ($r = +0.89$), thus devaluing it as an indicator of wetland performance. Treatment efficiency is preferred as a measure of wetland performance for iron retention, because it is significantly negatively correlated to flow rate ($r = -0.46$), iron load ($r = -0.74$), and inlet iron concentrations ($r = -0.44$). The density of cattail (*Typha latifolia*) shoots has generally increased through the years to a current density of 17 shoots/m^2. Plant diversity and non-cattail species cover, however, have declined since wetland inception. We postulate that the improvement observed with time in the ability of the Simco wetland to retain iron is a result of a combination of factors, namely the presence of moderate mine water quality (near neutral pH, [Fe] < 100 mg/L), sound wetland design and subsequent modifications, periodic site maintenance, and high vegetative cover.

Additional Key Words: acid mine drainage, constructed wetlands, iron, water treatment, *Typha latifolia*

Introduction

Constructed wetlands have been designed and implemented for the treatment of a variety of water pollutants over the last 10 yr. With respect to coal mine drainage, few of these wetlands have been monitored regularly since inception, and therefore data are scant regarding such important questions as longevity and vegetation patterns. In coal mine drainage, the water quality parameters of concern are pH and several metals. Of the metals, iron, manganese, and aluminum may exceed required or recommended outlet concentrations. Surveys indicate that while pH and Mn meet with varying degrees of success in wetland treatment systems, wetlands are usually capable of lowering iron concentrations significantly (Wieder 1989, Hellier 1989). Such wetland treatment is likely dependent on a few critical design parameters, namely the size of the wetland as compared to flow rate and influent metal concentrations, the net acidity of the influent water, and the metal load to the wetland system (Hedin and Nairn 1992).

In this paper, we report on patterns of iron retention and vegetation from a constructed wetland that has been in operation and continuously monitored since 1985. The Simco wetland was installed primarily to treat a seep that contained high levels of total iron and was initially planted with *Typha latifolia*.

---

[1]Paper presented at the International Land Reclamation and Mine Drainage Conference and the Third International Conference on the Abatement of Acidic Drainage, Pittsburgh, PA, April 24-29, 1994.

[2]Lloyd R. Stark, Senior Research Associate, Frederick M. Williams, Associate Professor of Biology, and David P. Eddy, Research Assistant, Pennsylvania State University, University Park, PA, USA.

[3]S. Edward Stevens, Jr., Chair of Excellence in Molecular Biology, Memphis State University, Memphis, TN, USA.

Methods

Design

In November 1985, construction of the Simco wetland in Coshocton County, OH, was completed. It consisted of three wetland cells in sequence separated by small ponds. The substrate consisted of a layer of crushed limestone (15 cm) covered with a layer of spent mushroom compost (45 cm). The total area of the system was 3,196 m^2 (including small ponds between cells and connecting ditches). Bed slope was 1%. Typha latifolia (common, broad-leaved cattail) rhizomes were transplanted from a donor site to an initial density of 3 to 4/m^2. In 1989, a fourth wetland cell was added, bringing the system area to 4,138 m^2 (fig. 1).

Water Sampling

Every 2 or 3 weeks, water samples were taken from the system inlet and outlet, as well as from individual wetland cell outlets and the site permit outlet (NPDES point). pH (electrometric), flow rates (flume), and temperature (electrometric) were taken in the field. Water samples were transported on ice to the laboratory, where standard methods (APHA 1985) were used to analyze total and dissolved Fe, total Mn, acidity, alkalinity, conductivity, sulfates, and total suspended solids.

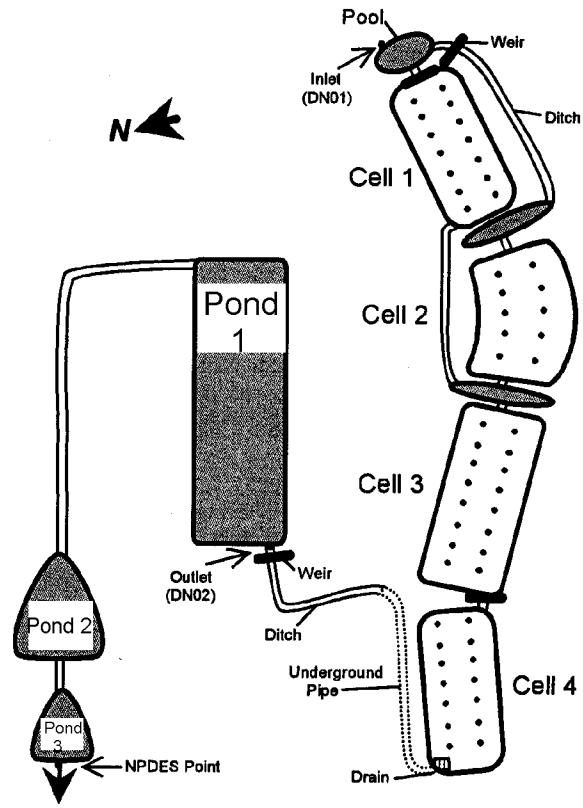

Figure 1. Diagram of the Simco wetland. Points within the cells represent the vegetation sampling stations.

Performance Indices

Two measures are commonly used in the assessment of wetlands treating metals: Treatment efficiency and Area-adjusted Fe retention. Treatment (or concentration) efficiency estimates the percentage of iron retained in a particular wetland:

$$\textit{Treatment Efficiency (\%)} = (100)([Fe]_{INLET} - [Fe]_{OUTLET}) \div [Fe]_{INLET}$$

Area-adjusted Fe retention (also AART, or mass retention) estimates the mass of Fe retained in the wetland per unit area:

Area-Adjusted Fe Retention ($g/m^2/d$) = $Q\,([Fe]_{INLET} - [Fe]_{OUTLET})\,(1.44) \div A$, where Q is flow rate, A is wetland area, and 1.44 is used to convert minutes to days and milligrams to grams.

At the Simco wetland, the wetland inlet and outlets are well marked; treatment efficiency is based on the iron concentrations found at stations DN01 and DN02 (fig. 1). Since the total area of the system changed in 1989, prior to October 1989, an area of 3,196 m^2 was used in the calculation of area-adjusted Fe retention. After October 1989, 4,138 m^2 was used in this calculation. Only dates where all three parameters were measured (i.e., inlet Fe, outlet Fe, and flow rate) were used in the area-adjusted Fe retention calculations.

Vegetation Sampling

Forty permanent, equidistant sampling stations were established along two parallel transects running the length of the original three-celled wetland system (fig. 1). Each summer (July or August), the percentage cover of vascular and non-vascular plants was assessed using a 0.5 m^2 quadrat. Visual estimates (to the nearest 10%) of cover were determined based on the canopy coverage method of Daubenmire (1970). Owing to the tall and slender nature of cattails, coverage was difficult to assess. As a result, beginning in 1987 stem counts of living cattails were taken in each quadrat, and density was calculated per unit area of wetland accordingly. Species diversity was estimated as the number of species occurring in the 40 sampling stations.

Results

Inlet and Outlet Water Chemistry

The principal pollutant entering the wetland is iron (table 1). Until early 1989, total manganese entering the wetland was above Federal (30-day average) standards (2.0 mg/L). However, since that time inlet Mn has been in compliance. Most other mine water parameters are decreased in concentration as a result of passage through the wetland (table 1).

Inlet and Outlet Iron Concentration. Although seasonal fluctuations occur, in general the inlet [Fe] has declined over the last ten yr (fig. 2) from about 200 mg/L to the current level near 75 mg/L. Upon wetland installation, water quality began to improve at the system outlet. Nevertheless, chemical treatment (sodium hydroxide) was required in addition to wetland treatment during the following periods.

Table 1. Mean (± 1 standard deviation) values for inlet and outlet water parameters at the Simco wetland, 1985-93.

Parameter	Inlet	Outlet	N
pH	6.56±0.16	6.58±0.75	190
Total iron (mg/L)	89.37±25.56	22.63±20.09	190
Total manganese (mg/L)	1.72±0.39	1.96±0.65	191
Acidity (mg/L)	133.80±61.81	28.04±22.94	191
Alkalinity (mg/L)	87.64±26.82	44.02±26.93	191
Conductivity (μomhos/cm)	1,790.10±360.71	1,701.97±336.17	189
Total suspended solids (mg/L)	37.60±16.87	29.71±22.05	190
Sulfate (mg/L)	984.07±233.79	912.63±219.27	174
Temperature (°C)	12.85±1.26	12.00±7.38	128
Flow Rate[1] (L/min)	451.29±272.70	427.50±270.90	95

[1]Paired data from 1987-93; previous to this only outflow data are available

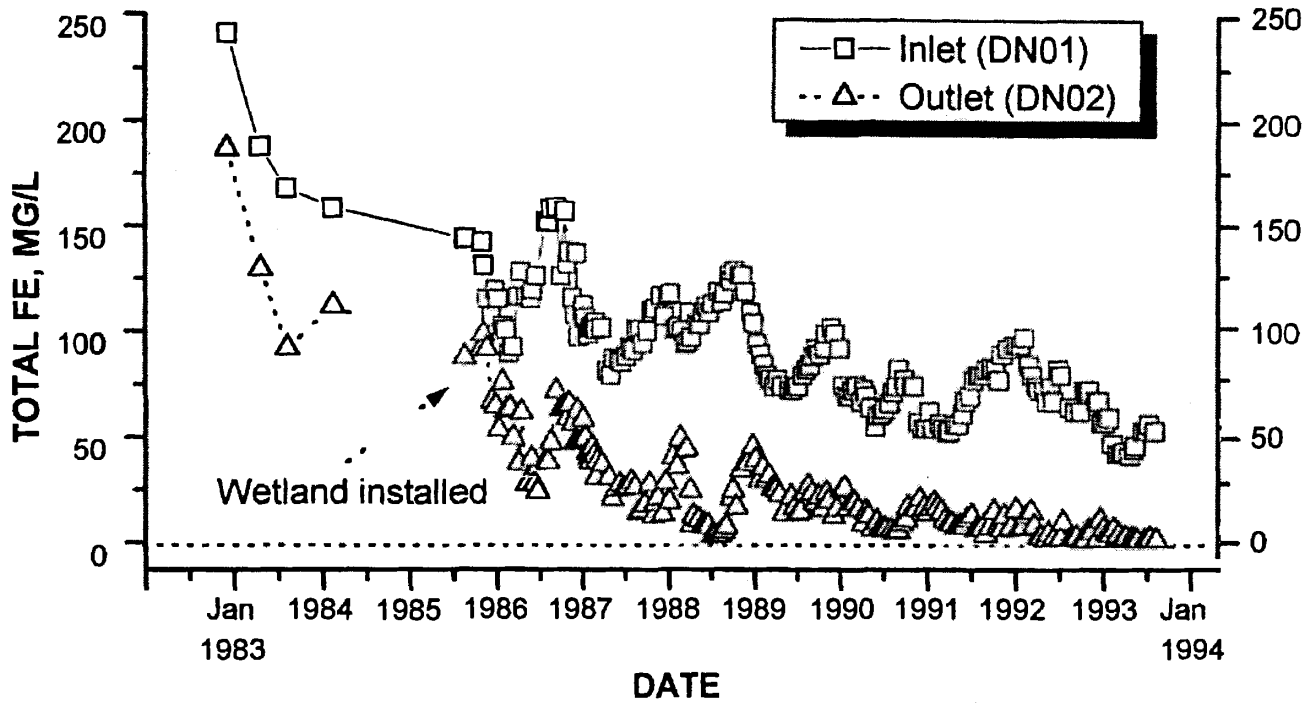

Figure 2. Inlet and outlet iron concentration over time at the Simco wetland. Pre-wetland values are shown from 1983 to 1985.

Chemical treatment and Duration

ON	Pre-wetland, 1980-85 ..... 5 yr.	ON	Dec. 1988 - May 1989 .....6 mos.
ON	Nov. 1985 - May 1987 ..... 19 mos.	OFF	June 1989 - Jan. 1990 .....8 mos.
OFF	June 1987 - Jan. 1988..... 7 mos.	ON	Feb. 1990 - Mar. 1990.....5 d.
ON	Feb. 1988 - Apr. 1988..... 3 mos.	OFF	Apr. 1990 - Jan. 1994.....3+ yr.
OFF	May 1988 - Nov. 1988 ..... 7 mos.		

During the last 3½ yr, no chemical treatment has been required of water discharging from the wetland. As of August 1993, the chemical treatment facility was removed, as supervised by the Ohio Department of Natural Resources.

Treatment Efficiency, Total Iron. The percentage of iron retained by the Simco wetland has increased over time (fig. 3). Generally, efficiency has been higher during the warmer months and lowest during the winter months. With one exception (the winter of 1991-92), the treatment efficiency has improved each succeeding winter.

Area-Adjusted Iron Retention. This measure has fluctuated widely since the wetland was installed, with a mean value at 10.54 g Fe/m^2/d ($\pm$5.57, N=167). The area-adjusted iron load to the wetland has averaged 15.14 g Fe/m^2/d ($\pm$10.16, N=167). Plotted against flow rate, area-adjusted retention mirrors the flow rate entering the Simco wetland: as flow rate increases, retention per unit area also increases (fig. 4).

Correlates of Performance Measures. A correlation analysis of the two measures of wetland performance and several iron and flow variables indicates that treatment efficiency and area-adjusted Fe retention are not closely related to one another. These two measures of wetland performance are correlated in opposite directions to iron concentrations, flow, load, and one another (table 2). High treatment efficiencies are attained when low iron concentrations and low flow rates occur (resulting in low iron loads). However, high area-adjusted iron retention occurs in the presence of high iron concentrations and high flow rates (resulting in high iron loads).

Vegetation Patterns

Cattail Stem Density. From the initial planting density of approximately 3.5 stems/m^2 (not measured), cattail density has generally increased with each summer in the upper three cells over the first 5 yr (fig. 5). Over the past three summers, density has been fairly stable near 17 living stems/m^2. In 1993, the mean biomass per cattail plant was 120 g (dry weight), partitioned between above-ground shoots (70 g) and below-ground rhizomes and roots (50 g; n=6). This equates to an approximate dry weight biomass of cattails of 2.04 kg/m^2, of which 850 g is below-ground.

Non-Cattail Coverage. With the exception of 1991, mean total coverage of non-Typha wetland plants has declined since 1987 (table 3). Coverage increased during the first two full summers, to a high of 40% (i.e., approximately 40% of the wetland surface was occupied by non-Typha species). However, currently this coverage has fallen to only 4%.

Shortly after the wetland was installed, a surge of growth by Leersia oryzoides (rice cut-grass) occurred, with this species accounting for a mean cover of 22% in 1987 (table 3). However, Leersia populations have since declined from co-dominant status in 1987 to incidental status by 1992. Only four genera are currently somewhat common in the Simco wetland besides Typha latifolia: Lemna (duckweed), Leersia, and two algal genera, Microspora (a filamentous green) and Oscillatoria (a filamentous blue-green).

Species Diversity. Diversity was highest during the first 2 yr of establishment (12 to 13 species) and has gradually declined from 1987 on, mirroring the decline in non-Typha coverage (table 3). During the last 3 yr, the number of species occurring in the Simco wetland has stabilized near five.

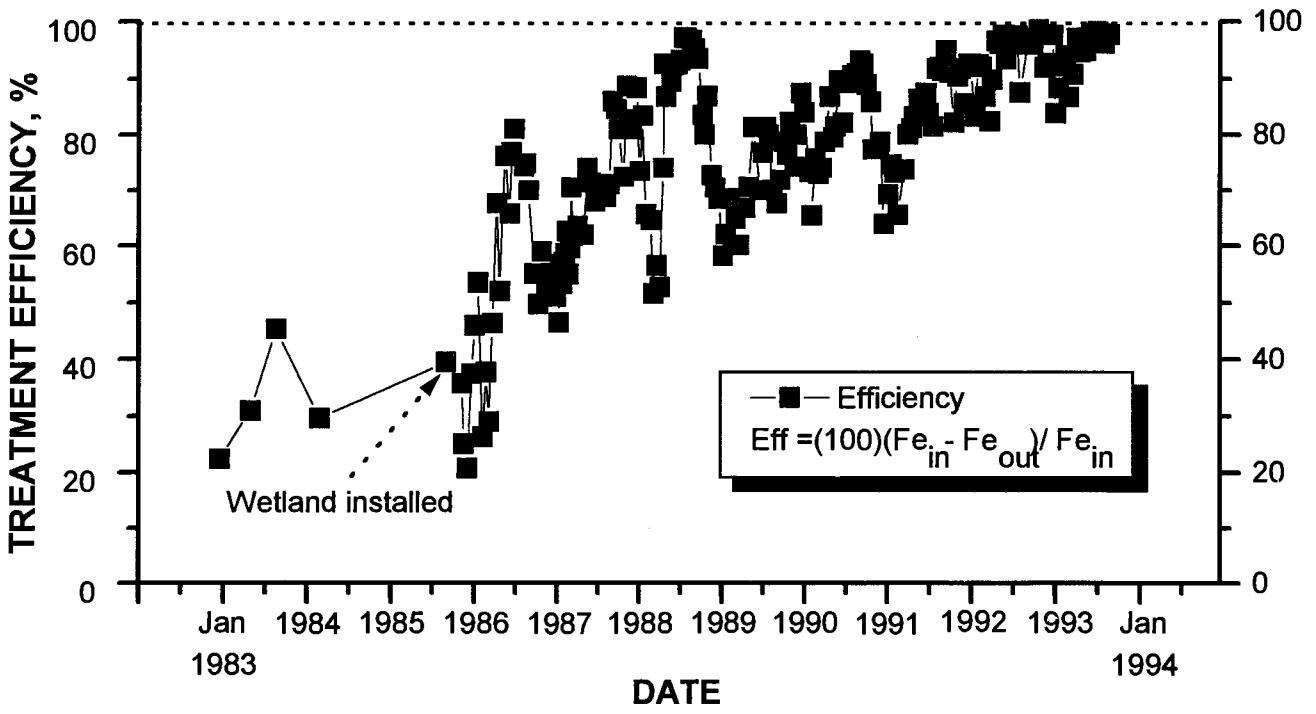

Figure 3. Treatment efficiency for iron at the Simco wetland over the life of the wetland. Pre-wetland values are shown from 1983 to 1985.

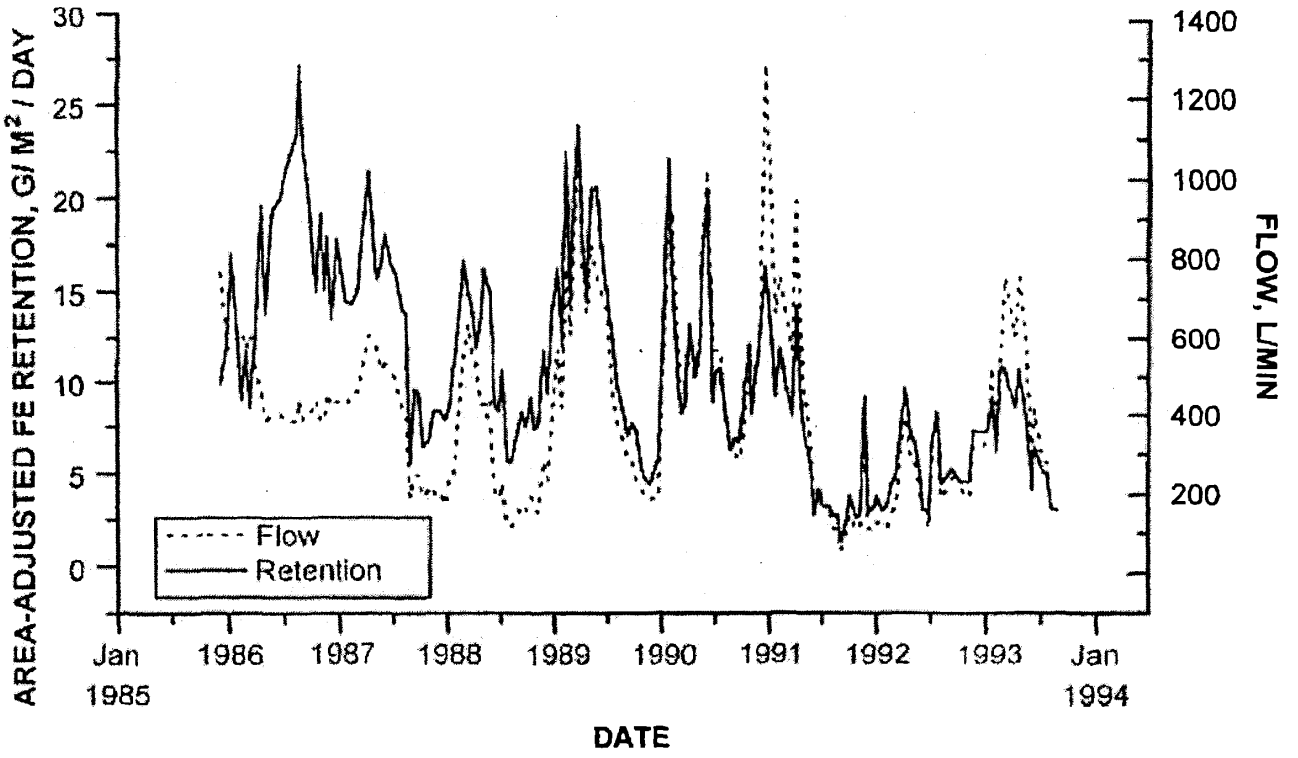

Figure 4. The relationship of area-adjusted iron retention and flow rate at the Simco wetland over the life of the wetland.

Discussion

Is Iron Treatment at Simco Improving With Age?

Evidence indicating that the Simco wetland has improved in its ability to retain iron over its 8-yr history is twofold. First, during the initial few years following installation, frequent chemical treatment of the discharge water from the wetland was necessary. The frequency and duration of chemical treatment has declined as the wetland has aged. Over the last 3½ yr, chemical treatment of the wetland discharge has not been necessary to meet Federal compliance for iron. Water treatment was judged by Ohio authorities as sufficient to warrant the removal of chemical treatment equipment in 1993. In addition, the site was previously declared a national urban wildlife sanctuary in 1990, and the Ohio Division of Wildlife accepted the wetland area as an official natural area in 1993.

Second, treatment efficiency for iron at Simco has improved over time to its current level above 90%. Two measures are commonly used to assess the performance of constructed wetlands with respect to mine water treatment: treatment efficiency and area-adjusted iron retention. We have shown here (and elsewhere, Stark 1990) that treatment efficiency is a better index of wetland performance for iron: the swamping effect of flow rate and iron load on area-adjusted Fe retention makes it an inappropriate evaluative tool (although a valuable design parameter). Iron load at Simco is very strongly positively correlated to area-adjusted Fe retention ($r = +0.88$, $p < 0.001$), such that a knowledge of the load of iron to the wetland explains 80% (r^2) of the observed variation in iron retention. Therefore, the findings that area-adjusted Fe retention at Simco has not changed significantly over the wetland history and has basically fluctuated with flow rate ($r = +0.68$, $p < 0.001$) are not surprising.

Evidence countering the contention that the observed improvement in iron treatment efficiency over time at Simco indicates an age-related wetland phenomenon is also twofold. First, the source water iron concentration has declined with time. From 1986 through 1988, inlet Fe concentration averaged near 125 mg/L. However, since

1991, inlet Fe concentration has averaged less than 100 mg/L. Outlet iron concentration has mirrored inlet iron concentration, such that lower outlet total iron levels are in part a product of lower inlet levels. A correlation of inlet and outlet iron concentration reveals that a strong correlation is present ($r = +0.65$) and that 43% (r^2) of the variation in outlet Fe is a product of inlet Fe.

Table 2. Pearson product moment correlation coefficients (r) between the two performance indices and a variety of water quality parameters for total iron.

Performance Index	Inlet [Fe]	Outlet [Fe]	Fe load	Flow rate	Treatment efficiency
Inlet [Fe]	—	—	—	—	—
Outlet [Fe]	+0.65**	—	—	—	—
Fe load	+0.31**	+0.70**	—	—	—
Flow rate	-0.23*	+0.29**	+0.82**	—	—
Treatment efficiency	-0.44**	-0.94**	-0.74**	-0.46**	—
Area-adjusted mass retention	+0.41**	+0.54**	+0.89**	+0.68**	-0.53**

*significant at $p < 0.01$
**significant at $p < 0.001$

Secondly, the addition of a fourth wetland cell at Simco in 1989 is probably at least partly responsible for the increase in treatment efficiency observed at Simco. However, a calculation of the treatment efficiency at Simco using outlet total iron values from Cell 3, rather than from the system outlet, reveals that (1) substantial increases in efficiency occurred in the first 3 yr, (2) efficiency stabilized over the next 3 yr, and (3) efficiency has increased during the last 2 yr. Thus it appears that the oldest three wetland cells improved in their ability to retain iron while becoming established wetlands, and then have, at the very least, maintained a level of retention without declining.

Why Has Simco Improved With Age?

After 8 yr of operation, the Simco wetland has shown no signs of declining iron retention or pH mitigation. This phenomenon is probably due to a variety of factors; several nonexclusive hypotheses are presented below.

Presence of Moderate Mine Water. Although acidity exceeds alkalinity at the source, the pH is near neutrality (6.5) and alkalinity is present in significant concentrations (88 mg/L). Iron concentrations have generally been < 100 mg/L, with most of the iron present in the ferrous form. Iron oxidation and precipitation of amorphous iron hydroxides (ferrihydrite) under these conditions are rapid (Ferris et al. 1989). The only water pollutant present is iron. Constructed wetlands have been shown to mitigate iron levels effectively at a variety of pH levels (e.g., Wieder 1989).

Wetland Design and Modifications. The Simco wetland was designed in 1985 to have a bed slope of 1%. This has resulted in a tendency of water to channelize during high flows and/or colonization by muskrats or beavers. To alleviate channelization and decrease the surface water depth in the wetland, the source water was split in 1987, effectively halving the flow rates to each of the upper two cells (fig. 1). Simultaneous with this, a series of straw dikes was installed in each cell (about five per cell), forcing the water to flow gently back and forth within each wetland cell. Following these modifications, treatment efficiency increased substantially for iron. Periodically the straw dikes have been reinforced, and about every 2 yr muskrats or beaver have had to be trapped out of the system in order to maintain the integrity of the study.

The configuration of Simco has proven to be effective in eliminating discharges of iron during the heaviest of summer storms. For example, during a storm lasting 3 days during which 13 cm of precipitation fell, iron concentrations at the NPDES point remained in compliance, despite an outflow rate that exceeded the inflow rate by a factor of 3 during the downpour. We attribute the presence of three ponds downstream of the wetland proper as a positive factor in ensuring effective iron retention during storms (Stark et al. 1994).

The Simco wetland is deeper, both by design and as a result of the aging process, than most constructed wetlands designed to treat iron. Initially, the depth of the compost at Simco was about 50 cm. Direct measurements of compost depth began in 1988 and indicate that substrate depth in the upper three cells has increased to 80 cm through 1993, for an average annual accumulation of 3.75 cm. However, most of this accumulation occurred during

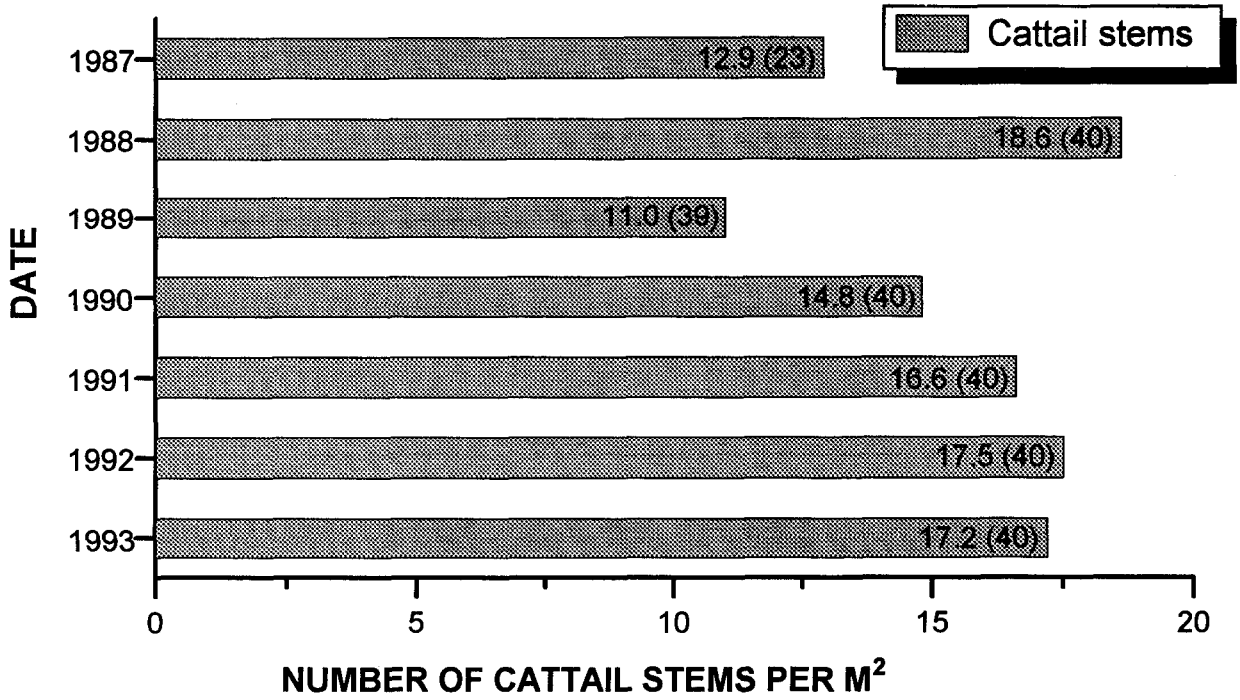

Figure 5. Mean cattail (Typha latifolia) stem density since 1987 at the Simco wetland (n-values in parentheses).

the first 4 yr of operation. The deep substrate creates a deep reducing zone that slowly transforms oxides of Fe into reduced iron (unpublished data). The canyon location assures that the gradual buildup of iron will not diminish treatment by providing a natural freeboard.

Role of Cattails. Cattail density may be related to treatment efficiency: the three highest annual mean treatment efficiencies (1988, 1992, 1993) correspond to the three highest mean cattail densities. The degradation of cattail biomass supplies the ultimate carbon source to the subsurface bacteria in the wetland, suggesting that there should be a lag time between summer density and peak treatment efficiency. However, this was not observed. A dense growth of cattails may result in better water treatment by encouraging a sheet flow rather than channelization, and diffusing the water flow. In addition, cattails remove water through transpiration, decreasing flow rates through the wetland, which should enhance treatment. For example, during the summer months, it is usual for the outflow rate to be 25% less than the inflow rate. Finally, the dense cattail growth may mirror overall temperature-dependent biological and chemical transformations within the wetland.

Vegetation Patterns at Simco

Aside from the anomalous year 1988, cattail density has generally increased each year, becoming fairly stable in 1991. It therefore required six growing seasons for the cattail productivity to reach a stable level at Simco. The timing corresponds roughly to a steady, high treatment efficiency level for iron.

Coverage of non-Typha species, however, has declined from a second summer high of 40% in 1987 to a current level of only 4% in 1993. This decline is principally a result of the surge in growth of Leersia to 22% in 1987, followed by a drop off in Leersia coverage to present levels of <1% in each of 1992 and 1993. There are currently no co-dominant species in the upper three cells: not a single species other than Typha latifolia occupies more than 1% of the wetland surface.

Table 3. Mean percentage cover and species diversity of non-cattail plant and algal species (grouped) at the Simco wetland, Cells 1-3; diversity includes Typha latifolia.

Species	1986	1987	1988	1989	1990	1991	1992	1993
Acer sp.	---	---	<1	---	---	---	---	---
Ailanthus altissima	---	<1	---	---	---	---	---	---
Alisma aquaplantago	---	1	<1	5	---	---	---	---
Epilobium sp.	---	1	---	---	---	---	---	---
Equisetum arvense	<1	<1	---	---	---	---	---	---
Impatiens sp.	---	---	---	---	---	<1	---	---
Leersia oryzoides	4	22	11	1	6	4	<1	<1
Lemna minor	4	2	5	1	1	2	1	1
Phalaris arundinacea	<1	2	---	---	---	---	---	---
Phleum pratense	---	---	<1	---	---	---	---	---
Polygonum sagittatum	<1	<1	---	---	---	---	---	---
Salix sp.	<1	---	---	---	---	---	---	---
Spirea sp.	---	---	---	---	---	<1	---	---
Verbena hastata	<1	---	---	---	---	---	---	---
ALGAE:								
Chlamydomonas sp.						---	---	---
Euglena sp.						---	---	---
Microspora sp.						12	---	1
Oscillatoria sp.						---	3	1
Total algae[1]	5	12	3	12	---	12	3	2
Total cover (non-*Typha*)	13	40	19	19	7	18	3	4
Species Diversity	12	13	10	8	7	6	4	5

[1]blanks indicate that individual algal species coverage was not determined prior to 1991.

Species diversity also reached a peak in the second summer (1987), with 13 species present. However, diversity has steadily declined to only five species in 1993. We can assume that the species initially showing up in the wetland were probably planted incidentally along with the cattails. As Kadlec (1989) found in constructed wetlands receiving municipal wastewater, species diversity has declined to favor almost exclusively cattails. The latter author suggested that the constant pollutant load and supply of water works against species diversity and favors

pollution-tolerant species. A constructed wetland receiving a steady supply of mine water will seldom "dry down," which is a phenomenon that encourages a variety of plant species to colonize. Rather, conditions are fairly stable with respect to water availability and water quality. Pollutants, in this case iron, are constantly present, providing a strong selection pressure for plant species tolerant of iron concentrations not normally found in natural wetlands. Along the periphery of the Simco wetland, a diverse emergent wetland plant community has developed, but nonetheless colonization of the wetland proper by this shore flora is not occurring.

The decline in non-cattail coverage and species diversity has had no negative effects on iron treatment at Simco. It is apparent that iron treatment is not related to the presence or the abundance of non-Typha species. However, the density of Typha latifolia shoots may be related to improved water treatment for iron; this contention remains to be demonstrated.

Acknowledgments

The authors acknowledge American Electric Power Service Corporation (Simco, Inc., contracts C-6900 and C-8161) for support. This project was also supported by federal funds from the U.S. Bureau of Mines and the National Mine Land Reclamation Center under Cooperative Agreement C0388026. We thank H. Webster, R. Hedin, W. Wenerick, and R. Nairn for insightful discussion; C. Urban, M. Ulrich, R. Ventorini, and R. Stark for field and laboratory assistance; R. Stark for assistance with figures and statistics; W. Bosworth and T. Romanoski for technical support throughout the project; and Dave DeVault and Jim Foster for field support.

Literature Cited

APHA. 1985. Standard Methods for the examination of water and wastewater, 16th ed. American Public Health Association, Washington, DC.

Daubenmire, R. F. 1970. Steppe vegetation of Washington. WA Agricultural Experiment Station Tech. Bull. 62.

Ferris, F. G., K. Tazaki, and W. S. Fyfe. 1989. Iron oxides in acid mine drainage environments and their association with bacteria. Chemical Geology 74: 321-330.

Hedin, R. S. and R. W. Nairn. 1992. Contaminant removal capabilities of wetlands constructed to treat coal mine drainage. In: Proceedings of the International Symposium on Constructed Wetlands for Water Quality Improvement. Lewis Publishers, Chelsea, MI.

Hellier, W. W. 1989. Constructed wetlands in Pennsylvania an overview. In: J. Salley, G.L. McCready and P.L. Wichlacz (eds.), Biohydrometallurgy, Proceedings of the International Symposium. Jackson Hole, WY.

Kadlec, R. H. 1989. Wetlands for treatment of municipal wastewater. In: S. K. Majumdar, R. P. Brooks, F. J. Brenner and R. W. Tiner, Jr. (eds.), Wetlands Ecology and Conservation: Emphasis in Pennsylvania. The Pennsylvania Academy of Science, Easton, PA.

Stark, L. R. 1990. A study of natural wetlands associated with acid mine drainage. Final Report, Contract No. H0378021, U.S. Department of the Interior, Abandoned Mine Lands Program, Pittsburgh, PA.

Stark, L.R., R. P. Brooks, F. M. Williams, and L. K. Davis. 1994. Water quality during storm events at two constructed wetlands receiving mine drainage. In review.

Wieder, R. K. 1989. A survey of constructed wetlands for acid coal mine drainage treatment in the eastern United States. Wetlands 9:299-315.

MANGANESE AND IRON REMOVAL FROM COAL MINE DRAINAGE BY USE OF A GREEN ALGAE-MICROBIAL MAT CONSORTIUM[1]

Peter Phillips,[2] Judith Bender,[2] Rachael Simms,[2] Susana Rodriguez-Eaton,[2] and Cynthia Britt[3]

Abstract: At the Tennessee Valley Authority's Fabius Coal Mine, Alabama, manganese was more effectively removed from a pond containing an algae mat consortium and limestone substrate than from ponds containing only limestone or pea gravel substrates. The algae mat resulted from the integration of a microbial mat and volunteer filamentous green algae. The microbial mat consisted of blue-green algae (predominately *Oscillatoria* spp.) and bacteria isolated from the site, cultured in the laboratory, and returned to the site. System operation ran from August 1992 through March 1993. Manganese and iron were consistently removed more efficiently in the algae mat pond (mean flow of 4.2 L/min) than through gravel-only ponds even as water temperatures dropped to less than 5° C in the winter.. Based on filtered water samples, during winter months, at 2 m from the influent point of each pond, the algae mat pond removed 2.59 g/d/m^2 manganese, compared with 0.80 in the limestone pond and 0.37 in the pea gravel pond. At 1 m from the influent pipe in the algae mat pond, 2.67 mg manganese and 34.25 mg iron were deposited in a gram of dried mat. In March 1993 two events likely caused the loss of much of the algae mat: (1) a 50-cm snowfall followed by a heavy runoff and (2) establishment of a snail population, as well as other possible invertebrate herbivores, which consumed the algae mat. The algae mat was reestablished in June 1993 and has persisted to date. A green algae and microbial mat consortium may be a cost- effective treatment technique for permanently removing metals from mine drainage.

Additional Key Words: acid mine drainage, blue-green algae, cyanobacteria, iron, manganese, metal removal, microbial mats, *Oscillatoria*.

Introduction

Manganese removal from acid mine drainage is a challenge due to the solubility of manganese sulfide and the alkaline conditions required to precipitate manganese as an oxide or carbonate. Therefore, it is common to find drainage with manganese above state or U.S. Environmental Protection Agency (U.S. EPA) standards (Gordon and Burr 1989). Additionally, in an oxygenated environment, ferric iron precipitates as $Fe(OH)_3$, and the consequent release of hydrogen ions will increase acidity (Caruccio and Geidel 1993). Thus the dual goal of simultaneously removing manganese and iron from mine drainage is complicated if the system does not have enough alkalinity and a high pH.

The Tennessee Valley Authority utilizes constructed wetlands technology to treat acid mine drainage. These wetlands have generally been effective in removing Mn (0.15 to 1.87 g/d/m^2) and Fe (0.4 to 21.3 g/d/m^2) (Brodie 1993). At one site within the Fabius coal mine in northeast Alabama, Mn and Fe levels are approximately 8 and 6 mg/L (0.45 μm filtered) after leaving an oxidation pond and before draining toward an extensive constructed wetland. At this point a pilot-scale field test was conducted to determine if a biological

---

[1]Paper presented at the International Land Reclamation and Mine Drainage Conference on the Abatement of Acidic Drainage, Pittsburgh, PA, April 24-29, 1994.

[2]Peter Phillips, Research Scientist, Judith Bender, Research Professor, Rachael Simms, Graduate Student, Susana Rodriguez-Eaton, Research Scientist, Research Center for Science and Technology, Clark Atlanta University, Atlanta, GA, USA.

[3]Cynthia Britt, Environmental Scientist, Tennessee Valley Authority, Knoxville, TN, USA.

consortium consisting of a microbial (dominated by cyanobacteria or blue-green algae) and green algae mat would effectively remove residual manganese and iron in a very small pond surface area.

Microbial mats are natural heterotrophic and autotrophic communities dominated by cyanobacteria (blue-green algae). They are self-organized laminated structures annealed tightly together by slimy secretions from various microbial components. The surface slime of the mats effectively immobilizes the ecosystem to a variety of substrates, thereby stabilizing the efficient internal microbial structure. Since mats are both nitrogen-fixing and photosynthetic (Paerl et al. 1989), they are self-sufficient, solar-driven ecosystems with few growth requirements.

In our laboratory, we have developed microbial mats, constructed with specific microbial components, for a variety of bioremediation applications (Bender and Phillips 1993). Mats have been found to reduce selenate to elemental selenium (Bender et al. 1991), to remove Pb, Cd, Cu, Zn, Co, Cr, Fe and Mn from water (Bender 1992, Bender et al. in press), and to remove Pb from sediments (Bender et al. 1989).

Degradation of recalcitrant organic contaminants has also been observed under both dark and light conditions (Bender and Phillips 1993). The following contaminants have been degraded in water and/or soil media by constructed mats: TNT (Mondecar et al. 1993), chrysene, naphthalene, hexadecane, and phenanthrene (Phillips et al. 1993), 2,4,4' trichlorobiphenyl (PCB) (Bender 1993), trichloroethylene (TCE), and the pesticides chlordane (Bender et al. 1993), carbofuran, and paraquat. Radio-labeled experiments with mat-treated carbofuran, petroleum distillates and TCE show that these three compounds are mineralized by mats and mat products, such as biofilms and bioflocculents.

Recently, our data confirm that the mats effectively treat mixtures of organics and a heavy metal by simultaneously sequestering Zn and mineralizing TCE and chrysene. Additional research, currently in progress, shows that U^{238} can be removed from ground water samples.

This project was designed to examine the feasibility of applying mats in a field remediation pilot project to remove residual manganese and iron from acid mine drainage. The broad goals were to assess the performance of mats under environmental conditions, such as determining seasonal survival and the efficiency of the mats in removing metals under day-night conditions. Comparisons in Mn and Fe removal were made among the three ponds: algae mat pond with limestone substrate, a pond with limestone substrate, and a pond with pea gravel substrate (the latter two without mat). Specific experiments in the present study compared the effectiveness of the algae mat and limestone pond compared with controls of limestone or pea gravel alone in removing manganese and iron. Parallel laboratory experiments determined, under more ideal conditions, manganese and iron removal under simulated field conditions.

Methods

Three 40-m^2 ponds were constructed by first lining with polyvinyl chloride. Two of the ponds had limestone substrate, and one had pea gravel substrate layered to create four rises separated by five troughs. Maximum trough water depth was 30 cm. Rises nearly broke the water surface. Mine drainage flowed from an oxidation pond to a trickling filter, both designed to precipitate $Fe(OH)_3$. From the trickling filter, one pipe fed all three ponds (fig. 1). Each pond was sampled for manganese and iron at six or seven points. The ponds operated continuously from August 1992 through March 1993 and again from June 1993.

Cyanobacteria-Algae Mat Pond (CGM)

A cyanobacterial-dominated microbial mat is an entire ecosystem containing several bacteria species, but dominated by cyanobacteria, in the multilayered mat structure. In this pond, microbial mat became enmeshed with volunteer green algae, thus forming an integrated green algae and microbial mat (CGM).

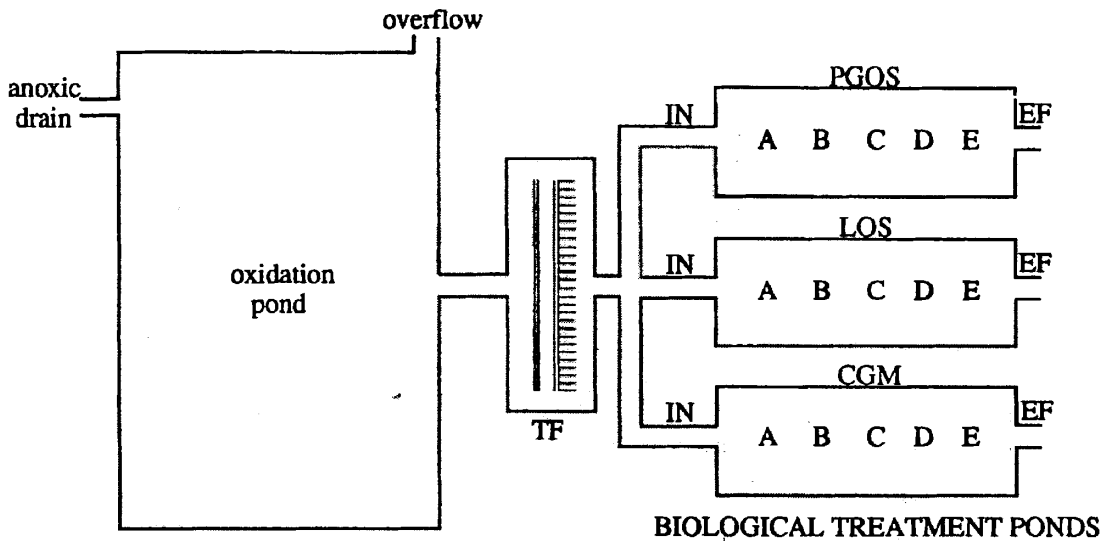

Figure 1. Oxidation pond, TF, trickling filter; IN, influent water; A-E, additional sample points for manganese and iron; CGM, cyanobacteria-algae mat pond; LOS, limestone-*Oscillatoria* pond; PGOS, pea gravel-*Oscillatoria* pond. Not drawn to scale.

Microbial strains, including *Oscillatoria* spp. and purple bacteria (likely a mixture of sulfur and nonsulfur species), were selected from the Alabama site during February 1992. Microbial mats were developed from these strains according to Bender and Phillips (1993). A microbial mat slurry (blended in water) was broadcast over the experimental pond at a rate of 1 to 1.5 L in three applications during a 4-week period. Silage, prepared from grass clippings, added organic acids and several species of ensiling bacteria to the water. Within 2 months a thick green mat covered the entire pond surface. Underneath this floating layer, the limestone itself was covered with a heavy green coating of cyanobacteria.

Limestone-*Oscillatoria* Pond (LOS)

Although no biological component was intentionally added, CGM pond cyanobacteria spread into this pond. Limestone was covered with a thin (<1-mm) film of cyanobacteria but did not develop a surface mat cover as in the CGM pond. Precipitated iron covered the entire limestone substrate of the pond including the pond, periphery beyond the effluent pipe.

Pea Gravel-*Oscillatoria* Pond (PGOS)

The pea gravel substrate in this pond also become thinly (<1 mm) covered with cyanobacteria. Additionally, there was a rapid buildup of precipitated iron at the effluent pipe by December 1992.

Flow Rate

Flow was set initially at 1 L/min and incrementally increased over a period of 2 months. Flow was adjusted on a daily basis owing to clogging by $Fe(OH)_3$. Ranges of flow rates (L/min) were 0.8 to 6.0, with the following mean values for each pond: CGM = 4.2, LOS = 3.8, PGOS = 2.8.

Mn could be removed by chemical precipitation in all ponds. By increasing the flow rate, we expected to reach a break point whereby the two ponds without the substantial biological component would no longer remove manganese as efficiently as the CGM pond. This would demonstrate the greater efficiency of Mn removal by the addition of the biological component.

Water Chemistry

Water samples were collected at the oxidation pond, the trickling filter, at each pond's influent and effluent pipes, and at five points within each pond in a horizontal profile from influent to effluent (fig. 1). If an effluent sample could not be effectively collected, the last point within the pond was considered the effluent sample.

In the field, the oxidation pond, trickling filter, and influent and effluent water was tested for pH (Orion GX series pH electrode; Orion 200 series portable pH and Eh meter), Eh (Corning platinum redox combination electrode; Orion 200 series portable pH and Eh meter), conductivity (Fisher Scientific digital conductivity meter), water temperature, and dissolved oxygen (Otterbine Sentry III dissolved oxygen meter).

For metal determination, water samples were filtered (0.45-μm cellulose acetate) and stabilized for transport with HNO_3. Oxidation pond iron was present mainly as $Fe(OH)_3$ and to a lesser extent as Fe^{+2}. Filtering removed $Fe(OH)_3$, thus only Fe^{+2} was determined. These were later analyzed for manganese and iron content by atomic absorption spectrometry (Varian, Spectra AA-20 BQ, double-beam). Reliability of manganese analysis was regularly verified (QA/QC) by comparing with a synthetic solution containing Mn and Fe (undiluted concentrations of 200 mg/L Mn and 100 mg/L Fe) and diluted with field pond water. The field pond water was a sample drawn directly from a pond.

Mn and Fe Concentration in CGM Mat

To determine the mg Mn and Fe per g algae mat, samples from the CGM pond were dried at 37° C for 24 h. Dried mats were pulverized by mortar and pestle. Triplicate 2 g samples were hydrolyzed by microwave digestion in concentrated HNO_3. Mn and Fe was determined by atomic absorption spectrometry.

Laboratory Comparison

Because it was not possible to keep the two field control ponds free of all biological material, controlled experiments for noting metal precipitation in the presence of a limestone substrate with and without attached microbes were performed in the laboratory.

Mn and Fe Removal. Bench-scale acrylic tanks, measuring 60- by 16.5-cm in surface area, were layered with 3.5-cm-depth limestone substrate. Three experimental tanks were inoculated with laboratory cultures of microbial mats, and three control tanks contained only limestone. The experimental tank microbial mats superficially covered the limestone.

Separate experiments examined Mn and Fe removal independently, as well as in a mixed Mn-Fe solution. The procedure was as follows. Two liters of a 10-mg/L Mn and/or Fe solution was added to a tank. The retention time in the closed tank was 2 min. The tank was elevated to 11 cm at one end. The solution was expelled in one batch. Liquid was collected, and Mn and Fe were measured by atomic absorption. Then the same solution was flowed through again. This was repeated 10 times for each of 6 tanks. Ten repeated flows with the same solution meant that the 2-L solution containing 20 mg total Mn or Fe passed through 1 m^2 (specifically 0.099 cm^2 x 10 flows = 0.99 m^2). Results are presented both graphically as a decrease in Mn and/or Fe in mg/L, and as a Mn and Re removal rate in $g/d/m^2$.

Results

Pond Characteristics

A floating mat (1 to 2 cm thick), composed of filamentous green algae mat and cyanobacteria,

predominantly *Oscillatoria* spp., grew well in the CGM pond after addition of silage amd mat inocula. A secondary mat of cyanobacteria also covered the limestone at the bottom. Thus the metal-contaminated water essentially flowed between a double layer of mat. Approximately 6 weeks were required to establish a full-pond mat cover, but effective metal removal began in the early stages of mat growth.

The thin layer of cyanobacteria covering the rocks of the two ponds designed as controls consisted of an *Oscillatoria* strain resembling that of the inoculated CGM pond cyanobacteria. Small amounts of green algae produced a floating mat, but the biomass remained low compared with that of the experimental pond.

Through winter 1993, the CGM pond maintained a viable algae mat. An approximately 1-m^2 bleached area (indicating cell death) developed during this time. Beneath this bleached algae, limestone was covered with viable cyanobacteria. Iron was evident in patches over the entire surface area of the pond, yet there were also large areas of viable green algae and microbial mat over the pond surface. In contrast to the control ponds, there was no visible evidence of iron precipitates beyond the effluent pipe.

In March 1993, after a 50-cm snowfall thawed, the mat was severely damaged. This may have been due to washout or snow shading. The algae mat pond was drained and reinoculated in June. Metal deposits were left in the troughs.

Water Quality

Table 1 summarizes daytime water quality parameters from August 1992 through April 1993. Dissolved oxygen values for the single nighttime (0530 h) sample were CGM, 4.2 mg/L; LOS, 6.1; and PGOS, 6.8. The low nighttime value for the algae mat pond is likely due to high oxygen consumption by the biological component.

Table 1. Mean daytime water quality parameters per pond.

	Parameters[2]						
Pond[1]	T(sd)	DO(sd)	pH(sd)	ORP(sd)	Cond(sd)	Alk(sd)	Flow(sd)
CGM	14.1(7.6)	7.3(1.3)	7.4(0.4)	413(56.4)	648(136.7)	167(50.8)	4.2(2.4)
LOS	14.7(8.4)	8.3(1.8)	7.6(0.4)	424(73.8)	618(94.7)	168(53.2)	3.2(1.0)
PGOS	14.8(8.5)	8.2(1.9)	7.2(0.5)	410(74.4)	580(92.3)	156(49.1)	2.2(1.6)

[1]CGM=cyanobacteria-algae mat pond; LOS=limestone-*Oscillatoria* pond; PGOS=pea gravel-*Oscillatoria* pond.

[2]T=temperature, Celsius; DO=dissolved oxygen, mg/L; ORP=oxidation-reduction potential (platinum combination Ag-AgCl electrode), mV; Cond=conductivity, μmho/cm; Alk=alkalinity, mg/L equivalent $CaCO_3$; Flow=L/min; sd=standard deviation.

Metals Removal

Manganese removal rates remained high as the flow rate increased in the CGM pond (fig. 2). This is especially significant because figure 2 data came from the winter months when water temperatures were between 4° and 6° C. In December 1992, the flow rate was 4.5 to 6 L/min in LOS and PGOS ponds, which was likely the reason for low Mn and Fe removal in those ponds. The CGM pond continued high-rate removal of Mn until 5 to 8 M from the inflow, while LOS and PGOS showed much lower removal rates, even though Mn concentration in the water remained high (table 2). At lower metal loading, the slower removal rates of LOS and PGOS were sufficient to remove most of the Mn before the effluent point. However, at flow rates of >4.5

L/min, the mechanisms of Mn removal present in these two ponds were saturated, and only the CGM pond continued effective removal. Ferrous iron removal patterns were similar but not as dramatic as for manganese since $Fe(OH)_3$ was removed in the 0.45-μm water filter during sample preparation.

Another way to distinguish the superior CGM pond metal removal efficiency was to determine differences between daytime and nighttime removal. Figure 3 shows the metal removal profiles in all ponds at a flow rate of 5 L/min, during light and dark periods. Mn was effectively removed beginning at 1 to 2 m from the inflow in the CGM pond. These data represent a time period after 4 months of continuous flow.

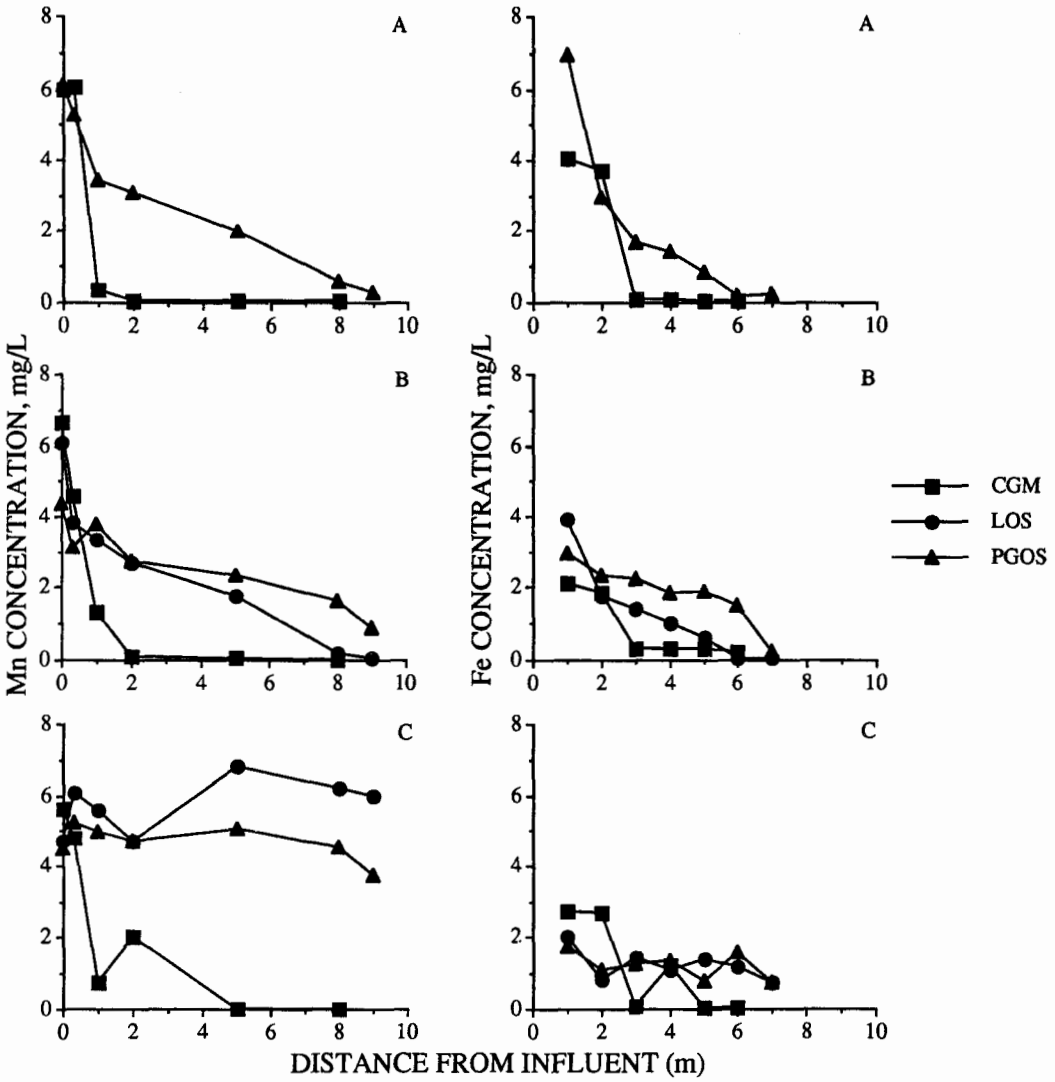

Figure 2. Comparison of Mn and Fe removal at varying rates: *A*, 1.5 L/min; *B*, 3 L/min; *C*, 4.5 to 6 L/min. CGM, cyanobacteria-algae mat pond; LOS, limestone-*Oscillatoria* pond; PGOS, pea gravel-*Oscillatoria* pond.

LOS and PGOS ponds with cyanobacteria covering only their rock substrate did demonstrate metal removal, although not as efficiently. Similar conclusions are difficult to reach with Fe because nighttime mg/L values were very low at the influent pipe (0.11 and 0.09) in the LOS and PGOS ponds. CGM pond filtered Fe enters at 4.39 mg/L and drops to 0.48 mg/L at 1 m.

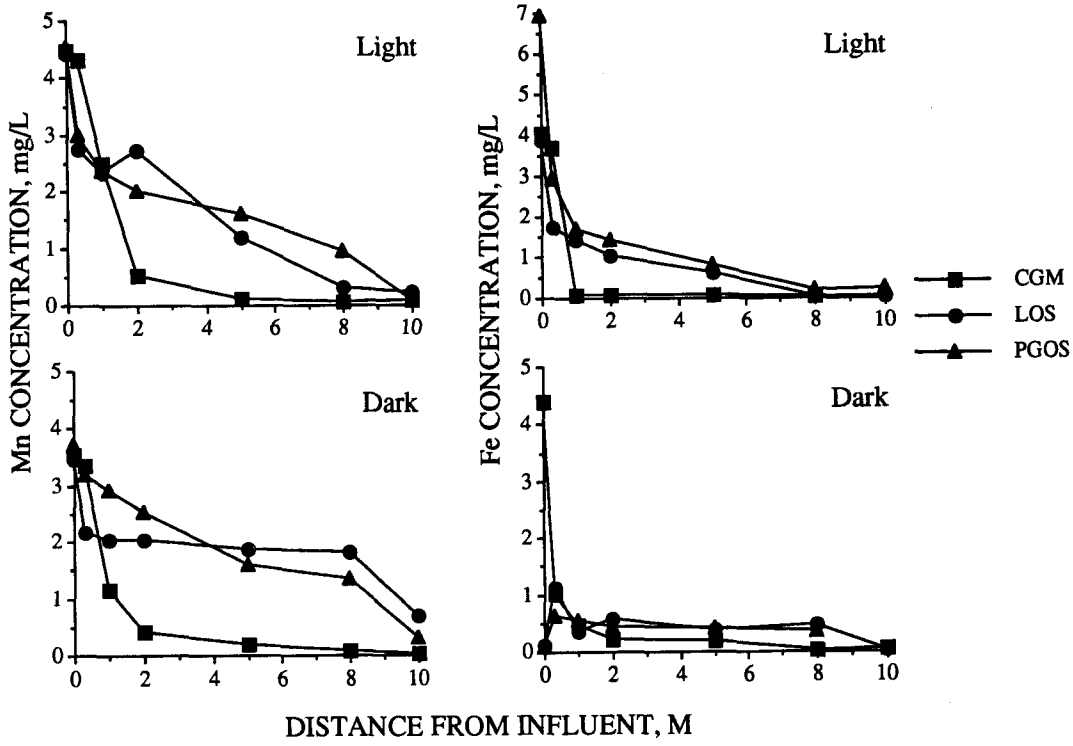

Figure 3. Day-night comparison of Mn and Fe removal among three ponds after 4 months of continuous flow. CGM, cyanobacteria-algae mat pond; LOS, limestone-*Oscillatoria* pond; PGOS, pea gravel-*Oscillatoria* pond.

Table 2. Manganese removal rates (g/day/m^2).[1]

Pond	Flow L/min	Influent Mn	2 m	5 m	8m
CGM	4.2	4.79	2.59	3.87	.74
LOS	3.8	3.78	.80	.55	.52
PGOS	2.8	4.47	.37	.86	.58

[1] Because of the plumbing design, it was not possible to standardize the three pond flows to the same rate.

[2] CGM=cyanobacteria-algae mat pond; LOS= limestone-*Oscillatoria* pond; PGOS=pea gravel-*Oscillatoria* pond.

[3] Two, 5, and 8 m represent points C, D, and E in figure 1.

Table 3. Metal concentration (mg metal per g dried mat) from CGM pond, January 1993.[1]

Location	Mn	Fe
1 m from Influent	2.67	34.25
Pond center	.98	11.20
Point E (near effluent)	.45	.79

[1] The highest concentration of metal was present as crystalline deposits in the pond troughs. Metal speciation of these precipitates is currently in progress (J. Neil, US Geological Survey).

Manganese Removal Rate. Mn removal rates presented in table 2 for the three ponds were calculated at 2, 5, and 8 m from the influent point. Five meters cooresponds to point D and 8 m point E in figure 1.

Mn and Fe Concentration in CGM Mat. Dried, ground, and hydrolyzed mat samples from the CGM pond revealed large decrease in manganese and iron concentration from influent to effluent points (table 3). Mn concentrations declined by 83% and Fe concentrations declined by 98%.

Laboratory Comparison

Figure 4 illustrates the removal of Mn and Fe in laboratory tanks by measuring the mg/L metal decrease in the effluent solution. Overall pH was approximately 8.0 in all tanks.

Mn Removal Alone. After 10 flows of an initial 10-mg/L Mn solution, data conversion to g/d/m² metal removal for three experimental tanks showed Mn removed at 1.93, 1.62, and 1.48 g/d/m² (overall average 1.68 g/d/m²). Three control tanks had removed Mn at 1.07, 1.34, and 0.88 g/d/m² (overall average 1.10 g/d/m²).

Mn-Fe Mixed Solution Removal. In another experimental set (fig. 4; right), Mn removal may have been inhibited by the presence of a similar 10-mg/L Fe concentration.

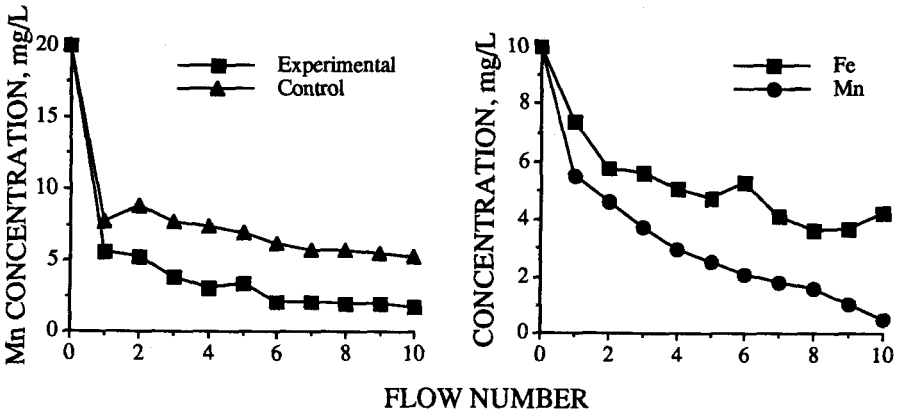

Figure 4. Left: Laboratory tank experiments in Mn removal without and with an algae mat. Right: Laboratory tank removal of Mn-Fe mixed solution.

Discussion

In the CGM pond, although there was manganese-cell binding tothe floating algae mat, visual observations indicated that even more manganese was deposited as precipitaates at the pnd bottom. Fe entered the treatment pond primarily as a flocculated precipitate which becme entrapped in the filamentous algae. in general, day-night and winter-summer meal removals were essentially the same for the CGM pond. The LOS and PGOS ponds showed Mn breakthrough (Mn outflow release > U.S. EPA regulations of 2 mg/L) during nighttime sampling or when mine drainage flow exceeded 4.5 L/min. $Fe(OH)_3$ accumulated at the end of the effluent pipes in the LOS and PGOS ponds. This did not occur at the effluent of the CGM pond.

The biological component and biological processes were responsible for the addition consistent metal removal in the CGM pond. In addition to the algae mat, all exposed limestone surfaces were effectively covered by cyanobacteria. Metals are known to complex with a wide range of organic material, including microbes and their organic releases. Dunbabin and Bowmer (1992) identify four dominant binding processes that incorporate metals into organic materials: (1) cation exchange, (2) adsorption, (3) precipitation and coprecipitation, and (4) complexation or chelation. Although metals that are adsorbed, precipitated, or complexed can be released back into solution in an equilibrium response, no such fluctuations were detected in the CGM pond. Additionally, conditions of neutral pH with high dissolved oxygen and redox levels (mediated by the biological component) favor the chemical precipitation of manganese oxides and iron

hydroxides. These oxides and hydroxides, in turn, act as reservoirs for additional metal deposit.

It is curious that, although LOS and PGOS do not function as well as CGM in Mn removal, they show high oxidation-reduction potential and dissolved oxygen levels. It may be important to consider the microzones present in the thick algal mat, which are absent in the LOS and PGOS ponds. While the gross water quality measurements were similar in the three ponds, the microlevel water quality conditions have shown large variability in previous laboratory research with microbial mats (Bender and Phillips 1993). Mats in the laboratory are known to entrap oxygen in their slime. If this occurred in the CGM pond, as the metal-laden water passed through the labyrinth of algae filaments, it was possibly exposed to elevated oxygen regions, which rapidly precipitated Mn. Examination of the underside of the mat showed that initial precipitation may occur in that location. As precipitation continues, sections of mat break and fall to the bottom, collecting in the troughs. These regions of concentrated manganese oxide deposits function as autocatalytic nuclei for further deposition of the Mn.

Although the conditions of high oxygen and high Eh generated in algae mat microzones as well as autocatalysis may be central to the deposit of Mn oxides, other factors may be functional as well. Other laboratory research has shown that specific bioflocculents were released by the mat in response to the presence of Mn^{+2} (Rodriguez-Eaton et al. 1993). These materials carried surface charges ranging from -58.8 to -65.7 mV. The charges changed to +1.8 in the presence of divalent metal, indicating metal binding to the bioflocculent.

The potential bioavailability of metals is favored by increases in acidity, reducing power, and salinity. Since the mat generally reduces acidity and sequesters certain anions from the water column, including chloride, the stability of the metal deposit is favored. Although anaerobic zones can be identified within the mat in laboratory experiments (Bender and Phillips 1993), the redox conditions of field water remained high. The purple sulfur bacteria, probably *Chromatium* spp.(positive identification not completed), was inoculated as part of the microbial mat group in order to maintain low-sulfide conditions. These autotrophs sequester H_2S instead of H_2O for photosynthesis, thereby decreasing the reducing power of the aqueous environment. Since *Chromatium* spp. typically colonizes in natural mats found in the environment, it can be expected to persist in the constructed field mats. Purple photosynthetic bacteria were also identified in the CGM pond.

It is likely that several mechanisms, including flocculation, cell sorption, autocatalysis, and mediation of the environmental conditions of pH, Eh, and oxygen concentration, contribute to the metal removal.

Acknowledgment

Funding for this project was received from the Tennessee Valley Authority, Chattanooga, TN (TVA Contract TV-89721V) and the U.S. Environmental Protection Agency (Grant No. CR81901); both grants were to Clark Atlanta University.

Literature Cited

Bender, J. 1992. Recovery of heavy metals with a mixed microbial ecosystem. Final report to the U.S. Bureau of Mines, Grant G0190028.

Bender, J. 1993. Biological effects of cultured cyanobacteria mats on water contaminants. Report #1 to the US Environmental Protection Agency, Grant CR8168901.

Bender, J., E. R. Archibold, V. Ibeanusi, and J. P. Gould. 1989. Lead removal from contaminated water by a mixed microbial ecosystem. Water Sci. & Tech. 21(12):1661-1664.

Bender, J., J. P. Gould, Y. Vatcharapijarn, and G. Saha. 1991. Uptake, transformation and fixation of Se(VI) by a mixed selenium-tolerant ecosystem. Water, Air and Soil Pollution 59:359-367.

Bender, J., R. Murray, and P. Phillips. 1993. Microbial mat degradation of chlordane. p. 135-139. In J.L. Means and R.E. Hinchee (eds.), Emerging Technology for Bioremediation of Metals, Lewis Publishers, Boca Raton.

Bender, J., and P. Phillips. 1993. Implementation of microbial mats for bioremediation. p. 85-98. In J.L. Means and R.E. Hinchee (eds.), Emerging Technology for Bioremediation of Metals, Lewis Publishers, Boca Raton.

Bender, J., J. R. Washington, and B. Graves. In press. Metal sequestering with immobilized cyanobacteria mats. Int. J. Water, Air and Soil Pollution.

Brodie, G. 1993. Aerobic constructed wetlands and anoxic limestone drains to treat acid drainage. Constructed Wetlands Workshop for Electric Power Utilities, Tennessee Valley Authority. (Chattanooga, TN, August 24-26, 1993). 10 p.

Caruccio, F. T., and G. Geidel. 1993. Acid-mine drainage/quality workshop manual. Constructed Wetlands Workshop for Electric Power Utilities, Tennessee Valley Authority. (Chattanooga, TN, August 24-26, 1993). 46 p.

Dunbabin, J. S., and K. H. Bowmer. 1992. Potential use of constructed wetlands for treatment of industrial wastewaters containing metals. Science of the Total Environment 111:151-168.

Gordon, J. A., and J. L. Burr. 1989. Treatment of manganese from mining seep using packed columns. J. Environ. Eng. 115(2):386-394.

Mondecar, M., J. Bender, J. Ross, W. George, and J. Preslan. 1993. Removal of 2,4,6-trinitrotoluene from contaminated water with microbial mats. p. 342-345. In R.E. Hinchee, D.B. Anderson, F. B. Metting, and G.D. Sayles (eds.), Applied Biotechnology for Site Remediation, Lewis Publishers, Boca Raton.

Paerl, H. W., B. M. Bebout, and L. E. Prufert. 1989. Naturally occurring patterns of oxygenic photosynthesis and N_2 fixation in a marine microbial mat: physiological and ecological ramifications. p. 326-341. In Y. Cohen and E. Rosenberg (eds.), Microbial Mats, American Society for Microbiology, Washington, DC.

Phillips, P., J. Bender, J. Word, D. Niyogi, and B. Denovan. 1993. Mineralization of naphthalene, phenanthrene, chrysene and hexadecane with a constructed silage-microbial mat. p. 305-309. In R.E. Hinchee, D.B. Anderson, F. B. Metting, and G.D. Sayles (eds.), Applied Biotechnology for Site Remediation, Lewis Publishers, Boca Raton.

Rodriguez-Eaton, S., U. Ekansmesang, and J. Bender. 1993. Release of metal-binding flocculents by microbial mats. p. 118-123. In J.L. Means and R.E. Hinchee (eds.), Emerging Technology for Bioremediation of Metals, Lewis Publishers, Boca Raton.

ARSENIC AND NICKEL REMOVAL BY WETLAND SEDIMENTS

Andrew Fyson[2], Margarete Kalin[2], and Les W. Adrian[3]

Abstract: Laboratory experiments were carried out to test the capacity of sediments from muskeg ponds to treat waste rock seepages with mean concentrations of As and Ni of 36 mg/L and 79 mg/L, respectively (1992 data). Seepage water was added to column reactors containing muskeg sediment, and additions of organic matter (alfalfa, potato waste and hydroseeding mulch) were made to the sediments to stimulate microbial activity. In the first experiment, arsenic concentrations in the water column of the reactors decreased to less than 1 mg/L from 50 mg/L, and Ni to less than 0.1 mg/L from 74 mg/L in 112 days. A second experiment established that the results are reproducible. More than 90% of As and Ni present at start-up is removed within 43 days. A third experiment indicated that alfalfa and potato waste increased the rate at which reducing conditions were established, which in turn resulted in increasing the rate of arsenic and nickel removal from the seepage water. The addition of alfalfa resulted in greater metal removal than when potato waste was used. These experiments have shown that muskeg sediments have the capacity to remove As and Ni from a waste rock seepage water through providing conditions that facilitate precipitation and adsorption with or without the addition of organic amendments.

Additional Key Words: acid mine drainage, passive treatment, sulfate reduction, iron reduction.

Introduction

Waste rock piles from metal mining operations often generate seepages with low pH and high concentrations of heavy metals. Depending on decommissioning methods chosen, contaminated seepage waters may emerge from waste rock piles for a long time. Treatment may therefore be required in perpetuity. Passive treatment systems, utilizing natural processes driven by bacteria, are attractive treatment alternatives, as opposed to maintaining a chemical treatment plant. Such systems would provide a low maintenance option and are environmentally sustainable.

Research on the utilization of wetlands for the treatment of a variety of wastewaters has been carried out in the past decade, including constructed wetlands treating acid mine drainage (AMD) from coal operations (Brodie 1988, Hammer 1989). Wetlands are considered passive treatment systems, since they have the capacity to regenerate themselves through continued growth.

Microbially-driven sulfate and iron reduction are processes occurring naturally in wetland sediments which facilitate the removal of metals from the AMD through increasing the pH, which in turn results in precipitation of the metals either as hydroxides or as sulfides (Wildeman 1993, Kalin 1993). Adsorption processes, which assist in metal removal, can also be active in wetlands. Wieder (1992) has provided some estimates quantifying different metal removal mechanisms in wetlands. Eger and Lapakko (1989) utilized peat in constructed wetlands to treat AMD with Ni concentrations up to 15 mg/L, following laboratory studies where peat was observed to adsorb up to 20 g Ni/kg dry weight.

Kalin (1993) reported Ni concentration reductions in an AMD tailings seepage from an initial concentration of 25 mg/L originally to less than 1 mg/L. The microbially-driven treatment system removes Ni likely by co-

---

[1]Paper presented at the International Land Reclamation and Mine Drainage Conference and the Third International Conference on the Abatement of Acidic Drainage, Pittsburgh, PA, April 24-29, 1994.

[2]Andrew Fyson, Microbiologist and Margarete Kalin, Ecologist, Boojum Research Ltd., Toronto, Ont, Canada.

[3]Les W. Adrian, Environmental Engineer, CAMECO Corp., Saskatoon, Saskatchewan, Canada.

precipitation with iron. When reducing conditions are established in the treatment system, Ni also potentially precipitates as a sulfide. Through additions of organic matter to the sediments, it should be possible to stimulate microbial activity and thereby maintain the capacity of the sediment to remove metals from water. If reducing conditions can be achieved in the sediment, a biological treatment system, for seepage waters which contact sediments in muskeg ponds, would be developed.

This paper presents the results of laboratory reactor experiments in which waste rock seepage water was added to sediments from muskeg ponds. The objective of this study was to determine the chemical and microbial processes which take place in the sediment and define the specific conditions necessary for metal removal.

Materials and Methods

Laboratory reactors were set up, constructed from acrylic columns with a diameter of 10 cm and a total volume of 2.5 L. The reactors were gas-tight and fitted with rubber stoppers as sampling ports. In the first set of experiments, sediment samples were supplemented with an amendment consisting of 10 % w/w of ground alfalfa and 90 % w/w of weathered hydroseeding mulch. Prior to addition to each column, 100 cm^3 of the amendment blend were mixed into 300 cm^3 of the sediment sample. The reactors were then filled with 1.0 to 1.5 L of test water, leaving approximately 0.5 litres of headspace in each reactor. The test water (station 6.11) is from a seepage collection pond next to the waste rock pile of a uranium mining operation in northern Saskatchewan, Canada. Three types of sediments from three different locations in two muskeg ponds in the same drainage basin of the waste rock pile were used in the first experiment. Water for the reactors was prepared by diluting waste rock pile seepage water with water to 20% of the original seepage concentration, since it was expected that, upon scale-up in the muskeg ponds, a dilution of the concentrations of most ions in the seepage would take place. To increase the arsenic concentrations in the seepage, the water was spiked with KH_2AsO_4 to a concentration of 50 mg/L arsenic to test the ability of the ecosystem to remove As at the maximum concentration likely to be encountered in the field.

A second experiment was set up using sediment from a single location. In this experiment, the same conditions were provided as in the first experiment, including the mixing of organic amendments into the sediment and using diluted (20%) seepage. This experiment was performed in order to establish whether the results obtained in the first experiment were reproducible.

During set-up of the third experiment, new samples of muskeg pond sediments without additions of organic matter (Control) and undiluted waste rock seepage water were added to the reactors. The sediments in the reactors were left for 6 days prior to addition of seepage water (760 mL), thereby allowing them to equilibrate. Those reactors receiving organic matter were treated with a surface layer of potato waste (5 g) or alfalfa (37.5 g). Application of a surface layer to the sediment surface was considered a realistic approach to simulating application of organic matter in field conditions.

To verify the function of sediments in the treatment process, 2 L glass jars with organic material but without sediment at the same ratio as used in the reactors were set up, using 760 mL of seepage water and 5 g potato waste or 37.5 g alfalfa. The quantities of organic matter added to the sediment were based on related work in base metal AMD (Kalin 1993).

Measurements of redox potential, electrical conductivity and pH were made using standard methods. The potential (Em), measured in the reactors, was converted to redox potential (Eh) by the following formula: Eh (mV) = Em (mV) + (241 - 0.66(T°C - 25)) to adjust for the potential of the reference electrode (Hem 1985). Water samples from above the sediment-water interface were extracted from the reactors through the sampling ports with a syringe. Samples were then filtered through 0.45 μm cellulose-acetate filters, acidified with concentrated HNO_3 and stored under ice or at 4°C until required for further analyses. Acidity and alkalinity were determined by titration with 0.01N NaOH (to pH 8.3) and 0.01N H_2SO_4 (to pH 4.5) respectively. Concentrations of Ni and As

were determined by inductively coupled plasma spectrophotometry (ICAP) analysis and total Fe, PO_4, NH_4 and NO_3 were determined by colorimetric methods (Hach). Nickel was determined by the diacetyldioxamine colorimetric method (Merck). Arsenic was determined by the Merck test strip method. Sulfate was determined by the $BaSO_4$ turbidometric method (ASTM 4500-SO_4^{2-}).

Adenosine triphosphate (ATP) concentration, a measure of biomass, was determined with a firefly luciferase test. Cells were lysed with ethanol, filtered, further lysed with acetone, filtered and then ATP was extracted in trisodium phosphate buffer containing Mg-EDTA to prevent inhibition of the luciferase enzyme by heavy metal ions. Sulfate reducers were enumerated with Rapidchek II tests (Conoco, Houston, Texas) which detect the presence of adenosine phosphosulfate (APS) reductase by a colour-linked immunological assay.

Results

The water chemistry of the seepage used in the experiments for 1991 and 1992 is summarized in table 1. The average pH of this water was 4.28. This water is characterized by high concentrations of Ni and As. The seepage water also contains very high nutrient concentrations (ammonium, nitrate and phosphate). The sample used for the laboratory experiments had a Ni concentration of 74 mg/L, an As concentration of 50 mg/L and pH of 3.85.

Table 1. Major chemical parameters in waste rock seepage pumping pond water, 1992.

Parameter		Mean	Standard deviation	Minimum	Maximum	Number of samples
pH	units	4.28	4.38	3.94	5.20	6
Conductivity	uS/cm	1,433	569	259	2,120	6
Total dissolved solids	mg/L	774	524	210	1,360	4
Chloride	mg/L	3.0	1.8	0.8	6.0	6
Bicarbonate	mg/L	2.7	2.1	0.0	5.0	3
Sulfate	mg/L	546	376	86	1,060	5
Calcium	mg/L	137	68	24	210	8
Iron	mg/L	3.3	4.4	0.1	9.6	3
Potassium	mg/L	23	11.9	5.0	46	8
Magnesium	mg/L	51	28	7	92	8
Manganese	mg/L	3.9	1.8	0.9	6.5	6
Sodium	mg/L	28	18.8	3.0	61	5
Ammonia-N	mg/L	4.6	2.4	0.8	7.2	6
Nitrate-N	mg/L	87	39	12.0	128	6
Phosphate	mg/L	34	30	1.0	89	5
Total arsenic	mg/L	36	32	5.4	97	5
Total nickel	mg/L	80	74	4.8	220	5
Aluminum	mg/L	14	27	0.1	68	5

The characteristics of the sediments are given in table 2. The sediments have a diverse microbial population. In two of the sediments, sulfate reducing bacteria could be quantified (1 to 50 x 10^4 cells/mL). Fine particulates plugged equipment which prevented quantification of sulfate reducing bacteria in the third sediment. The ATP values indicate the presence of active microbial populations in all 3 reactors at the time the reactors were set up.

The Ni and As concentrations after 87, 112 and 229 days in the first experiment are given in table 3 for each of the three sediment types used. Nickel concentrations declined in all three reactors to less than 0.12 mg/L by day 87. Thereafter, low Ni concentrations were maintained until the experiment was terminated after 237 days. Arsenic concentrations decreased substantially, in the presence of all three sediments, to 0.4 to 0.7 mg/L.

The results of the first experiment were encouraging. A second experiment was set up to determine the reproducibility of the results obtained. The data collected 115 days after set up are summarized in table 4. Eh values remained positive, but were sufficiently low that denitrification and dissimilatory nitrate reduction could proceed in the water column. These processes, which reduce nitrate to N_2O/N_2 and NH_4, respectively, can generate alkalinity and help establish conditions for further precipitation reactions, through lowering Eh and raising pH. The low NO_3 concentrations (0.41 to 1.94 mg/L) after 115 days also suggest that one or both of these processes has taken place. Sulfate reduction is indicated by the odour of H_2S and decline in the SO_4 concentration. As and Ni concentrations showed a rapid decline in all reactors. More than 90 % of both elements was removed within 44 days. After 115 days, As concentrations were in the range 0.1 to 1.3 mg/L and Ni concentrations were in the range of 0.05 to 0.14 mg/L. These values are in the same range as in the first experiment.

Table 2. Ecological and elemental characteristics of sediments.

Parameter		Sediment		
		BT1-200	BT2-250	BT2-350
Bacteria.....	/mL	86,000,000	140,000,000	170,000,000
Sulfate reducers...	/mL	1000	50,000	ND[1]
Molds.....	/mL	410,000	410,000	1,800,000
Algae.....	/mL	1,500,000	1,400,000	1,900,000
ATP.....	ng/mL	54	51	33
Arsenic.....	ug/g	21	57	411
Nickel.....	ug/g	<97	195	786
Sulfur.....	ug/g	678	2,335	982
Iron.....	ug/g	3,585	5,058	22,683
Phosphorus.....	ug/g	97	681	687
Aluminum.....	ug/g	10,756	13,132	102,121
Calcium.....	ug/g	1,647	4,961	5,990
Magnesium.....	ug/g	1,550	2,043	11,881
Loss on ignition....	%	38	84	11

ND[1] Not determined

Table 3. Arsenic and nickel removal by sediments.

	As, mg/L			Ni, mg/L		
Sediment	87	116	229 days	87	110	237 days
BT2-250	3.00	1.10	0.40	0.12	0.11	0.05
BT2-350	1.90	0.20	0.40	0.06	0.10	0.03
BT1-200	0.60	0.75	0.70	0.06	0.06	<0.01

Table 4. Reactor water chemistry 115 days after setup.

Parameter		Reactor						
		E6-1	E6-2	E6-3	E6-4	E6-5	E6-6	Mean
pH at set up.....	units	6.30	6.36	6.23	6.30	6.25	6.27	6.29
pH.....	units	6.44	6.55	6.73	6.07	7.00	7.00	6.63
Eh.....	mV	+88	+100	+163	+102	+129	+189	+129
Conductivity.....	uS/cm	639	620	585	715	523	554	606
Iron.....	mg/L	5.86	5.15	1.38	7.30	1.20	1.56	3.74
Arsenic.....	mg/L	1.30	0.40	0.10	0.30	0.60	0.60	0.55
Nickel.....	mg/L	0.05	0.05	0.08	0.08	0.06	0.14	0.07
Sulfate.....	mg/L	18	33	71	40	69	76	51
Acidity.....	mg/L	3.9	1.7	10.0	5.9	8.1	2.9	5.4
Alkalinity.....	mg/L	190	223	231	205	192	208	208
Phosphate.....	mg/L	0.29	0.26	0.33	0.37	0.76	0.49	0.42
Ammonium.....	mg/L	1.5	0.7	2.2	6.5	1.4	1	2.2
Nitrate.....	mg/L	1.94	0.48	0.88	0.41	0.75	1.36	0.97

A third experiment examined the amount of metal removal when organic material was added as a surface layer over sediments, rather than mixing the organic material into the sediment.

Control Reactors

In the control reactors, where organic amendments were not added, only minor changes in the water chemistry were observed in 70 days. The pH slightly increased in the first 16 days and thereafter declined slowly to original levels of 4.2 (fig. 1a). Acidity (fig. 1b) and Eh (fig. 1c) remained fairly constant. The iron concentration initially decreased, then abruptly increased (up to 21 days) and decreased again (by 34 days) to near initial levels (fig. 1d). Nickel concentrations declined steadily during the course of the experiment (fig. 1e). Arsenic concentrations remained steady for 21 days and then declined (fig. 1f). The NH_4 concentrations remained steady (fig. 1h) whereas the NO_3 concentrations (fig. 1i) declined from 63 to 12 mg/L (34 days). The PO_4 concentrations decreased somewhat (fig. 1j).

Potato Waste Reactors

In the potato waste reactors, there was an increase in pH from 4.1 to 5.1 (mean of 2 reactors) from day 8 onwards to 34 days after set-up (fig. 1a). This trend continued and by day 64, the mean pH of the two reactors was 6. The Eh decreased during the first 16 days of the experiment (fig. 1c). The abrupt decline in Eh between 10 and 14 days after set-up occurred at the same time as the dramatic increase in acidity (fig. 1b) due to release of reduced iron, and possibly organic acids (from microbial decomposition of starch), from the sediment.

The dramatic increase in iron concentration observed between day 10 and day 21 (fig. 1d) was likely due to ferrous iron concentration increases diffusing from the sediment, following microbial iron reduction, and likely accounts for the reduction in Eh. A much smaller increase in iron (from 0.45 mg/L at day 1 to 3 mg/L at day 20) was observed in the control jars, indicating that some oxidized iron precipitates initially present in the solution were reduced, and/or that the potato waste contains minor amounts of iron.

The observed decreases in phosphate concentrations (fig. 1j) are likely related to the increasing pH over the course of the experiment. As pH increased, more HPO_4^{-2} dissociated into PO_4^{-3} and precipitated primarily with aluminum. Increases in NH_4 during the first 10 days (fig. 1h) can be attributed to the decomposition of protein in the potato waste. Decreases in NO_3 observed between 7 to 10 days (fig. 1i) were likely due to denitrification, facilitated by the decline in Eh and the provision of organic acids as electron donors and carbon sources. A reduction in nitrate concentration was also observed in the absence of a sediment (table 5).

Table 5. Chemistry of control jars without sediments.

Treatment	Days	pH	Eh, mV	Cond, uS/cm	Temp, C	Fe, mg/L	Ni, mg/L	As, mg/L[2]	SO4, mg/L	NH4, mg/L	NO3, mg/L	PO4, mg/L	Acidity, mg/L[3]	Alkalinity mg/L[3]
Potato waste	1	4.12	445	1,620	21.9	0.45	74	50	ND	16	60	59	136	0
	3	4.37	425	1,660	21.8	3.10	74	50	ND	21	51	45	111	0
	8	5.53	90	1,670	13.2	1.10	74	50	594	21	57	59	97	59
	20	4.28	306	1,590	21.6	3.10	64	80	540	12	.3	47	ND	0
	51	6.42	181	1,536	21.9	0.10	73	100	100	18	0	96	103	116
Alfalfa	1	4.44	444	1,510	21.9	0.31	74	50	ND	18	60	48	87	0
	3	5.94	-237	4,100	21.8	0.52	40	50	ND	36	51	57	487	ND
	8	5.72	71	6,120	13.2	3.30	61	50	342	36	7	62	649	2,161
	20	5.69	-119	5,990	21.8	0.40	53	95	160	69	<.2	42	ND	ND
	51	6.83	111	6,110	21.9	ND[1]	17	75	400	500	ND	47	291	2,155

ND[1]Not determined.

[2]Interference with sulfides suspected in ASTM 3500-As Mercuric Bromide Stain method.

[3]mg/L CaCO3 equivalent.

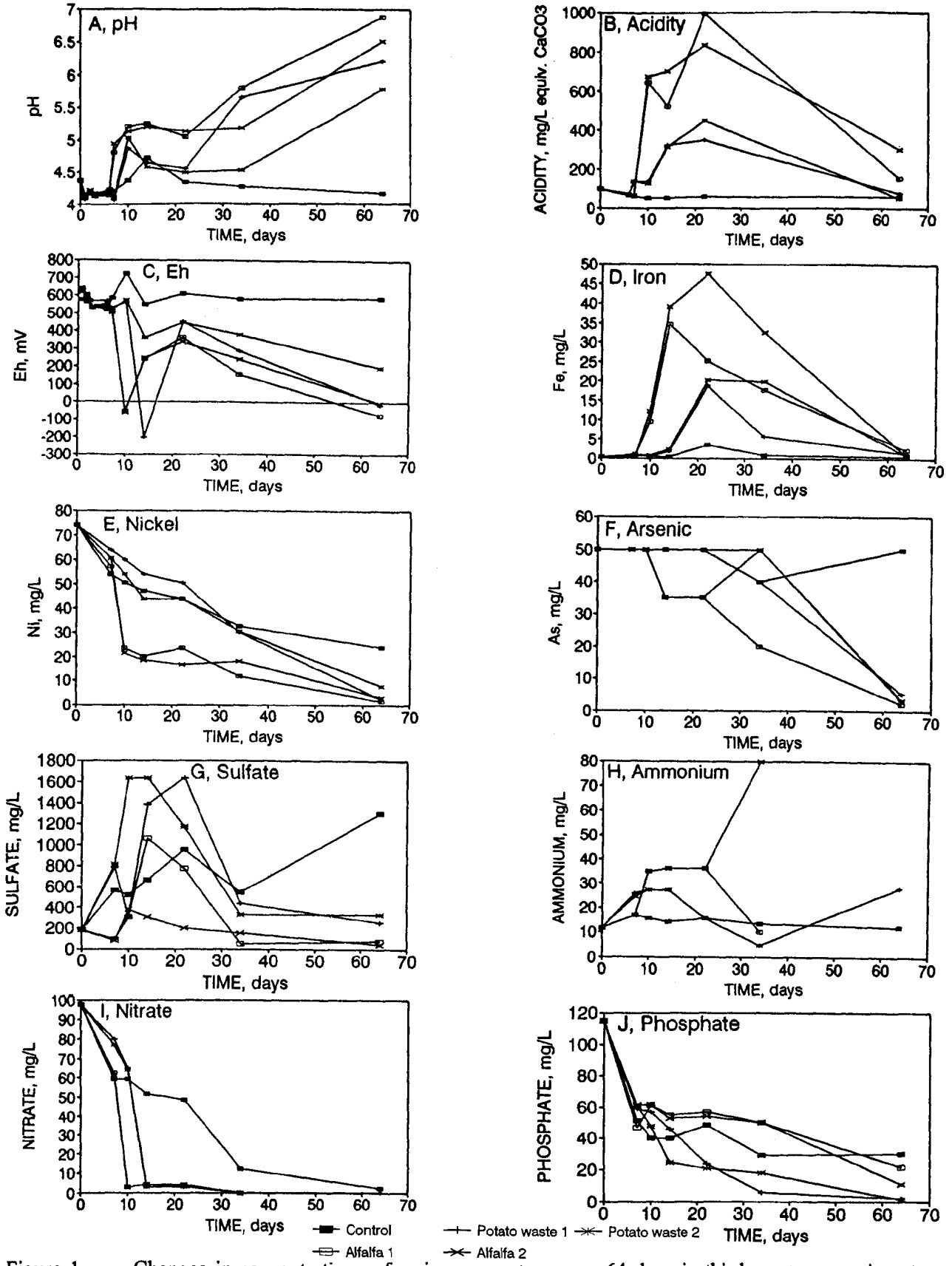

Figure 1. Changes in concentrations of major parameters over 64 days in third reactor experiment.

Ni concentrations decreased in the potato waste reactors over the course of the experiment at rates similar to those observed in the control reactor up to 30 days (fig. 1e). Arsenic concentrations held constant over the first 16 days (fig. 1f). From samples collected 63 days after set up, As concentrations had declined, averaging 4.1 mg/L. Sulfate concentrations increased in the reactors (fig. 1g). Sulfate was likely being released from both the potato waste and the sediments to the overlying water.

Alfalfa Reactors

Most trends of concentration changes in the reactors with added alfalfa were similar to those in the reactors with potato waste, except that concentration changes were more pronounced and changes occurred earlier in the experiment. The Eh decreased, within 2 to 3 days following set-up, to values much lower than in the potato waste reactors (fig. 1c). Greater NO_3 concentration decreases were observed (fig. 1i), more NH_4 was generated (fig. 1h) and higher pH's were reached (fig. 1a) than in the potato waste reactors. Phosphate concentrations declined more slowly than in the potato waste or control reactors, possibly due to release of phosphate from the decomposing alfalfa at a faster rate than precipitation (fig. 1j).

The measured iron concentrations increased (fig. 1d) and, according to the low Eh (fig. 1c), iron was likely in the reduced form, due to iron reduction by bacteria in the presence of alfalfa as a nutrient source. The nickel concentration decreases (fig. 1e) are likely related to production of large quantities of CO_2, with subsequent precipitation of Ni as $NiCO_3$. A consistent decrease in arsenic concentrations was not observed during the first 35 days of the experiment (fig. 1f). By 63 days however, the concentrations in the reactors had decreased to 2.49 mg/L As (mean of 2 reactors) with the exception of the control reactor. These decreases are likely related to the rate of microbial arsenate reduction and arsine production, which require low redox conditions for relatively long periods compared to precipitation reactions.

To determine the effects of the sediments in the metal removal process, and that of the organic material added to the sediment in the reactors, seepage water was tested in 1 L jars with additions of organic matter only. The results are summarized in table 5. After 51 days the organic matter had decomposed, the pH had increased and the concentrations of As, sulfate, nitrate, and phosphate, particularly in the jar with potato waste, had increased in the water. The possibility exists that interferences during colorimetric tests may account for the higher concentrations of As at this time.

Discussion

Arsenic Removal Processes

Arsenic may exist in natural systems as many chemical species, owing to the fact that it two major oxidation states: +V and +III. The oxidation state of arsenic is dependent on the pH and the redox potential (Eh) of the system. A pH-Eh diagram was constructed to show possible forms of arsenic in particular chemical conditions (fig. 2).

At high Eh and low pH, arsenic +V exists as arsenic acid (H_3AsO_4). At higher pH, the As +V species, hydrogen arsenate ions ($H_2AsO_4^-$, $HAsO_4^{-2}$, AsO_4^{-3}) predominate in water. Also, at higher pH, these As +V ions are predominant over an increasingly wide range of Eh; at pH greater than 11, hydrogen arsenate ions are the only arsenic species in a system at Eh between -350 mV and +750 mV (Kotz and Purcell 1987, Stumm and Morgan 1981). Different metals can precipitate with arsenate ions above specific pH's. The average concentrations of metals and arsenic in three field enclosures are taken to calculate the pH of precipitation for these various compounds, including Fe, Al, Ni, Mg, Ca and Zn. They are shown as dotted vertical lines in the diagram.

The Eh values from the reactor experiments are plotted as they were changing over the period of the experiment, from the time at set-up (day 1), on day 10 and on day 64. On day 1, all the reactors lay within the

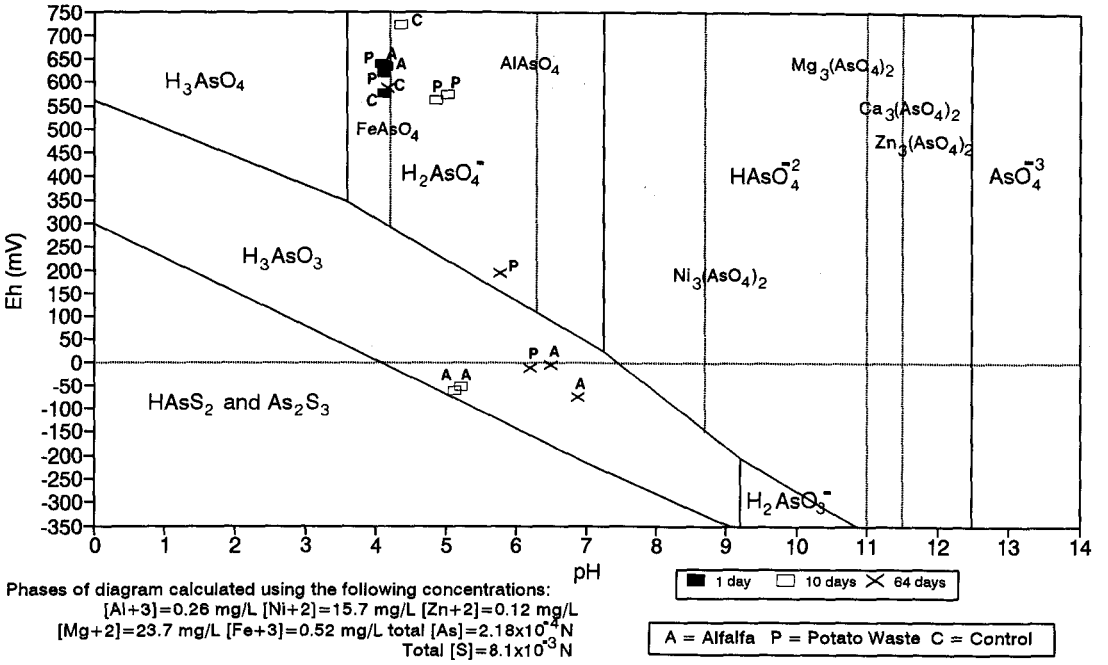

Figure 2. Redox-pH arsenic species phase diagram. Experiment 3 reactors' pH and redox on day 1, 10 and 64 are plotted.

zone where As occurs as $H_2AsO_4^-$. By day 10, the reactors which received organic material had changed considerably; the control and potato waste reactors were still in the $H_2AsO_4^-$ zone, whereas the alfalfa reactors were in the zone where the predominant form is H_3AsO_3. By day 64, one of the potato waste reactors had moved near to the AsO_3 zone, the zone where precipitation of As as sulfides is possible. The control reactor remained in the $H_2AsO_4^-$ zone for the entire 64 days.

Nickel Removal Processes

In aquatic ecosystems, the chemistry of nickel is less complex than arsenic, owing to its predominant oxidation state of +II. Therefore, there is both a more limited variety of chemical species of nickel, and fewer pathways by which dissolved nickel is removed from solution. Nickel is very mobile in acidic, high Eh water, while in high pH, reducing (low Eh) conditions, nickel sulfides can form. In addition, nickel is relatively amenable to adsorption onto iron and manganese hydroxides, clay particles and organic surfaces. Because of these properties, nickel removal can be anticipated in wetland environments with microbially active, reducing, organic sediments.

Summary and Conclusions

The reductions in arsenic and nickel concentrations observed in laboratory column experiments were also demonstrated in field enclosures installed in some of the same wetlands from which the reactor sediments were collected (Smith et al. 1993). Overall, field and laboratory estimates all fall within the same order of magnitude.

The laboratory experiments have established that muskeg sediments represent an effective micro-environment for removal of As and Ni from waste rock seepage water. The metal removal is associated with reducing conditions and is accelerated by the addition of readily degradable organic amendments which feed microbial processes.

The rate of arsenic removal was augmented by the presence of alfalfa, but not by potato waste. Both amendments reduced the Eh and augmented the supply of nutrients for anaerobic, alkalinity-generating microbial processes. This microbial community was active, as suggested by the decline in sulfate, the H_2S odour indicating sulfate reduction, the increases in dissolved iron (Fe III reduction), the dramatic decline in nitrate (denitrification) and the rise in pH. The removal of Ni in the reactors without amendments indicates that the processes involved were already present in the sediment. The addition of alfalfa increased the rates of As and Ni removal, compared to the other treatments. The rapid decline in Ni can be attributed to precipitation of $NiCO_3$ and/or NiS following the rise in pH generated by anaerobic microbial processes, including denitrification, iron reduction and sulfate reduction. Addition of alfalfa, both in the reactors and in the field, increased rates of Ni and As removal.

As a first approximation, the experimental results can be used to estimate the muskeg pond treatment capacity. A decrease of 49 mg in As concentration in the columns with a surface area of 0.005 m^2 in 65 to 110 days is equivalent to 151 $mg/m^2/day$ and 89 $mg/m^2/day$, respectively. For Ni, in all three reactors of the first experiment, nickel concentrations decreased from 12.9 mg/L to 0.2 mg/L in 40 days, equivalent to 64 $mg/m^2/day$. The rates for the third experiment range from 154 to 253 $mg/m^2/day$ for Ni and for As, 196 to 211 $mg/m^2/day$.

The data presented here, together with results from a field experiment (Smith et al. 1993), indicate that long-term exposure of seepage water to wetland sediments is a very promising approach to treatment of this wastewater. Ongoing experiments will determine the long-term stability of precipitates or other forms of the heavy metals held in the ecosystem.

Acknowledgment

The support of this work by CAMECO Corporation is greatly appreciated.

References

Brodie, G.A., D.A. Hammer, and D.A. Tomljanovich. 1988. Constructed wetlands for acid drainage control in the Tennessee Valley. p. 325-351 in Mine drainage and surface mine reclamation. Volume 1. Mine water and mine waste. U.S. Bureau of Mines Information Circular 9183, Washington D. C.

Clesceri, L.S., A.E. Greenburg and R.R. Trussell (eds.). 1989. Standard methods for the examination of water and wastewater. 17th edition. American Public Health Association, Washington D.C.

Eger, P. and K. Lapakko. 1989. Use of wetlands to remove nickel and copper from mine drainage. p. 780-787 in D.A. Hammer (ed.) Constructed Wetlands for Wastewater Treatment. Lewis Publishers, Chelsea, MI.

Hammer, D.A. (ed.). 1989. Constructed wetlands for wastewater treatment. Lewis Publishers, Chelsea,MI. 831 p.

Hem, J.D. 1985. Study and interpretation of the chemical characteristics of natural water. U.S. Geological Survey Water-Supply Paper 2254, 3rd. ed., 264 p.

Kalin, M. 1993. Treatment of acidic seepages using wetland ecology and microbiology. Final report of contract #23440-2-9217/01-SQ of the MEND program of the Canada Centre for Mining and Energy Technology, Energy, Mines and Resources Canada.

Kotz, J.C. and K.F. Purcell. 1987. Chemistry and chemical reactivity. Saunders College Publishing, Toronto. 1020 p.

Smith, M.P., L. Adrian, and M. Kalin. 1993. Arsenic and nickel removal in wetland sediments. In Proceedings of Saskatchewan Annual Conference on Environmental Management for Mining. (Saskatoon, Sask., October 27-29, 1993).

Stumm, W. and J.J. Morgan. 1981. Aquatic chemistry. Wiley-Interscience, New York.

Wieder, R.K. 1992. The Kentucky Wetlands Project: A field study to evaluate man-made wetlands for acid coal mine drainage treatment. Final Report. Agreement GR-896422 between the U.S. Office of Surface Mining, Reclamation and Enforcement and Villanova University.

Wildeman, T.R. 1993. Handbook for constructed wetlands receiving acid mine drainage. In T.R. Wildemann, G.A. Brodie and J.J. Gusek (eds.) Wetland design for mining operations. BiTech Publishers Ltd., Richmond, BC.

EARLY WEATHERING BEHAVIOR OF PYRITIC COAL SPOIL PILES INTERSTRATIFIED WITH CHEMICAL AMENDMENTS[1]

Joseph J. Donovan[2]
Paul F. Ziemkiewicz[3]

Abstract: An array of eleven 400-ton piles of sulfide-rich overburden rock was constructed and monitored in 1982 during the first year of leaching. Piles were constructed that had (1) no treatments, (2) layered base amendments (limestone, rock phosphate, lime), and (3) sodium lauryl sulfate (SLS). In conjunction with flow rate measurement, water samples were collected to determine major element chemistry and mass fluxes. The rate of pyrite oxidation obeyed pseudo-zero order kinetics of similar rate between piles (mean 0.0239 mol SO_4 per ton spoil per day). The ion ratio δ (dissolved SO_4 to Ca+Mg) was used as a surrogate measure of pyrite oxidation and carbonate dissolution. Observed δ was about 1.0, increasing to even higher values late in the first year in some piles; this is substantially lower than the "expected" value of 0.5 for neutralization at alkaline pH. One plausible explanation is that carbonate dissolution may be kinetically limited and exhibit different rates during the leaching period, due to more rapid dissolution of calcite than dolomite or to simple depletion of reactive calcite. Gypsum reaches saturation in mid-year and may have been a sink for Ca and SO_4, although this would not greatly alter the δ ratio. Acid produced was apparently buffered *in situ* by dissolution of natural carbonate disseminated in the spoil; most layered amendments demonstrated no unequivocal initial effectiveness. Acid conditions ensued within the first year for all non-amended and some amended piles with the ratio of neutralization potential to maximum potential acidity (NP/MPA) less than unity, but the speed and extent of acidity generation varied among these. Acidity also developed for some amended piles with NP/MPA's as high as 2.3. The layered amendments may not be as effective and rapidly available as natural carbonate disseminated throughout the spoil. More effective amendment may have been achieved had amendments been evenly distributed through the spoil.

Additional Key Words: aqueous geochemistry, acid mine drainage, coal spoil, kinetics, mineral equilibria

Introduction

Base amendments are commonly added to acidic minespoil as passive treatment agents. They are applied to supplement natural alkalinity of spoil materials in order to meet or exceed the rate of acid production from pyrite oxidation and associated reactions. Common basic amendments are crushed limestone, calcium oxyhydroxide, sodium hydroxide, and sodium carbonate. Other, non-basic amendments have been employed to slow down or prevent chemical or biological reactions leading to increased acidity or metals mobilization.

Rates and need for application of base amendments have been determined using acid-base balance of potential spoil materials. Acid-base accounting (Sobek *et al.*, 1978; Erickson and Hedin, 1988; Branham and Caruccio, 1991) uses various estimates of pyritic sulfur to calculate maximum potential acidity (MPA) in conjunction with an acid titration procedure to calculate base neutralization potential (NP). Attempts to quantitatively relate overburden acid-base balance to post-mining water quality, either *a priori* or *a posteriori*, have been only somewhat successful. DiPretoro and Rauch (1988) found poor correlation (R^2=0.16) between volume-weighted NP and alkalinity in AMD discharge from 30 West Virginia mines. While it has been noted that sulfate production of spoil correlates with pyrite sulfur content, the relationship between NP and sulfate production rates may be erratic and variable (Hedin and Erickson, 1988). Current research suggests that factors other than overburden characteristics may be important in determining post-mining water quality (Renton *et al.*, 1988; Hedin and Erickson, 1988); however, quantification of these factors is not straightforward.

---

[1]Paper presented at the International Land Reclamation And Mine Drainage Conference and theThird International Conference On The Abatement Of Acidic Drainage, Pittsburgh PA, April 24-29, 1994

[2]Joseph J. Donovan, Assistant Professor of Geology, West Virginia University, Morgantown, WV USA

[3]Paul F. Ziemkiewicz, Director, National Mine Land Reclamation Center, Morgantown, WV USA

There does, however, seem to be general correlation between acid generation and NP/MPA ratio for either large excesses or deficiencies of NP. DiPretoro and Rauch (1988) found that overburden with over 3% NP (expressed in weight percent neutralization as $CaCO_3$) produced alkaline drainage while those with <1% produced acidic drainage. Erickson and Hedin (1988) observed >8% and <2% NP as the limits for alkaline and acidic drainage, respectively. Lapakko (1988) found that 3% calcium carbonate neutralized an overburden material with 1.17% sulfur. Brady and Hornberger (1989) suggested NP threshold values of >3% and sulfur <0.5% as minimum guidelines for alkaline-producing strata. Brady *et al.* (1990) concluded that, even when alkaline additions are added to spoil with insufficient natural excess overburden NP ("net neutralization potential" or NNP), AMD was formed or persisted. A common thread in these investigations is that some excess of base is required to assure neutralization of acid potential. One or more physico-chemical mechanisms for "tying up" base or making it ineffective seems to be operating. The identities of these mechanisms, however, are not clear. The problem may be kinetic in nature, related to timely delivery of base, or physical, related to the mechanical distribution of base (Brady *et al.*, 1990), or statistical, related to uncertainty in estimation of NP and MPA. It is in fact possible that all of these factors may play a role.

In this investigation, we attempt to identify and measure mechanisms of base neutralization of acid-producing reactions. We examine short-term chemical behavior of both sulfide and carbonate reaction products in the initial phases of leaching of an acid-producing spoil pile. The dataset employed is a time series of geochemical and hydrologic measurements. The purpose is to assess (1) mechanisms of carbonate dissolution and acid production in the early phase of spoil weathering and (2) geochemical signature of early acid-pile evolution. We do not address the problem of long-term acid neutralization in the spoil, but only the issue of how piles first turn acid and what this tells us about the mechanisms and effectiveness of neutralization.

Study Area and methods

The study area is a reclaimed mine backfill in Upshur County near Buckhannon, WV, operated by Island Creek Corporation. This area has a humid climate, averaging 110 cm (45 in) of rain per year. In winter 1981-82, Island Creek personnel constructed 11 test piles with waste rock consisting of sandstone and shale overburden. The piles were flat-topped and roughly 16 x 16 m in area x 2 m high, each containing about 400 short tons of waste rock, sized to fall within the range of approximately 1 to 8 inches in diameter. Each pile was emplaced over a plastic liner for collecting basal drainage into an 8-inch-diameter perforated PVC underdrain. The underdrains discharged to a series of weirs where flow could be measured and samples of water collected.

Composition and construction methods were varied among piles. Four unamended "control" piles were used (1, 2, 3, 10), containing pure sandstone, pure shale, layered sandstone/shale/sandstone, and well-mixed sandstone and shale, respectively. Piles 6 and 7 were of shale composition, with 00.31 and 0.15 wt %, respectively, of phosphate rock amendment added in thin layers. Piles 4, 5, and 8 were of layered sandstone/shale/sandstone stratification, with additions of 0.46, 1.07, and 1.26 wt % crushed limestone, respectively, also added in thin lifts. Pile 9 was also layered sandstone/shale/sandstone, with addition of 0.15 wt % quicklime (CaO) in thin lifts. Pile 11 was composed of shale with a surface application of sodium lauryl sulfate (SLS), in addition to Microwet #2, a commercial surfactant. A summary of the materials and construction method for each pile is given in table 1. NP and MPA were determined on samples collected randomly from each truck during pile construction and batched along with the appropriate mass of amendment. The ratio NP/MPA was calculated from these values and includes both spoil material and any amendments added. Results of acid-base balance calculations are also listed in table 1.

The placement and composition of spoil materials simulated field conditions with one major difference. The screening to pass fines created a highly permeable spoil, with dominantly intergranular porosity. This material may therefore behave hydraulically quite differently from natural spoils, whose hydrogeologic characteristics have been described as dominated by highly transmissive fracture porosity (Hawkins and Aljoe, 1990). The Island Creek piles might therefore be expected to display higher recharge and fluid flow rates than natural spoils. Also, spatial variability in hydrogeologic characteristics is thought to have been largely controlled in these piles. Results, therefore, may differ

from full-scale spoil piles containing more typical unscreened overburden.

Samples for water chemistry were collected at approximately 2-week intervals during the first year of the experiment. Samples were analyzed for: dissolved calcium (Ca), magnesium (Mg), and sulfate (SO_4); total recoverable (raw acidified) iron (Fe) and manganese (Mn); and pH, alkalinity, and acidity. Analytical techniques employed included atomic absorption spectroscopy for cations, spectrophotometric determination of Ba-complexed SO_4, and titrimetric alkalinity and acidity. Measurements were made on site. Using measured fluid flows, mass fluxes of ionic species were estimated for interval periods by midpoint interpolation to calculate cumulative mass fluxes. These results were compiled for the first year of pile leaching by infiltration of natural precipitation. Equilibrium calculations were made using the mineral equilibrium solver WATEQ, ignoring redox reactions because no estimates of sample Eh could be made. Equilibria and speciation were calculated following simulated addition of a balance ion (either sodium or chloride) to make up charge imbalances. Samples with >10% initial charge imbalance were not employed in equilibrium calculations.

The dataset has several limitations. No measurements were taken of ions including dissolved sodium, potassium, chloride, fluoride, silica, or aluminum. This precludes full electrochemical balance of the chemical analyses to be checked, or rigorous mineral equilibrium calculations to be performed. Na and K concentrations could be favored by ion exchange or, at lower pH than about 5.0, by hydrolysis of silicates. The extent of these processes therefore cannot be evaluated. Also, no characterization of solid-phase mineralogy, extractable ions, or geochemical composition was performed either on the spoil and amendments (before the placement of the piles) or on the altered spoil (after leaching was performed). Finally, no characterization of heterogeneity in NP or MPA within each pile was performed.

Table 1. Experimental matrix for spoil piles showing spoil composition, placement methods, amendments, and acid-base accounting, with percentages are in mass %.

Pile	Sand-stone,%		Mixing method	Amendment Type	%			
1	100	0	n/a	None	n/a	1.23	0.31	3.94
2	0	100	n/a	None	n/a	0.08	0.97	0.08
3	57	43	Layer	None	n/a	0.10	0.56	0.18
4	53	47	Layer	Ls.	1.07	1.72	1.03	1.65
5	52	48	Layer	Ls.	0.46	1.11	2.00	0.56
6	0	100	n/a	Ph.	0.31	0.08	1.88	0.04
7	0	100	n/a	Ph.	0.15	0.08	0.91	0.09
8	54	46	Layer	Ls.	1.26	1.89	0.78	2.38
9	59	41	Layer	CaO	0.15	0.89	0.50	1.73
10	44	56	Blend	None	n/a	0.58	0.91	0.63
11	0	100	n/a	SLS	30 lb.	0.08	1.28	0.06

n/a: not applicable Ls.: crushed limestone Ph.: phosphate rock

Expected Stoichiometries Of Acid Mine Drainage

AMD-producing reactions may be written as some variation of the following (Stumm and Morgan, 1981):

$$FeS_2 + \frac{7}{2}O_2 + H_2O \xrightarrow{k_1} 2SO_4^{2-} + Fe^{2+} + 2H^+, \quad (1)$$

$$Fe^{2+} + \frac{1}{4}O_2 + H^+ \xrightarrow{k_2} Fe^{3+} + \frac{1}{2}H_2O, \quad (2)$$

$$Fe^{3+} + 3H_2O \xrightarrow{k_3} Fe(OH)_3 + 3H^+, \quad (3)$$

and

$$FeS_2 + 14Fe^{3+} + 8H_2O \xrightarrow{k_4} 15Fe^{2+} + 2SO_4 + 16H^+ \quad (4)$$

Under acid pH, rate constant k_3 is the slowest of the four reactions (Garrels and Thompson, 1960) and thus may limit the rate of additional acidity production in reactions (3) and (4). Oxidation of ferrous iron proceeds most rapidly at high pH and quite slowly at pH's below about 3, where half-reaction times are on the order of 1000 days (Stumm and Morgan, 1981). Thus Fe^{2+} oxidation may be a rate-limiting step for the potential acidity from oxidation of pyrite according to reaction (1).

The stoichiometry of reactions (1) to (4) gives the expected ratio of dissolved ions in AMD effluent. For example, in the absence of Fe^{2+} oxidation, the expected molar ratio of sulfate ion to acidity evolved is 2:2. Fe^{2+} oxidation consumes one mole of this acidity, but subsequent precipitation as $Fe(OH)_3$ produces an additional 3 moles of H^+, for a net acidity of 4 moles per mole of pyrite. Thus the expected molar SO_4/acidity ratio (per mole of pyrite) is 1:2. Catalytic oxidation of pyrite by Fe^{3+} may somewhat decrease this ratio, depending on the extent of Fe^{3+} reduction by pyrite. In general, however, a sulfate/acid ratio of 1:1 would accompany lack of oxidation of ferrous iron, while a ratio of 1:2 would ensue if $Fe(OH)_3$ is actively forming. Both assume, of course, that acid is not neutralized by other reactions and that dissolved SO_4 behaves conservatively.

Dissolution of calcite by evolved acid may be written as

$$CaCO_3 + 2H^+ \longrightarrow Ca^{2+} + H_2CO_3^\circ \qquad (pH <\sim 5.3), \qquad (5)$$

$$CaCO_3 + H^+ + HCO_3^- \longrightarrow Ca^{2+} + 2HCO_3^- \qquad (pH >\sim 7.3), \qquad (6)$$

while similar reactions may be written for dolomite dissolution, such as

$$CaMg(CO_3)_2 + 4H^+ \longrightarrow Ca^{2+} + Mg^{2+} + 2H_2CO_3^\circ \qquad (pH <\sim 5.3). \qquad (7)$$

The expected stoichiometric ratio of $(Ca^{2+} + Mg^{2+})/(H^+$ neutralized) is about 1:2 at low pH (mineralization to dissolved CO_2) and 1:1 at high pH (increase in bicarbonate alkalinity). Between these two extremes, the ratio will be intermediate between 0.5 and 1. The pH governing the extent of reactions (5) to (7) will be strongly influenced by pCO_2 and the ability of carbon dioxide to exsolve to the atmosphere. Depending on which neutralization reaction dominates, we may calculate the expected stoichiometry of $SO_4/(Ca+Mg)$, using the neutralization ratios in conjunction with the 2 moles of net acidity produced per mole of sulfate. We will refer to the rate of change in this ratio of dissolved acid products to base products as

$$\delta = \frac{d\{SO_4^{2-}\}}{d\{Ca^{2+} + Mg^{2+}\}} \qquad (8)$$

The index δ will have an expected value ranging from 0.5 (high pH) to 1.0 (low pH), with values between 0.5 and 1.0 at intermediate pH. δ values of less than the expected value under prevailing pH might indicate either (1) slower pyrite oxidation than base dissolution, (2) depletion of pyrite, or (3) neutralization by hydrolysis of Ca- or Mg-aluminosilicate minerals, such as clays or feldspars. A value of δ greater than expected could, on the other hand, suggest (1) slower carbonate dissolution than pyrite oxidation, (2) incomplete oxidation of ferrous iron resulting in less acid production, (3) ion exchange reactions transferring dissolved Ca or Mg to clays, or (4) depletion of carbonate minerals. Values of δ exactly equal to the expected value would suggest that reactions 1 through 7 are appropriate, i.e. acid is produced by both sulfide oxidation and metal-hydroxide formation and consumed by carbonate dissolution. The index δ thus provides a means to infer mechanisms of carbonate buffering within AMD-generating spoil. The sum of Ca + Mg is employed rather than Ca^{2+} alone because many natural carbonate rocks contain minerals of both calcitic (pure or magnesian) and of dolomitic composition. An inherent assumption in use of δ is that there is no source or sink for either sulfate or alkaline-earth cations (for example, acid sulfate salts, gypsum, sulfate reduction) not accounted for in reactions 1 through 7. Under specific conditions, this geochemical assumption may be reasonable.

Results

Plotted in figures 1-4 are the cumulative {SO_4} and {Ca+Mg} fluxes for groundwater effluent during the first year after placement of the piles. Also plotted is discharge pH. The results are grouped accorded to treatment types: control (no amendments: piles 1, 2, 3, and 10); limestone-amended (piles 4,5, and 8); phosphate rock-amended (piles 6 and 7); quicklime-amended (pile 9); and SLS-amended (pile 11). Table 1 details variations in the observed spoil materials composition and in their placement.

Figure 1 shows comparative results for the control piles. The NP for piles 2 and 3 are 0.08% and 0.10%, values typical for native carbonate composition in most of the unamended spoils. However, piles 1 and 10 had 1.23% and 0.58%, respectively, rather anomalously high values. The reason for the high "background" carbonate compositions in these latter two piles is unknown, but could be related to natural variability or to sampling error. All except pile 1 would be expected to be net acid producers based on the low values of NP/MPA observed (<0.65). Inspection of Figure 1 shows that all (including pile 1) did in fact at least start to turn acid, with the slowest rate of acid production coming from pile 10, the well-blended but unamended spoil pile. Pile 1 (unamended) gave the most rapid rate of acid evolution, with pH dropping below 5 within about four months. Near the end of year 1, pH in water from pile 1 appeared to be rising somewhat, but remained acid. For all four piles, the cumulative SO_4 and {Ca + Mg} fluxes show quite similar patterns, as do in fact nearly all of the piles.

Figure 2 shows the flux data for the limestone-amended piles, all composed of three horizontal layers of sandstone/shale/sandstone lithology. For these three, pile 5 (0.46% limestone, NP=1.11) shows a gradual decline to pH levels just above 5, while pile 8 (1.26% limestone, NP=1.89) dropped below pH 5 within 70 days. Pile 4 (1.07% limestone, NP=1.72) showed little variation in pH during this year.

Figure 3 shows the piles treated with rock phosphate from Florida deposits. This amendment consists largely of the minerals apatite ($CaPO_4$) as well as calcite ($CaCO_3$), a common impurity within phosphate deposits. Pile 7 (0.15% phosphate, NP=0.08) failed to turn acid, while pile 6 (0.31% phosphate, NP=0.08) turned acid near the end of the sampling period.

Figure 4 shows piles treated with quicklime (pile 9, CaO=0.15%, NP=0.89%) and SLS (pile 11; NP=0.08%). The former became acid within 5 months; the latter failed to turn acid and displayed relatively slow SO_4-production.

Figure 5 shows time versus pH (right axis) and molar Ca/Mg ratio, pCO_2 (atmospheres), and saturation indices for selected mineral phases (calcite, gypsum) in the leachate for pile 3, the

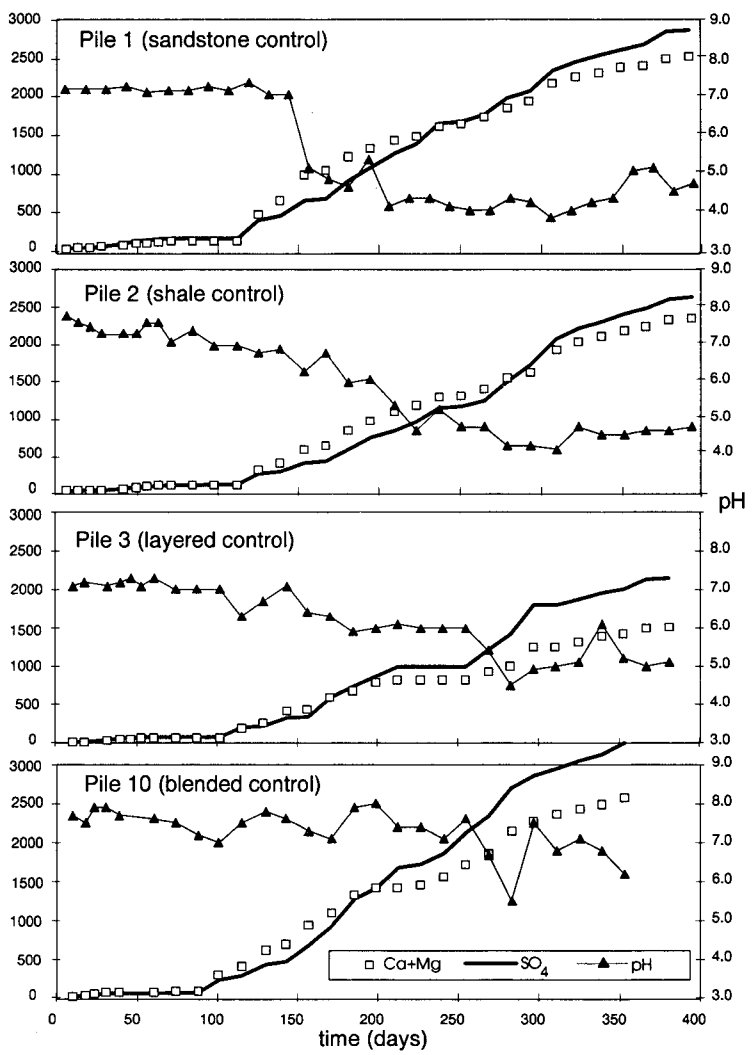

Figure 1. pH (right axis) and cumulative SO_4 and {Ca+Mg} fluxes (left axis, in mol) for leachate from unamended piles..

unamended layered mixture of sandstone and shale. Saturation index as used here is defined as SI = log [ion activity product/equilibrium constant]. A value of zero for SI indicates saturation with respect with the mineral phase. pH gradually declined in this pile to about 5, while Ca/Mg rose to a mid-year peak of about 4, dropping to about 2 in the latter half of the year. Gypsum reached saturation in mid-year, at about the same time Ca/Mg peaked. Calcite increased to about 3 to 4 orders of magnitude undersaturation by 300 days elapsed due to acid production in the pile. All other mineral phases of possible importance to the geological setting were also highly undersaturated.

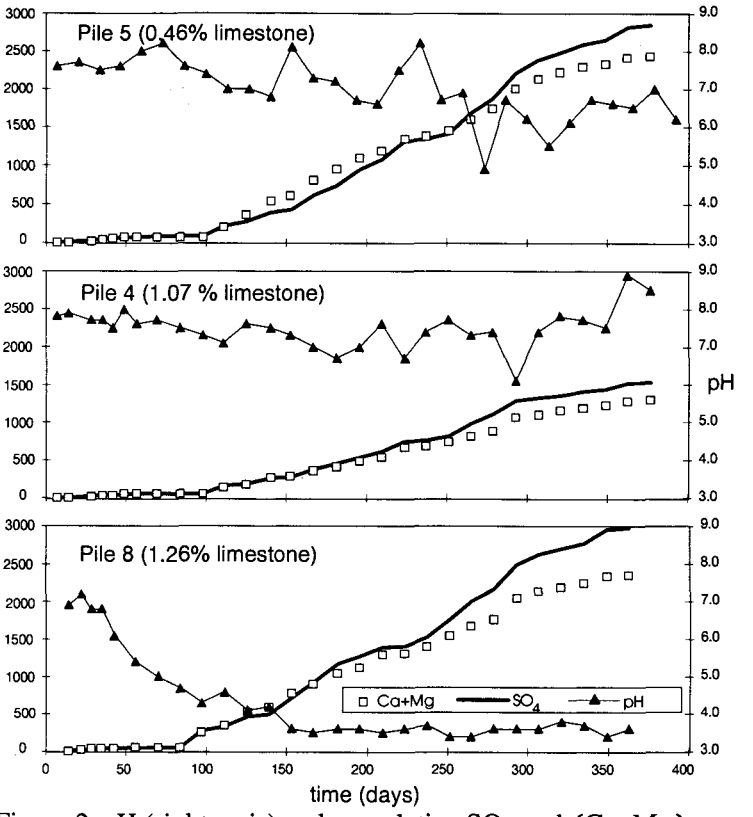

Figure 2. pH (right axis) and cumulative SO_4 and {Ca+Mg} fluxes (left axis, in mol) for leachate from limestone-amended piles, layered sandstone/shale/sandstone.

Interpretations

Shape of the ion flux time series

Cumulative SO_4 and {Ca + Mg} fluxes display grossly a similar pattern for all piles, irrespective of lithology, construction method, amendment, NP, and MPA. Several flux time-series show three characteristic features:

1. An initially flat curve for both fluxes, of 50-100 day duration

2 A slightly steeper slope of Ca+Mg flux than that for SO_4 between 100-300 days ($\delta<1$).

3. A later period of slower Ca+Mg flux ($\delta>1$) after about day 250, developing a gap for several piles between cumulative SO_4 and {Ca+Mg} fluxes.

The initial flat portion of the leaching curve (period 1) is interpreted as a period of saturation of the spoil with water and humidity, during which pyrite oxidation is incipient. The lag time may represent passage of the first pore volume through the piles.

The early Ca + Mg "bulge" (period 2) appears to reflect a transition from early base dissolution behavior, at the expected low ratio of $\delta \cong 0.5$, to the later period (period 3) where δ rises to and exceeds unity. The Ca/Mg molar ratio of in period 2 rises to above 3.0, higher than the ratio of 1.5 to 2.5 observed later in the year (fig. 5). This behavior was general to all the spoil piles and not related to any particular base amendment; it occurs for control piles also. The late decrease in Ca/Mg ratio suggests that a carbonate phase of approximately equal mass of dolomite and calcite may have been dissolving in this period, if the assumption is valid that all Mg is derived from carbonates as opposed to hydrolysis and ion exchange. During the earlier bulge period, the calcite percentage leached was likely >75%.

The unexpectedly high values of δ observed late in the year (period 3) may be interpreted in several ways, none of which may be unambiguously validated with available data. One possibility is that carbonate dissolution is kinetically slowed, due either to a net decrease in the ratio of calcite vs. dolomite or to a net decrease in surface area of the carbonate fraction. Another possibility is that the "effective" carbonate is simply near depletion, with some or much of the amendments added being hydraulically isolated from the leachate, as by ferric hydroxide armoring. The SO_4-Ca/Mg gap correlates with development of low pH in at least two of the piles, although this relationship is not

consistently observed. In several piles with low naturally-occurring carbonate NP (on the order of 0.1%, or about 2600-3600 moles of carbonate as $CaCO_3$ in various piles), cumulative carbonate flux approaches 80% or more of the available carbonate by the end of the sampling period.

Another possibility is transfer of Ca and/or Mg to other solid phases. Mineral equilibria indicate that no Ca- or Mg-bearing minerals are at or above saturation except gypsum, which reaches slight supersaturation for most of the piles following mid-year. Gypsum precipitation and ion exchange of Ca or Mg onto clays are both feasible reactions, but have not been confirmed by examination of reacted spoil. Gypsum precipitation would not by itself explain the anomalously-high δ values, although δ would vary somewhat under gypsum saturation.

The notable similarity between flux curves from different piles (both amended and unamended) suggests that base consumed in the first year of leaching was primarily native carbonate disseminated in spoil. The layered amendments cannot be demonstrated as ineffective but do not control flux behavior in early stage leaching.

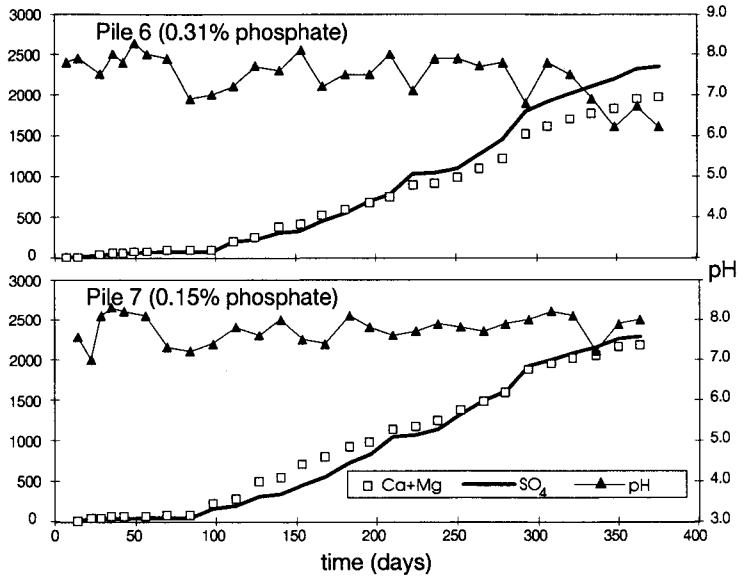

Figure 3. pH (right axis) and cumulative SO_4 and {Ca+Mg} fluxes (left axis, in mol) for leachate from phosphate-amended piles, all of uniform shale.

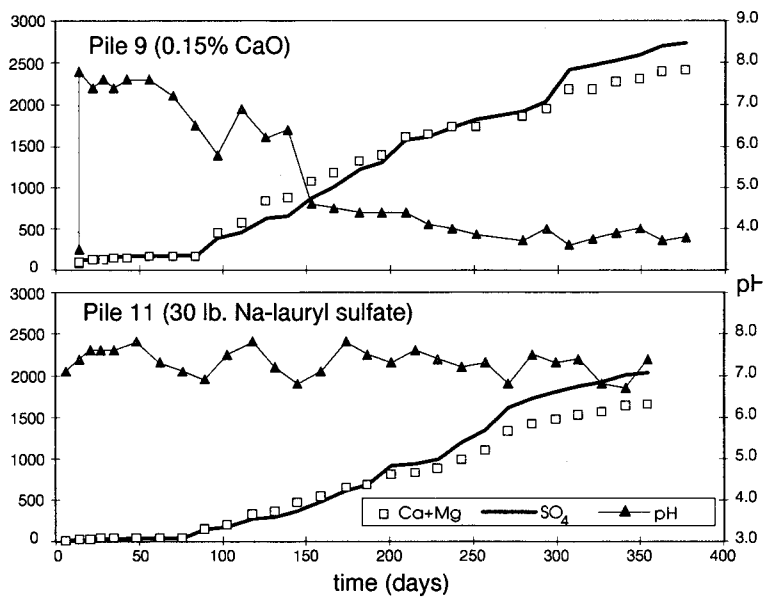

Figure 4. pH (right axis) and cumulative SO_4 and {Ca+Mg} fluxes (left axis, in mol) for leachate from CaO--and sodium lauryl sulfate-amended piles.

Effect of amendments

No clear relationship is indicated between presence/amount of base amendment and prevention of acid leachate. For example, all of the uniform or stratified control piles (pile 1, 2, 3) developed acid conditions readily, and the blended control pile 10 was on the verge of going acid near the end of the first year. On the other hand, one limestone-amended piles (pile 8, 1.25% limestone) and one apatite-treated piles (pile 6, 0.3% phosphate) went acid as well. These suggest that the initiation of acid conditions in these experiments was not strictly limited by the amendments and may have been influenced by the balance between pyrite oxidation and naturally-occurring carbonate. There appears to be enough variation in NP/MPA values (mean 1.04, standard deviation 1.28) to account for the observed variation in rate of acid generation. No data are available describing inter-pile heterogeneity of NP and MPA or the precision with which these were sampled and estimated.

The effect of differing spoil lithologies was not examined in these experiments due to the small number of piles examined. Only for the shale lithology (4 pure samples, piles 2, 6, 7, and 11) may natural variability be described. Shale (NP mean 0.08±0.003; MPA mean 1.26±0.44) exhibited almost no variance in NP and a coefficient of variation of about 0.35 in MPA. Higher NP values were observed in unamended piles containing sandstone, pile 1 (100%

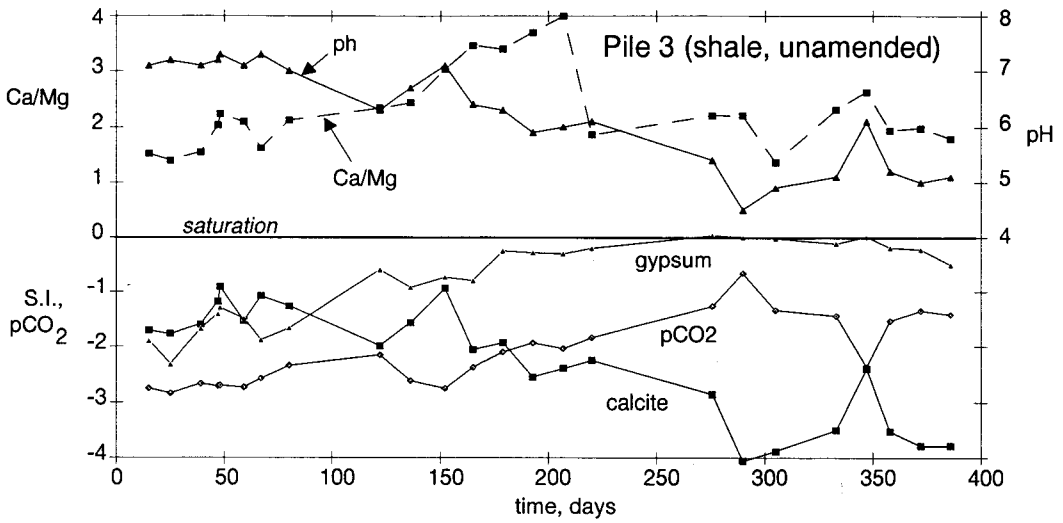

Figure 5. Leachate pH (right axis) and saturation indices, pCO_2, and molar Ca/Mg ratio (right axis).

sandstone) and pile 10 (44% sandstone), suggesting that sandstone contained higher NP than shale. From the limited data available, the shale had lower NP (<0.1%) and higher MPA (1.3%) than the sandstone (1.2% NP with MPA <0.5%).

Iron and manganese oxidation

Total recoverable iron concentrations were low in the great majority of effluent samples, exceeding 1 mg/L for only a very few. Manganese concentrations were somewhat higher (2 to 5 mg/L) for most piles and in the vicinity of 10 to 50 mg/L for piles 8 and 9, whose pH reached to below 4. It may be inferred that ferrous iron oxidation was rapid and led to precipitation of hydroxides in all piles. On the other hand, formation of manganese oxides may have become inhibited at lower pH. The ferrous/ferric redox couple was not analyzed, and so no estimates of oxidation potential could be made and mineral equilibria are not calculated for iron- and manganese-species.

Table 2. Zero-order pseudo-rate constants (mol SO_4/ton/day) based on sulfate fluxes. Confidence intervals based on T-distribution, α=0.05, 10 degrees of freedom.

Pile	Rate constant
1	0.0284
2	0.0259
3	0.0189
4	0.0150
5	0.0239
6	0.0230
7	0.0247
8	0.0239
9	0.0223
10	0.0358
11	0.0207
Mean	0.0239
Std. dev.	0.0053
Conf. limits	$0.0203<\mu<0.0275$

Pyrite oxidation kinetics

Cumulative sulfate flux is nearly linear with respect to time after the first 100 days or so; that is, dissolution of pyrite apparently obeys a pseudo-zero-order rate law. The mean rate is 0.0239 moles SO_4 per ton spoil per day, with rather small variance and narrow confidence limits (table 2). This low variance is striking considering the broad range of NP, MPA, amendments, lithologies, and construction methods employed. It appears that pyrite oxidation causes a uniform flux of dissolved sulfate, with rate controlled by oxygen availability, surface area of spoil fragments, pyrite reaction rind thickness, and other factors prominent in pyrite oxidation kinetics (Cathles and Apps, 1975). Hydraulic and transport factors may well be also important, but were not studied in this investigation.

Mineral Equilibria

pCO_2 values rise in groundwater within the pile from near-atmospheric levels at the onset of leaching to about 10^{-1} atm as carbonate dissolution begins. While some values of pH seem anomalously low with respect to measured alkalinities and may represent field errors and overestimation of pCO_2, high CO_2 pressures are nonetheless indicated by the data. Calcite (and dolomite, not shown) is at no point after mid-year less than 2 orders of magnitude undersaturated. Only gypsum approaches saturation, after about 200 days of leaching. SI_{gyp} reaches an apparent plateau that would be consistent with gypsum precipitation, although no x-ray observations of gypsum reaction products have been made to determine whether gypsum was in fact being formed. The observed decrease in Ca/Mg ratio late in the first year is consistent with gypsum formation.

Conclusions

Leachate samples collected during the first year of weathering of a large-scale field experiment yield insights into mechanisms of development of acid conditions in sandstone and shale spoil materials. Major conclusions are:

1. Dissolution of pyrite obeys a pseudo-zero-order kinetic rate law over a broad range of lithologies, NP, MPA, amendments, and pile construction. The mean rate constant is 0.0239 ± 0.0036 moles SO_4 per ton spoil per day.

2. SO_4 and {Ca+Mg} flux time series indicate that naturally-occurring carbonate disseminated through the spoil rocks neutralizes early acidity generated by acid reactions. Carbonate mineralogy (calcite, magnesian calcite, dolomite) may influence neutralization rates.

3. Amendments studied had no pronounced impact on early AMD evolution and were in some cases ineffective at preventing AMD for NP/MPA ratios as high as 2.3. One the other hand, in all cases for which NP/MPA was less than unity, acid leachate was generated within the year of study. Response in pH and acidity varies more between piles than SO_4 or {Ca+Mg} flux.

4. Layered base amendments appeared to have had no clear effect on leachate during the period of study. This may relate due to their inhomogeneous distribution, to heterogeneity in NP or MPA within the piles, to hydroxide armoring of amendment layers, or to time lag in their reaching the outflow.

5. Equilibrium calculations using WATEQ for a time series of samples from a typical pile indicate that gypsum reached a saturation plateau after about 200 days of leaching. Mineral equilibria support that gypsum or some calcium sulfate polymorph could precipitate in these piles. Calculated pCO_2 values ranged from an initial 10^{-3} atm to as high as about 10^{-1} atmospheres late in the year. Calcite ranged from 2 to 4 orders as acid production ensued in the first year of leaching.

Sampling of these piles was discontinued for a 10-year period following the first year; samples were not again collected until 1993. Current work on this site is focusing on the long-term impacts and success of the amendments on mitigating spoil-pile discharge, and on examination of the reacted spoil to determine mineralogical and chemical changes since mining.

Acknowledgements

Analytical chemistry and sampling was performed under supervision of Al Meek, of Island Creek Coal. John Sonderegger, Jack Renton, and an anonymous reviewer provided suggestions and technical comments that greatly improved the manuscript.

Literature Cited

Branham, W. S., and F. T. Caruccio, 1991. A comparative study of tailings analysis using acid/base accounting, cells, columns and soxhlets. p. 157-174 *In* Proceedings of the Second International Conference on the Abatement of Acidic Drainage (Montreal, P.Q.).

Brady, K., and R. J. Hornberger, 1989. Mine drainage prediction and overburden analysis in Pennsylvania. *In* Proceedings of the 1989 West Virginia Surface Mine Drainage Task Force Symposium. (West Virginia Mining and Reclamation Association, Morgantown, WV, April 1989).

Brady, K., M. W. Smith, R. L. Beam, and C. A. Cravotta, 1990. Effectiveness of the use of alkaline materials at surface coal mines in preventing or abating acid mine drainage: Part 2. Mine site case studies. p. 227-241 *In* Proceedings of the 1990 Mining and Reclamation Conference (Morgantown, WV).

Cathles, L. M., and J. A. Apps, 1975. A model of the dump leaching process that incorporates oxygen balance, heat balance, and air convection. Metall. Trans. 6B: 617-624.

Cravotta, C. A., K. Brady, M. W. Smith, and R. L Beam,., 1990. Effectiveness of the addition of alkaline materials at surface coal mines in preventing or abating acid mine drainage: Part I. Geochemical considerations. p. 221-225 *In* Proceedings of the 1990 Mining and Reclamation Conference (Morgantown, WV).

diPretoro, R. S. and H. W. Rauch, 1988. Use of acid-base accounts in pre-mining prediction of acid drainage potential: a new approach from northern West Virginia. *In* Mine Drainage and Surface Mine Reclamation. p. 2-10 *In* USBM Information Circular 9183.

Erickson, P. M., and R. S. Hedin, 1988. Evaluation of overburden analytical methods as means to predict post-mining coal mine drainage quality. p. 11-19 *In* Mine Drainage and Surface Mine Reclamation. USBM Information Circular 9183.

Garrels, R. M., and M. E. Thompson, 1960. Oxidation of pyrite by iron sulfate solutions. Amer. Jour. Sci., v. 258-A, p. 57-67.

Hawkins, J. W., and W. W. Aljoe, 1990. Hydrogeologic characterization and modeling of a heterogeneous surface coal mine spoil, Upshur County, West Virginia. p. 43-52 *In* 1990 National Symposium on Mining, Hydrology, Sedimentology, and Reclamation (University of Kentucky, Lexington, KY).

Hedin, R. S., and P. M. Erickson, 1988. Relationships between the initial geochemistry and leachate chemistry of weathering overburden samples.p. 21-28 *In* Mine Drainage and Surface Mine Reclamation. USBM Information Circular 9183.

Lapakko, K, 1988. Prediction of acid mine drainage from Duluth Complex mining wastes in northeastern Minnesota. *In* Mine Drainage and Surface Mine Reclamation. USBM Information Circular 9183, p. 180-190.

Renton, J. J., T. E. Rymer, and A. H. Stiller, 1988. A laboratory procedure to evaluate the acid producing potential of coal associated rocks. Min. Sci. and Technol. 7: 227-235.

Sobek, A. A., W. A. Schuller, J. R. Freeman, and R. M. Smith, 1978. Field and laboratory methods applicable to overburden and minesoils. U.S. Environmental Protection Agency Report No. EPA-600/2-78-054, 203 pp.

Stumm, W., and J. J. Morgan, 1981. *Aquatic Chemistry.* Wiley-Interscience, New York, 780 pp.

Ziemkiewicz, P.F. and F.A. Meek, 1994 (this volume). Long term behavior of acid-forming rock: results of twelve year field studies. *In* International Land Reclamation And Mine Drainage Conference and Third International Conference On the Abatement Of Acidic Drainage (Pittsburgh PA, April 24-29 1994).

EVALUATION OF NEUTRALIZATION POTENTIAL DETERMINATIONS FOR METAL MINE WASTE AND A PROPOSED ALTERNATIVE[1]

Kim A. Lapakko[2]

Abstract: Standard acid-base accounting (standard ABA), modified ABA, and B.C. Research initial static tests tended to overestimate the neutralization potential (NP) present as calcium carbonate and magnesium carbonate, with the extent of overestimation depending on the minerals present in the 10 metal-mine wastes examined. For 6 of the 10 samples the static test NP values were within about 10 kg/mt $CaCO_3$ of the calculated mineralogic NP. These samples were composed largely of quartz and sheet silicates (mica, chlorite, kaolinite, montmorillonite). The excess acid neutralization measured for these samples was apparently due to the presence of some (less than 10%) calcium feldspar in the samples. For the standard ABA and modified ABA methods, the NP overestimation was higher (13 to 47 kg/mt $CaCO_3$) for samples containing larger amounts of calcium feldspar, pyroxene, olivine, or iron carbonate minerals. The extent of overestimation for the B.C. Research initial NP was typically slightly higher than the standard ABA and modified ABA and was greatest for samples containing iron carbonate. The maximum overestimations by the standard ABA, modified ABA, and B.C. Research initial test NP values were 33, 31, and 49 kg/mt $CaCO_3$, respectively. A newly proposed method of NP determination, NP available above pH 6, was more accurate than these three methods. Six of the 10 NP values determined by this method were approximately equal to the mineralogic NP values. For the remaining 4 samples, this NP was within 3 kg/mt $CaCO_3$ of the mineralogic NP.

Additional Key Words: acid mine drainage, prediction, static tests, mine waste characterization

Introduction

The quality of mine waste drainage is the net result of dissolution of the minerals present in the mine waste. Acid is produced as the result of oxidation of iron sulfide minerals such as pyrite and pyrrhotite.

$$FeS(s) + (3/2)H_2O + (9/4)O_2(g) = FeOOH(s) + 2H^+(aq) + SO_4^{2-}(aq) \quad (1)$$

$$FeS_2(s) + (5/2)H_2O + (15/4)O_2(g) = FeOOH(s) + 4H^+(aq) + 2SO_4^{2-}(aq) \quad (2)$$

The most effective minerals for neutralizing (consuming, buffering) acid are those containing calcium carbonate and magnesium carbonate, examples of which are calcite, magnesite, dolomite, and ankerite ($CaCO_3$, $MgCO_3$, $CaMg(CO_3)_2$, and $CaFe(CO_3)_2$, respectively). Reactions 3 and 5 are dominant above approximately pH 6.3, while reactions 4 and 6 are dominant below this pH. The rate of magnesium carbonate dissolution is reported to be slower than that of calcium carbonate (Rauch and White 1977). Iron carbonates will provide no net neutralization of acid.

$$CaCO_3(s) + H^+(aq) = HCO_3^-(aq) + Ca^{2+}(aq) \quad (3)$$

$$CaCO_3(s) + 2H^+(aq) = H_2CO_3(aq) + Ca^{2+}(aq) \quad (4)$$

$$MgCO_3(s) + H^+(aq) = HCO_3^-(aq) + Mg^{2+}(aq) \quad (5)$$

$$MgCO_3(s) + 2H^+(aq) = H_2CO_3(aq) + Mg^{2+}(aq) \quad (6)$$

---

[1]Paper presented at the International Land Reclamation and Mine Drainage Conference and the Third International Conference on the Abatement of Acidic Drainage, Pittsburgh, PA, April 24-29, 1994.
[2]Kim A. Lapakko, Principal Engineer, MN Dept. of Natural Resources, Division of Minerals, St. Paul, MN, USA.

Dissolution of minerals such as anorthite (reaction 7, Busenberg and Clemency 1976) and forsterite (reaction 8, Hem 1970) can also neutralize acid, but their dissolution rate (and associated rate of acid neutralization) is slow in the neutral pH range. These minerals dissolve more rapidly as pH decreases and, therefore, provide more acid neutralization under acidic conditions.

$$CaAl_2Si_2O_8(s) + 2H^+(aq) + H_2O = Ca^{2+}(aq) + Al_2Si_2O_5(OH)_4(s) \quad (7)$$

$$Mg_2SiO_4(s) + 4H^+(aq) = 2Mg^{2+}(aq) + H_4SiO_4(aq) \quad (8)$$

Several static tests have been developed to estimate quickly and inexpensively if a mine waste will produce acidic drainage (Ferguson and Erickson 1987). The results are commonly used as a first-cut screening in the process of mine waste characterization. Standard acid-base accounting (standard ABA, Sobek et al. 1978), modified acid-base accounting (Lawrence 1990), and B.C. Research initial tests (Duncan and Bruynesteyn 1979) determine the maximum potentials for acid production (acid production potential or APP) and acid neutralization (neutralization potential or NP). The APP is based on sulfur analysis, and the NP is determined by the amount of acid neutralized when the sample is in contact with a solution in the approximate pH range of 1 to 3.5. Whether or not a mine waste will produce acidic drainage is determined by the difference (net NP) or ratio (NP/APP) of these values. Additional information on static testing is presented in Lapakko (1992a).

Technology for determination of sulfur species present in the solid phase is adequate to determine the maximum potential of a mine waste to produce acid. However, Lutwick (1986) contended that static tests overestimate NP available to maintain an environmentally acceptable drainage pH, owing to acid neutralization by host rock components under the strongly acidic conditions created in the NP determination. Lapakko and Antonson (1991) reported that the pH of drainage from a sample of Duluth Complex rock decreased below 6.0 after an NP depletion of only 0.5 kg/mt $CaCO_3$, considerably less than the 11 kg/mt $CaCO_3$ neutralization potential determined by standard ABA (Sobek et al. 1978). Apparently dissolution of plagioclase, pyroxenes, and olivine present in the host rock neutralized acid at low pH in the NP "digestion" but, during dissolution simulating that in the environment, the rate of acid neutralization was too slow to maintain drainage pH above 6.0. For similar reasons standard ABA (Sobek et al. 1978) overestimated the NP present as calcium carbonate and magnesium carbonate, or mineralogic NP, in 10 gold mine tailings (Lapakko 1992b). Inadequate quantification of ferrous iron acidity during the titration step may have further contributed to the overestimation of NP for a sample containing a large amount of siderite ($FeCO_3$). The modified ABA (Lawrence 1990) was reasonably accurate in quantifying the mineralogic NP of these samples.

Errors in NP measurement may result in the erroneous classification of acid-producing waste as non-acid producing, thereby creating an unexpected environmental liability. In such cases, the method of NP determination proposed in the present study may provide a more accurate mine waste assessment. Given the increased use of these tests for metal mine waste characterization and the potential magnitude of mine waste financial liabilities, this accuracy must be considered.

Objectives

The objective of this study was to assess the accuracy of NP measurements by standard ABA, modified ABA, and B.C. Research initial static tests. An alternative method for determining NP was also proposed, and its accuracy was evaluated.

Methods

Materials

Four waste rock samples, identified as RK1 to RK4, and six tailing samples, identified as TL1 to TL6, were collected for testing. The mine waste samples were split into different subsamples for subsequent chemical and mineralogical analyses, as well as static testing. The splitting procedure (ASTM E877-82) was tested by determining the sulfur (ASTM E395 using a Dietert furnace) and carbon dioxide contents (ASTM E350-89C) of three sample splits, to ensure uniformity of the samples generated. The standard deviations for the sulfur and carbon dioxide determinations on the triplicate splits ranged from 0 to 6.8% of the mean value, except for the carbon dioxide content of sample TL4 (17%, table 1).

Table 1. Sulfur, carbon dioxide, and mineral content (wt %) and mineralogic NP (kg/mt $CaCO_3$).

	RK-1	RK-2[1]	RK-3	RK-4	TL-1	TL-2	TL-3	TL-4	TL-5	TL-6
Sulfur	0.46	0.64	1.63	2.91	0.96	1.49	2.19	2.30	5.05	5.81
SD[2]	.012	.006	.111	.055	.040	.012	.025	.071	.308	.379
CO_2	.11	.03	1.41	1.42	.87	.80	4.06	.25	.65	2.01
SD	.006	.015	.095	.045	.031	.047	.104	.038	.023	.078
Quartz	24	-	41	34	38	53	42	45	21	12
Feldspar	24	54	29	29	39	30	12	13	52	5
Mica	6	4	12	4	14	10	10	30	10	2
Calcite	?	.1	.5	-	1.5	.7	.2	.6	-	4.6
Dolomite	?			3.0	.4	.8	-	-	1.10	-
Ankerite	-	-	-	-	-		1.9	-	-	-
Siderite	.3	-	3.2	-	-	.2	8.3	-	-	-
Rhodochrosite	-	-	?	-	<.1		-	-	-	-
Magnesite	-	-	-		-		-	-	.23	-
Mineral. NP	0	1	5	32	19	16	19	5	12	46
Error Int.[3]	0-2.9	0-2.3	1.9-9.7	28-37	17-23	13-21	8.1-33	3.7-6.6	9.8-17	35-52

? indicates probably present but not positively identified by XRD.
- indicates mineral not present.
[1] Trace amounts of copper carbonates were noted in TL-2.
[2] SD standard deviation.
[3] Error bar for mineralogic NP.

Silica and major metal components were extracted using borate fusion and analyzed using direct current plasma. The carbon dioxide content of the samples was used to determine the total carbonate mineral content. The carbonate minerals present were identified by X-ray diffraction (XRD, Phillips), and checked by scanning electron microscopy (Amray model 1200B) and energy dispersive spectroscopy (Noran Instruments model 2010). For some samples, optical microscopy (standard Zeiss petrographic microscope) was used for additional verification. Heavy mineral concentrates were separated using a Haultain Superpanner (Infrasizers Ltd.) and analyzed by XRD. These results were used to ascertain the presence of small amounts of siderite. The relative amounts of carbonate minerals present were determined by interpretation of the major peak heights based on the analyst's twenty years of experience. The potential error in the carbonate mineral determination was estimated as 20%; additional work is planned to further assess the potential error. XRD was also used to determine the amounts of other major minerals present in the samples and a potential 20% error is assumed for the values discussed.

Static Test Procedures

The static tests were conducted by consulting firms involved in mine waste characterization. For the standard acid-base accounting (Sobek et al. 1978) determination of neutralization potential (NP), samples were crushed to minus 60 mesh (diameter less than 0.25 mm). Approximately 0.5 g of sample was placed onto a piece of aluminum foil, and one or two drops of 1:3 hydrochloric acid (HCl) was added to the sample. Based on the extent of "fizzing" in this test, a volume and concentration of HCl were selected and added to 2 g of minus 60 mesh mine waste in a flask. The mixture of acid and mine waste was then boiled until the reaction ceased, as indicated by the termination of the production of bubbles. Distilled water was added to attain a total volume of 125 mL, and the contents of the flask were boiled for 1 min and then cooled to room temperature. The mixture was then titrated to pH 7.0 with sodium hydroxide to determine the amount of acid (as $CaCO_3$) neutralized by the sample. The NP (acid neutralization per unit mass rock) was expressed in units of metric tons $CaCO_3$ per 1000 metric ton mine waste or, equivalently, kilograms of $CaCO_3$ per metric ton of mine waste (kg/mt $CaCO_3$).

For the modified acid-base accounting (Lawrence 1990) determination of neutralization potential, the fizz test was also used to determine the volume and strength of HCl addition to a 2-g sample (minus 60 mesh). The acid-mine waste mixture was digested for 24 h at room temperature, at which time pH was measured. If pH was not in the range of 1.5 to 2.0, the digestion was rerun with an acid addition adjusted, based on the observed pH, until the pH range of 1.5 to 2.0 was attained. After the pH criterion was met, the amount of acid neutralized by the rock was determined by titrating the acid-mine waste mixture with NaOH until a pH of 8.3 was maintained for at least 30 seconds. The NP was then expressed in kilograms of $CaCO_3$ per metric ton.

The B.C. Research initial test (Duncan and Bruynesteyn 1979) uses different terminology and different units of quantification. The terminology and units were translated to be consistent with those of the standard ABA method for ease of presentation in this paper. The NP was determined by titrating, with 1.0N sulfuric acid, a stirred mixture of 10 g mine waste (70% minus 325 mesh or, equivalently, 70% of the particles having diameter less than 0.044 mm) and 100 mL distilled water. The titration was continued until pH 3.5 was reached and less than 0.1 mL of acid was added over a period of 4 h. Type 45 AR Chemtrix pH controllers with Cole Parmer electrodes were used for the titration.

The proposed alternative method of NP determination was the same as the B.C. Research initial test, except a titration endpoint of 6.0 was used in the present study rather than 3.5. pH 6 was selected since it is a commonly applied water quality standard. Therefore, the neutralization potential available above this pH represents the amount of acid that a mine waste could neutralize while maintaining drainage pH in a range that meets water quality standards. The test is referred to as the NP available above pH 6, or NP(pH6). Other pH values could also be used, depending on the drainage pH required at a specific site, and an endpoint pH of 5 was also examined in the present study.

Determination of Neutralization Potential Accuracy

Assessment of the accuracy of NP values is complicated by the fact that mineral dissolution, and the attendant acid neutralization, is a function of solution pH. To assess the accuracy of the static test NP values, the NP available to maintain a pH above 6.0 was calculated based on sample mineralogy. The mineralogic calculation assumed that the calcium carbonate and magnesium carbonate present in the mine waste samples, and only these minerals, would dissolve to maintain a drainage pH of least 6.0; that is,

$$\text{Mineralogic NP} = 10 \times (\%\ CaCO_3) + 11.9 \times (\%\ MgCO_3) \tag{9}$$

This approach assesses the accuracy of the various methods in determining the mineral content available to maintain a drainage pH of 6. It does not address how much of this neutralization is available nor the rate at which the neutralizing minerals will dissolve.

Error bars for the mineralogic NP values were established by different methods, all of which accounted for error contributed by splitting and determination of total carbon dioxide content. For most of the samples (RK1, RK2, RK4, TL1, TL2, TL4, TL5, TL6) the upper error bar was determined by assigning the maximum potential carbonate content, as indicated by carbon dioxide determination, to neutralizing minerals. The lower error bar for these samples (minimum amount of carbonate occurring with calcium and magnesium) was calculated as the minimum total carbonate content minus the maximum possible carbonate occurring with iron. For all of these samples except TL6, the maximum iron carbonate content was calculated based on the presence of less than 0.5% siderite (i.e. not detected) in the heavy mineral fractions. For TL6 a maximum iron carbonate content of 0.5% in the entire sample was used. For samples containing substantial siderite, RK3 and TL3, a potential 50% error in calcium carbonate and magnesium carbonate analysis was used.

Results

Sample Composition

Chemical and mineralogical analyses indicated the samples displayed a fair degree of compositional diversity. The carbon dioxide content of the 10 mine waste samples ranged from less than 0.1% to 4.1%. The reported calcium carbonate and magnesium carbonate mineral content of the samples ranged from trace amounts to a maximum of 4.6%. Siderite was also present in measurable amounts in four of the samples (table 1). Quartz, feldspar, and mica were the major host rock minerals in all samples except TL-6, in which pyroxene was dominant.

Accuracy of Standard Static Tests

There was good agreement among the NP values determined by the three standard tests for samples RK1, RK4, TL1, and TL2. For samples RK3, TL4, and TL5 the B.C. Research initial test values were roughly 10 to 15 kg/mt $CaCO_3$ higher than the standard ABA and modified ABA values. The variation among the three methods was greatest for samples RK2, TL3, and TL6, with no consistent trend in the relative magnitudes of the three values (table 2). For all samples except TL3 and TL6, there was good agreement between NP values determined by the standard ABA and modified ABA methods.

Table 2 Neutralization potential, kg/mt $CaCO_3$

Sample	Standard ABA	Mod ABA	B.C. Research	Mineralogic NP		Available above pH6
RK1	12	9.6	7.7	0	(0-2.9)[1]	3.0
RK2	35	33	11	1	(0-2.3)	2.8
RK3	15	14	25	5	(1.9-9.7)	3.3
RK4	28	28	33	32	(28-37)	28
TL1	27	27	30	19	(17-23)	24
TL2	18	20	25	16	(13-21)	16
TL3	46	61	82	19	(8.1-33)	30
TL4	3.8	2.9	15	5	(3.7-6.6)	3.8
TL5	7.5	3.2	20	12	(9.8-17)	15
TL6	99	72	58	46	(35-52)	55

[1] Error bar in parenthesis

The agreement between the static test NP values and the mineralogic NP was determined based on comparison with the error bars for the mineralogic NP. Samples within or below the error bars were assigned a value of zero, which indicated no error. It was assumed that NP values below the error bar were the result of acidic sulfide oxidation on the sample surface which were not accounted for by the mineralogic NP. The error for

the remaining values was calculated as the difference between the reported NP and the upper mineralogic error bar (table 3).

Table 3. Difference between static test NP and mineralogic NP, kg/mt $CaCO_3$ The method of calculation is presented in the preceeding paragraph.

Sample	Standard ABA	Mod. ABA	B.C. Research	Available above pH6
RK1	+9.1	+6.7	+4.8	+0.1
RK2	+33	+31	+8.7	+.5
RK3	+5.3	+4.3	+15	0
RK4	0	0	0	0
TL1	+4	+4.0	+7	+1
TL2	0	0	+4	0
TL3	+13	+28	+49	0
TL4	0	0	+8.4	0
TL5	0	0	+8.0	0
TL6	+47	+20	+6	+3

The standard ABA and modified ABA NP values were within the mineralogic NP error bars for samples RK4, TL2, TL4, and TL5 (table 3). The major rock-forming minerals in these samples were quartz, feldspar, and mica, although sample RK4 did contain a substantial amount of clay. Examination of the sample chemistry suggests that the feldspar was largely potassium feldspar. The NP values for these two tests were 4 to 10 kg/mt $CaCO_3$ above the upper mineralogic NP error bar for of samples RK1, RK3, and TL1. Once again the major rock forming minerals present in these samples were quartz, feldspar, and mica, with substantial chlorite and clay also present in sample RK1. The major difference between these samples and the samples mentioned above is that the feldspar is largely calcium feldspar.

The standard ABA and modified ABA NP values were least accurate for samples RK2, TL3, and TL6, exceeding the upper mineralogic NP error bar by 13 to 47 kg/mt $CaCO_3$. Samples RK2 and TL6 both contained pyroxene (18% and 55%, respectively), and sample RK2 also contained 11% olivine. No other samples contained these minerals. In addition, sample RK2 had the highest feldspar content, most of which was calcium feldspar, of the samples.

As was the case for the standard ABA and modified ABA NP values, the accuracy of the B.C. Research initial test NP for sample RK4 was good. However, on samples TL2, TL4, and TL5 (samples for which the standard ABA and modified ABA NP values were within the mineralogic NP error bars), the B.C. Research initial test NP values were about 4 to 9 kg/mt $CaCO_3$ higher than the upper mineralogic NP error bar (table 3). The B.C. Research initial NP error was also in this range for samples RK1, RK2, TL1, and TL6. Thus, the accuracy for samples RK1 and TL1 was similar to that for the standard ABA and modified tests, while the B.C. Research initial values were more accurate for samples RK2 and TL6.

The accuracy of the B.C. Research initial NP test was poor for samples RK3 and TL3, exceeding the upper mineralogic NP error bars by 15 and 49 kg/mt $CaCO_3$, respectively. These samples had iron carbonate contents of 3.2 and 8.7 wt %, respectively. Thus, the B.C. Research initial NP was less accurate than the standard ABA and modified ABA NP tests for samples with elevated iron carbonate contents.

Neutralization Potential Available Above pH 6

With the exception of samples TL3 and TL4, the NP available above pH 6 was lower than that determined by the three commonly applied static tests (table 2). The NP available above pH 6.0 was in good agreement with

the mineralogic NP (table 2). Six of these values were within the mineralogic NP error bars and the remaining four values were within 3 kg/mt $CaCO_3$ of the upper mineralogic NP error bar.

Discussion

The standard ABA and modified ABA NP values were in fairly good agreement, and the B.C. Research Initial NP was slightly higher than these values for most samples. The agreement of the NP values with the mineralogic NP was dependent on both the test and the sample composition. The NP values for the standard ABA and modified ABA were within the mineralogic NP error bars for samples RK4, TL2, TL4, and TL5. The B.C. Research initial NP was typically slightly higher than these values for these samples, with only one value (RK4) within the mineralogic NP error bars. These samples were comprised largely of quartz, feldspar (mostly potassium feldspar), and mica. The presence of these minerals apparently has little effect on the accuracy of the standard ABA and modified ABA NP determination. The smaller particle size used in the B. C. Research initial NP determination may have contributed to the slightly elevated NP values for TL2, TL4, and TL5. The tailings were crushed to minus-300 mesh, as opposed to being run "as received" in the standard ABA and modified ABA NP determinations. The minus-300 mesh fraction comprised roughly 50% of the each of the "as received" samples.

For three of the remaining samples the standard ABA and modified NP values were within 10 kg/mt $CaCO_3$ of the upper mineralogic NP error bar. As with the samples for which the NP values were within the mineralogic NP error bars, quartz, feldspar, and mica were the major minerals in these samples. However, the plagioclase was more calcic and the calcic plagioclase apparently neutralized some acid in the static tests. It should be noted that one of these samples (RK-3) contained 3.2 wt % siderite, which apparently contributed little error. For the standard ABA and modified ABA methods, the overestimation was higher yet (13 to 47 kg/mt $CaCO_3$ above the upper mineralogic NP error bar) for samples containing larger amounts of calcium feldspar, pyroxene, olivine (RK2, TL6), or iron carbonate minerals (TL3).

Apparently the pyroxene, olivine, or calcium feldspar present in samples RK2 and TL6 neutralized acid under the low-pH conditions in the NP tests. Whereas dissolution of these minerals can neutralize the acid produced by low-sulfur mine wastes (Lapakko 1988, Lapakko and Antonson 1993, Morin 1993), laboratory experiments and field data indicate that their dissolution may not be capable of maintaining a drainage pH above 6.0 for mine wastes of moderate sulfur content (Lapakko and Antonson 1991, Lapakko 1994). It should be noted, however, that dissolution of these minerals, and the attendant acid neutralization, will generally increase as particle size decreases.

The large discrepancy observed for TL3 was apparently due to interference from iron carbonate. The major rock-forming minerals present in sample TL3 are similar to those present in samples in closer agreement with the mineralogic NP values. However, this sample contained ankerite and siderite which yielded a total iron carbonate content of 8.6 wt % (table 1). The iron carbonate apparently contributed to the excessive static test NP. Such interference could be eliminated by enhancing the ferrous iron oxidation by using a higher endpoint pH, hydrogen peroxide addition during the titration (as prescribed in the ASTM method), or elevating the temperature.

The B.C. Research NP values were within 9 kg/mt $CaCO_3$ for the samples lacking substantial amounts of iron carbonate. This indicates that the pyroxene and olivine present in RK2 and TL6 (and calcium feldspar in RK2) did not dissolve as extensively as in the standard ABA and modified ABA NP tests. The lower pH conditions in the latter tests apparently resulted in the more extensive dissolution of these minerals. The extent of overestimation was considerably higher for samples containing iron carbonate (RK3, TL3). A maximum error of 49 kg/mt $CaCO_3$ above the upper mineralogic NP error bar was observed for a sample containing 8.6% iron carbonate.

This overestimation is likely due to incomplete oxidation of ferrous iron released from the carbonate minerals in the B.C. Research initial test. The B.C. Research initial NP determination involves only an acid addition, as opposed to an acid addition followed by a titration with a base. Oxidation of iron released from the mine waste during the acid addition is slower under the acidic conditions of the B. C. Research initial test, as opposed to the

higher pH conditions during the base titration in the standard ABA and modified ABA tests. Consequently, the B.C. Research initial test measures the acid neutralized by iron carbonate dissolution, but not the subsequent acid generation due to the oxidation of ferrous iron and precipitation of ferric hydroxide.

The newly proposed method, the neutralization potential available above pH 6, consisted of acid titration of a mixture of a mine waste sample and distilled water down to pH 6.0. This approach is designed to conservatively determine the neutralization potential necessary to meet water quality standards which typically require pH in excess of 6. This method yielded NP values which were within the error bars for the mineralogic NP for six of the ten samples and was within 3 kg/mt $CaCO_3$ of the upper mineralogic NP error bar for the four remaining samples. For the ten samples examined, the titration was generally more conservative in determining the neutralization potential available for maintaining drainage pH above 6.0. Although the titration slightly overestimated the mineralogic NP for some samples, the magnitude of this overestimation was less than that for the standard static tests. This technique merits additional examination as a viable technique for determination of neutralization potential.

Acknowledgments

Funding for this project was supplied by the US Environmental Protection Agency and administered by the Western Governors' Association. Chemical (sulfur, carbon dioxide) and mineralogical analyses were conducted by Lerch Brothers (Hibbing, MN) and Louis Mattson of the Midland Research Center (Nashwauk, MN), respectively. Standard acid-base accounting and modified acid-base accounting were conducted by Lawrence Consulting Ltd. (Vancouver, BC). The B.C. Research Initial Test and the neutralization potential available above pH 6 were conducted by B.C. Research (Vancouver, BC), under the direction of Rik Vos. Jennifer Wessels of the Minnesota Department of Natural Resources was responsible for data management and tables presented.

References

Busenberg, E. and C. Clemency. 1976. The dissolution kinetics of feldspars at 25°C and 1 atmosphere CO_2 partial pressure. Geochim. Cosmochim. Acta 40: 41-49.

Duncan, D.W. and A. Bruynesteyn. 1979 Determination of acid production potential of waste materials. Met. Soc AIME, paper A-79-29. 10 p.

Hem, J. D. 1970. Study and interpretation of the chemical characteristics of natural water. U.S. Geol. Sur. Water-Supply Paper 1473. 363 p.

Lapakko, K. A. 1988. Prediction of acid mine drainage from Duluth Complex mining wastes in northeastern Minnesota. p. 180-190. In Proceedings, 1988 Mine Drainage and Surface Mine Reclamation Conference, v. 1. BuMines IC#9183.

Lapakko, K. A. 1992a. Recent literature on static predictive tests. p. 109-119. In Emerging process technologies for a cleaner environment. Phoenix, AZ, February 24-27, 1992. Society for Mining, Metallurgy, and Exploration, Inc., Littleton, CO.

Lapakko, K. 1992b. Characterization and static testing of ten gold mine tailings. p. 370-384. In Proceedings, 1992 American Society for Surface Mining and Reclamation Meeting. (Duluth, MN, June 14-18, 1992).

Lapakko, K. A. 1994. Comparison of Duluth Complex rock dissolution in the laboratory and field. This volume

Lapakko, K. A. and D. A. Antonson. 1991. The mixing of limestone with acid producing rock. p. 343-358. In Proceedings, Second International Conference on the Abatement of Acidic Drainage. (Montreal, Canada, September 16-18, 1991).

Lapakko, K. A. and D. A. Antonson. 1993. Oxidation of sulfide minerals present in Duluth Complex rock: A laboratory study. In Environmental geochemistry of sulfide oxidation. ACS Symposium Series 550, American Chemical Society, Washington, DC. 15 p.

Lawrence, R.W. 1990. Prediction of the behaviour of mining and processing wastes in the environment. p. 115- 121. In F. Doyle (ed.), Proceedings, Western Regional Symposium on Mining and Mineral Processing Wastes. Society for Mining, Metallurgy, and Exploration, Inc., Littleton, CO.

Lutwick, G. D. 1986. Mineral composition and acid consuming potential of Nova Scotia shales Nova Scotia Research Foundation Corporation, Halifax, NS. 32 p.

Morin, K. A. 1993 Telephone conversation with Kevin Morin, Morwijk Enterprises, Vancouver, BC.

Rauch, H. W. and W. B. White. 1977. Dissolution kinetics of carbonate rocks 1 Effects of lithology on dissolution rate. Wat. Resour. Res. 13(2): 381-394.

Sobek, A.A., W. A. Schuller, J. R. Freeman, and R. M. Smith. 1978. Field and laboratory methods applicable to overburden and minesoils. EPA 600/2-78-054. 203 p.

EVALUATION OF ACID-BASE ACCOUNTING TO PREDICT THE QUALITY OF DRAINAGE AT SURFACE COAL MINES IN PENNSYLVANIA, U.S.A[1]

Keith B. C. Brady[2], Eric F. Perry[3], Richard L. Beam[4], David C. Bisko[5], Michael D. Gardner[4], and J. M. Tarantino[6]

Abstract: The effectiveness of Acid-Base Accounting (ABA) for predicting surface coal mine drainage quality in Pennsylvania was evaluated. Comparisons between ABA and mine drainage alkalinity, acidity, and sulfate were made for 38 mines in the bituminous coalfield. Neutralization Potential (NP), Maximum Potential Acidity (MPA), and Net Neutralization Potential (NNP) were evaluated with and without "thresholds." Calculations using "thresholds" counted only those values for NP greater than 30 mt CaCO3/1,000 mt and percent sulfur greater than 0.5%. "Without thresholds" computations included all values. Stoichiometric equivalence factors of 31.25 and 62.5 were used to compute MPA. NP and NNP are the best predictors of postmining drainage quality. Alkaline or acid drainage quality is controlled by as little as 1% to 3% carbonate in the overburden. NNP less than 1% generally results in acidic drainage, and NNP greater than 3% yields alkaline drainage. An empirical relation exists between alkalinity and NP. Postmining alkalinity can be estimated as 4 to 6 times NP (without thresholds). MPA is not a reliable predictor of drainage quality, except in the absence of calcareous strata, where a positive relation exists between acidity and MPA.

Additional Key Words: mine drainage, net alkalinity, neutralization potential, sulfate.

Introduction

Coal mine drainage is the greatest contributor of stream and ground water pollution in Pennsylvania, with more than 3,700 km of stream degraded by mine drainage (Pennsylvania Department of Environmental Resources, 1990). Pennsylvania laws and regulations require a premining evaluation of the probable hydrologic consequences of mining. Pennsylvania has been using acid-base accounting (ABA), since 1978 as one tool for the prediction of postmining water quality. ABA was developed at West Virginia University (Sobek et. al 1978) and is based on the following assumed stoichiometry of FeS_2 and $CaCO_3$ (Sobek et al. 1978, Williams et al. 1982, Cravotta et al. 1990):

$$FeS_2 + 2\ CaCO_3 + 3.75\ O_2 + 1.5\ H_2O \Longrightarrow Fe(OH)_3 + 2\ SO_4^{-2} + 2\ Ca^{+2} + 2\ CO_2 \qquad (1$$

Acidity produced from 1 mol of FeS_2 (64 g of sulfur) is neutralized by 2 mols of $CaCO_3$ (200 g), or 1 g sulfur to 3.125 g $CaCO_3$. On this basis, 31.25 mt

[1]Paper presented at the International Land Reclamation and Mine Drainage Conference on the Abatement of Acidic Drainage, Pittsburgh, PA, April 24-29, 1994

[2]Department of Environmental Resources (DER), P.O. Box 8461, Harrisburg, PA 17105; [3]Office of Surface Mining, 10 Parkway Center, Pittsburgh, PA 15220; [4]DER, R.D. 2, Box 603-C, Greensburg, PA 15601; [5]DER, Box 209, Hawk Run, PA 16840; [6]DER, White Memorial Building, Knox, PA 16232

of $CaCO_3$ will neutralize 1,000 mt of rock that contains 1.0 wt% pyritic sulfur. Thus, the total percent sulfur is multiplied by 31.25 to obtain a "maximum potential acidity" (MPA), which is in units of mt $CaCO_3$/1,000 mt of overburden material. This multiplication factor is intended to provide direct comparison with "neutralization potential" (NP) which also has units of mt $CaCO_3$/1,000 mt.

Cravotta et al. (1990) suggested that the original stoichiometric relationship shown in equation 1 underestimates the maximum potential acidity and proposed the following revised equation:

$$FeS_2 + 4\ CaCO_3 + 3.75\ O_2 + 3.5\ H_2O \Longrightarrow Fe(OH)_3 + 2\ SO_4^{-2} + 4\ Ca^{+2} + 4\ HCO_3^- \qquad (2)$$

In this reaction 1 mol of FeS_2 is neutralized by 4 mols of $CaCO_3$, which results in a mass ratio of 6.25 g of calcite to 1 g pyritic sulfur. MPA is therefore computed as percent sulfur times 62.5. A "net neutralization potential" (NNP = NP - MPA) can be determined for a stratum utilizing the stoichiometry of equation 1 or 2. In theory a positive NNP (surplus) would produce alkaline water and a negative NNP (deficiency) acidic water.

Early ABA interpretations defined "acid-toxic" overburden as any strata with a NNP less than -5 mt/1,000 mt of overburden material (Sobek et al. 1978). This criterion was developed mostly for agronomic purposes, and it was found to be not directly applicable for prediction of mine drainage quality. Some mines evaluated under this guideline produced acid mine drainage and stream pollution. Thus, in Pennsylvania, a more qualitative means of prediction evolved. By the mid-1980's alkaline strata were defined as strata with an NP greater than 30 mt/1,000 mt and a "fizz" (effervescence upon application of dilute HCl). Acidic strata were defined as strata with greater than 0.5% sulfur and an NP less than 30 mt/1,000 mt (Brady and Hornberger 1990).

In Pennsylvania ABA is used in conjunction with other predictive tools. These include consideration of premining water quality, adjacent mining water quality, paleodepositional environments and mine site hydrology.

The objectives of this study were to 1) examine relations among ABA data and postmining water quality parameters, and 2) evaluate the effectiveness of various ways of computing NP, MPA, and NNP for predicting postmining water quality.

Methods

The Pennsylvania Department of Environmental Resources (PaDER) bituminous surface coal mine files were canvassed for potential study sites. Each mine selected for evaluation had postmining ground water data (spoil seeps, monitoring wells, etc.) with multiple samples, and (with one exception) two or more ABA drill holes. Sites approved for refuse or flyash disposal, or having other unconventional conditions like gas well brines or preexisting pollutional discharges, which could complicate water quality interpretations were excluded. Thirty-eight mines in 15 counties were evaluated. Eleven different coal seam horizons are represented with 89% from the Allegheny Group, 7% from the Dunkard group, and the remaining 4% from the Conemaugh and Monongahela Groups.

There is an inherent bias in the sites selected for study. The group consists mostly of mines expected to produce acceptable water quality. A few mines with the worst water quality are older sites that had overburden analysis performed after permit issuance, generally to develop mitigation plans for water quality problems. The PaDER typically does not issue permits with negative NNP results, unless there are compelling reasons to the contrary. In addition to ABA data, the PaDER evaluates all available geologic and hydrologic information. The proposed mine plan and resources that could be affected are also considered in the decision making process. Thus sites at the extreme "bad" end are generally absent from our database. Likewise, where experience has shown that mining a certain seam invariably produces alkaline water (for example, the Redstone coal seam) ABA is rarely requested. Thus the "good" extreme is also missing from our database. This leaves the present study with a preponderance of sites with intermediate ABA properties that are difficult to predict using ABA alone.

Water quality parameters that were evaluated included pH, alkalinity, acidity, and sulfate. Metals data were also compiled but are not reported here. One representative ground water discharge or well was selected for statistical analysis. Selection for sites with multiple sample points was often simplified by one discharge being dominant in flow or all sample points being of similar quality. Water quality data were analyzed with nonparametric statistics because these methods are advantageous for analysis of mine drainage (Helsel 1987). Medians were evaluated as indicating central tendency. Water quality and ABA parameters were summarized and compared using graphical and statistical techniques.

ABA data were processed in an ORACLE database that resides on the PaDER's mainframe computer. This database performed ABA summary calculations using the algorithms and methods described in Smith and Brady (1990) with enhanced capabilities to represent site geometry. Areas of influence were planimetered for each overburden hole. ABA data summary numbers were weighted according to thickness, density, and areal extent of strata based on actual mined area to determine average NP, MPA, and NNP for each hole. MPA was calculated using percent sulfur times 31.25 and 62.5. Data for each hole were combined to obtain average values for the entire mined area.

NP, MPA and NNP were computed with and without "thresholds." Calculations with thresholds "counted" strata that have either a percent sulfur greater than 0.5 wt%, or NP greater than 30mt/1,000 mt with a "fizz." Other strata were considered insignificant in alkaline or acid potential and were assigned a percent sulfur or NP value of "0". Calculations "without thresholds" utilized all reported values for NP and percent sulfur for all strata.

Results and Discussion

Overburden Sampling

Reliable predictions of postmining water quality requires sampling to represent the geochemical and spatial properties of potentially acid-forming and alkaline-forming strata. As density of drill holes increased, the location of calcareous rocks could be determined more easily (fig. 1). Where hole density is less than 4 ha per hole, 93% of the sites had positive NNP and net alkaline drainage. For sites with hole densities greater than 4 ha per hole, only 65%

had positive NNP and only 43% had net alkaline water. This may reflect adjustments to the mine plan to selectively include areas with favorable ABA properties or exclude unfavorable areas on intensively sampled sites. A strong regional and stratigraphic bias exists in our data, as 14 of 15 intensively sampled mines are in one of the four PaDER mining districts.

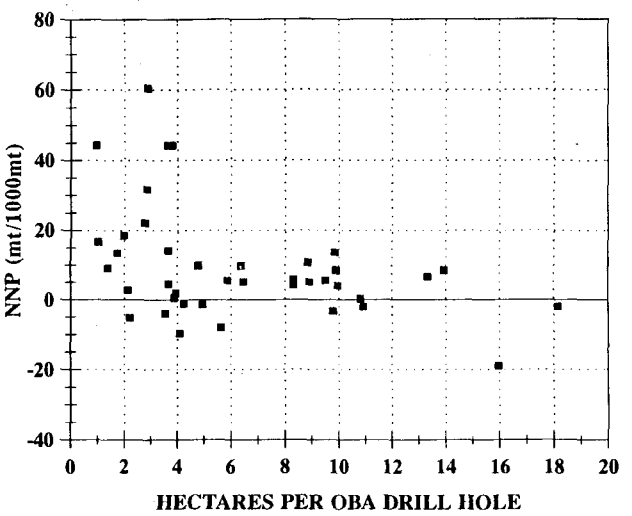

Figure 1. Plot of drilling density vs. net neutralization potential.

Calcareous rock can occur as laterally extensive units of fresh or marine limestones and calcareous sediments, discontinuous carbonate strata due to facies changes, and secondary cements and fracture fills. Superposed on these diagenetic and postdiagenetic processes are the effects of more recent weathering of carbonates (Brady and Hornberger 1990). Drilling programs and borehole locations should anticipate these depositional and post depositional processes.

Vertical sampling intervals are also important. Most intervals were less than 1.5 m and usually less than 1 m. Intensive vertical sampling is necessary for computation of reliable ABA summary parameters using "thresholds" for percent sulfur or NP. Large intervals can dilute high sulfur or high NP strata.

Net Neutralization Potential and Neutralization Potential

NNP and NP are reliable indicators of postmining water quality in this study. Figure 2 shows NNP (without thresholds and MPA = 31.25 X %S) and net alkalinity for the 38 sites evaluated. All sites with NNP greater than 15 mt/1,000 mt produced net alkaline water. Of the nine sites with NNP of 0 mt/1,000 mt or less, seven (78%) were acid producing. The "gray zone" in figure 2, where predictions were uncertain, appears to be between 0 and 15 mt/1,000 mt. Two mines that had positive NNP but negative net alkalinity were anomalies throughout this study. ABA analyses for these two sites may not represent the actual acid/base conditions.

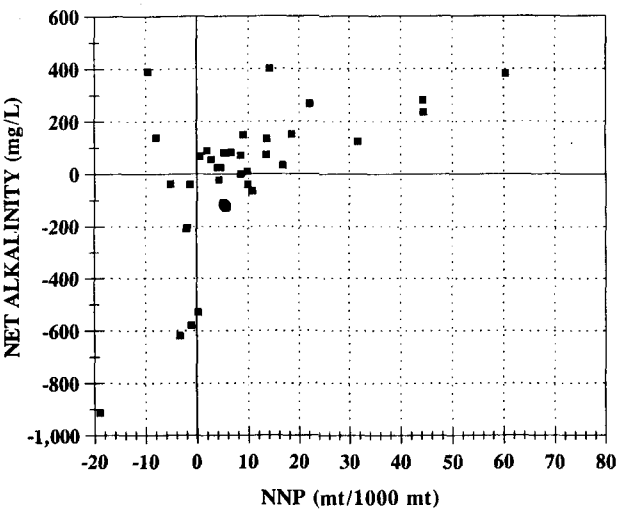

Figure 2. Net neutralization potential (no thresholds) vs. net alkalinity.

The same postmining water quality trends are evident when NNP is examined with thresholds. All sites with NNP greater than 5 mt/1,000 mt have

positive net alkalinity (fig. 3) and pH greater than 6.0. The "gray zone" of variable water quality extends from -5 to +5 mt/1,000 mt NNP.

Values of NNP above which alkaline water is consistently produced are lower in this study than in previous work. diPretoro and Rauch (1988), Erickson and Hedin (1988) compared net alkalinity and volume weighted NNP. MPA was computed the traditional way, using 31.25 times percent sulfur. Erickson and Hedin (1988) evaluated no sites with NNP between 20 and 80 mt/1,000 mt, however all sites greater than 80 mt/1,000 mt had net alkalinity. Nine of 11 sites (82%) with NNP less than 0 mt/1,000 mt had negative net alkalinity. Between NNP 0 and 20 mt/1,000 mt, 7 of 15 (47%) sites were alkaline.

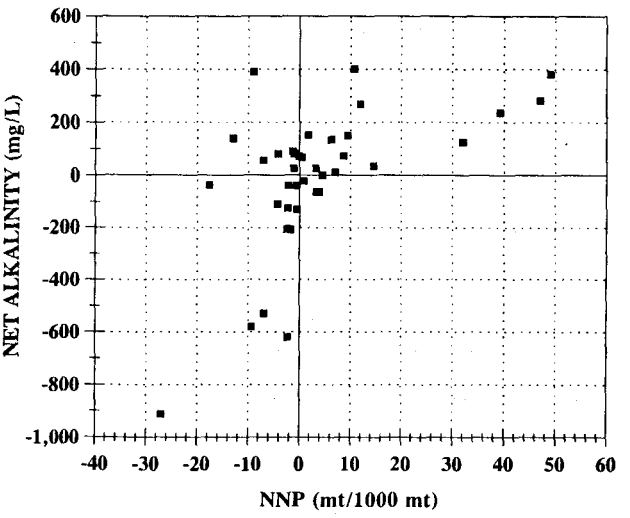

Figure 3. Neutralization potential (with thresholds) vs. net alkalinity.

diPretoro and Rauch found that sites with NNP greater than 30 mt/1,000 mt had net alkaline drainage and that sites with NNP less than 10 mt/1,000 mt had net acidic drainage. Between 10 and 30 mt/1,000 mt was a "gray zone" where 7 of 10 sites were alkaline. diPretoro and Rauch also found that all sites with NP greater than 40 mt/1,000 mt produced net alkaline drainage, while sites with NP less than 20 mt/1,000 mt were acidic (diPretoro and Rauch 1988).

Regardless of the specific values reported, this study and previous work point to the importance of carbonates in determining postmining drainage quality. The presence of as little as 1% to 3% carbonate content may determine whether postmining drainage is alkaline or acid. Different critical values among this and previous studies may reflect different methods of ABA data reduction to produce summary values. Earlier studies used "right triangle" approximations to volume weight their data. This study used a more precise method to produce mass-weighted ABA data (Smith and Brady 1990), and we used multiple ABA holes to define parameters. Different values may also reflect regional or stratigraphic variations in rock properties.

Correct prediction of net acidic or net alkaline water quality was most successful using NNP calculated without thresholds and a 31.25 multiplier, followed closely by NNP with thresholds and a 31.25 multiplier (table 1). A number of sites are clustered near the zero NNP line. The error types are also significant. The highest success rate (NNP, no thresholds, 31.25 multiplier) produced five of seven "errors" where a site was in fact acid when predicted to be alkaline (an undesirable consequence). The "errors" are reversed for NNP with thresholds and 31.25 multiplier. Here, seven of nine "errors" predicted acid sites that in fact were alkaline. This category therefore produced the least number of unanticipated acid sites.

For NP values computed with thresholds, all sites with NP greater than 10 mt/1,000 mt produced drainage with positive net alkalinity. Eight of nine sites

Table 1. Prediction of net alkalinity from net neutralization potential.

NNP calculation	Correctly predicted of 38 Mines	Errors in predicted water quality: Predicted acid, but alkaline	Errors in predicted water quality: Predicted alkaline, but acid
NNP, without threshold, 31.25 multiplier	31 (82%)	2 (5%)	5 (13%)
NNP, with threshold, 31.25 multiplier	29 (76%)	7 (18%)	2 (5%)
NNP, without thresholds, 62.5 multiplier	22 (58%)	11 (29%)	5 (13%)

(89%) having a computed NP less than 1 mt/1,000 mt, exhibited negative net alkalinity (fig. 4). One alkaline site with NP less than 1 is anomalous. NP values between 1 and 10 mt/1,000 mt include sites with both positive and negative net alkalinity, and comprises a "gray" zone, where mine drainage quality is not predictable from NP alone. Sites with NP values greater than 10 mt/1,000 mt also produced drainage of pH greater than 6.0, while "gray zone" sites exhibit variable pH.

Neutralization Potential and Alkalinity

Postmining alkalinity is related to NP (without thresholds) as shown in figure 5. A statistically significant relation at the 95% confidence level was found using simple linear regression. From this empirical relation, it may be

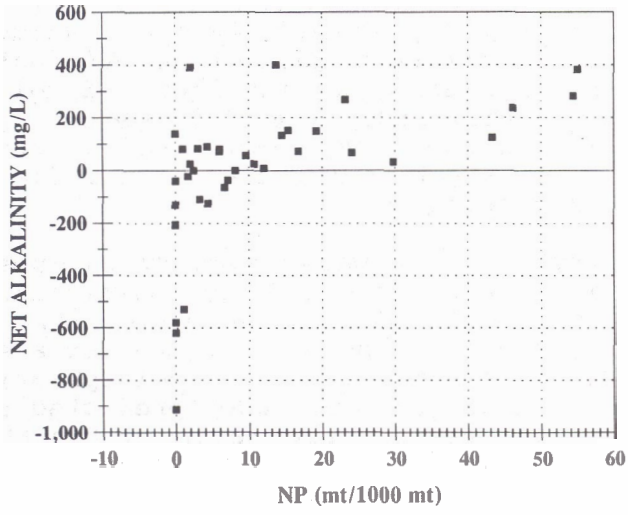

Figure 4. Plot of neutralization potential (with thresholds) vs. net alkalinity.

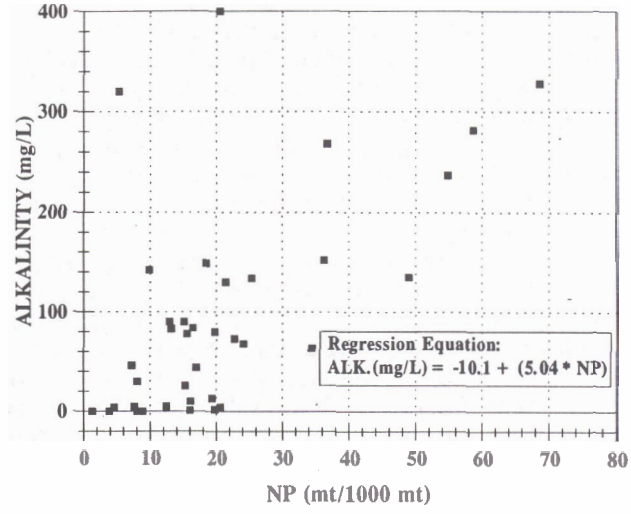

Figure 5. Plot of neutralization potential (no thresholds) vs. alkalinity.

possible to predict postmining alkalinity (in mg/l) as about five times the computed NP value. The predictive relation extends to maximums of about 70 mt/1,000 mt for NP and 400 mg/L alkalinity and has a range in slope of about four to six. The shape and slope of the plot may be explained by active dissolution of carbonate minerals. In addition to availability of carbonate minerals, alkalinity concentration is a function of partial pressure of carbon dioxide in spoil gases, pH, and ionic strength. We do not have mineralogical analyses of carbonate species, but assume that NP reflects mostly calcite with lesser amounts of dolomite, and possibly ankerite and siderite (Cravotta et al. 1994).

Maximum Potential Acidity

MPA, which is a measure of pyrite concentration, was compared against all postmining water quality parameters; no consistent or clear trends were apparent. Our results are similar to those reported by diPretoro and Rauch (1988). Figure 6 is a plot of MPA versus net alkalinity. We attribute the lack of trends to the mechanisms involved in acid generation and transport. Pyrite weathering is a multistep oxidation, dissolution and precipitation reaction with at least four reactions involved (Nordstrom, 1982; Kleinmann et al. 1980). Additionally, pyrite oxidation appears to be inhibited by the presence of carbonates, and many of the pyrite oxidation products are not conservative.

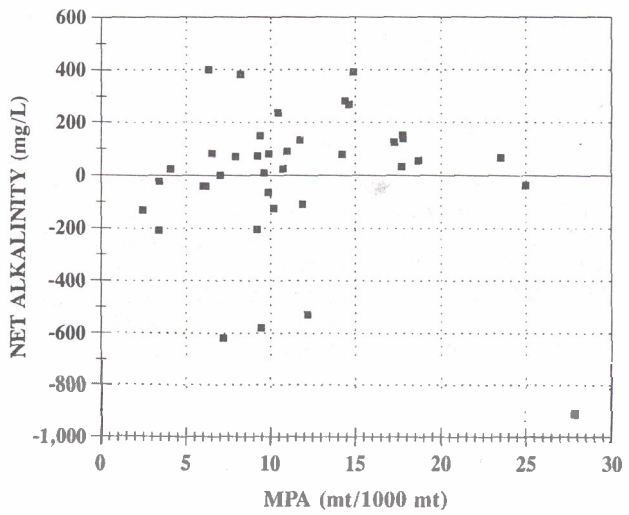

Figure 6. Maximum potential acidity (no threshold) vs. net alkalinity.

A significant positive linear relation between acidity and MPA was apparent for the eight acid sites that had NP's less than 1 (computed using threshold value of 30 mt/1,000 mt). Morrison et al. (1990), in laboratory weathering experiments of strata lacking carbonate minerals, also observed a linear relation. However, in similar experiments Williams et al. (1982) observed an exponential increase in acidity as sulfur increased. Our small sample size does not permit further evaluation.

Sulfate

Sulfate is a direct product of pyrite oxidation. Ambient sulfate levels in unmined areas of the Appalachian basin are usually low in surface and fresh ground waters. In mine drainage, sulfate usually acts conservatively in solution. Figure 7 is a plot of sulfate produced, normalized per unit mass of pyrite (expressed as percent sulfur), as a function of NP. When the data are normalized, a trend of declining sulfate concentration with increasing NP is apparent. Two sites are anomalous, exhibiting high sulfate values at high NP.

We interpret these data to indicate that pyrite oxidation is inhibited by the presence of carbonate minerals in quantities as low as 1% to 3% (10 to 30 mt/1,000 mt). Oxidation may be constrained by suppressing the activity of Thiobacillus sp. bacteria which catalyze the oxidation of ferrous to ferric iron (Singer and Stumm, 1970) or the low solubility of ferric iron at circumneutral pH. This is consistent with laboratory weathering studies conducted by Caruccio and Geidel (1982) and Williams et al. (1982), which indicated rocks containing several percent pyrite would produce less acidity and sulfate when carbonate content were only a few percent.

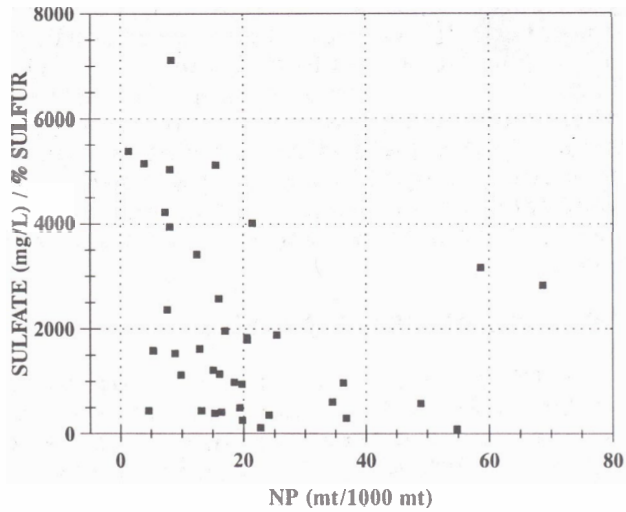

Figure 7. Plot of sulfate production (normalized) vs. neutralization potential.

Conclusions

In this study, the quantity of acid neutralizers (presumed mostly carbonates), represented by NP provides the most reliable and clearest demarcation of postmining water quality. At least one to three percent carbonate may be critical for alkaline producing conditions. Although sulfur content and MPA do not readily translate to postmine water quality predictions, they are still necessary to identify whether the risk of acid drainage exists. We do not report on metals concentrations and ABA parameters. Metals behavior is probably best described in terms of mineralogy and solution properties of pH and redox potential.

At the extremes of ABA values of large excesses or deficiencies, rock chemistry may dominate or overwhelm other mechanisms influencing water quality. In the "gray zone," where ABA properties are closely balanced, effects of other factors, such as hydrology, geology, or mining practices can cause variation in water quality among sites that have similar ABA properties. The principal findings and conclusions are:

1. The acid or alkaline character of postmining waters depends mainly on the carbonate or acid neutralizer content of the overburden. NP, a measure of carbonate content, most clearly predicted postmining water quality conditions.

2. The acid or alkaline character of postmining water can be controlled by carbonate content as low as 1 to 3%. Acid generation, as indicated by sulfate concentration, declines as NP values increase, i.e., carbonate minerals in quantities of a few percent can inhibit pyrite oxidation and acid generation. Other water quality impacts, such as increased dissolved solids or metals concentrations may still occur.

3. The use of "threshold" values for NP in processing raw ABA data improves prediction accuracy, especially for acid sites. Of sites where NP was less than 1 mt/1,000 mt, 89% produced net acid water. Sites where NP was greater than 10 mt/1,000 mt all produced net alkaline water.

4. Critical values of NP and NNP (without thresholds) were identified by which postmining waters can be differentiated. Mines with NP values greater than about 15 mt/1,000 mt and NNP greater than about 10mt/1,000 mt have net alkaline drainage.

5. A "gray zone" of ABA values exists where postmining drainage quality is variable. For NP (with threshold), the gray zone extends from about 1 to 10; for NNP (with thresholds) it extends from about -5 to +5 mt/1,000 mt. Within the "gray zone", the prediction of drainage quality cannot not be based on ABA alone. If a site falls in the ABA "gray zone" additional information is needed for mine drainage prediction. This information can include results of previous and adjacent mining, paleoenvironmental interpretations, baseline hydrologic data, proposed mining and operational plans, and other analytical procedures.

6. An empirical linear relation exists between median alkalinity and NP. A rough estimate of postmining alkalinity (mg/L) can be derived as five times the computed NP (without thresholds).

7. MPA alone is not a reliable predictor of postmining water quality, except where calcareous strata are absent. For acid sites with average NP less than 1 (with thresholds), acidity and MPA were positively related.

Results and conclusions discussed here are a product of using a certain method of data processing. The extent to which these findings are applicable to other areas with differing climate and geology is not known. However, our results show that the content of acid neutralizers strongly influences mine drainage quality. Future mine drainage prediction research should focus on the role of carbonates and other acid neutralizing minerals rather than sulfide reactivity.

Acknowledgements

The authors express appreciation for the enthusiastic support of our management and for assistance of PaDER staff in the mine selection and data acquisition process. Robert Peelor, programmer with PaDER Bureau of Information Services, developed the mainframe computer program for overburden data analysis. Funding for this study was provided by the PaDER, U.S. Department of Interior Office of Surface Mining, and U.S. Environmental Protection Agency

Literature Cited

Brady, K.B.C. and R.H. Hornberger. 1990. The prediction of mine drainage quality in Pennsylvania. Water Pollution Control Assoc. PA Magazine 23(5):8-15.

Caruccio, F.T. and G. Geidel. 1982. The geologic distribution of pyrite and calcareous material and its relationship to overburden sampling. BuMines IC 8863, p. 2-12.

Cravotta, C.A. III, K.B.C. Brady, M.W. Smith, and R.L. Beam. 1990. Effectiveness of the addition of alkaline materials at surface mines in preventing or abating acid mine drainage: Part 1. Theoretical considerations. p 221-225 In Proceedings of the 1990 Mining and Reclamation Conference and Exhibition. (Charleston, WV, April 23-26, 1990).

Cravotta, C.A. III, D.L. Dugas, and K.B.C. Brady. 1994. Effects of selective handling of pyritic, acid-forming materials on the quality of ground water at a reclaimed surface coal mine in Clarion County, Pennsylvania, U.S.A. (these proceedings).

diPretoro, R.S. and H.W. Rauch. 1988. Use of acid -base accounts in premining prediction of acid drainage potential: A new approach from northern West Virginia. p. 1-10. In Proceedings: Mine Drainage and Surface Mine Reclamation, Vol 1. Mine Water and Mine Waste. BuMines IC 9183.

Erickson, P.M. and R. Hedin. 1988. Evaluation of overburden analytical methods as a means to predict postmining coal mine drainage quality. p. 11-19. In Proceedings: Mine Drainage and Surface Mine Reclamation, Vol 1. Mine Water and Mine Waste. BuMines IC 9183.

Helsel, D.R. 1987. Advantages of nonparametric procedures for analysis of water quality data. Hydrological Sci. J. 32(2):179-190.

Kleinmann, R.L.P., D.A. Crerar, and R.R. Pacelli. 1980. Biogeochemistry of acid mine drainage and a method to control acid formation. Min. Eng. 33:300–306.

Morrison, J.L., B.E. Sheetz, D.W. Strickler, E.G. Williams and A.W.Rose. 1990. Predicting the occurrence of acid mine drainage in the Allegenian coal-bearing strata of western Pennsylvania; an assessment by simulated weathering (leaching) experiments and overburden characterization. p 249-256. In L.L. Chyi and C.L. Chou (eds), Recent advances in coal geochemistry. Geol. Soc. of America Special Paper 248.

Nordstrom, D.K., 1982. Aqueous pyrite oxidation and the consequent formation of secondary iron minerals. p 37-56. In Acid Sulfate Weathering, SSSA Special Publication Number 10.

Pennsylvania Department of Environmental Resources. 1990. Commonwealth of Pennsylvania 1990 water quality assessment (R.F. Frey, ed.). Harrisburg, PA. 206 p.

Singer,P.C. and W. Stumm, 1970. Acidic mine drainage:the rate determining step. Science 167:1121-1123.

Smith, M.W. and K.B.C. Brady. 1990. Evaluation of acid base accounting data using computer spreadsheets. p. 213-219. In proceedings of the 1990 Mining and Reclamation Conference and Exhibition (Charleston, WV, April 23-26, 1990)

Sobek, A.A., W. A. Schuller, J.R. Freeman, and R.M. Smith. 1978. Field and laboratory methods applicable to overburdens and minesoils. EPA-600/2-78-054. U.S. Environmental Protection Agency, Cincinnati, OH. 203p.

Williams, E.G., A.W. Rose, R.R. Parizek, and S.A. Waters. 1982. Factors controlling the generation of acid mine drainage. The Pennsylvania State University final report to the U.S. Bureau of Mines, Grant No. G5105086. 256 p.

OBSERVED PREFERENTIAL DEPLETION OF NEUTRALIZATION POTENTIAL OVER SULFIDE MINERALS IN KINETIC TESTS: SITE-SPECIFIC CRITERIA FOR SAFE NP/AP RATIOS[1]

Kevin A. Morin[2] and Nora M. Hutt[3]

Abstract: As the number of completed kinetic tests grows, an international database is forming on rates of acid generation, acid neutralization, and metal leaching. As the results become available and are compiled, valuable lessons are learned on the prediction of acidic drainage and on the variability of reaction rates caused by site-specific factors.

One of the more important lessons from the kinetic-test database pertains to acid-base accounting (ABA). A great deal of effort is expended on the development of universal ABA criteria to predict if a sample may eventually become net acidic. Based on the amount of carbonate or feldspar minerals (Neutralization Potential or NP) and sulfide minerals (Acid Potential or AP), the criteria are usually expressed as some form of Net Neutralization Potential (=NP-AP) or NP/AP ratio. Widely reported criteria for NP/AP state that a value above 2.5 to 3.0 can be considered non-net-acid-generating through time, but there is still some argument on the appropriate values. The Canadian database shows that one site required NP/AP>4.0 for the prediction of consistently neutral pH after 40 weeks of testing.

This paper presents some of the information in the Canadian database. In particular, the rates of NP and AP depletion are presented for several kinetic tests, showing that the amount of NP often has to exceed AP by a factor of 1.3 to 4.0 for the predicted maintenance of near-neutral pH into the distant future. This is in partial agreement with theoretical relationships that show the factor should often be between 1.0 and 2.0 for carbonate-based neutralization. In effect, the kinetic database shows that attempts to identify universal ABA criteria can be either too cautious or faulty for a particular minesite. Instead, appropriate ABA criteria should be determined on a site-specific basis, reflecting reaction rates of the acid-generating and acid-neutralizing minerals at the particular site.

Additional Keywords: acidic drainage, geochemical predictions, kinetic tests, acid-base accounting

Background and Objectives

From a geochemical perspective, acidic drainage can be viewed as the result of competition between acid-generating and acid-neutralizing minerals, with the dominant mineral(s) regulating the chemistry of water passing over the material. A problem arises from the recognition that the dominant mineral at one point in time may not be the dominant one at a later time. These issues can be summarized in the pointed question: Will the sample generate net acidity *at any point* in time? The answer to this question carries major implications for mine planning, operation, closure, and bonding.

A person unfamiliar with acid-drainage prediction, but aware of acid-drainage impacts, would likely be surprised to discover that current techniques do not typically yield predictions with which mining companies and regulatory agencies are comfortable. This is understandable in light of past technical failures in prediction and

---

[1]Paper presented at the International Land Reclamation and Mine Drainage Conference and the Third International Conference on the Abatement of Acidic Drainage, Pittsburgh, PA, USA, April 24-29, 1994.

[2]Kevin A Morin, Morwijk Enterprises Ltd, 47-115 Kamehameha Highway, Kaneohe, Hawaii, USA 96744 (address until 2/28/94).

[3]Nora M. Hutt, Normar Enterprises, Box 357, Wildwood, Alberta, Canada T0E 2M0

control and because of the philosophical issues surrounding human limitations. Focusing on technical matters, past failures in prediction can be traced to two basic problems: insufficient data and incorrect interpretation.

Insufficient data is not an acceptable excuse for erroneous predictions, as additional effort would eliminate the problem. Incorrect interpretation of the data, on the other hand, is more complicated and, for this paper, we are concerned with general misinterpretation rather than individual weakness. Furthermore, we limit our discussion here to the common predictive tools for acidic drainage often labelled "static" and "kinetic" tests. Other highly specialized, research-level tools are available, but they are not as widely used and accepted as the aforementioned tests.

Predictions of acid drainage are commonly based on suites of static and kinetic tests. Static tests typically comprise bulk analyses of minerals, metals, and nonmetals that characterize a sample at one point in time. Such tests include the popular acid-base accounting (ABA), for which there are several variations (e.g., Coastech Research 1989). By their nature, static tests cannot reliably yield long-term trends in chemistry.

Kinetic tests consist of repetitive cycles of leaching and monitoring either under laboratory conditions or in the field. The trends through time in aqueous concentrations issuing from the tests yield long-term production rates of metals, nonmetals, and titration-based parameters such as acidity, which static tests cannot provide. However, kinetic tests alone often do not indicate how long the long-term production rates can be maintained, unless the tests are run for years or decades. More often, static tests on the sample provide the total mass and balances of acid-generating and acid-neutralizing minerals that are being consumed in the kinetic test. Consequently, static and kinetic tests form a codependent suite of predictive testwork, and each test must be conducted for proper interpretation of all tests. This opposes earlier views that kinetic tests were only "confirmatory" in nature and were only necessary if static tests suggested a potential problem (e.g., B.C. AMD Task Force et al. 1989).

The idea that kinetic tests are only needed if static tests like ABA suggest a problem assumes that static tests can accurately "suggest a problem". The literature abounds with efforts to improve, refine, and properly interpret ABA results (e.g., Coastech Research 1989; Morin 1990; Lapakko and Lawrence 1993). In particular, the focus of many papers has been the proper criteria for identifying acid-drainage potential through the Acid Potential (AP or similar parameter) and Neutralization Potential (NP or similar parameter). The net potential for acid drainage is often expressed through subtraction (Net Neutralization Potential = NP - AP) or through division (NP/AP). Various criteria that have appeared include: (1) any sample with an NNP value less than -20 ppt $CaCO_3$ will be net acid generating at some point in time, (2) any sample with NP/AP less than 1.0 will be net acid generating, and (3) any sample with NP/AP greater than 1.0 and less than 2.5 is "uncertain" in its potential and requires further (kinetic) testwork. We find these criteria particularly interesting because our unpublished work has provided samples with negative values of NNP that are not expected to generate net acidity at any time, as well as samples with NP/AP > 4.0 that are expected to generate net acidity within several years.

The worldwide search for universal ABA criteria is useful, but an "uncertain" range seems to develop from any large compilation of ABA data. This actually means that "uncertain" samples at some mines will produce acidic drainage, whereas similarly classified samples at other mines will not. Careful examination of the preceding sentence reveals that the sample's potential is not "uncertain" at all; it is simply site-dependent. In other words, each site has its own ABA criteria for estimating acid-drainage potential, and it is only the search for universal criteria that creates the uncertain status.

The first objective of this paper is to show how kinetic tests empirically provide the critical or "safe" NP/AP ratio above which there is no predicted potential for acidic drainage at any point in time. This is obtained by comparing the consumption rate of NP to the oxidation of sulfide. For example, if NP is consumed 2.3 times faster than sulfide oxidizes, then samples with reactive, available NP and AP at ratios above 2.3 would be predicted not to generate acidic drainage at any time. The second objective of this paper is to provide examples of "safe" NP/AP ratios at particular minesites that lie within the "uncertain" range in any universal ABA criteria. We conclude with

the recommendation that static and kinetic tests should always be conducted as one suite so that the results of all testwork can be interpreted more accurately .

Theory

Since the focus of this paper is on the relative reaction rates of acid-generating and acid-neutralizing minerals, the relevant theory addresses the geochemical reactions of the minerals and the manner in which one mineral can affect another. In this paper, the acid-generating minerals are limited to pyrite (FeS_2), and the acid-neutralizing minerals are limited to calcite ($CaCO_3$) and a suite of feldspar minerals. The conclusions reached for these minerals may not necessarily apply to other minerals and the appropriate reactions for other minerals should be checked independently. Furthermore, site-specific environmental conditions can sometimes invalidate the following conclusions as illustrated below.

The "standard" reaction for pyrite oxidation is:

$$FeS_2 + 7/2\ H_2O + 15/4\ O_2 \rightarrow Fe(OH)_3 + 2\ SO_4^{2-} + 4\ H^+ \qquad (1)$$

Equation 1 assumes much about mineralogy, reaction pathways, and local environmental conditions. These assumptions include: (1) all sulfur occurs in the solid phase only as S_2^{2-}, (2) S_2^{2-} oxidizes completely to sulfate, (3) pyrite is the only oxidizing sulfide mineral, (4) molecular oxygen and water are the only oxidants, (5) all iron oxidizes to the ferric (Fe^{3+}) state, and (6) all iron precipitates as $Fe(OH)_3$. Obviously, these assumptions on mineralogy, reaction pathways, and environmental conditions are not always met, and thus alternative equations would apply (Morin 1990; Morin 1993). For simplicity, this paper assumes equation 1 is applicable to a site.

Where calcite is present and reactive, the overall oxidation-neutralization reaction depends on pH (Ferguson and Morin 1991). Two simplified neutralization reactions with calcite, assuming no calcium and sulfate are lost to secondary mineral precipitation, are:

<u>for pH < 6.3</u>:

$$FeS_2 + 7/2\ H_2O + 15/4\ O_2 + 2\ CaCO_3 \rightarrow Fe(OH)_3 + 2\ SO_4^{2-} + 2\ H_2CO_3^0 + 2\ Ca^{2+} \qquad (2)$$

<u>for 6.3 < pH < 10.3</u>:

$$FeS_2 + 7/2\ H_2O + 15/4\ O_2 + 4\ CaCO_3 \rightarrow Fe(OH)_3 + 2\ SO_4^{2-} + 4\ HCO_3^- + 4\ Ca^{2+} \qquad (3)$$

Equations 2 and 3 show that twice as much calcite is needed to neutralize the pyrite-derived acidity to neutral levels than to slightly acidic levels. Additionally, the resulting aqueous ratio of calcium to sulfate is 1:1 at acidic levels and 2:1 at neutral levels. Again, equations 2 and 3 are simplifications of mineral-water reactions; potentially important factors such as aqueous complexation and chemical activity are ignored and other complications are discussed below.

If carbonate is absent or non-reactive, slower-reacting feldspar and accompanying mafic minerals can provide some neutralization of acidity (Lapakko 1988; Lapakko and Antonson 1993; Moss and Edmunds 1992). However, the stoichiometry of these neutralization reactions can be complex and site-specific (Melchoir and Bassett 1990; Stumm 1990) and the understanding of the mineral-dissolution mechanisms is evolving quickly (Schott 1990). In general, the rates and nature of feldspar neutralization are dependent on several factors (Sverdrup and Warfvinge 1993) and complete neutralization may only be possible where mineral-surface areas are high, feldspar minerals comprise a significant percentage of the overall mineralogy, and the rate of acid generation is relatively low. Such a case is discussed below as Mine "E". In many cases, though, only partial neutralization can be expected from feldspar and accompanying mafic minerals.

Due to the complexity of feldspar dissolution, only simplified examples will be discussed here. For these examples, (1) all sulfur in pyrite oxidizes fully to sulfate, (2) iron from pyrite oxidizes and precipitates as $Fe(OH)_3$, (3) the silicon from the feldspar forms aqueous $H_4SiO_4^0$ or solid-phase SiO_2, (4) aluminum does not hydrolyze between pH 3.5 and 4.5, but hydrolyzes and precipitates as $Al(OH)_3$ around pH 7, and (5) the alkali metals do not hydrolyze and do not precipitate between pH 3.5 and 7.0. Consequently, the neutralization reactions for the three most common end-member feldspar minerals are:

<u>at 3.5<pH<4.5</u>:

$$FeS_2 + 13/2\ H_2O + 15/4\ O_2 + 1/2\ CaAl_2Si_2O_8 \rightarrow Fe(OH)_3 + 2\ SO_4^{2-} + 1/2\ Ca^{2+} + Al^{3+} + H_4SiO_4^0 \quad (4)$$

$$+ 15/2\ H_2O + 15/4\ O_2 + KAlSi_3O_8 \rightarrow Fe(OH)_3 + 2\ SO_4^{2-} + K^+ + Al^{3+} + 3\ H_4SiO_4^0 \quad (5)$$

$$+ 15/2\ H_2O + 15/4\ O_2 + NaAlSi_3O_8 \rightarrow Fe(OH)_3 + 2\ SO_4^{2-} + Na^+ + Al^{3+} + 3\ H_4SiO_4^0 \quad (6)$$

<u>around pH 7</u>:

$$FeS_2 + 13/2\ H_2O + 15/4\ O_2 + 2\ CaAl_2Si_2O_8 \rightarrow Fe(OH)_3 + 2\ SO_4^{2-} + 2\ Ca^{2+} + 4\ Al(OH)_3 + 4\ H_4SiO_4^0 \quad (7)$$

$$+ 15/2\ H_2O + 15/4\ O_2 + 4\ KAlSi_3O_8 \rightarrow Fe(OH)_3 + 2\ SO_4^{2-} + 4\ K^+ + 4\ Al(OH)_3 + 12\ H_4SiO_4^0 \quad (8)$$

$$+ 15/2\ H_2O + 15/4\ O_2 + 4\ NaAlSi_3O_8 \rightarrow Fe(OH)_3 + 2\ SO_4^{2-} + 4\ Na^+ + 4\ Al(OH)_3 + 12\ H_4SiO_4^0 \quad (9)$$

Based on equations 2 through 9, the ratios of the cation from the neutralizing mineral (calcium, potassium, or sodium) to sulfate range from 1:1 to 2:1 around neutral pH and from 1:1 to 4:1 at acidic pH (table 1). These ratios represent the depletion rate of neutralizing minerals relative to that of the sulfide mineral, which in turn reveals the relative amount of reactive NP to AP needed to ensure the maintenance of pH-neutral conditions into the future.

Table 1 Ratio of cation (Ca, K, Na) to sulfate during selected neutralization reactions[1].

Mineral	~ pH 4	~ pH 7
CALCITE	1.00	2.00
ANORTHITE (Ca feldspar)	0.25	1.00
ALBITE (Na feldspar) . . .	0.50	2.00
K FELDSPARS (various) .	0.50	2.00

[1] See equations 1 through 9

At this point, two complications should be considered. First, if feldspar minerals provide significant neutralization in a sample, their contents should be converted into $CaCO_3$ equivalent for comparison to ABA values. One mole of calcium feldspar (anorthite) around neutral pH neutralizes two moles of acidity (equation 7) and thus this mineral can be twice as effective per mole as calcite at neutral pH (equation 3). Consequently, $NP_{feldspar\ as\ CaCO3}$ = 2 x Ca-feldspar content on a molar basis, or $NP_{feldspar\ as\ CaCO3}$ = 5.56 x Ca-feldspar content on a weight basis such as tonnes/1000 tonnes (not the same as visual and volume percent). Other conversion factors apply depending on

the mineralogy and environmental conditions (e.g., table 2). Second, there is no reason that the ratios of cation to SO_4 should match exactly those of table 1. For the mineralogy and environmental conditions involved in equations 1 through 9, the actual value of the ratio can lie anywhere within a factor of two for calcite (1.0 to 2.0) and a factor of four (0.25 to 1.00, or 0.50 to 2.00) for the feldspar minerals. Also, additional reactions such as the exsolution of CO_2 gas from the water upon neutralization by calcite can prevent the ratio from reaching 2.0 at pH>6.3 (Ferguson and Morin 1991), and minerals other than those examined here can produce other ratios. Furthermore, carbonate and feldspar minerals can be dissolved and leached even in the absence of sulfide oxidation by dilute water. The point being brought forward here is that there are definable ratios based on simplified theory, but the actual ratios of cation to SO_4 could be higher or lower than expected. Therefore, it is more appropriate and more reliable to now examine actual ratios obtained from kinetic testwork for some Canadian mines.

Table 2. Conversion of parts-per-thousand weight measurements of a neutralizing mineral to $NP_{mineral\ as\ CaCO3\ equivalent}$ as tonnes $CaCO_3$/1000 tonnes of sample[1].

Mineral	~ pH 4	~ pH 7
CALCITE	1.00	0.50
ANORTHITE (Ca feldspar)	11.12	5.56
ALBITE (Na feldspar) . . .	5.56	2.78
K FELDSPARS (various) .	5.24	2.62

[1] See equations 1 through 9.

Examples of Geochemical Ratios of Neutralization

The first example is drawn from the extensive testwork of the Cinola Gold Project in British Columbia (City Resources/Norecol 1988). This testwork included over 200 acid-base accounts, 44 humidity cells, 13 laboratory-scale leach columns, and 4 on-site 30-mt leach pads. Although the mine application is no longer pursued, the British Columbia AMD Task Force and the Canadian MEND Program continued some tests for a total period of 5 years, and a draft report has recently been submitted (Norecol, Dames, and Moore 1993). Geochemical molar ratios were calculated for initial humidity cells that were pH-neutral and had analyses for one or more of calcium, magnesium, manganese, strontium, and barium (fig. 1). These cations are taken as indicators for dissolution of all potential

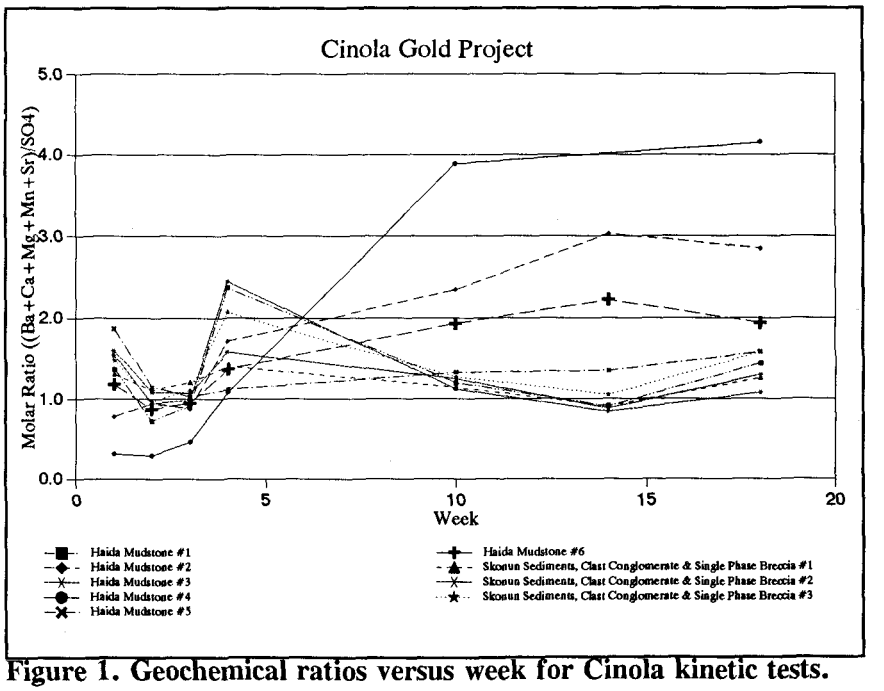

Figure 1. Geochemical ratios versus week for Cinola kinetic tests.

carbonate minerals, although calcium dominated the sum. Pyrite was the dominant sulfide mineral.

After the Cinola humidity cells began stabilizing by Week 5, the geochemical ratios usually exceeded 1.0 for most of the Skonun rock type and 2.0 for three samples of Haida mudstone (fig. 1). The ratios above 1.0 for $Ca:SO_4$ suggested neutralization was derived from calcite (table 1), which was consistent with other information that indicated calcium-dominated carbonate minerals were present and available in the rock. Furthermore, in agreement with figure 1, later studies of limestone addition to Skonun sediments showed that NP/AP values close to 1 were not sufficient to maintain pH-neutral conditions over decades, but that a ratio of 2.0 should indefinitely maintain neutral conditions (Norecol, Dames, and Moore 1993). The higher ratios for some Haida mudstone over the Skonun show that the carbonate minerals can be more quickly leached relative to sulfide in this rock type. As a result, a "safe" NP/AP ratio from ABA would be a maximum of 4.2 based on figure 1.

The second example in this paper is taken from a copper mine in Canada in which five humidity cells contained pH-neutral samples of waste rock and tailings with known calcium-based carbonate minerals and pyrite. The geochemical ratios from these cells (fig. 2) showed that there was often an accelerated depletion of neutralizing minerals relative to sulfide oxidation beyond that attributable to sulfide oxidation alone (table 1). Interpretation of results by Week 40 suggested a safe NP/AP ratio for this site was approximately 4.0, and continuation of two cells beyond Week 40 continued to support this value as a maximum. Although the samples were pH-neutral and were expected to remain so for years, their ABA ratios were less than 4.0. Consequently, eventual net acid generation was predicted for them.

The third example is a coal-tailings area with no known occurrences of acidic drainage in the tailings area, but acidic seepage was common in nearby waste piles due to oxidation of pyrite. The geochemical ratios from the one pH-neutral cell remained relatively consistent during the 40-week period, around values of 1.0 to 1.5 (fig. 3). The safe NP/AP ratio for this sample in the long term is 1.4. This relatively

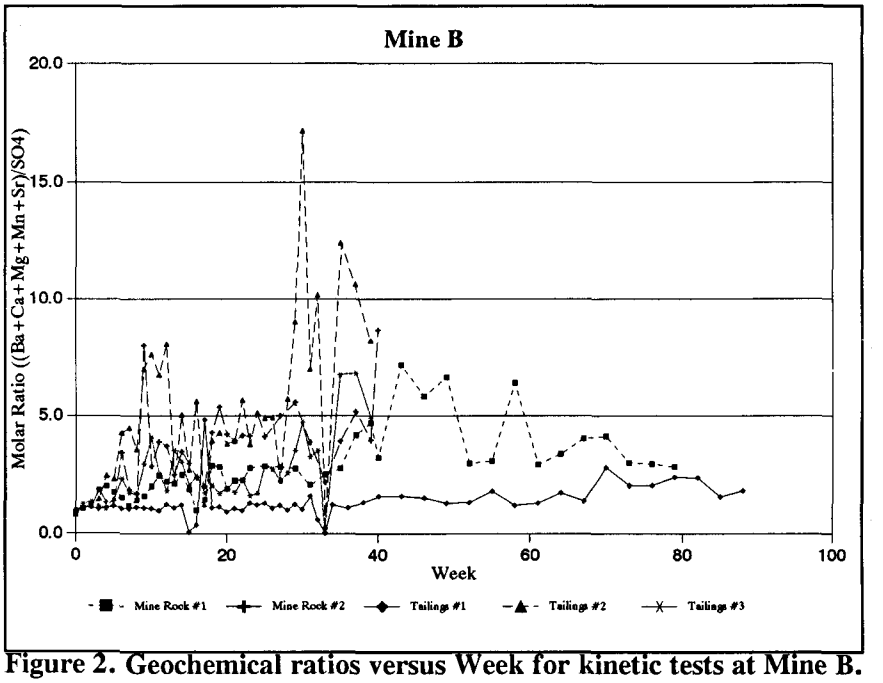

Figure 2. Geochemical ratios versus Week for kinetic tests at Mine B.

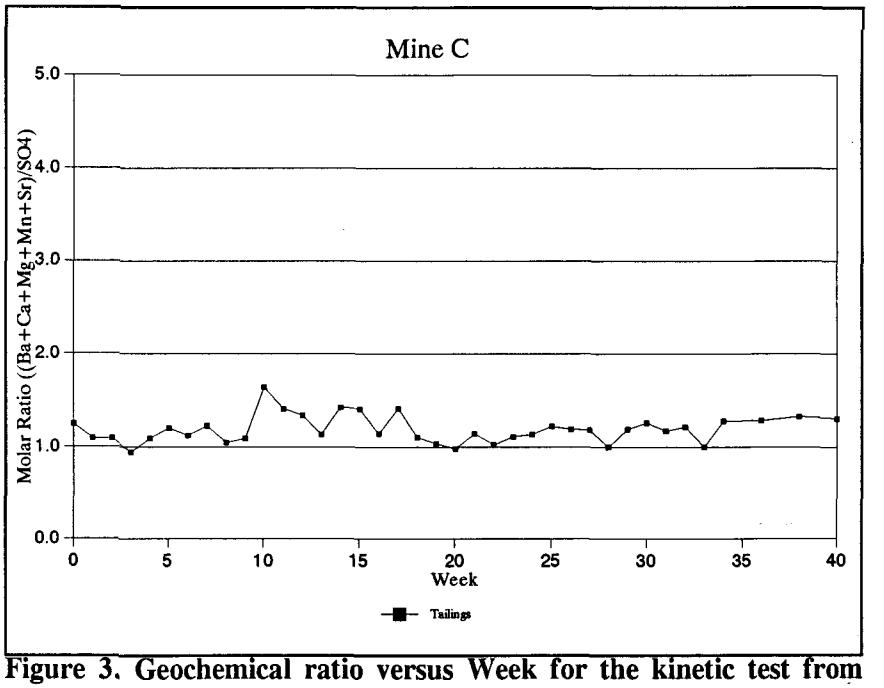

Figure 3. Geochemical ratio versus Week for the kinetic test from Mine C.

low value is attributed to the loss of CO_2 gas during neutralization within the cell (Ferguson and Morin 1991), but the safe value may have to be raised to 2.0 or more if CO_2 is not similarly lost under field conditions.

The fourth example in this paper is drawn from a Canadian copper mine with no known occurrences of acidic drainage, although elevated sulfate values in mine drainage point to active oxidation of the pyrite. Geochemical ratios from the four pH-neutral rock types placed in humidity cells were less than 3.0 after the cells began stabilizing by Week 10 (fig. 4). After 40 weeks, the ratios indicated each rock type could be assigned its own safe value, but the overall value for the minesite could be set at 2.3 at Week 40.

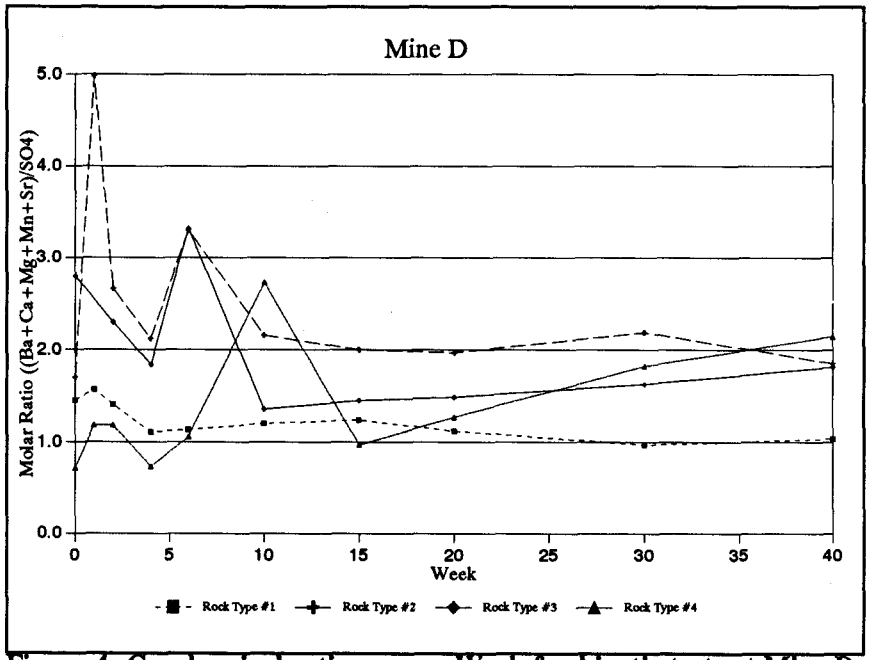

Figure 4. Geochemical ratios versus Week for kinetic tests at Mine D.

The fifth and last example is taken from a Canadian mine with little to no carbonate minerals in the rock and tailings. This mine has been closed for over a decade and no acidic drainage has appeared despite the general lack of carbonate minerals since closure. There is one dominant rock type and this rock and its tailings contain 50% feldspar, 1%S as pyrite, and most of the remainder is quartz with minor magnetite and hornblende. Two geochemical ratios were calculated from the humidity-cell results: a carbonate ratio including calcium and magnesium and a feldspar ratio including calcium, potassium, and sodium (fig. 5). Because calcium was the dominant cation, both ratios are similar. Although there were apparently some occasional errors in analyses of the cations and/or anions, the ratios often centered around 1.0, which is the theoretical value for dissolution of calcium feldspar under pH-neutral conditions (table 1). However, due to erratic values towards the end of the testwork, a conservative safe NP/AP ratio would be 1.5. This, however, is not an important issue since the conversion of the 50% feldspar to an NP value (table 2) far exceeds the potential acidity from 1%S sulfide.

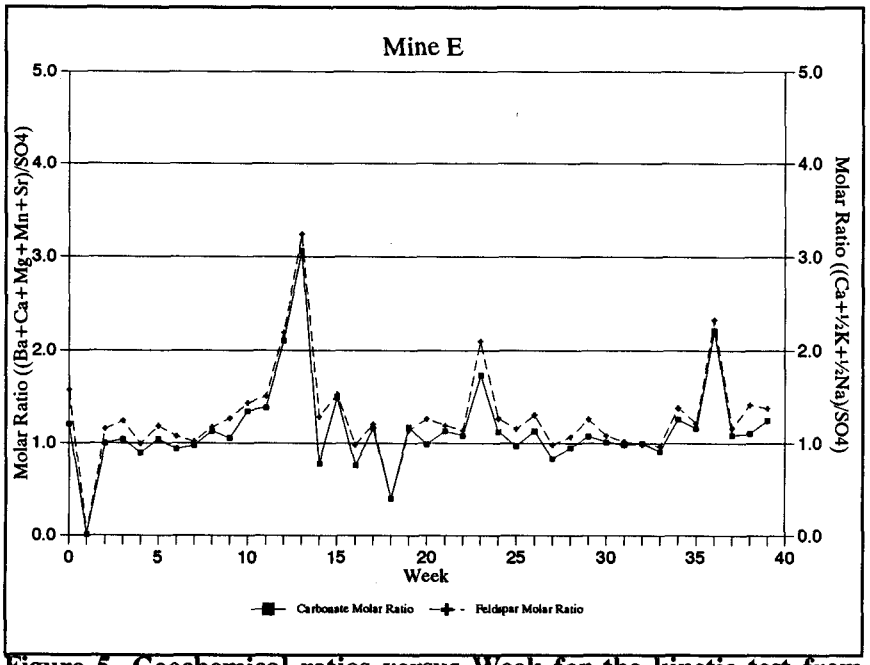

Figure 5. Geochemical ratios versus Week for the kinetic test from Mine E.

Conclusion

This paper has examined the simplified dissolution reactions of carbonate and feldspar minerals through theory and through examples from common predictive testwork known as "kinetic" tests. When the dissolution of carbonate or feldspar is driven by pyrite oxidation, the aqueous ratios of the cations to sulfate can occur within theoretically definable ranges. The occurrence of a value within or beyond a theoretical range can sometimes reveal an important aspect of the mineralogy or environmental conditions within the test chamber. When the mineralogy and environmental conditions are known, the ratio identifies the relative rate at which neutralizing minerals are consumed relative to the acid-generating minerals, which leads two important conclusions. First, in association with the results of static tests which define the total amounts of all relevant minerals, the eventual "winner" in the geochemical competition between acid-generating and acid-neutralizing minerals can be predicted, and the times to complete consumption can be calculated. Second, the long-term ratio from the testwork indicates the "safe" NP/AP ratio needed from ABA to declare a specific sample to be net acid-generating or acid-consuming indefinitely. Such an assessment should ensure that environmental conditions in the test chamber, like the exsolution of CO_2 gas, resemble those in the field.

Based on these observations, static and kinetic tests should be performed as one suite of testwork because each relies on information from the other for proper interpretation. Additionally, the search for universal criteria in this situation, where site-specific factors dominate, can lead to the delineation of an "uncertain" range that will grow as the worldwide database grows. However, the "uncertainty" is simply the result of the search for universal criteria in the first place, and gives the false impression that predictive tests for acidic drainage are not dependable or appropriate.

Acknowledgements

We thank the mining companies of Canada that recognize the continually evolving state of acid-drainage prediction and are committed to conducting the best practical predictive testwork available. We are grateful to the three anonymous reviewers, who improved the quality and clarity of this paper, and to the conference coordinators, particularly Ms. Lowanse, who managed manuscript submissions.

'Ua mau ke ea ō ka 'āina i ka aloha 'āina

References

British Columbia AMD Task Force, Steffen Robertson Kirsten (B.C.) Inc., Norecol Environmental Consultants, and Gormely Process Engineering. 1989. Draft Acid Rock Drainage Technical Guide, Volume 1.

City Resources (Canada) Limited and Norecol Environmental Consultants Ltd. 1988. Cinola Gold Project, Stage II Report, Volume V and Volume V Appendices. Submitted to the British Columbia Ministry of Energy, Mines, and Petroleum Resources.

Coastech Research Inc. 1989. Investigation of prediction techniques for acid mine drainage. MEND Project 1.16.1a.

Ferguson, K.D., and K.A. Morin. 1991. The prediction of acid rock drainage - Lessons from the database. p.86-106. In Volume 3, Proceedings of the Second International Conference on the Abatement of Acidic Drainage. (Montreal, Quebec, September 16-18).

Lapakko, K. 1988. Prediction of acid mine drainage from Duluth Complex mining waste in northeastern Minnesota. p.180-190. In Proceedings of the 1988 Mine Drainage and Surface Mine Reclamation Conference, American Society of Surface Mining and Reclamation. (Pittsburgh, PA, April 17-22).

Lapakko, K., and R.W. Lawrence. 1993. Modification of the net acid production (NAP) test. p. 145-159. In Proceedings of the Seventeenth Annual British Columbia Mine Reclamation Symposium. (Port Hardy, British Columbia, May 4-7).

Lapakko, K., and D.A. Antonson. 1993. Oxidation of sulfide minerals present in Duluth Complex rock: A laboratory study. In Environmental Geochemistry of Sulfide Oxidation, ACS Symposium Series No. 550., American Chemical Society, Washington, D.C., USA.

Melchoir, D.C., and R.L. Bassett, eds. 1990. Chemical modeling of aqueous systems II. American Chemical Society, Washington, D.C., USA. 556 p.

Morin, K.A. 1993. Rates of sulfide oxidation in submerged environments: Implications for subaqueous disposal. p.235-247. In Proceedings of the Seventeenth Annual British Columbia Mine Reclamation Symposium. (Port Hardy, British Columbia, May 4-7).

Morin, K.A. 1990. Problems and proposed solutions in predicting acid drainage with acid-base accounting. In Acid Mine Drainage - Designing for Closure, Geological Association of Canada/Mineralogical Association of Canada Conference. (Vancouver, British Columbia, May 16-18).

Moss, P.D., and W.M. Edmunds. 1992. Processes controlling acid attenuation in the unsaturated zone of a Triassic sandstone aquifer (U.K.) in the absence of carbonate minerals. Applied Geochemistry, 7, p.573-583.

Norecol, Dames, and Moore. 1993. Long term kinetic acid generation studies Cinola Project, Queen Charlotte Islands British Columbia [sic]. Report for the British Columbia Acid Mine Drainage Task Force.

Schott, J. 1990. Modeling of the dissolution of strained and unstrained multiple oxides: The surface speciation approach. p.337-365. In W. Stumm, ed., Aquatic Chemical Kinetics, Wiley-Interscience, Toronto.

Stumm, W., ed. 1990. Aquatic chemical kinetics. Wiley-Interscience, Toronto. 545p.

Sverdrup, H., and P. Warfvinge. 1993. Calculating field weathering rates using a mechanistic geochemical model PROFILE. Applied Geochemistry, 8, p.273-283.

CHEMICAL PREDICTIVE MODELING OF ACID MINE DRAINAGE FROM WASTE ROCK: MODEL DEVELOPMENT AND COMPARISON OF MODELED OUTPUT TO EXPERIMENTAL DATA[1]

William W. White III,[2] Edward M. Trujillo,[3] and Cheng-Kuo Lin[3]

Abstract: The U.S. Bureau of Mines (USBM) is developing a geochemical predictive model for acid mine drainage (AMD) from waste rock associated with metal mining. The model will identify AMD potential during property exploration and development and will facilitate planning of waste-rock handling. This paper presents results on model development and comparison of model output with 90 weeks of kinetic tests (humidity-cell data) for three selected samples. The existing model successfully matched experimental data collected from humidity-cell effluent during the 90-week period. The model (1) predicted the progressive development of acid as well as the decrease in aqueous sulfate and iron concentrations as jarosite precipitated and (2) demonstrated good agreement between modeled output and actual effluent pH, total iron, and sulfate concentrations from the three different samples of waste rock. Sulfide contents of these three samples were 3, 6, and 24 wt %. Although acid-base accounting classified all three samples as potential acid producers, effluent pH from the 3% pyrite sample was neutral to slightly basic during 90 weeks of accelerated weathering. Samples containing 6% and 24% pyrite continuously produced acidic effluent during the same 90-week period. Sulfate-release rates resulting from sulfide oxidation increased with solid-phase sulfide content and decreasing pH. Calcium and magnesium release-rates determined from accelerated weathering of the 3% pyrite sample were projected beyond 90 weeks. This projection suggests that the 3% pyrite sample should develop AMD after 110 to 130 weeks of laboratory-accelerated weathering. The mathematical model also predicts that AMD will occur after 130 weeks.

Additional Key Words: acid mine drainage, metal-mine waste rock, laboratory-accelerated weathering, geochemical predictive model.

Introduction

The purpose of the USBM's AMD predictive-modeling research is to (1) assist Federal land-managing agencies and industry with this assessment during the exploration and feasibility-study stages of a project and (2) apply the resulting model to the assessment of proposed AMD-treatment and -control scenarios. Model development is a cooperative effort between the USBM and the University of Utah Chemical and Fuels Engineering Department (University). Static and kinetic laboratory tests are being conducted by the USBM on samples of three different waste-rock types designated as 1-B, 1-C, and 1-D. Sulfide contents of these three samples are 3, 6, and 24 wt %, mainly as mixtures of euhedral and/or subhedral and framboidal pyrite (White and Jeffers 1994). The resulting experimental data from the USBM's laboratory tests are used by the University in the development of the mathematical model.

---

[1]Paper presented at the International Land Reclamation and Mine Drainage Conference and the Third International Conference on the Abatement of Acidic Drainage, Pittsburgh, PA, April 24-29, 1994.

[2]William W. White III, Geologist, U.S. Department of the Interior, Bureau of Mines, Salt Lake City Research Center, Salt Lake City, UT, USA.

[3]E. M. Trujillo, Associate Professor, and Cheng-Kuo Lin, Ph.D. Candidate, Department of Chemical and Fuels Engineering, University of Utah, Salt Lake City, UT, USA.

Several recent reviews discuss the development of AMD modeling and summarize available models (Nicholson 1992, British Columbia Acid Mine Drainage Task Force 1989). The dominant reaction for AMD production is oxidation of the common iron sulfide minerals pyrite (Stumm and Morgan 1981) and pyrrhotite (Lapakko 1980, 1988). Therefore, many of the AMD models focus on (1) oxygen as the main oxidant and (2) the various associated transport mechanisms thought to be common in waste-rock dumps. This emphasis has been successful for modeling oxidation rates and related thermal effects in site-specific applications (Davis and Ritchie 1986, Cathles and Apps 1975). However, realistic prediction of acid production (hydrogen ion concentration) and dissolution and transport of toxic metals (e.g., copper and zinc) to the receiving environment is unlikely unless oxygen-diffusion models are coupled with geochemical and hydrologic models (MEND International Workshop Proceedings 1992). A more complete AMD field model is one that couples gas transport and thermal effects with chemical kinetics and aqueous-transport mechanisms.

To facilitate understanding of AMD's complex nature, the USBM and University have chosen to first model the AMD-producing potential of discrete waste-rock types under the fixed conditions characteristic of accelerated-weathering humidity-cell tests. While conditions common to humidity-cell kinetic tests differ from those encountered in actual waste-rock dumps, reaction-controlling conditions within each cell can be fixed at predefined limits. Humidity-cell experiments (1) are essentially isothermal, (2) have an ample supply of oxygen, and (3) are characterized by well-defined gas-transport and water-flow systems. These conditions not only accelerate the weathering process but also have potential to identify rate-limiting steps characteristic of both chemical and physical processes, rather than physical processes alone (i.e., diffusion of oxygen).

The objective of the current modeling effort is to (1) predict humidity-cell effluent quality for a specific rock type and have it match experimental data for the same rock and (2) better understand the dominant geochemical mechanisms active under restricted experimental conditions.

Methods and Materials

Humidity-Cell Apparatus Description and Test Protocol

A single humidity-cell array is comprised of 16 individual cylindrical cells, each 20.3 cm long, with an inside diameter (I.D.) of 10.2 cm. Waste-rock charges for each cell are comprised of 1,000 g of sample crushed to 100% passing 1/4 in. The test protocol is comprised of weekly leach cycles that include 3 days of dry air and 3 days of wet air pumped up through the sample (at the rate of 1 L/min), followed by a drip-trickle leach with 500 mL of de-ionized water on day 7 (Lawrence 1990). Duration of the leach is approximately 2 h. Data collected weekly from each humidity cell are described in White and Jeffers (1994).

Geochemical Predictive Model

The University, under contract to the USBM, has designed a preliminary model that simulates chemical changes that occur in the weekly interstitial water remaining in each humidity cell (see White and Jeffers 1994). Rather than solve the customary diffusion and convective-transport equations for a packed column of reacting particles, a different approach has been taken. The humidity cell is conceptualized as 20 continuous-stirred tank reactor's (CSTR's) in series. Twenty CSTR's are used because this number approaches the same effluent results as a packed-bed model with axial dispersion. Currently, the model uses 10 simultaneous chemical reactions and 14 different chemical species to describe the generation and neutralization of acid in the humidity cell. Solid species include pyrite, calcium carbonate, ferric hydroxide, jarosite, and feldspar. Aqueous species include sulfate, ferrous and ferric ion, oxygen, calcium, potassium (shown as A^+ in later equations), carbonate ion, and hydrogen ion (pH). Bacterial catalysis of AMD is modeled by using a modified Monod-type relationship for the growth phase that accounts for pH dependency and includes a term that accounts for the death phase. The weekly cycle of leaching with 500 mL of de-ionized water (1 day), dry air (3 days), and then water-saturated air (3 days) is modeled, taking into account the volume change in interstitial water and the resulting evaporation.

The kinetic parameters in the model are assumed constant and dependent only on temperature, which is not a variable in these experiments. Kinetic parameters were obtained by comparing the experimental effluent compositions collected during the water-leaching phase of the weekly cycle with those predicted by the model. Input to the model includes the following parameters:

Weight percent of total waste rock contributed by each of the major mineral constituents determined from mineral characterization

Volume of interstitial water remaining in the humidity-cell waste-rock charge at the end of the leaching step

Evaporation rate of interstitial water determined from the dry-air period of the weekly cycle

Weighted-average particle size estimated from screen analysis of each sample

Packed volume and void fraction of the humidity-cell waste-rock charge.

Once these parameters have been entered, the model calculates (1) the transient compositional changes in each CSTR with time and (2) the aqueous concentrations (including hydrogen ion as pH) predicted for the effluent sample obtained during the drip-trickle leach. The modeled effluent concentration can then be compared with experimental data.

Geochemical Reactions Included in the Model

Oxidation of Pyrite. Several mechanisms have been proposed for abiotic (Stumm and Morgan 1981, Lowson 1982) and biotic (Kleinmann et al 1981, Nordstrom 1982) oxidation. Pyrite oxidation is modeled using the four reactions listed below (equations 1-4; kinetic parameters such as KSO, KF(2), etc. listed here and in following equations are described in table 2).

$$\frac{1}{3.5}FeS_{2(s)} + O_{2(aq)} + \frac{1}{3.5}H_2O_{(l)} \xrightarrow{KSO} \frac{1}{3.5}Fe^{2+}_{(aq)} + \frac{2}{3.5}SO^{2-}_{4(aq)} + \frac{2}{3.5}H^{+}_{(aq)}$$

$$Fe^{2+}_{(aq)} + \frac{1}{4}O_{2(aq)} + H^{+}_{(aq)} \xrightarrow{KF(2)} Fe^{3+}_{(aq)} + \frac{1}{2}H_2O_{(l)}$$

$$\frac{1}{14}FeS_{2(s)} + Fe^{3+}_{(aq)} + \frac{8}{14}H_2O_{(l)} \xrightarrow{KSF} \frac{15}{14}Fe^{2+}_{(aq)} + \frac{2}{14}SO^{2-}_{4(aq)} + \frac{16}{14}H^{+}_{(aq)} \qquad (3)$$

$$Fe^{2+}_{(aq)} + \frac{1}{4}O_{2(aq)} + H^{+}_{(aq)} + ?X^{?}_{(aq)} \xrightarrow{MMAX} Fe^{3+}_{(aq)} + \frac{1}{2}H_2O_{(l)} + ?X^{?}_{(aq)}$$

An expression for the viable bacterial population density (X) (equation 5) is derived using a modified Monod equation for the growth phase and a simple kinetic expression for the death phase. Although several rate expressions have been proposed for these types of bacteria, *Thiobacillus ferrooxidans* in particular (Shrihari 1990, Hanson 1989, Asai et al 1992, Yun and Meyerson 1982), very few account for pH effects and death rates. The growth term is a function of pH and the limiting substrate concentration, which is assumed to be the ferrous ion. The death term is a function of population density and implies that populations cannot sustain

unlimited growth because living space is limited. Additionally, the death term is implicitly related to surface area because bacteria population is also a function of ferrous ion concentration, which in turn is a function of available particle surface area. Equation 5 also provides limits to viable bacterial population densities and makes the organisms somewhat responsive to environmental conditions, although this expression is obviously not a comprehensive model. More experimental work, specifically the study of viable bacterial population densities obtained under these experimental conditions, is needed. It is also likely that a mixed culture exists in these humidity cells. If significant quantities of bacteria other than *T. ferrooxidans* are present, other expressions and reactions must be included.

$$\frac{d[X_{(aq)}]}{dt} = \mu_{max}[X_{(aq)}]\left(\frac{[H^+]}{K_{M7a} + [H^+]}\right)\left(\frac{[Fe^{2+}]}{K_{M7b} + [Fe^{2+}]}\right) - k_d[X_{(aq)}]^2 \tag{5}$$

<u>Neutralization</u>. Chemical-weathering reactions not only affect metallic sulfide minerals, but also result in partial or complete dissolution of some silicate and carbonate gangue minerals comprising the bulk of the waste rock. Some of the more important gangue minerals are those that neutralize the acid being produced. Carbonates, in particular, are quite reactive and, if present in large amounts, can delay propagation of acid. Calcite and dolomite are the most common carbonate minerals, but others may also be present. The current model only considers the reaction of calcite and converts all other carbonates (except for siderite) into an equivalent amount of calcite. The reaction is given in equation 6. Calcium and carbonate are the only ions that are considered to be solubilized as a result of this neutralization reaction.

$$\frac{1}{2}CaCO_{3(s)} + H^+_{(aq)} + \frac{1}{2}H_2O_{(l)} \xrightarrow{KSCA} \frac{1}{2}Ca^{2+}_{(aq)} + \frac{1}{2}H_2CO_{3(aq)} + \frac{1}{2}H_2O_{(l)} \tag{6}$$

For some waste-rock materials, carbonate minerals are present in trace amounts and do not contribute significantly to acid neutralization. However, once the pH reaches relatively low values, other minerals (e.g., some silicates) can begin to solubilize and react with the acid. Feldspars fall into this category and can prevent the pH from dropping to even lower values. There are many different types of feldspars with various compositions. In the present model, all feldspar-like minerals will be represented as AW; A represents the monovalent ion that is released after being solubilized (commonly potassium), and W represents the silicate component. The chemical reaction for silicate neutralization is represented by equation 7.

$$AW_{(s)} + H^+_{(aq)} \xrightarrow{KSAW} A^+_{(aq)} + HW_{(s)} \tag{7}$$

<u>Shrinking-Core Models</u>. Reactions involving a solid phase are treated using the "shrinking-core" model(Fogler 1992, Levenspiel 1972). For most solid reactions, the diffusion of the reactant(s), and the counter diffusion of products through the reacted portion of the particle are rate controlling. This applies to the reactions for pyrite (equations 1 and 4), carbonate (equation 6), and feldspar (equation 7) as the radius of the shrinking core decreases appreciably. The effective diffusivities of ferric ion, dissolved oxygen, and hydrogen ion are included in the rate expressions for these solids. The amount of reactive surface area available for reaction for each of the solid species is a function of the amount of jarosite, calcium sulfate, ferric hydroxide, and ferrous carbonate that have precipitated from the interstitial water.

<u>Precipitation</u>. Oxidation of pyrite produces sulfate ion in solution. This ion would increase indefinitely were it not for the presence of metallic ions, particularly iron. The eventual precipitation of these sulfate salts removes metal and sulfate ions from solution, but, more importantly, produces a solid that can coat reactive pyritic surfaces. Because chemical reactions involving a solid material are a function of the reactive surface area, this coating can significantly affect the overall kinetics by providing a physical barrier between reactants. While a variety of metallic salts are possible as a result of precipitation, four species are considered significant for waste-rock samples 1-B, 1-C, and 1-D (described in White and Jeffers 1994, and shown here in table 1).

They are ferric hydroxide, jarosite, ferrous carbonate, and calcium sulfate (equations 8-11). Note that the production of ferric hydroxide is reversible, while the others are considered irreversible.

$$Fe^{3+}_{(aq)} + 3H_2O_{(l)} \xleftrightarrow[KF(-3)]{KF(3)} Fe(OH)_{3(s)} + 3H^{+}_{(aq)} \tag{8}$$

$$A^{+}_{(aq)} + 3Fe^{3+}_{(aq)} + 2SO^{2-}_{4(aq)} + 6H_2O_{(l)} \xrightarrow{KF(10)} AFe_3(SO_4)_2(OH)_{6(s)} + 6H^{+}_{(aq)} \tag{9}$$

$$Fe^{2+}_{(aq)} + CO^{2-}_{3(aq)} \xrightarrow{KF(9)} FeCO_{3(s)} \tag{10}$$

$$Ca^{2+}_{(aq)} + SO^{2-}_{(aq)} \xrightarrow{KF(5)} CaSO_{4(s)} \tag{11}$$

The precipitation of jarosite (equation 9) is affected by the solution concentrations of ferric, sulfate, and A^+ (mainly potassium) ions. As these concentrations increase, the rate of precipitation increases, forming an increasing total amount of precipitate. The jarosite precipitate presumably covers the solid materials and decreases the available surface area for the solid reactions (shrinking-core reactions), which affects the overall oxidation of pyrite.

Physical Considerations

Simulation of Humidity-Cell Weathering Cycle. The weekly cycle of the humidity-cell test has been described and is particularly challenging to model mathematically. The following assumptions have been made in order to simplify the calculations.

> During the dry-air and wet-air periods, the water in the cells is saturated with air at the appropriate temperature
>
> The volume of interstitial water in the humidity cell exhibits the same changes from week to week
>
> During the dry-air period, water is being evaporated at a constant rate
>
> The drip-trickle leaching step consumes 2 h each week.

The oxidation rate of pyrite, when kinetically controlled, should be a function of the liquid volume since aqueous species' concentrations are determined by the amount of water present. In some experimental settings, liquid volume is relatively constant and, thus, unimportant. However, this is not true under the conditions required for accelerated-weathering tests using humidity cells. Interstitial water volume in the waste-rock charge changes throughout the week owing to air drying and resaturation with de-ionized water. Consequently, concentrations of the various aqueous species contained in the interstitial water vary considerably over the weekly cycle. This is taken into consideration by adjusting concentrations within the cell based on the amount of interstitial water. The critical volumes are those after the drying cycle and those associated with the leaching step and subsequent elution.

Oxygen Diffusion. Because air is pumped continuously through each humidity cell at 1.0 L/min for both the wet- and dry-air cycles, the concentration of oxygen in the interstitial water is assumed to be constant at saturated conditions during this time period. During the leaching step, however, air is not being pumped and oxygen in the aqueous phase is allowed to decrease in accordance with its consumption for the designated

chemical reactions. As stated earlier, the solid reactions include the effects of oxygen diffusion through the reacted portion of the particles.

Particle Size Versus Reactive Surface Area. Most cells have a rather broad distribution of particle sizes depending on how the sample is taken and if only a certain size fraction is used. The description of the particles within the cell has been simplified by using a weighted average particle size for each rock type based on experimentally-determined weight and size distributions.

Numerical Techniques

One-dimensional, unsteady-state material balances are calculated for each species in each CSTR. The 280 simultaneous differential equations (20 CSTR's times the number of species, which is 14 at this point) were solved for each time increment using the Runge-Kutta fourth-order method coded in FORTRAN. The model predicts the effluent concentrations for the aqueous species from the last CSTR as a function of time during the drip-trickle leach step. These point concentrations are then integrated over the appropriate time period to give an average concentration in the collected effluent for each species, which can then be compared with experimental data.

Results and Discussion

Geochemical Predictive Model

Input Parameters. The most critical input to the model is the suite of dominant mineral species contained in each waste-rock type that comprises the bulk of the waste dump. The major mineral species comprising samples 1-B, 1-C, and 1-D are contained in table 1; weight-percent estimates for these minerals were determined by image analysis and are also summarized.

Table 1. Weight-percent estimates of major mineral constituents in waste-rock samples 1-B, 1-C, and 1-D.

Mine sample	Rock type	Major mineral constituents (est. wt %)						
		Qtz[1]	K-spar[2]	Plag[3]	Clay	$CaCO_3$[4]	Pyrite	Po[5]
	Latite porphyry	30	26	22	2	0	6	ND
1-C	Massive-sulfide mudstone	30	12	8	5	.2	24	ND
1-D .	Mudstone	40	18	20	2	.3	3	Tr

ND Not detected.
Tr Trace.
[1]Quartz.
[2]Potassic feldspar.
[3]Plagioclase.
[4]White and Jeffers (1994), table II
[5]Pyrrhotite.

Although all three samples are from the same mine, minerals common to each vary markedly in abundance (especially pyrite). While carbonate is present in two of the three samples, its presence is minimal compared with the amount of pyrite contained in all three samples. A more detailed presentation and discussion of the mineral-characterization results for each of the three samples is contained in White and Jeffers (1994).

Another important model input is the average particle-size diameter for each sample. Average particle-size diameters for samples 1-B, 1-C, and 1-D are 1.3, 2.9, and 3.4 mm, respectively.

Kinetic Parameters. Fifteen kinetic parameters have been derived for the current model and are shown in table 2.

Table 2. Kinetic parameters used in geochemical model

Parameter	Description	Model value	Literature value(s)	Reference(s)
	Abiotic oxidation of ferrous ion.			
	Formation of ferric hydroxide.			
	Equilibrium constant for ferric hydroxide.			Stumm (1981)
KF(5)	Precipitation of calcium sulfate.	1.0×10^{-5} mmol/L/h	NAp	
KF(9)	Precipitation of ferrous carbonate.	1.0×10^{-3} mmol/L/h	NAp	
KF(10)[1]	Precipitation of jarosite.	4.07×10^{-15} mmol/L/h	NAp	
	Monod-type constant for hydrogen ion in bacteria growth equation.	0.1 mmol/L	NAp	
	Monod-type constant for ferrous ion in bacteria growth equation.	2.0 mmol/L	2.2 mmol/L 2.5 mmol/L 2.55 mmol/L 2.2 to 5.4 mmol/L	Ehrlich (1990) Yun (1982) Myerson (1984) Schnaitman (1969)
	Maximum growth rate.	0.1/h	0.183/h 0.05 to 0.25/h 0.104/h 0.1085/h	Shrihari (1990) Hanson (1989) Asai (1992) Yun (1982)
K_d	Bacteria death-phase constant.	5.0×10^{-2} mmol/L/h	NAp	
$Y_{X/Fe}$	Yield coefficient.	0.4 mg bacteria/ (mmol Fe^{+2})	0.09 to 0.5 mg bacteria/ (mmol Fe^{+2})	Hanson (1989)
KSO	Direct oxidation of pyrite by dissolved oxygen.	1.5×10^{-11} L/cm^2/sec	NAp	
KSF	Oxidation of pyrite by ferric ion.	5.0×10^{-11} L/cm^2/sec	NAp	
	Reaction of calcium carbonate with acid.	1.0×10^{-7} L/cm^2/sec	8.65×10^{-6} L/cm^2/s for pure calcite	Busenberg (1986)
	Reaction of feldspars with acid.	8.0×10^{-12} L/cm^2/sec	2.28×10^{-13} L/cm^2/s for pure albite	Blum (1988)

NAp Not applicable.
[1]For sample 1-B, a value of 2.33×10^{-10} was used.
[2]For samples 1-B and 1-C, a value of 2.0×10^{-12} was used.

The magnitude of each kinetic parameter was initially established by applying trial and error curve-fitting techniques to the experimental data. Sensitivity analysis was then performed to assess the importance of each kinetic parameter on the modeled output. The resulting calculated parameters have been compared with corresponding kinetic parameters available in the literature and demonstrate reasonable agreement. Note that all but two of the kinetic-parameter values are the same for each of the three samples. The two exceptions are for the precipitation of jarosite and the dissolution of calcium carbonate (constants KF(10) and KSCA, respectively).

The value of the jarosite precipitation rate constant for sample 1-B was changed from 4.07×10^{-15} (used for 1-C and 1-D) to 2.33×10^{-10}. Rationale for this change is the possibility that other species are being precipitated in sample 1-B, but not in the other two samples.

The rate constant for the reaction of calcium carbonate with acid was changed from 1.0×10^{-7} to 2.0×10^{-12} for samples 1-B and 1-C. This change is more difficult to justify. Carbonate content in each of the three samples was too low to identify discrete mineral composition by X-ray diffraction (XRD) analysis. Because sample 1-D contained the only visually-observed carbonate (White and Jeffers 1994), it has been assigned a value closer to the calcite rate constant until further characterization can be completed, and more published carbonate-rate constants can be found.

Correlation of Modeled Output With Experimental Data. Preliminary fit of model-generated data to corresponding experimental data from 90 weeks of humidity-cell testing is encouraging. Figures 1 through 3 compare model-predicted pH, total iron, and sulfate concentrations with corresponding weekly effluent

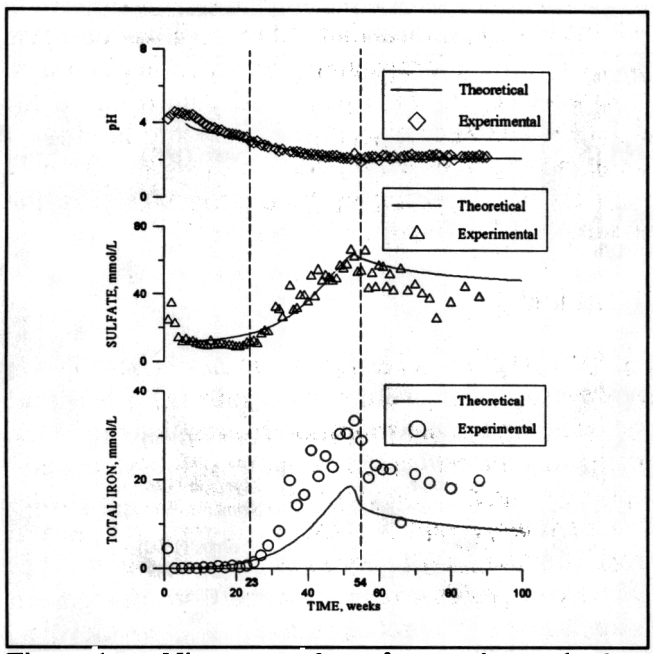

Figure 1. Ninety weeks of experimental data obtained from sample 1-C compared with modeled output.

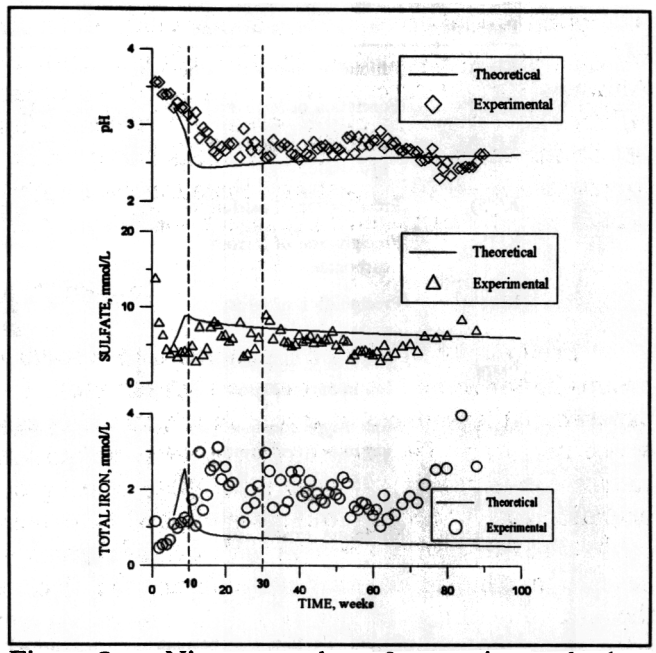

Figure 2. Ninety weeks of experimental data obtained from sample 1-B compared with modeled output.

concentrations from samples 1-B, 1-C, and 1-D.

The model duplicated two critical experimental responses, which are illustrated by sample 1-C in figure 1. The first is transition of the pyrite-oxidation mechanism from abiotic (oxygen only) to biotic (bacteria catalyzed) oxidation at pH 3. The second is the effect of jarosite precipitation on pH, sulfate, and total-iron concentrations at week 54. Elapsed time required for weekly effluent to reach a pH of 3 was 23 weeks. A correlative increase in sulfate and total iron concentrations also occurred at week 23. These concentrations continued to increase until week 54, when they started to decrease. By week 54, a yellow precipitate was visible in sample 1-C, and later identified as jarosite by XRD. Total iron and sulfate concentrations continued to decrease from week 54 to week 90. This decrease in concentration is from the coating of exposed pyrite surfaces by jarosite precipitate and consequent reduction in the pyrite-oxidation rate.

Output from the model is generally in good agreement with these experimental data from sample 1-C, and in fair agreement with samples 1-B and 1-D. This is encouraging considering that with two exceptions, all the kinetic rates have been held constant for all three samples. Modeled output for sample 1-B

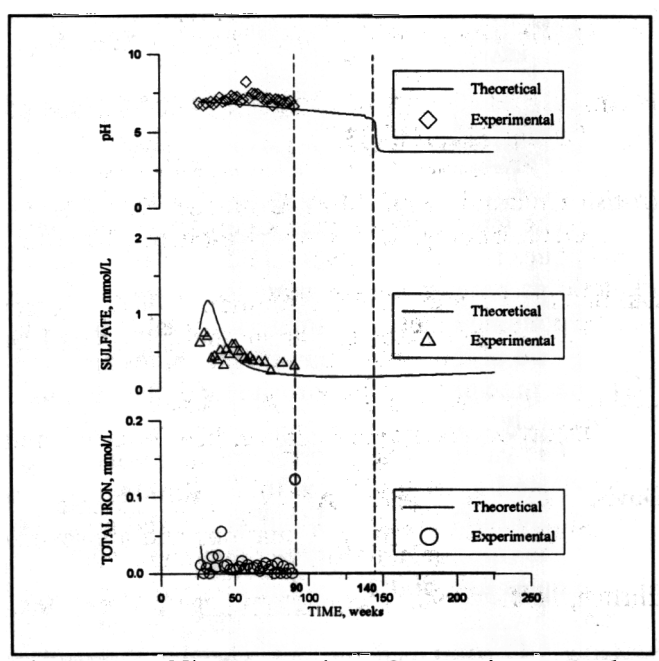

Figure 3. Ninety weeks of experimental data obtained from sample 1-D compared with modeled output.

predicted that pH would drop below 3 near weeks 8 to 10 with concurrent increases in total iron and sulfate concentrations; effects of jarosite precipitation (i.e., concurrent reduction in total iron and sulfate concentrations) would start within the same time frame. Experimental data from sample 1-B effluent closely matched modeled output for pH, but demonstrated a significant lag time between modeled effects of jarosite precipitation and actual effects at 30 weeks. For sample 1-D, the model predicts that effluent pH will decrease very slightly, but remain in the neutral range until after week 130, when it drops precipitously from pH 6 to 4. Although current experimental data are only available for 90 weeks of testing, existing pH data from weekly effluent closely match model-predicted values. White and Jeffers (1994) predicted a similar drop in effluent pH during the period 110 to 130 weeks based on experimental calcium plus magnesium release rates from 51 weeks of humidity-cell testing. Because these rates have not changed appreciably from 51 to 90 weeks, the estimate is still expected to match modeled predictions for sample 1-D effluent.

Summary and Conclusions

Preliminary fit of model-generated data to 90 weeks of humidity-cell accelerated-weathering test data is promising for three different waste-rock samples. The current version of the model has duplicated two critical experimental responses observed in the humidity-cell testing. The first is the transition from abiotic to biotic pyrite oxidation. The second reflects the precipitation of jarosite and the concurrent reduction of total iron and sulfate concentrations due to precipitate coating of rock particles and consequent reduction in the pyrite-oxidation rate. Modeled output is in good agreement with experimental data for one waste-rock sample and exhibits reasonable agreement with two additional waste-rock samples. With two exceptions, these matches have been achieved without manipulating the 15 calculated rate constants for respective reactions that govern the operation of the current model. To enhance the model's application to a broader range of waste-rock types, additional solid- and liquid-phase species will be added to the model as new waste-rock types are characterized. Examples include the minerals chalcopyrite and pyrrhotite, elemental sulfur, and aqueous species of copper and zinc.

Literature Cited

Asai, S., Y. Konishi, and K. Yoshida. 1992. Kinetic model for bacterial dissolution of pyrite particles by *Thiobacillus ferrooxidans*. Chemical Eng. Sci. 47(1):133-139.

Blum, A. and A. Lasaga. 1988. Role of surface speciation in the low-temperature dissolution of minerals. Nature 331:431-433.

British Columbia Acid Mine Drainage Task Force. 1989. Draft acid rock drainage technical guide. Dept. Energy, Mines, and Resources, Vancouver, BC, Canada, v. 1, 260 pp.

Busenberg, E. and L. N. Plummer. 1986. A comparative study of the dissolution and crystal growth kinetics of calcite and aragonite. U.S. Geol. Surv. Bull. 1578.

Cathles, L. M. and J. A. Apps. 1975. Model of the dump leaching process incorporates oxygen balance, heat balance, and air convection. Metall. Trans. B 6B:617-624.

Davis, G. B. and A. I. M. Ritchie. 1986. A model of oxidation in pyritic mines wastes: Part 1, Equations and approximate solution. Appl. Math. Modelling 10:314-322.

Ehrlich, H. L. 1990. Geomicrobiology, 2d ed. Marcel Dekker, Inc. Ch 14.

Fogler, H. S. 1992. Elements of chemical reaction engineering, 2d ed. Prentice Hall International, NJ. p. 582-589.

Hanson, J. S. 1989. Kinetic model of the bacteria leaching of chalcopyrite concentrates. Dep. Mat. Sci. and Min. Eng. Univ. of CA-Berkeley.

Kleinmann, R. L. P., D. A. Crerar, and R. R. Pacelli. 1981. Biogeochemistry of acid mine drainage and a method to control acid formation. Min. Eng. 33:300-305

Lapakko, K. A. 1980. Kinetics and mechanisms of the oxidative dissolution of metal sulfide and silicate minerals present in the Duluth Gabbro. M.S. Thesis. Univ. of MN, Minneapolis, MN. 199 p.

Lapakko, K. A. 1988. Prediction of acid mine drainage from Duluth Complex mining wastes in northeastern Minnesota. p. 180-190. In Proceedings of 1988 Mine Drainage and Surface Mine Reclamation Conference, v.1. BuMines IC 9183.

Lawrence, R. W. 1990. Prediction of the behaviour of mining and processing wastes in the environment. p. 115-121. In Proceedings of the Western Regional Symposium on Mining and Mineral Processing Wastes. (Berkeley, CA, May 30-June 1, 1990).

Levenspiel, O. 1972. Chemical reaction engineering, 2d ed. Wiley, New York. p. 361-374.

Lowson, R. T. 1982. Aqueous oxidation of pyrite by molecular oxygen. Chem.Reviews 82(5):461-497.

Mine Environment Neutral Drainage (MEND) Program. 1992. 52 p. In Proceedings of the International Workshop on Waste Rock Modelling. (Toronto, ON, September 29-October 1, 1992).

Myerson, A. S. and P. C. Kline. 1984. Continuous bacterial coal desulfurization employing *Thiobacillus ferrooxidans*. Biotechnol. and Bioeng. 26:92-99.

Nicholson, R. V. 1992. A review of models to predict acid generation rates in sulphide waste rock at mine sites. p. 41-52. In Proceedings of the International Workshop on Waste Rock Modelling. (Toronto, ON, September 29-October 1, 1992).

Nordstrom, D. K. 1982. Aqueous pyrite oxidation and the consequent formation of secondary iron minerals. p. 37-56. In Acid sulfate weathering. J. A. Kittrick, D. S. Fanning, and L. R. Hossner (eds.), Soil Sci. Soc. America Spec. Pub. 10.

Schnaitman, C. A. , M. S. Korczynski, and D. G. Lundgren. 1969. Kinetic studies of iron oxidation by whole cells of *Thiobacillus ferrooxidans*. J. Bacteriology 99:552-557.

Shrihari, R. K. and K. S. Gandhi. 1990. Modelling of Fe2+ oxidation by *Thiobacillus ferrooxidans*. Appl. Microbiol.and Biotechnol. 33:524-528.

Stumm, W. and J. J. Morgan. 1981. Aquatic Chemistry. Wiley-Interscience, New York. p. 241, 469-471.

White, W. W. and T. H. Jeffers. 1994. Chemical predictive modelling of acid mine drainage from metallic sulfide-bearing waste rock. p. 608-630. In Proceedings of American Chemical Society Symposium Series 550.

Yun, C. C. and A. S. Myerson. 1982. Growth models of the continuous bacterial leaching of iron pyrite by *Thiobacillus ferrooxidans*. Biotechnol. and Bioeng. 24:889-902.

WEATHERING BEHAVIOUR OF MINE TAILINGS AND WASTE ROCK: A SURFACE INVESTIGATION[1]

Serena J. Domvile[2], Michael G. Li[2], Diana D. Sollner[2], and Wayne Nesbitt[3]

Abstract: A study focussing on the ion movement in the near surface of sulphide minerals was conducted to better understand the weathering mechanisms of mine waste materials. Tailings and waste rock samples from Canadian mines were subjected to controlled weathering studies using various chemical leachants. Leachates were analyzed for various parameters, and petrographic analyses were conducted on the solid residues. Laboratory oxidation studies of pure pyrrhotite and arsenopyrite were carried out using the surface techniques X-ray photoelectron spectroscopy (XPS) and auger electron spectroscopy (AES). The data derived from the weathering study and the surface techniques were correlated to determine mechanisms of oxidation. Several results were observed during the project: Ferric iron constitutes one third of the iron present in pyrrhotite, sulphide oxidation is initiated when rock is blasted, sulphide sulphur is oxidized to di- and poly-sulphides prior to forming sulphates, and significantly more sulphate is produced upon exposure to aqueous environments than to air alone.

Introduction

Acid rock drainage (ARD) is a significant environmental concern to the mining industry. Much effort has been expended over the last decade to develop methods of preventing, predicting, controlling and treating ARD. An important starting point for all ARD research is understanding the mechanisms of ARD. The objective of this research is to expand our knowledge of ARD fundamentals.

A study of ion movement in the near surface of pyrrhotite and arsenopyrite revealed some of the mechanisms involved in ARD development. This study was carried out by conducting X-ray photoelectron spectroscopy (XPS) and auger electron spectroscopy (AES) on pure minerals and petrographic analyses on laboratory-weathered tailings and waste rock. The results of the petrographic analyses served as a link between the two sets of information obtained from the laboratory-weathered material and from the pure minerals.

This paper will focus on the pyrrhotite experiments.

Methodology

The project was conducted as two parallel research programs: Examination of pyrrhotite surfaces using XPS and AES, and controlled laboratory weathering of tailings and waste rock containing pyrrhotite. The analytical procedures used are presented in two subsections, representing each program.

Mineral Surface Investigations

Three different analytical techniques were considered in this research: secondary ion mass spectrometry (SIMS), X-ray photoelectron spectroscopy (XPS), and auger electron spectroscopy (AES). As a result of the limitations encountered with SIMS, only XPS and AES were employed in surface investigations conducted on pyrrhotite.

---

[1]Paper presented at the International Land Reclamation and Mine Drainage Conference and the Third International Conference on the Abatement of Acidic Drainage, Pittsburgh, PA, April 24-29, 1994.

[2]Serena J. Domvile, Director, Environmental Science Division, Michael G. Li, Environmental Engineer, and Diana D. Sollner, Environmental Engineer, Klohn-Crippen Consultants Ltd., Richmond, BC, Canada.

[3]Harold W. Nesbitt, Professor of Geochemistry, University of Western Ontario, London, ON, Canada.

Sample Preparation of Pyrrhotite and Arsenopyrite. Research-grade pyrrhotite from Santa Eulalia, Chihuahua, Mexico was used in this study. Crystallographic properties were investigated by X-ray diffraction methods. Mineral composition was determined by repeated electron microprobe analyses.

Mineral fragments approximately 2 to 3 mm^3 were cleaved from the research-grade samples. Fragment faces were polished with P 800 silicon carbide paper to provide quick recognition of fresh fracture faces. Following polishing, the grains were ultrasonically cleaned for 2 min with methanol. Samples were dried in a low-vacuum desiccator.

Characterization of initial mineral surface chemistry was achieved by analyzing samples fractured under high vacuum in the XPS instrument. Transfer to the AES instruments was performed using a nitrogen-filled glove bag to prevent reaction with the atmosphere. Pyrrhotite samples were also analyzed after exposure to air at room temperature and atmospheric pressure for periods of 6.5 and 50 h, after 8 h of distilled water leaching, and after 8 h of sulphuric acid solution leaching.

Experiments Employing XPS. In the XPS experiment, X-ray photons interact with surface atoms to eject core level electrons. The atoms from which photo-ejected electrons originate are determined by the binding energies of the ejected electrons. Photoelectrons typically originate in the first 5 to 50 Å below the surface.

Survey scans were used to determine the elements present at the pyrrhotite surface. Emphasis was placed on the variations in the surface composition between samples rather than the absolute composition of each particular sample surface. Chemical state information was obtained from narrow-region photoelectron spectra, resolved by a peak-fitting routine using a Shirley-type background (Shirley 1972) and an 80% Gaussian, 20% Lorentzian peak model. Photoelectron binding energies for the vacuum-fractured sample were assigned relative to the monosulphide (S^{2-}) peak at 161.25 eV.

Experiments Employing AES. In the AES experiment, a high energy electron beam (1 to 10 kV) is focused at a sample surface, resulting in the inner shell ionization of a surface atom. As the ionized surface atom relaxes, excess energy is dissipated by either fluorescence or the ejection of an electron with characteristic kinetic energies of the donor atom (Auger 1975).

Acquisition of AES spectra was accomplished using a scanning Auger microprobe, equipped with a secondary electron detector and an Ar^+ ion gun. AES data collection was in two modes, survey and profile. Semiquantitative surface compositions were calculated using peak heights and sensitivity factors of data collected in survey mode. AES depth profiles were collected with reference to sputter time rather than depth. Time was converted to depth using the sputter erosion rate. The standard sputter rate for iron oxides is approximately 100 Å min^{-1} ±20% (Nicholson et al. 1990). The sputter rate of unoxidized pyrrhotite surfaces was measured to be approximately 0.4 Å min^{-1}.

Controlled Laboratory Weathering Tests

Samples of tailings and waste rock were subjected to several controlled laboratory weathering tests. These tests are described below.

Acid Base Accounting (ABA). ABA tests were conducted in duplicate on all samples, according to standard procedures (Sobek et al. 1978). Neutralization potential was determined by a modified method by employing hydrochloric acid digestion at ambient temperature for 24 h.

Humidity Cell Program. One kilogram of tailings was added to each of six humidity cells (HC-1, HC-2, HC-3, HC-4, HC-5, HC-6), and 1 kg of waste rock, crushed to -¼ in, was added to each of six additional humidity cells (HC-7, HC-8, HC-9, HC-10, HC-11, HC-12). The tailings and waste rock contained in all cells were weathered according to a 30-week, three stage program:

- 2-week leaching program using deionized water as the leachant, according to standard humidity cell protocol;
- 8-week leaching program using six different chemical solutions for each of the six cells containing tailings and waste rock, according to the standard wet-dry humidity cell protocol; and
- 20-week leaching program in which the same solutions employed in the 8-week program are maintained as continuous covers for each of the respective tailings and waste rock cells.

The standard protocol for humidity cell tests is outlined in the BC Draft ARD Technical Guide (1989): (1) dry air is passed over the samples from day 1 to day 3; (2) humidified air is passed over samples from day 4 to day 6; and (3) the sample is leached on day 7. The leachants used to simulate disposal conditions were selected from Engler et al. (1976) and modified in strength for the purpose of this study (table 1).

Table 1. Leaching conditions

Test	Leachant	Simulated Disposal Environment
HC-1 HC-7	Deionized water	Natural precipitation.
HC-2 HC-8	Dilute acetic acid (pH 3.5)	Landfills, water bodies with high organic content, and fermentative waters/bogs.
HC-3 HC-9	Oxalic acid (0.004M) and ammonium oxalate (0.004M)	Bottom and middle region of deep water disposal environments.
HC-4 HC-10	Sulphuric acid (pH 2.5)	Acidic drainage, pore water, lakes, and tailings ponds.
HC-5 HC-11	Hydrogen peroxide solution (0.1% w/w)	Oxygenated waters and sulphide-oxidizing environment.
HC-6 HC-12	Sodium hydroxide (pH 11.0)	Alkaline drainage, pore water, mill effluent, and some environments.

Leachate samples collected from the 12 humidity cells were analyzed for pH, Eh, conductivity, acidity, alkalinity, sulphate, and dissolved metals. The pH of leachates was measured with a combination electrode, and Eh was measured with a combined platinum-reference electrode. Sulphate was measured gravimetrically. Dissolved metal levels were determined by inductively coupled plasma optical emission spectrometry (ICP-OES) upon filtration of leachates through a 0.45 μm-filter.

Quality-control methods, including calibration programs for each method, duplicate analyses, standard solution analyses, and blanks were implemented to ensure the integrity of results collected on leachates.

Cumulative release of sulphate and metals were plotted against time to identify trends.

The saturation indices for 214 minerals were calculated using the geochemical modelling software package SOLMINEQ.88. Using leachate data and established thermodynamic data, relationships between solid and liquid phases were established.

Petrographic Analysis. Upon completion of the 30-week weathering program, a sample from each of the tailings and waste rock humidity cells was subjected to petrographic analysis. Tailings samples consisted of vertical cross-

sections of the tailings bed and waste rock samples consisted of grab samples from the humidity cells. Waste rock samples consisted of material from various depths in the cells, however, vertical layering was not preserved.

Thin sections were examined, in transmitted and reflected light modes, using a petrographic microscope. Mineral identifications were made by standard observations of optical and physical properties. Observations of particle size were made using a calibrated eyepiece scale. Mineral abundances were estimated. Conclusions were based on observations of spatial distributions and textural relationships of the identified components.

Results

Surface Investigations

Data obtained from the XPS and AES analyses of research-grade pyrrhotite are summarized in tables 2 and 3.

Table 2. Iron, sulphur and oxygen species identified by XPS experiments on pyrrhotite, percent.

Spectrum	Vacuum Fractured	Air oxidized (6.5 h)	Water leached (8 h)	Sulphuric acid leached (8 h)	
				Smooth textured	Mosaic textured
Iron:					
Fe(II)-S	63.86	37.78	32.77		11.93
Fe(III)-S	33.18		23.84		19.55
Fe(III)-O		51.90	43.39	100.00	68.52
Sulphur:					
Monosulphide	77.40	64.00	61.45	7.71	31.10
Disulphide	12.00	18.80	21.27	12.00	20.75
Polysulphide	10.60	6.80	9.23	15.17	12.69
Elemental sulphur		3.40		7.01	3.29
Sulphite		3.30		4.12	
Sulphate		3.80	4.93	53.99	32.17
Iron sulphate			3.12		
Oxygen:					
Oxide-oxygen	20.00	29.10	25.28	31.52	17.28
Hydroxide	55.40	57.10	51.61	54.92	56.49
Adsorbed water	24.60	13.80	18.49	13.56	26.23
Iron sulphate			18.49		

Table 2 contains three components: the iron spectrum, the sulphur spectrum and the oxygen spectrum. Percentages represent contributions of a particular chemical species towards the overall spectrum for an element. The concentration of elements at the mineral surface is summarized in table 3.

Table 3. Atomic concentrations of surface atoms in pyrrhotite determined by AES, percent.

	Pyrrhotite					
	Vacuum fractured	Air oxidized (6.5 h)	Air oxidized (50 h)	Water leached (8 h)	Sulphuric acid leached (8 h)	
					Smooth textured	Mosaic textured
Carbon				49.00	37.00	14.00
Oxygen	12.00	29.00	37.00	24.00	30.00	48.00
Sulphur	46.00	24.00	15.00	6.00	16.00	11.00
Iron	40.00	47.00	48.00	21.00	17.00	27.00

Several points are noted from these results. First, iron is present in both ferric and ferrous ionic forms. Second, oxidized species of sulphur were detected in the vacuum-fractured pyrrhotite in the upper layers. The amount of sulphide sulphur decreases as the oxidizing potential of the environment increases. As sulphide sulphur decreases, the amount of oxidized sulphur species increases. Finally, iron is present predominantly as the ferric ion in all the experiments except the vacuum-fractured pyrrhotite experiment.

Controlled Laboratory Weathering Tests

Acid Base Accounting. ABA data are summarized in table 5. Samples of unweathered, naturally weathered, and laboratory-weathered tailings were analyzed. Naturally weathered tailings have been exposed for approximately 10 years. Both unweathered and naturally weathered tailings have a net neutralization potential (NNP) of -90 t $CaCO_3$ equivalent per 1 000 t waste. Except for the sodium hydroxide leached cell, NNP results for tailings weathered in the laboratory for 30 weeks show no significant changes in comparison to values obtained for unweathered and naturally-weathered tailings. The laboratory-weathered tailings exhibit decreases in total percent sulphur.

Table 5, Acid base accounting analysis of laboratory-weathered tailings.

Sample	Total S, %	Paste pH	NP	MPA	NNP
Unweathered	3.13	7.8	7.8	97.8	-90.0
HC-1	3.07	6.8	6.1	95.9	-89.8
HC-2	3.09	6.9	5.6	96.6	-91.0
HC-3	3.06	6.5	5.4	95.6	-90.2
HC-4	3.00	6.0	4.0	93.8	-89.8
HC-5	3.01	6.7	4.5	94.1	-89.6
HC-6	2.87	7.5	6.2	92.8	-86.6

HC-1= deionized water leached
HC-2= acetic acid leached
HC-3= ammonium oxalate/oxalic acid leached
HC-4= sulphuric acid leached
HC-5= hydrogen peroxide leached
HC-6= sodium hydroxide leached
NP = neutralization potential in t $CaCO_3$ equivalent per 1 000 t waste
MPA= maximum potential acidity in t $CaCO_3$ equivalent per 1 000 t waste
NNP = net neutralization potential in t $CaCO_3$ equivalent per 1 000 t waste

Waste rock materials collected from a waste rock pile were analyzed before and after the laboratory weathering program, as summarized in table 6. Unweathered waste rock produced a net neutralization potential (NNP) of -7.6 t $CaCO_3$ equivalent per 1,000 t waste. Four of the six laboratory-weathered samples had NNP values equal to or less than the value obtained for unweathered material, while the remaining two samples had an NNP value greater than the unweathered material.

Table 6. ABA analysis of laboratory-weathered waste rock.

Sample	Total S, %	Paste pH	NP	MPA	NNP
Unweathered	0.56	7.8	9.9	17.5	-7.6
HC-7	0.40	6.8	4.8	12.5	-7.7
HC-8	0.31	6.9	3.3	9.7	-6.4
HC-9	0.42	6.5	3.8	13.1	-9.3
HC-10	0.35	6.0	3.0	10.9	-7.9
HC-11	0.47	6.7	3.2	14.7	-11.5
HC-12	0.66	7.5	4.8	20.6	-15.8

HC-7 = deionized water leached
HC-8 = acetic acid leached
HC-9 = ammonium oxalate/oxalic acid leached
HC-10 = sulphuric acid leached
HC-11 = hydrogen peroxide leached
HC-12 = sodium hydroxide leached

Humidity Cell Program. The results of the humidity cell program on tailings and waste rock material are summarized in tables 7 and 8, respectively.

Table 7, Physical and chemical characteristics of tailings leachates.

Physical and chemical characteristics	Trends
pH	· Alkaline or alkaline-to-neutral throughout tests in all cells, except the sulphuric acid cell. · In the sulphuric acid cell, pH increased gradually upon establishment of saturated conditions, reaching 4.5 in the final cycle. · Aside from the sulphuric acid cell, the most significant drop in pH (from 7.8 to 5.4) was observed in the hydrogen peroxide cell in the 14th week (this decline was not accompanied by a significant increase in SO_4 levels). A slight drop in pH (from 8.3 to 7.5) was accompanied by a peak in SO_4 levels in week 10 during unsaturated conditions in the sodium hydroxide cell. · Large fluctuations in pH during saturated leaching conditions (aside from the sulphuric acid cell) were observed in the hydrogen peroxide cell.
Eh	· An oxidizing environment dominated in all cells, the highest Eh values being measured in the sulphuric acid cell.

Table 7, Physical and chemical characteristics of tailings leachates (continued).

SO_4 levels	· Cumulative SO_4 curves indicate that SO_4 production in the first 10 weeks was as follows (cumulative SO_4 values at week 10 are given in brackets): SO_4 hydrogen peroxide cell (2162 mg/kg) > SO_4 sodium hydroxide cell (2054 mg/kg) > SO_4 sulphuric acid cell (1879 mg/kg) > SO_4 ammonium oxalate/oxalic acid cell (1230 mg/kg) > SO_4 deionized water cell (1017 mg/kg) > SO_4 acetic acid cell (798 mg/kg). · During maintenance of continuous solution covers, beginning with week 12, SO_4 production was highest in the sulphuric acid cell and decreased as follows (cumulative SO_4 values at week 30 are given in brackets): SO_4 sulphuric acid cell (4960 mg/kg) > SO_4 hydrogen peroxide cell (3994 mg/kg) > SO_4 sodium hydroxide cell (2767 mg/kg) > SO_4 ammonium oxalate cell (2072 mg/kg) > SO_4 deionized water cell (1749 mg/kg) > SO_4 acetic acid cell (1031 mg/kg).
Acidity	· Minority acidity measured throughout tests in all cells, except the sulphuric acid leached cell.
Alkalinity	· Largest variations in the hydrogen peroxide cell. · High alkalinity levels in the ammonium oxalate/oxalic acid cell.
Metal levels	· Iron levels lower than 10 ppm were reported in all cells except the sulphuric acid cell. · The highest arsenic levels were reported for the ammonium oxalate/oxalic acid cell. · Calcium concentrations lower than the deionized water cell were measured only in the ammonium oxalate/oxalic acid cell.

Table 8. Physical and chemical characteristics of waste rock leachates.

Physical and chemical characteristics	Trends
pH	· Alkaline, acidic and neutral-to-alkaline in the leachates from sodium hydroxide, sulphuric acid and deionized water, respectively. · Ammonium oxalate/oxalic acid and acetic acid leachates initially acidic, then upon establishment of saturated conditions, neutral. · Leachate from the hydrogen peroxide cell initially alkaline, then acidic. Indication of acid generation throughout the weathering program.
Eh	· An oxidizing environment dominated in all cells, the highest Eh values being measured in the sulphuric acid cell.
SO_4 levels	· Noticeably higher cumulative sulphate levels in the sulphuric acid (356 mg/kg) and hydrogen peroxide (646 mg/kg) cells compared to the acetic acid, ammonium oxalate/oxalic acid, and sodium hydroxide cells (206 - 218 mg/kg) at week 30. De-ionized water cell was intermediate at 308 mg/kg. · A 10-week lag in sulphate production observed in the hydrogen peroxide cell (138 mg/kg at week 10). Other cells showed low cumulative sulphate levels.

Table 8. Physical and chemical characteristics of waste rock leachates (continued).

Metal levels	· With the exception of ammonium oxalate/oxalic acid and sulphuric acid cells, iron concentrations were less than 2 ppm. · Arsenic levels remained below 0.1 ppm in all cells except the ammonium oxalate/oxalic acid cell where it reached levels of 0.14 ppm. · Sulphuric acid, ammonium oxalate/oxalic acid, and hydrogen peroxide leachates show cumulative calcium concentrations of 100 and 45 ppm, respectively.

Petrographic Analyses. Petrographic analyses were conducted on unweathered, naturally weathered and laboratory-weathered tailings and waste rock material. These studies revealed varying degrees of red-brown stains on fragments of waste rock. The sulphuric acid leached cell displayed the most strongly developed staining. However, no effects on the sulphides were recognizable in any of the six laboratory-weathered waste rock samples.

Tailings material clearly showed the effects of laboratory weathering. All samples, except the sodium hydroxide cell, displayed brown staining. The depth of this staining was consistent in the deionized, acetic acid, and ammonium oxalate/oxalic acid leached cells at 1 to 2 mm. Unoxidized sulphides were present throughout the samples, including the zone of staining. Sulphuric acid and hydrogen peroxide leached tailings had the thickest zones of brown staining (approximately 5 mm). These two samples were the only cells to display appreciable sulphide destruction. Sulphides in the upper four-fifths of the stained zone in the hydrogen peroxide leached tailings were almost completely destroyed. In the sulphuric acid leached tailings, unoxidized sulphides were present at the surface, but sulphides were completely oxidized in the slimes-enriched areas of the stained zone.

The naturally weathered tailings were obtained from the same mine as the tailings material used in the laboratory weathering program. Several differences were observed between this material and the unweathered material. The sulphide content of naturally weathered tailings was 0.5%, compared with 17% in unweathered material, based on observations during the petrographic analyses. Also, the particle size was in the range of 10 to 50 μm, as opposed to fresh tailings, which had a size range of 10 to 200 μm. Ferruginous secondary minerals occurred as diffuse stains and coatings on silicates, and as discrete, diffuse-margined grains probably representing the oxidized remnants of the original sulphide particles. Surviving sulphides typically displayed encapsulation by limonite.

Discussion

Although direct correlations between mineral surface chemical studies and leachate chemistry studies could not be made, valuable information was still obtained. Petrographic analyses of laboratory-weathered materials provided a valuable link to relate information obtained from the surface studies of pure minerals and from the leaching studies of natural waste materials.

Initiation of Oxidation - Ferric Iron Sites

The data from XPS and AES studies provide evidence that ferric iron is present in pyrrhotite, as opposed to pyrite, which contains ferrous iron only. The initiation of oxidation is expected to occur in the vacant cation sites within in the pyrrhotite crystal structure. Oxidation continues through redox reactions involving ferric iron. The vacuum-fractured mineral experiments suggest that the process begins at the fracturing stage.

Exposure-Related Weathering Behaviour

According to surface investigations and petrographic analyses, surface appearance and structure of alteration layers appear to vary according to exposure conditions. The tailings material leached by hydrogen peroxide and

sulphuric acid displayed the greatest depletion in sulphide content, limnotization, and staining compared with other humidity cell leaching conditions. Naturally weathered tailings also showed considerable sulphide destruction. Air-oxidized pyrrhotite produced surface iron oxide, while deionized water and sulphuric acid leached pyrrhotite produced surface iron oxyhydroxide.

Sulphate Production

Different surface layers were produced as a result of air-oxidation and deionized water leaching. It was also observed that deionized water leaching produced twice as much sulphate as air-oxidation according to XPS. Sulphuric acid-leaching produced the most sulphate according to surface investigations (XPS) conducted on pyrrhotite. Net sulphate levels in the sulphuric acid cell leachates for tailings were significantly higher than from other tailings cells. Compared to sulphate generated in the hydrogen peroxide cells, these higher levels are assumed to be due to the presence of ferrous rather than ferric iron sulphates. The rate of sulphate release remained constant or decreased in five of the six cells after the samples were immersed after week 10. Sulphate production decreased after week 20 in the sulphuric acid-leached cell. The cumulative sulphate in the tailings leachates account for the reduction of sulphur required to reduce the maximum potential acidity (MPA) values reported in the tailings ABA results. The hydrogen peroxide-leached waste rock was the only sample reporting increased sulphate release rate after the samples were immersed. Cumulative sulphate levels did not account for all the sulphur reductions suggested by the waste rock MPA results.

Release of Iron

The extensive depletion of sulphides in the hydrogen peroxide leached tailings compared with those from other cells did not correspond to higher dissolved iron levels. Hydrogen peroxide and sodium hydroxide cell leachates contained the lowest iron levels, while the sulphuric acid cell leachates contained the highest. High iron, sulphate and acidity levels in the sulphuric acid cell leachates are expected to be due, in part, to bacterial catalysis, although this was not confirmed. The low iron levels observed in hydrogen peroxide cell leachates can be attributed to the low solubility of Fe(III) under the prevailing pH conditions. The iron levels in ammonium oxalate/oxalic acid cell leachates is expected to be due to the chelating effects of the leachant.

Conclusions

Oxidation state and depth profile information obtained from the experiments conducted on research-grade pyrrhotite produced some very significant and relevant findings with respect to understanding and predicting ARD potential. Some of the following conclusions will require further work to verify their validity.

The vacuum fractured pyrrhotite experiment provided many insights into the initiation of the oxidation process. One-third of the iron in pyrrhotite is present as Fe(III). The first step in the ARD process may begin with the redox reaction between sulphur (oxidizing) and ferric iron (reducing). This first step is initiated when the rock is blasted, not upon exposure to air. Upon exposure to air, the reduction of molecular oxygen to oxide oxygen may be facilitated by the vacant cation sites created by the presence of ferric iron in the crystal structure. The presence of ferric iron in addition to ferrous iron provides a possible explanation for the higher reactivity of pyrrhotite relative to pyrite.

Sulphide sulphur is oxidized to di- and poly-sulphides prior to forming sulphate.

Exposure to oxygenated aqueous environments during the XPS and AES experiments produced significantly more sulphate than exposure to air at room temperature and pressure. Exposure to aqueous environments also produced hydrated iron oxides rather than iron oxide. Previous isotope studies (Taylor et al. 1984, Reedy et al. 1990, and Van Everdingen and Krouse 1985) indicate the involvement of water-derived oxygen in the formation of sulphate

in addition to atmospheric-derived oxygen. Directed studies involving mine waste materials are required to confirm suggestions that water is an important source of oxygen in the production of sulphate.

Literature Cited

Arkensteyn, G. F. M. W. 1980. Pyrite oxidation in acid sulphate soils: The role of microorganisms. Planet and Soil 54: 119-134.

Auger, P. 1975. The auger effect. Surface Science. 48: 1-8.

Engler, R. M., J. M. Brannon, J. Rose and G. Bigham. 1976. A practical selective extraction procedure for sediment characterization. In T. F. Yen, and Ann Arbor (eds), Chemistry of Marine Sediments. Science Publ. Inc. p.163-171.

Harris, J. J. 1993. Petrographic analysis - Tailings and waste rock. Unpublished.

McKibben, M. A. and H. L. Barnes. 1986. Oxidation of pyrite in low temperature acidic solutions: Rate laws and surface textures. Geochim. Cosmochim. Acta 50:1509-1520.

Moses, C. O., D. K. Nordstrom, F. S. Herman and A. L. Mills. 1987. Aqueous pyrite oxidation by dissolved oxygen and by ferric iron. Geochim. Cosmochim. Acta 51:1561-1572.

Nicholson, R. V., R. W. Gillham and E. F. Reardon. 1990. Pyrite oxidation in carbonate-buffered solution: 2 rate control by oxide coatings. Geochim. Cosmochim. Acta 54:395-402.

Reedy, B. J., J. K. Beatie and R. T. Lowson. 1990. Determination of sulphate isotopomers by vibrational spectroscopy. Spectrochimica Acta 10A:1513-1519.

Shirley, D. A. 1972. High-resolution X-ray photoemission spectrum of the valence bands of gold. Physical Review B 5:225-237.

Sobek, A. A., A. W. Schuller, J. R. Freeman and R. M. Smith. 1978. Field and laboratory methods applicable to overburdens and minesoils. EPA 600/2-78-054, p. 45-55.

Taylor, B. E, M. C. Wheeler and D. K. Nordstrom. 1984. Stable isotope geochemistry of acid mine drainage: experimental oxidation of pyrite. Geochimica et Cosmochimica Acta 48:2669-2678.

Van Everdingen, R. O. and H. R. Krouse. 1985. Isotopic composition of sulphates generated by bacterial and abiological oxidation. Nature 315:395-396.

DEVELOPMENTS IN PREDICTING AND MANAGEMENT OF ACID FORMING MINE WASTES IN AUSTRALIA AND SOUTHEAST ASIA[1]

Stuart D. Miller, John J. Jeffery, and Theresa A. Donohue[2]

Abstract: The acid-base account (ABA) is the most commonly used procedure for identifying potentially acid-forming materials at mine sites in Australia and Southeast Asia. The ABA is a very useful screening tool for classifying materials as either potentially acid-forming or non-acid forming. Confirmation of the ABA calculation usually requires a kinetic leaching test, which may run for a long period and require a major commitment of resources. Environmental Geochemistry International Pty Ltd have been developing a simple hydrogen peroxide oxidation procedure for quantifying the acid-generating capacity of a sample. This procedure, known as the net acid generation (NAG) test, provides a direct measure of the net amount of acid produced by a sample. The procedure is simple and low in cost and is currently used to identify potentially acid-forming materials at a number of mine sites in Australia, New Zealand, Papua New Guinea, and Indonesia.

The NAG test provides information on the risk of acid formation by mine waste materials, the relative reactivity of the contained sulfides, a measure of the amount of acid a material can generate. This information can then be used for planning and implementing waste rock and tailings disposal operations.

Research funded through the Australian Mining Industry Research Association (AMIRA) and sponsored by individual mining companies in Australia is currently being carried out to refine the net acid generation (NAG) procedure for predicting the acid-generating potential of mine waste materials. A component of this research is aimed at evaluating the kinetics of the NAG test reaction using pH and temperature profiles of the effect of rapid oxidation on a range of mine rock and process residue samples. This information will be related to the leaching characteristics and acid formation reaction kinetics (or lag period) observed in column tests and in the field.

The study commenced in September 1993 and will run over 18 months. Waste rock and tailings samples from 17 mine sites in Australia, New Guinea, and Indonesia are included in the program. This paper provides some background on developments of the NAG procedure to date and also outlines the research program being undertaken to further refine the method. Examples of pH and temperature profiles during the NAG test are given and related to ABA results.

Additional Key Words: acid mine drainage, prediction, hydrogen peroxide test, net acid generation test, acid-base account, lag period.

Introduction

Acid-forming rock and process wastes are a common occurrence at many base metal, gold, and coal mines in Australia and Southeast Asia. If poorly managed, acid-forming material can be difficult to rehabilitate and can produce drainage of unacceptable quality for discharge to the environment. Treatment of acid drainage is often difficult and costly.

---

[1]Paper presented at the International Land Reclamation and Mine Drainage Conference and the Third International Conference on the Abatement of Acidic Drainage, Pittsburgh, PA, April 24-29, 1994.

[2]Stuart D. Miller, Managing Director, John J. Jeffery, Principal, and Theresa A. Donohue, Environmental Scientist, Environmental Geochemistry International Pty Ltd, Balmain, NSW, Australia.

Incorrect identification and inappropriate management of acid-forming mine wastes has significant cost as well as environmental implications for the mining industry. In the Southeast Asia context, acid drainage can directly affect the livelihood of downstream communities which heavily depend on natural streams and rivers for food, transport, and domestic uses.

The process of acid generation from geological materials is well documented. When materials containing sulfide minerals are exposed to air and water, the sulfides become chemically unstable and react to form sulfuric acid and iron salts. The sulfuric acid may subsequently react with other minerals in the rock, reducing the amount of acidity formed. If the amount of acid generated by sulfide oxidation exceeds the inherent acid neutralization capacity of the rock, then acid conditions will be established; water flowing through such materials will have a low pH, high acidity, and high salt content and may contain elevated concentrations of metals.

Acid-forming mine waste materials include waste rock, mine overburden, and process tailings and acid-forming materials often occur in exposed mine faces in opencut pits and underground workings. Appropriate design and implementation of a waste management plan for the correct placement and disposal of the waste types (i.e. acid generating/acid neutralising) can overcome many of the problems associated with acid forming mine rock and waste. However, such planning requires not only an appreciation of the geochemistry of the materials but also an understanding of the location, nature, and extent of the various waste rock types to be mined and placed within the waste storage area. Therefore a means to accurately predict and identify acid-forming materials on a routine basis is essential for an effective management operation.

Net Acid Producing Potential

At the present time, the acid-base account (ABA) procedure is the most commonly used method for assessing the acid-forming potential of mine waste materials (Ferguson and Erickson 1988). This procedure provides a theoretical estimate of the net acid-producing potential (NAPP) of the waste and is based on the difference between the acid-forming and acid-neutralizing capacities of the material (Miller and Murray 1988). The acid-forming capacity is estimated from the total sulfur (or pyritic sulfur) content of the material, and the acid neutralization capacity (ANC) is measured directly in the laboratory. The NAPP is calculated as follows--

$$\text{NAPP} = \text{Total sulphur} \times 30.6 - \text{ANC}$$

While the NAPP indicates the potential for acid formation to occur, it does not provide any indication on the likely time it will take. Furthermore, the NAPP procedure is not suited to field applications, such as in-pit identification of potentially acid-forming waste rock types because the analyses required to calculate the NAPP are relatively time consuming and require specialized laboratory equipment.

The use of total sulfur for estimation of the total acid generation capacity presumes that all sulfur can participate in the acid generation processes. This may result in an overestimate of the acid generation capacity (Miller et al. 1991a). The laboratory procedures used for measurement of ANC can also overestimate the availability of ANC in the field, particularly when carbonate minerals such as dolomite and ferroan dolomite are present. These minerals often have limited solubility at the pH of acid sulfate systems and may not contribute significantly to the true ANC in the field.

Net Acid Generation Test

Preliminary investigations of the net acid generation (NAG) test have been carried out by Environmental Geochemistry International Pty Ltd (EGI) to assess its suitability for identification of acid-forming rock and mining wastes. These preliminary investigations have produced promising results (Miller et al. 1991b) that suggest the NAG test could be used in conjunction with

the acid-base account to identify and predict acid rock drainage for new mining ventures. The NAG test also has potential as a "stand alone" method for field identification and operational monitoring of waste types at existing mines. This field capability makes the NAG test a very attractive procedure and worthy of further development.

The NAG procedure is based on a test developed by Finkelman and Giffin (1986) in which hydrogen peroxide was used to quantify the pyrite content and acid mine drainage potential of overburden sediments and spoil materials from coal mining operations. Other researchers have also investigated the use of peroxide for assessing sulfide content and acid potential of mine waste materials (Smith et al. 1974, Sobek et al. 1978, O'Shay and Hossner 1984, Coastech 1989, O'Shay et al. 1990).

The hydrogen peroxide reacts with sulfide minerals, generating heat and acid. The acid in turn reacts with any inherent acid-neutralizing minerals in the material. Therefore, the amount of acid remaining in solution at the completion of the reaction, which is quantified by titration, represents the net acid generated. The final pH of the NAG solution also provides a measure of the activity of hydrogen ions in solution and an indirect measure of the acidity generated. To date, the NAG test has been mainly used to verify the findings of the ABA procedure; for example, to test whether a material classified as potentially acid-forming on the basis of the sulfur and ANC contents does in fact produce acid when the sulfide minerals are oxidized.

NAG Method

The NAG working procedure (which will be further developed in this study) is presented here. The NAG test involves the addition of 250 ml of 15% hydrogen peroxide (unstabilised 30% hydrogen peroxide diluted 1:1 with deionised water) to a 2.5 ± 0.1 g sample of pulverised waste rock or tailings. 500 ml conical glass beakers covered with watchglasses are used for the testwork and samples are kept in a fume hood during the test. The oxidation reaction results in the production of heat in some samples. Samples are considered to have finished reacting when: (1) the sample solution boils and then cools, or (2) after at least 12 hours has elapsed. Any excess hydrogen peroxide left in the sample solution is broken down by heating all NAG solutions on a hotplate at 100 ^{o}C until all effervescence ceases and the solution boils. Samples which react violently resulting in lost sample solution are repeated using a 1 litre beaker.

After the solution has cooled, the pH and acidity of the solution is measured. Measurement of the acidity involves titrating the NAG solution with standardised NaOH (0.100 N NaOH if pH > 2.5 and 0.500 N NaOH if pH <2.5) to an endpoint of pH 7.0 using an Orion 960 autochemistry system. Samples with a NAG result of > 25 kg/mt H_2SO_4 are repeated using 1.0 g of sample.

Monitored samples record pH and temperature over the reaction period of the test. pH and temperature probes are placed in the sample solution and the pH, temperature and time are recorded using a MacLab analog digital instrument, which transfers the data onto a MacIntosh computer. Parameters are measured continuously and the average reading each 10 seconds is recorded and plotted.

NAG Test Development

Research funded through the Australian Mining Industry Research Association (AMIRA) and sponsored by individual mining companies in Australia is currently being carried out to refine the net acid generation (NAG) procedure for predicting the acid-generating potential of mine waste materials. The main objectives of the current study are -

1. To develop the NAG procedure as a simple low cost test for identifying acid-forming mine rock and waste materials for use in premining and operational phases of mining ventures.

2. To study the kinetics of the NAG reaction on monitored samples and evaluate whether they can be extrapolated to the field situation for prediction of the kinetics of the acid generation and neutralization reactions in the field and the exposure time necessary before acid formation occurs (i.e., the lag period).

3. To assess on-site application of the NAG test, including in-pit monitoring of acid-forming materials.

The study is being sponsored by 8 mining companies and includes 119 waste rock and tailings samples from gold, nickel, base metal, iron ore, and coal mining projects. The study will compare NAG, NAPP, and leach column results for an extensive and wide-ranging group of mine rock and process residue samples. Table 1 shows the types of samples available for the NAG testwork.

Table 1. Samples available for NAG testwork program

Sample Type	Number of Samples	Number of Mines	Ore Deposit				
			Gold	Iron Ore	Nickel	Base metal	Coal
Tailings	23	11	8	-	11	1	3
Waste Rock	78	15	54	8	6	3	7
Ore	18	8	13	-	3	2	-

Results to date

119 samples have been analysed for ABA and NAG including final pH of NAG solution. Total sulfur results range from 0.1 to 40%S, ANC from 0 to 425 kg/mt H_2SO_4 and NAPP from - 390 to 1230kg/mt H_2SO_4. Figure 1 shows NAPP vs NAG results and the results from 0 to 60 kg/mt H2SO4 are shown in more detail in figure 2. The results indicate that the calculated NAPP is predominantly higher than the acid generated by oxidation. The NAG solution pH for the samples in figure 2 are plotted in figure 3 and show that samples with a slightly positive NAPP can produce neutral or alkaline NAG solutions and samples with an NAPP of >10 all have a pH <4.5. These results will be further evaluated via changes to the NAG procedure, kinetic studies, column leaching and field observation.

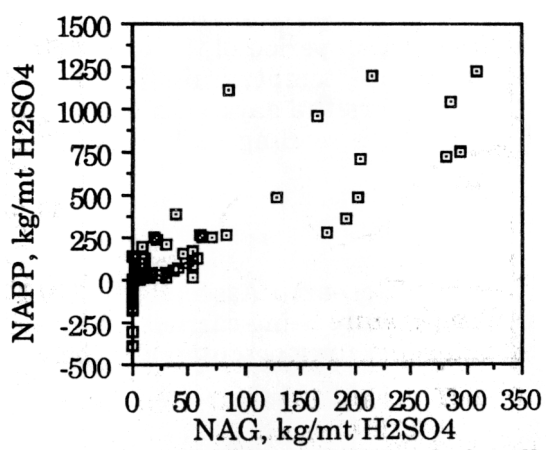

Figure 1. NAPP vs NAG result for all samples.

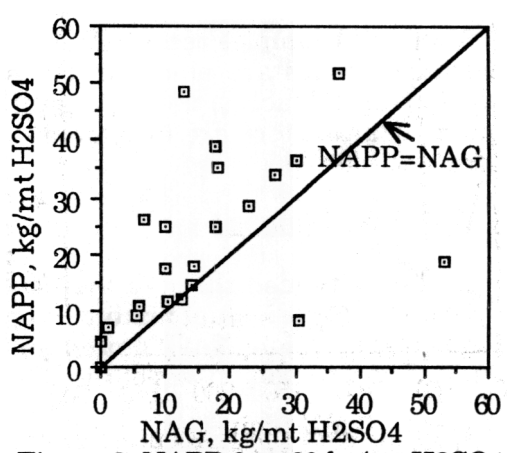

Figure 2. NAPP 0 to 60 kg/mt H2SO4 vs NAG result.

Monitored NAG solutions

Monitored NAG tests provide information regarding the pH and temperature change over time and preliminary investigations suggest that the time to reach the temperature maximum during the NAG test is a function of sulfur content, sulfur reactivity and ANC of the material (Miller et al. 1991b). These properties all affect the length of the lag period that precedes acid formation in the field.

Figures 4 to 8 show NAG test profiles of pH and temperature for five mine waste samples that are classified as potentially acid-forming by the standard ABA procedure. The ABA results for the five samples are given in table 2.

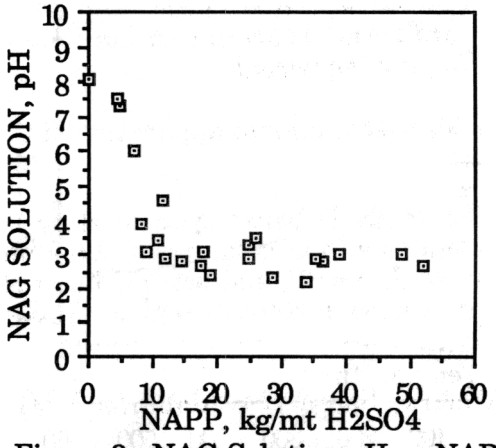

Figure 3. NAG Solution pH vs NAPP 0 to 60 kg/mt H2SO4.

Although all samples are classified as potentially acid-forming by the ABA method, the NAG test results demonstrate significantly different oxidation kinetics and rates of acid formation. For example, sample 1 is a high S-low ANC material that reacts rapidly under NAG test conditions. Figure 4 indicates that the NAG solution effectively boiled within 55 min of commencement of the test from the heat generated by the exothermic oxidation of the sulfides in the sample. Simultaneously, the pH of the solution decreased to around pH 2.5.

Sample 2 contains less S and has a greater ANC than sample 1. In this case the time to react was slower, taking approximately 160 min for the solution to boil (fig. 5).

Sample 3 also has a lower S content than sample 1 as well as a low ANC. This sample did not produce a "boiling peak", but the pH of the solution did steadily decrease to approximately pH 3 in about 500 min.

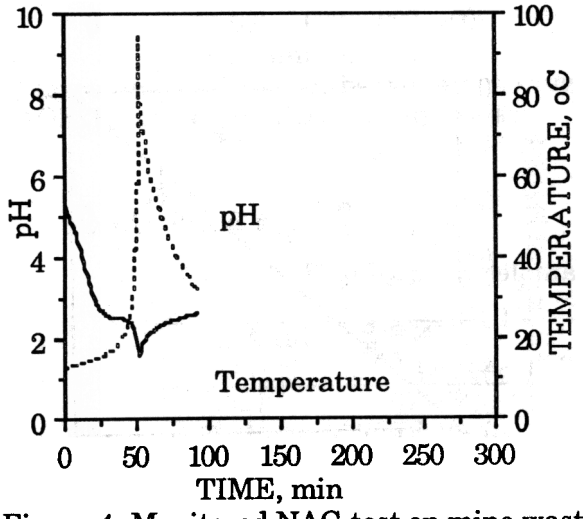

Figure 4. Monitored NAG test on mine waste rock sample 1 (NAPP=125 kg/mt H2SO4).

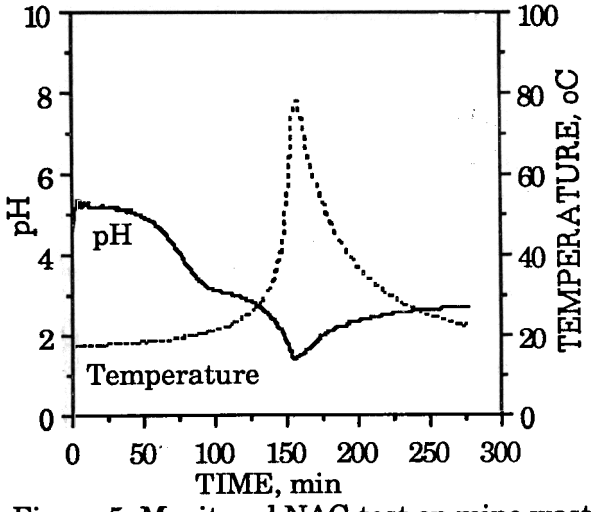

Figure 5. Monitored NAG test on mine waste rock sample 2 (NAPP=55 kg/mt H2SO4).

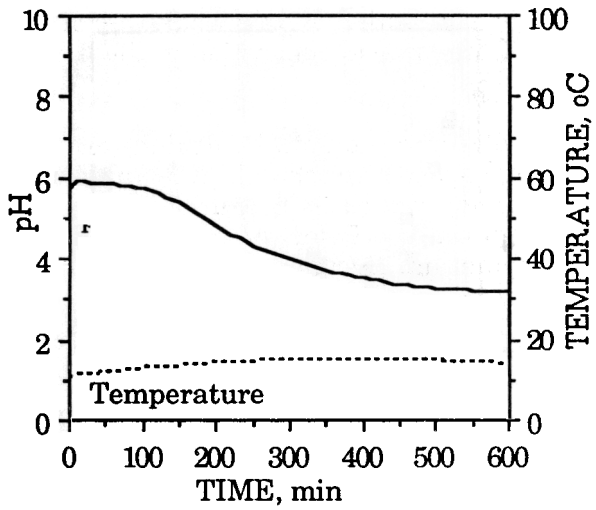

Figure 6. Monitored NAG test for mine waste rock sample 3 (NAPP=33 kg/mt H2SO4)

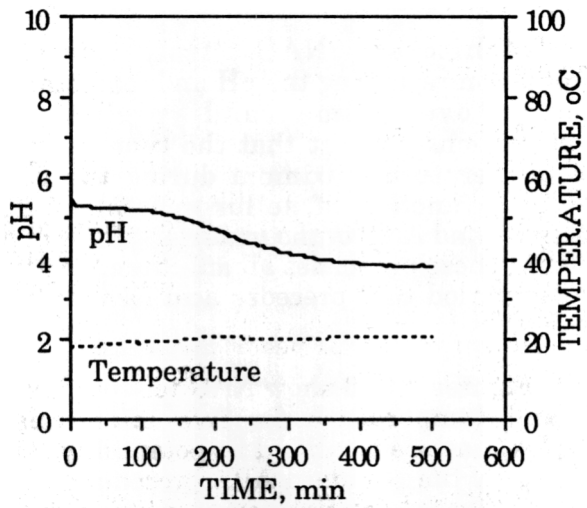

Figure 7. Monitored NAG test for mine waste rock sample 4 (NAPP=11 kg/mt H2SO4).

Samples 4 and 5 contained only slightly less S than sample 3, but the ANC's were significantly greater. Although samples 4 and 5 were classified as potentially acid-forming by the ABA, neither sample generated significant heat and the final pH's of the NAG tests were only weakly acidic at around pH 4 and 5.5, respectively.

The results for these five samples provide an indication of the range of reaction kinetics that occur under NAG test conditions. On the basis of both the ABA and NAG test results, samples 1 and 2 would be described as potentially acid-forming and high risk because of their high NAPP's and the strongly acidic NAG tests.

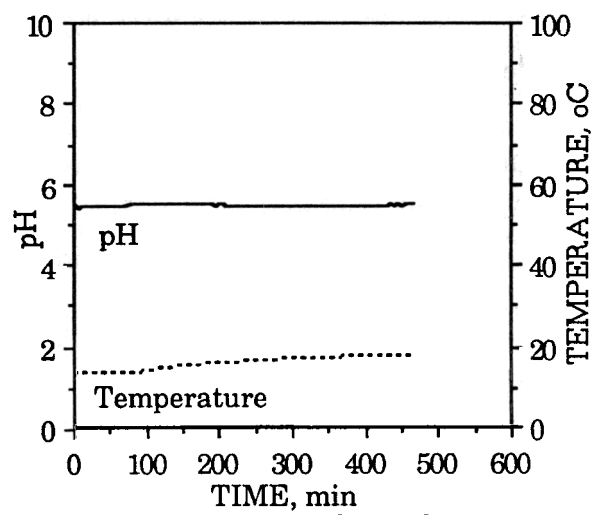

Figure 8. Monitored NAG test for mine waste rock sample 5 (NAPP=6.5 kg/mt H2SO4).

Table 2. ABA results for mine waste rock samples referred to in figures 1 to 5.

Sample	Total S, %S	ANC, kg/mt H_2SO_4	NAPP*, kg/mt H_2SO_4	NNP* kg/mt $CaCO_3$	MPA/ANC* ratio
1	4.1	0.1	125	-125	1255
2	2.4	18	55	-55	4.1
3	1.2	3.9	33	-33	9.4
4	0.89	16	11	-11	1.7
5	0.80	18	6.5	-6.5	1.4

* NAPP= total S x 30.6 - ANC = -NNP, MPA = total S x 30.6

Samples 3 and 4, on the other hand, would be classified as potentially acid-forming but low risk because of their much slower reaction times and/or the generation of only weakly acidic NAG liquors. Sample 5 would be described as non-acid-forming because acid generation in the NAG test was insignificant and the NAPP was close to zero.

As the results for the five waste rock samples indicate, most potentially acid-forming rocks and mine wastes contain some inherent acid neutralizing capacity which delays or inhibits acid generation for a period of time following exposure. This delay, which is measured in minutes in the NAG test, may relate to a real time of months or years in the field. Also, the reactivity of sulfide varies, which in turn affects the time to acid formation. Because of these factors, acid generation may not be observed until the material has been exposed for months or even years. This lag period is an important consideration for waste management operations because it will determine if materials need to be treated or buried immediately or can be left exposed for a period of time before covering.

Conclusions

At present, there is no rapid routine laboratory procedure for assessing the kinetics of acid formation by sulfidic waste materials. Batch and leaching column tests are sometimes used, but these may need to be maintained for 12 months or longer to provide meaningful results. Consequently there is often a reluctance to use column tests, particularly in the premining phase when time constraints do not allow for long-term waste rock testing. Also, there is often concern in regard to extrapolating column test results to field conditions.

Preliminary testwork has indicated that a relationship may exist between the kinetics of the NAG test and the lag period observed in the field. The current research is aimed at evaluating this relationship; if it is established, it may be possible to provide a time factor for use in waste management design.

An added advantage of the NAG test is that it requires minimal laboratory equipment to carry out and can be completed within hours. This means the NAG test is suited to on-site use and is currently used at mines in Australia and Southeast Asia.

Acknowledgments

The authors wish to thank AMIRA and its members for their sponsorship of this research program. The companies supporting this research are Billiton Australia, BHP Coal Limited, Carpentaria Gold Pty Limited, Hammersley Iron Pty Limited, Peak Gold Pty Limited, Placer Pacific Limited, P.T. Kelian Gold, and Western Mining Corporation Limited - Kambalda Nickel Operations.

Literature Cited

Coastech Research Inc. 1989. Investigation of prediction techniques for acid mine drainage. Report prepared for Canada Centre for Mineral and Energy Technology, Energy Mines and Resources Canada, DSS File No. 30SQ.23440-7-9178.

Ferguson, K.D., and P.M. Erickson. 1988. Pre-mine prediction of acid mine drainage. p. 24-43. In W. Salomons and U. Forstner (eds.), Environmental management of solid waste - dredged material and mine tailings. Springer-Verlag, Berlin.

Finkelman, R.B., and D.E. Giffin. 1986. Hydrogen peroxide oxidation: an improved method for rapidly assessing acid-generating potential of sediments and sedimentary rocks. Reclamation & Reveg. Res. 5:521-534.

Miller, S.D., J.J. Jeffery, and J.W.C. Wong. 1991a. Use and misuse of acid-base account. p. 489-506. In Proceedings of the Second International Conference on the Abatement of Acidic Drainage. (Montreal, PQ, September 16-18, 1991).

Miller, S.D., J.J. Jeffery, J.W.C. Wong, and A.J. Goldstone. 1991b. In-pit identification and management of acid-forming waste rock at the Golden Cross Gold Mine, New Zealand. p. 137-152. In Proceedings of the Second International Conference on the Abatement of Acidic Drainage. (Montreal, PQ, September 16-18, 1991).

Miller, S.D., and G.S.C. Murray. 1988. Application of acid-base analysis to wastes from base metal and precious metal mines. p. 29-33. In Proceedings of Mine Drainage and Surface Mine Reclamation Conference, v.1. (Pittsburgh, PA, April 17-22, 1988). BuMines IC 9183

O'Shay, T.A., and L.R. Hossner. 1984. The determination of potential acidity of overburden sediments. p. 13-14. In Proceedings of Surface Mine Reclamation Workshop. TX Agric. Ext. Service and TX A. & M. Univ. (San Antonio, TX, October 9-10, 1984).

O'Shay, T.A., L.R. Hossner, and J.B. Dixon. 1990. A modified hydrogen peroxide oxidation method for determination of potential acidity in pyritic overburden. J. Environ Qual. 19:778-782.

Smith, R.M., W.E. Grube, Jr., T. Arkle, Jr., and A. Sobele. 1974. Mine spoil potential for soil and water quality. U.S. Department of Commerce, EPA-670/2-74-070. 101 p.

Sobek, A.A., W.A. Schuller, J.R. Freeman, and R.M. Smith. 1978. Field and laboratory methods applicable to overburdens and mine soils. U.S. Environmental Protection Agency, Cincinnati, OH, EPA 600/2-78-054.

THE EFFECTS OF ANOXIC LIMESTONE DRAINS ON MINE WATER CHEMISTRY[1]

Robert S. Hedin and George R. Watzlaf[2]

Abstract: Construction and water quality characteristics of 21 anoxic limestone drains (ALDs) were studied in order to identify and evaluate factors responsible for the variable performance of these passive treatment systems. Nineteen of these ALDs discharged water that contained bicarbonate alkalinity ranging from 69 to 469 mg/L as $CaCO_3$. In addition to adding alkalinity to the mine water, some ALDs decreased the mineral acidity of the mine water. Acidity removal ranged from 0 to 5,901 mg/L. Large changes in acidity were primarily associated with retention of ferric iron and aluminum. Equilibrium calculations indicated that all of the ALD effluents were undersaturated with respect to calcite and oversaturated with siderite. Retention of ferrous iron, however, was only indicated at two sites when retention times were longer than 25 days. Half of the ALD effluents were in equilibrium with rhodochrosite, however, retention of manganese was not indicated at any sites. Two of the ALD effluents were saturated with gypsum. One of these sites retained 4,500 mg/L sulfate. At two sites, where mine water could be sampled at points along the flow path within the ALDs, concentrations of alkalinity were found to plateau at maximum values well before the end of the ALD. These maximum values of alkalinity were developed after 14 to 23 hours of retention time. An ALD sizing technique is suggested that incorporates the minimum retention time findings.

Additional Key Words: acid mine drainage, passive treatment, carbonate chemistry, calcite.

Introduction

Since Turner and McCoy (1990) first described the use of buried beds of limestone to treat acid mine drainage (AMD), dozens of similar passive treatment systems have been constructed in Appalachia. Commonly called "anoxic limestone drains" or "ALDs," the systems function by promoting the contact of acid mine drainage with limestone gravel under anoxic conditions. The anoxic conditions limit the oxidation of ferrous iron, thereby minimizing the armoring of limestone with ferric hydroxide.

Anoxic limestone drains are generally used to treat acid mine drainage (AMD) before it flows into a constructed wetland. The ALD raises the pH of the water to circumneutral levels (pH 6 to 7) and introduces bicarbonate alkalinity. Upon exiting the ALD, the circumneutral pH level promotes metal precipitation and the bicarbonate alkalinity neutralizes the acidity produced by metal hydrolysis (Hedin and Nairn 1993).

ALDs can be a tremendously cost-effective water treatment technique. The Tennessee Valley Authority (TVA) has used ALDs to enhance the performance of existing constructed wetlands and avoid hundreds of thousands of dollars of chemical treatment costs (Brodie 1991). In western Pennsylvania, chemical treatment has been eliminated at several sites where the mine waters are treated with ALDs before flowing into constructed wetlands (Nairn et al. 1992, Hedin and Nairn 1993).

The concentration of alkalinity contained in the ALD effluents varies considerably (Faulkner and Skousen 1993, Nairn et al. 1991). This variation has important repercussions for the design and sizing of the total passive treatment system. When an ALD does not generate enough alkalinity to totally neutralize the acidity contained in the mine drainage, additional alternative alkalinity-generating treatments are necessary.

In this paper we report the chemical characteristics of the effluents of 21 ALDs located in Appalachia. We evaluated the alkalinity-generating and acidity-neutralizing processes to better understand the chemical changes occurring in these systems.

---

[1]Paper presented at the International Land Reclamation and Mine Drainage Conference and the Third International Conference on the Abatement of Acidic Drainage, Pittsburgh, PA, April 24-29, 1994.

[2]Robert S. Hedin, Research Biologist, and George R. Watzlaf, Environmental Engineer, U.S. Department of the Interior, Bureau of Mines, Pittsburgh, PA, USA.

Methods

Water samples of the final effluent were collected from all ALDs. Alkalinity and pH were measured in the field. The pH was measured with a calibrated Orion SA270 or 290A pH/ISE meter. Alkalinity determinations were made with the Orion Total Alkalinity Test Kit and a pH meter. The results of this method agree well with results obtained by the standard titration procedure (Watzlaf and Hedin 1993). Concentrations of Fe, Mn, Al, Ca, and Mg were determined for samples acidified in the field (2 mL of 12.1N HCl per 250 mL of sample) using inductively coupled argon plasma spectroscopy (ICP). Ferrous iron concentrations were determined for acidified samples by titration with $K_2Cr_2O_7$ (Fales and Kenny 1940). Ferric iron was calculated from the difference of total iron and ferrous iron measurements. Sulfate concentrations were determined by either ion chromatography or ICP. The net acidity or alkalinity of each sample was determined in the laboratory by boiling 50 mL of raw sample with 1 mL of 30% H_2O_2 and titrating acidic solutions to pH 8.3 with 0.1N NaOH and alkaline solutions to pH 4.8 with 0.1N H_2SO_4 (American Public Health Association 1985). All concentrations of alkalinity and acidity are reported as mg/L as $CaCO_3$. Analyses of duplicate and spiked samples indicated an analytical error of less than 3% for all parameters.

Partial pressures of CO_2 and mineral saturation indices were calculated from the results of water analyses using the U.S. Geological Survey WATEQ, version 4F, computer model (Ball et al. 1987). A bicarbonate input to the model was estimated by assuming that field alkalinity resulted entirely from HCO_3^-. This assumption is reasonable for the pH range of alkalinity-containing water samples collected in this study (pH 5.5 to 6.7). Flow rates were determined at the effluents of ALDs by measuring the time necessary to collect a known volume of water. The theoretical retention or detention time (t_d) of mine water within each ALD was estimated using the equation:

$$t_d = \frac{M\,V_v}{\rho_b\,Q}$$

where M is the mass of limestone, V_v is the bulk void volume expressed in decimal form, ρ_b is bulk density of the limestone, and Q is the volume flow of the mine water. For the ALDs studied in this paper, the bulk density for limestone was assumed to be 1,600 kg/m^3 (2,700 lb/yd^3) and a void volume of 45 to 50% (based on measurements of limestone used at three sites) was used.

Results and Discussion

The chemical compositions of the effluents of 21 ALDs are shown in table 1. Pre-ALD water quality is also shown. Two types of pre-ALD water quality were collected. At 10 sites, the mine water was able to be sampled before it flowed into the ALD at the same time that ALD effluent samples were collected. At eight sites, sampling of the raw water was not possible, therefore, the existing water quality data for the acidic discharges before the ALDs were constructed are reported. For most sites, the pre-ALD samples predate the ALD effluent samples by several years. Comparisons of the chemical compositions of the current ALD effluents and the historic raw water quality at these eight sites may be partly compromised by recent changes in the raw water chemistry unrelated to the construction and performance of the ALDs. We were unable to chemically characterize pre-ALD water at three ALD sites. The original water at the Ohio site was reportedly highly acidic with pH values less than 3. The original water at the REM-L ALD was reportedly similar to the REM-R discharge (which was sampled previous to ALD construction). No information exists on the water quality at the Maud site prior to construction of the ALD.

Concentrations of alkalinity in the effluents of the ALDs ranged from 0 to 469 mg/L. Of the 21 ALDs sampled, 19 discharged water that contained alkalinity. These effluent alkalinity concentrations, the amount of limestone used, the average effluent flow rate, and calculated theoretical retention times (t_d) for each ALD are presented in table 2. We were unable to obtain construction information for six of the 21 ALDs.

Changes in Water Quality at the ALD Sites

For all of the ALDs that produced alkalinity, the chemistry of the effluent water samples differed from that of the raw water (table 1). Differences in the water quality between the raw water and ALD effluent could arise from three general reasons. First, at sites where the raw water was characterized by samples collected several years ago, differences between these old analyses and analyses of recently collected ALD effluents samples may arise from recent changes in the chemistry of the raw mine water.

Table 1. Influent (In) and effluent (Out) water chemistry of 21 anoxic limestone drains in Appalachia. Values of pH in standard units. All concentrations in mg/L; alkalinity concentrations expressed in mg/L of calcium carbonate. "NA" indicates data is not available.

Site	Alkalinity		pH		Ca		Fe		Al		Mn		Sulfate	
	In	Out	In	Out	In	Out	In	Out	In	Out	In	Out	In	Out
Rid-2L[1]	0	469	2.3	6.2	97	855	1416	202	486	<1	23	11	6,719	2,227
Ohio	NA	400	NA	6.1	NA	592	NA	625	NA	<1	NA	80	NA	4,250
Hathaway[2]	0	385	3.3	6.5	NA	445	195	54	23	<1	44	14	2,237	1,303
TVA-AROAD[1]	0	350	2.8	6.6	57	87	16	38	19	<1	4	2	430	55
Rid-2R[1]	0	306	3.7	6.3	92	316	217	164	31	<1	7	7	979	957
Rid-1[1]	3	290	4.7	6.5	215	400	5	27	2	<1	23	27	711	992
TVA-2[3]	0	280	3.5	6.7	NA	111	40	24	<2	<1	13	7	NA	210
Morrison[1]	23	271	5.3	6.3	119	230	216	151	1	<1	51	42	1,340	1,081
Schnepp[2]	0	191	3.3	6.3	NA	240	92	61	7	<1	28	39	980	908
Willi[4]	0	187	2.7	6.3	145	360	48	<1	62	<1	45	34	1,538	1,185
Empire[5]	0	180	4.0	6.2	NA	176	37	67	NA	<1	22	29	1,155	1,025
Jennings[1]	0	177	3.3	6.3	86	215	81	62	21	<1	9	9	691	680
Howe-2[1]	24	174	5.9	6.5	162	229	276	271	<1	<1	39	39	1,298	1,309
Howe-1[1]	33	161	5.6	6.2	159	211	279	277	<1	<1	41	40	1,323	1,329
Maud	NA	155	NA	6.5	NA	153	NA	<1	NA	<1	NA	2	NA	333
REM-L	NA	138	NA	6.0	NA	223	NA	184	NA	<1	NA	45	NA	1,247
Shade[4]	0	123	3.5	6.6	132	254	3	1	22	<1	32	36	1,042	1,300
TVA-4[3]	NA	120	4.9	6.7	NA	85	135	<1	NA	<1	24	3	NA	155
REM-R[4]	0	69	4.3	5.5	258	257	589	507	5	3	136	132	2,825	2,655
Fawn[1]	0	0	3.5	3.7	346	379	417	445	103	152	25	29	5,000	5,432
Ohiopyle[1]	0	0	3.3	3.6	209	178	10	3	112	87	79	63	2,345	2,043

[1]"In" samples collected at the same time that "Out" samples were collected.
[2]"In" samples describe discharge before construction of ALD; data supplied by PA Dept. of Environmental Resources.
[3]"In" samples describe discharge before construction of ALD; data from Brodie (1991).
[4]"In" samples describe discharge before construction of ALD; data collected by U.S. Bureau of Mines.
[5]"In" samples describe discharge before construction of ALD; data from Turner and McCoy (1990).

Table 2. Selected parameters of the 21 ALD sites. Alkalinity concentrations in mg/L as calcium carbonate as measured at each field site. "NA" indicates data is not available.

Site	Limestone mass, mt	Flow, L/min	Mass per flow, mt/(L/min)	t_d[1], h	Alkalinity, mg/L
Rid-2L	114	0.8	142.5	698	469
Ohio	NA	NA	NA	NA	400
Hathaway	945	NA	NA	NA	385
TVA-AROAD	NA	265	NA	NA	350
Rid-2R	162	0.5	324.0	1,588	306
Rid-1	108	5	24.0	118	290
TVA-2	NA	NA	NA	NA	280
Morrison	64	7	9.4	46	271
Schnepp	132	57	2.3	11	191
Willi	182	5	36.4	178	187
Empire	NA	NA	NA	NA	180
Jennings	364	92	4.0	19	177
Howe-2	132	53	2.5	12	174
Howe-1	455	92	4.9	24	161
Maud	NA	NA	NA	NA	155
REM-L	125	82	1.5	7	138
Shade	35	15	2.3	11	123
TVA-4	364	131	2.8	14	120
REM-R	124	115	1.1	5	69
Fawn	NA	NA	NA	NA	0
Ohiopyle	225	218	1.0	5	0

[1]Theoretical detention time.

Second, the ALD may collect water that was not originally intended to be collected by the ALD prior to construction. When ALDs are intended to collect contaminated seepage (as well as treat it), the ALD likely collects nontarget water as well. If these nontarget waters are uncontaminated, dilution of contaminant concentrations in the ALD will occur. If these nontarget inputs are more contaminated than the sampled raw water, it is possible that contaminant concentrations will increase with flow through the ALD.

We evaluated the significance of nontarget inputs of mine water at four ALD sites by comparing influent and effluent concentrations of conservative ions (table 3). The conservative ions compared were magnesium (Mg), manganese (Mn), and sulfate. Magnesium does not form any solids under the chemical conditions that exist in ALDs. Because all of the limestones used at the ALD sites were high-calcium/low magnesium, and because the solubility of dolomite is low, magnesium levels do not change appreciably as water flow an ALD. Manganese and sulfate

concentrations were also compared because we have found these ions to behave conservatively in ALDs where the solubility product of gypsum is not exceeded. At the Jennings, Howe-1, and Howe-2 ALDs the raw water is piped to the ALD from a discrete source and thus these ALDs were not intended to collect any other water. At these sites, there is little or no change in Mg, Mn, or sulfate concentrations. At the Morrison site, which is designed to collect mine drainage along the toe of the spoil, the raw water was diluted by an average 18%. When the site was sampled in conjunction with rainstorms, changes in Mg and Mn were as high as 50%. Clearly, this ALD collects uncontaminated water as well as the targeted acid mine drainage. We suspect that when ALDs are constructed for both collection and treatment of AMD, the collection of uncontaminated water may often occur. At these sites, improvements in water quality may be partly attributable to dilution of contaminants and the true performance of the ALD can only be assessed when dilution is quantified and taken into account.

Table 3. Percentage change in magnesium, manganese, and sulfate concentrations at sites where water can be sampled before it enters the ALD and from the effluent.

Site	Mg	Mn	SO_4
Morrison	-18%	-18%	-19%
Jennings	0%	-1%	-2%
Howe-2	+1%	0%	+1%
Howe-1	0%	-1%	0%

Faulkner and Skousen (1993) report that some ALDs in West Virginia have unintentionally collected nontarget acid mine drainage. Two of the ALDs sampled in our study collected nontarget waters that were more contaminated than the original target waters. The Rid-1 site discharged water that contained 440% more Fe and 40% more sulfate than the influent water (table 1). The Fawn site discharged water with contaminant concentrations that were 7% to 48% higher than those of the influent water. These unexpected inflows have most likely contributed to the failure of this ALD. The interception of nontarget contaminated water may also be a common feature of ALDs that are constructed to collect mine water. During construction of the Schnepp ALD, excavations intercepted and collected acid mine drainage that was not originally targeted.

The third reason that the chemistry of the raw mine drainage and the ALD effluent differ is due to chemical reactions within the ALD. These reactions will determine the performance and ultimate longevity of the ALD system. The chemical reactions that occur in an ALD fall into two types: reactions that increase the concentrations of alkalinity in the water and reactions that decrease the acidity of the water (table 4). Alkalinity is increased primarily by reactions that increase concentrations of bicarbonate ion, HCO_3^-. In natural systems, the principal reaction that generates bicarbonate alkalinity is the reaction of carbonic acid (H_2CO_3) with calcite. The acidity of mine water is decreased in ALDs through the neutralization of proton acidity (H^+) and the precipitation of iron, manganese, and aluminum. Ferric iron and aluminum potentially precipitate as hydroxides, while ferrous iron and manganese potentially precipitate as carbonates.

Alkalinity-generating and acidity-removing reactions are linked by several reactions. The neutralization of proton acidity associated with free H^+ and metal hydrolysis reactions generates carbon dioxide which, through the formation of carbonic acid, increases the generation of alkalinity. Bicarbonate produced by calcite dissolution potentially reacts with Fe^{2+} and Mn^{2+} to form siderite ($FeCO_3$) and rhodochrosite ($MnCO_3$).

Alkalinity-generating and acidity-removing reactions occur in a predictable order that is consistent with the solubility products of the solids. When highly acidic, metal contaminated water contacts limestone, the first reaction that occurs is the neutralization of proton acidity. This reaction raises the pH, which decreases the solubility of metal hydroxides. Between pH 3 and 4, ferric iron precipitates as ferric hydroxide. Between pH 4 and 5, aluminum precipitates as aluminum hydroxide. As the pH rises above pH 4.5, bicarbonate begins to accumulate in appreciable amounts. As bicarbonate concentration increases, the solubility of metal carbonates may be exceeded, causing the precipitation of siderite and then rhodochrosite. With each of these reactions, calcium is released into solution. As the concentration of calcium increases, the potential for gypsum ($CaSO_4$) precipitation increases.

Table 5 shows the concentrations of alkalinity generated and calculations of the decrease in acidity for the ALDs. Variation of the alkalinity generated was less than the variation in the decrease in acidity. The generation of alkalinity in an ALD is limited to a maximum value by the solubility of calcite. High partial pressures of carbon dioxide increase the equilibrium concentrations of bicarbonate; however, even under very high CO_2 partial pressures,

Table 4. Chemical reactions involving calcite that can occur in anoxic limestone drains.

Alkalinity-generating reactions:
$CaCO_3 + H^+ \text{ ---> } Ca^{2+} + HCO_3^-$
$CaCO_3 + H_2CO_3 \text{ ---> } Ca^{2+} + 2HCO_3^-$
$CaCO_3 + SO_4^{2-} + H_2O \text{ ---> } CaSO_4 + OH^- + HCO_3^-$
Acidity-lowering reactions:
$CaCO_3 + 2H^+ \text{ ---> } Ca^{2+} + H_2O + CO_2$
$3CaCO_3 + 2Fe^{3+} + 6H_2O \text{ ---> } 3Ca^{2+} + 2Fe(OH)_3 + 3H_2CO_3$
$3CaCO_3 + 2Al^{3+} + 6H_2O \text{ ---> } 3Ca^{2+} + 2Al(OH)_3 + 3H_2CO_3$
$CaCO_3 + Fe^{2+} \text{ ---> } Ca^{2+} + FeCO_3$
$CaCO_3 + Mn^{2+} \text{ ---> } Ca^{2+} + MnCO_3$

the concentrations of alkalinity that develop in ALDs rarely exceed 500 mg/L (table 6). Changes in acidity at the ALD sites, however, ranged as high as 5,900 mg/L. Large changes in acidity values were generally a result of retention of ferric iron and aluminum. ALDs have a high potential to retain Fe^{3+} and Al^{3+} because at circumneutral pH, the metal hydroxide of ferric iron and aluminum rapidly precipitate. Precipitation of these metal solids within the ALD may armor limestone and/or decrease the permeability of the system - both of which could decrease the performance and theoretical longevity of the ALD (Nairn et al. 1991).

All but one of the ALD effluents that contained iron were supersaturated with siderite (table 6); however, little removal of ferrous iron (Fe^{2+}) was observed (table 5). This is likely due to the kinetics of siderite formation and that equilibrium has not been reached. WATEQ is used only to identify those solids that are supersaturated and therefore have the potential for forming. Changes in Fe^{2+} concentrations at the Morrison ALD were largely consistent with a dilution effect. Changes in Fe^{2+} concentrations at the REM-R ALD are subject to uncertainties associated with comparing pre-ALD water quality (collected 3 years ago) with the current ALD effluent. Retention of Fe^{2+} definitely occurred at the Rid-2L and Rid-2R sites. At both sites, samples of the raw water were collected in conjunction with samples of the ALD effluent. Both of these ALDs were characterized, at the time of sampling, by very long retention times (table 2). While most ALDs had retention times of less than two days, retention times at the Rid-2 sites were more than a month. If siderite forms in ALDs, the reaction appears to be slow and only becomes important when the systems are constructed to have extremely long retention times. Half of the ALD effluents were saturated with rhodochrosite (table 6). No strong evidence was found to suggest that Mn was being retained in any of the ALD systems. The absence of retention of Mn may be due to kinetic limitations, like those proposed for siderite; also rhodochrosite is more soluble than siderite and is unlikely to form until ferrous iron concentrations decrease.

Only two of the ALD effluents were saturated with gypsum (table 6). Both of the mine waters at these sites contained concentrations of sulfate > 4,000 mg/L. At the Ohio site, influent sulfate concentrations are not available. At the Rid-2L ALD, sulfate concentrations of the mine water as it flowed through the ALD decreased from 6,719 to 2,227 mg/L. Several hundred milligrams per liter of the sulfate removal may be attributed to adsorption of sulfate to ferric hydroxide solids (Winland et al. 1991), but most of the loss in sulfate is likely due to gypsum formation. Formation of gypsum in ALDs appears to be limited to sites with very high concentrations of sulfate. For alkalinity-generating ALDs, gypsum saturation was not indicated when sulfate concentrations were less than 2,000 mg/L.

Retention Time and Alkalinity Generation

Calcite dissolution is not an instantaneous chemical process. For uncontaminated ground water to become saturated with calcite, months of contact time between the water and limestone is necessary (Deines and Langmuir 1974). Most ALDs have retention times that are less than 2 days (table 2) and discharge waters that are

Table 5. Change in concentrations (mg/L) of alkaline and acidic water quality parameters as the mine drainage flows through the ALDs. Alkalinity and acidity concentrations in mg/L as calcium carbonate. Sites with unknown influent water quality are not included in this table. "NA" indicates data is not available.

Site	Alkalinity[1]	Acidity[2]	Fe^t	Fe^{3+}	Fe^{2+}	Al	Mn
Rid-2L	+469	-5,901	-1,214	-680	-534	-486	-12
Hathaway	+385	-595	-141	NA	NA	-23	-30
AROAD	+350	-78	+23	-10	+33	-19	-2
Rid-2R	+306	-236	-53	-1	-52	-31	0
Rid-1	+287	+60	+22	-1	+23	-2	+4
TVA-2	+280	-32	-16	NA	NA	0	-6
Morrison	+248	-102	-65	0	-65	-1	-9
Schnepp	+191	-190	-35	NA	NA	-7	+11
Willi	+187	-639	-48	-48	0	-62	-11
Jennings	+177	-146	-11	-10	-1	-21	0
Howe-2	+134	-16	-5	0	-5	0	0
Howe-1	+128	+19	-2	0	-2	0	-1
Shade	+123	-193	-2	0	-2	-22	+4
TVA-4	+120	-278	-135	NA	NA	0	-21
REM-R	+69	-148	-82	-32	-50	-2	-4
Fawn	0	+370	+28	0	+28	+49	+5
Ohiopyle	0	-143	-7	-6	-1	-25	-16

[1]Calculated by (field alkalinity out) - (field alkalinity in).
[2]Calculated to represent change in acidity only (increases in alkalinity were removed from this value): [(net acid out) + (field alk out)] - [(net acid in) + (field alk in)].

undersaturated with calcite (table 6). The kinetics of calcite dissolution are strongly influenced by degree of undersaturation (Berner and Morse 1974). Calcite dissolution is fast for highly undersaturated waters (pH < 4), but decreases dramatically as the waters approach saturation.

At the Howe-1 and Morrison ALDs, the presence of sampling wells within the ALDs allowed an evaluation of alkalinity generation. At both ALDs, concentrations of alkalinity plateau at maximum values within the limestone bed, significantly before the ALD discharge (fig. 1A). While the concentration of alkalinity at which the two sites plateau differs, the waters have similar calcite saturation indices; $10^{-1.1}$ at Howe-1 and $10^{-0.9}$ at Morrison (fig. 1B). Interestingly, at both sites the alkalinity plateau occurs when rhodochrosite has reached saturation levels (fig. 1B). The decrease in the rate of alkalinity generation at both ALDs may result from inhibition of calcite dissolution by manganese carbonate complexes (Terjesen et al. 1960). If this hypothesis is correct, then the concentration of alkalinity that an ALD is capable of producing may be controlled, in part, by the concentrations of Mn in the raw water. The retention time necessary for the mine water to reach an alkalinity plateau was 14 hours for Howe-1 and 23 hours for Morrison (fig. 1A). These patterns indicate that retention time will primarily affect the generation of alkalinity in ALDs at low retention times. If retention times are less than 14 hours, concentrations of alkalinity in

Table 6. CO_2 partial pressures and mineral saturation indices for the ALD effluent water samples. "NA" indicates data is not available.

Site	pCO_2, %	Saturation index (log)				Alkalinity, mg/L
		$CaCO_3$	$CaSO_4$	$FeCO_3$	$MnCO_3$	
Rid-2L	26.8	0.246	+0.153	+0.930	-0.378	469
Peabody	22.9	-0.830	+0.119	+1.061	+0.121	400
Hathaway	11.1	-0.155	-0.192	+0.722	NA	385
AROAD	8.3	-0.472	-1.796	+0.907	-0.365	350
Rid-2R	7.9	-0.364	-0.328	+1.161	-0.287	306
Rid-1	8.3	-0.263	-0.280	+0.375	+0.327	290
TVA-2	5.4	-0.531	-1.176	+0.586	+0.029	280
Morrison	11.2	-0.819	-0.477	+0.834	+0.231	271
Schnepp	9.6	-0.905	-0.495	+0.305	+0.093	191
Willi	8.1	-0.790	-0.255	NA	-0.001	187
Empire	11.1	-1.173	-0.604	+0.247	-0.158	180
Jennings	8.2	-0.870	-0.610	+0.392	-0.472	177
Howe-2	4.7	-0.770	-0.434	+1.141	+0.251	174
Howe-1	7.2	-1.239	-0.466	+0.748	-0.141	161
Maud	5.2	-0.900	-0.880	NA	NA	155
REM-L	10.8	-1.482	-0.441	+0.315	-0.345	138
Shade	2.2	-0.914	-0.372	NA	+0.073	123
TVA-4	2.2	-0.899	-1.318	NA	-0.574	120
REM-R	14.2	-2.418	-0.271	-0.215	-0.850	69
Fawn	NA	NA	NA	NA	NA	0
Smith	NA	NA	NA	NA	NA	0

in the effluent water may be limited by insufficient contact time between the water and limestone. For example, the two ALDs with the shortest known theoretical retention times, Ohiopyle and REM-R, with retention times of 5 hours each, produced the lowest alkalinity values - 0 and 69 mg/L, respectively. In these cases where retention time is a limiting factor, the addition of more limestone (and more retention time) will likely increase the effluent concentrations of alkalinity. If retention times are greater than 23 hours, the concentration of alkalinity in the ALD effluent will be primarily affected by chemical factors such as dissolved CO_2, metal, and sulfate concentrations. The addition of more limestone to these systems to increase retention time will have little effect on effluent concentrations of alkalinity.

Implications for Sizing ALDs

Previously proposed ALD sizing methods have been based on the drainage flow rate, the anticipated calcite

dissolution rate, and the desired lifetime of the ALD (Nairn et al. 1991, Brodie et al. 1991). An improved sizing technique should also incorporate the concept of minimum retention time. Data presented in this paper indicate that, in order to produce a maximum concentration of alkalinity, retention time of mine water in the ALD must be ~15 hours. To achieve this 15-hour retention time, the requirement for the mass of limestone (M) can be expressed as:

$$M = \frac{Q\,\rho_b\,t_d}{V_v}$$

where Q is the volume flow of the mine water, ρ_b is bulk density of the limestone, t_d is the detention time and is set equal to 15 hours, and V_v is the bulk void volume expressed in decimal form. In addition to the mass of limestone required for a 15-hours retention time, enough limestone must be added to satisfy the dissolution losses expected over the proposed treatment period. This can be expressed as:

$$M = \frac{Q\,C\,T}{x}$$

where Q is the volume flow of the mine water, C is the predicted concentration of alkalinity in the ALD effluent, T is the design life of the ALD (i.e. proposed treatment period), and x is the calcium carbonate content of the limestone in decimal form. The summation of these two equations represents the total requirement of limestone. For example, an ALD is to contain limestone that has a bulk density of 1600 kg/m^3, contains 90% calcium carbonate, and has a bulk void volume of 50%. The ALD is expected to deliver 300 mg/L of alkalinity to a flow of 25 L/min of AMD for 20 years. The mass of limestone (M) required is calculated by:

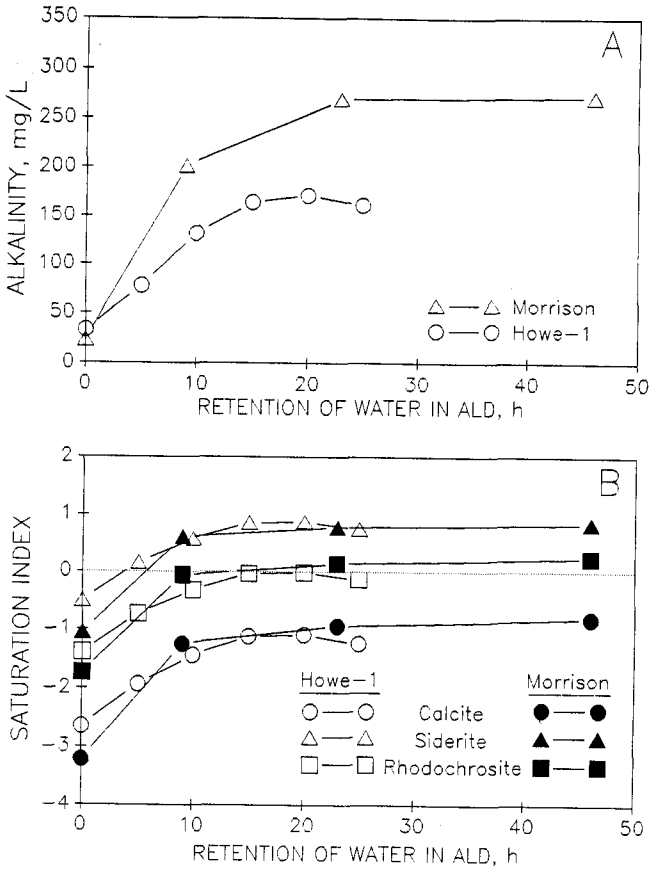

Figure 1. Changes in alkalinity (*A*) and calcite, siderite, and rhodochrosite (*B*) saturation indices as the water flows through the Howe-1 and Morrison ALDs. Retention of water in ALD is based on the average mine water flow rate at each site and the position of sampling wells within the ALD.

$$M = \frac{Q\,\rho_b\,t_d}{V_v} + \frac{Q\,C\,T}{x} = \frac{(25\text{ L/min x 60 min/hr})\,(1600\text{ kg/m}^3\text{ x m}^3/1000\text{ L x mt/1000 kg})\,(15\text{ hr})}{0.50} + \frac{(25\text{ L/min x 60 min/hr})\,(300\text{ mg/L x mt/}10^9\text{ mg})\,(20\text{ yr x 8766 hr/yr})}{0.90}$$

$$= 72.0\text{ mt} + 87.7\text{ mt} = 159.7\text{ mt}$$

As the limestone dissolves, the hydraulic integrity of the system should decrease. Since these systems have only recently been used in the treatment of AMD, no data exists describing how this dissolution may affect the performance of the ALD. If the ALD is expected to remove acidity as well as generate alkalinity (through retention of Fe^{3+} or Al^{3+}), the demands of these reactions on calcite dissolution should be added into the sizing calculation. However, the effects on the generation of alkalinity and longevity of the ALD by ferric and aluminum hydroxide precipitation and retention can not be confidently predicted. Any ferric iron and aluminum in the raw mine water has the potential to significantly and adversely affect the performance of ALDs.

Conclusions

1) The variation in alkalinity generation was less than the variation in acidity removal.
2) Large changes in acidity resulted from retention of ferric iron and aluminum.

3) Ferrous iron was not significantly retained unless retention times were greater than 650 hours.
4) Manganese was not retained in any ALD.
5) Sulfate was not retained and gypsum was not supersaturated (based on WATEQ) at any drain which received water with less than 2000 mg/L of sulfate.
6) Concentration of alkalinity reached maximum levels after 14-23 hours of contact.
7) Retention times over 23 hours will not markedly increase alkalinity concentrations.
8) The mass of limestone required for treatment can be calculated by:

$$M = \frac{Q\,\rho_b\,t_d}{V_v} + \frac{Q\,C\,T}{x}$$

where Q is the volume flow of water, ρ_b is bulk density of the limestone, t_d is the detention time and is set equal to 15 hours, V_v is the bulk void volume expressed in decimal form, C is the predicted concentration of alkalinity in the ALD effluent, T is the design life of the ALD, and x is the $CaCO_3$ content of the limestone in decimal form.

Literature Cited

American Public Health Association. 1985. Standard methods for the examination of water and wastewater. Washington, DC. 1,268 p.

Ball, J. W., D. K. Nordstrom, and D. W. Zachmann. 1987. WATEQ4F - a personal computer translation of the geochemical model WATEQ2 with revised database. USGS Open File Report 87-50.

Berner, R. A. and J. W. Morse. 1974. Dissolution kinetics of calcium carbonate in sea water, 4, theory of calcite dissolution. Am. J. Sci. 274:108-134.

Brodie, G. A. 1991. Achieving compliance with staged, aerobic, constructed wetlands to treat acid drainage. p. 151-174. In Proceedings of the American Society for Surface Mining Reclamation Meeting, Princeton, WV.

Brodie, G. A., C. R. Britt, T. M. Tomaszewski, and H. N. Taylor. 1991. Use of passive anoxic limestone drains to enhance performance of acid drainage treatment wetlands. p. 211-222. In Proceedings of the Annual Meeting of the American Society for Surface Mining Reclamation, Princeton, WV.

Deines, P. and D. Langmuir. 1974. Stable carbon isotope ratios and the existence of a gas phase in the evolution of carbonate ground waters. Geochim. et Cosmochim. Acta 38:1147-1164.

Fales, H. A. and F. Kenny. 1940. Inorganic quantitative analysis. D. Appleton Century Co., New York.

Faulkner, B. B. and J. G. Skousen. 1993. Monitoring of passive treatment systems: an update. In Proceedings of the 14th Annual West Virginia Surface Mine Drainage Task Force Symposium. WV Univ., Morgantown, WV.

Hedin, R. S. and R. W. Nairn. 1993. Contaminant removal capabilities of wetlands constructed to treat coal mine drainage. p. 187-195. In G. A. Moshiri (ed.), Constructed wetlands for water quality improvement. Lewis Publishers, Boca Raton, FL.

Nairn, R. W., R. S. Hedin, and G. R. Watzlaf. 1991. A preliminary review of the use of anoxic limestone drains in the passive treatment of acid mine drainage. In Proceedings of the 12th West Virginia Surface Mine Drainage Task Force Symposium. WV Univ., Morgantown, WV.

Nairn, R. W., R. S. Hedin, and G. R. Watzlaf. 1992. Generation of alkalinity in an anoxic limestone drain. p. 206-219. In Proceedings of the American Society for Surface Mining and Reclamation Meeting. (Duluth, MN, June 14-18, 1992).

Terjesen, S. G., O. Erga, G. Thorsen, and A. Ve. 1960. Phase boundary process as rate determining steps in reactions between solids and liquids: the inhibitory action of metal ions on the formation of calcium bicarbonate by the reaction of calcite with aqueous carbon dioxide. Chem. Eng. Sci. 14:277-289.

Turner, D. and D. McCoy. 1990. Anoxic alkaline drain treatment system, a low cost acid mine drainage treatment alternative. p. 73-75. In D. H. Graves and R. W. DeVore (eds.), Proceedings 1990 National Symposium on Mining. (Lexington, KY, May 14-18,1990).

Watzlaf, G. R. and R. S. Hedin. 1993. A method for predicting the alkalinity generated by anoxic limestone drains. In Proceedings of the 14th Annual West Virginia Surface Mine Drainage Task Force Symposium. WV Univ., Morgantown, WV.

Winland, R. L., S. J. Traina, and J. M. Bigham. 1991. Chemical composition of ochreous precipitates from Ohio coal mine drainage. J. Environ. Qual. 20:452-460.

SUCCESSIVE ALKALINITY-PRODUCING SYSTEMS (SAPS) FOR THE TREATMENT OF ACIDIC MINE DRAINAGE[1]

Douglas A. Kepler and Eric C. McCleary[2]

Abstract: Constructed wetland treatment system effectiveness has been limited by the alkalinity-producing, or acidity-neutralizing, capabilities of the systems. Anoxic limestone drains (ALD's) have allowed for the treatment of approximately 300 mg/L net acidic mine drainage, but current design guidance precludes using successive ALD's to generate alkalinity in excess of 300 mg/L because of concerns with dissolved oxygen. "Compost" wetlands designed to promote bacterially mediated sulfate reduction are suggested as a means of generating alkalinity required in excess of that produced by ALD's. Compost wetlands create two basic needs of sulfate reducing bacteria; anoxic conditions resulting from the inherent oxygen demand of the organic substrate, and quasi-circumneutral pH values resulting from the dissolution of the carbonate fraction of the compost. However, sulfate reduction treatment area needs are generally in excess of area availability and/or cost effectiveness. Second generation alkalinity-producing systems demonstrate that a combination of existing treatment mechanisms has the potential to overcome current design concerns and effectively treat acidic waters ad infinitum. Successive alkalinity-producing systems (SAPS) combine ALD technology with sulfate reduction mechanisms. SAPS promote vertical flow through rich organic wetland substrates into limestone beds beneath the organic compost, discharging the pore waters. SAPS allow for conservative wetland treatment sizing calculations to be made as a rate function based on pH and alkalinity values and associated contaminant loadings. SAPS potentially decrease treatment area requirements and have the further potential to generate alkalinity in excess of acidity regardless of acidity concentrations.

Additional Key Words: acid mine drainage, passive alkalinity generation, anoxic limestone dissolution.

Introduction

Ferrous iron (Fe^{2+}) is the most common and typically most abundant contaminant found in coal mine drainage. The oxidation and subsequent hydrolysis of Fe^{2+} is the single greatest contributor to the production of mineral acidity associated with coal mine drainage and is the basis of the commonly used term, acid mine drainage (AMD). Any water containing Fe^{2+} is considered to contain a proportional amount of mineral acidity, although a more broad based characterization of the same water may or may not justify the qualifying term of AMD.

Coal mine drainage may be characterized as net acidic, or as net alkaline. Net acidic mine drainage lacks adequate buffering capacity to neutralize the entire complement of protons produced (in this example) by the oxidation and hydrolysis of Fe^{2+}. Net alkaline mine drainage contains sufficient neutralizing potential, generally as bicarbonate (HCO_3^-), to accept any proton acidity generated by the described reactions. Manganese and aluminum are also common mineral-acidity-producing components of coal mine drainage and require consideration in the balancing of net acidic versus net alkaline discharges.

Any coal mine drainage treatment scenario must be predicated on the ultimate neutralization of acidity, resulting from naturally net alkaline drainage, or from the active addition or passive generation of alkaline substances. Constructed wetlands can passively generate alkalinity through either dissimilatory sulfate reduction, carbonate dissolution, or a combination of these two processes. Much attention has been directed toward the functioning of these two processes within the substrate of constructed wetlands (Hedin et al. 1988, McIntire and Edenborn 1990), although a shifting emphasis is being placed on more direct passive alkalinity generation in anoxic limestone drains (ALD's) (Brodie et al. 1991, Skousen and Faulkner 1992).

---

[1]Paper presented at the International Land Reclamation and Mine Drainage Conference and the Third International Conference on the Abatement of Acidic Drainage, Pittsburgh, PA, April 24-29, 1994.

[2]Douglas A. Kepler, Restoration Ecologist, and Eric C. McCleary, Restoration Ecologist, Damariscotta, Clarion, PA, USA.

ALD's promote carbonate dissolution by placing a relatively large source of carbonate material; e.g., $CaCO_3$, in the flow path of AMD. ALD's are designed to maintain and promote anoxic conditions, and produce alkalinity as HCO_3^-. As AMD exits an ALD and is exposed to atmospheric oxygen, iron oxidation and hydrolysis reactions occur until the entire complement of iron is removed from the discharge, or until the neutralizing potential of the discharge is utilized (the drainage remains net acidic) and the pH of the flow decreases to a level inhibiting further iron precipitation.

ALD's have a finite potential to produce alkalinity that cannot exceed equilibrium with available CO_2; i.e., any increase in CO_2 leads directly to an increase in HCO_3- (Stumm and Morgan 1970). Proton acidity (H_3O^+) is also converted to alkalinity in ALD's, leading to increased pH values. ALD's must be designed large enough to detain the flows to be treated for a period sufficient for the above reactions to occur (the hydration of CO_2 is a relatively slow process), but there is little empirical evidence that beyond a certain detention time, alkalinity concentrations can be increased (Hedin et al. 1993). The generation of 300 mg/L of alkalinity is considered to be the maximum capability of current ALD design, and although greater alkalinity concentrations have been reported, the median alkalinity production of operating ALD's is likely less than 300 mg/L (personal observations).

Dissolved oxygen and ferric iron (Fe^{3+}) are considered to be the two factors limiting the broader utilization of ALD's. Dissolved oxygen concentrations in the contaminated discharge should preferably be less than 1 mg/L to prevent the oxidation of ferrous to ferric iron, which can armor limestone and limit any further dissolution of the stone. Ferric iron can also be present in flows with pH values less than 3.5, even with low dissolved oxygen concentrations, again presenting armoring concerns. Aluminum presents an additional concern in that aluminum hydroxide formation is strictly pH dependent and can occur within an ALD in the absence of oxygen. Aluminum hydroxides do not appear to armor stone in the fashion of ferric hydroxides, but concerns over physical plugging of the available void space within the stone exist.

ALD implementation has been generally relegated to point of discharge mine flows meeting these guidelines. Mine drainage exposed to atmospheric oxygen typically exceeds 1 mg/L of dissolved oxygen; for this reason, the assumption has been that ALD's cannot be constructed in succession where there is an intermediate aerobic treatment step (Hedin et al. 1993). This assumption has limited attempts to passively treat discharges requiring alkaline additions in excess of net 300 mg/L.

Wetlands referred to as compost wetlands, designed to generate HCO_3^- through sulfate reduction, are recommended to provide additional alkalinity in these instances. Compost wetlands are amenable to further alkalinity generation because they create two basic needs of sulfate reducing bacteria; anoxic conditions as a result of the inherent oxygen demand of the organic matter, and quasi-circumneutral pH values as a result of the dissolution of the carbonate fraction of the compost. However, bacterially mediated sulfate reduction treatment area needs are generally in excess of area availability and/or cost effectiveness, based on the rate and seasonal production of alkalinity generation.

The oxygen demand associated with the bacterial decomposition of organic rich waters is well documented and exaggerated at the water-sediment interface (Stumm and Morgan 1970). It is equally well documented that the underlying described sediments become anoxic, resulting in the reduction of oxidized metals and a shift to anaerobic bacterial metabolism (Wetzel 1975). It is both readily conceivable and well documented that the biogeochemical cycling of nutrients is strongly controlled by oxidation-reduction states that are in turn strongly mediated by bacterial metabolism. Sulfate-reducing sediments in wetlands are always associated with atmospheric oxygen in the sense that they underlie open water and require organic carbon as an energy source. It is a logical progression to investigate the potential development of limestone dissolution zones beneath reduced organic zones.

We will document in this paper that oxygen concentrations are a design consideration rather than a limiting factor to utilizing the benefits of limestone dissolution in passive treatment systems, and that limestone dissolution is already an integral function of many passive treatment systems constructed in open environments. We will report that limestone dissolution after the fashion of ALD's can be and has been incorporated into passive treatment systems after the subject mine drainage has been exposed to the open atmosphere. We will also suggest that successive alkalinity-producing systems (SAPS) can significantly reduce the currently accepted area treatment needs of passive treatment systems. SAPS technology represents another phase in the evolution of passive treatment systems (fig. 1).

The aerobic wetland shown in "A" is an emergent marsh, surface flow system. The compost wetlands referenced in "B" and "C" are also surface flow systems, additionally dependent on anaerobic treatment utilizing microbial sulfate reduction. Relatively large surface areas are required to even theoretically meet the effluent quality depicted in these two scenarios. The SAPS treatment pictured in "D" combines aerobic an anaerobic treatment in vertical flow systems, potentially requiring significantly less area to achieve the goals of "B" and "C".

Site Descriptions

Three passive treatment systems were evaluated for this study. The wetlands are all located in Jefferson County, PA roughly 10 km northwest of the town of Brookville. The Howe Bridge system was constructed in October 1991 and modified in July 1993, the REM system was built in September 1989 and modified in March 1992, and the Schnepp Road system was constructed in July 1992. The Howe Bridge system treats two artesian flow, abandoned gas well discharges, while the REM and Schnepp Road systems treat abandoned deep mine flows.

Each wetland treatment system incorporates an ALD at the point of AMD discharge, followed by an aerobic treatment area, and then additional anoxic and aerobic treatment components. The performance of the ALD's in these systems is reported elsewhere in these proceedings (Hedin and Watzlaf). (The Howe Bridge, REM, and Schnepp Road ALD's were constructed with a greater cross-sectional area than typical ALD designs, averaging 7 m in width and roughly 1.5 m in depth.) This study focuses on the ability to create effective anoxic limestone dissolution treatment components for AMD abatement in open atmospheres. An overview of the dimensions and composition of the three study SAPS is provided in table 1. A typical cross-sectional view of a SAPS treatment component is shown in figure 2.

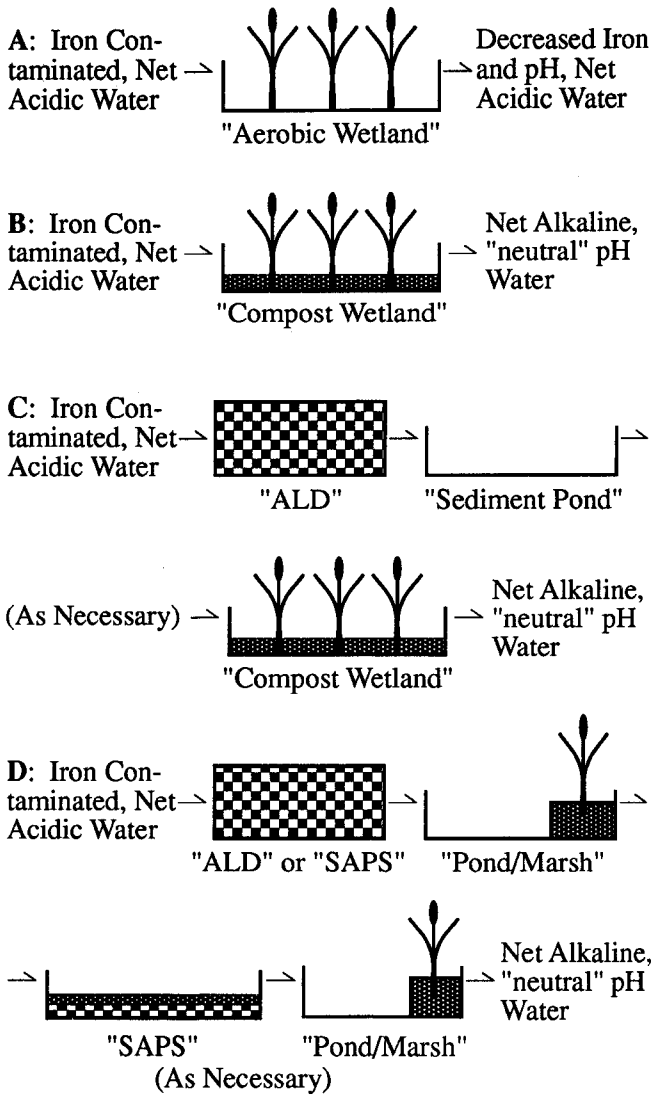

Figure 1. Evolution of passive, wetland treatment technology.

Table 1. Study SAPS treatment component dimensions and materials.

Location	Surface dimensions, m	Freestanding water, m	Substrate composition[1]
Howe Bridge.....	60 x 25	1.9	45 cm compost, 45 cm limestone
REM.....	10 x 15	1.6	45 cm compost, 60 cm limestone
Schnepp Road....	10 x 20	1.8	45 cm compost, 60 cm limestone

[1] Spent compost from mushroom industry, limestone (minimum 90% $CaCO_3$) at 1.3 to 1.9 cm diameter.

Methods

Each wetland has been evaluated regularly since its construction. The reported data reflect temporal and spatial characterizations of the treatment processes examined. Chemical and physical analyses were made directly in the field and in the authors' laboratory facilities. Field pH and Eh determinations and temperatures were made with an Orion model 250A meter and an Orion temperature compensating pH triode. Alkalinity was determined directly in the field with the same meter using an Orion total alkalinity test kit. Sample acidity was determined in the laboratory by boiling with hydrogen peroxide and titration to pH 8.3 using a Fisher ACCUMET model 230A pH/Ion meter. Alkalinity and acidity are reported in milligrams per liter as $CaCO_3$ equivalents. Dissolved oxygen was determined directly in the field with a YSI model 50B temperature compensating dissolved oxygen meter and polarographic probe. Total iron and ferrous iron were determined using the 1,10-phenanthroline method with a Milton Roy Co. Spectronic 20 D spectrophotometer. Manganese was determined by the periodate oxidation method, aluminum by the aluminon method, and sulfate by the barium sulfate turbidmetric method, all using the referenced spectrophotometer. Calcium was directly titrated by the EDTA titration method. All analyses follow Standard Methods for the Examination of Water and Wastewater (American Public Health Association 1985). Flows were determined by "bucket and stopwatch".

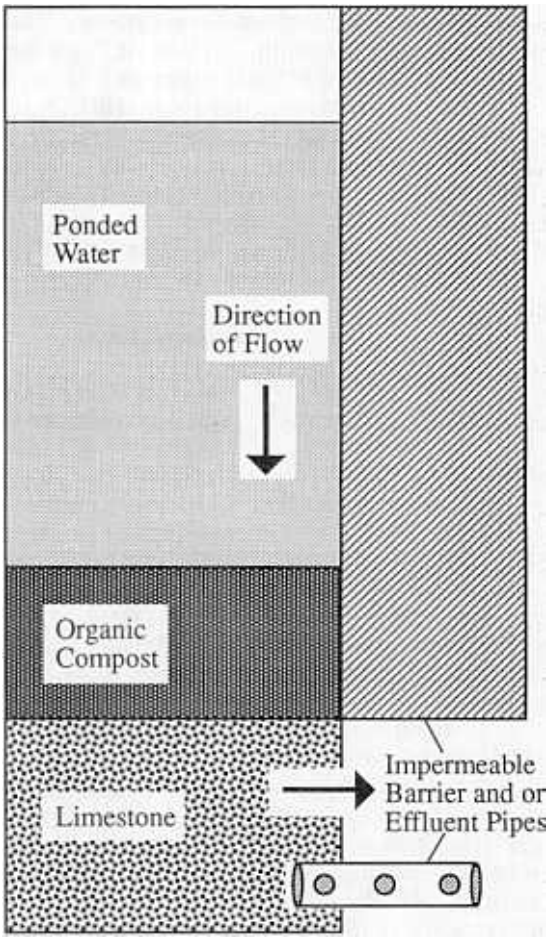

Figure 2. Typical cross-sectional view of a successive alkalinity producing system (SAPS) treatment component.

This study also utilizes data collected by the U.S. Bureau of Mines (BOM) Pittsburgh Research Center . Iron, manganese, aluminum, magnesium, and calcium were determined in the BOM laboratory in 0.45-*u*m membrane filtered and acidified samples using inductively-coupled argon plasma spectroscopy. Ferrous iron was determined by the BOM on acidified samples following the potassium dichromate method, and sulfate was determined through reactions with barium chloride and thorin as an endpoint indicator (Hedin et al., in press). Field pH and alkalinity were determined as above.

Results

The study results are predicated on several basic principles and assumptions. Increases in alkalinity and/or decreases in acidity are considered to be equal for these discussions. Any measured increase in calcium concentration between two sample locations is assumed to be proportionally related to alkalinity production, as in equation 1. This fraction of alkalinity will be referred to throughout this study as "calcium alkalinity".

$$H_2CO_3 + CaCO_3 \text{ ----> } Ca^{2+} + 2HCO_3^- \qquad (1)$$

Alkalinity production associated with sulfate reduction can similarly be determined directly by decreases in sulfate concentrations between two points, as in equation 2.

$$2CH_2O + SO_4^{2-} \text{ ----> } H_2S + 2HCO_3^- \qquad (2)$$

Sulfate, however, can also coprecipitate with ferric hydroxides and is prone to more analytical variation (less accurate measure) than many parameters. More weight is therefore placed on net changes in acidity associated with limestone dissolution for this study.

The physical construction of the study sites does not allow for direct and/or accurate measurement of flow at all sample locations. While significant perturbations to the treatment systems are not known for these sites, water gains and losses do occur. The effects of these gains and losses have been compensated for through the measurement of magnesium, a conservative ion in wetland treatment systems. The effluent magnesium concentrations for this study have been divided by the influent magnesium values to determine a reasonable dilution-concentration factor. The effluent parameters have been "corrected" by dividing the effluent concentrations by the applicable dilution-concentration factors. The dilution-concentration factors were typically slightly less than 1 and had a minor effect on the reported data. The purpose of this study is to report treatment principles and trends. Treatment comparisons are not made between the systems, so concentrations rather than loadings (as in grams per day) were used. Passive treatment based on biological mechanisms decreases with decreasing temperatures. The emphasis of this study has been placed on winter treatment data to provide a conservative and accurate assessment of SAPS applicability.

Table 2 displays the increases in alkalinity and concurrent decreases in acidity attributable to $CaCO_3$ dissolution in the Howe Bridge SAPS for two consecutive winters. Data from two consecutive summer samples have been included to demonstrate the seasonal effectiveness of the biological component of alkalinity production through microbially mediated sulfate reduction. Table 3 displays the means and ranges of other measured parameters within the Howe Bridge SAPS for the same sample dates.

Table 2. Alkalinity produced and acidity removed through limestone dissolution, Howe Bridge SAPS, January 23, 1992 through July 27, 1993.

Sample Date	Calcium Alkalinity[1]	Acidity[1] Removed	% Removal Attributable to Calcium Alkalinity
January 23, 1992.....	174.5	207	84
February 21, 1992...	134.8	202	67
July 15, 1992.....	174.5	366	48
January 18, 1993.....	125.0	134	93
February 22, 1993...	90.3	118	77
July 27, 1993.....	148.0	344	43

[1] Alkalinity and acidity are presented as mg/L of $CaCO_3$ equivalent.

Periodic measurements of dissolved oxygen in the Howe Bridge SAPS consistently displayed values less than 0.2 mg/L in the effluent, while the influent concentrations ranged between 5 and 10 mg/L. The entire complement of iron in the effluent is reduced, indicating that armoring of the limestone within the SAPS should not be of concern. Measurements of Eh at the effluent discharge pipe were generally less than 20 millivolts, subject to atmospheric interference. The discharge pipe of this system has never accumulated any typically orange ferric hydroxide precipitates, while the exposed surface area of the SAPS component is characteristically orange. The discharge pipe does accumulate black deposits of iron monosulfides, which are converted to ferric hydroxides when exposed to oxygen.

The chemistry of the influent sample changes dramatically over a course of 3 to 10 m and is not totally representative of the level of treatment occurring within the Howe Bridge SAPS. The influent sample location is at the discharge point of a settling pond and provides a convenient sampling station. The AMD falls roughly 1 m over a rock spillway to a shallow aerobic wetland (compost substrate) that is approximately 20 m wide by 30 m long and sparsely planted with *Typha latifolia*. The remaining alkalinity in the reported influent sample is utilized by the precipitation of an additional amount of iron at the base of the spillway and within the shallow marsh area, with a consistent chemistry at the actual SAPS surface of zero alkalinity and a pH of roughly 3.0. This observed decrease in pH is a common phenomenon that has limited the passive treatment of decidedly net acidic discharges, so it is significant to note that the SAPS discharge of this water reflects a pH of about 6.0.

Table 4 displays the increases in alkalinity and concurrent decreases in acidity attributable to $CaCO_3$ dissolution in the REM SAPS over the course of 1 yr. Seasonal variations resulting from microbially mediated sulfate reduction are not nearly as evident in this SAPS as at Howe Bridge, possibly because of the much smaller

relative treatment area at REM. Table 5 presents the means and ranges of other measured parameters within the REM SAPS for these same sample dates.

Table 3. Influent-effluent water quality, Howe Bridge SAPS, January 23, 1992 through July 27, 1993, effluent corrected for dilution-concentration.

	(Influent)			(Effluent)		
Parameter[1]	n	Mean	Range	n	Mean	Range
pH, s.u.....	6	NA	3.29 - 6.14	6	NA	5.84 - 6.49
Acidity.....	6	321.0	207 - 396	6[2]	92.6	0 - 278.8
Calcium.....	6	182.4	136.0 - 230.8	6	230.2	192.2 - 279.4
Magnesium....	6	94.8	67.1 - 114.6	6	99.8	77.8 - 123.6
Sulfate.....	6	1,189	875 -1,407	6	1,033	621 -1,258
Fe^{2+}.....	6	193.0	149 - 231	6	102.0	47.7 - 159.0
Fe^{3+}.....	6	1.6	0 - 9.6	6	0	0

NA Not applicable.
[1] Acidity is presented as mg/L of $CaCO_3$ equivalent; all other values are in mg/L.
[2] n = 3 < 10 mg/L readings, calculated as zeroes.

Periodic measurements of dissolved oxygen at this system also consistently displayed values less than 0.2 mg/L in the effluent, and concentrations ranging between 5.0 and 10 mg/L in the influent. The majority of iron at the effluent point is reduced, although a measurable amount of ferric iron remains, raising design concerns with potential armoring of the limestone. This SAPS component was designed with the capability to regulate water levels, and the system was completely drained and the substrate examined in November 1993. The surface of the organic substrate had accumulated up to 5 cm of iron hydroxides, but these precipitates did not extend to any degree into the compost substrate, and examination of the limestone over its entire depth did not indicate any armoring of the limestone. The measurable ferric iron found in the effluent may result from a complexing of soluble ferric iron with humic derivatives common to the rich organic compost substrate (Shapiro 1957), or may be the result of the analytical method in that ferric iron is measured indirectly.

As a demonstration of the potential effectiveness of SAPS technology, we have included data from the aerobic treatment system immediately upflow of the REM SAPS (table 6). This treatment component carries 10 cm of water above a 30 cm compost substrate and is densely vegetated with *Typha latifolia*. This marsh component has 50% more surface

Table 4. Alkalinity produced and acidity removed through limestone dissolution, REM SAPS, July 15, 1992 through July 13, 1993.

Sample Date	Calcium Alkalinity[1]	Acidity[1] Removed	% Removal Attributable to Calcium Alkalinity
July 15, 1992.....	78.8	83.5	94
August 19, 1992.....	66.8	89.9	74
January 18, 1993.....	78.6	81.1	97
February 8, 1993.....	71.5	89.5	80
March 4, 1993.....	80.2	82.0	98
May 4, 1993.....	108.7	90.8	120
July 13, 1993.....	74.7	79.1	82

[1] Alkalinity and acidity are presented as mg/L of $CaCO_3$ equivalent.

treatment area than the associated SAPS treatment unit, yet removes approximately 85% less acidity than the SAPS on a mean basis for these sample dates. The surface of the compost in this area is coated with up to 10 cm of ferric hydroxide, while the compost is black and rich in hydrogen sulfide odor when disturbed. The presence and dissolution of limestone within the anoxic compost (the compost contains approximately 10% limestone by weight) is an important treatment factor in wetlands dependent on alkalinity generation through sulfate reduction. Sulfate reducing bacteria, with *Desulfovibrio* being the most ubiquitous in AMD affected areas, are not effective at pH values less than 5.0 (Postgate 1984). However, the relatively small decrease in acidity here suggests that there is limited potential for mixing of the substrate pore waters with the discharging surface waters.

Table 5. Influent-effluent water quality, REM SAPS, July 15, 1992 through July 13, 1993, effluent corrected for dilution-concentration.

	(Influent)			(Effluent)		
Parameter[1]	n	Mean	Range	n	Mean	Range
pH, s.u.....	7	NA	2.97 - 3.30	7	NA	3.61 - 4.22
Acidity.....	7	173.0	146 - 208	7	87.9	65 - 117
Calcium.....	7	187.5	171.0 - 209.7	7	213.7	196.8 - 243.6
Magnesium....	4	94.2	80.8 - 110.0	4	95.8	84.4 - 107.0
Sulfate.....	7	1,008	895 -1,029	7	972	883 -1,203
Fe^{2+}.....	7	2.5	0.8 - 5.4	6	14.7	3.6 - 31.7
Fe^{3+}.....	7	21.3	13.6 - 30.5	6	1.8	0 - 5.6

NA Not applicable.
[1] Acidity is presented as mg/L of $CaCO_3$ equivalent; all other values are in mg/L.

Table 6. Influent-effluent water quality, REM "Compost Wetland", July 15, 1992 through July 13, 1993, effluent corrected for dilution-concentration.

	(Influent)			(Effluent)		
Parameter[1]	n	Mean	Range	n	Mean	Range
pH, s.u.....	7	NA	3.02 - 3.32	7	NA	2.96 - 3.21
Acidity.....	7	207.4	161 - 234	7	195.4	163 - 228
Calcium.....	7	209.0	182.0 - 225.9	7	210.8	185.6 - 230.8
Magnesium....	4	106.6	92.5 - 120.0	4	98.3	86.2 - 113.0
Sulfate.....	7	1,180	963 -1,314	7	1,114	970 -1,313
Fe^{2+}.....	7	55.0	36.4 - 73.0	7	4.1	1.8 - 11.9
Fe^{3+}.....	7	8.5	2.0 - 17.1	7	26.0	15.7 - 32.3

NA Not applicable.
[1] Acidity is presented as mg/L of $CaCO_3$ equivalent; all other values are in mg/L.

The Schnepp Road SAPS also produces a significant measure of calcium alkalinity in an open environment (tables 7 and 8). The significant feature once again is that aerobic surface waters with dissolved oxygen values ranging from roughly 5 to 9 mg/L are made anoxic within the SAPS, discharging at measured values of 0.2 mg/L or less.

The results from these three SAPS indicate that the limitations dissolved oxygen places on ALD design can be eliminated in SAPS through the combined use of open water and high organic content substrate overlying a limestone treatment zone. The SAPS design provides a relatively sound assurance that the AMD contacting the limestone will be anoxic. SAPS design mimics natural lake biogeochemistry in much the same way that aerobic wetland treatment mimics natural marshes. The oxygen content of the hypolimnion, or deeper portion, of natural lakes rich in organic matter is rapidly depleted through bacterial respiration. Oxygen consumption is greatest at the sediment-water interface, and even in well aerated surface waters, oxygen does not generally diffuse more than several centimeters into the sediments of a standing body of water (Mortimer 1971).

Table 7. Alkalinity produced and acidity removed through limestone dissolution, Schnepp Road SAPS, July 26, 1992 through July 13, 1993.

Sample Date	Calcium Alkalinity[1]	Acidity[1] Removed	% Removal Attributable to Calcium Alkalinity
July 15, 1992.....	79.3	85	93
August 19, 1992.....	76.2	84	91
January 18, 1993.....	70.1	69	102
July 13, 1993.....	79.3	75	106

[1] Alkalinity and acidity are presented as mg/L of $CaCO_3$ equivalent.

The oxygen demand, chemical and biological, per unit area of the SAPS substrate will determine the depth of penetration and the concentration of oxygen available to the sediments. These same assurances cannot necessarily be made for an ALD whose water supply may undergo periodic fluctuations in quality and/or dissolved oxygen concentrations within the associated mine pool or mine spoil. Additionally, with ferric iron converted to ferrous iron in the reducing zone of the sediment-water interface of the SAPS treatment area, a water chemistry consistent with present ALD design criteria is met. Table 9 compares the calcium alkalinity production realized at both the Howe Bridge SAPS and the Howe Bridge ALD for the same dates to emphasize both the potential of SAPS treatment and the consistency with ALD alkalinity generation.

Table 8. Influent-effluent water quality, Schnepp Road SAPS, July 15, 1992 through July 13, 1993, effluent corrected for dilution-concentration.

	(Influent)			(Effluent)		
Parameter[1]	n	Mean	Range	n	Mean	Range
pH, s.u.....	4	NA	5.86 - 6.20	4	NA	6.29 - 6.88
Acidity.....	4	83.5	69 - 102	4	5.2	0 - 18
Calcium.....	4	196.2	184 - 212	4	221.2	207 - 237
Sulfate.....	4	750	654 - 846	4	717	622 - 810
Fe^{2+}.....	4	1.6	0.4 - 3.6	4	1.0	0.6 - 1.2
Fe^{3+}.....	4	19.0	16.5 - 21.2	4	0.1	0 - 0.2

NA Not applicable.
[1] Acidity is presented as mg/L of $CaCO_3$ equivalent; all other values are in mg/L.

Variations in alkalinity production and pH adjustment within the three study SAPS are believed to be a function of detention time within the limestone treatment zones. Limestone dissolution in ALD's is viewed as a rate function with 12 hrs. currently purported as a minimum detention time for maximum alkalinity production (Hedin et al. 1993 and personal observations by the authors). The Howe Bridge SAPS approaches this detention time, while the REM and Schnepp Road SAPS have variable detention rates of 4 to 8 hrs.

Table 9. Alkalinity produced through limestone dissolution, Howe Bridge SAPS and ALD, January 23, 1992 through July 27, 1993.

Sample Date	Calcium Alkalinity SAPS[1]	Calcium Alkalinity ALD[1]
January 23, 1992.....	174.5	179.5
February 21, 1992....	134.8	149.6
July 15, 1992.....	174.5	163.6
January 18, 1993.....	125.0	167.2
February 22, 1993....	90.3	164.1
July 27, 1993.....	148.0	168.7

[1] Alkalinity is presented as mg/L of $CaCO_3$ equivalent.

Physical plugging of the limestone within the study SAPS has not presented any known hydraulic problems. The pressure exerted by the downward force of the freestanding pool above the substrate materials in the SAPS should actually reduce the risk of physical plugging as compared to waters flowing laterally through conventional ALD's or other subsurface treatment systems. Lateral flow systems are designed to maintain their entire flow beneath the surface and have historically failed because of substrate pore plugging with subsequent water mounding and a surface expression of the waters to be treated. The SAPS design, with adequate freeboard, allows for any build up of static head required (if any) to continue "pushing" water downward and through the substrate material. Additionally, the bottom discharge of a SAPS design in essence creates a treatment pond with a bottom or breastwork that leaks, further maintaining the integrity of the designed flow path.

Discussion and Conclusions

Most constructed wetlands of generic design to date have been limited in their effectiveness by the alkalinity-producing, or acidity-neutralizing, capabilities of the systems. Alkalinity generation for decidedly net acidic AMD based on microbially mediated sulfate reduction is simply not practical or cost effective. The ability to develop SAPS as alkalinity generating systems capable of producing an essentially infinite amount of alkalinity obviously broadens the scope of passive treatment.

Iron oxidation and hydrolysis reactions are strongly controlled by solution pH and dissolved oxygen. Rate constants for the formation of iron complexes increase from minutes and hours at circumneutral pH values, to months and years as pH values decrease below 4 (Sung and Morgan 1980, Stumm and Morgan 1970). The greater the buffering capacity of a given water, the greater the ability of that water to maintain a pH amenable to rapid metal removal. Adequate alkalinity must be made available in treatment situations to at least effectively neutralize the acid producing capabilities of the target metal contaminants. In that metal oxidation and hydrolysis reactions produce acidity, what is considered adequate alkalinity can be site specifically calculated from the sum equivalents of measured acid producing metals.

Current passive treatment sizing criteria for iron are based on an iron removal rate per given area. This method of sizing passive treatment systems applies a linear function (area) to a nonlinear function (removal rate). Iron removal is a function of area only as area relates to detention time and should be determined instead as a removal rate per rate limiting functions; i.e., pH and dissolved oxygen. Diffusion of oxygen into any given body of water can be assumed to be relatively constant for that body of water and can be determined and used as a constant for sizing considerations.

Sizing calculations can therefore be based upon the pH and buffering capacity of the AMD. Conservative a priori sizing calculations can be made for expected pH and alkalinity values, independent of whether those values are the result of ALD or SAPS origin. Iron, and therefore acidity, removal can and should occur within settling ponds designed to retain the flows for the period necessary to utilize the alkalinity buffer and decrease the

pH to a range of 4.0 to 4.5. At this point, again through a priori calculations, SAPS can be implemented to the degree necessary to effectively neutralize the required amount of acidity for a given discharge.

Treatment based on detention can be more cost effectively managed in open water ponds than in constructed, shallow marsh wetlands because of obvious volume to area ratio advantages. Acidity neutralization of AMD (through the removal of iron) can be based on rate functions dependent on known levels of pH, alkalinity, and dissolved oxygen. Sizing calculations for iron removal and acidity neutralization therefore become a product of the contaminant loading, which is dependent on concentrations and flows (Kepler and McCleary, unpublished research).

SAPS provide a heretofore lacking component of effective AMD treatment based on existing and proven principles. Conventional *Typha* dominated wetland areas should be utilized between SAPS components to aid in suspended solids removal and to provide a sustainable supply of oxidizable organic matter to the SAPS units. Ongoing efforts are being directed towards maximizing detention time within the SAPS while minimizing the area necessary to utilize the alkalinity produced by the SAPS in the removal of target metals, particularly iron.

Literature Cited

American Public Health Association. 1981. Standard methods for the examination of water and wastewater. 15th Ed. American Public Health Association, Inc., Washington, DC, 676 p.

Brodie, G.A., C.R. Britt, T.M. Tomaszewski, and H.N. Taylor. 1991. Use of passive anoxic limestone drains to enhance performance of acid drainage treatment wetlands. p. 211-222. In W. Oaks and J. Bowden (eds.), Proceedings of Reclamation 2000: Technologies for Success. (Durango, CO, 1991).

Hedin, R.S., D.M. Hyman, and R.W. Hammack. 1988. Implications of sulfate reduction and pyrite formation processes for water quality in a constructed wetland: preliminary observations. p. 382-388. BuMines IC 9183.

Hedin, R.S., R.W. Nairn, and R.L.P. Kleinmann. 1993. The passive treatment of coal mine drainage. p. 38-41 BuMines IC, in press.

Kepler, D.A. and E.C. McCleary. 1993. personal observations.

McIntire, P.E. and H.M. Edenborn. 1990. The use of bacterial sulfate reduction in the treatment of drainage from coal mines. p. 409-415. In J. Skousen, J. Sencindiver, and D. Samuel (eds.), Proceedings of the 1990 Mining and Reclamation Conference and Exhibition. (WV Univ., Morgantown, WV 1990).

Mortimer, C . H. 1971. Chemical exchanges between sediments and water in the Great Lakes, speculations on probable regulatory mechanisms. Limnol. Oceanogr. 16: p. 387-404.

Postgate, J.R. 1984. The Sulphate-reducing bacteria. 2 ed., Cambridge University Press, New York. 208 p.

Shapiro, J. 1957. Chemical and biological studies on the yellow organic acids of lake water. Limnol. Oceanogr. 2: p. 161-179.

Skousen, J. and B. Faulkner. 1992. Preliminary results of acid mine drainage treatment with anoxic limestone drains in West Virginia. In Proceedings of the 13th Annual West Virginia Surface Mining Task Force Symposium. (Morgantown, WV, 1992).

Stumm, W. and J.J. Morgan. 1970. Aquatic chemistry. Wiley, New York. 583 p.

Sung, W. and J.J. Morgan. 1980. Kinetics and products of ferrous iron oxygenation in aqueous systems. Environ. Sci. and Technol. 14(5): p. 1-8.

Wetzel, R. G. 1975. Limnology. Saunders College Publishing, Philadelphia, PA. 743 p.

THE BIOSULFIDE PROCESS: INTEGRATED BIOLOGICAL/CHEMICAL ACID MINE DRAINAGE TREATMENT - RESULTS OF LABORATORY PILOTING[1]

Michael V. Rowley, Douglas D. Warkentin, Vita T. Yan, and Beverly M. Piroshco[2]

Abstract: The need for an economically viable treatment alternative to lime neutralization of acid mine drainage (AMD) has led to the investigation of many processes, including those utilizing biological sulfate reduction. Realization of the limitations imposed by conventional sulfate reduction motivated the development of the Biosulfide process over the last six years. The Biosulfide process separates the chemical precipitation of sulfides from the biological conversion of sulfate to sulfide. Metals can be removed selectively and separately, allowing for the recovery of saleable products and the isolation of hazardous sludges. This paper concerns the evaluation of the process in a 75 hour continuous pilot run of a 100 L system at the Triton Development Corporation laboratory. The objective of this demonstration was to operate and evaluate a continuous, integrated chemical/biological AMD treatment system depending solely on microbially-generated products for stream treatment. Results are included that demonstrate the effectiveness of the process in treating a strong AMD sample (pH 2.45, 20 g/L $SO_4^=$, 4 g/L total metals) to strict discharge requirements while isolating metal co-products. In addition to being an effective AMD treatment method, the Biosulfide process has also demonstrated exceptional reliability and ease of operation through more than a year of uninterrupted bioreactor operation, and ten months of semi-continuous and continuous chemical stage operation in the 100 L pilot system.

Additional Key Words: acid mine drainage treatment, sulfate reduction, resource recovery, sulfide precipitation

Introduction

In the mining industry, there is an increasing need for an economically viable and environmentally sound method of managing acid mine drainage and other sulfate-laden waste streams. This need is the result of the short-comings of the lime treatment process and the increasing trend toward more stringent, government-imposed discharge guidelines.

Conventional AMD treatment with lime produces large volumes of unstable metal hydroxides mixed with gypsum. The sludges are voluminous and costly to dispose of, especially when toxic metals content classifies it as a hazardous waste.

The application of sulfate reducing bacteria (SRB) to sulfate-containing wastes has been studied for many years in substantial detail (Barnes et al 1991, Dvorak et al 1991, Gyure et al 1990, Hammack et al 1993 and 1994, Maree et al 1986 and 1987, and Tuttle et al 1969). Conventional sulfate reduction utilizes a bioreactor where SRB grow on some form of solid support or in a sludge bed. Sulfate is metabolized according to equation 1, below. Hydrogen sulfide generated by the SRB contacts metal cations, forming insoluble metal sulfides which precipitate in the bioreactor, according to equation 2.

$$SO_4^= + \text{Nutrients} + H_2O \rightarrow H_2S + HCO_3^- \quad (1)$$

$$M^{++} + S^= \rightarrow MS_{(s)} \quad (2)$$

---

[1]Paper presented at the International Land Reclamation and Mine Drainage Conference and the Third International Conference on the Abatement of Acidic Drainage, Pittsburgh, PA, April 24-29, 1994.

[2]Michael V. Rowley, Process Microbiologist, Douglas D. Warkentin, Process Engineer, Vita T. Yan, Chemical Engineer, and Beverly M. Piroshco, Research Associate, Triton Development Corporation, Vancouver, BC, Canada.

Conventional sulfate reduction processes treat the entire stream in a bioreactor, resulting in significant limitations in terms of both application and effectiveness in treatment. The sensitivity of the bacterial population to low pH and high metal loading necessitates prohibitively long retention times for the treatment of highly contaminated streams. In addition, because the entire AMD stream enters biological treatment, the bioreactor is subjected to widely varying conditions of flow and feed stream strength with seasonal fluctuations, making it difficult to maintain the chemostat conditions necessary for optimum bioreactor performance. The sludge produced by conventional sulfate reduction processes also presents some problems. Firstly, sulfide sludge is precipitated in the bioreactor, which may cause problems of plugging, abrasion, and toxicity. Secondly, the sludge contains a mix of metals. Metals of concern are mixed with those of lesser concern, creating a greater volume of sludge to be classified as toxic, and incurring a greater disposal expense. The sludge also contains biomass (lost from the bioreactor) which further increases the volume of sludge for disposal. Conventional sulfate reduction processes are, however, well suited to certain specific applications, particularly those concerning the treatment of streams with low metals concentrations (Barnes et al, 1992).

Attempts to overcome the limitations inherent in conventional sulfate reduction treatment of AMD resulted in the development of the Biosulfide Process and the subsequent design, construction, and operation of a 100 L laboratory-scale pilot system. Developed over the last six years, the Biosulfide process differs from conventional sulfate reduction by the combination of the following features: 1) the biological component of the process is separated from the chemical precipitation/neutralization stage; 2) only a fraction of the stream volume, as determined by sulfide and/or alkalinity requirements, enters the bioreactors; 3) AMD treatment to discharge quality is achieved entirely with bacterially generated products, and; 4) metal concentrates, metal sludge, and biomass can be produced separately for sale or disposal.

The Biosulfide process completely separates the chemical precipitation of sulfides from the biological conversion of sulfate to hydrogen sulfide. Raw AMD enters the chemical circuit and is contacted with hydrogen sulfide generated in the biological circuit. Some fraction of the volume of treated AMD enters the biological circuit for the biologically catalyzed conversion of sulfate to sulfide. In this manner, the sulfide sludges are isolated in the chemical circuit, eliminating the problems experienced due to their build-up in the bioreactor and effectively separating them from the biomass. In addition, by operating a multi-stage chemical precipitation circuit the Biosulfide process permits metals to be removed and isolated selectively. Selective separation is achieved by pH manipulation in the reactors, as specific metals begin to precipitate as sulfides at different pH ranges. Alkalinity requirements for the stepwise pH manipulations are supplied by the biological circuit. Alkalinity is produced simultaneously in the biological conversion of sulfate to sulfide in the form of carbonate (equation 1).

The precipitation of metals as sulfides has many advantages over hydroxide precipitation. Sulfides form more rapidly, create a denser sludge, are more stable, and are less soluble than hydroxides (Bhattacharyya et al 1981, and Kim 1981). These benefits are shared by conventional sulfate reduction processes. However, by isolating the toxic fraction of the AMD stream in a sulfide sludge separate from the biomass sludge and from the metals deemed valuable, the Biosulfide process can significantly reduce the volume of sludge requiring expensive disposal. In addition, the cost of treatment can be offset or eliminated in streams with significant recoverable metals through the sale of metal sulfide concentrates to smelters. Metals readily removed as sulfides include copper, cadmium, zinc, arsenic, nickel, iron, lead, and antimony, among others. Molybdenum can also be removed in this manner, although the reaction kinetics are slower. Aluminum, which does not form a sulfide can be precipitated as an hydroxide at a pH of 4 to 4.5.

This paper summarizes the methods of Biosulfide process piloting conducted since August 1992. Piloting was conducted in a 100 L, fully integrated biological/chemical system that has been operated extensively with five different AMD samples and sulfate sources to date. In order to demonstrate and evaluate the Biosulfide process prior to on-site demonstration, the 100 L system was operated for a 75 hour continuous run treating a strong AMD sample (table 1). The objective of the 75 hour run was to treat the AMD to discharge quality using only bacterially-generated products in a stand-alone laboratory pilot system. To do this, all pH adjustment was done

with bioreactor products, and all precipitation was done with bioreactor off-gas. Data included here is from the 75 hour demonstration. Discharge requirements are listed in table 2.

Table 1. Head analysis of AMD treated.

Parameter	Units	Assay	Parameter	Units	Assay	Parameter	Units	Assay
pH	-	2.45	sulfate	mg/L	20000	Al	mg/L	1200
As	mg/L	12	Ca	mg/L	400	Cd	mg/L	2
Co	mg/L	8	Cu	mg/L	190	Fe	mg/L	2300
Mg	mg/L	1500	Mn	mg/L	313	Ni	mg/L	18
Zn	mg/L	273						

Table 2. Discharge requirements.

Parameter	Units	Value	Parameter	Units	Value	Parameter	Units	Value
pH	-	> 5.5	Cu	mg/L	< 0.05	Zn	mg/L	< 0.2

Methods and Materials

Description of Apparatus -100 L Pilot System

Overview. A Biosulfide process schematic is shown in figure 1.

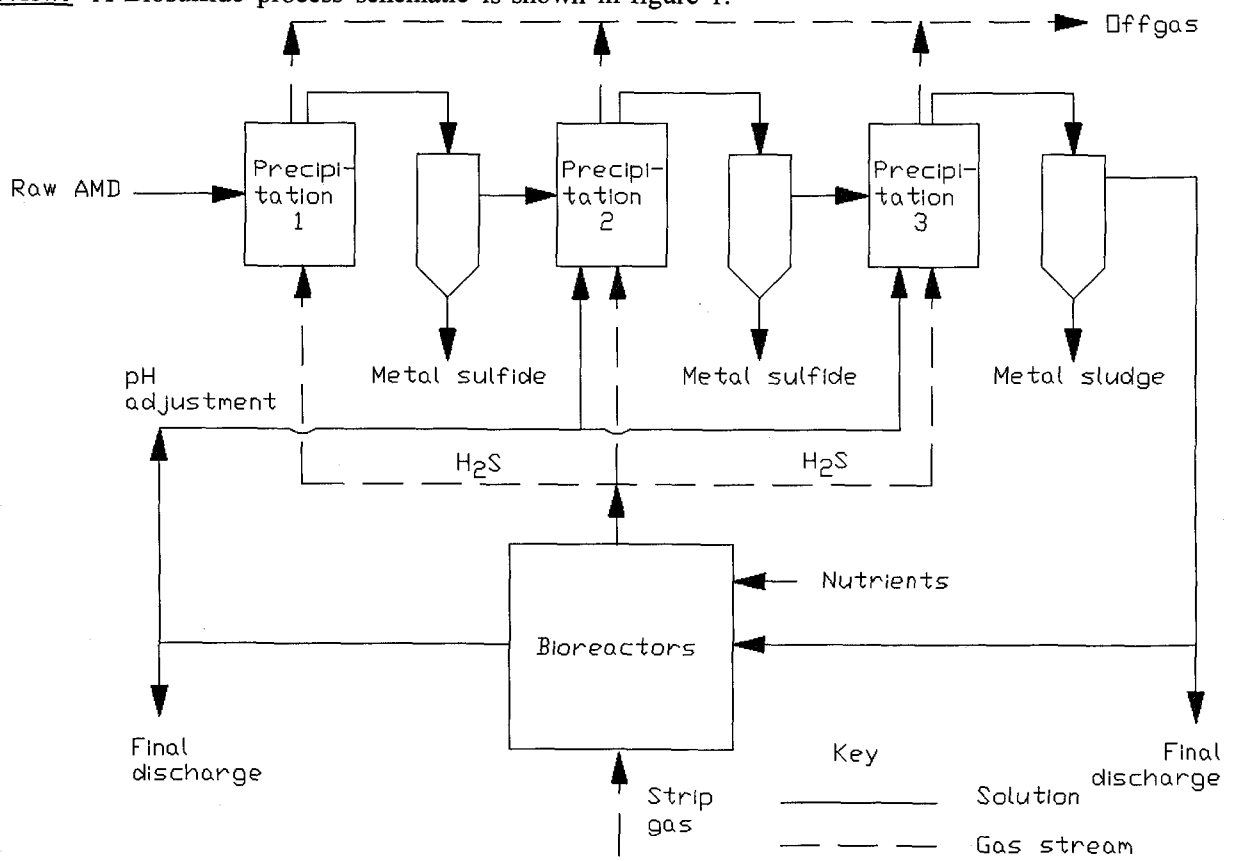

Figure 1. Biosulfide process schematic.

Chemical Stage. The chemical precipitation circuit consisted of three series-configured acrylic reactors of 6 L, 5 L, and 6 L, respectively. Each of these vessels was agitated by a magnetic stirring plate, and was followed in the circuit by a 1.5 L cylindrical glass settling vessel (thickener) with a conical base. The first precipitation reactor was pH-monitored, whereas the final two were pH-controlled at desired values. Peristaltic pumps transferred the AMD through the circuit for contacting with bioreactor off-gas.

Biological Stage. The biological stage of the pilot system consisted of two 40 L polyvinylchloride (PVC) anaerobic bioreactors developed specifically for the Biosulfide process during bioreactor comparison tests in 1990 and 1992. Solution exiting the chemical precipitation stage was mixed with nutrients (table 3) in batches of 20 to 50 L to be fed to the bioreactors. A single peristaltic pump moved solution through the series-configured bioreactor stage. Nitrogen gas travelled through the system to carry the product hydrogen sulfide to the chemical precipitation circuit. Bioreactors were maintained at 30°C with submersible heaters.

The mixed bacterial culture used throughout Biosulfide process development and piloting was originally obtained from bog water in 1988. This culture has been utilized continuously in Biosulfide development research for over six years, and has been adapted to a variety of specific operating conditions.

Table 3. Nutrient additions used in testwork.

Nutrient	Source	Addition
N	NH_4Cl	0.35 g/L
P, K	KH_2PO_4	0.06 g/L
C, H	90/10 Ethanol/Methanol	1g/g $SO_4^=$

Analyses

Dissolved sulfate was determined by turbidimetric analysis with a spectrophotometer at an absorption wavelength of 420 nm, following barium sulfate precipitation at low pH. Bioreactor off-gas analyses were performed using an SRI 8610 Gas Chromatograph equipped with a nine foot long, 1/8" O.D. teflon column packed with 100/120 mesh Hayesep D material, and a Thermal Conductivity Detector. Solid and solution samples were analyzed by ICP for trace metal concentration analysis, and by Atomic Absorption Spectrophotometry for particular metals present in high concentrations.

Results

In this section, figures and tables are presented that demonstrate the effectiveness of the Biosulfide process at AMD treatment. All results were obtained during the 75 hour continuous, integrated pilot run.

Prior to the commencement of the 75 hour continuous run the system had been operated extensively with different AMD samples and sulfate streams. The two bioreactors had been operated continuously for seven months and four months, respectively, while the precipitation circuit had been operated for shorter periods over a four month period to determine the optimum system configuration. In the week preceding the 75 hour run the bioreactors began treating pure (non-diluted) chemical stage discharge solution, and the chemical stage completed multiple shorter runs sufficient to ensure a complete change-over from previous AMD testing.

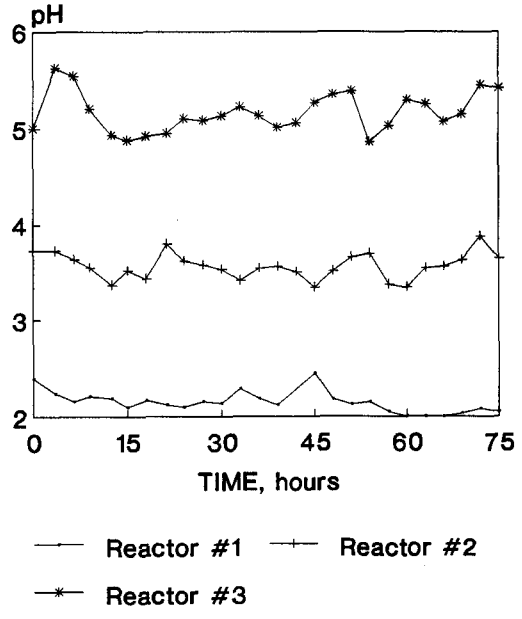

Figure 2. Chemical stage pH values during 75 hour continuous AMD treatment.

The system performed well throughout the

demonstration, experiencing no mechanical upsets or failures, and meeting the strict discharge requirements for the duration utilizing only microbially-generated products. As shown in figure 2, chemical stage pH values were held near the target values of 2.0, 3.5, and 5.2 in reactors one, two, and three, respectively. It is important to note that the pH of third precipitation reactor does not need to meet the discharge requirement of greater than 5.5. As shown in the process schematic (fig. 1), remaining bioreactor product solution and treated AMD are mixed to form the final discharge of the process. With this addition, the pH of Biosulfide process final discharge solution during the pilot run was consistently greater than 5.5.

Chemical stage copper, zinc, and iron concentrations are shown for the duration of the pilot run (fig. 3, 4, and 5). Together these graphs demonstrate the precipitation trends within the three-reactor chemical stage.

Prior to hour 60 of operation the formation of copper sulfide was occurring primarily in the second and third reactors, not in the first reactor as intended (fig. 3). Similarly, zinc sulfide was forming primarily in the third reactor and not in the second, as intended (fig. 4). On hour 60 the flow rate of AMD through the chemical stage was decreased (table 4). Following this change a substantial improvement in the selective precipitation of copper and zinc can be noted, with copper sulfide forming in the first precipitation reactor, and zinc sulfide in the second. Iron precipitated primarily in the third reactor for the duration of the demonstration (fig. 5). Aluminum hydroxide also precipitated primarily in the third reactor, as evidenced by the product concentrate/sludge analyses (table 5).

The composition of the final discharge solution is determined by the third precipitation reactor, as this solution forms the greatest fraction of the ultimate discharge solution. As shown in figure 1, third precipitation reactor solution is diluted with bioreactor product solution, which contains no metals.

Table 4 shows a summary of the pilot run, presenting the volumes and flow rates of AMD treated, as well as the volume of bioreactor product solution added to meet the alkalinity requirements of AMD neutralization in the chemical stage.

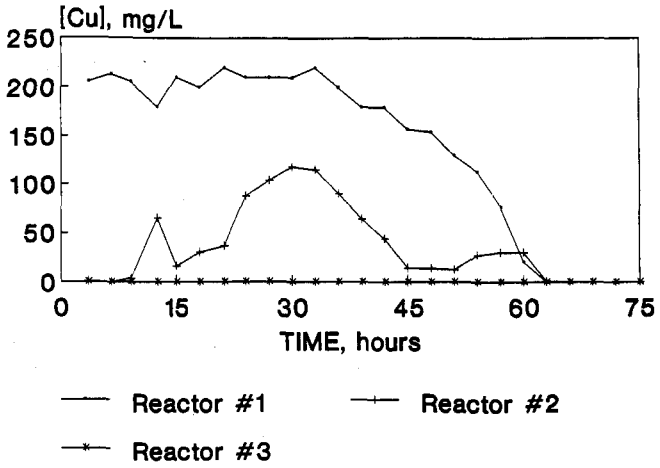

Figure 3. Chemical stage dissolved copper levels during 75 hour continuous AMD treatment.

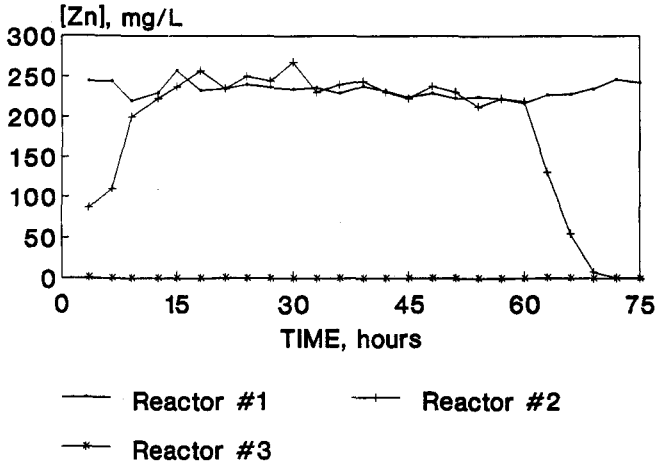

Figure 4. Chemical stage dissolved zinc levels during 75 hour continuous AMD treatment.

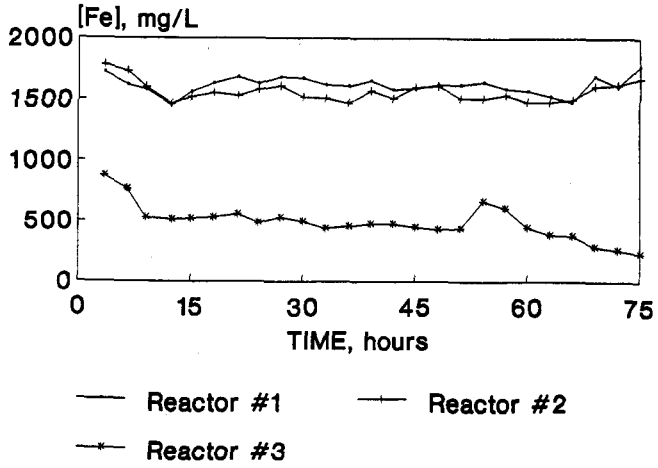

Figure 5. Chemical stage dissolved iron levels during 75 hour continuous AMD treatment.

Product precipitate grades from the final (optimum) 15 hours of operation are presented in table 5. The formation of isolated copper and zinc concentrates for sale, along with a mixed (aluminum and iron) waste sludge for disposal, is demonstrated.

As shown in table 6, bioreactor performance was reliable and consistent throughout the pilot run, maintaining an average sulfate reduction of 85 % at retention times of approximately 40 hours each. Biological data is presented from the time at which the bioreactors began feeding pure (non-diluted) chemical stage discharge on day 245 to day 255. The 75 hour run spanned days 252 to 255. Bioreactor percent sulfate reduction values presented in table 6 consider the influent and effluent sulfate of each bioreactor only and are therefore not cumulative. Overall sulfate reduction is presented in the product data section of table 6.

Table 4. Summary of 75 hour continuous operation.

Parameter, units	Hour 0 to 60	Hour 60 to 75
AMD treated, L	44.30	7.30
AMD feed rate, L/hr	0.74	0.49
Chemical stage retention, hrs	22.30	33.70
Bioreactor solution added, L	63.60	13.90
Recirculating load, %	144	190

Table 5. Precipitate analyses in %.

Residue	Al	Cu	Fe	S	Zn
Precipitation #1	-	10.0	0.24	89.8	0.06
Precipitation #2	2.5	13.1	10.70	25.8	6.18
Precipitation #3	8.5	0.3	8.95	24.9	2.11

Table 6. Biological operating data prior to and during the 75 hour pilot run.

		Days 245 to 251			Days 252 to 255		
Parameter	Units	High	Low	Average	High	Low	Average
Feed							
pH	-	6.40	6.00	6.13	6.21	6.04	6.14
rate	L/d	24.5	22.0	23.3	24.7	21.5	23.2
sulfate	mg/L	8271	6810	7482	7364	5780	6597
First bioreactor							
pH	-	5.89	5.14	5.42	5.36	5.17	5.27
sulfate	mg/L	4560	4105	4294	4830	3462	4239
sulfate reduction	%	50.4	33.0	42.0	46.6	24.2	35.5
sulfate reduction rate	mg/L/d	2457	1269	1850	2175	889	1415
retention time	hrs	42.5	38.2	40.2	43.5	37.8	40.5
Second bioreactor							
pH	-	8.30	7.67	7.94	7.84	7.44	7.63
sulfate	mg/L	1385	1167	1289	1380	268	933
sulfate reduction	%	74.4	67.2	69.8	92.3	69.5	78.6
sulfate reduction rate	mg/L/d	2085	1789	1889	2577	1890	2137
retention time	hrs	39.1	35.5	36.9	40.0	34.7	37.2
Product data							
pH	-	8.46	7.90	8.15	8.39	7.88	8.16
sulfate	mg/L	1170	757	995	1700	337	1024
overall sulfate reduction	%	90.8	84.1	86.5	94.2	75.3	84.9
off-gas hydrogen sulfide	%	4.8	1.2	3.0	3.1	2.0	2.6

Discussion

The biological stage of the system performed well throughout the duration of continuous testing, providing a reliable source of hydrogen sulfide and alkalinity for use in the chemical stage. In fact, one of the two bioreactors in the 100 L Biosulfide pilot system has been operating continuously at retention times of 21 to 44 hours for 14 months without interruption or a decline in performance. The dependability of the biological stage is a result of both the bioreactor design and the configuration of the Biosulfide process. By placing the chemical stage prior to the biological stage, the bioreactors receive an almost metal-free solution, and sulfate loading can be controlled to maintain optimum bioreactor performance.

Like the biological stage, the chemical stage performed reliably throughout the pilot run. However, it was only with a substantial reduction of chemical stage feed rate that the precipitation of sulfides occurred in the desired vessel. While not altering the effectiveness of the treatment in terms of meeting discharge requirements, the precipitation of all metals in one reactor detracted from the potential for metal recovery. Due to the rapid formation of metal sulfides observed in batch tests conducted since 1988 (Warkentin et al, 1992), it was suggested that inadequate hydrogen sulfide/AMD contacting resulted in the slowed reaction kinetics observed in the pilot run. Improvements in precipitation reactor design have been incorporated since that should bring a substantial increase in the rate of sulfide formation as well as in the efficiency of sulfide utilization.

Three product sludges were isolated from the AMD. The first two, copper and zinc sulfide concentrates, are intended to be sold to smelters to offset treatment costs during commercial-scale operation. A third sludge, intended for disposal, consisted primarily of iron, aluminum, and sulfur. A substantial reduction in disposal sludge volume is achieved by the combination of recoverable metals isolation with the benefits of sulfide precipitation over lime precipitation. The result is a higher density sludge that contains fewer of the metals present in the AMD. All sludges produced have the additional benefit that sulfides are much less prone to re-dissolution than their hydroxide counterparts, resulting in increased long-term sludge stability.

The copper and zinc grade of the product concentrates were not as high as previous batch testwork has demonstrated to be possible. This was due primarily to dilution of the precipitates by the formation of large quantities of elemental sulfur. Sulfur was formed by the reaction of sulfide and ferric iron, as shown in equation 3. In addition to diluting and increasing the volume of the product sludges, the reaction also incurs substantial losses of sulfide, placing greater demand on the bioreactors.

$$S^{=} + 2Fe^{+++} \rightarrow S^{0}_{(} + 2Fe^{++} \qquad (3)$$

The occurrence of this reaction was verified by the presence of ferrous iron and elemental sulfur in the precipitates. This problem could be addressed in part by utilizing 'fresh' AMD. The sample tested had been stored for approximately two months, permitting the slow, ongoing oxidation of ferrous iron to ferric to become significant. Substantial quantities of ferric hydroxide were noted in the storage drums as a result of this oxidation followed by precipitation at the pH of the AMD sample (2.45). Utilization of 'fresh' AMD (with a more favourable Fe^{++}:Fe^{+++}) would reduce sulfide losses to this reaction. Also, an additional precipitation reactor added to precede the copper precipitation reactor would convert ferric iron to ferrous prior to copper sulfide precipitation to permit the production of a higher grade copper concentrate. The additional precipitation reactor would produce a high sulfur sludge, and would necessitate the production of greater amounts of hydrogen sulfide.

Conclusions

The results of continuous Biosulfide process piloting in a 100 L system demonstrate the process to be a potential alternative to conventional AMD treatment, particularly lime treatment. A strong AMD (2.45, 20 g/L $SO_4^{=}$, 4 g/L dissolved metals) sample was treated to discharge requirements utilizing only bacterially-generated reagents in a reliable, consistent manner. Dissolved metal levels were reduced to below discharge requirements

for the duration of the run. Furthermore, metal concentrations in Biosulfide process discharge were consistently far below those of conventional lime treatment because metal sulfides are much less soluble than their hydroxide counterparts, most often by several orders of magnitude. The treatment was also successful in meeting discharge pH requirements throughout the run.

In addition to treating the stream successfully, copper and zinc sulfide concentrates were isolated to demonstrate the potential for the process to offset or eliminate operating costs through production of saleable co-products.

Throughout nearly a year of operation the 100 L Biosulfide pilot system has demonstrated remarkable reliability and consistency of performance while treating five different AMD samples and sulfate sources to date. This stability results from the two-stage nature of the treatment. The biological stage is able to maintain optimum and chemostat conditions due to separation of the bioreactors from the raw AMD. Similarly, the chemical stage is able to precipitate metals from and neutralize the stream independent of the specific operating requirements of the biological stage. With the successful conclusion of laboratory pilot demonstration, design work is underway for a 3 m^3 on-site demonstration system scheduled to commence operation in mid-1994.

Literature Cited

Barnes, L. J., F. J. Janssen, J. Sherren, J. H. Versteegh, R. O. Koch, and P. J. H. Scheeren. 1991. A new process for the microbial recovery of sulphate and heavy metals from contaminated waters extracted by a geohydrological control system. Chemical Engineering Research and Design 69:184-186.

Barnes, L. J., F. J. Janssen, P. J. H. Scheeren, J. H. Versteegh, and R. O. Koch. 1992. Simultaneous microbial removal of sulphate and heavy metals from waste water. Transactions of the Institution of Mining and Metallurgy 101:C183-C199.

Bhattacharyya, D., G. Sun, C. Sund-Hagelberg, and K. Schwitzgebel. 1981. Precipitation of heavy metals with sodium sulfide: Bench-scale and full-scale experimental results. AIChE Symposium Series 77(209):31-38.

Dvorak, D. H., H. M. Edenborn, R. S. Hedin, and P. E. McIntire. 1991. Treatment of metal-contaminated water using bacterial sulfate reduction: results from pilot-scale reactors. In Proceedings of the 1991 SME Annual Meeting. (Denver, CO, February 25-28,1991).

Gyure, R. A., A. Konopka, A. Brooks, and W. Doemel. 1990. Microbial sulfate reduction in acidic (pH 3) strip-mine lakes. FEMS Microbiology Ecology 73:193-202.

Hammack, R. W., D. H. Dvorak, and H. M. Edenborn. 1993. The use of biogenic hydrogen sulphide to selectively recover copper and zinc from severely contaminated mine drainage. Biohydrometallurgical Technologies, Proceedings of the International Biohydrometallurgy Symposium, Jackson Hole, WY. Edited by A. E. Torma, J. E. Way, The Minerals, Metals and Materials Society. p. 631-639.

Hammack, R. W., D. H. Dvorak, and H. M. Edenborn. 1994. Selective metal recovery using biogenic hydrogen sulfide: Rio Tinto mine, Nevada. In Proceedings of the International land Reclamation and Mine Drainage Conference and the Third International Conference on the Abatement of Acidic Mine Drainage. (Pittsburgh, PA, April 24-29, 1994).

Kim, B. M. 1981. Treatment of metal containing wastewater with calcium sulfide. AIChE Symposium Series 77(209):39-48.

Maree, J. P., A. Gerber, and W. F. Strydon. 1986. A biological process for sulphate removal from industrial

effluents. Water SA 12(3):139-144.

Maree, J. P., G. Hulse, D. Dods, and C. E. Schutte. 1987. An integrated process for biological treatment of sulfate-containing industrial effluents. Journal Water Pollution Control Federation. 59 (12): 1069-1074.

Tuttle, J. H., P. R. Dugan, and C. I. Randles. 1969. Microbial sulfate reduction and its potential utility as an acid mine water pollution abatement procedure. Applied Microbiology 17(2):297-302.

Warkentin, D. D., M. V. Rowley, P. E. Elson, and P. B. Marchant. 1992. Development of the Biosulphide Process. In Proceedings of the 31st C.I.M. Conference of Metallurgists, Edmonton, Alberta, August 1992.

BENCH-SCALE TEST TO SELECTIVELY RECOVER METALS FROM METAL MINE DRAINAGE USING BIOGENIC H_2S[1]

R. W. Hammack[2], D. H. Dvorak[2], and H. M. Edenborn[2]

Abstract: Hydrogen sulfide generated by the anaerobic respiration of sulfate-reducing bacteria was used to treat samples of pH 2.2 water from the abandoned Rio Tinto copper mine in Nevada. The untreated water contained 550 mg/L Fe, 140 mg/L Al, 92 mg/L Cu, 76 mg/L Mn, 60 mg/L Zn, 4 mg/L Co, and 2 mg/L Ni. H_2S was generated in a bench-scale bioreactor and bubbled into the mine water in three precipitator-clarifier units, where metal sulfide precipitation and recovery took place. The treatment system reduced the concentrations of all metals except Mn to less than 0.1 mg/L. Manganese concentrations were reduced by 96% to 3.3 mg/L. A CuS-S° concentrate (33% Cu) and a ZnS-S° concentrate (28% Zn) were produced that may be suitable for metal recovery at existing smelters.

Introduction

Certain anaerobic bacteria are capable of reducing SO_4^{2-} and other sulfur oxyanions to H_2S when provided with a suitable carbon source (Postgate 1984). This reaction can be expressed as

$$2CH_2O + SO_4^{2-} \text{-------}> H_2S\uparrow + 2HCO_3^-, \qquad (1)$$

where CH_2O represents labile organic matter. This naturally occurring biological process can potentially remediate acidic, metal-contaminated waste waters by producing H_2S, which reacts with many dissolved metals to form insoluble metal sulfides; by adding alkalinity in the form of HCO_3^-; and by lowering dissolved SO_4^{2-} concentrations. However, to obtain these benefits, an environment must be created and sustained that is conducive to the growth and activity of the sulfate-reducing bacteria.

Many investigators have proposed the use of bacterial sulfate reduction to treat metal-contaminated mine waters (Tuttle et al. 1969, Wakao et al. 1979, Pugsley et al. 1970), but few field demonstrations have been documented in the literature. Artificial wetlands built to treat coal mine drainage in the Eastern United States have sometimes made use of biological sulfate reduction, although at first this application was inadvertent. Constructed wetlands were often built with a thick layer of organic compost to foster plant growth. Once the compost became saturated with sulfate-rich mine water, it became an ideal environment for a community of anaerobic organisms, including sulfate-reducing bacteria. Biological sulfate reduction occurring in the compost was found to contribute significantly to water treatment, primarily because of the bicarbonate alkalinity generated (Kleinmann et al. 1991). Bacterial sulfate reduction-based treatment systems have also been constructed using compost-filled containers (Dvorak et al. 1992, Hammack and Edenborn 1992), and mine entries filled with organic compost. Other low-cost organic materials, such as composted municipal and yard waste, hay, corn meal, and chicken manure, have also been used to fuel biological sulfate reduction in similar passive treatment systems.

In May 1992, a commercial-scale, bacterial sulfate reduction treatment plant began treating zinc-contaminated ground water at the Budelco Smelter site in the Netherlands using ethanol as the carbon source

---

[1]Paper presented at the International Land Reclamation and Mine Drainage Conference and the Third International Conference on the Abatement of Acidic Drainage, Pittsburgh, PA, April 24-29, 1994.

[2]Richard W. Hammack, Geologist, Darryl H. Dvorak, Research Biologist, Harry M. Edenborn, Supervisory Research Biologist, U.S. Bureau of Mines, Pittsburgh Research Center, P.O. Box 18070, Pittsburgh, PA 15236.

for the sulfate-reducing bacteria (Scheeren et al. 1992). This plant uses a sludge blanket bioreactor to treat 3,000 L/h of water with a 4-to-6 h residence time. The ZnS sludge that settles to the bottom of the bioreactor is sent to a nearby smelter for zinc recovery.

Sulfate reduction-based treatment systems have generally used a single bioreactor for both the generation of H_2S and the precipitation of metal sulfides (Dvorak et al. 1992, Scheeren et al. 1992, Barnes et al. 1991). These simple systems may be suitable if all components in a waste stream are nontoxic to the bacterial population, and if the production of a mixed-metal sludge or a sludge that contains organics as well as metals is acceptable. However, metal concentrations in mining or mineral processing waste streams often exceed the tolerance levels of anaerobic bacteria (Mueller and Steiner 1992), and mixed-metal precipitates are of less value to potential smelters. An approach that avoids these problems is the use of an inert carrier gas to sparge H_2S from the bioreactor and transport it to one or more separate precipitation reactors (Marchant and Lawrence 1989, Hammack et al. 1993). In the precipitation reactors, H_2S reacts with the waste water to form insoluble metal sulfides. The advantages of this approach are that

1. Potentially inhibitory or toxic metals in the wastewater do not contact the sulfate reducing bacteria,
2. Metal sulfide precipitation reactions can be carried out under conditions that are not conducive to the growth of sulfate-reducing bacteria,
3. Individual metal sulfides can sometimes be selectively precipitated by controlling the pH of the wastewater within the precipitators,
4. Metal sulfides that are processed for metal recovery are not contaminated or diluted with biomass or organic substrate.

In this study, we evaluated a bench-scale bacterial sulfate reduction treatment system for the treatment of a low-pH mine drainage that contained Fe, Al, Cu, Mn, Zn, Co, and Ni. The performance goals for the treatment system were to produce an effluent having a circumneutral pH and containing less than 0.1 mg/L of any heavy metal. In addition, the treatment system was expected to recover both a copper and a zinc concentrate that could be processed at existing smelters for metal recovery.

Experimental Work

The water treated in this study was obtained from the Rio Tinto Mine, an abandoned copper mine located about 80 miles north of Elko, NV, near Mountain City. Active mining was conducted at the site between 1932 and 1947, and in situ leaching operations were carried out in the early 1970s. A chemical analysis of the water (as received) is shown in table 1.

System Design

The bench-scale treatment system consisted of a bioreactor and three precipitator-clarifier units (fig. 1). H_2S generated by sulfate-reducing bacteria was sparged from the bioreactor by an inert N_2 carrier gas and bubbled through untreated mine water in precipitator 1. Here, the H_2S reacted with copper and ferric iron in the mine water to form copper sulfide (equation 2) and elemental sulfur (equation 3):

$$Cu^{2+} + H_2S \rightarrow CuS\downarrow + 2H^+. \quad (2)$$

$$2Fe^{3+} + H_2S \rightarrow S^\circ + 2Fe^{2+} + 2H^+. \quad (3)$$

The combined gas-liquid effluent from precipitator 1 flowed into clarifier 1 (C-1), from which a CuS-S° concentrate was recovered. The gas-liquid effluent from C-1 then flowed into precipitator 2, where the pH of the solution was maintained between 2.2 and 4.0 by the addition of NH_4OH (aqueous solution containing 3%

Table 1. Chemical analysis of Rio Tinto Mine water.

Parameter	Concentration (mg/L)
Fe	550
Al	140
Cu	92
Mn	76
Zn	60
Co	4
Ni	2
pH[1]	2.2

[1] pH in standard units

NH_3). Zinc sulfide formed in precipitator 2, and a ZnS concentrate was recovered from clarifier 2 (C-2). From C-2, the combined gas-liquid effluent flowed into precipitator 3, which was maintained at pH 7.6 to 8.0, again with NH_4OH. The precipitator-clarifier 3 (PC-3) was installed to remove any remaining heavy metals before the combined gas-liquid stream flowed into the bioreactor.

Precipitators and clarifiers were constructed from 5-cm-ID translucent polyvinyl chloride (PVC) pipe. Details of the precipitators and the single-baffle clarifiers used in this treatment system are shown in figure 2. The volume and hydraulic residence time for these units are given in table 2. A diaphragm pump with Teflon-wetted parts was used to pump mine water through the treatment system at a rate of 2.5 mL/min. The carrier gas was recirculated at a rate of 150 to 250 mL/min using a single-piston, vacuum-pressure pump.

Bioreactor

The sulfate reduction bioreactor was a 15.4-cm-ID by 162-cm-long, translucent PVC column packed with crushed steel mill slag (2 cm by 2 cm). The slag was added to provide additional surface area for bacterial attachment (Maree et al. 1987, 1990). With the slag in place, the void volume of the bioreactor was 15 L. The liquid-gas effluent from clarifier 3 was combined with a nutrient solution (described in the following section) and was pumped into the base of the bioreactor. The recirculated carrier gas, the metal depleted but sulfate-rich mine water, and the nutrient solution then flowed up through the bioreactor and exited at the top in a combined liquid-gas stream that flowed into a liquid-gas separator (fig. 1).

The bioreactor was initially inoculated with a mixed culture of anaerobic microorganisms that had been obtained from composted manure and maintained on Postgate's "B" medium (Postgate 1984) for more than 1 yr. A nutrient solution containing 2 g/L beet molasses (specific gravity = 1.3), 4 g/L $CaCl_2 \bullet 2H_2O$, 6 g/L $MgCl_2 \bullet 6H_2O$, 2 g/L $FeSO_4 \bullet 7H_2O$, 2 g/L KH_2PO_4, and 2 g/L yeast extract was added at a rate of 1.6 mL/min using an FMI piston pump. There is no evidence in the literature that suggests that sucrose, which comprises about 50% of beet molasses, can be used directly by sulfate-reducing bacteria. However, bacteria present in the mixed anaerobic culture would be expected to hydrolyze sucrose and ferment it further to simpler organic acids, such as lactate and pyruvate (Maree et al. 1987). These simpler organic compounds can be directly used as carbon sources by sulfate-reducing bacteria (Postgate 1984, Fauque et al. 1991). The sulfate needed for cell respiration and the NH_3-N needed for cell growth were provided by the mine water that flowed into the bioreactor from clarifier 3.

Table 2. Void volumes and residence times for reactors used in this study.

Unit	Void volume, L	Flow rate mL/min	Residence Time h
Precipitator 1	0.9	2.5	6
Precipitator 2	1.6	2.5	11
Precipitator 3	1.8	2.5	12
Clarifiers	.24	2.5	1.6
Bioreactor	15	4.1	60
Entire system	20	--	94

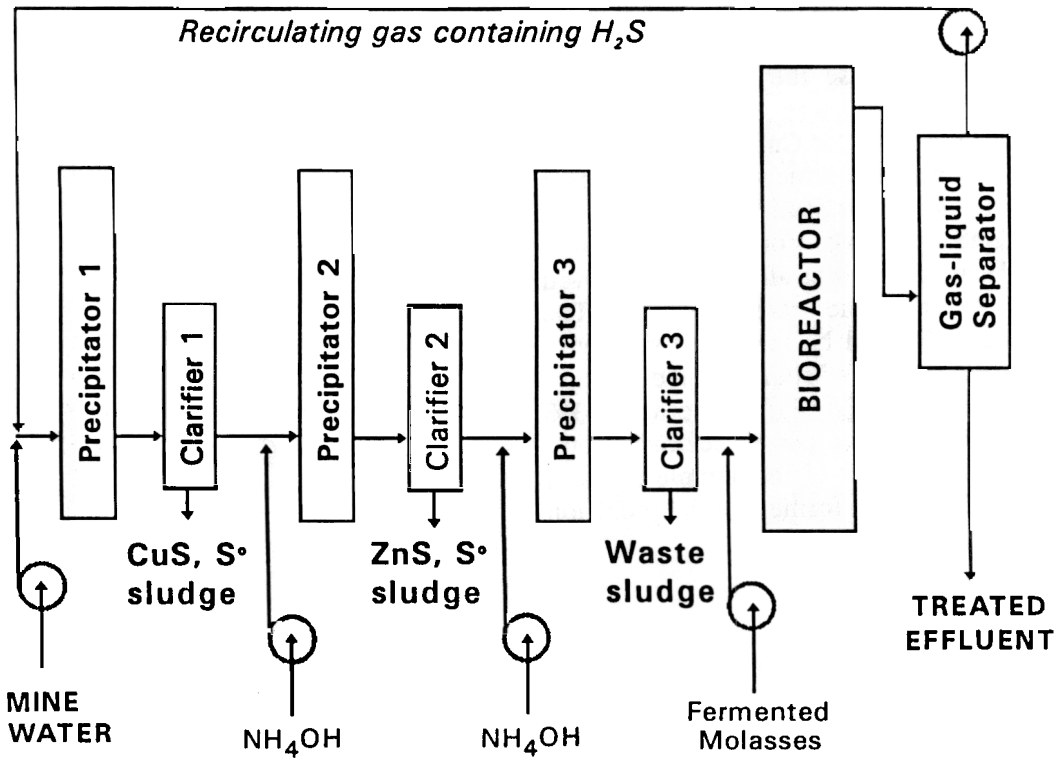

Figure 1. Schematic for bench scale biogenic H_2S treatment system.

Analytical Methods

Influent, effluent, and samples from each clarifier were collected 2 to 3 times a week during the continuous operation of the treatment system. All samples were filtered using 0.45-μm acetate filters. The filtrate was analyzed for Fe, Cu, Zn, Mn, Al, Co, Ni, Cd, and Pb using inductively coupled argon plasma emission spectrometry (ICP). Precipitates from the clarifiers were dried at 102°C for 12 h, weighed, and digested with aqua regia. The aqua regia solution was filtered, diluted to a known volume, and submitted for ICP analysis as above. All chemical analyses were carried out according to U.S. Environmental Protection Agency guidelines (1979).

Results and Discussion

In the bench-scale treatment system tested in this study, the recirculated carrier gas contained about 0.3% H_2S when it exited the bioreactor. Assuming this concentration to be constant throughout the system, the pH ranges for metal sulfide formation were calculated based on the pH-dependent dissociation of H_2S and the solubility of each metal sulfide. Figure 3 shows the pH range where each metal present in Rio Tinto Mine water would theoretically form metal sulfides when reacted with the H_2S-containing carrier gas. The low-pH boundary for each metal indicates the lowest pH at which a sulfide of that metal would form, given the concentration of the metal in the mine water and the H_2S concentration of the carrier gas. The right boundary indicates the minimum pH that must be maintained to reduce the concentration of that metal to less than 0.1 mg/L. In reality, the H_2S concentration of the carrier gas is depleted as it flows through the treatment system, and the solubility of the newly formed metal sulfide is often significantly higher than the published values for the sulfide mineral (Peters et al. 1984). Therefore, we expected the experimentally determined pH ranges to be shifted towards the higher pH.

Precipitator-Clarifier 1

CuS was expected to form in precipitator-clarifier 1 (PC-1) because the pH of Rio Tinto Mine water (pH 2.2) was higher than the theoretical minimum pH for CuS precipitation (fig 3). However, because the mine water pH was near the low-pH boundary for ZnS formation, it was uncertain if ZnS would also form. Experimental results (fig. 4) indicated that all Cu was removed from the Rio Tinto Mine water in PC-1. The concentrations of Fe and Ni increased slightly in PC-1 owing to corrosion of stainless steel fittings. The metal content of PC-1 sludge averaged 33% Cu and 0.3% Zn, with no other detectable metals. Sulfur comprised the bulk of the sample and was present as both S^{2-} and S^{o}, formed by the reduction of ferric iron (equation 3).

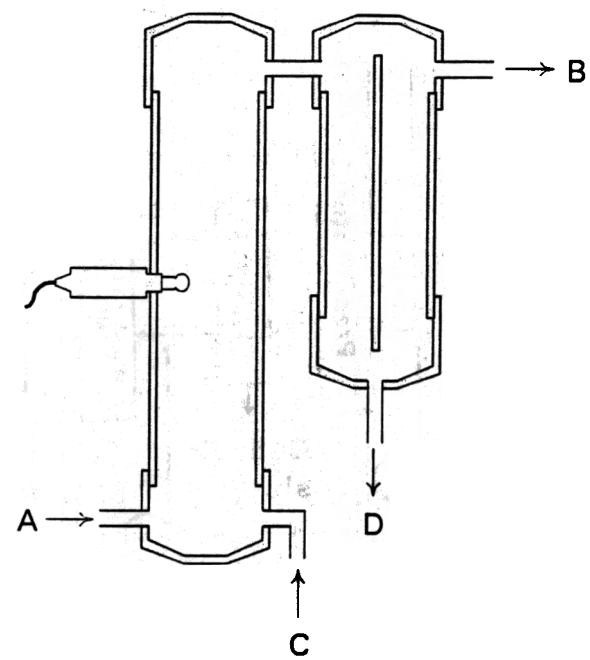

Figure 2. Detailed drawing of a precipitator/ clarifier unit showing: A) the liquid/gas inflow; B) the liquid/gas outflow; C) the NH_4OH addition port; and D) the sludge removal port.

Precipitator-Clarifier 2

During the study, the pH in precipitator-clarifier 2 (PC-2) was maintained between 2.2 and 4.0, the predicted pH range for ZnS formation (fig. 3). This pH range seemed appropriate for the precipitation of a relatively pure ZnS concentrate because Cu should have been completely removed in PC-1, and CoS, NiS, FeS, and MnS should not theoretically form below pH 4.5 (fig. 3). However, our initial attempts to operate at pH 3.8 to 4.0, where Zn removal was maximized, resulted in significant precipitation of $Al(OH)_3$. In addition, operation at pH greater than 3 resulted in the precipitation of $Fe(OH)_3$, since Fe^{3+} was not completely reduced in PC-1. In consideration of these constraints, the potential operating range was then limited to pH 2.2 to 3.0. Figure 5 shows the Zn concentration of PC-2 effluents when operated at selected pH's between 2.2 and 3.8. The performance of PC-2 was optimal at pH 2.8, where more than 99% of the Zn was recovered, but Fe and Al remained in solution. The PC-2 sludge formed at pH 2.8 contained 28% Zn, 0.7% Fe, 0.4% Ni, 0.3% Co, and no detectable Al or Mn. As in the PC-1 sludge, S^{o} and S^{2-} comprised most of the PC-2 sludge. The presence of Co and Ni in this sludge was unexpected because these elements should not precipitate as sulfides at pH 2.8 (fig. 3). However, Co and Ni may have adsorbed to precipitating ZnS particles. This possibility was not investigated further.

Precipitator-Clarifier 3

Precipitator-clarifier 3 (PC-3) was included in this treatment system to provide a metal-depleted but sulfate-rich feed to the bioreactor by removing Zn, Co, Ni, Fe, and Al from the effluent of PC-2. Therefore, PC-3 was operated at pH 7.6, a pH where the effluent concentration of all remaining metals, except Mn, should be less than 0.1 mg/L. We did not expect to be able to remove Mn because of the high solubility of MnS ($K_{sp} = 5.6 \times 10^{-16}$). As expected, the effluent concentrations of all metals except Mn were less than 0.1 mg/L. Surprisingly, Mn concentrations were reduced from 71 mg/L to 3.3 mg/L, presumably due to rhodochrosite ($MnCO_3$) precipitation. Because anaerobic fermentation reactions produce HCO_3^- or CO_2 as products, the P_{CO2}

in the recirculated carrier gas would be high compared with that in ambient air. Since a significant proportion of the CO_2 dissolved in the pH 7.6 mine water would have been present as CO_3^{2-}, it is likely that $MnCO_3$ formation (K_{sp} = 6.31 X 10^{-11}) was responsible for most of the observed decrease in Mn concentration.

Conclusions

The bench-scale, biogenic H_2S treatment system tested in this study was effective in the removal of Cu, Zn, Co, Ni, Fe, Mn, and Al from Rio Tinto Mine water. In addition, this treatment system produced a CuS-S° concentrate (33% Cu) and a ZnS-S° concentrate (28% Zn) that may be suitable for metal recovery at existing smelters.

New mine water treatment technologies must ultimately be compared with conventional lime treatment in terms of performance, cost, and reliability. Potential advantages of biogenic H_2S treatment over conventional lime treatment include the ability to achieve lower metal concentrations in treated effluent, the potential for metal recovery, and the production of metal sludges that are faster settling, denser, and more stable.

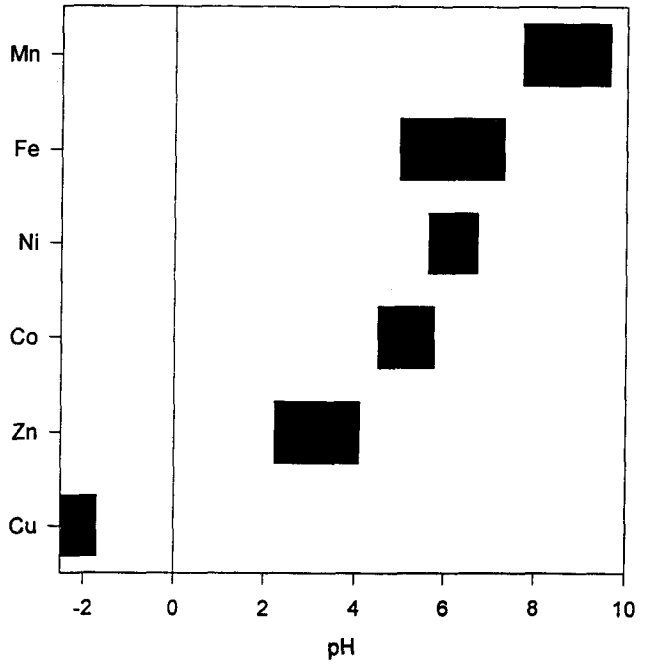

Figure 3. Theoretical pH ranges for the precipitation of different metal sulfides with biogenic H_2S. The low-pH limit is the minimum pH at which a metal sulfide will form given the concentration of that metal in Rio Tinto Mine water. The high-pH limit is the minimum pH that must be maintained to reduce the concentration of that metal to less than 0.1 mg/L.

The operating cost of a biogenic H_2S treatment system will likely vary greatly depending on application and location. Although the beet molasses used as an organic food source for bacterial sulfate reduction in this study cost about $83 per metric ton, the value of recovered metals may more than offset this cost. In many cases, no-cost or low-cost organic wastes could be used as carbon sources for sulfate-reducing bacteria. For example, anaerobic digestors at existing sewage treatment facilities can be modified for H_2S production (Butlin et al. 1956).

Biogenic H_2S treatment may be the method of choice in applications where there are

1. High concentrations of salable metals,
2. Low-cost carbon sources or existing anaerobic sewage treatment facilities,
3. Concerns about sludge volume and toxicity,
4. Strict discharge standards for heavy metals and sulfate.

The treatment plant at the Budelco Smelter established biogenic H_2S treatment as a technology for treating slightly acidic waste waters containing a single metal on a commercial scale (Scheeren et al. 1992). The present study suggests that the application of biogenic H_2S treatment to acidic waste waters containing several metals, and their selective recovery, is also feasible.

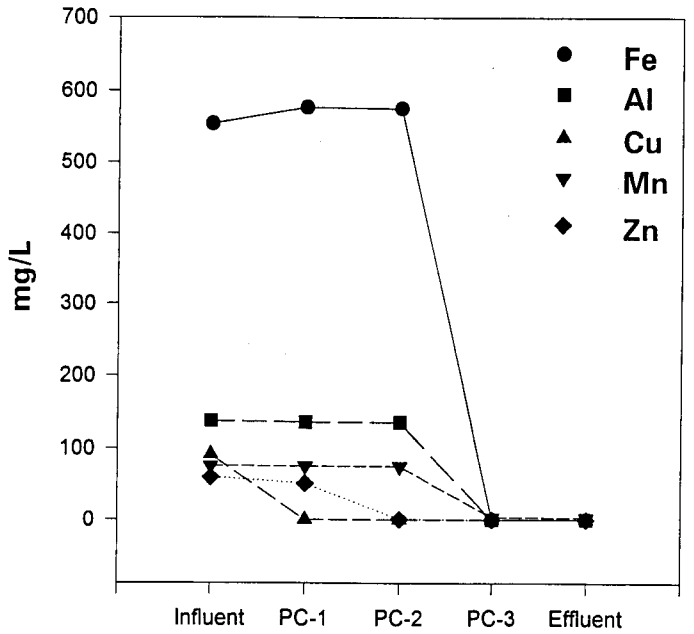

Figure 4. Dissolved metal concentrations at different points in the biogenic H_2S treatment system.

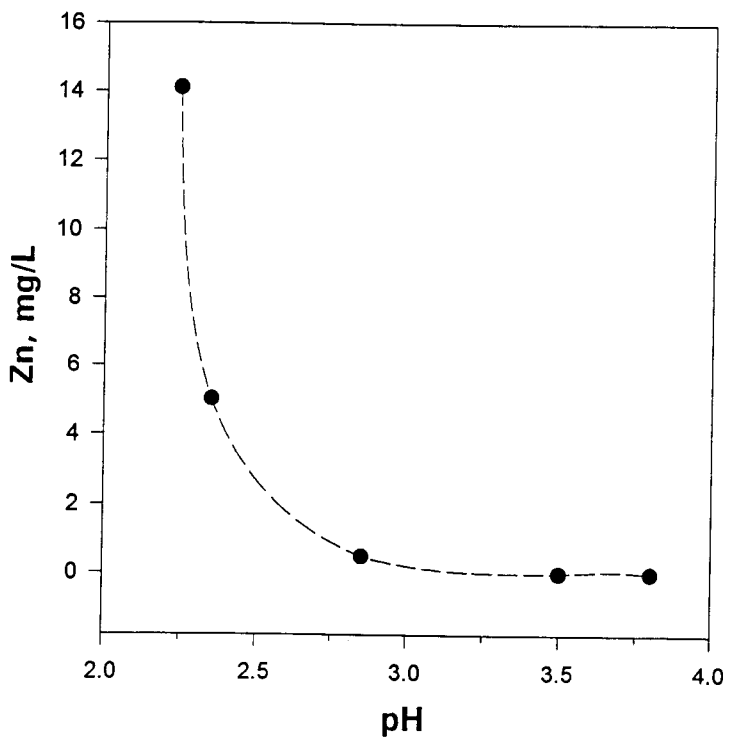

Figure 5. Zinc concentrations remaining in solution in precipitator/clarifier 2 when operated in the pH range 2.2-3.8.

Literature Cited

Barnes, L. J., F. J. Janssen, J. Sherren, J. H. Versteegh, R. O. Koch, and P. J. H. Scheeren. 1991. A new process for the microbial removal of sulphate and heavy metals from contaminated waters extracted by a geohydrological control system. Chem. Eng. Res. and Design 69:184-186.

Butlin, K. R., S. C. Selwyn, and D. S. Wakerley. 1956. Sulphide production from sulphate-enriched sewage sludge. J. Appl. Bacteriology 19:3-15.

Dvorak, D. H., R. H. Hedin, H. M. Edenborn, and P. E. McIntire. 1992. Treatment of metal-contaminated water using bacterial sulfate reduction: results from pilot-scale reactors. Biotechnol. and Bioeng. 40:609-616.

Fauque, G., J. LeGall, and L. L. Barton. 1991. Sulfate-reducing and sulfur-reducing bacteria. p. 271-337, In Variations in autotrophic life. Academic Press, New York.

Hammack, R. W. and H. M. Edenborn. 1992. The removal of nickel from mine waters using bacterial sulfate reduction. Appl. Microbiol. and Biotechnol. 37:674-678.

Hammack, R. W., D. H. Dvorak, and H. M. Edenborn. 1993. The use of biogenic hydrogen sulfide to selectively recover copper and zinc from severely contaminated mine drainage. p. 631-640. In Biohydrometallurgical technologies. I. Bioleaching processes. The Minerals, Metals, and Materials Society, Warrendale, PA.

Kleinmann, R. L. P., R. S. Hedin, and H. M. Edenborn. 1991. Biological treatment of mine water-an overview. p. 27-42. In Proceedings of the Second International Conference on the Abatement of Acidic Drainage. (Montreal, PQ, September 16-18, 1991).

Marchant, B. and R. W. Lawrence. 1989. Integrated biological processing of complex sulphides for metal extraction and waste treatment. P. 205-220. In Biohydrometallurgy. CANMET, Ottawa.

Maree, J. P., A. Gerber, A. R. McLaren, and E. Hill. 1987. Biological treatment of mining effluents. Environ. Technol. Letters 8:53-64.

Maree, J. P., G. Hulse, D. Dods, and C. E. Schutte. 1990. Pilot plant studies on biological sulphate removal from industrial effluent. Water Sci. and Technol. 23:1293-1300.

Mueller, R. F. and A. Steiner. 1992. Inhibition of anaerobic digestion caused by heavy metals. Water Sci. and Technol. 26:835-846.

Peters, R. W., Y. Ku, and T-K. Chang. 1984. Heavy metal crystallization kinetics in an MSMPR crystallizer employing sulfide precipitation. AIChE Symp. Series 80:55-75.

Postgate, J. R. 1984. The sulphate reducing bacteria. Cambridge University Press, New York.

Pugsley, E. B., C. Y. Cheng, D. M. Updegraff, and L. W. Ross. 1970. Removal of heavy metals from mine drainage in Colorado by precipitation. Chem. Eng. Prog. Symp. Series 67:75-89.

Scheeren, P. J. H., R. O. Koch, C. J. N. Buisman, L. J. Barnes, and J. H. Versteegh. 1992. New biological treatment plant for heavy metal contaminated groundwater. p. 403-416. In Proceedings EMC '91: Non-ferrous metallurgy-present and future. (Brussels, Belgium).

Tuttle, J. H., P. R. Dugan, and C. I. Randles. 1969. Microbial sulfate reduction and its potential utility as an acid mine water pollution abatement procedure. Appl. Microbiol. 17:297-302.

U.S. Environmental Protection Agency. 1979. Handbook for analytical quality control in water and wastewater laboratories. EPA 600/4-79-015.

Wakao N., T. Takahashi, Y. Sakurai, and H. Shiota. 1979. The treatment of acid mine water using sulfate-reducing bacteria. J. of Fermentation Technol. 57:445-452.

PROSPECT OF METAL RECOVERY /RECYCLE FROM ACID MINE DRAINAGE[1]

S. R. Rao[2], N. Kuyucak[3], T. Sheremata[3], M. Leroux[2], J. A. Finch[2], and K. G. Wheeland[3]

Abstract: Experimental investigations were conducted to determine the prospect of recovering valuable metals from acid mine drainage (AMD) from a Canadian source. In particular, potential for the recovery of zinc as sulfide for recycling to a zinc roaster has been examined. Several chemical methods were evaluated to selectively precipitate and recover metal ions, and a conceptual flowsheet, consisting of a three-step process, was developed. The process comprised oxidation of Fe(II) and precipitation of iron as ferric hydroxide in the first step, precipitation of Zn and Cu as sulfides in the second step, and the removal of the residual metal ions by lime neutralization in the third step. Alternative methods for selective precipitation that were evaluated included a two-step process in which ferric iron was precipitated with limestone, followed by precipitation of zinc and copper hydroxides and other metals using sodium hydroxide. The precipitation of sulfides was studied using sodium sulfide, sodium hydrosulfide and hydrogen sulfide. The results to date showed that almost 100% iron is precipitated in step 1, more than 90% zinc recovery with greater than 50% Zn grade can be obtained in step 2, and a discharge effluent with less than 1 mg/L heavy metals (Fe, Cu, Mn, Al) is obtained in step 3. The zinc grade was superior to that obtained by other methods evaluated which produced only 30% Zn grade. Economical and technical constraints of the three step process are reagent costs and solid-liquid separation. Acceptability of zinc hydroxide for recycling is uncertain. Alternative approaches for metal recovery based on these findings are suggested.

Additional Key Words: acid mine drainage, metal recovery, selective precipitation.

Introduction

Acid mine drainage (AMD) generated in sulfide-ore-processing regions is a serious environmental concern. The standard treatment is by mixing lime to precipitate the dissolved metals and disposing of the resulting sludge. This practice inevitably results in the loss of metals, some of which, if recovered, could provide revenue to offset in part the treatment and disposal costs while decreasing the sludge volume.

The present project was initiated to investigate methods for the treatment of AMD with the objective of recovering some of the base metals while maintaining or improving the effluent quality. Earlier work was done with AMD from Mattabi Mines Ltd., Ignace, Ontario (Rao and Finch 1992). Precipitation of the metals as hydroxide, sulfide, and by cementation in the case of copper, was investigated. Two multistep treatment options were demonstrated. In both options iron was first precipitated as ferric hydroxide at about pH 3.5. The possible use of this product as feedstock for producing a ferric sulfate coagulent was also considered (Rao et al. 1992). Contamination of the iron hydroxide with Cu and Zn was significantly reduced by introducing dodecylamine, $C_{12}H_{25}NH_2$ (DDA). This had the added benefit of reducing the loss of Cu and Zn. DDA was tried because it is known to adsorb on iron hydroxides (Iwasaki et al. 1960) and thus may act to "block" the adsorption site for metal ions.

---

[1]Paper presented at the International Land Reclamation and Mine Drainage Conference and the Third International Conference on the Abatement of Acidic Drainage, Pittsburgh, PA, April 24-29, 1994.

[2]S. R. Rao, Research Associate, M. Leroux, Research Technician, and J. A. Finch, INCO-NSERC Research Professor, Department of Mining and Metallurgical Engineering, McGill University, Montreal, PQ, Canada.

[3]N. Kuyucak, Project Leader, T. Sheremata, Research Scientist, and K. G. Wheeland, Program Manager, Noranda Technology Centre, Pointe Claire, PQ, Canada.

The present work was conducted with AMD from Les Mines Gallen, Rouyn Noranda, Quebec. This contained zinc in high concentration (~14 g/L) and ~30 g/L iron. Concentration of copper was very low (~0.2 g/L) relative to that of zinc. The work was therefore aimed at the recovery of zinc. Precipitation as the sulfide was selected because the precipitation as the hydroxide required raising the pH to about 7, which caused contamination with manganese and calcium sulfate precipitates. Zinc sulfide is also the common feed material to a zinc extraction plant.

The recovery of zinc as sufide was investigated by a three-step process:
Step 1. Removal of iron as hydroxide with preoxidation of Fe(II) to Fe(III),
Step 2. Precipitation of zinc sulfide,
Step 3. Production of a final discharge effluent using lime treatment.

The precipitation of zinc sulfide was studied with hydrogen sulfide, sodium sulfide, and sodium hydrosulfide. Sodium sulfide was chosen as it is a readily available industrial chemical. Hydrogen sulfide was used to study the precipitation at lower pH and investigate the action of lime to set the pH to higher values. Sodium hydrosulfide was used as an alternative to sodium sulfide. It is recognized that the equilibrium concentrations of Na_2S, NaHS, and H_2S are a function of the pH only.

This treatment procedure was compared with other options, including straight precipitation of all metals in one step and a two-steps option comprising precipitation of iron as hydroxide at pH 3.5 followed by precipitation of other metals as hydroxides by sodium hydroxide.

Experimental Work

Material Description

The AMD received was a seep water, pH about 1.8. It was diluted five times to correspond to more typical conditions; this is referred to as the "original" AMD (table 1). For experiments involving biological oxidation of Fe(II), the seep water was diluted 23 times.

Table 1. Composition of the original AMD from Les Mines Gallen.

Metal	mg/L	Metal	mg/L
Fe(II)	16,700	Al	3,520
Fe(III)	13,100	Mg	2,790
Total Fe	29,800	Ca	5.0
Cu	191	Pb	1.8
Zn	13,800	Cd	45.3
Mn	146	As	50.0

Oxidation of Fe(II)

Using Hydrogen Peroxide. The stoichiometric quantity of hydrogen peroxide required to oxidize the iron present as Fe(II) was added as a 30% solution to 20 L AMD. The mixture was stirred for 15 min and left for 12 h to allow for the dissipation of any residual peroxide.

Using Thiobacillus ferrooxidans (Tf bacteria). The bacteria were enriched from waste rock at a mine site using 9K

medium (Payant and Siwik 1987). Then 1.5 L AMD was inoculated with the isolated bacteria, and the nutrients (1.605 g KNO_3 and 0.525 g K_2HPO_4) were added. The solution was agitated for 6 days, samples were drawn for Fe(II) determination initially and after 1, 2, and 6 days.

Treatment Procedure for the Three-Step Process.

The basic experimental approach described before (Rao and Finch 1992) was followed with some modifications. The process flowsheet is shown in fig.1.

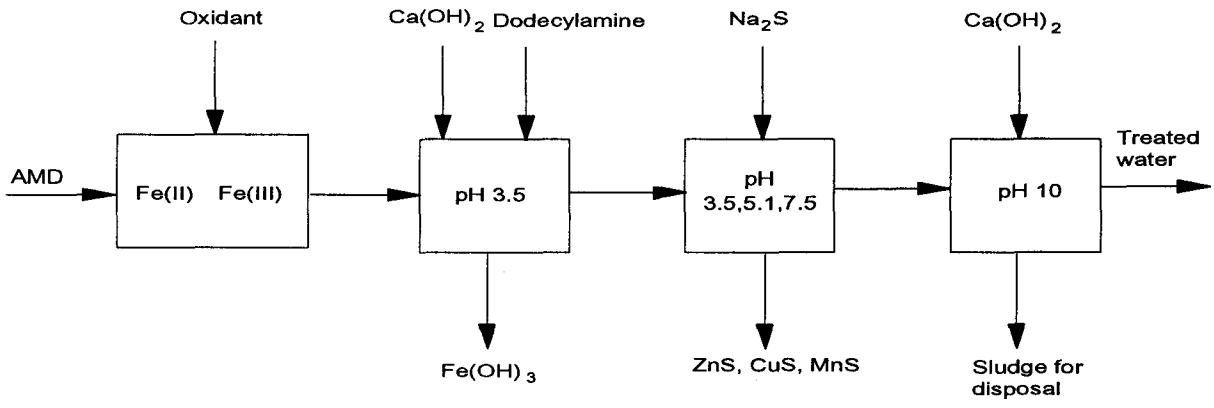

Figure 1. Flowsheet for three-step precipitation process.

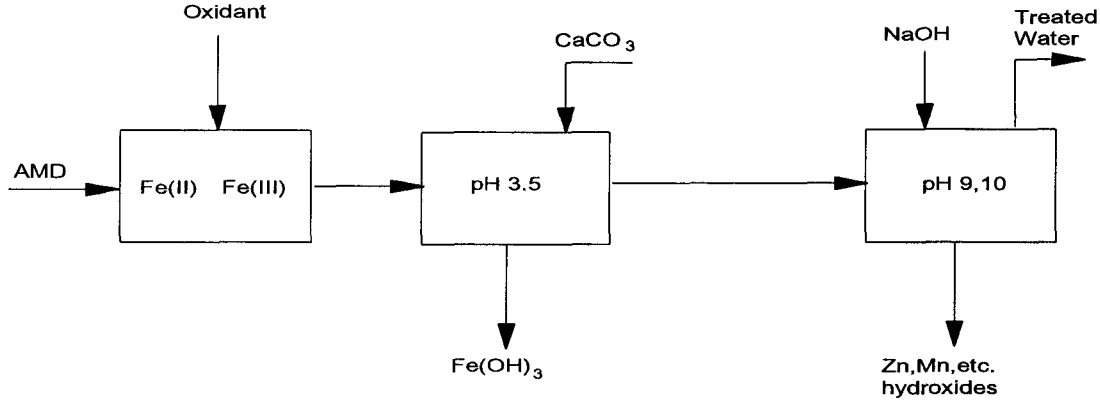

Figure 2. Flowsheet for alternative two-step precipitation process.

Step 1. Removal of iron as the hydroxide. After oxidation, dodecylamine (DDA) in concentrations up to 20 mg/L was added to the AMD. Experiments were conducted in a 1.5- L flotation cell with impeller speed at 800 r/min. Following the mixing of DDA, iron hydroxide was precipitated by adding calcium hydroxide until the pH reached 3.5 to 3.7. The precipitate was allowed to settle, enhanced by adding an anionic flocculant (0.05% solution) at an optimum dosage of 3.75 mg/L AMD, as established by settling rate studies. The precipitate was filtered to retrieve the effluent, which is feed to step 2.

Step 2. Recovery of zinc as the sulfide. Zinc was precipitated from the effluent of step 1 using sodium sulfide, hydrogen sulfide, or sodium hydrosulfide. The pH was adjusted using sodium hydroxide or calcium oxide. A calculated amount

(stoichiometric to precipitate Zn) of sodium sulfide or hydrosulfide was added from a 10% solution. For precipitation by hydrogen sulfide, the gas was bubbled through 1 L of solution at a rate of 35 mL/min for 2 h.

Treatment with sodium sulfide was studied at pH 3.9, 5.1, and 7.5. Treatment with hydrogen sulfide was conducted at pH 3.5, 5.1, and 7.5. Additional experiments were conducted by treatment with sodium sulfide, followed by the required amount of lime to reach a pH of 4.5. In another modification, sodium sulfide and the lime were mixed and added together to the AMD. The sulfide precipitate in each case was allowed to settle, and the solution was clarified by filtration through 0.45 μm millipore filter.

Step 3. Production of a final discharge effluent by lime treatment. Each effluent from the various step 2 treatments was treated with lime to pH 10.

Two Step Precipitation Process.

The process sheet for this option is shown in fig.2. After the oxidation of Fe(II), ferric hydroxide was precipitated by calcium carbonate; 13.5 g was required to raise the pH of 1 L to 3.5. After the separation of ferric hydroxide as described before, 4N sodium hydroxide solution was added to the filtrate to raise the pH to 9 and 10 in two separate batches. The precipitate of metal hydroxides was flocculated using anionic flocculant and separated by filtration.

Base line Test.

For the purpose of comparison, the pH of the original AMD was raised directly to pH 9.5, as is done in the conventional lime treatment process.

Leachability Tests.

These were conducted on precipitates from steps 1 and 3 according to the Ontario Regulatory Extraction Procedure (1985).

Results

Oxidation of Fe(II) to Fe(III).

A comparison of the three methods of oxidation showed that the residence times required for chemical oxidation were significantly shorter than that required for biological oxidation (table 2).

Table 2. Residence times for the oxidation of Fe(II) to Fe(III) in AMD.

Method	Reagent	Residence time
Chemical	Hydrogen peroxide	15 min- 2 h.
Biological	T. ferrooxidans	2-6 days.

Removal of Iron as the Hydroxide (Step 1).

Effect of Dodecylamine (DDA). The results obtained with different quantities of DDA are shown in table 3, which records the concentration of metal ions in the effluent. The precipitation of iron was virtually complete at pH 3.5; above 5 to 10 mg DDA/L, zinc contamination in the precipitate is reduced.

The DDA created a reddish froth, which retained some solids; analysis showed that they were mainly calcium sulfate with very little ferric hydroxide (despite the color).

Table 3. Precipitation of ferric hydroxide: effect of DDA.

DDA, mg/L	Concentration, mg/L									
	Fe	Cu	Zn	Mn	Al	Mg	Ca	Pb	Cd	As
Original	5,880	38	2,840	29	704	562	1.0	0.4	9.1	10.0
0	10.3	34.3	2,448	28	396	450	244	0.4	8.0	5.5
5	10.8	36.7	2,752	29	426	554	248	0.4	8.1	5.5
10	12.0	47.1	2,750	29	438	556	248	0.4	8.2	5.0
20	12.8	37.1	2,746	29	445	556	248	0.4	8.2	5.0

Table 4. Composition of the ferric hydroxide sludge in step 1

Reagent	Composition (dry basis),%								
	Fe	Zn	Cu	Mn	Mg	Al	Cd	Ca	As
$Ca(OH)_2$	16.720	1.61	0.03	0.004	0.12	1.00	0.002	0.03	0.019
$Ca(OH)_2$ + DDA, 5 mg/L	18.430	0.64	0.02	0.003	0.09	0.80	0.002	0.02	0.018
$CaCO_3$	18.380	0.03	0.02	0.001	0.001	1.10	0.003	0.02	1.100

Purity of Ferric Hydroxide Sludge. The composition of the sludge produced by various reagents are summarized in table 4. The sludge produced with calcium carbonate had the lowest levels of As, Cd, Mg, Mn, and Zn compared with the sludge obtained with calcium hydroxide. With calcium hydroxide the zinc loss was reduced in the presence of DDA, but it was still higher than that with calcium carbonate. Therefore, calcium carbonate is the most effective reagent for the production of a metal-free ferric hydroxide sludge for disposal or possible reuse.

Recovery of Zinc as the Sulfide.

Effect of pH Adjusted With Sodium Hydroxide. The effluents from step 2 show (table 5) that zinc was selectively precipitated below pH 4. More complete precipitation was observed at higher pH, but the selectivity was reduced. Composition of the precipitates showed that the Zn grade was 55% to 60% at pH<4, decreasing to <50% at pH 7.4, with Al as the main contaminant.

Comparison of Lime and Sodium Hydroxide to Adjust pH. Adjustment of pH with lime in place of sodium hydroxide also produced selective precipitation of zinc but with significantly greater recovery, the effluent showing lower concentration of zinc (table 6). The grade of the precipitate was lower owing to contamination by calcium sulfate.

Two-Step Precipitation Process. When sodium hydroxide was used for the two-step precipitation process, the Zn grade ranged from 27.3% to 29.7% at pH 9 and 10. However, the main advantage of this option is that the step 3 lime treatment may be eliminated, thereby reducing the volume of sludge requiring disposal, and sodium hydroxide precipitation is more easily controlled compared to sulfide precipitation.

Table 5. Step 2- Precipitation of zinc sulfide: Effect of sulfide reagents[1].

Description	Concentration, mg/L									
	Fe	Cu	Zn	Mn	Al	Mg	Ca	Pb	Cd	As
Original	5,880	38	2,840	29	704	562	1.0	0.4	9.1	10.0
Effluent after step 1	10.8	36.7	2,752	29	426	554	248	0.4	8.1	5.5
H_2S: pH 3.5	8.8	ND[2]	965	28	329	554	246	ND	1.0	4.0
pH 5.1	3.1	ND	697	28	10	550	246	ND	ND	4.0
pH 7.4	1.0	ND	4.0	1.9	ND	534	246	ND	ND	3.5
Na_2S: pH 3.9[3]	5.8	ND	542	28	316	556	250	ND	1.0	4.5
pH 5.1	2.1	ND	356	26	11	552	248	ND	ND	4.0
pH7.4	1.0	ND	3.3	11	ND	517	246	ND	ND	3.5
NaHS: pH 3.8[3]	3.9	0.1	1,142	42.4	211	632	423	0.3	11	1.8

[1]Conditions: DDA (10 mg/L) in step 1; NaOH used for pH adjustment.
[2]ND Not detected.
[3] Natural pH.

Base line Test. The effluent from this simulation of the conventional lime treatment of AMD showed metal concentrations similar to those in the effluent of the three-step process.

Sludge Stability.

The leachability test results (table 7) on unfiltered ferric hydroxide sludge from step 1, with and without DDA, showed that it contained Cu and Zn above the regulatory limit of 5 mg/L. In filtered sludge, the level of leached Cu is below the regulatory limit; however, the level of Zn did not meet the regulatory limit. Leaching tests were not conducted for step 1 ferric hydroxide precipitate formed with calcium carbonate. However, the results of the leaching tests on sludges from other tests indicate that filtration of the sludge reduces the degree to which metals are leached from the sludge.

Final Water Quality.

Chemical analysis of discharge water from various process options showed that in each case the water quality was sufficiently good for discharge; total metal levels ranged from 0.1 to 11 mg/L.

Discussion

Oxidation of Fe(II).

In comparing chemical versus biological oxidation for the conversion of Fe(II) to Fe(III), it was found that although residence time required for biological oxidation was excessive (2-6 days), an examination of the economics of the process (to be discussed below) shows the cost of biological oxidation is 72% to 97% lower than that of the options examined for chemical oxidation. To improve the efficiency of biological oxidation, process parameters such as temperature, rate of oxidation, rate of aeration, and inoculum ratio should be examined.

Table 6. Comparison of lime and sodium hydroxide in the precipitation of zinc sulfide.

Description	Zn in products			
	Effluent, mg/L		Precipitate, %	
	NaOH	Lime	NaOH	Lime
H_2S: pH 3.5	965	306	59.2	43.8
pH 5.1	697	2	46.4	21.1
Na_2S: pH 5.1	356	ND[1]	48.3	ND
pH 4.5	ND	1.1	ND	56.4
pH 4.5	ND	2.4	ND	54.8

[1]ND Not detected

Table 7. Sludge stability of ferric hydroxide sludges.

	Leachable metals, mg/L					
	Zn	Fe	Cu	Mn	Al	Mg
Settled sludge:						
no DDA	950	1.98	15.8	10.2	144	207
10 mg/L DDA	830	1.66	10.5	8.4	92	145
Filtered sludge:						
no DDA	130	0.10	2.46	0.91	6.2	18.4
10 mg/L DDA	105	0.10	1.80	0.65	6.0	15.6

Precipitation of Ferric Hydroxide (Step 1).

The results (table 3) showed that while the precipitation of iron as ferric hydroxide was practically complete, the precipitate is contaminated with Cu, Zn and Al ions. The extent of coprecipitation is reduced in the presence of DDA, but the precipitate still failed the leachability test. Of the chemical precipitants tested, calcium carbonate yielded the least contaminated ferric hydroxide precipitate. It is also cost effective; the estimated cost of calcium carbonate is 4 to 22 times lower than that of the other precipitants on cost-per-unit volume basis.

Precipitation of Zinc Sulfide (Step 2).

Sulfide precipitation of zinc at pH 3.5 using sodium sulfide yielded the highest grade of zinc, but the effluent from this process still carried about 1,000 mg/L Zn.

The recovery of zinc at pH 3.5 with hydrogen sulfide is enhanced using lime in place of sodium hydroxide to set the pH. In addition to pH control, the Ca(II) ions precipitate the sulfate ion in solution. This facilitates the dissociation of $ZnSO_4$ to free additional Zn(II) ions, which are then precipitated (Huang and Tahija 1990). The product, however, then contains about 8 to 9% Ca as $CaSO_4$, but remains free of other metals, which confirms the high degree of selectivity.

A possible alternative route is to use sodium sulfide and lime. Setting the pH at 4.5 yielded essentially 100% Zn recovery (table 6) from the effluent of step 1 with high selectivity and a product much lower in Ca than that obtained with hydrogen sulfide and lime. The use of calcium sulfide as a precipiant for zinc has been described (Kim and Amodeo 1983). This will be explored as a cheaper alternative for the precipitation of zinc.

Zinc Recovery as Hydroxide by Two Step Option.

Precipitation of Fe-free effluent from step 1 with sodium hydroxide at pH 10 yielded a sludge with almost 30% Zn with dissolved metals in the overflow that were sufficiently low for discharge. Use of lime to precipitate zinc as hydroxide resulted in a low Zn grade (11 to 20%) owing to contamination by calcium sulfate.

Comparison of the ZnS precipitate formed at pH 3.5 and $Zn(OH)_2$ formed at pH 10 indicates that each has certain advantages. In the latter case, although there is no sludge for disposal, there are concerns of high moisture content and elevated levels of Al and Mg. The impact of moisture content and impurities on recycling to the zinc roasters or in pressure leaching should be determined.

Although the fine nature of sulfide precipitates may result in carryover of material from a zinc roaster, the precipitate would be suitable for pressure leaching. A sedimentation-flocculation-filtration scheme should be considered for solid-liquid separation of the sulfide precipitates. On the basis of economics the feasibility of the process involving calcium carbonate for iron precipitation at pH 3.5 and sodium hydroxide for zinc precipitation at pH 10 depends on the costs associated with solid-liquid separation.

Economics.

Reagent costs. The available costs for the two oxidizing agents tested are , in dollar-per-cubic-meter, 5.85 for hydrogen peroxide and 0.32 for T. ferrooxidans. The costs for various reagent combinations are summarized in table 8. All costs are in Canadian dollars.

Table 8 Reagent costs for various precipitation steps

Precipitation step	Reagent	Cost, $/m^3
Step 1 Fe precipitation.	$CaCO_3$	0.16
	Na_2CO_3	2.40
	$Ca(OH)_2$	0.75
	CaO	0.65
Steps 2+3 in 2 steps.	Na_2S (pH 3.5)	3.20
	$Ca(OH)_2$ (pH 10)	0.39
	Total	3.59
Steps 2+3 in 1 step.	NaOH (pH 10)	2.78
Step 2+3 in 1 step.	$Ca(OH)_2$ (pH 10)	NA[1]

[1]NA Not available.

The least expensive oxidant is biological catalyst T.ferrooxidans. However, the residence time observed for Fe(II) oxidation in these preliminary tests was 2 to 6 days and must be optimized, and the effect of process parameters (e.g., temperature) must be determined.

For step 1 precipitation of ferric hydroxide, calcium carbonate is the least expensive neutralizing agent. For zinc precipitation and final water treatment, sodium hydroxide is the least expensive reagent.

Lime Treatment versus the Proposed Flowsheet. The operating costs for the 1992 season at Les Mines Gallen plant were $487,000 (P.Godbehere, internal memo, 1992). The costs associated with lime treatment and sludge handling would be eliminated by recycling all of the zinc and iron. Therefore, in conducting a preliminary cost-benefit analysis, a credit for lime and sludge handling will be assumed.

The estimates of reagent costs, reported in table 10 are based on the experimental results for dilute seep water. However, owing to stratification of the rock, the concentration of the pit water increases continuously throughout the operating season, which must be taken into account for an accurate cost-benefit analysis.

Based on the zinc loading during the operating season of the plant (22,221 kg), the zinc credit was calculated as $9,675 assuming 50% of the zinc value, $1,046.72 per mt.

To estimate the feasibility of the project, possible benefits (credits) associated with replacing lime treatment with the costs (debits) of the zinc value recovery process are detailed in table 9.

The costs of chemicals used in full operation will be higher owing to lower efficiency. Also, the cost of solid-liquid separation is not taken into account. Although the credits otherwise outweigh the debits, the feasibility of the proposed value recovery project will depend on the costs associated with soild-liquid separation.

Table 9. Possible credits and debits associated with replacing lime treatment with the two-step recovery process of $CaCO_3$-NaOH.

Description	Credit	Debit
Zn credit (22,221 kg Zn)	$9,675	NAp.[1]
Lime	150,000	NAp.
Sludge handling	55,000	NAp.
Fe credit from $Fe_2(SO_4)_3$ from weak acid plant	120,000	NAp.
$CaCO_3$/NaOH for Fe and Zn precipitation from AMD.	NAp.	$21,477
Total	334,675	21,477

[1]NAp. Not applicable.

Conclusions

The present work has demonstrated on a laboratory scale the technical feasibility of a three step process for recovering zinc from AMD. The three-step process gives superior grade zinc sulfide, but it is less economic, owing to the cost of sodium sulfide, than the two-step process, which gives higher recovery and lower, but still acceptable, grade of zinc hydroxide.

Future work directed toward the following areas for improving the efficiency and economics of the process is recommended in the following areas:

1. Solid-liquid separation studies on ferric hydroxide and zinc sulfide and hydroxide precipitates.
2. Use of calcium sulfide as a precipitant for zinc sulfide.
3. Sulfate reducing bacteria as the sulfide ion source.

4. Separation of zinc sulfide and calcium sulfate by selective flotation.
5. Separation of zinc hydroxide and calcium sulfate by selective flotation.

Sulfide precipitation appears to have a growing application because it yields improved effluent quality compared to lime. The incremental costs of metal recovery by using an alternative, cheaper source of sulfide (e.g., calcium sulfide) should be evaluated. The perception of the mining industry as involved with recycling metals and extending natural resources may have important social and economic consequences.

Literature Cited

Huang, H. H. and D. Tahija. 1990. Characteristics and surface treatment problems of surface and underground waters. p. 261-270. In Mining and Mineral Processing Wastes. Editor, F. M. Doyle. Soc. Min. Eng., Littleton, CO.

Iwasaki, I., S. R. B. Cooke, and H. S. Choi. 1960. Flotation characteristics of hematite, goethite and quartz. Trans. AIME 217:237-245.

Kim, B. M. and P. Amodeo. 1983. Calcium sulfide process for treatment of metal containing wastes. Environmental Progress 2:175-180.

Kuyucak, N., D. Lyew, P. St. Germain, and K. G. Wheeland. 1991. In situ bacterial treatment of AMD in open pits. p. 335-353. In Proceedings of the Second International Conference on the Abatement of Acidic Drainage. (Montreal,PQ, September 16-18, 1991).

Payant, S. and R. Siwik. 1987. Control of acid generation on Brunswick Mining waste rock with the use of chemicals. N-8616, RR 87-1, Noranda Technology Centre Research Report, July 1987.

Rao, S. R. and J. A. Finch. 1992. Resource recovery from acid mine drainage; bench scale studies. p. 3-11. In Waste Processing and Recycling in Mining and Metallurgical Industries. Editors, S. R. Rao, L. M. Amaratunga, D. A. D. Boateng, M. E. Chalkley. CIM, Montreal.

Rao, S. R., R. Gehr, M. Riendeau, D. Lu, and J. A. Finch. 1992. Acid mine drainage as a coagulant. Minerals Engineering 5:1011-1020.

PIPELINE TREATMENT OF A METAL MINE DRAINAGE CONTAINING COPPER AND ZINC[1]

Craig C. Hustwit[2] and Richard G. Sykes[3]

Abstract: A pipeline treatment system, previously used to treat coal mine drainage, was tested at pilot- and full-scale to determine its effectiveness in treating a copper-zinc bearing metal mine drainage in northern California. The 37.85 liters per minute (L/min) (10 gpm) system consisted of a jet pump and static mixer, arranged in series. Three alkaline reagents were each evaluated at four treatment pH values. An additional reagent mixture was evaluated at one treatment pH value. Initial copper, zinc, and cadmium concentrations were 100, 450, and 1.7 milligrams per liter (mg/L), respectively. Post-treatment concentrations for these metals were below detection limits for soluble metals using the inductively-coupled plasma spectroscopy (ICP) method, regardless of reagent used, when the treatment pH was in the 9.0 to 10.0 standard unit range. A full-scale version of the pipeline system was constructed and operated at 1,136 L/min (300 gpm) for approximately 5 months. Calcium hydroxide slurry was introduced at the jet pump to achieve a pH of 9.5 to 10.0 standard units. The system removed between 97% and 99% of copper, zinc, cadmium. Based on these studies, it was concluded that 1) pipeline treatment is a viable approach to metal mine drainage treatment, 2) establishing a treatment pH in the 9.0 to 10.0 standard unit range was critical for metals removal, and 3) treatment in the In-Line System (ILS) may involve coprecipitation mechanisms.

Additional Key Words: pyrite, acid mine drainage, heavy metals, treatment, ILS

Background

This study was undertaken as part of an effort led by East Bay Municipal Utility District (EBMUD) and the California Regional Water Quality Control Board (CRWQCB) to minimize the impacts of acidic drainage from the abandoned Penn Mine. EBMUD is a public utility that provides water and wastewater service to over 1 million people in Oakland, Berkeley, Alameda, and several other cities and communities east of the San Francisco Bay. The U. S. Bureau of Mines' (USBM) interests were in investigating metal mine drainage treatment options.

The purpose of this study was to evaluate the performance of an in-line treatment system (ILS) for treating metal mine drainage. While the chemical compositions of metal mine drainage vary, they are typified by elevated acidity and the presence of heavy metals and sulfates. They often constitute a threat to the environment if the water is not hydrologically isolated, diluted, and/or treated. The evaluation of ILS treatment is consistent with an EBMUD goal of protecting its water resources. Additionally, it is part of the USBM's ongoing effort to developing new technologies for protection and remediation of the environment.

The Penn Mine Site

This study was conducted at the Penn Mine in Calaveras County, CA. The site is located in a remote section of the western foothills of the Sierra Nevada mountains approximately 40 kilometers (km) east of Lodi, CA. Two watersheds converge on the site: Hinkley Run and Mine Run. The site is 79 meters (m) above mean

---

[1] Paper presented at the International Land Reclamation and Mine Drainage Conference and the Third International Conference on the Abatement of Acidic Drainage, Pittsburgh, PA, April 24-29, 1994.

[2] Craig C. Hustwit, Civil Enginner, U.S. Bureau of Mines, Pittsburgh Research Center, Pittsburgh, PA 15236.

[3] Richard G. Sykes, Senior Engineer, East Bay Municipal Utility District, Oakland, CA 94623-1055.

sea level and lies approximately 152 m east of the Camanche Reservoir on the Mokelumne River (fig. 1).

The Penn Mine is one of several copper mines in this region. Chalcopyrite and sphalerite were discovered there in 1861 as adjacent land was being placer-mined for gold. Ore extraction of the copper began shortly thereafter, using the stope method. Mining continued intermittently until 1953, when the mine was finally closed. Remnants of various ore concentrator facilities are still present, including a copper cementation launder. The site is marred by numerous piles of waste rock, concentrator tailings, slag, and unprocessed ore. Many of these materials retain residual chemical reactivity (CRWQCB 1993).

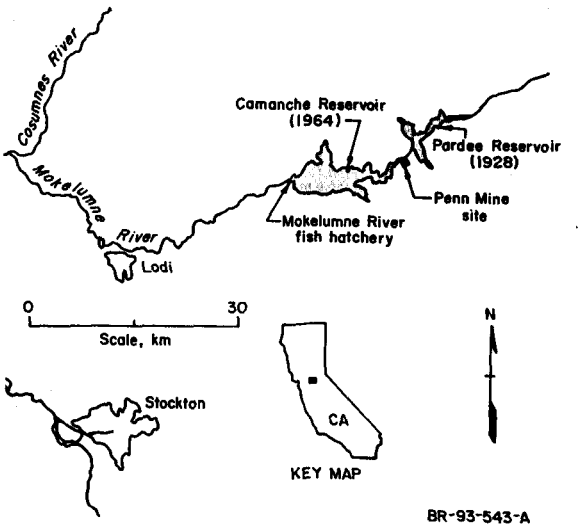

Figure 1. Area Map.

The historic and current reactivity of these materials has resulted in the production of classic metal mine drainage: acidified water with elevated concentration of soluble metals. Fish kills in the Molkumne River were first recorded in 1937 and occurred regularly following heavy rainstorms. During the 1960's, EBMUD constructed the Camanche Dam on the Molkumne River to increase their water storage capacity. The dam is located 12 kilometers downstream of the Penn Mine. A steelhead and salmon hatchery is located adjacent to the dam. In conjunction with this project, EBMUD purchased a narrow piece of the mine property that would be affected by the reservoir formation. After repeated administrative and legal efforts to force the owners of the Penn Mine to clean up the site and halt uncontrolled releases of mine drainage, the CRWQCB, EBMUD, and the California Department of Fish and Game embarked on a cooperative effort to install interim pollution control measures. In 1978, EBMUD constructed Mine Run Dam at the foot of the site and CRWQCB reconstructed six dams upstream on Mine and Hinkley Runs (fig. 2) These control measures eliminated the fish kills in the Camanche Reservoir and the Mokelumne River. However, during wetter than normal winters, the ponds' 67,849 cubic meters (m^3) (17,925,706 gal) capacity is exceeded, and controlled and uncontrolled releases have occurred. Evaporation is the principal method by which impounded water volumes are reduced each year.

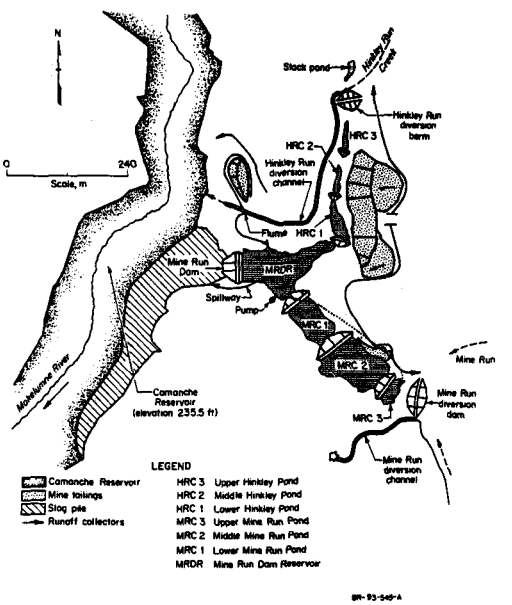

Figure 2. Site Map.

Mine Drainage Formation

The mineral pyrite, FeS_2, is the principal source of dissolved iron and acidity in the Penn Mine drainage. Pyrite is associated with the ore body and is subject to chemical weathering upon exposure to atmospheric oxygen and water. When this exposure occurs, pyrite releases soluble ferrous iron and sulfuric acid into the environment (Stumm and Morgan 1981). Pyrite's reaction with oxygen proceeds according to

$$FeS_{2(s)} + 7/2\ O_2 + H_2O \Rightarrow Fe^{2+} + 2S0_4^- + 2H^+.$$

Note that the iron released is initially in the reduced, ferrous form.

The presence of a naturally occurring, acidophilic bacteria, *Thiobacillus ferrooxidans*, is known to accelerate the chemical weathering of pyrite by oxidizing the ferrous iron to ferric iron, which in turn reacts with pyrite:

$$FeS_2 + 14Fe^{3+} + 8H_2O \Rightarrow 15\ Fe^{2+} + 2SO_4^{2-} + H^+.$$

Additional acidity is also generated as Fe^{3+} that fails to react with pyrite, hydrolyzes, and forms ferric hydroxide.

Once an acidic environment is created, other less soluble sulfide minerals are chemically weathered, resulting in additional metals being mobilized. In the Penn Mine drainage, the metals of most environmental concern are copper, zinc, and cadmium.

Mine Drainage Treatment

The most common method of treating acidic mine drainage is the chemical precipitation process. In this process, an alkaline reagent, i.e., hydrated lime ($Ca(OH)_2$), quick lime (CaO), or caustic soda ($NaOH$), is added and mixed with the mine drainage. The added alkalinity removes free, excess acidity from the process stream and raises the ambient solution pH. Each metal precipitate has a pH at which its solubility is minimized. By adjusting the solution pH into the range of a metal's minimum solubility, the metal is substantially removed from solution through a hydrolysis precipitation process. However, the minimum solubility pH's for the metals are not concurrent. Since mine drainage typically contains multiple metals, the solution pH must be carefully selected. This is normally determined through bench-scale tests where the drainage is adjusted to different pH levels and the metal concentrations are evaluated.

Coprecipitation is a secondary metal removal mechanism that can occur during treatment. In coprecipitation, precipitation seeds (metal hydroxide particles, called floc) form and adsorb additional metals out of solution through a heterogeneous reaction.

Precipitation of metals in a conventional treatment system would normally take place in a basin or pond. While in the basin, the alkaline reagent would be added and mechanical mixers would provide sufficient agitation to thoroughly distribute the reagent and maintain the metal floc in suspension.

Following the precipitation of the metals, the metal floc must be separated from the water. A gravity separation method is normally employed for solid/liquid separation. In gravity separation the water-metal floc stream is directed to a quiescent pond or clarifier. Chemical additives, typically polyelectrolytic polymers, are sometimes added prior to solid/liquid separation to accelerate the settling rate. When the floc has separated, the clarified water can be drawn off. The metal floc, called sludge, from this process is a voluminous by-product with unstable chemical and physical properties. At present, the disposition of sludge is one of the most expensive components in metal mine drainage treatment. Although this study does not address sludge disposal issues a subsequent study is being conducted on a new method for chemically and physically stabilizing the Penn Mine metal sludge.

As an alternative to conventional mine drainage treatment systems that employ basins or ponds, the USBM invented the ILS. The ILS consists of two off-the-shelf components: a jet pump or eductor, and a static mixer. These are arranged in series in a pipeline carrying mine drainage. The drainage is pumped or gravity fed through the ILS at upstream pressures between 14,062 kilograms per square meter (kg/m^2) (20 psi) and

42,186 kg/m^2 (60 psi). An alkaline reagent is pulled in by the suction port of the jet pump and mixed with the drainage downstream in the static mixer. Atmospheric air is also introduced in the jet pump. The air bubbles assist in the mixing action and provide oxygen for the oxidation of any reduced metals present. The ILS replaces the basin-mixer unit where the chemical precipitation step occurs in conventional treatment systems.

Originally, the ILS was designed to treat coal mine drainage that contained acidity and dissolved metals (Ackman and Erickson 1986). The dissolved metals most common in coal mine drainage are iron, manganese, and sometimes aluminum. Currently, the ILS is being used at approximately 20 coal mines in the United States.

Methods

Pilot-scale Study

Treatment Plant Description. A 2.54 cm (1 inch) PVC jet pump was arranged in series with an 20 cm (8 inch) x 1.22 m (4 foot) (diameter x length) static mixer. The static mixer was constructed of polyethylene pipe and packed with 2.54 cm (1 inch) trickling media. Sampling ports were provided immediately upstream of the jet pump and immediately downstream of the static mixer discharge. Pressure gauges were installed upstream and downstream of the jet pump. A chemical feed unit was used to deliver the alkaline reagents into the suction port of the jet pump. The feed unit consisted of a 208 L (55 gal) barrel equipped with a portable mixer and a metering pump with flow control. Water from MRC3 was used in the study to prepare the alkaline slurries. Figure 3 is a schematic of the ILS pilot system.

The pilot unit was positioned on the dam that forms MRC3. Drainage from MRC3 was pumped through the ILS with a gasoline-powered centrifugal pump and then discharged into MRC2. The pump was equipped with a foot valve and strainer and provided a nominal 28,124 kg/m^2 (40 psi) at the gauge upstream of the ILS. The flow rate of the drainage through the system was approximately .63 liters per second (L/s) (10 gpm).

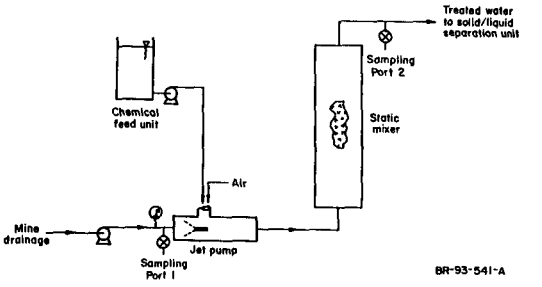

Figure 3. Schematic of the pilot-scale ILS.

Test Description. The study consisted of batch treatments of mine drainage using four alkaline reagents: hydrated lime, quick lime, caustic soda, and a mixture of hydrated lime and Type C fly ash. Slurries were prepared from the dry reagents and a dilute solution prepared from 50% caustic soda. Each reagent, with the exception of the hydrated lime/fly ash mix, was then evaluated at four effluent pH's: 7, 8, 9, and 10 standard units. A complete pH spectrum with the hydrated lime/fly ash was not possible due to an insufficient supply of the fly ash. With this exception, each reagent was evaluated at all treatment pH's before proceeding to the next reagent. After the desired effluent pH was established, three sample pairs were taken at the ILS discharge. All sample bottles were filled to the brim and tightly capped. The samples were then placed in an ice chest and delivered to the analytical laboratory. Each sample pair consisted of an acidified and unacidified sample. Acidified samples were filtered through a 0.45 micron filter prior to acidification. A similar sampling protocol was used on the inlet side of the ILS to establish the pretreatment water quality conditions.

The acidified samples were analyzed for dissolved metals by inductively-coupled plasma (ICP) spectroscopy (American Public Health Association et al 1985). Determinations of acidity/alkalinity and pH were performed on the unacidified samples using Standard Methods 402 and 403 respectively.

Full-scale Study

In early February 1993, it appeared that the capacity of the Penn Mine storage ponds would soon be exceeded for the first time since May 1986. This was due to high rainfall levels during the winter months. In response to a potential overflow of acid mine drainage from the site, EBMUD wrote to the U. S. Environmental Protection Agency (EPA), Region IX, suggesting several measures to prevent or mitigate the impacts of a release. One of the measures was installation of an ILS treatment plant.

On February 11, 1993, EPA directed EBMUD to begin construction of an ILS plant. EPA set a treatment goal for the plant of 98% removal for heavy metals (measured as total metals for Al, Cd, Cu, Fe, Ni, Pb, and Zn). Using the data collected from the June 1992 pilot study, EBMUD designed a full-scale ILS plant. The plant was completed within 8 weeks and went into operation on April 13, 1993.

Treatment Plant Description. Figure 4 is a process flow diagram and a list of the major equipment used in the ILS plant. Mine drainage from Mine Run Dam Reservoir (MRDR) was pumped into two parallel treatment units. Each 9.46 L/s (150 gpm) capacity unit consisted of a 7.62 cm (3 inch) diameter jet pump, 7.62 cm (3 inch) diameter static mixer, and 79,500 L (21,000 gal) settling basin. The two clarifier overflow streams were recombined in a common outfall which discharged to Camanche Reservoir via the MRDR spillway. Two 3.16 L/s (50 gpm) sludge pumps drained the clarifiers. Sludge was disposed of in an arm of the MRDR upstream of a sediment curtain.

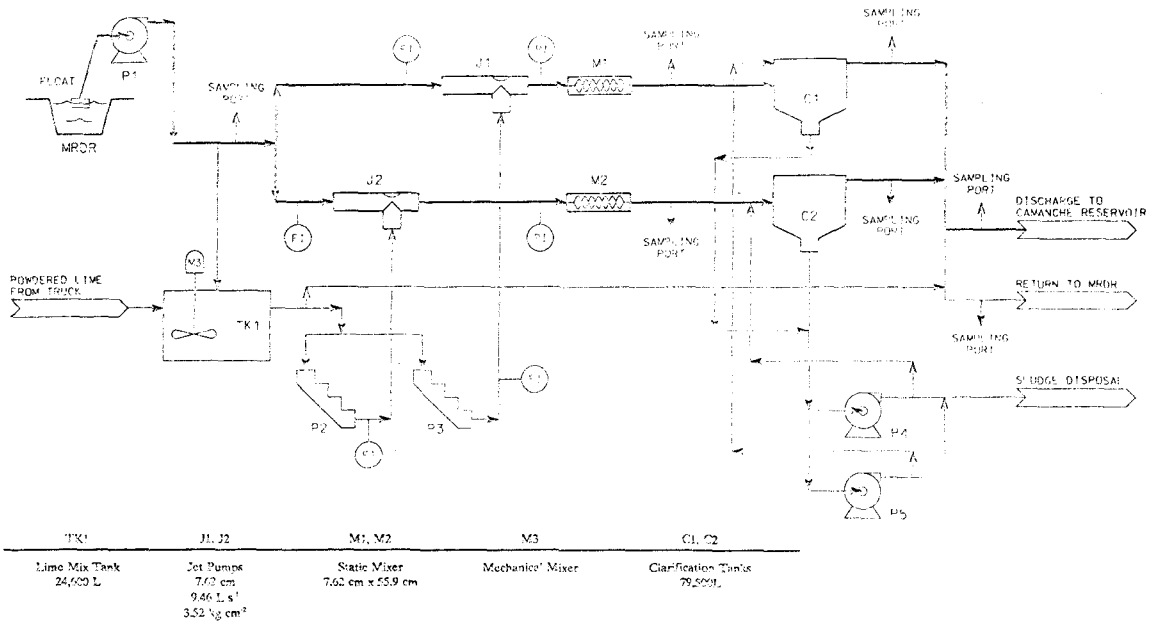

Figure 4. Schematic of the full-scale ILS.

Hydrated lime was selected as the pH adjustment reagent because it was the safest and easiest to use of the three reagents that were successful at the pilot plant level. The lime feed system consisted of a 24,600 L (6,500 gal) slurry tank and two chemical metering pumps. Lime slurry was injected into the jet pumps at a manually controlled rate to achieve a pH of between 9.5 and 10.0 units immediately following the static mixers. This range was originally selected based on the pilot studies and was reconfirmed as full-scale plant data became available.

Plant Operation. The ILS treatment plant was operated on 54 days between April 13 and September 17, 1993. For approximately half of these days, the plant discharged treated mine drainage to Camanche Reservoir. On

the other days, the system was operated in a testing mode and treated water was returned to MRDR. In April, May, and June, EBMUD determined optimum system control parameters for metals removal and devised solutions to lime feed and scale formation problems. The system was shut down during July so that several minor modifications could be constructed. Plant operations resumed in August and continued through the third week of September.

Results

Pilot-scale Study

Untreated mine drainage from MRC3 had a pH of 2.6 standard units and an acidity of 4,100 mg/L as $CaCO_3$. Copper, zinc, and cadmium concentrations in MRC3 were 100, 450, and 1.7 mg/L, respectively. Table 1 shows the quality of untreated drainage from MRC3.

Table 1. Water quality from the pilot-scale study.

Conc.:[1]	Mine Drainage Quality	at pH = 7.0			at pH = 8.0			at pH = 9.0			at pH = 10.0			
Reagent:		Hydrated Lime	Quick Lime	Caustic Soda	Hydrated Lime	Quick Lime	Caustic Soda	Hydrated Lime	Quick Lime	Caustic Soda	Hydrated Lime	Quick Lime	Caustic Soda	Hydrated Lime/Fly Ash
pH, field, std. units[2]	2.6	7.0	7.0	7.0	8.0	8.0	8.0	9.0	9.0	9.0	10.0	10.0	10.0	10.0
pH, laboratory, std. units	2.6	5.0	3.3	4.0	6.1	3.9	NA[3]	3.4	4.5	9.1	3.1	5.4	9.8	9.8
Copper	100	<.002	<.002	<.002	<.002	<.002	<.002	<.002	<.002	.010	<.002	<.002	.006	<.002
Zinc	450	.590	.011	1.6	.061	.009	<.008	<.008	<.008	.010	<.008	<.008	<.008	1
Cadmium	1.7	.028	<.008	.110	<.008	<.008	<.008	<.008	<.008	<.008	<.008	<.008	<.008	<.008
Sulfate	8,600	2,900	2,400	7,300	2,800	2,400	7,100	2,100	1,700	1,500	1,500	1,500	7,100	1,800
Acidity, as $CaCO_3$	4,400	35	54	63	32	88	49	100	66	98	130	43	0	0
Alkalinity, as $CaCO_3$	0	4.8	0	0	10	0	0	0	0	110	0	0	91	29
Conductivity, umho cm^{-1}	8,400	3,540	3,180	9,410	3,390	3,150	9,880	2,950	2,400	NA	2,560	2,270	NA	2,530

[1] All units in mg/L unless noted. Metals data are for the dissolved fraction.

[2] +/- 0.2 standard units.

[3] NA indicates data is not available.

The pilot study indicated that, in general, the higher the treatment pH (up to 10 standard units) in the ILS, the greater the removal efficiency for metals. Metal concentrations in the ILS effluent were lower than would be expected based on the theoretical solubilities of metal hydroxides. This suggested that coprecipitation was occurring during treatment, although there was no direct confirmation of this. Additionally, there was no evaluation made of other metal removal mechanisms, such as insoluble carbonate formation. Table 1 also presents the post-treatment water quality results. Hydrated lime, quick lime, and caustic soda appeared to be suitable reagents for metals removal.

Cadmium removal clearly increased with increased treatment pH. At pH 7, cadmium removal ranged from 94% to 98%. Cadmium concentrations decreased to the ICP detection limit for all reagents at a pH of 8 or greater. At the ICP detection limits of .008 mg/L, the cadmium removal would be 99%. The minimum solubility of cadmium hydroxide ($Cd(OH)_2$) occurs at a pH of approximately 10.5. The significant reduction in cadmium at lower pH values may be attributable to coprecipitation or other unidentified removal mechanisms.

Virtually complete removal (>99.99%) of soluble copper was achieved for hydrated lime, quick lime, and caustic soda at all four pH ranges tested. The post-treatment copper concentration was two orders of magnitude less than the theoretical solubility of copper hydroxide for the hydrated lime, quick lime, and caustic

soda reagents at pH 7. Coprecipitation is postulated as the explanation for this increased level of copper removal. Theoretical solubility and actual concentrations were not significantly different at the higher pH values.

Successful zinc removal (>99%) occurred at all four pH ranges tested for the lime and caustic soda treatments. Hydrated lime with fly ash achieved a 99.8% removal at a treatment pH of 10.0. In many cases of successful zinc removal, the actual concentrations of zinc were below the theoretical minimum concentration for the respective pH. Coprecipitation, again, is the suspected mechanism for the enhanced level of zinc removal.

Full-scale Study

Table 2 presents the ILS influent and effluent water quality data for cadmium, copper, and zinc. The data indicate the three distinct periods of system operation.

Table 2. Water quality from the full-scale study.

Period of Operation	1st			2nd			3rd		
Conc.:[1]	In	Out	% Removal	In	Out	% Removal	In	Out	% Removal
Copper, avg.	4.94	.612	87.6	15.3	.284	98.1	28	.129	99.5
Copper, min.	3.8	.52	86.3	7.4	.09	98.8	22	.02	99.9
Copper, max.	5.7	.69	87.9	20	1.2	94.0	30	.29	99.0
Zinc, avg.	27.6	7.04	74.5	72	3.03	95.8	156	1.48	99.1
Zinc, min.	23	5.9	74.4	35	.88	97.5	140	.17	99.9
Zinc, max.	31	9.1	70.7	100	16	84.0	170	2.9	98.3
Cadmium, avg.	.12	.064	46.7	.30	.026	91.3	.64	.012	98.1
Cadmium, min.	.1	.049	51.0	.15	.006	96.0	.56	.006	98.9
Cadmium, max.	.13	.085	34.6	.43	.11	74.4	.72	.019	97.4

[1] All concentration units in mg/L. Metals data are for the dissolved fraction.

First Operational Period. The first period, from April 14 to April 21, was the initial start-up period when the plant was operated to achieve an effluent pH of between 7.5 and 8.5 units. As predicted from the ILS pilot-scale study, metal removal during this period was limited, ranging from approximately 86% to 88% for copper, 71% to 74% for zinc, and 35% to 51% for cadmium.

Second Operational Period. During the second period of operation, from April 28 to June 24, the system was operated to achieve an effluent pH of between 9.5 and 10 units. The increased pH resulted in substantially

improved metals removal. Copper removal averaged 98.1% with a range from 94.0% to 98.8%. Zinc removal averaged 95.8% with a range from 84.0% to 97.5%. Average removal of cadmium was 91.3% and ranged from 74.4% to 96.0%.

Third Operational Period. The third period of operation occurred from August 13 through September 17 and followed the completion of several plant modifications performed in July. The plant was operated to achieve a pH of between 9.5 and 10.0 units. During this operation period, the ILS effluent consistently met the EPA goal of 98% metals removal. Copper removal ranged from 99.0% to 99.9% with an average of 99.5% being removed from solution. The average reduction in zinc concentration was 99.1% with a range from 98.3% to 99.9%. The average cadmium reduction was 98.1% with a range from 97.4% to 98.9%.

Table 2 also shows that influent to the ILS plant was becoming more concentrated through the spring and summer owing to evaporation. This had no observable negative impact on ILS plant effluent quality; conversely, ILS effluent quality improved as the summer progressed.

Conclusions

Pilot-scale study of the ILS indicated that it was appropriate for treating metal mine drainage at the Penn Mine. Additionally, the pilot study permitted the selection of an optimum treatment pH and several acceptable reagents for pH adjustment. In many instances, metals removal in the pilot study was below theoretical solubility for metal hydroxides. This may have been the result of coprecipitation within the ILS.

Pilot study results were successfully used as a basis of design and operation of a full-scale ILS treatment plant. The ILS plant was designed, installed, and put in operation in a remote site within approximately 8 weeks. After approximately 30 days of operation, the full-scale plant was achieving the goal of removing 98% of influent heavy metals while a treatment pH range of 9.5 to 10.0 was maintained.

Literature Cited

Ackman, T. E. and P. M. Erickson. 1986. In-Line Aeration and Neutralization System (ILS) - Summary of Eight Field Tests. In Proceedings of the AIME/SME/TMS 115th Annual Meeting. (New Orleans, LA, March 2-6, 1986).

American Public Health Association, American Water Works Association, and Water Pollution Control Federation. 1985. Standard Methods for the Examination of Water and Wastewater 16th ed. American Public Health Association, Washington, DC.

California Regional Water Quality Control Board, Central Valley Region. 1993. Penn Mine Site Technology Evaluation Report, prepared by Davy Environmental, San Ramon, California.

Stumm, W. and J. J. Morgan. 1981. Aquatic Chemistry. Wiley-Interscience, New York. p. 469-471

TREATMENT OF ACID MINE DRAINAGE BY THE HIGH DENSITY SLUDGE PROCESS

by D.J. Murdock, J.R.W. Fox and J.G. Bensley[2]

Abstract: The oxidation of sulphide minerals in moist, aerobic conditions leads to the formation of acid and the mobilization of metals. This process is aided by bacterial action and gives rise to acid mine drainage. The most commonly applied technology for chemical neutralization of acid mine drainage is the use of lime which not only neutralizes the acid but also precipitates metals as their oxides or hydroxides. The processes that have been used to date for lime neutralization include simple neutralization, neutralization with aeration to oxidize iron, and neutralization with aeration and sludge recycle. A refinement of the third method, based on aeration and sludge recycle can produce a dense sludge of 20%+ solids with free drainage properties, which rapidly achieves 40% to 50% solids in the impoundment area. Because of these advantages, this method, otherwise known as the high-density sludge (HDS) process, has been selected for treatment of acid mine drainage at several mining operations in Canada and the United States. The stability of the sludge is naturally high but can be further improved by the addition of a slight lime excess before impoundment.

Additional Key Words: acid mine drainage, high density sludge, water treatment, effluent treatment, impoundment.

Introduction

The dissolution of soluble metal compounds from ore, waste rock, and tailings results in metal-contaminated effluent commonly known as acid mine drainage. Properly, acid mine drainage (AMD) refers to water mobilization of sulfide oxidation products. Depending on the type of host rock, sulfide content, and degree of oxidation, such effluents range from near neutral pH with a few milligrams of metal content to highly acidic with metal content measured in grams. The most commonly applied technology in the North American base metal mining industry for the treatment of AMD is chemical neutralization and precipitation using lime. Other technologies may find site-specific application, but there are valid reasons for the dominance of lime treatment. Chemical precipitation is controllable and predictable. Lime is widely available, inexpensive, and easily handled. In some cases, additional reagents are required to fix metals mobilized during sulfide decomposition, including iron salts to remove arsenic and antimony.

The first application of a process in Canada based on neutralization and recirculation of the precipitated sludge was reported by Kuit (1980). The process was installed at the Sullivan Mine of Cominco Ltd. at Kimberley, B.C. As described by Kuit, based on considerable pilot-plant work, a plant had been successfully designed to treat AMD, and the process produced sludge that was substantially denser than that achieved with simple neutralization. At that time, the plant had been operating for only 1 year, but the quality of effluents produced met or fell under the limits set by the Provincial and Federal environmental authorities. It was stated that several years would be required to confirm water management and treatment plant capabilities under the complete range of operating conditions, as well as to confirm the long-term environmental acceptability of the treated sludge.

---

[1] Paper presented at the International Land Reclamation and Mine Drainage Conference and the Third International Conference on the Abatement of Acidic Drainage, Pittsburgh, PA, April 24-29, 1994.

[2] D.J. Murdock, Manager, Process Technologies, J.R.W. Fox, Principal Engineer, Metallurgy, J.G. Bensley, Principal Engineer, Process Control, Cominco Engineering Services Ltd., Vancouver, B.C. Canada

Kuyucak et al (1991) have studied similar variations of the lime neutralization process in a laboratory setting and have reported extensively on the results. These papers are cited here for interested readers but will not be reviewed.

The purpose of this paper is to discuss some of the unique features of the HDS process, to provide an update on the operations and stability of the first plant in Kimberley and provide some practical knowledge on full scale implementation of HDS at several industrial locations.

Process Fundamentals

A wide variety of techniques have been considered for the treatment of AMD. Genes et al (1991) presented the following alternatives for the treatment of 400 L/min of acidic drainage from an abandoned lead-zinc mining area in the United States:

- Carbon adsorption.
- Ion exchange.
- Reverse osmosis.
- Electrodialysis.
- Ozonation.
- Engineered wetlands.
- Lime neutralization-precipitation.

Apart from lime neutralization, the only technique that has been applied to any great extent has been engineered wetlands (Norton 1993). Lime neutralization has been the preferred technique for the following reasons:

- Capability of treating severe waste rock drainage.
- A wide range of flows can be accommodated.
- Capital and operating costs are moderate.
- It is generally considered the best practical technology

The near-complete precipitation of the metals as hydroxides in the neutralization process proceeds according to the following reactions:

$$M^{++} + SO_4^{=} + Ca^{++} + 2(OH)^{-} + H_2O \rightarrow M(OH)_2 + CaSO_4 \cdot 2H_2O, \text{ and}$$
$$M^{+++} + 3(SO_4)^{=} + 3Ca^{++} + 6(OH)^{-} + 6H_2O \rightarrow 2M(OH)_3 + 3CaSO_4 \cdot 2H_2O.$$

As implied by the equations above, the products of these reactions are metal hydroxide precipitates and calcium sulfate (gypsum). It is hypothesized that if the sulfate concentration of the wastewater is high enough, there will be sufficient gypsum produced to exceed its solubility and it will precipitate with the sludge. The presence of the gypsum increases the buffering capacity of the sludge and may be partially responsible for the sludge's improved chemical stability. Wasserlauf (1987), Higgs (1990) and Kuyucak (1991) have all studied this issue and found gypsum does indeed exist in the sludge although at ambient temperatures, treated solutions are often supersaturated in gypsum. These findings tend to support the author's hypothesis.

Complete oxidation of the ferrous hydroxide to the more stable ferric hydroxide is required for optimum process chemistry, as follows:

$$Fe^{+++} + 2(OH)^{-} + 1/4\ O_2 + 1/2\ H_2O \rightarrow Fe^{+++} + 3(OH)^{-}$$

Incomplete ferrous oxidation during treatment can result in chemical instability of impounded sludge and redissolution of heavy metals. Simplified lime treatment flowsheets are shown in figure 1. For the most part, metal hydroxides are compatible with effluent objectives. However, the supplemental addition of iron salts and/or minor

sulfides can compensate for most deficiencies in metals removal by lime. The first scheme shown in figure 1 essentially involves the addition of lime and mixing the solids with the tailings discharge. This process is low in cost and was successfully applied at Heath Steele Mines in New Brunswick (Busse 1974). The process is also used at Equity Silver Mines Ltd. in British Columbia (Gormely 1989). Although this process can produce acceptable effluent quality, the precipitated sludge produced is voluminous, rarely exceeding 2.5% solids, and difficult to handle. Sludge stability is questionable, and redissolution of precipitated metals is a concern. Furthermore, the volume of sludge produced can approach the volume of the original effluent treated.

The second scheme requires an independent plant for lime reaction and aeration to oxidize Fe^{++} to Fe^{+++}, followed by a clarifier or settling pond. Chemical stability of the sludge is improved, but given the low density, disposal is still a concern.

These disadvantages are largely overcome by using the third scheme, the HDS process, which produces a thickener underflow sludge of 20%+ solids with free drainage properties, which rapidly achieves 40% to 50% solids. The stability of the sludge can be further improved by the addition of a slight lime excess before impoundment.

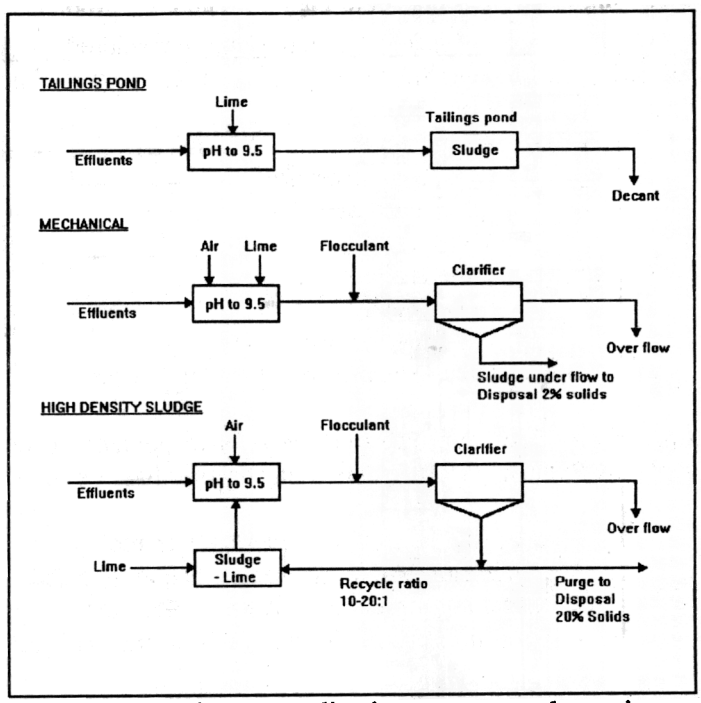

Figure 1. Lime neutralization treatment alternatives.

The effective removal of base metals in a stable form in the HDS process is caused by the formation of a precipitate of calcium and coprecipitate with iron on the surface of a recycled particle. The stability of the precipitates is favorably influenced by a high-iron-to-total-metal ratio. Simple recycle is not enough to change metal ratios, and in extreme examples iron may have to be added, or the storage site for sludge produced must allow for the possibility of longer term instability. In all cases the oxidation of ferrous to ferric iron is the principal oxygen-consuming cation reaction. Anions containing sulfur (such as thiosulfate) and arsenic (as arsenite) may also require oxidation. However, if air is sparged into the reactor for oxidation, the oxygen transfer may well be controlling the reaction and hence the reactor tank sizing. Oxygen transfer will be dominant in agitator design and power requirements.

Design plant throughput is influenced by the volume of water to be treated: for example, seasonal changes will determine runoff, much of which may have to be treated. Increased flow may be accompanied by a dilution of contaminants, both acid and metal, and the resulting plant influent may require reduced oxidation and/or residence time.

High-Density Sludge Process

A simplified flowsheet for the HDS process is shown in figure 2. The main features of the process have been reported previously by a variety of authors such as Kuit (1980) and can be summarized as follows: A combination of lime and recycled sludge is added to the sludge-lime mix tank at the head of the process. This mixture is discharged to the rapid mix tank, to which is also added the influent. Thereby achieving a partial neutralization. This mixture is fed to the main lime reactor where a combination of aggressive aeration and high shear agitation ensures optimum process chemistry and clarifier performance. The discharge from the lime reactor is treated with flocculant prior to entering the flocculant mix tank. The clarifier separates the treated effluent from the sludge, a portion of which is recycled to the head of the process.

The HDS process is normally run at a pH between 9 and 9.5, as most metals encountered in the process precipitate at or below this concentration of hydroxide ions. This pH is also required for ferrous iron oxidation. Oxidation of ferrous to ferric iron takes place quite rapidly at this pH, and oxygen is the most usual oxidizing agent. There is no reason why other agents cannot be used for oxidation, although all the plants built by the authors so far have used air for oxidation.

The process itself depends upon sludge recycle from the treated effluent, and in most plants this has been achieved in a thickener style clarifier, which offers a pumpable sludge as the separated solids product. Clearly, recycle from a settling pond presents some material-handling problems, as do filter-style clarifiers, but both could be used.

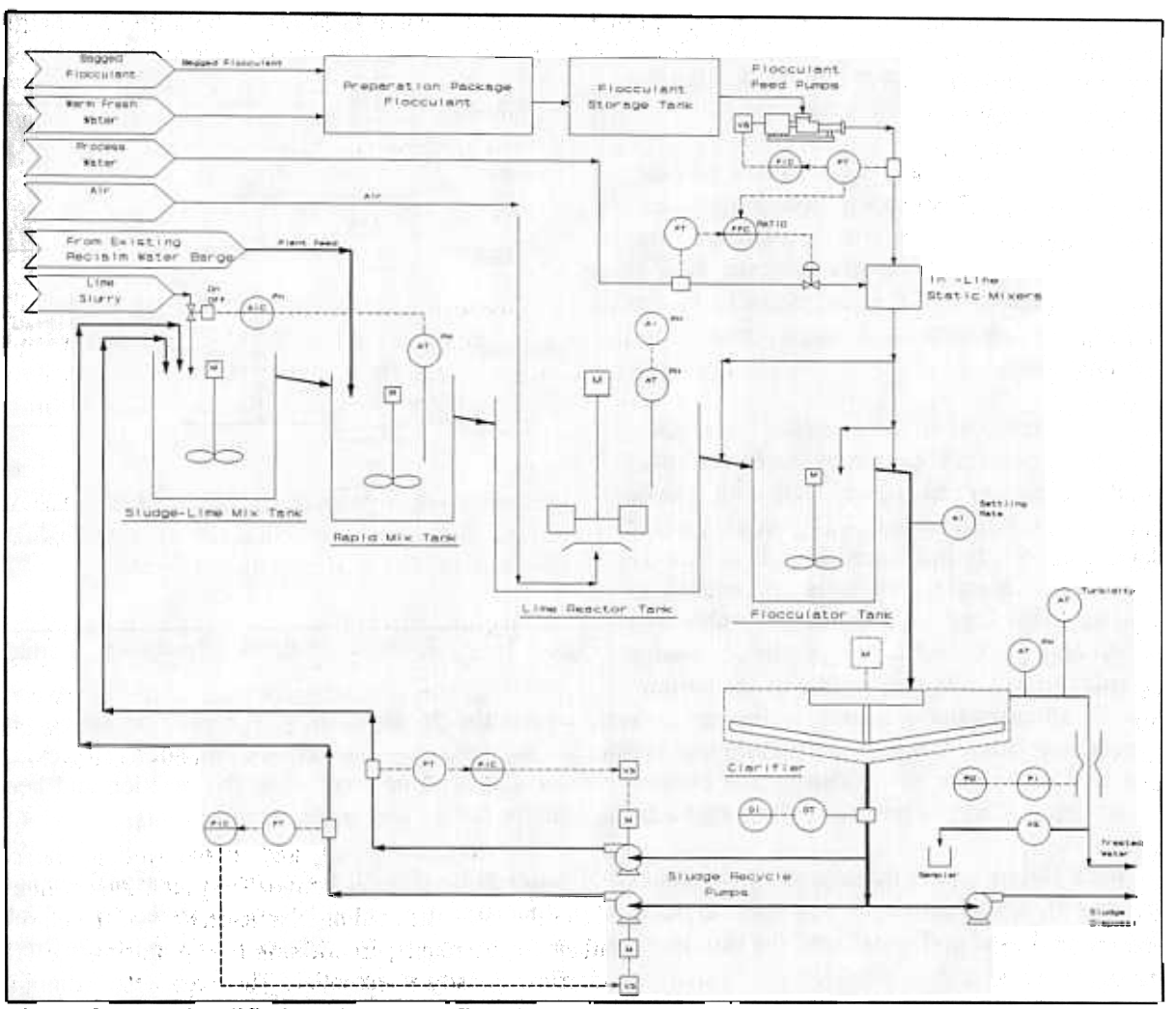

Figure 2 Simplified HDS process flowsheet

Design Parameters and Plant Features

Some general comments on the materials of construction and design parameters are as follows:

Untreated water supply — All pumps in contact with this water should be 316 SS because of the acid pH of the water. Any surge tanks should also be 316SS. Pipelines are best in high density polyethylene. Scaling conditions of the water must be evaluated so that pipeline descaling can be provided if required. The propensity of water to cause scale in pipelines is governed by the concentration of scale forming compounds such as sulfates and

carbonates. Analysis for these compounds in conjunction with their respective solubility curves and information on typical temperatures and pH's expected will provide insight regarding the extent of scaling problems to be expected. The process water flow rates and contaminant levels must be fully known in order to develop a proper design.

Sludge-lime mix tank — This vessel is normally made of carbon steel since the vessel contents are at a high pH. The agitator must be able to supply adequate mixing power to get sufficient shear in the vessel.

Rapid mix tank — This vessel must be made of 316 SS because of the corrosive nature of the untreated water being put into the tank. The agitator and shaft should be 316SS or rubber covered.

Lime reactor — This tank can be either concrete or mild steel. Concrete is preferred because of the high power input requirements of the agitator. The final selection is dependent on an economic analysis and the need to prevent freezing in the plant. The agitator gear reducer must be of a very heavy duty design to handle the difficult process requirements of keeping solids in suspension, dispersing the air into small bubbles, and contacting the air, water and solids. Designing for a low-maintenance requirement is also an important factor.

Flocculent mix tank — This vessel can be concrete or mild steel. The agitation is gentle to avoid breaking any of the flocs produced.

Clarifier — This vessel can be either steel or concrete. Site objectives and location will form part of the economic evaluation to determine steel or concrete. This vessel is not a thickener but a clarifier, and so thixo-posts are required rather than shoes to move the sludge. The introduction of the flocculated feed into the clarifier must be gentle to avoid breaking up the flocs. The clarifier overflow must be properly collected to reduce the problems of freezing.

Sludge disposal — This may require pumping over a long distance. The line loss characteristics of the sludge must be known to properly size the pumps required. Proper startup and shutdown of this batch pumping operation are important to avoid plugging or freezing during wintertime operation. The sludge lines can be HDPE or steel.

The principal control parameters for the HDS process are also illustrated in figure 2. The pH in the rapid mix tank is the primary parameter used to control lime addition to the sludge-lime mix tank. Optimum operation is achieved through time-proportional control of a pinch valve, which taps a small proportion of the slurry circulating in a loop from the lime slurry storage tank. The pH in the lime reactor is monitored and may be used to adjust the set-point of the primary pH control loop based on operating parameters such as feed rate, metals loading, and sludge recycle rate.

Flocculant may be added at various locations prior to the flocculator tank and in the feed to the clarifier. Flocculant flow is measured prior to dilution and controlled to an operator determined set-point. An on-line settling rate analyzer is commercially available that can be used to determine the settling characteristics of the clarifier feed and thus speed up the establishment of optimum flocculant requirements, in addition to monitoring the effects on clarifier overflow turbidity. Monitoring of clarifier underflow density is essential. This parameter combined with sludge recycle flow rate determines recycle mass flow, the control of which is paramount in achieving optimum process performance. Duplication of the sludge recycle circuit with the use of variable-speed pump controllers and automatic line-flush sequencing has been found to provide good operating flexibility.

Clarifier overflow turbidity and pH are monitored, and can be used to shut down plant feed in the event that they exceed operational limits. Final discharge flow is monitored and grab samples are taken automatically for analysis and reporting. Fresh water consumption can be reduced through the use of treated water (from clarifier overflow) for lime slaking, flocculant dilution, and line flushing.

In order to minimize labor costs, various automatic sequences for equipment operation can be included that are controlled through programmable logic controllers. For example, operation of lime slakers can be automated based on the drawdown of slurry from the lime slurry storage tank, and flocculant preparation can be similarly controlled. At remote sites where the plant is mainly unattended, an automatic power on-restart sequence (which can restart the plant in the event of a brief power interruption) has been found to be beneficial.

Case Studies

Cominco Ltd., Kimberley BC, Canada

This plant was one of the first applications of the HDS process in Canada. The plant was started up in 1979 and has been operating more or less continuously since that time. The plant treats on average 11,500 L/min of AMD at a ph of 4.0. The normal maximum that the plant is designed to treat is 18,000 L/min, which can be forced to 27,000 L/min. Some comparative data are presented in tables 1 and 2, which show the design basis originally selected and the performance achieved shortly after startup, compared with that achieved during the 12-month period from June 1992 to May 1993. The values shown for 1992-93 are the averages of the monthly composite performance.

Table 1. Kimberley HDS plant, comparative plant performance.

	1979		1992-93	
Species, ppm	Influent	Effluent	Influent	Effluent
Iron	250	<1.0	144	0.02
Zinc	22	<0.2	28	0.01
Lead	5	<0.1	4.9	0.02
Suspended solids	75	<15	73	10
pH	4.5	9.5	4.0	9.3

Table 2. Typical comparative operating parameters, per unit volume of water treated.

	1980	1992-93
Lime consumption, g/L	1.0	.5
Flocculent consumption, g/m^3	3.0	2.1
Sludge production, g/m^3	1.3	.66

Trends in treated water flow, soluble zinc concentration in the treated water (plant effluent in figure 3 below) and soluble zinc concentration from water wells surrounding the sludge impoundment site for the period June 1992 to May 1993, are shown in figure 3. The soluble zinc content of the well water provides an indication of the extent to which heavy metals are re-released by the sludge over time and therefore, a measure of long-term sludge stability.

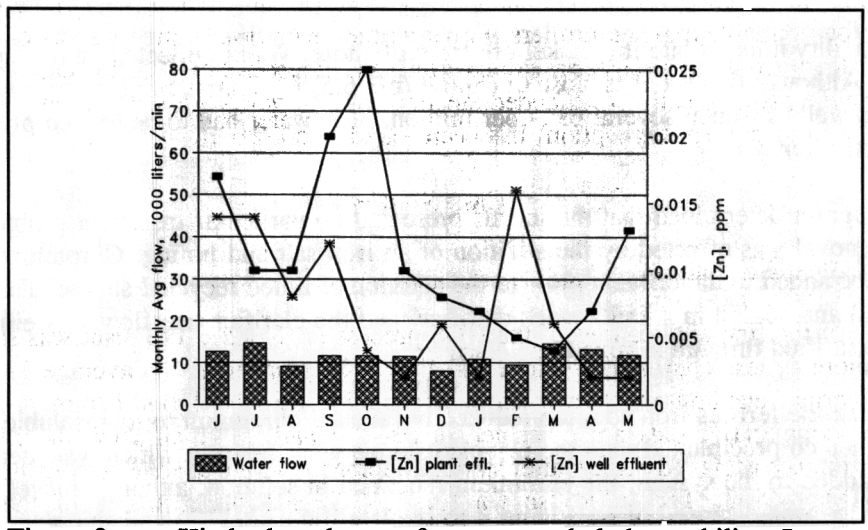

Figure 3. Kimberley plant performance and sludge stability, June 1992 to May 1993

The data plotted in figure 3 shows conclusively that after 13 years of operation, the plant still produces an effluent that contains metal concentrations substantially below current government regulations. Regulations in Canada for zinc are a maximum of 0.5 to 1 ppm in discharged effluent. Furthermore, the low content of metals in the well water from around the impounded sludge indicates that, to date, re-release of the metals to the ground water is not occurring, due to sludge stability.

Brunswick Mining and Smelting, Bathurst, N.B., Canada

The Brunswick Mining and Smelting Company operates a mine in the Province of New Brunswick, Canada. The ore contains considerable amounts of pyrite as well as the valuable sulfides of copper, lead, and zinc. Mining operations on current reserves are planned for another 30 years. A water treatment plant based on the HDS process was commissioned in the fall of 1993.

The topography of the property is such that although tailings and waste dump seepage could be conveniently collected, the catchment area for contaminated surface runoff was quite large and hydrological studies indicated that the 100-year event was expected to produce 750,000 L/min from the potentially contaminated catchment area, although a normal peak of 40,000 L/min was expected during spring runoff.

At the average feed rate of 22,000 L/min, metals at 150 ppm Fe, 100 ppm Zn, and pH 3.5 are expected with the worst case designed for 40,000 L/min with 230 ppm Fe, 200 ppm Zn and pH 2.0. The main HDS plant is designed to accept flows up to 60,000 L/min but at these flows metal loadings would be below the peak (and close to the average quoted above). Flows above 60,000 L/min may be possible but at very significantly reduced metal loadings.

At time of writing (November 1993) the plant was functioning well at a feed rate of 30,000 L/min producing a sludge of greater than 20% solids. Treated water discharge was meeting design specifications. The plant started treating water at reduced flows in order to make sludge for recycle. When sludge reached 12% solids, full operation was instituted. It took about 1 week to reach 18% solids in full operation, and 20% was exceeded by the second week.

Glenbrook Nickel Co., Coos Bay, OR, U.S.A.

The Coos Bay facility imports lateritic nickel ore from offshore. Water collected on the site includes runoff from ore storage piles. Although this water is close to neutral (pH 6.5) it contains soluble copper, nickel, and chromium at 1-ppm levels, as well as iron at several parts per million. The water had to be treated prior to discharge into the estuary of a salmon river.

A laboratory program determined that the metals presented no particular treatment problem, with the exception of chromium. Removal was effected by the addition of an iron salt and liming. Chromium removal required that a ferrous iron salt be added to the effluent prior to the addition of limed recycled sludge. The resulting mixture was aerated, flocculated and settled in a Delta stack clarifier, and the clarifier overflow was either discharged directly to the estuary, or clarified through a mixed-bed clarifier.

It is postulated that the ferrous iron addition reduced hexavelant chromium to its insoluble trivalent state and that this material was then co-precipitated onto the recycled sludge with the iron, which was then all oxidized to ferric. If ferric iron was added to the system, the chromium remained in solution, although nickel, iron and copper were removed. The sludge was disposed of by adding it to the lateritic nickel ore and shipping it to the smelter.

Tiwest, Kwinana, W.A., Australia

Tiwest is a titanium pigment plant treating mainly natural rutile in an acidic chloride digestion system. The iron-containing waste streams were previously neutralized with lime and thickened to about 6% solids. The Tiwest plant was operating a straight lime neutralization plant for the treatment of effluent from various waste waters emanating from its chloride based titanium pigment plant. Densities of the sludges were less than 6% and storage space was becoming a problem. Cominco Engineering Services Ltd. was retained to carry out test work and demonstrated in the mini-pilot plant sent to Australia that sludges of 20% solids could be made.

A flowsheet was produced that utilized as much as possible of the existing plant, in essence the only new requirement was the reactor tank where aeration of the slurry took place. Other modifications to the plant took place, such as the piping in of a slurry recycle line, and the utilization of tankage from the old liming plant as mix and reactor vessels. The gas dispersion agitator selected was of the "gas shear turbine" type, which has a significantly lower power requirement than the Rushton design. The plant has been running successfully since April 1992.

Conclusions

Based on applications in Canada and elsewhere, the HDS process has been shown to be an effective and economical method for the treatment of AMD. Experience to date suggests that the associated sludge is both dense and stable, and that no significant re-release of the precipitated metals to the environment takes place. The applicability of the technology is not limited to the treatment of mine drainages only, but the technology can be effectively applied to other industrial effluents that have significant quantities of dissolved heavy metals.

Acknowledgements

The authors wish to gratefully acknowledge the contributions of Walter Kuit, John Knapp, and Alan Humber.

Literature Cited

Busse, E. Acid drainage control and water treatment at Heath Steele. CIM Bulletin, November, 1974.

Genes,B.R., Scheibach, R.B., Jarman, R. Treatment technologies to abate acid mine drainage. Proceedings from National Conference on Environmental Engineering, February, 1991, Denver CO.

Gormely, L., Review of long term acid mine drainage costs at Equity Silver Mines. Report Prepared for the Province of British Columbia, Ministry of Energy, Mines, and Petroleum Resources, 1989.

Higgs, T.W, 1990 ARD, Treatment plant sludge-chemical stability and disposal considerations. GAC/MAC Joint Annual Meeting, Vancouver, B.C., May 16-18, 1990.

Kuit, W.J., Mine and tailings effluent treatment at the Kimberley, B.C. Operations of Cominco Ltd. CIM Bulletin, December, 1980.

Kuyucak, N., Mikula, R.J., Wheeland, K. Evaluation of improved lime neutralization processes. Part III. Interpretation of properties of lime sludge generated by different processes. Second International Conference on the Abatement of Acidic Drainage, September 16-18, 1991, Montreal, Quebec

Kuyucak, N., Sheremata, T., Wheeland, K., Evaluation of improved lime neutralization processes. Part I. Lime sludge generation and stability. Second International Conference on the Abatement of Acidic Drainage, September 16-18, 1991, Montreal, Quebec.

MacDonald, R.J.C., Kondos, P.D., Crevier, S., Rubinsky, R. and Wasserlauf, M. Generation of, and disposal options for Canadian mineral industry effluent treatment sludges. CANMET Mineral Sciences Laboratories Divisional Report MSL 89-45 (OP&J), 1989.

Norton, P.J., Engineered wetlands and AMD. Mining Environment Management. September, 1993, London, U.K.

Wasserlauf, M., Generation and stability of Canadian mine/smelter effluent treatment sludges. DSS Contract No. 14SQ.23440-5-9161 GML Project 7227-R-1, 1987.

SUBAQUEOUS DISPOSAL OF REACTIVE MINE WASTE: AN OVERVIEW AND UPDATE OF CASE STUDIES - MEND/CANADA[1]

W. Wayne Fraser[2] and James D. Robertson[3]

Abstract: A study of subaqueous disposal of reactive tailings started in 1988 with an initial overview of all known Canadian sites. A work plan was developed in 1989, which consisted of evaluating four lakes (Buttle and Benson Lakes, BC, Anderson and Mandy Lakes, MB) over 2-year periods for each lake. The initial year consisted of evaluating the biophysical features of each lake as a preliminary exercise in preparation for the second year of work. The second year consisted of performing detailed geochemical work on interstitial water at two or three sites in each lake. Each phase resulted in the preparation of a separate report.

At the request of MEND, a scientific and technical peer review of all work was done in 1992. This and presentations made to regulatory agencies provided feedback on the merits of use of subaqueous disposal to control reactive materials. Information deficiencies were also documented. Additional research work was undertaken to address these and support application of this method. A planning team of technical and scientific experts met in January 1993 and outlined a program which incorporated the peer review recommendations. Two lakes were selected to continue the field program and work has been undertaken to obtain additional data. Companion studies include technical literature reviews, comparison of field techniques, and the establishment of quality assurance and quality control programs.

A planned outcome is a manual on how to employ the technique for final disposal of reactive tailings.

Introduction

Worldwide research is in progress to find an economic and effective solution to acid mine drainage (AMD). Two coordinated programs have been initiated in Canada: the National Mine Environment Neutral Drainage (MEND) program and the British Columbia Mine Acid Drainage Task Force.

Disposal of tailings materials under a water barrier, such as in a lake, is thought to be one way to prevent acid generation, by preventing oxygen and bacterial action on the sulfide surfaces. Similar disposal may offer benefits in the handling of potentially acid-generating waste rock, although studies to date have not addressed this.

Random deposition of reactive tailings under water has been used at various mines in Canada. However, a thorough review has not been done of long-and short-term impacts at these historic sites, which could provide an understanding of the physical, chemical, and biological processes taking place.

This paper provides an overview of studies conducted and general results from each of four studied lakes, major collective results, and additional work required to develop criteria for applying this technology. Perhaps

---

[1] Paper presented at the International Land Reclamation and Mine Drainage Conference and the Third International Conference on the Abatement of Acidic Drainage, Pittsburgh, PA, April 24-29, 1994.

[2] W. Wayne Fraser, Director Environment, Hudson Bay Mining and Smelting Co., Ltd., Flin Flon, MB, Canada

[3] James D. Robertson, Manager Environmental Engineering, Placer Dome Inc., Vancouver, BC, Canada

as important, the paper outlines the planning process used to ensure that the concepts are properly understood and fairly reviewed by all those involved.

Public Policy Issues

The concept of disposing of tailings materials in lakes is controversial and in the past has generally not been acceptable to regulatory agencies or the public. Consequently, this study was initiated with the recognition that the possible scenarios for the application of subaqueous disposal were: not being acceptable in any lake, being of limited application in biologically barren (low productivity) lakes, or being applicable to biologically productive lakes under rigorous conditions. These scenarios are still valid. However, the policy that sets acceptable scenarios is only partly determined by technical and scientific evidence. The need for a comprehensive review program and consequent endorsement from regulators and other sectors was recognized in the original planning of this project.

Project Evolution and Study Schedule

The subaqueous study started in 1988 with an initial overview report, consisting of a literature review and case histories of historic mining activities in Canada where subaqueous disposal had been used for tailings materials (Rescan, June 1989). The intention was to identify and assess sites where detailed studies could help develop complete case histories. This report provided a basis for subsequent work planned in 1989 and performed from 1989-92 on four lakes. Buttle and Benson Lakes in British Columbia and Mandy and Anderson Lakes in Manitoba. (Figure 1) Information on mine history and tailings characteristics were reported as part of each of these investigations (Rescan, March 1990a,b,c,d).

Table 1. Subaqueous tailings disposal project study lakes.

Lake	Mineral mined	Tailings deposited (mt)	Tailings minerals and metals	Tailings discharge
Mandy, MB	copper,zinc.	73,000	pyrite, chalcopyrite, sphalerite.	1943-45
Anderson, MB	copper,lead, zinc.	7,300,000	pyrite, pyrrhotite, galena, sphalerite, chalcopyrite, arsenopyrite.	1979-present
Buttle, BC	copper,lead, zinc.	5,000,000	chalcopyrite, pyrite, galena, sphalerite.	1966-84
Benson, BC	N/A	N/A	chalcopyrite, pyrite.	1962-73

N/A not available

Study consisted of two phases conducted over two consecutive years for each lake. The first phase consisted of a preliminary surveillance of the biophysical conditions in each. It was recognized that, to withstand rigorous scientific scrutiny, more comprehensive studies of the chemical and physical lake dynamics would ultimately be required. The second phase was a detailed sampling program to core sediments under controlled conditions that prevented the oxidation and changes in the chemistry of the pore water. These geochemistry studies were to determine the general reactivity of tailings materials at the sediment/water interface, as determined by the chemistry profiles through the upper sediment layers. If initial results indicated that the tailings had been rendered unreactive, it could be concluded that this disposal method had high

potential for control of reactive tailings. Additional work would then be warranted to provide technical understanding of the overall natural system, and design and operating criteria for application of this methodology. The schedule for the studies is shown in Table 2.

Table 2. Study schedule

Topic	Phase	Year of Study	Phase	Year of Study
General overview of Canadian mines.	Planning	1988		
Buttle Lake.	Biophysics	pre 1989	Geochemistry	1989
Mandy Lake.	Biophysics	1989	Geochemistry	1990
Anderson Lake.	Biophysics	1989	Geochemistry	1990
Benson Lake.	Biophysics	1990	Geochemistry	1991

Study Results

Study results have been compiled (Rescan March 1990a,b,c,d) and summarized (Pederson et al. 1991).

Mandy Lake Studies

The preliminary studies (Rescan March 1990a) provided numerous observations:

- Mandy Lake is a small meso-eutrophic lake (area 239,000 m^2) with a mean depth of 3.6 m.
- Water quality in the lake was good and metals release from sediments appears to be minimal.
- Mandy Lake has diverse and abundant biota.
- Metals do not appear to be bioaccumulating in fish.
- Although metal levels are elevated in sediments in areas where tailings were deposited, an organic layer covering these sediments appears to reduce oxygen concentrations at the water-sediment interface and provide a barrier to metal release.
- Mandy Lake has rehabilitated naturally and speculation is that this will continue to do so.

The detailed geochemical studies (Rescan September 1990b) revealed the following:

- Despite the cessation of mining many years previous, tailings are widely distributed (possibly owing to slumping of the tailings fan) in modern sediments on the lake floor.
- Natural sediments underlying the tailings are organic-rich.
- The tailings-bearing deposits are suboxic or anoxic at very shallow depth below the sediment/water interface. Near shore, oxic conditions are indicated in at least the upper 5 mm.
- Concentrations of Zn, Cu and Pb in pore waters are very low. There is no apparent outflow of metals from the mixed tailings and natural organic-rich sediments.
- Tailings on the lake floor show little or no evidence of chemical reaction 46 yr after discharge.

Anderson Lake Studies

The preliminary studies (Rescan March 1990b) showed the following:

- Anderson Lake is a small biologically productive (meso-eutrophic) lake with a mean depth of 2.1 m.
- Present tailings discharges are adversely affecting water quality near the outfall and to a lesser extent in the whole lake. Drainage from exposed tailings (access roads) adjacent to the lake probably contributes to deterioration of water quality, as do hydroxide salts suspended in the water used to transport tailings to the lake. The relative contribution of these factors has not been determined.
- Petrographic and mineralogical examination of submerged and fresh tailings indicated a high sulfide content, mainly pyrite, and little oxidation of the sulfides.
- Benthic invertebrate densities were generally lowest near the tailings discharge point but comparable to those observed prior to tailings deposition. Although natural sediments near the outfall are initially buried by the tailings discharge, a veneer of organic material is deposited over time allowing benthic communities to re-establish.
- Fisheries resources in the lake have always been limited, possibly owing to winter kills or restricted stream access to the lake. Metal levels were higher in fish near the tailings outfall, particularly for Cu, Pb and Zn. High Zn in the fish correspond to high levels in the sediments.

The detailed geochemical studies (Rescan September 1990a) revealed:

- Mine tailings are widely distributed on the floor of Anderson Lake, not only near the discharge outfall but also in distal regions some 2 km from the discharge.
- Natural sediments underlying the tailings are extremely organic-rich.
- Tailings and sediments are suboxic or anoxic at very shallow depths below the sediment-water interface.
- Dissolved metals and sulfate are high in Anderson Lake, reflecting contamination from tailings slurry water and non-tailings sources.
- Despite high metal levels in lake water, metals in pore waters of both tailings and natural sediments are extremely low. This depletion must reflect continuous removal of metals from interstitial solution at very shallow depths at all sites.
- There is no evidence that tailings on the lake floor are releasing Zn, Cu or Pb to the overlying water. In fact, metals may be diffusing into the tailings and natural sediments from metal-rich bottom water.
- Once tailings discharge to Anderson Lake stops, organic-rich deposits will likely progressively blanket the tailings, ensuring that they remain stored in an anoxic state.

Buttle Lake Studies

A preliminary information base on Buttle Lake (Rescan March 1990a), compiled prior to 1988, allowed immediate planning for geochemistry work which was conducted in 1989. The results were:

- Buttle Lake is oligotrophic and is 35 km long. The tailings deposit is in the south basin (7 km long with maximum depth of 87 m), separate and effectively confined from the north basin by a shallow sill.
- Tailings are widely distributed across the south basin, and are being covered with a veneer of organic-rich sediments at a rate of about 4 mm $year^{-1}$. High solid-phase metal concentrations are still observed in the upper 5 mm, which presumably reflects upward mixing of tailings by burrowing infauna.
- The deposits are anoxic below depths of about 2 or 3 cm.
- Dissolved metals levels in pore waters in methane-bearing natural sediments underlying the tailings are extremely low, probably due to precipitation of authigenic sulfide minerals.

- Dissolution of Fe oxyhydroxides may be releasing heavy metals to interstitial waters at shallow depths. However, an Fe and Mn oxide-rich veneer at the core top is providing an absorbent veil which reduces upward diffusion of dissolved heavy metals from enriched zones below.
- In south basin deep water, metals are diffusing into the tailings; at other locations, there are very small effluxes of metals in most cases. The largest efflux - Zn - could increase the steady-state Zn content in deep water by <0.2 parts per trillion.
- Now-buried tailings in the south basin had a negligible impact on water quality.

Benson Lake Studies

Background studies (Rescan March 1990c) characterized the lake adequately for additional geochemistry studies. The results of this work were:

- Benson Lake is a reasonably small, deep (mean depth 25.5 m) soft-water oligotrophic coastal lake.
- Studies in 1967 and 1973 found the lake bottom covered by tailings and devoid of benthic life. The outlet river had a fine sediment bottom layer and was populated by turbid-water benthic invertebrates.
- The lake supports some fish, which feed on drift organisms carried by lake inlet streams. The fish have high zinc in their tissues; equally high concentrations were found in a nearby control lake (Keogh Lake).

Benson Lake studies (Rescan June 1992) followed the format of the other studies. Conclusions were:

- Pyrite-rich mine tailings were discharged into Benson Lake from 1962 to 1973.
- A thin veneer of manganese and iron oxyhydroxide-rich material mantles the deposits; natural sediments are suboxic or anoxic at very shallow depths below lake bottom.
- Dissolved metals are low in bottom waters; there is no evidence of efflux to overlying water.

Summary of Results

The following basic conclusions were developed from the initial studies of the four lakes:

- Reactivity of the tailing materials is low as illustrated by extremely low dissolved metals in interstitial pore water. This verifies the hypothesis of reduced reactivity due to submerged conditions.
- Preliminary estimates of metal flux rates from the sediments indicate that these are low and should have no significant impact on overall metal balances within the lakes.
- Basic physical conditions detected in each lake have allowed estimates of the chemical mechanisms acting to maintain low-reactivity in and around the tailings deposits.
- Biological communities exist in some of the lakes.
- Metal levels in water and fish are variable and depend on the history of the lake (active or abandoned). Some levels appear to be elevated while others are typical of background levels.

Scientific, Regulatory and Public Review; Planning Group

A strategy was evidently needed to review the results of studies. Elements were determined to include scientific peer review of completed and proposed work, government regulatory agency review of work and final reports, and public review of the overall concept and scientific database.

Following completion of work through 1991, the MEND Board of Directors requested a peer review of all work. Clearly, if subaqueous disposal is to be used, it has to be scientifically sound and well justified.

The Rawson Academy of Aquatic Science, an independent consulting group, was chosen to do the review. They, in turn, chose an expert panel (Appendix A). The objectives of the review were to conduct a technical and scientific review of all of the MEND studies on subaqueous disposal of tailings and to define additional requirements to establish the scientific credibility of the approach.

A scope for the review was developed (Rescan July 1992); the review established a number of key points.

- Subaqueous disposal of tailings appears to offer physico-chemical advantages over terrestrial disposal, particularly in preventing and/or controlling sulphide oxidation and generation of acid waters.
- The process of tailings disposal is potentially highly disruptive of lake ecosystems. Natural sedimentation would take decades to insulate the ecosystem from the potential influence of the tailings. However, remedial measures could perhaps limit the extent of impact and accelerate recovery.
- The MEND literature review of geochemical processes was comprehensive through 1992, but was inadequate on toxic effects, particle behaviour, field and analytical techniques, biological indices of whole lake effects, and the role of wetlands in metal stabilization.
- Background limnologies of the case-study lakes were adequate for gross comparisons but did not support clear interpretation of cause and effect.
- Data were sufficient to assess whether reactivity of tailings disposed under water remained low; the data were insufficient to address effects during disposal and long term ecosystem adjustment.
- Methods used for porewater extractions from the cores, and quality assurance/quality control (QA/QC) were of concern.
- More detailed studies of metal fluxes, rates of accumulation, whole lake response and seasonal variations should be done.
- Preferences for subaqueous tailings disposal would be, in order, infilling a small headwater lake, disposal in a manmade structure, and in-lake disposal where tailings represent a small part of total lake volume.

Following the peer review, presentations on the studies were made at a meeting of representatives of various federal and provincial agencies. No "fatal" technical flaw was identified by the representatives. Consequently, it was felt additional research work could proceed to address peer recommendations.

Future information sessions involving regulators will be held when enough new information is available to present. Meetings with the public and other interest groups are felt to be premature at this time.

A Planning Group of technical and scientific experts (Appendix B) has been assembled to ensure that the objectives of the program are being met. This group is not to be concerned about program costs or the sources of finances while developing a sound and complete program.

The planning team has focused on field and analytical techniques to improve measurement of metal fluxes at the sediment/water interface, and selected two lakes for continuing study: Buttle as a deep lake and Anderson as an active, relatively shallow site. The group planned a program to clarify understanding of the reactivity of the substrate, and to study the seasonal spectrum. Improved techniques to estimates metal flux, involving use of small dialysis chambers, or peepers, located at the water/tailings interface. The group also recommended at least three locations would be sampled in each lake for each sampling campaign, and duplicates of all cores and peepers would be required.

1993 Field Program

As recommended in the peer review, a literature review on metal toxicology was completed. (INRS-EAU March 1993).

Based on the Planning Group directions, detailed design was done for the 1993 field and laboratory programs. Formal documents for each study campaign were reviewed and signed-off by each group member. Through this, consensus on campaign strategy and technical details was achieved prior to field work. Each work plan had a detailed work scope and methods manual for field work (Rescan February 1993, Rescan et al. July 1993, Rescan October 1993) and QA/QC procedures for field methods. An equally detailed lab QA/QC manual (ASL and U BC March 1993) was prepared; this is the subject of a separate paper (Maynard April 1994).

Three major campaigns were conducted in 1993 - two on Anderson Lake and one on Buttle Lake. Timing of the Anderson campaigns was critical in that the metallurgical operation using the site, the only active disposal site available for study, was scheduled for shutdown in late 1993/early 1994. A further post-production campaign will be performed after operations cease. For Buttle, a fall 1993 study was conducted and a spring 1994 program is scheduled. Another - probably during winter 1994-95 - will complete seasonal gaps.

The various campaigns include water column sampling, sediment cores, and peepers, as well as measurement of field parameters. A special water column sampler was designed and applied to the winter and summer campaigns at Anderson Lake. A group of special studies is being run as well. At Anderson, manual diurnal temperature profiles are being obtained, and in-situ recording termister strings will provide a full data set of water column temperature profiles with changing seasons. Two weather stations erected to obtain temperature, wind and precipitation data, will assist in interpreting the other data and in developing future generic application criteria. For both the Buttle and Anderson programs, a cross-comparison is being done of two methods of handling samples from the peepers: under inert atmosphere or sample extraction under normal atmosphere. Preliminary results from the 1993 programs, particularly the high-resolution water column sampling, confirm the tentative findings from earlier studies (Pederson et al. April 1994).

Budget

Due to the duplicity of data collection required for QA/QC, recent campaigns cost approximately $0.25 million (Canadian) each. The completed program will, in total, cost $1.5 to $2.0 million (Canadian).

Proposed Additional Future Work

The basic elements of the original hypothesis have been successfully addressed, as the reactivity of the tailings studied has been demonstrated to be low. In addition, biological communities have been demonstrated to be present in the adjacent environment in some of the lakes studied. To more fully understand these systems, and to develop case history information that will withstand scientific, regulatory and public scrutiny, additional extensive technical supportive work is underway. Ideally, additional disposal lakes in other geographical and geological settings and operating mines utilizing a biological-active lake could be studied. Appropriate sites have not been found, and are not part of current planning.

Design and operating criteria for an application manual is also required. With continuing positive results from recent study campaigns, work on this should commence in 1994 in parallel with ongoing studies.

Conclusions

Completed work has demonstrated that subaqueous disposal has technical justification. Additional work requirements have been outlined, and are underway. Additional case histories would be useful to extend the findings geologically and geographically, but candidate lakes for study have not been found.

Scientific and regulatory review and planning is a major part of the program, and is assisting in achieving a fair and objective study of the concept and methodology for subaqueous disposal of reactive tailings in lakes. Though complex, it is as important as the technical study for the acceptance and application of this promising method of acid drainage control, and will continue over the entire program to the final objective of a design and application manual.

Acknowledgement

This work was supported by the British Columbia Ministry of Energy, Mines and Petroleum Resources, CANMET, Environment Canada, Hudson Bay Mining and Smelting and Placer Dome through the Mine Environment Neutral Drainage (MEND) Program and the British Columbia Acid Mine Drainage Task Force.

Appendix A

Members of Scientific Review Team

Dr. P.G.C. Campbell, INRS-Eau, 2700 rue Epstein, Ste. Foy, Quebec, G1V 4C7
Dr. P. Dillon, OME Research Station, POB 39, Dorset, Ontario, P0A 1E0
Dr. R. Hecky, Freshwater Institute, 501 University Crescent, Winnipeg, Manitoba, R3T 2N6
Dr. R.A. Ryder, Fisheries Research Section, OMNR, PO 2089, Thunder Bay, Ontario, P7B 5E7
Dr. P.G. Sly, Director Science Program, Rawson Academy of Aquatic Science, Ottawa, Ontario, K1A 7B7
Dr. R.L. Thomas, Director, Great Lakes Institute, University of Windsor, Ontario, N9B 3P4

Appendix B

Subaqueous Disposal Planning Group

W.W. Fraser, Hudson Bay Mining and Smelting, PO Box 1500, Flin Flon, MB, R8A 1N9
Dr. R. Hecky, Freshwater Institute, 501 University Crescent, Winnipeg, MB, R3T 2N6
Dr. J. Lawrence, National Water Research Institute, 867 Lakeshore Rd, Burlington, ON, L7R 4A6
Dr. T. Pedersen, University of BC, Dept. of Oceanography, 6270 University Blvd., Vancouver, BC, V6T 1Z3
C. Pelletier, Rescan Environmental Services Ltd., 510-1111 West Hastings Street, Vancouver, BC, V6E 2J3
J.R. Robertson, Placer Dome Inc., PO Box 49330, Bentall Postal Station, Vancouver, BC, V7X 1P1
Dr. P.G. Sly, Rawson Academy of Aquatic Sciences, Suite 404, 1 Nicholas Street, Ottawa, ON, K1N 7B7
G.A. Tremblay, CANMET/MEND, 555 Booth Street, Ottawa, ON, K1A 0G1

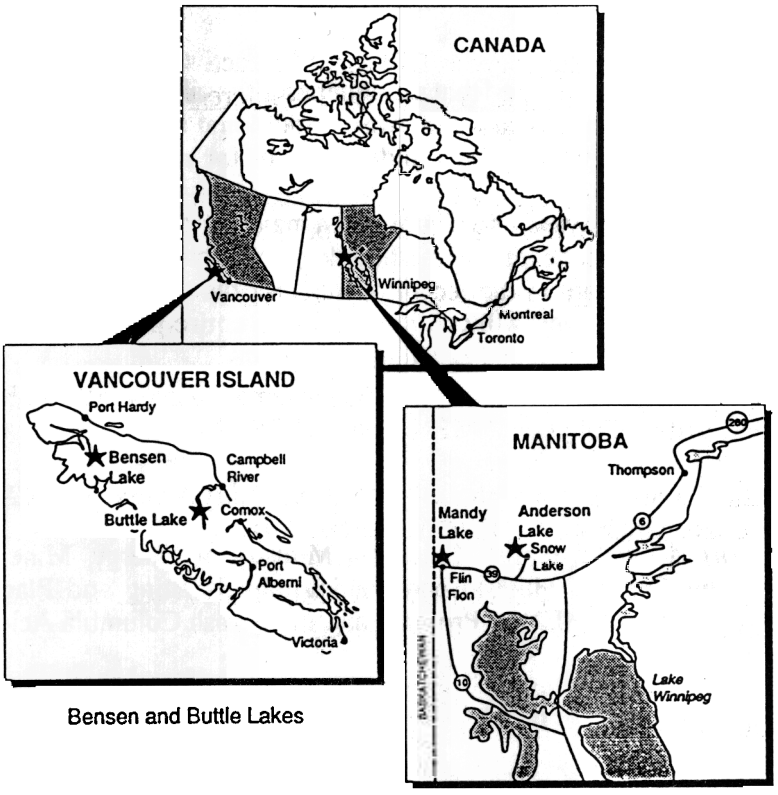

Bensen and Buttle Lakes

Mandy and Anderson Lakes

Figure 1. Location of project sites

Literature Cited

ASL Analytical Service Laboratories Ltd., University of British Columbia Department of Oceanography, March 1993, "Laboratory Analysis and Quality Assurance/Quality Control for the MEND Project - Anderson Lake Winter Survey." For: Placer Dome Inc.

INRS-EAU, March 1993, "Literature Review Report: Possible Means of Evaluating the Biological Effects of Sub-Aqueous Disposal of Mine Tailings." For: Placer Dome Inc.

Maynard, A.W., ASL Analytical Service Laboratories Ltd. "The Laboratory Component of Environmental Monitoring: A Case Study Involving Sub-Aqueous Tailings Research.) In: Third International Conference on the Abatement of Acidic Drainage. April 1994, Pittsburgh, PA.

Pedersen, T.F., Mueller, B., McNee, J.J., Department of Oceanography, University of British Columbia, Pelletier, C., Rescan Environmental Services, "Diagenetic Reactivity of Mine Tailings in Mesotrophic and Oligotrophic Lakes in Manitoba and British Columbia." In: Second International Conference on the Abatement of Acidic Drainage. September 1991. Montreal, Quebec.

Pedersen, T.F., McNee, J.J., Mueller, B., Department of Oceanography, University of British Columbia, Flather, D., Pelletier, C.A., "Geochemistry of Reactive Tailings in Anderson Lake, Manitoba and Buttle Lake,

British Columbia." In: Third International Conference on the Abatement of Acidic Drainage. April 1994, Pittsburgh, PA.

Pelletier, C.A., September 1991, "Subaqueous Disposal of Reactive Mine Waste: An Overview of the Practice with Case Studies". In: Second International Conference on the Abatement of Acidic Drainage, September 1991, Montreal, Quebec.

Rawson Academy of Aquatic Science, July 1992, "A Critical Review of MEND Studies Conducted to 1991 on Subaqueous Disposal of Tailings." MEND Report 2.11.1d.

Rescan Environmental Services Ltd. June 1989, "Subaqueous Disposal of Reactive Mine Wastes: An Overview." MEND Report 2.11.1a.

Rescan Environmental Services Ltd. March 1990a, "Geochemical Assessment of Subaqueous Tailings Disposal in Buttle Lake, British Columbia." MEND Report 2.11.1a.

Rescan Environmental Services Ltd. March 1990b, "A Preliminary Assessment of Subaqueous Tailings Disposal in Anderson Lake, Manitoba." MEND Report 2.11.1a.

Rescan Environmental Services Ltd. March 1990c, "A Preliminary Assessment of Subaqueous Tailings Disposal in Benson Lake, British Columbia." MEND Report 2.11.1a.

Rescan Environmental Services Ltd. March 1990d, "A Preliminary Assessment of Subaqueous Tailings Disposal in Mandy Lake, Manitoba." MEND Report 2.11.1a.

Rescan Environmental Services Ltd. September 1990a, "Geochemical Assessment of Subaqueous Tailings Disposal in Anderson Lake, Snow Lake Area, Manitoba." Mend Report 2.11.1b.

Rescan Environmental Services Ltd. September 1990b, "Geochemical Assessment of Subaqueous Tailings Disposal in Mandy Lake, Flin Flon Area, Manitoba." MEND Report 2.11.1b.

Rescan Environmental Services Ltd. June 1992, "Chemical Diagenesis of Submerged Mine Tailings in Benson Lake and Natural Sediments in Keogh Lake, Vancouver Island, British Columbia." MEND Report 2.11.1c.

Rescan Environmental Services Ltd. February 1993, "Subaqueous Tailings Disposal Study - Scope of Work for Anderson Lake Winter Survey (1993)." For: MEND.

Rescan Environmental Services Ltd., National Water Research Institute, Environment Canada, July 1993, "Subaqueous Tailings Disposal Study - Scope of Work for Anderson Lake Summer Survey (1993)." For: MEND.

Rescan Environmental Services Ltd. October 1993, "Subaqueous Tailings Disposal Study - Scope of Work for Buttle Lake Summer Survey (1993)." For: MEND.

Anyone wishing to obtain copies of the MEND reports in this list should contact: MEND Secretariat, Telephone 613-995-4681, Fax 613-996-9673.

THE LABORATORY QUALITY ASSURANCE COMPONENT OF ENVIRONMENTAL MONITORING: A CASE STUDY INVOLVING SUBAQUEOUS TAILINGS RESEARCH[1]

By Allan W. Maynard and Katherine B. Thomas[2]

Abstract: Assessments concerning the environmental impact of mining projects are highly dependent on reliable low-level analyses of samples collected from the receiving environment. The analytical program must be designed to maximize the reliability of the data and also provide information concerning the reproducibility, accuracy, specificity, and sensitivity of test results.

In Canada, the MEND (Mine Environment Neutral Drainage) Program has sponsored projects pertaining to comprehensive monitoring of subaqueous tailings disposal. Lake sediments, lake water, and interstitial water samples were collected and then analyzed for a host of parameters (metals, anions, physical tests, etc.). The analyses were carried out using state-of-the-art procedures and instruments. A comprehensive quality assurance-quality control (QA-QC) program was incorporated into the study with all QA-QC subsequently reported. The studies provide an ideal example of what is required, in terms of analytical approach, for projects that require extremely low detection levels and are subject to rigorous scrutiny by regulatory agencies, the scientific community, and the public.

This paper presents the QA-QC approach taken for the subaqueous tailings disposal work by discussing method selection, determination of detection limits, use of reference materials, laboratory and field QC samples, and criteria for assessing QC results. Representative QC data are presented to demonstrate validation of methodology and to show that pre-determined criteria were met. The results on all blanks were below limits of detection, the results on reference materials met suppliers 95% acceptance criteria and replicate results agreed to within ±15% of a calculated mean.

Additional Key Words: quality assurance, quality control, chemical analyses, detection limits, monitoring.

Introduction

The demand for high quality environmental laboratory services has grown rapidly, especially during the past 10 yr. Significant technical advances have been made with services and capabilities now routinely available that only a few years ago were the domain of research. There has been a dramatic trend toward multi-component determinations at very low concentrations in complex sample matrices. These requirements place an increasing burden on the laboratory and its ability to produce quality results.

The field of environmental analytical chemistry is no doubt a scientific field that has become vitally important to society by providing the required data to support environmental studies. The work produced by environmental laboratories is "under a lens", and this close scrutiny has been increasing over the years.

Government regulations have been the driving force in the rapid growth of the field of environmental analytical chemistry. In North America this sector is sophisticated and is dominated by regulatory, research, and private-sector laboratories. Laboratory managers have had to become increasingly proactive in educating industry, regulators, and the public about the field of measurement science. This has been especially important as regulators establish new

[1]Paper presented at the International Land Reclamation and Mine Drainage Conference and the Third International Conference on the Abatement of Acidic Drainage, Pittsburgh, PA, April 24-29, 1994.

[2]From ASL Analytical Service Laboratories Ltd., Vancouver, B.C., V5L 1K5.

envir..mental standards, compliance limits, and criteria. The setting of compliance limits will undoubtedly be based on many factors; the capability to measure must be among such considerations.

As users of environmental laboratories become more educated, their expectations become enhanced. Laboratories must now routinely provide evidence that they are accredited and/or certified and that they incorporate a comprehensive quality assurance program with all work programs.

Defining Laboratory Credibility

Laboratory credibility is established through "good laboratory practice" (GLP) which involves the complete management system for laboratory operation. While laboratories will, on their own initiative, establish GLP, it is necessary to obtain official recognition in the form of certification and accreditation. Certification is the formal recognition of the proficiency of a laboratory to carry out specific tests. It is determined by a procedure of submitting proficiency samples and defining the standards that must be met by the laboratories. Accreditation is a more comprehensive system that includes, along with a proficiency component, formal site visits by properly trained laboratory auditors.

In Canada, a national accreditation program has been established by CAEAL, or the Canadian Association of Environmental Analytical Laboratories (CAEAL 1993). In the United States, the ultimate goal is a national accreditation program, but at present accreditation is offered only in some of the individual States (IAETL 1993).

Defining Laboratory Quality

The U.S. Environmental Protection Agency (EPA) defines quality assurance (QA) as the total program for assuring the reliability of monitoring data. Quality control (QC) is defined as "the routine application of procedures for controlling the measurement process" (U.S. EPA 1986). In other words, QC consists of the technical, day-to-day activities used to assess the quality of the measurement process, while QA is the overall management system that ensures a QC program is in place and is working effectively.

Quality control is primarily concerned with the tools of the measurement system. This includes internal laboratory activities or quality control steps, and the preparation and analysis of quality control samples. Analysis of quality control samples allows the determination of precision, accuracy, sensitivity, and contamination control for the sampling and analysis process. There are two types of quality control (QC) samples: internal and external. Internal or laboratory quality control samples are prepared in the laboratory and include blanks, replicates, surrogates, spikes, and reference materials. These are defined in table 1. External or field quality control samples (table 1) are prepared in the field and should be handled exactly the same way as the collected environmental samples. The data produced from these samples provide information on the sampling techniques, sampling precision and bias, analyte stability, and cleanliness of sample containers.

The results of analysis of the QC samples provide valuable information on the precision (or repeatability) and the accuracy (how close the measurement is to the true value) of the analyses. The relationship between precision and accuracy is depicted in figure 1. It is the goal of analytical chemists to utilize analysis protocols that are both accurate and precise (category B of figure 1), but some tests required for regulatory purposes do not meet such criteria (Maynard 1990).

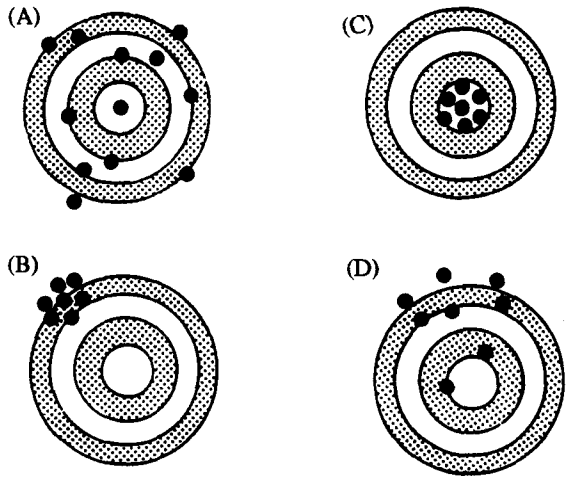

Figure 1. Relationship between precision and accuracy of analytical measurements. A, Poor precision, mean accuracy acceptable; B, good precision, good accuracy; C, good precision, poor accuracy; D, poor precision, poor accuracy.

Table 1. Definitions of laboratory and field QC samples

QC Sample	Definition	Purpose
Laboratory		
Method blank	Distilled water or "clean sample matrix" with added reagents, which is carried through procedure.	To monitor laboratory contamination.
Laboratory replicate	A homogenous sample that is split in the laboratory.	To monitor precision.
Surrogate compounds	Primarily used in organics analysis-consists of deuterium-labelled compounds or non-naturally-occurring fluorinated or brominated compounds which are added to the samples prior to their extraction or purging.	Quantified independently of the authentic compounds to monitor accuracy.
Sample spike	A sample to which a known amount of analyte is added.	To provide information on matrix effects and apparent accuracy.
Standard reference material (SRM)	A material that contains a known concentration of the analyte in question.	To determine accuracy.
Field		
Transportation blank	A sample container that contains distilled or de-ionized water and accompanies the sample containers into the field and is returned to the laboratory unopened.	To monitor contamination from the sample or shipping container.
Field blank	Distilled and de-ionized water that has been exposed to the same conditions and treatment as the environmental samples.	To monitor potential field sampling contamination.
Field analyte spike	Distilled and de-ionized water and preservation chemicals that are spiked in the field with a supplied solution containing a known concentration of the analytes of interest.	To monitor analyte degradation from the time of sampling.
Field replicate	A homogenous sample that is split in the field.	To monitor precision.

Defining Sensitivity

Sensitivity is an important component of monitoring programs required by the mining industry because ambient samples must be analyzed to detect trace (i.e., parts per billion or even parts per trillion) levels of certain analytes (especially metals). Sensitivity is defined by the detection limit, which is defined as the smallest amount of an analyte that can be measured with a stated confidence.

The American Chemical Society established a clear distinction between the detection and quantitation of an analyte (Keith et al. 1983). The limit of detection (LOD) was defined as the concentration equivalent to three times the standard deviation of the "noise" or background signal of an instrument. The limit of quantitation (LOQ) was defined as 10 times the standard deviation of the background signal.

The U.S. EPA further assessed this definition and stated that the signal-to-noise ratio provides a basis for estimating the sensitivity of the instrument alone (U.S. EPA 1985). The U.S. EPA protocols therefore required that detection limits be defined as full "method detection limits" or MDL's. The MDL is considered the most realistic approach to calculating a detection limit because it is based on a complete analytical procedure. The process involves an actual determination of detection limit by analyzing a number of low-level spikes in reagent grade water. The MDL method has been adopted by the U.S. EPA (U.S. EPA 1985) and the Canadian Association of Environmental Analytical Laboratories (Maynard 1992) and was used to define detection limits for the present program.

Summary of Monitoring Requirements for Subaqueous Tailings Disposal Project

In Canada, research has been undertaken to assess the potential impact of subaqueous disposal of mine tailings. Disposal of tailings materials under a water barrier, such as a natural lake, is thought to be one solution to stopping acid generation by preventing oxygen and bacterial action on the sulfide surfaces (Fraser and Robertson 1994).

The 1993 monitoring program involved two Canadian lakes: Anderson Lake in Manitoba and Buttle Lake in British Columbia. Both receive tailings from copper-lead-zinc mines. Details covering these studies are presented by Fraser and Robertson (1994) and by Pedersen et al. (1994).

The primary objective of the subaqueous tailings disposal monitoring program is to provide an estimation of the metal fluxes between the sediment and the water. The comprehensive sample collection process is described by Pedersen et al. (1994) and was carried out by designated field personnel. The samples collected include sediment cores, lake waters from various depths, and interstitial waters. The latter was collected by two techniques: (1) from a process involving coring, extrusion, and centrifugation and (2) utilizing in situ dialysis chambers.

All sample storage containers were cleaned and prepared by the laboratory, and the collected samples were subsequently returned within 1 to 2 days of collection. The analyses undertaken on these various samples are presented in table 2. In all cases, the methods were selected on the basis of providing optimum sensitivity, especially with respect to the various water samples, given that some parameters were expected to be at or below detection. The water quality methods are described in APHA (1992) and the sediment methods were based on EPA (1986).

Quality Program for Subaqueous Tailings Disposal Project

The subaqueous tailings disposal monitoring program requires extremely low detection limits, and the generated results are subject to rigorous scrutiny by regulatory agencies, the scientific community, and the public. For this reason the quality assurance program was expanded beyond what would be considered normal for routine environmental monitoring.

Laboratory QC

Laboratory QC samples were included with each analytical batch at a target level of about 40%, as outlined in table 3. Although batch sizes varied for different parameters and sample types, this approximate level of QC was maintained throughout the program.

Most of the interstitial water samples had insufficient volumes to replicate all of the analyses. It was, however, possible to replicate those analyses that only required low volumes (i.e., metals by graphite furnace atomic absorption spectrophotometry).

The reference materials used for this project are presented in table 4 and were selected on the basis that their matrix and concentration levels would approximate those of the actual samples. It was known, however, that these reference materials would not readily match the matrix of the interstitial water samples analyzed. For this reason, analyte spiking (for metals) was employed as additional QC.

Table 2. Analysis requirements for subaqueous tailings disposal project.

Parameter	Lake water	Sediments	Interstitial waters
Physical tests	✓	—	—
Anions	✓	—	—
Nutrients:			
NH3—N	✓	—	—
NO3—N	✓	—	—
Total N	—	✓	—
Total P	✓	—	—
Carbon (organic)	✓	—	—
Elements:			
As	✓	✓	✓
C	—	✓	—
Ca	✓	—	—
Cd	✓	✓	✓
Co	—	✓	—
Cr	—	✓	—
Cu	✓	✓	✓
Fe	✓	✓	✓
Hg	✓	✓	✓
K	✓	✓	—
Mg	✓	✓	—
Mn	✓	✓	✓
Na	✓	✓	—
Ni	—	✓	—
Pb	✓	✓	✓
S	—	✓	—
Zn	✓	✓	✓

✓ = analysis performed; — = analysis not performed.

Table 3. Incorporation of quality control (QC) samples: target batch.

Sample type	Number per batch[1]
Actual samples	20
Method blanks	2
Sample replicates	3
Reference materials	3
% QC samples	40

[1] Total numbers varied for different parameters and sample types, but percentage QC was consistent.

For samples with analyte concentrations near or below the detection limit, a spike level of approximately four to five times the detection limit was employed. For samples with higher concentrations, the spike was carried out at two to three times the concentration in the actual sample.

The quality control data were evaluated on a batch-by-batch basis and were reported along with the sample results. Predetermined criteria were adopted for data acceptability as presented in table 5. If data did not meet the target criteria, but met the warning criteria, also listed in table 5, they were accepted, but detailed explanations were provided. If data had not met the warning criteria, the analytical batch would have been repeated.

The results of all the QC analyses were presented in the reports. A typical presentation showing blanks and reference materials is shown in table 6. These results are representative of the findings throughout the study. With few exceptions, the target criteria outlined in table 5 were met.

Table 4. Reference materials used for subaqueous tailings disposal project.

Reference material	Description
Sediments	
NRC[1] PACS-1	Harbour sediment certified for trace metals.
NRC[1] MESS-2	River estuary sediment certified for trace metals.
NRC[1] BSCC-1	River sediment certified for trace metals.
Waters	
NWRI[2] ANI-04	Lake water certified for general water quality.
NRWI[2] ION-96	Lake water certified for general water quality.
NWRI[2] TM-02	Lake water certified for trace metals.
NWRI[2] TM-21	Lake water certified for trace metals.
APG[3] (current lot)	Prepared water certified for trace metals.

[1] NRC = National Research Council of Canada (Ottawa, ON); [2] NWRI = National Water Research Institute (Burlington, ON); [3] APG = Analytical Products Group (Belpre, OH).

Table 5. Pre-determined criteria for data acceptability.

QC sample	Predetermined criteria
Target criteria	
Method blank	Below detection limit.
Laboratory replicate	Agree to within ±10% of a calculated mean[1].
Reference material	Meet manufacturers and/or suppliers' 95% acceptance criteria.
Warning criteria	
Method blank	Less than 5 times the detection limit[2].
Laboratory replicate	Agree to within ±15% of a calculated mean.
Reference material	Meet calculated 99% acceptance criteria.

[1] Only when sample concentrations are greater than 10 times the detection limit; [2] Method blank results must be less than the lowest reported result.

Table 6. Representative results for laboratory blanks and reference materials.[1]

Parameter	Results-analysis of blanks (range)[2]	Results-analysis of reference materials (range)[3]	Reference material target values
Conductivity	1.3-2.7	[4]597-617	607.3±33.7
Alkalinity	<1.0-<1.0	[4]84.6-86.8	79.6±5.52
Chloride	<.5 -<.5	[4]57-2-57.9	56.8±3.59
Sulfate	<1.0-<1.0	[4]114-116	112.3±10.2
Nitrate	<.005-<.005	[4]1.96-2.02	2.03±0.6
Cd	<.0002-<.0002	[5].0205-.0215	0.0210±0.0035
Cu	<.0005-<.0005	[5].0500-.0610	0.0541±0.0098
Fe	<.003-<.003	[5].043-.053	0.050±0.016
Pb	<.0005-<.0005	[5].0219-.0285	0.0259±0.0052
Hg	<.00001-<.00001	[6].00170-.00190	0.00173±0.00039

[1] All results are expressed as milligrams per liter (ppm); < = less than the stated detection limit; [2] n = 4; [3] n = 5;
[4] NWRI RM-ANI-04 - see table 4; [5] NWRI TM-02 - see table 4; [6] APG Lot 10369 - see table 4.

Detection Limit Validation

It was recognized that very low detection limits would be required for the subaqueous tailings disposal monitoring project. The methods employed were selected to provide optimum detection limits. All detection limits quoted for this project are MDL's. In most cases they were reverified specifically for this project. To determine the MDL's, or method detection limits, a laboratory standard, containing the analyte of interest was prepared at a concentration of five times the proposed detection limit. Eight replicates were then processed through the entire analytical procedure. Using the eight measurements obtained, the mean and standard deviation were calculated, and the MDL was computed as follows (EPA 1985):

$$MDL = S \bullet t\ (n-1, \alpha=0.99),$$

MDL = the method detection limit,
t = the Student's t value appropriate for a 99% confidence level and a standard deviation estimate with n-1 degrees of freedom (for eight replicates, t=2.996),
S = standard deviation of the replicate analyses.

Table 7 lists the reverified MDL's.

Field QC

The sampling program for the subaqueous tailings disposal monitoring required extensive field handling of the samples. All samples were prepared in an oxygen-free environment to prevent rapid oxidation of reduced species. This handling included filtration of lake waters, coring and extrusion to prepare interstitial waters, and sediment core fractionations. It was necessary to employ a rigorous field QA-QC program to demonstrate adequate contamination control and representative sample preparation.

Table 7. Validation of detection limits for trace metals.[1]

Parameters	Target detection limit[2]	Spike Level[3]	Number of Replicates	Mean	Standard deviation (S)	Calculated method detection limit
Cd	.0002	.0010	8	.00091	.00004	.0001
Cu	.0005	.0020	8	.0021	.0001	.0004
Fe	.001	.005	8	.006	.001	.003
Pb	.0005	.0020	8	.0019	.0001	.0003
Mn	.001	.005	8	.0045	.0000	.0001
Zn	.001	.005	8	.0042	.0001	.0003

[1] All results are in milligrams per liter (ppm); [2] As agreed to prior to initiating project; [3] Concentration into reagent- grade water.

Transportation blanks (normally 2 for every 20 samples) were prepared in the laboratory and sent to the field. These samples were analyzed upon their return to the laboratory. Sample replicates were collected in the field (about 2 to 3 for every 20 samples) and submitted to the laboratory as blind samples. Field filter blanks were also prepared using field filtration equipment (approximately 1 for every 20 samples).

Due to the ice on the surface and the shallow nature of the lake being studied (Anderson Lake, MB), a unique water column sampler was designed for this project. This sampler contained long lines of tubing to obtain samples from specific depths. There was concern that metals could become adsorbed onto the tubing during this process. It was also necessary to investigate the possibility of cross contamination between samples. Prior to sample collection the following laboratory-prepared solutions were pumped through one of the sampling lines:

Distilled and de-ionized water (SAMPLER BLANK #1).
A solution of known metal concentrations (0.2 to 5 ppb) to assess possibility of adsorption (SAMPLER SPIKE #1).
Then, after rinsing, a second volume of distilled and de-ionized water (SAMPLER BLANK #2).
A solution of known concentrations that matched the more contaminated locations in Anderson Lake to assess possibility of carryover (SAMPLER SPIKE #2).
Then, after rinsing, a third volume of distilled and de-ionized water as a second step in assessing carryover (SAMPLER BLANK #3).

All of the resulting solutions were then analyzed, and the results are presented in table 8.

Table 8. Representative results of analysis of field sampler blanks and spikes.[1]

Parameter	Blank #1	Spike #1 (low)	Blank #2	Spike #2 (high)	Blank #3
As	<.0001	.0049 (98)	<.0001	—	<.0001
Cd	<.0002	.0060 (120)	<.0002	—	<.0002
Cu	<.0005	.0047 (94)	<.0005	.052 (104)	<.0005
Fe	<.003	.005 (100)	<.003	—	<.003
Pb	<.0005	.0048 (96)	<.0005	—	<.0005
Mn	<.001	.004 (80)	<.001	—	<.001
Hg	<.00001	.00025 (71)	<.00001	—	<.00001
Zn	<.001	.002 (100)	<.001	.496(99)	<.001

[1]All results are expressed as milligrams per litre (ppm); < = less than the stated detection limit; values in parentheses are % recovery for the spike.

Summary

The subaqueous tailings disposal monitoring program described in this paper provided unique challenges with respect to sampling design, sample collection, sample analysis, and data management. Specifically, concerning the laboratory component, the procedures had to provide optimum detection limits on complex sample matrices, many of which (the interstitial water samples) were extremely low in volume. It was necessary to incorporate a comprehensive quality program to ensure that these challenges were properly met. The quality control data generated from these studies provided reliable information concerning the precision, accuracy, and sensitivity of the test procedures selected.

Literature Cited

American Public Health Association (APHA). 1992. Standard methods for the examination of water and wastewater. 18th ed. American Public Health Association, Inc., Washington DC.

Canadian Association of Environmental Analytical Laboratories (CAEAL). 1993. Laboratory accreditation program. Ottawa, ON.

Fraser, W.W. and J.D. Robertson. 1994. Subaqueous disposal of reactive mine waste: An overview and update of case studies. (These proceedings.)

International Association of Environmental Testing Laboratories (IAETL). 1993. Panel discussion on the status of national accreditation. 1993 annual meeting of the IAETL. (San Diego, CA, 1993).

Keith, L.H., W. Crummett, J. Deegan Jr., R.A. Libby, K.K Taylor, and G. Wentler. 1983. Principles of environmental analysis. Anal. Chem. 55: 2210-2220.

Maynard, A.W. 1992. Environmental standards and limits: Consideration of results at or near detection limits. Env. Sci. and Eng. Feb. - Mar. 1992, p. 44-49.

Maynard, A.W. 1990. Environmental tests: Are they valid? Chemtech. March 1990, p. 151-155.

Pedersen, T., J. McNee, B. Mueller, D. Flather, and C. Pelletier. 1994. Geochemistry of reactive tailings in Anderson Lake Manitoba and Buttle Lake British Columbia. (These proceedings.)

U.S. Environmental Protection Agency (EPA). 1985. National primary drinking water regulations; volatile synthetic organic chemicals: final rule and proposed rule. U.S. EPA, 40 CFR Parts 141 and 142 (Nov. 1985).

U.S. Environmental Protection Agency (EPA). 1986. Test methods for evaluating solid wastes. Office of Solid Waste and Emergency Response.

Acknowledgements

This work was supported by the British Columbia (BC) Ministry of Energy, Mines and Petroleum Resources, CANMET, Environment Canada, Hudson Bay Mining and Smelting, and Placer Dome through the BC Acid Mine Drainage and Mine Environment Neutral Drainage (MEND) task forces.

We gratefully acknowledge the support of individuals involved in the actual study: W. Fraser of Hudson Bay Mining and Smelting, J. Robertson of Placer Dome, T. Pedersen and J. McNee of University of BC, and D. Flather of Rescan Environmental Services. We also acknowledge the assistance of Carol Hyde, who prepared this manuscript.

SUBAQUEOUS DISPOSAL OF MINE WASTE: LABORATORY INVESTIGATION[1]

Kim A. Lapakko[2]

Abstract: Laboratory experiments were conducted for 120 weeks to examine the effect of three different subaqueous disposal techniques on the oxidation of sulfide minerals present in Virginia Formation hornfels rock containing about 14 wt % pyrrhotite ($Fe_{0.9}S$). The subaqueous techniques were unmodified subaqueous disposal, subaqueous disposal with alkaline addition, and pretreatment (rinsing and neutralization) of rock prior to subaqueous disposal and subsequent alkaline addition. The pH of drainage from the two controls, representing on-land disposal, ranged from 3.7 to 4.2 during the initial 100 weeks, then decreased rapidly to 3.2 at 120 weeks. During the first 100 weeks the sulfate release rates averaged roughly 2.0×10^{-12} mol per gram rock per second; concurrent with the pH decrease, rates for controls increased to 5.6×10^{-12} and 13×10^{-12} mol per gram rock per second. For unmodified subaqueous disposal, pH declined steadily from 4.5 initially to 3.5 after 120 weeks. The pyrrhotite oxidation rates for the three subaqueous disposal techniques were 1.5×10^{-12}, 1.7×10^{-12}, and 2.2×10^{-12} mol per gram rock per second, respectively. With the exception of some initial rapid sulfate release from rock that was not pretreated, these rates were relatively constant over the course of the experiment. The rates observed in the laboratory were used, in conjunction with existing knowledge on oxygen transport, to determine rates of acid production for subaqueous disposal of similar mine waste in an open pit.

Additional key words: acid mine drainage, pyrrhotite, oxidation, rates, kinetics

Introduction

Subaqueous disposal has been gaining favor as a preferred option for mine waste disposal. This trend is the result of documentation of cases in which the oxidation of the sulfide minerals present in tailings has been retarded as a result of their disposal in lakes (Rescan Environmental Services Ltd 1989, Pedersen et al. 1990, Pedersen et al. 1991, Robertson 1991) and in mines (Rescan Environmental Services Ltd 1989). Ritcey (1991) cautioned that subaqueous disposal of partly oxidized waste, such as this waste rock, would result in release to the water of acidic reaction products that had accumulated on the mine waste surface. Disposal of partly oxidized waste in pits in British Columbia (Equity Silver Ltd. 1988) and the Yukon (Morin 1993b) resulted in acidification of the mine pit water. In another case, waste rock that produced acidic drainage while stored on land was relocated, along with a limestone amendment, into an open pit in 1988. The pit was subsequently flooded, and Veillette and Desrochers (1991) reported that the results through 1990 were favorable.

Although the rate of oxidation may be inhibited, sulfide minerals can oxidize in a subaqueous environment (City Resources Limited and Norecol Environmental Consultants Ltd. 1988, Moses and Herman 1991, Yanful and Payant 1992). The rates of oxidation and the resultant water quality are dependent upon site-specific conditions (Morin 1993a). Empirical determination of sulfide mineral oxidation rates for specific mine wastes in the laboratory, in conjunction with the existing knowledge on the diffusion of oxygen in water, allows calculation of site specific oxidation rates and the resultant water quality. Morin (1993a) used this approach to calculate rates of pyrite oxidation, and the attendant acid production, under various subaqueous disposal conditions.

In the present study the subaqueous oxidation of pyrrhotite ($Fe_{0.8\text{-}1}S$) present in mineralized Virginia Formation hornfels is examined. The complete oxidation of $Fe_{0.9}S$ is expressed as follows:

---

[1]Paper presented at the International Land Reclamation and Mine Drainage Conference and the Third International Conference on the Abatement of Acidic Drainage, Pittsburgh, PA, April 24-29, 1994.
[2]Kim A. Lapakko, Principal Engineer, Minnesota Department of Natural Resources, Division of Minerals, St. Paul, MN, USA.

$$10Fe_{0.9}S + (87/4)\ O_2 + (47/2)\ H_2O = 9\ Fe(OH)_3 + 10\ SO_4^{2-} + 20\ H^+ \quad (1)$$

The water quality associated with this oxidation and the rates of oxidation under laboratory conditions are compared for on-land (subaerial) disposal and three variations of subaqueous disposal. The rates determined in conjunction with existing knowledge of oxygen transport are used to extrapolate the laboratory data to in-pit disposal in the field.

Objectives

The objectives of this experiment were to describe the oxidation of sulfide minerals present in mineralized Virginia Formation rock under the following conditions:

In a subaerial (on-land disposal) environment in which the mine waste is subjected to wet-dry cycling,
2. In a submerged environment,
3. In a submerged environment with regular alkaline addition, and
4. In a submerged environment with regular alkaline addition, after removal of trace metal and acid reaction products from the hornfels surface.

The final objective was to extrapolate laboratory results to conditions of in-pit disposal in the field

The wet-dry cycling environment represents disposal of the hornfels on land, with alternate periods of oxidation and flushing of oxidation products. The second condition represents the disposal of partly oxidized rock in an underwater environment, with no subseqent mitigation. The third condition includes addition of alkalinity after the disposal described by condition 2. The fourth condition includes "pretreatment" of the hornfels by removing the metals and acid on the rock surface. The rock is then handled as described in condition 3. This pretreatment was investigated as a means of removing acid and trace metals from partly oxidized wastes prior to subaqueous disposal.

Methods

Materials

The rock used in the experiment was mineralized Virginia Formation hornfels (VFH) which was collected, crushed, and wet-sieved in March 1989. The plus 270-minus 100-mesh fraction (0.053 < particle diameter ≤ 0.149 mm) was retained for experimental use and stored in plastic bags until the inception of this experiment in September 1990. Sulfur contents, as determined by LECO furnace, of the two samples used in the study were 5.13% and 5.96%, respectively. Acid digestion (U. S. Bureau of Mines 1980) and digestate analysis by atomic absorption spectrophotometry (Perkin Elmer 603) indicated that over 97% of the sulfur was associated with iron (table 1). X-ray diffraction and electron microscopy (SEM/EDS) of a heavy mineral concentrate indicated the

Table 1. Sulfur, trace metal, and pyrrhotite content of mineralized Virginia Formation hornfels samples. (All values in wt %.)

Sample	S	Cu	Ni	Co	Zn	Pyrrhotite
			0.052			
			[3].068			

[1] Used for on-land, unmodified subaqueous, and subaqueous with alkaline addition simulation
[2] Used for pretreated subaqueous with alkaline addition.
[3] Average of analyses of duplicate samples.

presence of both hexagonal ($Fe_{0.9}S$) and monoclinic ($Fe_{0.875}S$). The pyrrhotite content of the samples was calculated based on the chemical analyes and the hexagonal pyrrhotite formula. Transmitted light microscopy of a similar

mineralized VFH sample (Graber 1990) indicated the rock contained 32% quartz, 32% opaques (sulfides, oxides, and graphite), and 19% of a clay mineral, probably kaolinite. Feldspar and chlorite each contributed 5%, and phlogopite and muscovite each contributed 4%.

Dissolution Procedures

To simulate on-land disposal, duplicate 75-g samples were placed onto a perforated plastic plate (covered by a glass fiber filter) in the upper segment, or reactor, of a two-stage filter unit (fig. 1). Prior to the inception of the experiment, the reactor was placed onto the lower segment (receiving flask) of the unit, upon which was placed a 0.45-μm filter. Samples were then rinsed with three distilled water volumes of 200 mL, to remove products that accumulated from oxidation during sample storage. To each reactor, 200 mL of distilled water was added and allowed to stand for 5 min; it was then drawn by vacuum through the mine waste sample and 0.45-μm filter into the receiving flask. This rinsing was repeated weekly for 120 weeks.

Between rinses the solids were retained in the reactors to oxidize further and stored in individual compartments of a wooden housing. A thermostatically controlled heating pad was placed beneath the housing to control temperature. The reactors were stored in a small room equipped with an automatic humidifier and dehumidifier, to maintain a stable range of humidity. Temperature and relative humidity were monitored two to three times a week. The average weekly temperature ranged from 21.7° to 28.6° C, with an average of 25.8° C and a standard deviation of 1.1° C (n=118). The relative humidity ranged from 38% to 67%, with an average of 53.6%, and a standard deviation of 5.6%.

The volume of rinse water, or drainage, was determined by weighing the receiving flask. pH was analyzed directly in the lower stage of the reactor, and aliquots were withdrawn for on-site determinations of specific conductance, acidity, and alkalinity Samples were also taken for subsequent analysis of metals and sulfate. Samples taken for metal analyses were acidified with 0.2 mL AR Select nitric acid (Mallinckrodt) per 50 mL sample.

The three underwater disposal conditions were all examined in duplicate. In each case 200 g hornfels and 1.8 L of distilled water were added to a 2-L Erlenmeyer flask. Glass wool was placed in the mouth of the flask to retard evaporation while allowing oxygen transport into the flask. The flasks were stored in the same controlled temperature and humidity room as the wet-dry cycle reactors. The pH of the solution was measured directly by inserting the electrode into the flask. Samples were withdrawn from a depth of about 8.3 cm in the flasks, which had an average water depth of 13 cm, for determination of specific conductance and alkalinity or acidity. The remaining sample was filtered (0.45 μm) for subsequent determination of sulfate, calcium, and magnesium. Samples taken for metal analyses were

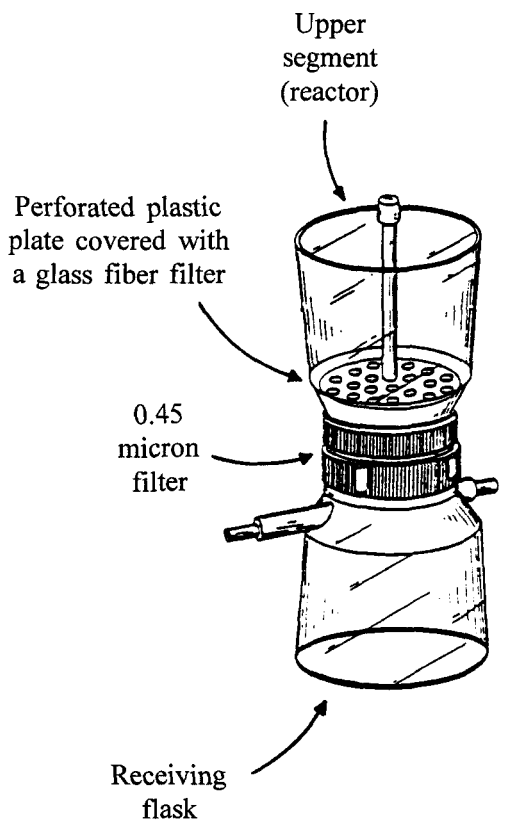

Figure 1. Reactor design.

acidified with 0.2 mL AR Select nitric acid (Mallinckrodt) per 50 mL sample. Distilled water was added to maintain a constant volume within the flasks.

For the first subaqueous disposal condition, untreated rock was placed into the flasks with no further modification. For the second disposal condition, untreated rock was placed into the flasks, and an alkaline solution (hydrated lime dissolved in distilled water) was added when the pH in the flask dropped below 7.25. The alkalinity of this solution typically ranged from 1,400 to 2,000 mg/L as $CaCO_3$.

For the third subaqueous disposal condition, the 200-g rock samples were first rinsed with approximately 5.7 L of distilled water to remove acid and other products generated by weathering. The samples were next rinsed with 4.1 L of a solution of hydrated lime and distilled water (average alkalinity 1,030 mg/L as $CaCO_3$). A subsequent rinsing with 6.4 L of a solution of sulfuric acid and distilled water (average acidity 310 mg/L as $CaCO_3$) because the alkaline solution rinses produced a pH in excess of 11 on the rock sample surface. In total, each sample was subjected to 151 rinses of 100 to 120 mL. For the final rinse, 100 mL of distilled water was passed through the solids bed, and the pH of the effluent was between 7.6 and 7.8.

Analysis

An Orion SA 720 pH meter with a Ross combination pH electrode (8165) was used for pH analysis, and a Myron L conductivity meter was used to determine specific conductance. Alkalinity and acidity were analyzed using standard titration techniques (APHA et al. 1992). Sulfate was analyzed using an HF Scientific DRT-100 nephelometer for the barium sulfate turbidimetric method (APHA et al. 1992). Calcium and magnesium were analyzed at the MN DNR Minerals Office in Hibbing using a Perkin Elmer 603 atomic absorption spectrophotometer in the flame mode.

Results

The drainages from the duplicate reactors simulating on-land disposal exhibited similar temporal variations in quality over the 120-week period of record. The drainage quality clearly indicated that the rock was a fairly strong acid producer. During the initial 90 to 105 weeks the drainage composition was fairly stable, with pH ranging from 3.6 to 4.0 and sulfate concentrations typically between 40 to 65 mg/L (fig. 2). It should be noted that sulfate concentrations were highest in the initial rinse and decreased until

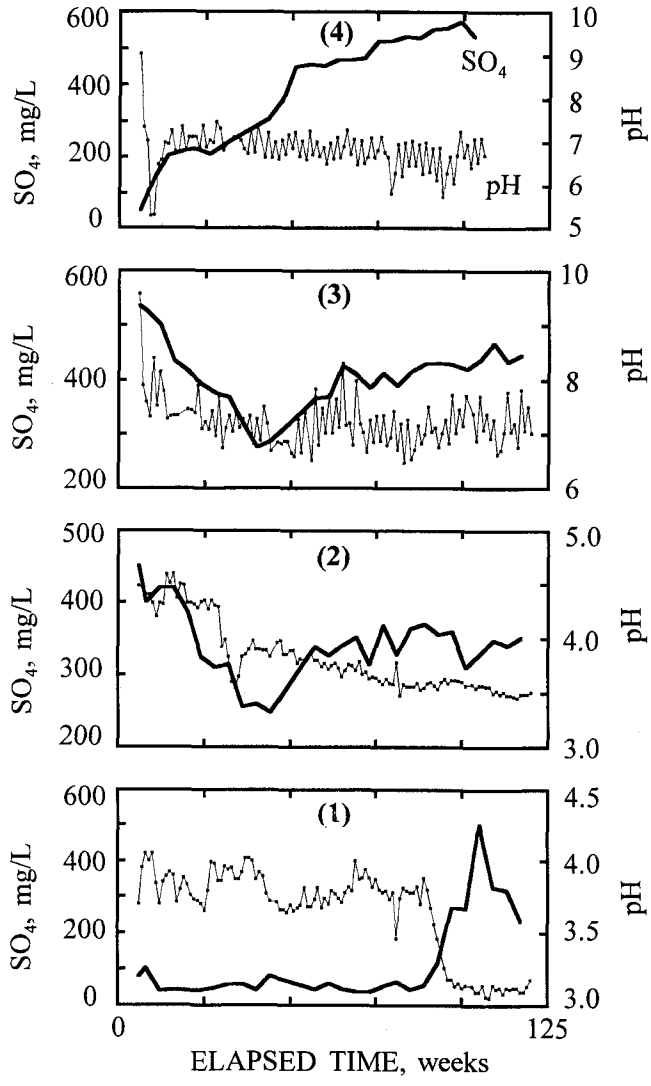

Figure 2. Solution pH and sulfate concentrations for (1) on-land disposal, (2) unmodified subaqueous disposal, (3) subaqueous with alkaline addition, (4) pretreated rock, subaqueous disposal with alkaline addition. Acidic solutions were produced by (1) and (2).

week 10, reflecting the release of oxidation products which accumulated between sample crushing and the inception of the experiment. For all four experimental conditions the amount of sulfate on the rock surfaces ranged from 5 to 8 mg per gram rock. Subsequently, the aqueous sulfate observed was the product of sulfide mineral oxidation, since no sulfate minerals were present in the rock. Between weeks 90 and 100 drainage pH decreased to 3.1 while sulfate concentrations increased to the neighborhood of 300 mg/L. This transitional phase was followed by a period of fairly stable drainage quality during which drainage pH was lower and sulfate concentrations were greater than the corresponding values in the initial phase.

The rates of sulfate release in the final phase were three and six times higher than those in the initial phase for the two on-land reactors (table 2). This accelerated release was probably due to increased biologically mediated ferric iron oxidation of the sulfide minerals in the lower pH range. The rate of chemical oxidation also may have increased, but this increase would be slight relative to the increase in the rate of biological oxidation (Nordstrom 1982).

For the unmodified subaqueous disposal, pH declined steadily from 4.5 initially to a value of 3.5 after 120 weeks. The initial sulfate concentrations were about 450 mg/L. These elevated concentrations and the initial low pH reflected the release of acidic reaction products that had accumulated on the rock owing to oxidation prior to the experiment. During the initial 40 weeks sulfate concentrations decreased from roughly 450 to 250 mg/L; they \subsequently increased and stablized in the approximate range of 350 to 400 mg/L (fig. 2). The initial decrease in sulfate concentrations was due to dilution by the distilled water added to replace the sample volume withdrawn. During the first 40 weeks this volume averaged 75 mL/week. Subsequently the sample volume was reduced to about 44 mL/week.

The sulfate release for the unmodified subaqueous disposal was relatively rapid during the initial 10 weeks, owing to release of oxidation products accumulated on the solids prior to the experiment. Subsequent sulfate release was fairly linear and was the result of oxidation of pyrrhotite present in the rock. The rate of this oxidation was about 75% of that during the initial phase for the on-land disposal environment (table 2).

The pH of water in the two flasks simulating subaqueous disposal with subsequent alkaline addition was maintained in the typical range of 6.7 to 7.5. Sulfate concentrations followed the same trend observed for the unmodified subaqueous disposal. Concentrations decreased from about 520 to 300 mg/L during the first 40 weeks and subsequently increased to around 450 mg/L (fig. 2). As was the case for the unmodified subaqueous disposal, the initial elevated sulfate concentrations were the result of release of reaction products that had accumulated on the rock surface. Similarly, the subsequent decrease in concentrations was due to dilution by the distilled water used to replace the sample volume withdrawn.

The linear rate of release, representing the oxidation of pyrrhotite, was slightly faster than that observed for the unmodified reactors, and was about 88% of the initial rate for the on-land disposal simulation (table 2). The rates of alkalinity addition and the sum of calcium and magnesium release were in good agreement with the sulfate release rates.

For the rock that was treated prior to subaqueous disposal, the initial pH values were elevated due to some residual alkalinity on the solids. The solution pH declined steadily, decreasing below 6.0 at week 9. Alkalinity was added subsequently at regular intervals to maintain neutral pH. Sulfate concentrations were near 20 mg/L at the beginning of the experiment, indicating, as did the elevated initial pH, that the pretreatment was effective in removing reaction products from the rock surfaces. Subsequently, sulfate concentrations increased steadily over the course of the experiment (fig. 2).

Sulfate release for the pretreated subaqueous disposal was linear throughout the period of record (fig. 3) The rate of sulfate release per gram rock was higher than that observed for the other subaqueous disposal reactors, and was slightly higher than that during the initial phase of the on-land disposal simulation (table 2). When

normalized for the difference in pyrrhotite content (table 1), the rate of oxidation per unit area pyrrhotite approximated that observed for the on-land disposal simulation (table 3). The sum of the calcium and magnesium release rates was within 6% of the sulfate release rate (table 2). However, the rate of alkalinity addition was about 20% less than the sulfate release rate. Some of the acid generated as a result of iron sulfide oxidation was apparently neutralized by dissolution of host rock components and/or by the release of alkalinity accumulated on the solids during their pretreatment.

The data indicate that pyrrhotite can oxidize in a subaqueous environment with a consequent generation of acid and provide rates for that oxidation. The oxidation rates expressed as a function of the mathematically derived pyrrhotite surface area (table 3) also allow extrapolation of the data to particles larger than those used in the present study. For the sample masses used in this experiment, the rate of oxidation in the subaqueous setting was approximately equal to that observed in the intial phase for the wet-dry cycling environment. This indicates that, under the experimental conditions, oxygen transport was not the rate-limiting step for sulfide mineral oxidation. However, as the depth of pyrrhotite-bearing rock increases, oxygen transport would become limiting.

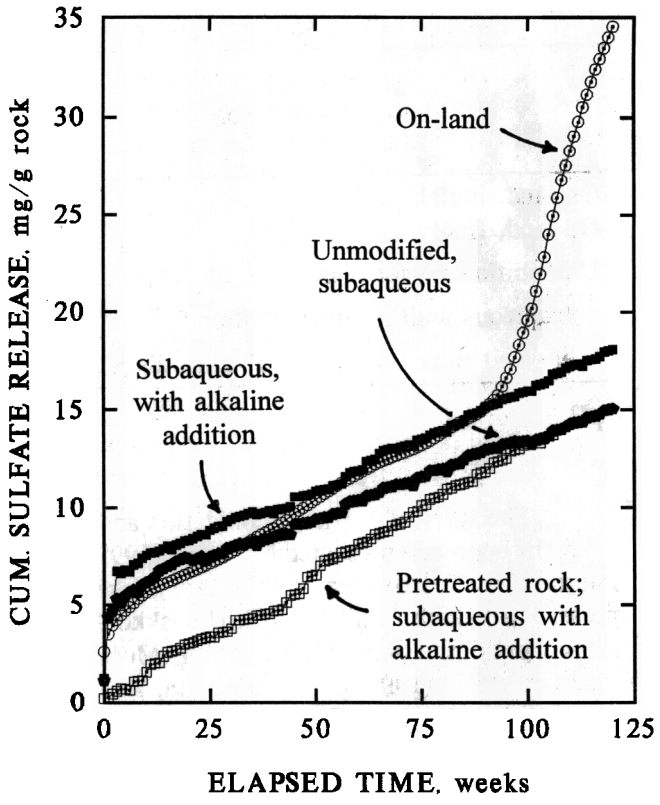

Figure 3. Cumulative sulfate release for on-land and subaqueous disposal. The rates of sulfate release and attendant acid production for the disposal options did not differ greatly. Data presented are from the second replicates.

Table 2. Rates of sulfate, calcium, and magnesium release and alkalinity addition (moles per gram rock per second x 10^{-12}.)

Simulation	Replicate	Sulfate	Calcium	Magnesium	Alkalinity Addition[1]
On-land initial	A	1.9	0.41	0.46	0
	B	2.1	.40	.46	0
On-land final	A	5.6	.13	.86	0
	B	13	.20	2.7	0
Unmodified subaqueous	A	1.6	.20	1.1	0
	B	1.4	.18	1.0	0
Subaqueous with alkaline addition	A	1.8	[2]1.3	.40	1.7
	B	1.7	[2]1.2	.38	1.7
Pretreated subaqueous with alkaline addition	A	2.1	[2]1.9	.01	1.7
	B	2.3	[2]2.0	.01	1.7

[1] Rate of alkalinity addition as equivalent moles $CaCO_3$.
[2] Includes calcium released to solution from rock and that supplied by the addition of alkalinity.

Table 3. Pyrrhotite oxidation rates expressed as a function of mathematically derived pyrrhotite surface area. (d = 1 x 10^{-4} m, specific gravity = 4.6, specific surface area = 0.013 m^2/g.)

Simulation	Rate: nmol $Fe_{0.9}S$ per m^2 $Fe_{0.9}S$ per second		
	Replicate 1	Replicate 2	Average
On-land, initial[1]	1.1	1.2	1.2
On-land, final[2]	3.3	7.5	5.4
Unmodified subaqueous	.92	.77	.84
Subaqueous with alkaline addition	1.0	1.0	1.0
Pretreated subaqueous with alkaline addition	1.1	1.2	1.1

[1] pH 3.6 to 4.0.
[2] pH 3.1.

The rates of pyrrhotite oxidation and acid generation, when oxygen transport is limiting, can be calculated using the approach presented by Morin (1993a). This approach assumed a first-order dependence of pyrite oxidation rate on dissolved oxygen concentration, a relationship that was previously reported for the oxidation of pyrrhotite present in Duluth Complex rock (Lapakko 1980). Examination of the equations presented by Morin (1993a) and subsequent discussion with the author (Morin 1993b) led to the conclusion that the following corrections should be made in Morin (1993a). Equation 7(a) should read $J = DO(pond)(kDe)^{0.5}$; FACT1=1.00 and FACT2=1.67 for equation 1; FACT1=1.07 and FACT2=0.90 for equation 2.

The aforementioned corrections were incorporated to calculate the rates of acid production for pyrrhotite-bearing tailings and waste rock disposed under water in a mine pit. The calculation assumes the water overlying the mine waste is saturated with dissolved oxygen and the water within the mine waste pores is stagnant. Under these conditions pyrrhotite oxidation and the consequent acid production will occur only as oxygen diffuses into the mine waste. As mentioned by Morin (1993a), it is necessary to characterize the physical and chemical hydrology of the system to ensure that these assumptions are correct.

Oxygen saturation at 26° C temperature in the present study would be approximately 8 mg/L and at 5° C would be near 13 mg/L (APHA 1992). For the calculation the following values were used: dissolved oxygen = 10 mg/L; pyrrhotite oxidation rate = 1 nmol/m^2 $Fe_{0.9}S$/s; average porosity = 0.3; pyrrhotite content = 14%; tailings diameter = 0.0001 m; and waste rock diameter = 0.1 m. The calculated acid production rates for tailings and waste rock were 1 x 10^{-3} mg $CaCO_3/m^2$ horizontal cross-sectional area/s and 5 x 10^{-5} mg $CaCO_3/m^2$ horizontal cross-sectional area/s, respectively. The value for tailings is slightly less than the observed laboratory value of 2 x 10^{-3} mg $CaCO_3$ /m^2/s. Despite the approximations applied in the calculation, the similarity of values suggests that observed laboratory rate is close to being limited by oxygen transport. This seems curious since the depth of solids in the laboratory was less than 3 cm. The equations used will be examined further and additional laboratory study will be undertaken to evaluate the implication of oxygen-transport limitation in the laboratory.

The rates of acid generation for subaqueous conditions must be considered to ensure that acid conditions would not develop in a pit upon disposal of pyrrhotite-bearing mine wastes. The potential for residual acid salts on the mine wastes prior to disposal must also be taken into account. The neutralization required for the acid inputs can then be quantified. Sources of neutralization include alkaline water inputs to the pit, dissolution of alkaline components in the pit walls, and addition of alkaline amendments. The possibility of placing an oxygen consuming material above the mine waste could also be considered as a means of slowing the acid generation. Furthermore, the release of trace metals from sulfide minerals into neutral waters must be assessed.

Acknowledgments

Solid-phase chemical and mineralogical analyses were conducted by Don Schnortz of Lerch Brothers (Hibbing, MN) and Louis Mattson of Midland Research (Nashwauk, MN), respectively. The dissolution experiments were conducted by Kathleen Willis under the direction of David Antonson. Sulfate was analyzed by Jean Matthew, while calcium and magnesium were analyzed by Albert Klaysmat at the Hibbing office of the Minnesota Department of Natural Resources. Jon Wagner was responsible for data management as well as production of tables and figures for this publication.

References

American Public Health Association (APHA), American Water Works Association, Water Environment Federation. 1992. Standard Methods for the Examination of Water and Wastewater, 18th edition. American Public Health Association, Washington, D. C.

Cathles, L. M. 1982. Acid mine drainage. Earth and Mineral Sciences 51: 37-41

City Resources (Canada) Limited and Norecol Environmental Consultants Ltd. 1988. Cinola gold project, stage II report, v. V and v. V appendices. Submitted to British Columbia Ministry of Energy, Mines, and Petroleum Resources. (cited in Morin 1993).

Equity Silver Ltd. 1988. Decommissioning and closure report. Houston, BC.

Graber, R. 1990. Telephone conversation with Ron Graber, Pickands Mather Services, Inc., Research Center, Hibbing MN.

Lapakko, K. A. 1980. The kinetics and mechanisms of the oxidative dissolution of metal sulfide and silicate minerals present in the Duluth Gabbro. M.S. Thesis, Univ. MN, Minneapolis, MN. 199 p. plus appendices.

Morin, K. A. 1993a. Rates of sulfide oxidation in submerged environments: Implications for subaqueous disposal. p. 235-247. In Proceedings Seventeenth Annual British Columbia Mine Reclamation Symposium. (Port Hardy, BC, May 4-7, 1993).

Morin, K. A. 1993b. Telephone conversation with Kevin Morin, Morwijk Enterprises Ltd., Vancouver, BC.

Moses, C. O. and J. S. Herman. 1991. Pyrite oxidation at curcumneutral pH. Geochimica et Cosmochimica Acta 55: 471-482.

Nordstrom, D. K. 1982. Aqueous pyrite oxidation and the consequent formation of secondary iron minerals. p. 37-56. In Acid Sulfate Weathering. Soil Sci. Soc. Am. Madison, WI.

Pedersen, T. F., B. Mueller, and J.J. McNee. 1991. Diagenetic reactivity of mine tailings in mesotrophic and oligotrophic lakes in Manitoba and British Columbia. p. 199-226 In Proceedings Second International Conference on the Abatement of Acidic Drainage, v. 4. (Montreal, PQ, September 16-18, 1991).

Pedersen, T. F., B. Mueller, and C. A. Pelletier. 1990. On the reactivity of submerged mine tailings in fjords and a lake in British Columbia. p. 285-293. In Acid Mine Drainage: Designing for Closure. Proceedings GAC/MAC Joint Annual Meeting. (Vancouver, BC, May 16-18, 1990).

Rescan Environmental Services Ltd. 1989. Subaqueous disposal of reactive mine wastes: An overview. Report to British Columbia Ministry of Energy, Mines, and Petroleum Resources. Vancouver, BC.

Ritcey, G. M. 1991. Deep water disposal of pyritic tailings. p. 421-442. In Proceedings Second International Conference on the Abatement of Acidic Drainage, v. 1. (Montreal, PQ, September 16-18, 1991).

Robertson, J. D. 1991. Subaqueous disposal of reactive mine waste: An overview of the practice with case studies. p. 185-200. In Proceedings Second International Conference on the Abatement of Acidic Drainage, v. 3. (Montreal, PQ, September 16-18, 1991).

United States Bureau of Mines. 1980. A simple low-cost method for the dissolution of metal and mineral samples in plastic pressure vessels. BuMines RI 8480. 14 p.

Veillette, G. and C. J. Desrochers. 1991. Reclamation of the Solbec Mine by flooding waste rock in open pit. p. 219-238. In Proceedings Second International Conference on the Abatement of Acidic Drainage, v. 3. (Montreal, PQ, September 16-18, 1991).

Yanful, E. K. and S. C. Payant. 1992. Evaluation of techniques for preventing acidic rock drainage First Milestone Research Report submitted to MEND.

WATER COVERS FOR THE DECOMMISSIONING OF SULFIDIC MINE TAILINGS IMPOUNDMENTS[1]

Luc St-Arnaud[2]

Abstract: Covering sulfidic mine tailings with water effectively reduces oxygen influx to the tailings and the resulting acid generation. However, metals present in porewater solutions or in soluble mineral phases may still be released from the flooded tailings impoundment. Several laboratory leach tests are performed to evaluate metal release rates and times.

Results from 20-day laboratory tests where fresh, unoxidized sulfide tailings are leached under controlled hydraulic and chemical conditions show limited metal releases even as pH changes occur in the leach water. Metal release times are generally of short duration. Monitoring of tailings seepage and surface waters is recommended for detecting sudden metal releases which could occur from natural pH variations.

Results from a 3-month column experiment where oxidized tailings are covered by 1 m of water showed that transfer of zinc, sulfate, and iron from the tailings to the water column could occur. This transfer could be controlled by the addition of a protective sand layer over the tailings. Results for this case suggest that removal of zinc by treatment of surface and seepage water is still required for a long period after implementation of the water cover.

The construction costs for artificial hydraulic containment structures to obtain an adequate water storage over the tailings are always high. It is therefore necessary, before deciding to commit to these costs, to evaluate treatment and maintenance requirements using laboratory and field testing, such as described herein.

Introduction

Water covers have been proposed at several Canadian mine sites as a long term decommissioning measure for sulfide tailings impoundments. Covering the tailings with water reduces oxygen influx to the tailings and the resulting acid generation. The main advantage of water covers is that implementation costs are less dependent on surface area than other oxygen barriers such as soils, which require more transport and handling. As the most abundant and available oxygen barrier, water can sometimes be controlled to cover large surfaces with relatively little effort. However, the benefits of implementing a water cover are highly site-dependent. Some of the influencing factors are the geochemical history of the tailings, the degree and quality of natural or manmade containment in place at the time of decommissioning, and the physical and hydrogeological setting of the tailings disposal area.

This paper presents results from laboratory simulations of tailings disposal scenarios and provides details on some of the acting principles and processes occurring in water-covered tailings systems. Factors that can influence decision making at the time of decommissioning are discussed.

---

[1]Paper presented for the Third International Conference on the Abatement of Acidic Drainage, April 25-29, Pittsburgh PA.

Noranda Technology Centre, Pointe-Claire, Québec Canada H9R 1G5

Chemical Evolution of Unsaturated Tailings

Sulfide oxidation results from the exposure of mined rock to geochemical conditions that are different from those in which it originated and is described by the following reaction:

$$2\ MeS_{(s)} + 7/2\ O_2 + H_2O \Rightarrow 2\ Me^+ + 2\ SO_4^{2-} + 2\ H^+ \qquad (1$$

where Me represents a metal such as iron, lead, zinc, or nickel. Tailings oxidation models (for example Senes 1991) suggest that, in most cases, the oxidation of unsaturated tailings slows down with time, as sulfide minerals become depleted near the tailings surface and oxygen transport paths to fresh sulfide particles become longer. This was verified during controlled oxidation experiments in 1-m columns presented earlier by Yanful and Payant (1993). Figure 1 shows acid fluxes decreasing by approximately 37% in a period of approximately 600 days as the downward movement of the oxidation front reached a depth of approximately 40 cm below surface. This decrease in acid production would be slower under field conditions because oxidation rates in colder temperatures are slower. After many years, the downward progression of the oxidation front should reach the water table; at that point, acid production should cease.

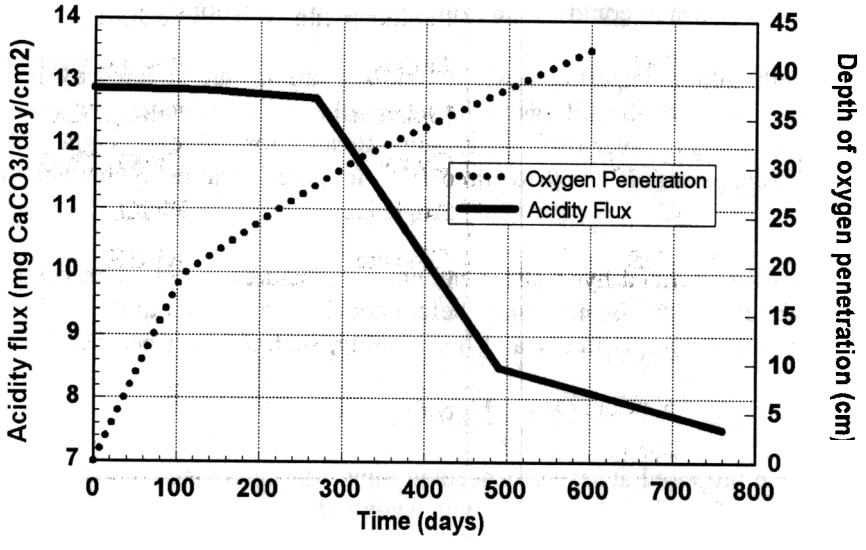

Figure 1. Acidity flux and oxygen penetration in laboratory column

Metal release from tailings is also influenced by the precipitation and dissolution of minerals below the oxidation front. The net resulting acid generation is therefore a complex function of the overall chemical composition of the tailings solids, as described, for example, by Dubrovsky et al. (1984) and Blowes et al. (1990). Table 1 lists some of the minerals that commonly constitute fresh, unoxidized, tailings solids (primary minerals) produced from the mining of Canadian sulfide base-metal ore bodies, and minerals that have been found to appear as a result of reactions occurring after tailings deposition (secondary minerals). As the mineralogy of tailings deposits evolves toward equilibrium with atmospheric geochemical conditions, sulfide minerals are replaced by secondary minerals which eventually form a major proportion of metallic constituents. The evolution rate is a function of factors such as the sulfide mineral type and abundance, tailings grain size, and temperature.

The placement of a water cover induces changes in geochemical conditions which will promote reactions other than those generally described above. The importance of these reactions depends on the length of time during which the tailings were exposed to atmospheric conditions. If tailings exposure to atmospheric conditions is not long enough to allow the formation of a significant quantity of secondary minerals, reactions with primary minerals will dominate effluent quality from the flooded tailings. These conditions were observed in previous laboratory studies described in Ritcey (1986) and in field studies by Rescan (1990). Morin (1993) recently reviewed the theory of sulfide oxidation rates under water.

Table 1. Minerals commonly found in Canadian base metal mine tailings.

Primary minerals		Secondary minerals	
Name	Formula	Name	Formula
Pyrite	FeS_2	Ferrihydrite	$Fe(OH)_3$
Chalcopyrite	$CuFeS_2$	Goethite	FeOOH
Pyrrhotite	$Fe_{(1-x)}S$	Lepidocrocite	FeOOH
Sphalerite	ZnS	Jarosite	$KFe_3(SO_4)_2(OH)_6$
Galena	PbS	Melanterite	$FeSO_4.7H_2O$
Arsenopyrite	FeAsS	Gypsum	$CaSO_4.2H_2O$
Chalcocite	Cu_2S	Anglesite	$PbSO_4$
Covellite	CuS	Gibbsite	$Al(OH)_3$
Magnetite	Fe_3O_4		
Calcite	$CaCO_3$		
Dolomite	$MgCa(CO_3)_2$		
Siderite	$FeCO_3$		

On the other hand, if the tailings are exposed long enough to allow the formation of significant quantities of secondary minerals, the geochemistry of the effluent may be dominated by reactions with these minerals. In general, the dissolution of sulfate and hydroxide minerals occurs more readily in aqueous solutions than that of sulfides and silicates (Stumm and Morgan 1981). The following sections give two examples where laboratory simulations of water cover conditions have been done.

Flooding of Fresh Tailings

In this case example, highly acid-generating tailings, typically containing 45% pyrite and less than 1% of other sulfide minerals, are produced from the milling of polymetallic ore. It is planned to deposit the tailings in an engineered disposal cell and to maintain the tailings in saturated conditions throughout the active life of the impoundment. The tailings will be deposited in a slurry at a pH above 10. After closure, a 1-m water cover will be permanently maintained over the tailings.

Variations in the chemistry of water above the tailings are expected, as atmospheric water will replace the mill water in the impoundment. Typical rain water for the region shows a pH near 5, and it is therefore expected that chemical conditions in the water-covered tailings system will become less alkaline, and that pH will decrease to

values closer to the rain water pH. In addition, there is the risk that some tailings may be exposed for longer times, allowing some oxidation, which could further decrease the pH.

Standard shake flask tests conducted at a pH of 4.8 (EPA procedure 1311) suggested the possible release of zinc and manganese from the tailings. These tests give only a rough estimate of possible metal releases from the tailings, because of the large water-solid ratio (approx 100:1) and the large amount of energy applied to the flask (18-hr shake). Other tests, such as humidity cell tests, are not applicable because they allow air to freely contact the sample, a condition that should not occur under water-cover conditions.

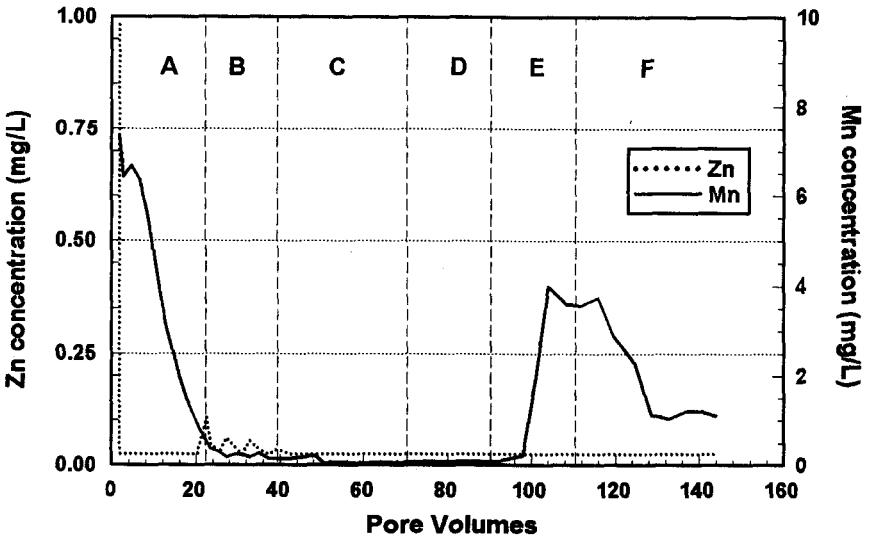

inflow	A	B	C	D	E	F
pH	10	7	5	5	5	3
Fe (mg/L)	0	0	0	0	100	0

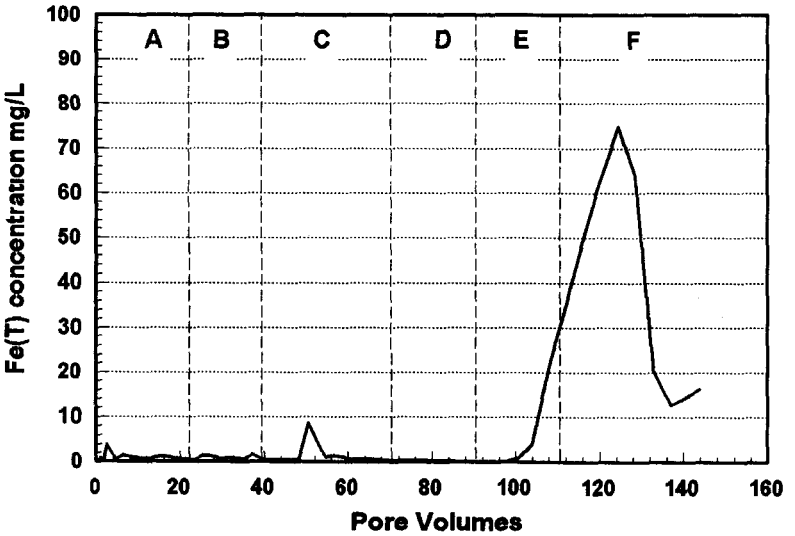

Figure 2. Metal concentrations in column effluent

To more realistically assess the possibility of metal leaching from the tailings, a column test was initiated. The test involved the percolation of water through a 15 cm long by 10 cm diameter tailings sample. Saturated conditions were maintained in the sample throughout the test, and water was percolated from a reservoir placed at a height of 50 cm above the sample (hydraulic gradient equal to 5). Possible pH fluctuations were reproduced in the test by modifying the distilled water influent pH between 10 and 5 using NaOH or HCl addition. Figure 2 shows concentrations of some of the metals dissolved in the column effluent plotted with respect to the number of pore volumes that passed through the sample. After respectively 21 pore volumes of influent at pH 10, 18 at pH 7, and 49 at pH 5, no zinc release was measured in the effluent. Manganese release occurred during the initial flushing of 21 pore volumes at pH 10, then decreased. Toward the end of the test period (at 88 pore volumes), 21 pore volumes of a 100 mg/L ferrous iron (Fe^{2+}) solution were introduced in the inflow as iron sulfate. As the solution passed through the sample, a rise in manganese concentrations up to 5 mg/L was produced.

The conclusion of the preliminary column test is that leaching of zinc and other metals from the minerals contained in the tailings would not occur under normal conditions in which the tailings would be deposited. Some release of manganese could occur as an association with the mobilization of iron. Possible chemical mechanisms for manganese release are dissolution of manganese carbonates due to changes in redox conditions, and replacement of manganese by iron in hydroxide mineral structures.

The changes in pH and iron concentration in the influent water correspond to chemical variations that could probably occur in the field. However, the simulated flow rates, which are governed by the hydraulic conductivity of the sample and the hydraulic gradient, could be quite different under field conditions. While the measured laboratory hydraulic conductivity of 6×10^{-6} cm/s could resemble field conditions, the hydraulic gradient in the field could likely be as much as 50 to 100 times lower than the one simulated in the laboratory. Pore water could therefore flush the tailings at a rate which could be 50 to 100 times slower than in the laboratory column. The flushing of 88 pore volumes across the tailings sample could thus correspond to 176 yr of actual conditions. However, this last affirmation is not exactly true because the effect of flow rate on the resulting water chemistry depends on the availability of source minerals and on the rate of transfer of metals into the pore water. It is likely that the rate of metal transfer to the pore water is very slow, and that metal concentrations in the tailings pore water become higher as the residence time of water in the tailings pores increases.

Flooding of Oxidized Tailings

In this case, tailings from the milling of polymetallic sulfide ore containing 33% pyrite, 1.5% sphalerite, and 1% of other sulfide gangue minerals have been deposited in a small lake. Additional containment was provided by dams constructed of cycloned tailings spilled over waste rock "starter dams"—a construction technique typically used at most Canadian mineral processing sites prior to the mid-1970's. These dams offered only physical support to the tailings mass, allowing the tailings to drain freely and to develop an unsaturated zone. Oxidation and geochemical evolution occurred during a period of approximately 20 yr, as generally described in the first section of this paper.

As a consequence of tailings oxidation, seepage from the tailings exhibited the high levels of dissolved metals and sulfate and low pH typical of acid mine drainage. Decommissioning work at the site included interception of all seepage and removal of metals by lime treatment. Decommissioning plans are to treat water and store treatment sludges on site. A water cover is being considered as an option to reduce future tailings oxidation, to reduce future water and sludge management, and to generally decrease postclosure operational requirements.

A description of the laboratory model used to simulate the water-covered tailings was presented earlier in St-Arnaud and Yanful (1993). The model consisted of 2-m-high by 30-cm-diameter plexiglass columns. The bottom 1-m section was filled with 60 cm of unoxidized and 35 cm of oxidized tailings. The top 1-m column section was filled with clean water. Sampling ports allowed the pore water in the tailings and water above the tailings to be sampled with time.

In the first stage of the laboratory simulation, the water column was maintained stagnant over the tailings. Figure 3 shows that zinc concentrations reached 20 mg/L in the water column after 152 days. Iron concentrations were controlled by the rapid and sustained formation of hydrous ferric oxide precipitates at the surface of the tailings. These precipitates are commonly formed as ferrous iron dissolved in the pore water seeps to surface; the iron is then oxidized to ferric and rapidly hydrolyzes to form the reddish solid. The chemical reaction describing the hydrolysis of ferric iron is

$$Fe^{3+} + 3H_2O = Fe(OH)_3(s) + 3\ H^+. \tag{2}$$

Dissolved iron levels can be so high that the reaction, by producing hydrogen ions, may significantly contribute to water acidification. Acidification of the water cover is undesirable because additional water treatment would be required if release to the environment became necessary and because leaching of the tailings solids could be increased if acidic water would seep into the tailings. Measured pH in the laboratory column was near 4.

It was demonstrated that upward diffusion of ferrous iron present in the pore water prior to flooding of the tailings can account for only part of the iron release to the water column. Another apparent mechanism affecting metal

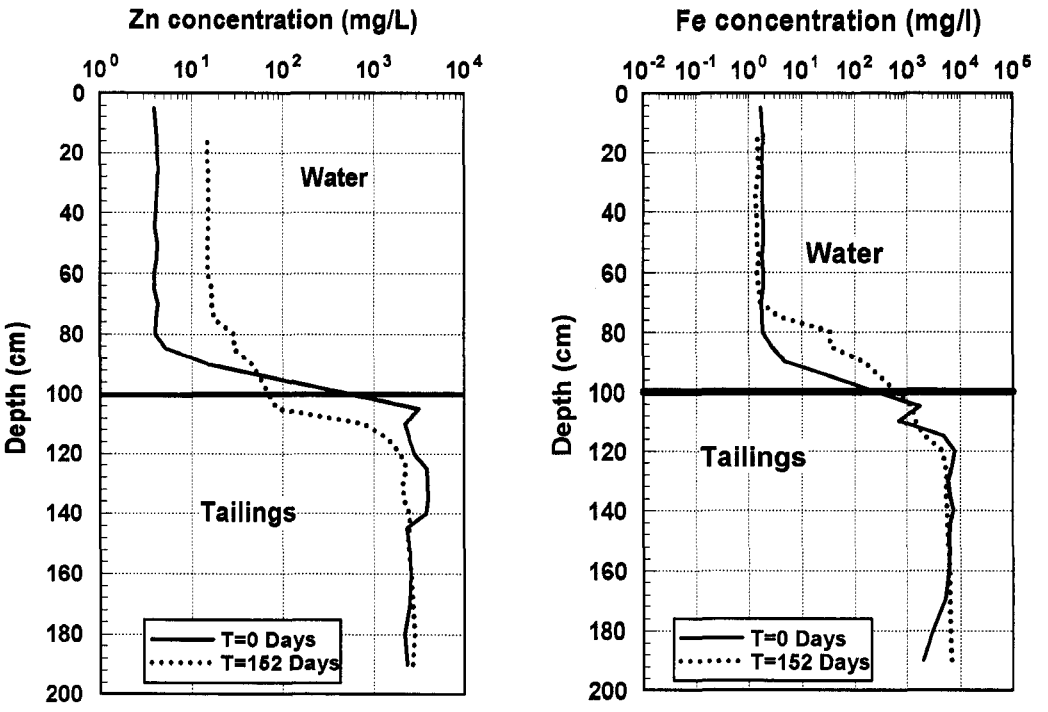

Figure 3. Zinc and iron concentration profiles in laboratory columns

transfer is the dissolution of iron sulfate and hydroxide secondary minerals present in the oxidized part of the column, followed by advection due to the consolidation effect created by the change in volume induced by the dissolution. In addition to the release of iron, the dissolution of secondary mineral phases induces the release of other metals, which are commonly adsorbed or coprecipitated on amorphous hydroxide phases. The chemical kinetics of metal sorption on amorphous metal hydroxides were described by Gadde and Laitinen (1974) and Kinniburg et

In the first stage of the laboratory simulation, the water column was maintained stagnant over the tailings. Figure 3 shows that zinc concentrations reached 20 mg/L in the water column after 152 days. Iron concentrations were controlled by the rapid and sustained formation of hydrous ferric oxide precipitates at the surface of the tailings. These precipitates are commonly formed as ferrous iron dissolved in the pore water seeps to surface; the iron is then oxidized to ferric and rapidly hydrolyzes to form the reddish solid. The chemical reaction describing the hydrolysis of ferric iron is

$$Fe^{3+} + 3H_2O = Fe(OH)_3(s) + 3\ H^+. \tag{2}$$

Dissolved iron levels can be so high that the reaction, by producing hydrogen ions, may significantly contribute to water acidification. Acidification of the water cover is undesirable because additional water treatment would be required if release to the environment became necessary and because leaching of the tailings solids could be increased if acidic water would seep into the tailings. Measured pH in the laboratory column was near 4.

It was demonstrated that upward diffusion of ferrous iron present in the pore water prior to flooding of the tailings can account for only part of the iron release to the water column. Another apparent mechanism affecting metal

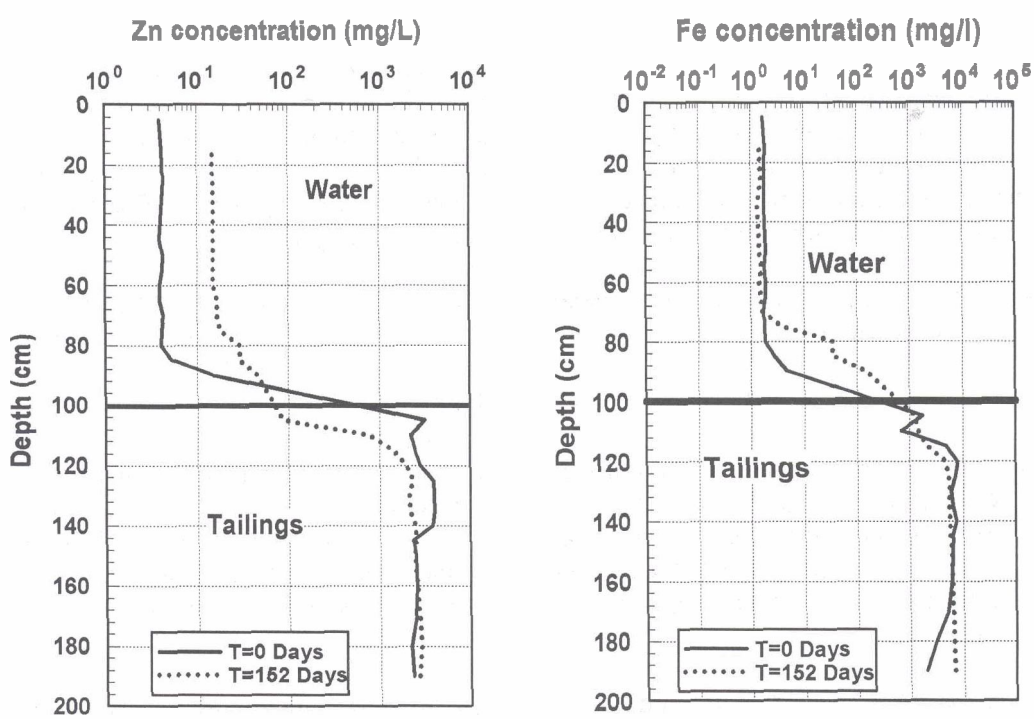

Figure 3. Zinc and iron concentration profiles in laboratory columns

transfer is the dissolution of iron sulfate and hydroxide secondary minerals present in the oxidized part of the column, followed by advection due to the consolidation effect created by the change in volume induced by the dissolution. In addition to the release of iron, the dissolution of secondary mineral phases induces the release of other metals, which are commonly adsorbed or coprecipitated on amorphous hydroxide phases. The chemical kinetics of metal sorption on amorphous metal hydroxides were described by Gadde and Laitinen (1974) and Kinniburg et

al. (1976). More recent reports by Music and Ristic (1992) and Morel and Hering (1993) state that, in general, heavy metal retention by amorphous minerals is highly reversible and pH-dependent. Blowes and Jambor (1990) found that sorption and coprecipitation with hydroxide and sulfate minerals was a major removal mechanism for zinc in oxidized tailings. It is likely that metal transfer will last for a long period of time, as the relative proportion of secondary minerals available for dissolution could be important. The metal transfer should decrease with time, however, and should cease after the dissolution of soluble minerals is complete. The composition and proportion of secondary mineral phases in the oxidized tailings are presently being evaluated.

As secondary mineral dissolution and the associated metal releases occur in the oxidized tailings, the subsequent migration and reformation of iron hydroxides at the surface of the tailings is also associated with heavy metal sorption. In the water-covered tailings system, sorption of metals by the observed iron hydroxide coating would effectively intercept upward-moving dissolved metals, thereby reducing loading to the water cover. However, because of the reversible nature of the sorption, the metals could remain available for release if, for example, pH changes occur in the water. As reported in St-Arnaud and Yanful (1993), iron hydroxide precipitate was visible on the field wherever ponding occurred on the tailings. Analysis of the precipitate revealed the presence of 0.2% of zinc in the sample, and zinc mobility was confirmed by shake flask tests. Since downward infiltration of water into the tailings which occurs in the field probably counteracts upward metal transfer by diffusion, dissolution followed by consolidation is probably the only mechanism that could be responsible for the metal transfers observed in the field.

To modify the mobility of metals from the tailings to the water body, additional laboratory columns were installed as described above, with the addition of a 10-cm layer of sand on top of the tailings. The results, plotted on figure 4, show that zinc and iron concentrations decreased to values lower than 0.02 mg/L in the water column during the 4-month (122-day) test period. It appears that the transfer of zinc and iron is limited significantly by the sand protective layer because iron hydroxide precipitated rapidly at the sand-tailings interface, filling the sand pore spaces and limiting further transfer of metals. The benefit of the sand is to offer a stable physical support for hydroxide gels, which, once in place, can become an effective barrier to upwardly moving metals. The same benefit could also be obtained by using other granular materials, such as clean, coarse tailings.

Further chemical monitoring under conditions where the water column is allowed to infiltrate through the tailings is ongoing in order to measure the duration of metal transfers into downward-moving pore waters.

Discussion

The laboratory simulations of tailings disposal scenarios presented above demonstrate that (1) tailings oxidation in unsaturated conditions slows down with time, (2) if the tailings are placed under water while still fresh (unoxidized), metal releases should be very low compared to uncovered tailings, (3) metal releases from water-covered oxidized tailings could be significant and could last for long time periods; they should however decrease with time; (4) upward metal release from water-covered oxidized tailings may be controlled by a layer of clean, granular material such as sand.

The environmental benefits of placing a water cover over sulfide tailings before they can oxidize were discussed. Economic benefits are also possible if the chemistry of the water-covered tailings system can be controlled so there is no requirement for extensive water treatment.

In the case where oxidized sulfide tailings are to be decommissioned, water capture and treatment are often necessary, leading to significant labor, capital, and operation costs. The physical limit to unsaturated tailings oxidation suggests that operation costs should slowly decrease with time even when the tailings remain uncovered. In addition, operation costs for a lime neutralization plant and sludge disposal become less significant when distributed over long time periods because economic evaluations normally discount future cash flows (positive or negative) at a rate equal to the average cost of capital, which in turn is related to the opportunity to use capital to generate revenues. Consequently, the real cost of operating treatment facilities decreases with time, and, depending

on the economic situation, costs to be incurred 15 or 20 yr in the future may become quite small when discounted to present values. Of course, the real costs may be greatly increased by legislative requirements for the advanced payment of financial assurances to cover future operation costs for decommissioned sites.

Placing a water cover over oxidized tailings may require immediate investments for the upgrade of dams to obtain an adequate water storage over the tailings and for the emplacement of protective layers on the tailings surface for

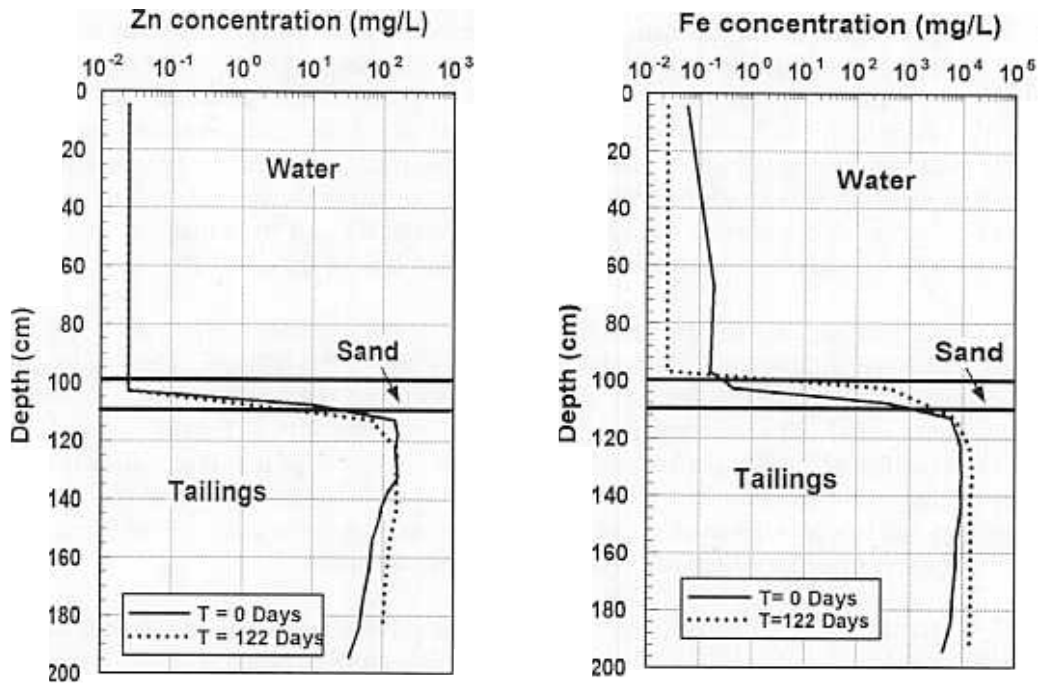

Figure 4. Zinc and iron profiles in laboratory column with sand layer

physical stability and to limit metal transfer. For the water cover to be environmentally and economically acceptable, reduction in metal releases would have to occur within 15 to 20 yr after implementation. The evaluation of treatment and maintenance requirements using laboratory and field testing such as described in this paper is therefore necessary before decision making on final decommissioning can be done.

Acknowledgements

The laboratory work described in this paper is part of ongoing studies sponsored by Noranda Minerals Inc. and are part of the MEND program. Technical contributions by personnel of the Noranda Technology Centre, in particular B. Aubé, S. Payant, and P. Tibble, are acknowledged. Comments from V. Coffin of Noranda Minerals, A. Condy of Noranda Technology Centre, and from two other anonymous reviewers are gratefully acknowledged.

Literature Cited

Blowes, D. W. and J. L. Jambor. 1990. The pore water geochemistry and the mineralogy of the vadose zone of sulphide tailings, Waite Amulet, Quebec. Appl. Geochem. 5:327-346.

Dubrovsky, N. M., J. A. Cherry, E. J. Reardon and A. J. Vivyurka. 1984. Geochemical evolution of inactive pyritic tailings in the Elliot Lake Uranium District:1, The groundwater zone. Can. Geotech. J. 22:110-128.

Gadde, R. R. and H. A. Laitinen. 1974. Studies of heavy metal adsorption by hydrous iron and manganese oxides. Anal. Chem. 46(13):2022-2026.

Kinniburg, D. G., M. L. Jackson, and J. K. Syers. 1976. Adsorption of alkaline earth, transition, and heavy metal cations by hydrous oxide gels of iron and aluminum. Soil Sci. Soc. America J. 40:796-799.

Morel, F. M. M. and J. G. Hering. 1993. Principles and applications of aquatic chemistry. NY: Wiley Interscience.

Morin, K. A. 1993. Rates of sulphide oxidation in submerged environments: implications for subaqueous disposal. In proceedings of the 17th Annual Mine Reclamation Symposium (Port Hardy, BC, November 1993)

Music, S. and M. RISTIC. 1992. Adsorption of zinc(II) on hydrous iron oxides. J. radioanalytical and nuclear chem., Articles 162(2):351-362.

RESCAN. 1990. Geochemical assessment of subaqueous tailings disposal in Mandy Lake, Flin Flon area, Manitoba. MEND report.

Ritcey, G. M. 1986. Tailings management, Ch. 14: Methodology and plan for investigating weathering, migration, and close-out: the model. Amsterdam: Elsevier.

SENES. 1991. The reactive acid tailings assessment program (RATAP.BMT3), Volumes 1 and 2.

St-Arnaud, L. C. and E. K. Yanful. 1993. Water covers for the decommissioning of sulphidic mine tailings impoundments: Mattabi mines case study. p. 275-285. In proceedings of the 32d Annual Conference of Metallurgists of the Canadian Institute of Mining, International Symposium on Materials Processing Technology and Environmental Protection in Mining and Metallurgy, Part II.

Stumm, W. and J. J. Morgan. 1981 Aquatic chemistry, 2nd edition. NY: Wiley Interscience.

Yanful, E. K. and S. Payant. 1993. Laboratory acid fluxes from covered and uncovered sulphidic tailings. p. 259-274. In proceedings of the 32d Annual Conference of Metallurgists of the Canadian Institute of Mining, International Symposium on Materials Processing Technology and Environmental Protection in Mining and Metallurgy, Part II.

GEOCHEMISTRY OF SUBMERGED TAILINGS IN ANDERSON LAKE, MANITOBA: RECENT RESULTS[1]

Thomas F. Pedersen[2], J.Jay McNee[2,3], Bert Mueller[2], David H. Flather[3] and Clem A. Pelletier[3]

Abstract: Sulfide-rich zinc-, copper-, and lead-bearing tailings have been deposited via floating pipeline into shallow (< 8 m) Anderson Lake in north-central Manitoba since 1979. The lake water contains elevated levels of dissolved metals which are derived mainly from an acid-generating roadway along the north shore. Water-column sampling and sediment coring were carried out through the ice on Anderson Lake in April 1993. Two sites were occupied, one proximal to the tailings discharge (Station B, the "pure tailings" site) and the other about 2 km away (Station A, the "natural sediments" site). Interstitial waters were extracted from duplicate cores collected at each location. The water column was strongly stratified at both locations, exhibiting four layers at the natural sediments site (two of which were dysaerobic or anoxic), and two layers near the tailings outfall, the lower being dysaerobic. The unusual multiple layering probably reflects the influence of laterally variable advective processes. High concentrations of dissolved iron in shallow pore waters indicate that the sediments at both locations were anoxic at shallow subsurface depths. Concentrations of Zn, Cu, Pb and Cd were very low or undetectable in the pore waters. There was no evidence of release of Cu, Cd or Pb from the deposited tailings, although there was evidence of possible minor release of Zn from surface sediments in one of the tailings cores. Metals were removed from pore waters below the upper 10 cm at both sites, which is attributed to precipitation of authigenic sulfide phases.

Additional Key Words: subaqueous disposal, diagenesis, sulfide.

Introduction

A growing body of information suggests that the permanent storage of unoxidized, sulfide-rich mine tailings under water and their eventual burial by natural sediments may serve to inhibit significantly the dissolution of metals from such deposits. This emerging view stands in marked contrast to terrestrial tailings disposal operations where combined chemical and biological oxidation of tailings often results in the generation of acidic, metal-bearing drainage. Subaqueous disposal offers promise as a waste management technique that minimizes the environmental effects of mining by inhibiting the release of dissolved metals to surface and ground waters. The most tenable hypothesis that accounts for this inhibition is that ambient oxygen concentrations within natural waters and sedimentary pore waters are too low to effect significant oxidation within the tailings deposit. Results from an increasing number of published studies of both marine and lacustrine subaqueous disposal operations support this hypothesis in general (e.g., Drysdale 1990, Pedersen 1983, 1985, Pedersen and Losher 1988, Pedersen et

---

[1]Paper presented at the International Land Reclamation and Mine Drainage Conference and the Third International Conference on the Abatement of Acidic Drainage, Pittsburgh, PA, April 24-29, 1994.

[2]Thomas F. Pedersen, Professor, J. Jay McNee, Ph.D. candidate, and Bert Mueller, Research Scientist, Department of Oceanography, University of British Columbia, Vancouver, B.C., Canada V6T 1Z4.

[3]J. Jay McNee, Consultant, David H. Flather, Consultant, and Clem A. Pelletier, President, Rescan Environmental Services, 6th Floor, 1111 West Hastings St., Vancouver, B.C., Canada V6E 2J3.

al., 1993); however, the basic tenet that tailings are essentially unreactive in submerged environments has not been fully established. Moreover, previous studies have not addressed the role of seasonal variations in hydrography and oxygenation on the reactivity of the submerged deposits. Recognizing that such seasonal effects are poorly understood, a program has commenced in which tailings reactivity is being investigated in detail in the winter and summer in Anderson Lake, Manitoba. In this paper, we present an abbreviated description of new results from the recent winter survey carried out in Anderson Lake, when the water column was rather remarkably stratified. A more comprehensive description and interpretation will be published elsewhere.

Environmental Setting and Background

Anderson Lake is located approximately 2 km south of the townsite of Snow Lake in central Manitoba (fig. 1). It is a small, shallow, highly productive (mesotrophic to eutrophic) Precambrian Shield lake, which was floored originally by organic-rich sediments (Pedersen et al. 1993). Since 1979, about 8 million t of tailings have been discharged at the surface, mostly to the western basin of the lake, via a movable, floating Sclair pipe.

Water quality in the lake is very poor (Pedersen et al. 1993), due to dissolved metals and salts being added from acid rock drainage issuing from an old roadway built of waste rock and tailings along the north shore of the lake. Dissolved solids are also added to a much lesser extent from the process water discharged from the pipeline.

Sampling and Methods

Two locations were sampled in April, 1993 (fig. 1), one (Station B) near the tailings outfall in nearly 4 m of water, and the other (Station A) some 2 km to the southeast. At both sites the water column was sampled by submerging in place a 3.8 m long plexiglass pipe studded with sampling ports. About 50 cm of ice was cut through with a gas-powered auger. At least 48 h after emplacement of the pipe, water samples were drawn through each port by peristaltic pumping at a rate slow enough (<1 mL/s) to minimize flow-field distortion. The samples were drawn into a nitrogen-filled glove bag to eliminate potential oxidation and immediately filtered through 0.45 μm polycarbonate membrane filters. Oxygen and temperature profiles were collected through a separate hole in the ice within 5 m of the water sampling location, using a YSI meter and submersible probe. The oxygen probe was field-calibrated with respect to air.

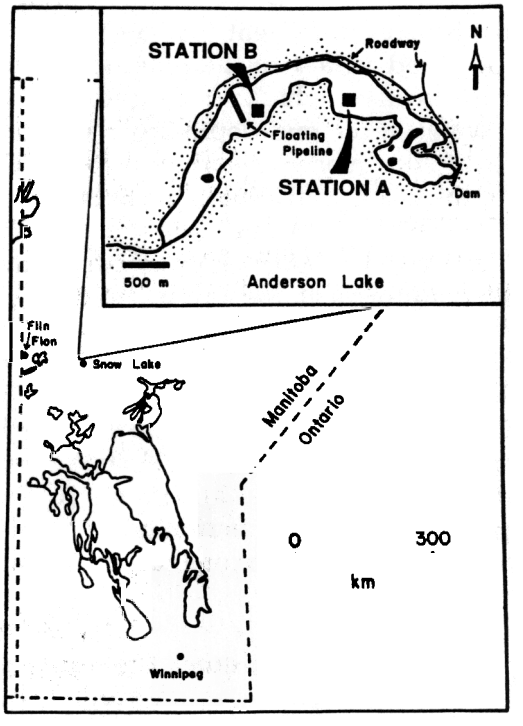

Figure 1. Lake and station locations.

Duplicate cores for sediment and interstitial water analyses were collected through holes about 3 m apart and 5 m from the water column sampler at Station A,

and about 12 m apart and ~10 m from the water column sampler at Station B. The lightweight gravity corer described by Pedersen et al. (1985) was used, and the quality of all four cores was excellent. Immediately after collection, each core was transported upright to nearby Snow Lake for processing. Interstitial water samples were extracted from the upper 30 cm of each of the cores by centrifugation under N_2 as described by Pedersen et al. (1993).

Analytical procedures for the interstitial water samples followed those described previously (Pedersen et al., 1993). Water column samples were analyzed by Analytical Services Laboratories (ASL) of Vancouver, as described by Maynard and Thomas (this volume). Sedimentary organic carbon (C_{org}), nitrogen, sulphur and $CaCO_3$ concentrations were determined at the University of British Columbia as described by Pedersen et al. (1993), while concentrations of a suite of major and minor elements in splits of the same homogenized sediment samples were measured by ASL (Maynard and Thomas, this volume).

Results

Water Column

Water column profiles of dissolved O_2 and temperature are shown in figure 2. Both the temperature and O_2 data at Station A indicate a four-layer stratification below the ice in April 1993. Relatively high O_2 contents (up to 4.6 mg/L) were limited to a cold water layer 20 cm thick immediately under the ice. The oxygen concentration decreased sharply between 60- and 80-cm depth, where the temperature increased from <1° to >6 °C. A mid-depth warm layer between 90 and 250 cm deep was characterized by a near-zero oxygen content. Up to ~1.5 mg/L O_2 occurred in a 1-m-thick aerobic zone near the bottom, which was slightly cooler than water in the mid-depth layer. Oxygen was again depleted in a warmer (by ~0.4 °C) 20-cm-thick layer adjacent to the bottom.

Less complex profiles characterize the water column near the tailings outfall at Station B (fig. 2). Oxygenated water was confined to a thin horizon immediately below the base of the ice and to the water in the 50-cm-deep hole through the ice, which must have been aerated (at both sites) when the holes were cut. As at Station A, the oxygen-depleted layer was much warmer than the relatively oxygenated waters above.

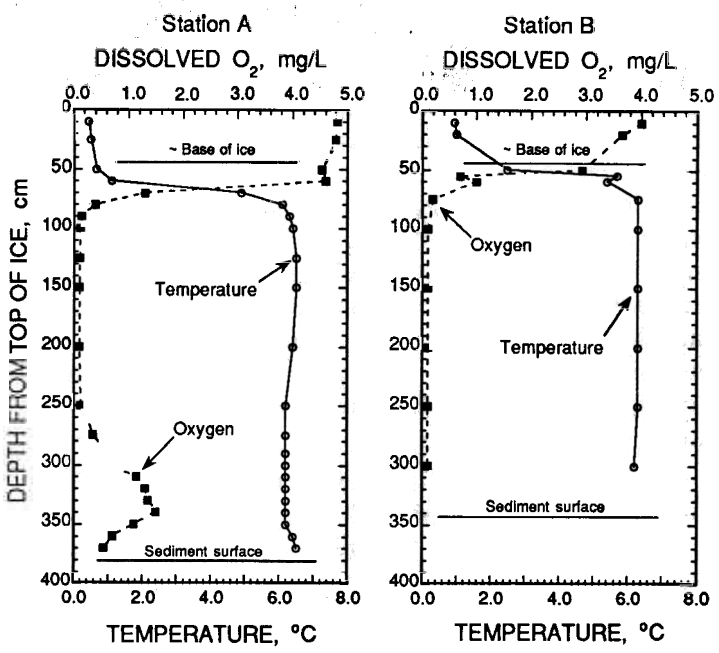

Figure 2. Oxygen and temperature profiles measured through the ice. Station locations are shown in fig. 1.

Variations in the concentrations of dissolved metals paralleled the stratification. Dissolved Fe contents, for

example were low (< 0.08 mg/L) in the oxic waters between 300- and 370-cm depth at Station A, but relatively high (up to ~9.5 mg/L) in the anaerobic layers (fig. 3). The oxygen-depleted waters at Station B hosted dissolved Fe contents of ~2 mg/L between 50- and 250-cm depth; below this horizon, the concentrations increase steadily and markedly toward the bottom, reaching ~70 mg/L in the deepest sample.

The distribution of dissolved Zn in the water columns at both sites was antipathetic to that of Fe; high Zn values of up to ~400 mg/L occurred where iron contents were low, and diminished sharply in the Fe-rich intervals (fig. 3). The contrast between the two elements was particularly pronounced in the lower 20 cm at Station A where abrupt changes in both the Fe and Zn contents occur 10 cm above the bottom.

Arsenic distributions in the water column were very similar to those of iron at both sites, although the absolute As concentrations near the tailings outfall (0.3 to 0.6 mg/L) were only about one-third of those at the natural sediments site (fig. 3).

Sediments and Interstitial Waters

Cores A1 and A2 collected ~3 m apart at the natural sediments site were visually and compositionally very similar. Both cores were veneered by a 2- to 3-mm-thick cap of rusty-brown noncohesive fine-grained sediment which contained abundant organic fragments. Small copepods (Daphnia?) were abundant in the water immediately above the sediment-water interface and were observed burrowing into the rust-colored surface layer. The surface veneer was underlain by about 10 cm of charcoal-gray fine-grained gelatinous ooze, which graded into the brown, gelatinous, homogeneous, organic-rich ooze that characterized the lower 40 cm of both cores. Small (presumably) methane bubbles developed below 30 cm depth in both cores shortly after collection. Both cores raised about 12 m apart at Station B consisted of undifferentiated fine-grained gray tailings which contained a very high proportion of glistening, very fresh-looking pyrite grains. The lake floor at this location was irregular with differences of more than 1 m depth between sites only 12 to 15 m apart. Observations made by divers during the

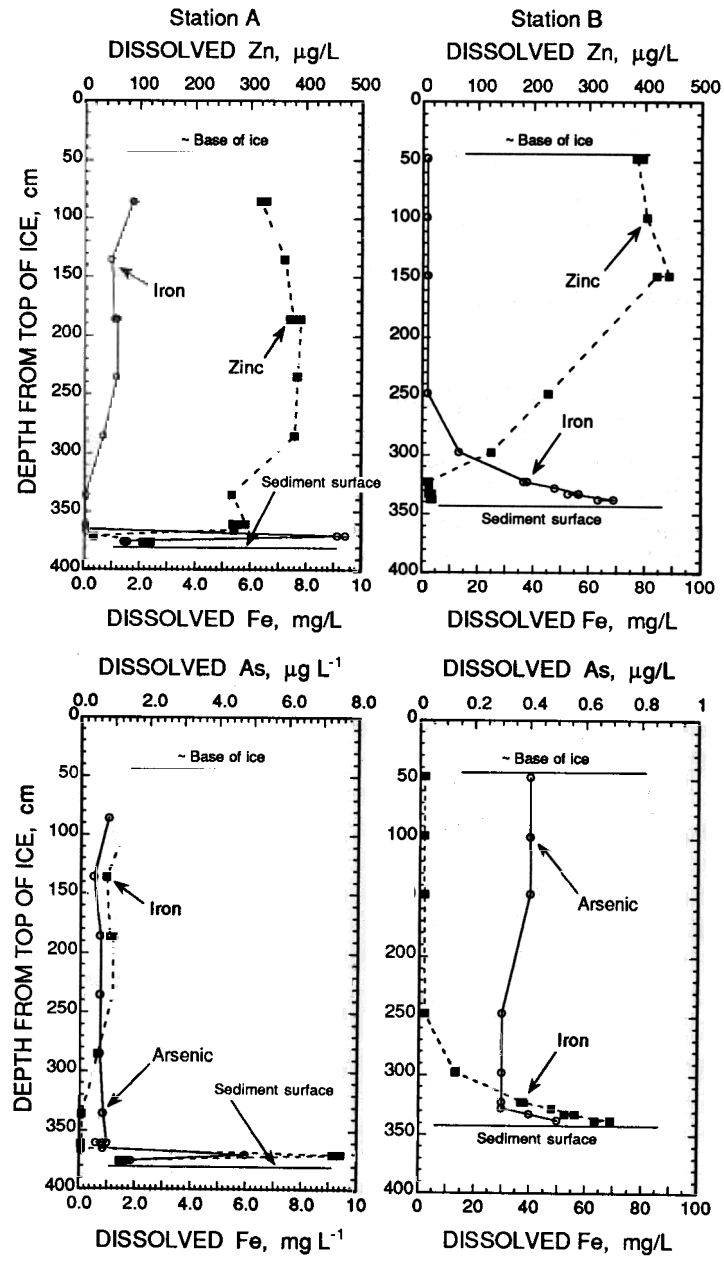

Figure 3. Dissolved iron, zinc, and arsenic profiles in the water column at the two sampling sites.

August 1993 survey of the lake confirmed that the sediment surface near the tailings outfall is hummocky. Lobes of tailings appear to account for the observed differences in local relief.

Cores A1 and A2 consist of essentially tailings-free, organic-rich sediments below about 12 cm deep, as shown by C_{org}, Fe/Al, S, Zn, Cu, Pb, As, and Cd data (not shown, but the distributions are very similar to those reported by Pedersen et al. 1993). The upper stratum in both cores is composed of a mixture of tailings and natural sediments with metals concentrations reaching maxima between 1- and 2-cm depth. The marked compositional similarity of cores A1 and A2 is not matched by the pair of cores from Station B. Organic carbon, Fe/Al, S, Zn, Cu, Pb, As, and Cd distributions in cores B1 and B2 show differences with depth, which apparently reflect significant local-scale lateral inhomogeneities in the tailings deposit in the lake. This inhomogeneity is not inconsistent with the variable composition of the ore feedstock and the frequent changing of the location of the discharge outfall.

All filtered pore water samples from all four cores were analyzed for a suite of dissolved metals. We report here the distributions of Fe, Mn, Zn, Cu, Pb, and Cd. Total dissolved sulfide was measured in selected aliquots where volume permitted.

Dissolved Fe profiles are shown in figure 4 along with concentrations measured in the lowermost sample (5 cm above the bottom) collected with the water column sampler. The "duplicate" profiles are similar in form at each site: high concentrations characterize the pore waters in the upper several centimeters, particularly in the Station B cores; below the upper 10 cm, concentrations fall to very low values. Dissolved Mn distributions are fundamentally different (fig. 4): there is no significant increase with depth in the upper 10 cm, and there is no depletion toward the base of the cores as is evident for iron. Dissolved zinc concentrations at the natural sediments site sharply decrease with depth in the upper 2 cm of the deposits (fig. 5), similar to the tailings in core B1, whereas in B2, a peak in concentration (~25 μg/L) occurs between 0.5 and 2 cm depth.

Dissolved copper (fig. 5) was essentially undetectable (≤ 0.12 μg/L) in all pore waters extracted from the pure tailings cores (as well as in the overlying bottom water). In cores A1 and A2,

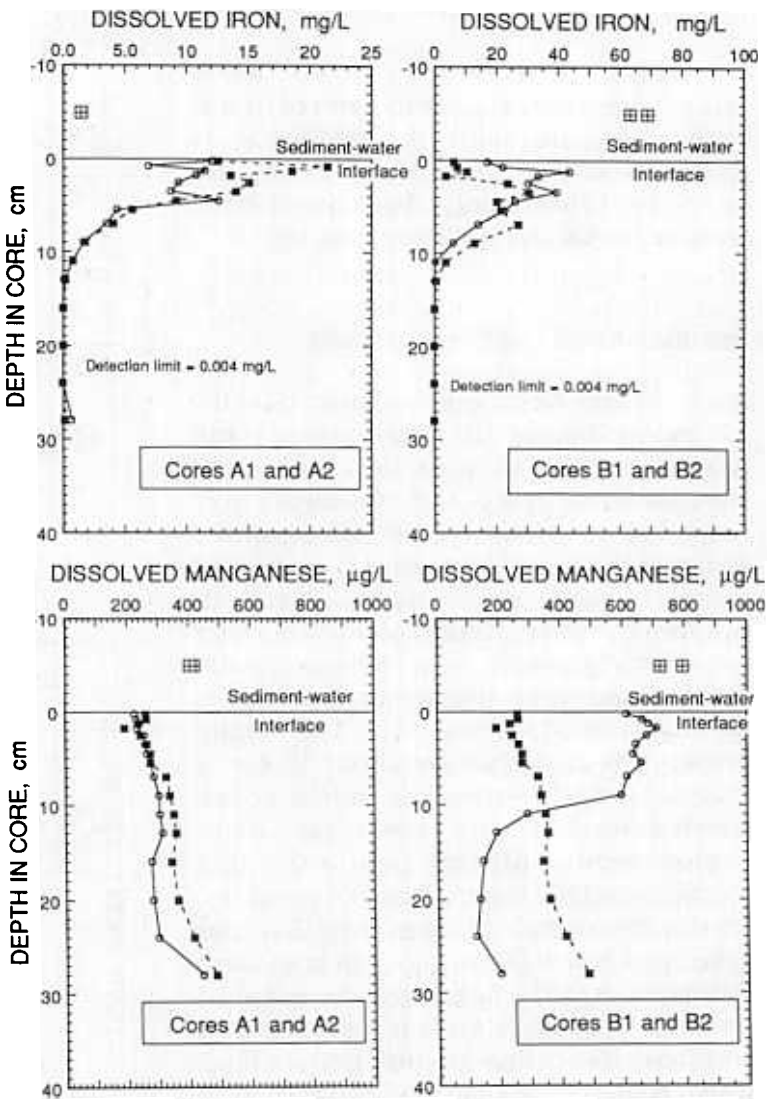

Figure 4. Dissolved interstitial iron and manganese distributions in duplicate cores from the sampling sites. Cores A1 and B1 are designated by open circles, and A2 and B2 by open squares.

maximum concentrations of 2.8 µg/L are observed in the upper 2 cm, with very low or undetectable values at greater depths. Neither Pb nor Cd was detectable in any of the pore water samples at either station (fig. 6), excepting the 1.25-cm sample in Core A1 where the Cd concentration marginally above the detection limit. Lead and cadmium were primarily undetectable in the bottom waters at either site. Dissolved sulfide was not detectable in pore waters from the tailings cores, in contrast to the measurable but low levels (up to 25 µmol/L) recorded at the natural sediments site (fig. 7). The decline in dissolved sulfate concentration with depth in the natural sediments is consistent with the sulfide profile. Increases in interstitial sulfate with depth at the tailings site (Station B, fig. 7) indicate that the tailings release sulfate to pore waters; Pedersen et al. (1993) attributed this to dissolution of sulfide alteration products formed during milling, and pointed out that the addition of sulfate to the pore waters at depth does not rule out the co-occurence of sulfate reduction.

Discussion

Pedersen et al. (1993) described the distribution of dissolved metals in pore waters collected in summer 1990 at three sites in Anderson Lake. Their principal conclusion was that the submerged deposited tailings in Anderson Lake were not releasing metals to the overlying water column at that time. Indeed, the opposite appeared to be true: sharp decreases with depth in the concentrations of dissolved Zn, Cu, Pb, and Cd in the upper few centimeters of the deposits were interpreted as representing consumption of metals from the contaminated overlying lake water. Precipitation of authigenic sulfide phases at shallow depths in anoxic tailings and natural sediments was suggested as an explanation for the very low metals concentrations in the pore waters.

The winter survey results presented here confirm that the water column in Anderson Lake undergoes a pronounced seasonal change in hydrography and chemistry. When the lake is ice covered and wind-driven mixing is eliminated, the development of water column anoxia appears likely. We do not know how long such a water-column condition might persist in any given year nor whether episodes of anoxia or dysaerobia recur annually. However, the contrast in water column stratification

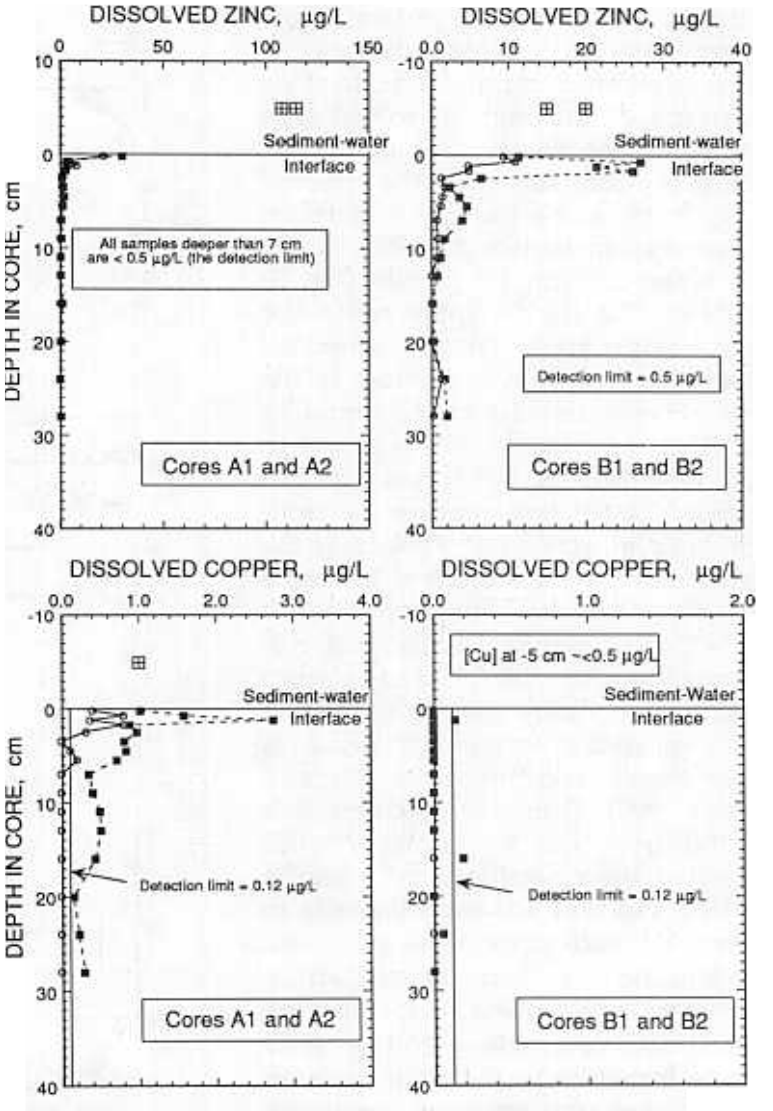

Figure 5. Dissolved zinc and copper distributions in duplicate cores. Symbols as in fig. 4.

between the 1990 summer survey, when the water column was warm and oxygen replete, and the wintertime observations presented here suggests that the conclusions of Pedersen et al. (1993) are applicable to the summer season only.

Several conclusions can be drawn from these preliminary results. First, steady state does not exist in Anderson Lake as it might in deeper water bodies; this complicates the interpretation of chemical exchange between the sediments and the overlying waters. The seasonal development of a multilayer stratification, which appears to vary both horizontally and vertically, adds additional complexity. Despite these difficulties, these data indicate that there was no measureable release of dissolved Cu, Pb, or Cd from the rapidly-deposited tailings near the floating outfall in early April 1993, despite the tailings being highly enriched in each of these metals. Similarly, there was no apparent release of dissolved Cd or Pb from "natural" but tailings-contaminated sediments" cored at Station A.

Second, although anaerobic water occupied almost three-quarters of the water column at Station A, a thin layer of oxygenated water was present in the lower meter. This poses a thermodynamic conundrum in that occurence of the high dissolved iron content observed 10 cm above the bottom is inconsistent with the presence of O_2 in the same water. We have no obvious explanation for this observation. The water-column Fe profile (fig. 3) indicates that the Fe spike could not have originated from reductive dissolution of Fe oxyhydroxides in the underlying sediments at the sampling site. Also, the spike could not be due to slow oxidation of Fe^{2+} at a low pH because the pH measured in the iron-rich interval was ~7.5. However, the high dissolved As content at the same horizon 10 cm above the bottom does imply that oxyhydroxide dissolution is responsible for the Fe peak, since arsenate ion readily adsorbs to FeOOH and is released when the latter dissolves under anoxic conditions (Belzile and Tessier 1990). Thus, we speculate that the thin iron- and As-rich layer could have had been produced at a nearby location and was advected laterally to Station A. If such phenomena are indeed active in the lake, than any comparison of the bottom-water metals concentrations with core-top pore waters becomes problematic: neither chemical nor compositional continuity would exist between the pore and

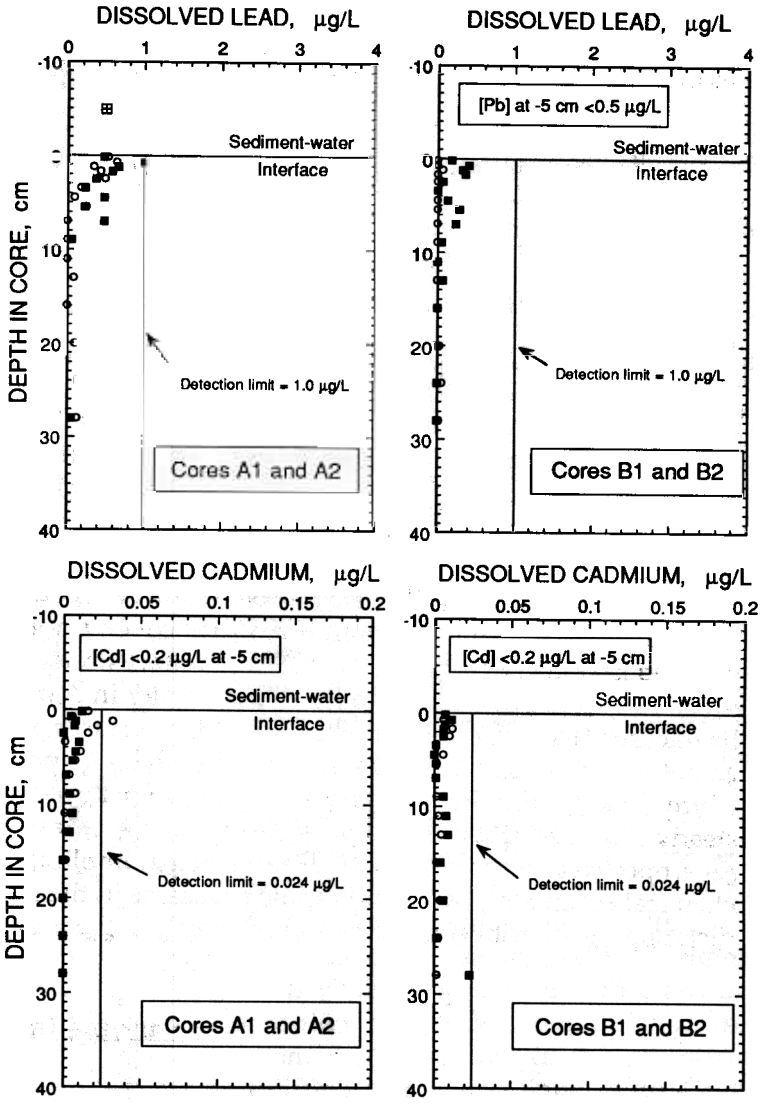

Figure 6. Dissolved lead and cadmium distributions in duplicate cores. Symbols as in fig. 4.

bottom waters under these circumstances. This implication might explain the contrast between the high iron concentration in the bottom water at Station B (fig. 3) and the minimum in the pore water Fe profiles seen at the surface in both cores raised from this site (fig. 4).

The high iron content observed in the near-surface pore waters at Station A may be attributed to reductive dissolution at shallow depths in the sediment column; this is consistent with the presence of the thin rusty-brown veneer on the core tops at that site, and the black colour of the immediately underlying deposits. The steep decline in dissolved Fe below about 5 cm depth in both cores plainly reflects precipitation of FeS or FeS_2. As noted earlier, free dissolved sulfide is present in the pore waters in both cores below the upper several centimeters (fig. 7).

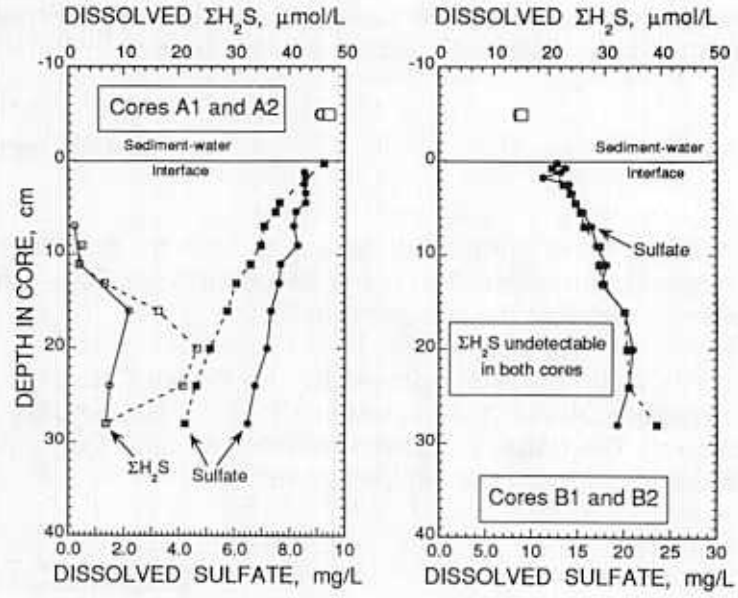

Figure 7. Dissolved sulfide and sulfate distributions in duplicate cores. Cores A1 and B1 are indicated by circles and A2 and B2 by squares.

Third, although the data from the tailings site (Station B) unequivocally indicate no copper release to the overlying water, the profiles in the "natural sediments" (Station A) imply that Cu was being released to pore solution at about 1.25 cm depth and was diffusing both upward and downward from this maximum. More problematic is the subsurface dissolved zinc maximum seen in core B2, which is shallower than the pore water Fe maximum in the same core. Although this distribution could reflect a diffusive efflux of Zn out of the tailings, the maximum may be somewhat artificial: a change in the bottom water zinc content not long before the cores were collected could have induced a perturbed profile that does not reflect steady-state diagenesis. An additional ambiguity is that the tailings were overlain by oxygen-poor water in April 1993, and under such conditions, no Zn should be released (for example, via oxidation of the surfaces of ZnS particles. The spatial disparity between the dissolved zinc and iron maxima in the shallow pore waters of Core B2 tends to rule out iron oxyhydroxide dissolution as an explanation for the apparent zinc release. On balance, we prefer non-steady state perturbation as a possible explanation for the zinc efflux implied by the dissolved Zn data in the upper centimetre of Core B2. The principal implication of this suggestion is that temporally-varying chemical reactions and hydrographic processes in the overlying water column may play a major role in dictating the distributions of dissolved metals in the near-surface pore waters.

Summary and Implications

Pedersen et al. (1993) noted that Anderson Lake is essentially a sediment-starved basin, but it is also mesotrophic to eutrophic in character. Thus, the natural flux of sediments to the bottom of the lake is characterized by little silicate detritus and an extremely high organic content. Therefore, anoxia develops at very shallow subbottom depths. Mine tailings are now widely distributed on the floor of the lake, and

all available results are consistent in indicating that no Cd, Pb or Cu is being released from the submerged tailings. Unlike the summertime survey of Pedersen et al. (1993), however, the winter survey data discussed here do not rule out the possibility that there was a very small efflux of dissolved zinc from the tailings to the overlying water in April 1993.

These results confirm that metal release from fresh, sulfide-rich tailings is limited by submerged storage, in contrast to the behavior of sulfide-bearing tailings deposits stored subaerially. Along the north shore of Anderson Lake, subaerial tailings deposits have become acidic and are releasing substantial quantities of metals to surface drainage.

Acknowledgments

We are very grateful for the assistance in the field of Brian Levia (Hudson Bay Mining and Smelting Company, Flin Flon). We thank Maureen Soon, Raja Ganeshram, and Iain Watson for their careful analytical work in the laboratory at UBC.

This work was supported by the British Columbia Ministry of Energy, Mines and Petroleum Resources, CANMET, Environment Canada, Hudson Bay Mining and Smelting Co. Ltd., Placer Dome Inc., and The Canada/British Columbia Mineral Development Agreement through the MEND (Mine Environment Neutral Drainage) Program.

Literature Cited

Belzile, N., and A. Tessier. 1990. Interactions between arsenic and iron oxyhydroxides in lacustrine sediments. Geochim. Cosmochim. Acta 54: 103-109.

Drysdale, K. 1990. Geochemistry of a buried mine tailings deposit, Howe Sound, B.C M.Sc. thesis, University of British Columbia.

Pedersen, T. F. 1983. Dissolved heavy metals in a lacustrine mine tailings deposit - Buttle Lake, British Columbia. Marine Pollution Bulletin, **14**: 249-254.

Pedersen, T. F. 1985. Early diagenesis of copper and molybdenum in mine tailings and natural sediments in Rupert and Holberg Inlets, British Columbia. Canadian Journal of Earth Sciences, **22**: 1474-1484.

Pedersen, T. F., and A. J. Losher. 1988. Diagenetic processes in aquatic mine tailings deposits in British Columbia. *In* Chemistry and Biology of Solid Waste. *Edited by* W. Salomons and U. Forstner. Springer-Verlag, Berlin, pp. 238-258.

Pedersen, T. F., S. J. Malcolm and E. R. Sholkovitz. 1985. A lightweight gravity corer for undisturbed sampling of soft sediments. Canadian Journal of Earth Sciences, **22**: 133-135.

Pedersen, T. F., B. Mueller, J. J. McNee, and C. A. Pelletier. 1993. The early diagenesis of submerged sulphide-rich tailings in Anderson Lake, Manitoba. Canadian Journal of Earth Sciences 30: 1099-1109.

WATER COVER ON ACID GENERATING URANIUM TAILINGS - LABORATORY AND FIELD STUDIES[1]

Nand K. Davé[2] and Albert J. Vivyurka[3]

Abstract: Under the Mine Environmental Neutral Drainage (MEND) program, a joint research project between CANMET, Elliot Lake Laboratory and Rio Algom Limited, Elliot Lake, Ontario, Canada, was established to investigate the feasibility of establishing a shallow water cover on pyritic uranium tailings as a close-out option for controlling acid generation and release of contaminants. The program consisted of: 1) laboratory lysimeter studies to investigate oxidation and leaching characteristics of coarse and homogenized total mill tailing with and without a water cover, 2) field evaluation of a partially submerged wetland tailings basin for its geochemical and biological controls on acid generation, and 3) establishment of a 65 ha flooded field demonstration site, and evaluations of its hydrological and geochemical control parameters. The laboratory lysimeter studies indicated that both control tailings without a water cover oxidized rapidly producing acidic drainage. However, the oxidation rate for the well drained coarse tailings was approximately two orders of magnitude higher than that for the homogenized total mill tailings which retained high degree of moisture saturation. Coarse tailings with a shallow water cover had a near neutral drainage effluent for a period of three years. Dissolved iron concentrations in the effluent were either below detection or less than 1 mg/L for the initial three year period and increased slightly thereafter. Results from the partially submerged tailings basin showed that the overall wetland/water cover system was effective in controlling acidic drainage from this site with effluent pH>7 and dissolved iron concentrations ~ 0.1 mg/L. A description of the 65 ha flooded field test program is presented including some initial water quality data. The results indicated that acid generation could effectively be controlled using a shallow water cover (0.5- 1.0 m in depth).

Additional Key Words: acid mine drainage, uranium mine/mill tailings, uranium wastes

Introduction

Water with its low oxygen diffusion coefficient ($2x10^{-9}$ m^2/s) and low oxygen solubility (8.6 g/m at 25° C), is probably the most cost effective and readily available oxygen- limiting cover for controlling acid generation in reactive wastes. In the absence of convective transport, the rate of oxygen diffusion through water is too slow to be significant (Davé 1992). A water cover on reactive wastes: 1) limits available oxygen and hence controls acid generation, 2) eliminates surface erosion by wind and water action, and 3) creates a reducing environment for bacterial reductions of nitrates and sulphates.

Under the Canadian Mine Environmental Neutral Drainage (MEND) program, a joint research project entitled "Development of wet barriers on pyritic uranium tailings" was undertaken by the Elliot Lake Laboratory, CANMET, Energy, Mines and Resources Canada and Rio Algom Limited, Elliot Lake, Ontario. The objective of the study was to evaluate the feasibility of establishing a shallow water cover on pyritic uranium tailings, as a decommissioning option, for controlling acid generation and release of contaminants.

---

[1]Paper presented at the International Land Reclamation and Mine Drainage Conference and the Third International Conference on the Abatement of Acidic Drainage, Pittsburgh, PA, April 24-29, 1994.

[2]Nand K. Davé, Senior Environmental Research Scientist, Elliot Lake Laboratory, CANMET, Energy, Mines and Resources, Canada, Elliot Lake, Ontario, Canada.

[3]Albert J. Vivyurka, Senior Environmental Engineer, Rio Algom Limited, Elliot Lake, Ontario, Canada.

The uranium mill tailings in the Elliot lake region are acid generating, low level radioactive wastes, containing approximately 5 to 7% pyrite and low concentrations (10 to 15 Bq/g) of uranium decay series radionuclides. The tailings were discharged at neutral to alkaline pH's but have low buffering capacity because of an acid leach process used in uranium extraction.

With water cover as an emerging technology for controlling acid generation, Rio Algom Limited, for their Elliot Lake operations, has proposed decommissioning two inactive tailings sites at Quirke and Panel Mines by large scale flooding and an in situ water cover. These sites are ideally situated in valleys with cross-valley engineered dams and favourable topography for flooding and maintenance of a water cover. At the Quirke site, an experimental 65 ha test site has been developed for a large scale flooding demonstration.

The present study was initiated in 1989 to evaluate the performance of a water cover on pyritic uranium tailings, both under laboratory controlled conditions and in the field. Preliminary results of this study were reported in 1990 by Davé et al. (1990).

Experimental Study

The experimental study consisted of three parts: 1) laboratory lysimeter column tests, 2) field evaluation of a wetland basin containing partially submerged pyritic uranium tailings, and 3) establishment of a 65 ha flooded field demonstration site.

Column Leaching Tests

Column lysimeter leaching tests were conducted to determine oxidation and leaching characteristics of pyritic uranium tailings under unsaturated (control) and flooded conditions. For these tests, two types of tailings were chosen. The first one consisted of fresh and homogenized total mill tailings (control-1, approximately 50% less than 74 μm or -200 mesh), obtained from the tailings filtration circuit of Rio Algom's Quirke mill. The second consisted of fresh and predominantly coarse tailings (94% greater than 74 μm or +200 mesh), obtained from the Quirke tailings area. For flooded conditions, only coarse tailings were used representing a worst case scenario. Tests were also conducted for evaluating the effects of coarse and fine grained limestone mixed with the two types of tailings.

Figure 1 shows a typical experimental arrangement of a column leaching lysimeter with a water cover. The column, 122 cm in height and 15.2 cm nominal diameter (I.D. 14.5 cm), was made from a schedule 80 (thickness 1.25 cm) PVC pipe. In total, 24 columns were filled with tailings or tailings and limestone mixtures and each column contained approximately 14.3 kg of material. Columns 1 to 15 consisted of five sets, all in triplicates. Set 1 contained only total mill tailings and was used as a first control (control-1). The other four sets contained total mill tailings mixed with 7.5% (by weight) limestone of grain sizes -6.3 mm (-4 mesh), -2.4 mm (-8 mesh), -0.84 mm (-20 mesh) and wet ground limestone, respectively. The amount of limestone added was approximately equivalent to the net acid generation potential of the tailings.

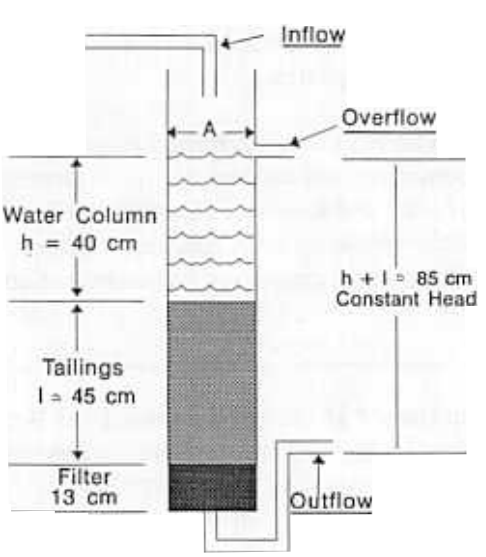

Figure 1. Experimental arrangement of a flooded leaching column.

Columns 16 to 21 consisted of three duplicate sets which contained coarse tailings as a second control

(control-2). The first set (columns 16 and 17), contained coarse tailings, while the other two sets contained coarse tailings mixed with 7.5% (by weight) of coarse grain size 6.3 mm (-4 mesh) or wet ground limestone, respectively.

Columns 22 to 24 contained only coarse tailings with no limestone and were filled with distilled water to a height of 40 cm above the tailings, providing a shallow water cover.

Initially, all the columns were inoculated with 100 mL of acidic leaching solution obtained from an underground leaching stope of the Quirke Mine. The columns were then allowed to acclimatize for a few days. All columns from 1 to 21 were batch leached under unsaturated conditions by adding, every two weeks, 1 L of well aerated natural lake water collected from Gravel Pit Lake near the Quirke tailings. For each column, the effluent sample was collected every two weeks and its volume and primary water quality parameters: pH, redox potential (Eh), electrical conductance (Ec), acidity, alkalinity were measured. On a monthly basis, individual column samples were composited and analyzed for total dissolved Al, Ca, Fe, Mg, Mn, Ra-226, Th, U and SO_4^{-2} concentrations. Initially for the first year, the columns were leached by adding 100 mL of the lake water daily and the samples were composited weekly for analysis.

Column 22 to 24 with a water cover were leached with distilled water under flooded conditions. Distilled water was continuously added at the top of each column at a sufficient flow rate to maintain the water cover and allow pore water drainage of approximately 1L per day for the first two years and then to 1 L per week. Over a four year period, approximately 250 pore water volumes were exchanged. The initial high ground water flow was simulated to rapidly leach and remove soluble minerals like gypsum to further study the oxidation and leaching characteristics of other residual minerals and radionuclides.

Partially Submerged Tailings and Wetland Basin: Field Evaluations

This study consisted of an extensive environmental monitoring survey of an existing natural wetland basin, called Panel wetland, containing partially submerged pyritic uranium tailings. It was undertaken to establish whether the existing natural wetland and water cover system was providing any treatment to acid mine drainage, and to evaluate its hydrologeochemical and biological controls on acid generation and migration of contaminants associated with the oxidation process.

The survey included: determination of the site hydrology and its flow conditions, measurements of surface and ground water quality parameters and their seasonal fluctuations, characterization of substrate solid/tailings and sediment for oxidation- reduction profiles, bacterial enumeration, and vegetation uptake of metals and radionuclides.

The Panel wetland site is a small basin located in a bedrock valley containing partially submerged pyritic uranium tailings. It has a total area of 14.5 ha and contains approximately 236,000 tonnes of tailings spread over 12.9 ha. Approximately 88% of the total tailings area is under water, leaving 1.6 ha in the western part of the basin where the tailings are exposed. The average thickness of the tailings in the basin is 0.92 m. The depth of water cover varies from shallow, 0.1 to 0.5 m, in the western and central parts to slightly deeper ponded water, 0.4 to 1.4 m in depth, in the east. The basin supports a dense vegetation cover consisting of cattails, marshland grasses, sedges, sphagnum and other acidophilic mosses. The deep ponded water contained submergent vegetation such as pond weeds.

The surface water hydrology and chemistry of the basin were studied for three seasons, spring, summer and fall. Water samples were collected along selected transacts throughout the basin and at various depths. For ground water monitoring, the site was instrumented with a series of multi-level piezometers along selected transacts parallel to surface and ground water flow regimes and at shallow depths of 0.3, 1.0, 1.5 m at each location. The ground water hydrology and chemistry was only determined for summer and fall seasons.

The water samples were analyzed for pH, redox potential (Eh), electrical conductance (Ec), dissolved oxygen, acidity, alkalinity, total dissolved solids, SO_4^{-2}, and total dissolved metal concentrations for Al, Ca, Cu, Fe, Mg, Mn, Ni, Pb, Th, U, Zn and Ra-226.

Soil/tailings substrate and sediment samples were collected from shallow depths (up to 0.3 m) for solid phase characterization of metals and radionuclides, sulphur speciation and bacterial enumeration for Thiobacillus ferrooxidans (TF) and Sulphate Reducing Bacteria (SRB). Composite vegetation samples were also collected for individual plant species. All substrate, sediment and vegetation samples were analyzed for total Al, Ca, Cu, Fe, Mg, Mn, Ni, Pb, Th, U, Zn and Ra-226 contents.

Field Demonstration and Flooded Test Site: Quirke Tailings Concept

A large scale flooded test site, 65 ha in area, has been developed at the Quirke Mine tailings site to demonstrate flooding of tailings using a terraced cell concept, and to evaluate its performance based on the site hydrological and geochemical monitoring results. Figure 2 shows a general plan of the flooding concept at the Quirke mine waste management area.

The tailings basin contains approximately 48 million tonnes of uranium mine tailings and waste rock and covers an area of 190 ha with a drainage basin of 275 ha. There is a 15 m elevation difference between the west end of the Quirke tailings and the east end effluent discharge area. To enable covering the tailings with water, the basin was developed in a terraced manner by construction of four internal dykes and dividing the basin into a series of internal cells (14 to 18) which effectively dealt with a drop in tailings surface elevation from west to east. This represented an overall average gradient of about 0.5%. The drop in elevation from cell to cell is about 4 m. These internal cells are retained by dykes constructed of mine waste rock, tailings and glacial till. Figure 3 shows a typical cross-section of the tailings basin, internal dykes and external dams. The overall basin hydrology is such that a minimum of 0.6 m water cover could be maintained over the tailings in each cell. Detailed design concepts and geotechnical aspects of the Quirke tailings site are given by Balins et at. (1991).

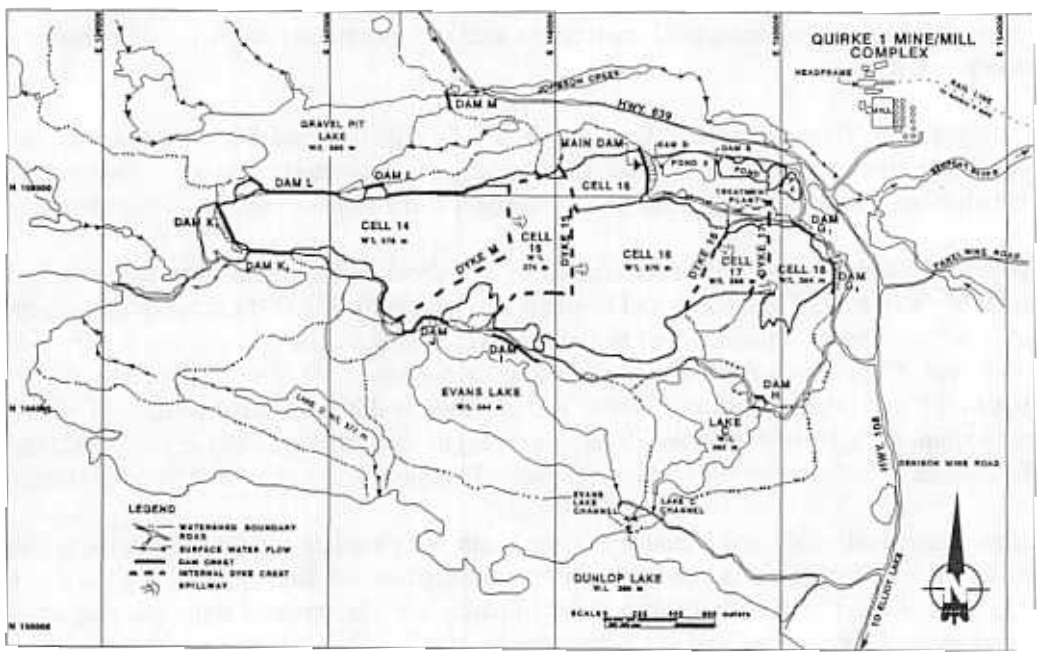

Figure 2. General plan of flooding concept at the Quirke mine waste management area.

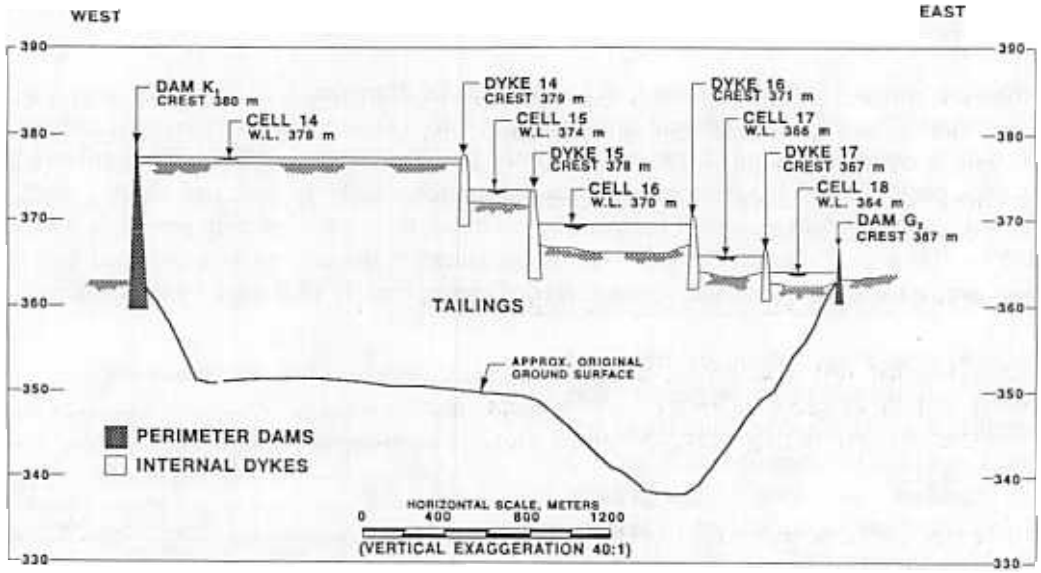

Figure 3. Schematic profile of flooding concept, Quirke mine waste management area.

The initial decommissioning and flooding concept is being tested at Cell #14 located at the highest elevation in the west end of the basin. The cell has an area of approximately 65 ha. An internal dyke #14, together with other containment dams completes the field demonstration test site. Water from a nearby Gravel Pit Lake is used for initial flooding.

The monitoring program for cell #14 consisted of obtaining a water balance for evaluating seepage losses through the site, measurements of piezometric pressure heads across the dyke for calculating seepage losses through the dyke and monitoring of surface and ground water quality parameters.

Results and Discussion

Column Leaching Tests

The column leaching results for unsaturated coarse tailings (control-2, column 16 and 17), unsaturated coarse tailings with coarse limestone (column 18 and 19), unsaturated total mill tailings (control-1, column 1 to 3) and flooded coarse tailings (column 22 to 24) are shown, respectively, in figures 4 to 7 for pH, SO_4^{-2}, and Fe. The results are presented in decreasing order of acidic drainage from the columns.

Initially for the first year, when the leaching scheme consisted of daily additions of 100 mL of natural lake water to the columns, no acidic drainage was observed from any of the columns. Although the tailings in columns 16 and 21 were coarse grained, they appeared to retain appreciable amounts of moisture to maintain near saturation conditions due to a shallow

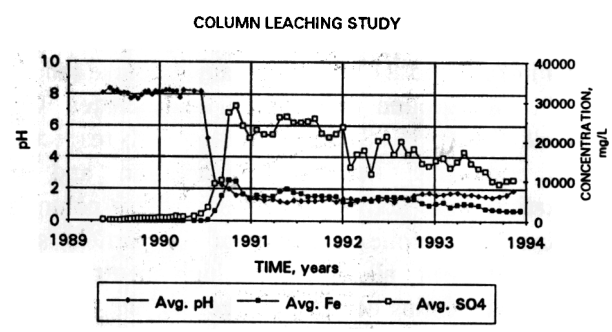

Figure 4. Leaching profiles of coarse pyritic uranium tailings, columns 16 and 17 (control-2), variations of pH, Fe and SO_4^{-2} with time.

water table and frequent water additions. This condition was altered by modifying the leaching scheme in June 1990 to batch additions of 1L of water every two weeks.

The control-2, columns 16 and 17, were first to show acidic drainage, 1 to 2 months after the new leaching scheme was implemented. The pH of the effluent dropped from 8 to 2 during this short interval and continued to fall slowly to pH 1.2 over a two year period. It recovered slowly to 1.8 afterward. All other parameters also indicated severe oxidation with peak Fe and SO_4^{-2} concentrations of approximately 10,000 and 28,000 mg/L, respectively (Fig. 4). From the water quality data and mass balance for the initial three year leaching period, it was estimated that approximately 275 to 300 g or 70 to 75% of the total Fe contained in the tailings was oxidized and removed. This corresponded to an average iron oxidation and removal rate of approximately 18.3 mg Fe per kg tailings per day.

In addition to the mobilization of iron and sulphate, the acidification of these columns also mobilized other metals, e.g., Al, Ca, Mg, Mn, Th, U and rare earths Y and Ce, etc. The control-2 tailings also contained some residual limestone and gypsum precipitate following limestone neutralization of leached tailings in the mill. With the onset of acid generation, all the available alkalinity was consumed and Ca leached out within the first year and a half. After approximately four years of leaching, the columns are still producing very acidic leachates with Fe and SO_4^{-2} concentrations on the order of 4,000 and 15,000 mg/ L, respectively.

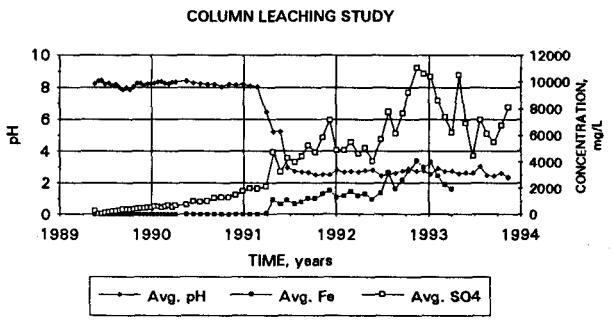

Figure 5. Leaching profiles of coarse pyritic uranium tailings mixed with 7.5% +6.5 mm size limestone (columns 18 and 19), variations of pH, Fe and SO_4^{-2} with time.

Columns 18 and 19, which contained coarse tailings and 7.5% limestone, also produced acidic drainage, but its onset was delayed for a period of one year from the start of acidic drainage from control-2 columns (Fig. 5). The acidic discharge rates were also lower for these columns than control-2 columns. Although sufficient limestone alkalinity was present in these columns, the data showed that it was not readily available for total acid neutralization probably because of its coarse grain size and surface armouring. The leachates were also saturated with respect to gypsum (Ca concentrations ~600 mg/L).

For the entire leaching period, no acidic drainages were observed from columns 3 to 15 which contained total mill tailings mixed with 7.5% limestone and columns 20 and 21 which contained coarse tailings and 7.5% wet ground limestone. The leachates were slightly alkaline (pH ~ 8) and saturated with respect to gypsum, indicating that acid generation and its neutralization were active processes in these columns. Wet ground limestone, because of its particle size, provided sufficient alkalinity or high neutralization potential in preventing acidic drainage.

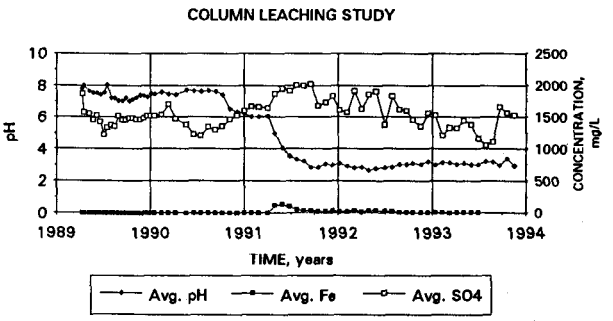

Figure 6. Leaching profiles of homogenized pyritic uranium total mill tailings , columns 1, 2 and 3 (control-1), variations of pH, Fe and SO_4^{-2} with time.

The control-1, columns 1 to 3, which contained homogenized total mill tailings also produced acidic drainages but at pH's ~ 3 containing lower concentrations of Fe and SO_4^{-2} than those for the control-2 columns (Fig. 6). The maximum Fe and SO_4^{-2} concentrations of the leachates were in the ranges of

50 to 400 mg/L and 1400 to 2800 mg/L, respectively. These values were significantly lower than corresponding concentrations of 10,000 to 12,000 mg/ L for Fe and 25,000 to 32,000 mg/L for SO_4^{-2} in control-2 column leachates. From the leachate Fe concentrations, it was calculated that for the homogenized total mill tailings (control-1), on an average a total of approximately 2.5 g or less than 0.7% of the total Fe contained in the tailings was oxidized and mobilized over the entire leaching period.

These tailings had a permeability on the order of $1x10^{-7}$ m/s and were characterized by a high capillary suction which, under the present water table configuration, maintained them near complete saturation conditions. The acid generation and metal migration rates for such tailings were thus low. Deposition of well mixed and homogenized total mill tailings without further segregation of its particle distribution could significantly reduce total acid generation and metal loadings.

In columns 22 to 24, which contained coarse tailings under water, soluble sulphates of Ca, Mg and trace amounts Mn leached out rapidly with approximately 50 L of water applied over an initial period of three months. The drainage from these columns remained at near neutral pH for a period of over three years and thereafter the pH dropped slightly to ~ 6.5 (Fig. 7).

Dissolved iron concentrations were either below detection or less than 1 mg/L for these columns for the initial three year period, then increased slowly to 1 to 2 mg/L for columns 22 and 23 and between 5 to 20 mg/L for column 24. Occasionally there have been flow control and drainage problems with the last column, which at times resulted in an excessive drainage, and hence, a drop in the water cover height over the tailings. The effluent concentrations of other metals during that period were less than 1 mg/L.

Because of its continuous flow, the water column above the tailings was well oxygenated (~ 8 to 10 mg/L of dissolved oxygen). In the drainage effluent, the dissolved oxygen concentrations were depleted to 2 to 4 mg/L. Consumption of oxygen by tailings and/or by other oxygen-consuming micro-organisms may lead to oxidation of tailings. The observed increase in the effluent Fe concentration could indicate the start of such a process which can only be verified by further monitoring.

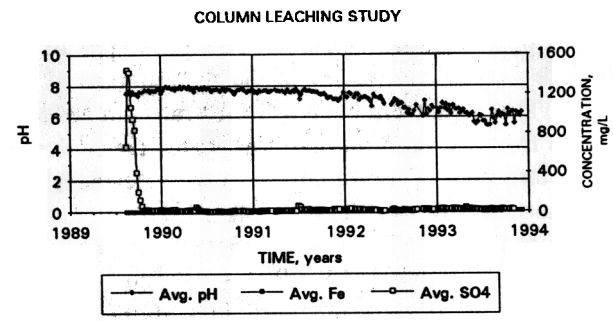

Figure 7. Leaching profiles of coarse pyritic uranium tailings under flooded conditions (columns 22,23 and 24), variations of pH, Fe and SO_4^{-2} with time.

With the depletion of dissolved Ca and Mg sulphates, the flooded columns also started to release increased concentrations of Ra-226, increasing from 1000 mBq/L to approximately 5,000 mBq/L.

Partially Submerged Tailings and Wetland Basin

Figure 8 shows the surface water quality profiles for pH, and dissolved Fe and SO_4^{-2} concentration for the Panel wetland basin along its length. The surface water in the basin was slightly to moderately acidic in the exposed and vegetated part of the basin with low to medium concentrations of dissolved solids (600 to 2000 mg/L), Fe (1 to 80 mg/L), Ca (150-500 mg/L) and SO_4^{-2} (50 to 1000 mg/L).

In the central and eastern parts of the basin, where a permanent water body existed, the surface water was near neutral to moderately alkaline, pH (6.2 to 9.8), with low concentrations of dissolved solids (100 to 300 mg/L), Fe (0.1

to 0.4 mg/L), Ca (30 to 50 mg/L), and SO_4^{-2} (50 to 100 mg/L). The surface water quality of the basin was seasonally independent except for pH in the central and eastern parts of the basin, which increased from 7.5 to 9.8 in the summer. The drainage water volume was estimated to be six times the volume of the water contained in the basin which represented a dilution factor of 6.

Figure 9 shows the ground water quality profiles for pH, and dissolved Fe and SO_4^{-2} concentrations at 1 m below the tailings/sediment surface. The ground water at shallow depths in the basin was mostly tailings derived pore water with slightly acidic to near neutral pH (5.7 to 7.8), low to moderate acidity (10 to 200 mg $CaCO_3$/L), low to high alkalinity (0 to 1400 mg $CaCO_3$/L), low to moderate Fe (0.5 to 70 mg/L), high Ca (400 to 800 mg/L), high SO_4^{-2} (800 to 1500 mg/L), and high Ra-226 (280 to 10,900 mBq/L). There was no seasonal dependence except for dissolved Fe concentrations, which were variable.

The soil substrate in the basin consisted mainly of tailings except near the far east end where the original peat sediment existed. The paste pH of the substrate varied from highly acidic to near neutral, 2.1 to 7.5. TF were present in all soil substrate and sediment samples from exposed and shallow water cover sites in the western part of the basin. At deep water sites near the center and towards the east, the bacterial counts for TF reduced drastically to insignificant numbers (0 to 100 MNP). Sulphate Reducing Bacteria (SRB) populations at these sites exceeded those for TF. Sulphate reduction was clearly evidenced by a strong smell of H_2S gas in the ground water at these locations.

Tailings were oxidizing in the exposed and shallow water covered and vegetated part of the basin. In exposed areas, oxidation was taking place near the surface in the unsaturated zone and in the vicinity of the water table. In vegetated areas, oxidation of both organic matter and tailings was taking place from surface to the root zone of the substrate. The tailings in the basin were fine grained and retained high degree of moisture saturation. The exposed tailings were thus oxidizing slowly producing moderately low pH (3.4 to 5.5) surface drainage and sub-surface water.

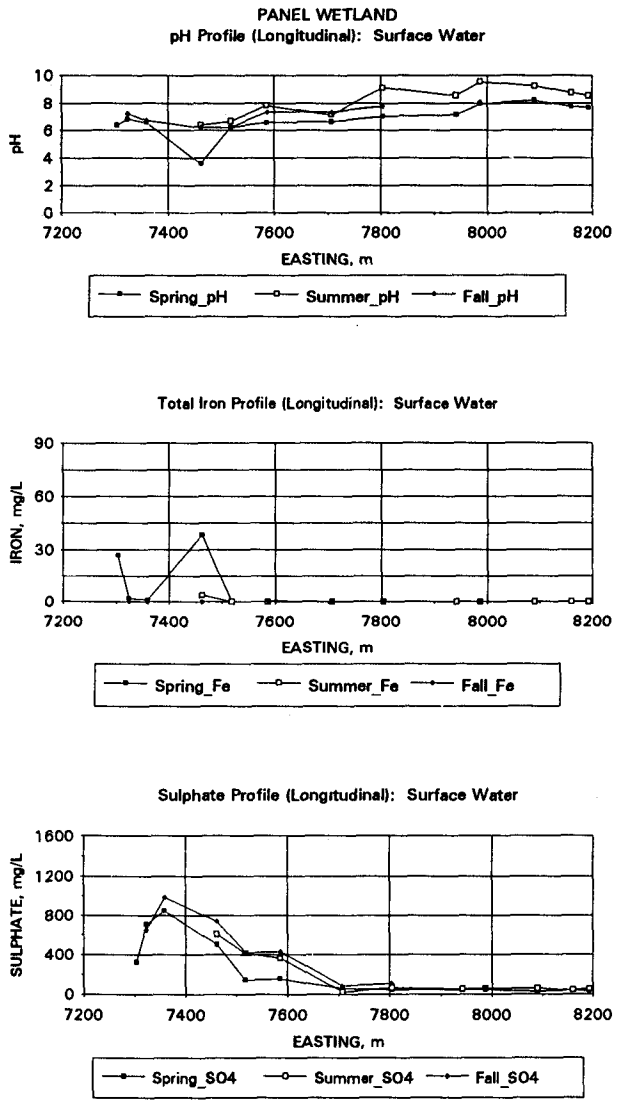

Figure 8. Panel wetland: surface water quality profiles and their seasonal variations for pH, Fe and SO_4^{-2}.

In the vegetated zone, no improvement in the quality of the surface water was noted as it drained from exposed areas towards the ponded water. Both the surface and ground water data indicated that the vegetation was associated with oxidation of the substrate rather than providing treatment for acid mine drainage. Some iron was precipitated and removed as ferric hydroxide in the vegetated zone.

The acidic surface drainage from exposed tailings and vegetated areas was diluted by a factor of 6 to 10 as it drained and mixed with the ponded water in the central part of the basin. The ground water from western and central

sections of the basin also discharged in the ponded water where it neutralized the acidic surface water. Dissolved iron, aluminum and manganese were thus precipitated when the waters mixed.

The pH of the ponded water increased from 7.5 to 9.5 in the summer which was attributed to the bacterial reduction of nitrates in the organic sediments and photosynthetic process of some submergent vegetation (pond weeds) producing ammonia alkalinity and hydroxyl ions, respectively. This phenomenon needs to be further investigated.

From water quality data for surface drainage from exposed, shallow water cover and vegetated areas, and for pond water near the discharge end, the annual rates of total iron production, as a result of pyrite oxidation, and iron discharged from the system were calculated at 183.7 kg/y and 9 kg/y, respectively. These values corresponded to annual pyrite oxidation and iron discharge rates of 1.11 and 0.04 mg Fe per kg of tailings in the basin per year.

The existing wetlands system, because of its various physical , chemical and biological controls, retained or recycled approximately 96% of the total iron produced as a result of pyrite oxidation. It was estimated that at these rates, it will take approximately 31,700 years for all the pyrite to oxidize and 926,000 years for all the mobilized iron to leave the system. For calcium and Ra-226, the corresponding times for their complete removal from the system were calculated as approximately 708 and 40,000 years, respectively.

For cattails and grasses, the observed metal uptake levels were similar to those observed at other pyritic uranium tailings, base metal and gold tailings sites. High concentrations of Fe, Al, Ca and other heavy metals were observed in pond weeds and sphagnum moss, but their contribution to the total bio-mass production and metals retention and removal load was very small compared to cattails and grasses which were the most abundant species. In all vegetation species, the observed metal concentrations were below plant toxicity levels with little or no significant accumulation. There should, therefore, be little concern related to wind dispersion or animal forage. No symptoms of plant toxicity were observed in the basin.

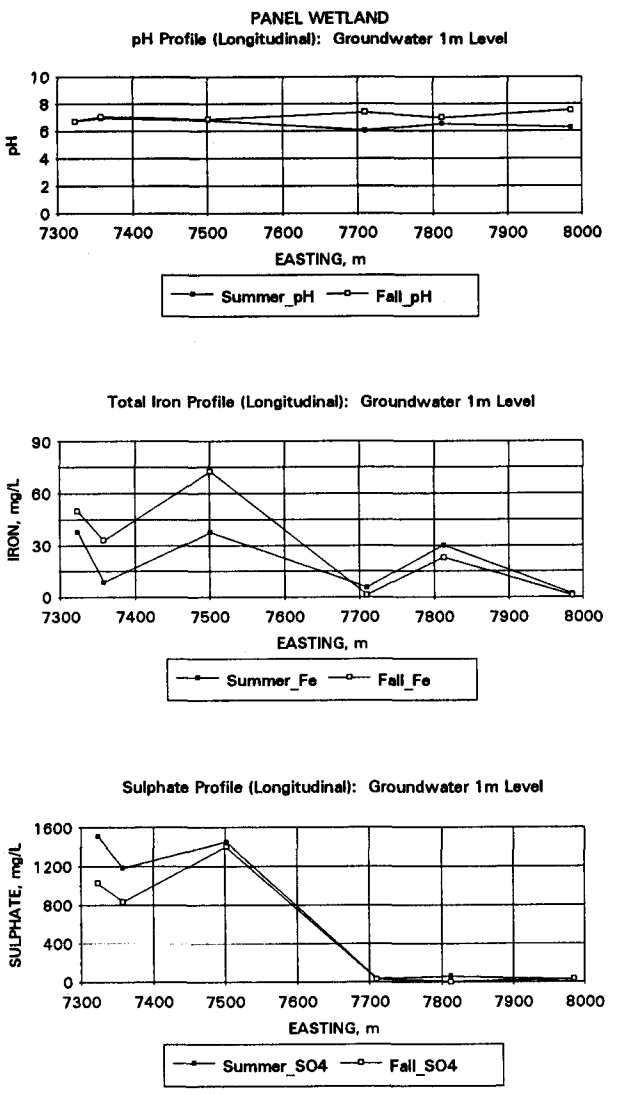

Figure 9. Panel wetland: ground water quality profiles and their seasonal variations for pH, Fe and SO_4^{-2}.

In general, the wetland/water system in the Panel wetland basin was effectively controlling the acidic drainage from partially submerged pyritic uranium tailings. The system should continue to function as long as the water cover is maintained. Its performance could be improved further if all the tailings were completely submerged.

Field Demonstration Test Site

Full scale flooding of the field demonstration test site, Cell #14, began in October 1992 using Gravel Pit Lake water. There was approximately 0.4 m of water cover over shallow areas at the end of flooding in 1992. In April 1993, the flooding of the cell resumed again. The site is being maintained at a constant water cover by periodically adding, when required, more water from Gravel Pit Lake. During 1993, a detailed water balance for the cell has been carried out and the site is being monitored continuously for its surface and ground water quality.

Figure 10 shows the surface water quality results for Cell #14 from October 1992 to September 1993. Previous to flooding in 1992, Cell #14 contained some water which had turned acidic with pH ~ 3.3 and acidity levels of 100 mg/L $CaCO_3$. The acidity was produced from exposed tailings in the basin which were not surface treated with limestone. Approximately 50% of the basin area had been leveled off and limestone was incorporated in the top 15 cm of the tailings to neutralize any acidity produced when exposed.

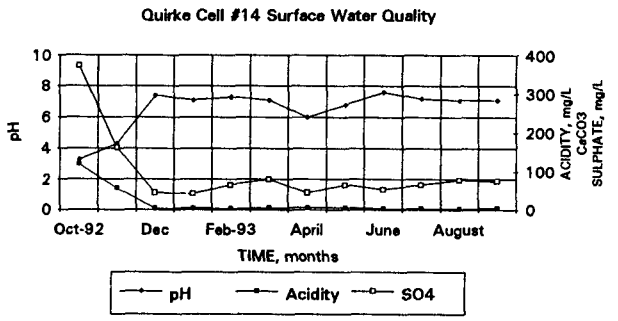

Figure 10. Surface water quality in the flooded Cell #14 at the Quirke mine tailings, variations of pH, acidity and SO_4^{-2}.

During the recent flooding, lime slurry was added to the inflow water for additional neutralization. At the end of flooding in December 1992, the surface water pH in the cell was 7.0 with acidity and alkalinity levels in the range of 6 to 8 mg/L $CaCO_3$. The water has maintained that general quality since. For comparison, the inflow water from Gravel Pit Lake had an average pH of 6.4, acidity of 5 mg/L $CaCO_3$, alkalinity of 4 mg/L $CaCO_3$, total dissolved solids at 40 mg/L and SO_4^{-2} concentration at 4 mg/L.

At the Quirke tailings site Cell #14, using a terraced cell concept, a shallow water cover has been successfully established and maintained for over a year. The site is being continuously monitored for its hydrological and water quality parameters throughout 1993.

Literature Cited

Balins, J. K., D. E. Welch, R. A. Knapp, C. F. Ashley and J. W. Maltby. 1991. Decommissioning of the Quirke Mine uranium tailings basin to eliminate acid production. p. 379-398. In Proceedings of the Second International Conference on the Abatement of Acidic Drainage. (Montreal, Quebec, Canada, September 16 - 18, 1991).

Boucher, Y. M. , N. K. Davé and T. P. Lim. 1989. Surface environmental research at the Elliot Lake Laboratory, a compilation of papers. Division Report MRL 89-79 (LS), CANMET, Energy, Mines and Resources, Canada, 1989.

Davé, N. K. and T. P. Lim. 1988. Environmental research at the Mining Research Laboratory, CANMET, Elliot Lake, Ontario, Canada. Division Report MRL 88-84 (OPJ), CANMET, Energy, Mines and Resources, Canada, 1988.

Davé, N. K., T. P. Lim, A. J. Vivyurka, B. Bihari and D. A. Kay. 1990. Development of wet barriers on pyritic uranium tailings, Elliot Lake, Ontario: Phase 1. Division Report MRL 90-050 (OPJ), CANMET, Energy, Mines and Resources, Canada, 1990.

Davé, N. K. 1992. Water cover on acid generating mine/mill wastes- a technical review. Division Report MSL 92-38 (CR), CANMET, Energy, Mines and Resources, Canada, November 1992.

SEDIMENT QUALITY ASSESSMENT NEAR TWO ONTARIO MINE SITES: HOW RELEVANT ARE THE PROVINCIAL GUIDELINES?[1]

Robert Prairie[2] and Paul McKee[3]

Abstract: Sediment quality guidelines have recently been issued in Ontario. These guidelines provide methodologies to assess the degree of impact, as well as outlining contaminant criteria for remedial action. Results from recent environmental studies carried out near two Noranda mine sites in Ontario were used to assess the relevance of these guidelines for river sediments near mining operations. Site-specific results (solid-phase total metal concentrations, porewater metal concentrations, sequentially extracted metal phases, benthic community assessment, and sediment toxicity testing) are presented and compared with the Ontario Ministry of the Environment and Energy (MOEE) Provincial Sediment Quality Guidelines (PSQG). Results from one particular site were used to predict lowest effect level (LEL) and severe effect level (SEL) values for sediment Cu, Pb, Cd, and Zn concentrations, using the MOEE PSQG development approach for metals. These site-specific LEL and SEL values are much greater than the PSQG values. Solid-phase sediment toxicity tests showed that increased mortality or reduced growth in test animals occurred at sediment metal concentrations well above PSQG SEL. This study suggests that the PSQG numerical criteria may be too conservative for some metals and should be used as a screening tool only, while site-specific data should be used to confirm the actual environmental effects on the benthic biota.

Introduction

As part of their environmental management program, many of the Noranda group operations have carried out studies to assess the degree and extent of impacts of their operations on the nearby environment. These studies have mainly focused on aquatic environment aspects such as water and sediment quality, along with effects on the resident biota (fish populations and benthic communities). The enrichment of aquatic sediment by various metals can be important in the vicinity of some mine sites. The resident benthic fauna could be directly affected by this contamination, depending on its degree and possibly on the forms of metal in the sediment.

Sediments quality guidelines have been recently issued by Ontario MOEE (Persaud et al. 1992) to protect the aquatic environment, and to provide guidance during the decision-making process in relation to sediment contamination, ranging from preventive to remedial action. The guidelines describe numerical values developed for the protection of aquatic biological resources (i.e., benthos), which can be directly impacted by contaminated sediments. Among the various approaches considered for developing sediment quality guidelines (Persaud et al. 1992, Chapman 1989, Procéan 1991, MacDonald et al. 1992), the Ontario MOEE PSQG have used the screening level concentration approach (developed by Neff et al. 1986) to derive their numerical criteria. Two levels of effects are described: the lowest effect level (LEL) and the severe effect level (SEL). The historical level of the contamination observed near some Noranda mine sites would be considered severe because sediment metal levels are much higher than the numerical guideline values (Prairie 1993).

Since these guidelines could potentially impact on Noranda mining activities in terms of regulatory response, it became important that the available information (on metal-contaminated sediments and the related effects on the

---

[1]Paper presented at the International Land reclamation and Mine Drainage Conference and the Third International Conference on the Abatement of Acidic Drainage, Pittsburg, PA., April 24-29, 1994.

[2] Robert Prairie, Environmental Biologist, Centre de technologie Noranda, Pointe-Claire, Québec, Canada.

[3]Paul McKee, Associate, Aquatic Ecologist, Beak Consultants Ltd., Brampton, Ontario, Canada.

benthic biota) be reviewed and updated (via supplementary sampling and testing). Many of the Noranda group mine sites have recently carried out environmental studies to determine current environmental conditions as a baseline for the development of their closure plans. The objective of this paper is to describe some of the sediment chemical analyses and biological response results obtained from the testing of several river sediments collected downstream of discharges from two Noranda mine sites affected by acid mine drainage (AMD): Mattabi Mines Ltd (Mattabi) and Noranda Minerals Ltd. Geco Division (Geco), both located in northern Ontario.

Methods

Figure 1 illustrates the sampling site locations near Mattabi and Geco mine sites, between 1989 and 1992. Table 1 summarizes the number of samples and the type of analysis or tests carried out at Mattabi Mines and Geco along with the methods and protocols used for each of the parameters studied.

Table 1 Number of sites sampled or tested for the various topics near two Noranda mine sites, 1989-92.

Topics	Sampling methods	Mattabi	Geco	Laboratory analyses / methods
Solid-phase chemistry	KB Corer	66	21	Zn, Cu, Pb, Cd, Fe by graphite furnace or inductively coupled plasma (ICP)
Porewater chemistry	Peepers	6	4	Zn, Cu, Pb, Cd, Fe, by ICP
Sequential extraction analysis	Ekman grab	1	4	Zn, Cu, Pb, Cd, Fe, plus others; modification of Tessier et al. (1979) method, ICP
Simultaneously extracted metals / acid-volatile sulfide	Ekman grab	5	4	Simultaneously extracted Zn, Cu, Pb, Cd, and Ni by ICP; AVS, DiToro et al. (1992)
Benthic community structure	Ekman grab	66	21	Benthic identification at genus level
Sediment toxicity tests	Ekman grab			
Hyalella azteca		6	-	10-day mortality ; ASTM (1991a)
Chironomus riparius		4	-	8-day mortality and growth; ASTM (1992)
Chironomus tentans		2	7	10-day mortality and growth; Bedard et al. (1992)
Hexagenia limbata		-	7	10-day mortality and growth; Bedard et al. (1992)
Pimephales promelas		-	7	10-day mortality and growth; Bedard et al. (1992)

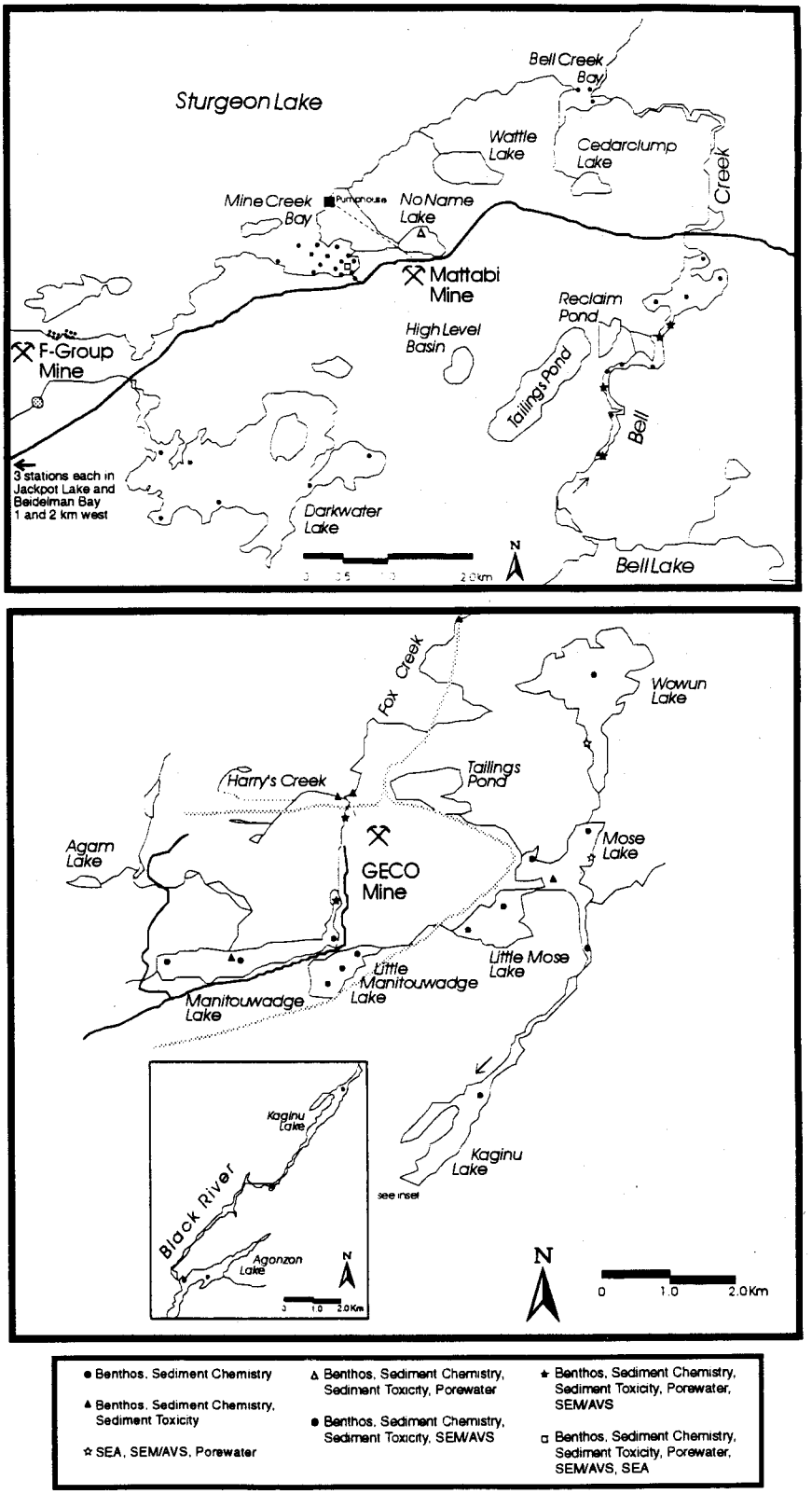

Figure 1. Location of sampling sites near Mattabi and Geco mine sites, 1989-92.

Data described here were collected near the two Noranda mine sites between 1989 and 1992. The 1989 data for the Mattabi mine site were gathered by Noranda Technology Centre (NTC) during an extensive preclosure environmental study (Prairie et al. 1990, 1992). At both sites, Beak Consultants Ltd. (BEAK) carried out environmental studies during the 1991-92 period (Beak Consultants 1993a, 1993b) to assess current environmental conditions as a baseline to predict postclosure improvements.

Sediment Analysis

Sediment samples were collected for chemical analysis using a K-B corer; a total of 10 sub-samples were pooled for each desired depth. Cores were extruded within eight hours of collection and the outer smear zone removed. Samples were then placed in polyethylene bags and frozen within 48 hours. **Total metal concentrations** were determined on aqua regia extracts of the solid phase of the sediments at various depth increments, and are all reported on a dry weight basis. For the purpose of the present document, the surficial sediment (typically 0 to 5 cm) data will be used, as benthic communities are found generally in the top portion of the sediments.

Interstitial water (or **porewater**) concentrations of contaminants are good tools to predict toxic effects to the benthic biota (DiToro et al. 1991, Ankley et al. 1990). Peepers (technique described in Mudroch and MacKnight 1991), which collect in situ porewater by dialysis, were selected to sample the sediment interstitial water at both sites. Samples for dissolved metal determinations were removed in the field with a hypodermic syringe and preserved with HNO_3. Metal determinations were done by ICP (BAS 1992).

Sequential extraction analysis (SEA) is an operationally defined procedure which provides a convenient means of determining major accumulation phases for metals in sediments. The SEA procedure identifies five fractions in the bulk sediment-exchangeable, carbonate bound, Fe-Mn oxide bound, organic complexes and residual metals. The Tessier sequential extraction procedure (Tessier et al. 1979) was used to evaluate metal (particularly zinc) chemical speciation in key sediment samples from both sites. In all cases, surficial sediments were collected by Ekman grab, transferred immediately to air-tight polyethylene bags and frozen. The Tessier et al (1979) extraction procedure was modified by keeping the sediment frozen until extraction and samples were thawed for analysis under N_2 to avoid oxidation and altered metal partitioning (Thomson et al. 1980; Rapin et al. 1986). Residual metals in the extraction series were extracted by aqua regia rather than hydrofluoric acid. The metals analyzed in the SEA included Zn, Cu, Pb, Cd, and Ni, and determinations were made by ICP (BAS, 1992).

Acid-volatile sulfide (AVS) is an operationally defined sediment parameter that consists of sediment sulfides that are cold acid soluble. Although acid-volatile sulfide has been studied for several years, it only recently has been recognized as a possible indicator of metal toxicity in sediments. Several recent studies (DiToro et al. 1990, 1992; Ankley et al. 1991) have identified a link between the toxic potential of trace metals such as Pb, Cd, Zn, Cu, and Ni to benthic invertebrates in sediment deposits and the amount of acid-volatile sulfur present in the sediments. They have found that no significant mortalities occurred relative to controls if the AVS concentration is greater, on a molar basis, than the simultaneously extracted metals (SEM). The above hypothesis was tested by BEAK at both sites by determining the AVS and SEM, and by carrying out sediment toxicity tests on a total of nine samples.

Biological Responses

The resident **benthic community** (insect larvae, clams, worms) which has been used extensively in past decades to assess impacts of effluents on the aquatic fauna has been also sampled during the various surveys at both sites. In these studies, benthic samples were sieved using a 500-µm mesh and preserved in the field with 10% buffered formalin. All Mattabi samples were sorted using a microscope, identified and enumerated by L.Cloutier, University of Montréal. Geco samples were sorted by Ontario Ministry of Environment and Energy (MOEE) and were identified and enumerated in BEAK's biological laboratory; all stations were sampled and analyzed in triplicate. The identification of benthic organisms was carried out down to the genus level (whenever possible). To allow comparisons between stations, the enumeration and identification results were assessed according to the number of taxa, the total density (number of organisms per square meter), the relative density of organisms (%) in categories of pollution sensitivity, and the diversity index.

Although benthic community structure assessments are widely used, they have several limitations (e.g. different types of substrate, natural variations, ...). Therefore, the presence and absence of benthic invertebrates alone does not give much insight into the toxicity of sediments (Geisy and Hoke 1990). Specific benthic macroinvertebrate species have often been described as the optimal assessment tool in determinations of sediment toxicity. The close contact of tested organisms with bottom sediments and with interstitial and overlying waters, for extended periods, permits adverse effects to occur in the presence of contaminated sediments (Burton 1992). During our studies, different types of **sediment toxicity tests** were carried out (not systematically) at key locations near the two mine sites: *Hyallela azteca* (ASTM 1991a), *Chironomus riparius* (ASTM 1992), *Chironomus tentans* (Bedard et al. 1992), Hexagenia limbata (Bedard et al. 1992), and fathead minnows, *Pimephelas promelas* (Bedard et al. 1992). Sediment collection, handling and storage protocols were consistent with ASTM (1991b) standard guide.

Sediments from Mattabi were tested in BEAK's toxicity laboratory. Geco sediments were tested by the Ontario MOEE, although samples from two sites (identified as toxic by the MOEE in 1991) were resampled and tested by BEAK in 1992 to confirm the initial finding. All sediments sampled by BEAK were tested fresh (sediments collected and tests set up within 96 hours). Sediments were wet sieved without the addition of freshwater (overlying water present with the sediments used as wash water). Tests carried out by the MOEE were wet sieved as described in Bedard et al. (1992).

Results and Discussion

Although the concentrations of metals other than zinc in sediments (such as Pb, Cd, and Cu) have been determined during these studies and may very well be involved in the toxicity to the benthic biota, the following section uses zinc as a tracer for metal contamination in sediments. Of all the metals tested in these sediments, zinc shows the greatest degree of elevation in comparison with natural background. Also, the concentrations of the other metals were all significantly correlated with zinc (e.g., for Mattabi, $n=66$, $p<0.05$, $r>0.7$).

The 1991-92 resident benthic community results from the Mattabi mine site (Prairie et al. 1990, 1992; Beak Consultants Ltd 1993a) showed effects (reduced number of taxa and diversity along with increased proportion of tolerant organisms) as total metal levels in the sediments increased; the same observation was made using the 1989 data. Figure 2 illustrates the fluctuations of the number of taxa in relation to the total zinc concentrations (log scale) in the sediments, using all data pairs (Zn levels and number of benthic taxa) from 1989 and 1991-92 studies near

the Mattabi site. A majority of samples exhibited zinc concentrations above the PSQG Zn SEL values (820 µg/g); the total range of Zn concentrations in sediments samples (66) was 30 to 46,000 µg/g (including reference sites). Also relatively high numbers of species are observed (up to 19 benthic taxa) at zinc levels above MOEE PSQG severe effect level. Although wide variations in the number of taxa can be observed, a linear inverse relationship exist between the log Zn concentration and the number of benthic taxa (n=66, $p<0.05$, r=0.48).

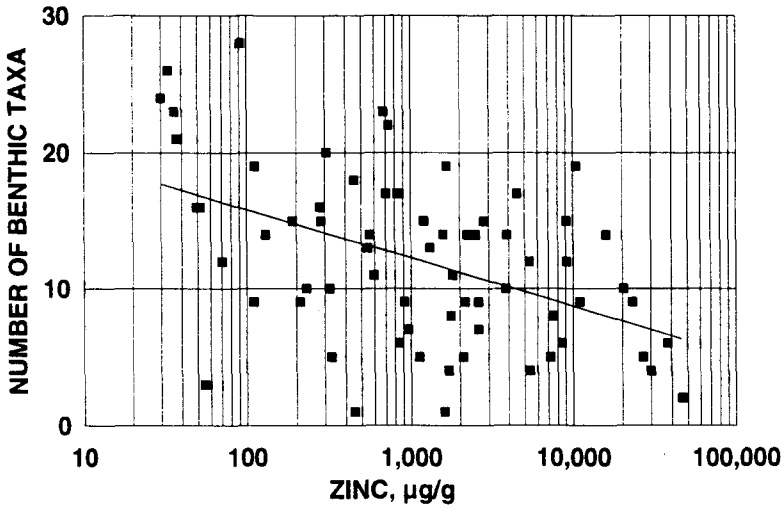

Figure 2. Zinc concentrations in sediments versus number of benthic taxa, Mattabi, 1989-92.

The toxicity tests results showed that no significant differences in mortality rates occurred (relative to controls) using *Hyalella azteca* ($p>0.05$); significantly higher mortality rates occurred with *Chironomus* only when total zinc concentrations in the sediments reached 30,000 µg/g ($p<0.05$). *Chironomus* growth rates were affected at zinc concentrations >5,000 µg/g ($p<0.05$).

The benthic community data collected near the Geco mine site (Beak Consultants Ltd 1993b) showed similar trends where total zinc concentrations in the sediments samples (21) ranged between 54 and 9,600 µg/g (including reference sites). A comparison of benthic responses (number of taxa and diversity index) to total zinc concentrations in the sediments was made using data from Mattabi and Geco. No significant differences between regression slopes for the two sites were observed ($p>0.05$). The toxicity tests carried out by Ontario MOEE in 1991 on seven key sediment samples collected near the Geco site (using *Chironomus tentans*, *Hexagenia limbata*, and *Pimephales promelas*) showed no significant differences in mortality rates (Tukey's multiple range test) relative to the control test, except for two sites where low surface water pH (3.9) and high un-ionized ammonia probably contributed to the observed mortalities (probably not related to metal levels in sediments). The range of total zinc concentration in the seven sediment toxicity tests was 30 to 6,000 µg/g.

The sequential extraction analysis (SEA) results from one Mattabi sample (3,400 µg/g Zn), showed that most of the zinc (and also other metals such as Pb and Cd) was found in the Fe-Mn oxides phase. No toxicity (using *Hyalella* and *Chironomus*) was found for that sample, although the resident benthic community from that collection station appeared to be slightly impaired (lower number of taxa but relatively high diversity index values). The four Geco SEA results showed about the same conclusions, i.e. most of the metals, especially zinc, were found mainly in the Fe-Mn oxides phase (and 20 to 40% in the organic phase). At locations where samples were analyzed for both SEA and toxicity, none showed sediment toxicity values significantly different than the control test values, except for one sample where the fathead minnow test showed 100% mortalities and could probably be attributed to the high un-ionized ammonia levels. Therefore, the SEA results from the Mattabi and Geco are consistent with the nontoxic response observed since zinc was in a relatively non bio-available form (Fe-Mn oxide and organic phase).

Contrary to the AVS hypothesis (i.e. the ratio of [simultaneously extracted metals]/[acid-volatile sulfide] greater than 1 predicts potential toxicity to benthic organisms), our [SEM]/[AVS] ratios calculated from the Mattabi and Geco sediment sample results were ineffective in distinguishing toxic and nontoxic sediments. Figure 3 illustrates that most of the samples analyzed showed SEM/AVS ratios greater than 1, and yet only two significantly higher mortality rates (relative to controls) were observed (one point being most probably related to un-ionized ammonia, not metals).

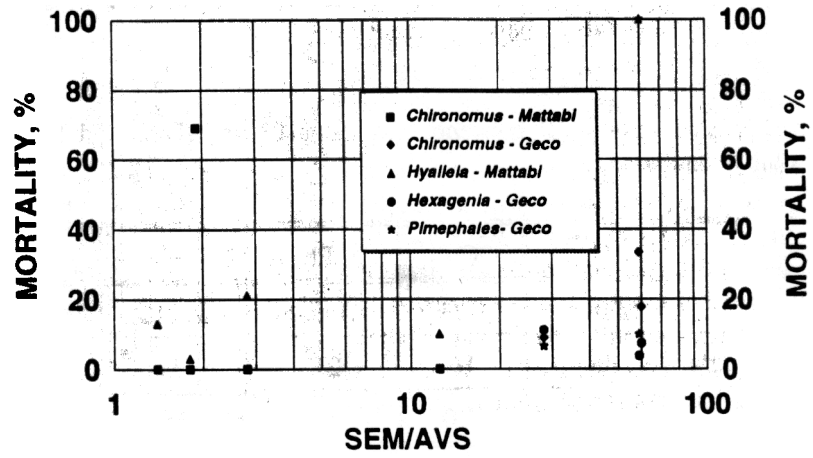

Figure 3. SEM/AVS ratios versus sediment toxicity test results (mortality rates) near Mattabi and Geco mine sites, 1991-92.

The porewater zinc levels determined in a limited number of surficial sediment samples from Mattabi and Geco sediments were compared with some benthic community structure parameters (number of taxa and diversity index values) and sediment toxicity test results. Although there are no data points between 0.1 and 1.0 mg/L Zn, it seems that a clear effect on the benthic responses occurs when zinc porewater concentrations are above 1 mg/L: the number of taxa, the diversity values and the growth rate of *Chironomus* are generally low, while the *Chironomus* mortality rate is generally higher at porewater concentrations of >1 mg/L.

The information collected at these sites suggests that effects of zinc (and possibly other metals such as Cu, Cd, and Pb) in the sediments on the benthic organisms and community are occurring at levels greater than the Ontario PSQG. Considering the importance of the database collected in water bodies located near the Mattabi mine site, it was possible to derive site-specific LEL and SEL values (for Zn, Cu, Pb, and Cd) using the **screening level concentration** (SLC) approach (developed by Neff et al. 1986) utilized by the Ontario MOEE for the development of PSQG. The LEL is identified as the sediment contaminant concentration at which toxic effects may be expected in the most sensitive benthic species, and is calculated as the 5th percentile of the SLC. The SEL is the sediment metal concentration which may be expected to eliminate most benthic organisms, and is calculated as the 95th percentile of the SLC. The SLC uses field data on the co-occurrence of benthic species and different concentrations of contaminants, and is an estimate of the highest concentration of a contaminant that can be tolerated by a specific proportion of benthic species in a community. This method assumes that the data cover the full range of species tolerance and, as a rule of thumb, should span at least two orders of magnitude of chemical concentration. The MOEE developed LEL and SEL values for a range of metals, principally using a data set developed from benthic and sediment quality sampling in the Great Lakes.

The site-specific values are described in Table 2 along with the Ontario PSQG. A comparison between these two sets of values indicates that the newly derived LEL and SEL values are considerably greater than the MOEE PSQG. Many reasons could explain these differences. The range of metal concentrations observed in the Mattabi database is much greater than the one obtained in the Great Lakes database used for the PSQG calculations (Jaagumagi 1992). Another difference between the sediments from the two databases (MOEE and Mattabi) is the

proportion of total organic carbon; Mattabi sediments TOC values averaged 8%, while MOEE sediments' TOC values were closer to 2% (Hart et al. 1988). The differences in biological responses from the two sets of SLC values could be explained by the fact that a high organic carbon content in the sediments may bind metals and therefore inhibit toxic effects of metals to benthic organisms.

Table 2. Screening level concentration calculations (LEL and SEL) using MOEE (Great Lakes) and Noranda (Mattabi) databases.

Metal	Cu	Cu	Pb	Pb	Cd	Cd	Zn	Zn
Database	Mattabi	MOEE	Mattabi	MOEE	Mattabi	MOEE	Mattabi	MOEE
LEL, µg/g	388	16	213	31	5.2	0.6	1,600	120
SEL, µg/g	1,946	110	840	250	48.4	10	21,500	820

Conclusions

The current sediment quality guidelines encourage an assessment on a site-specific basis of the effects of elevated sediment metal concentrations on biota when concentrations exceed the specific numerical values. These studies suggest that, for some metals (particularly zinc), exceedance of numerical criteria should not mean automatic implementation of a specific remedial action or program. Based on the studies undertaken on sediment quality conditions at the two Noranda mine sites, it can be concluded that benthic studies, combined with confirmatory sediment toxicity tests, may be the most effective means of evaluating sediment quality impacts near mine sites. Reliance solely on MOEE PSQG values for assessment of bulk sediment chemistry data for Zn (and possibly Pb, Cu and Cd) near the mine sites considered would lead to exaggerated conclusions on impact. It is therefore concluded that the MOEE PSQG values for some metals should be used only as a screening tool for sediment quality evaluation near mine sites.

Literature Cited

Ankley G. T., A. Katko, and J. W. Arthur. 1990. Identification of ammonia as an important sediment-associated toxicant in the Lower Fox and Green Bay, Wisconsin. Environ. Toxicol. and Chem. 9:313-322.

Ankley G. T., G. L. Phipps, E. N. Leonard, D. A. Benoit, V. R. Mattson, P. A. Kosian, A. M. Cotter, J. R. Dierkes, D. J. Hansen, and J. D. Mahony. 1991. Acid-volatile sulfide as a factor mediating cadmium and nickel bioavailability in contaminated sediments. Environ. Toxicol. and Chem. 10:1299.

ASTM. 1991a. Standard guide for conducting sediment toxicity tests with freshwater invertebrates. Vol. 11.04.E1383-90.

ASTM. 1991b. Standard guide for collection, storage, characterization and manipulation of sediments for toxicological testing. Vol. 11.04.E1391-90.

ASTM. 1992. Guide for conducting sediment toxicity tests with freshwater invertebrates. Annual Book of ASTM Standards. Vol. 11.04.E1383--92, p. 1085-1104.

BAS Laboratories Limited. 1992 BAS Analytical methods manual. BAS Laboratories Limited, 14 Abacus Road, Brampton, Ontario, Canada.

Beak Consultants Ltd. 1993a. 1991-1992 Mattabi Mines environmental studies, Report to Mattabi Mines.

Beak Consultants Ltd. 1993b. 1991-1992 Environmental studies in the vicinity of Noranda Minerals Inc. Geco Division, Draft report.

Bedard, D., A. Hayton, and D. Persaud. 1992. Laboratory sediment biological testing protocol, Ontario Ministry of Environment. Toronto, ON, 23p.

Burton G. A. 1992. Sediment toxicity assessment. Lewis Publishers Inc., Boca Raton, FL, 457 p.

Chapman, P. M. 1989. Current approaches to developing sediment quality criteria. Environ. Toxicology and Chem. 8:589-598.

DiToro, D. M., J. D. Mahony, D. J. Hansen, K. J. Scott , M. B. Hicks, S. M. Mayr, and M. S. Redmond. 1990. Toxicity of cadmium in sediments: the role of acid volatile sulfide. Environ. Toxicology and Chem. 9:1487.

DiToro, D. M., C. S. Zarba, D. J. Hansen, W. J. Berry, R. C. Swartz, C. E. Cowan, S. P. Pavlou, H. E. Allen, N. E. Thomas, and P. R. Paquin. 1991. Technical basis for establishing sediment quality criteria for nonionic organic chemicals using equilibrium partitioning. Environ. Toxicology and Chem. 10:1541-1583.

DiToro D. M., J. D. Mahony, D. J. Hansen, K. J. Scott, A. R. Carlson, and G. T. Ankley. 1992. Acid volatile sulfide predicts the acute toxicity of cadmium and nickel in sediments. Environ. Science and Technology 26:96-101.

Giesy, J. P. and R. A. Hoke. 1990. Freshwater sediment quality criteria: toxicity bioassessment, p. 265-347. In Baudo, R., J. P. Geisy, and H. Muntau, Sediments: Chemistry and toxicity of in-place pollutants. Lewis Publishers, Inc., Chelsea, MI, 405 p.

Hart, D. R., J. Fitchko, and P. McKee. 1988. Development of sediment quality guidelines - Phase II - Guideline development, Final report for Ontario Ministry of the Environment, Beak Consultants.

Jaagumagi, R. 1992. Development of the Ontario provincial sediment quality guidelines for arsenic, cadmium, chromium, copper, lead, manganese, mercury, nickel, and zinc. Ontario Ministry of Environment, Toronto, 46p.

MacDonald D. D., S. L. Smith, M. P. Wong, and P. Mudroch. 1992. Élaboration des recommandations pour la qualité de l'environnement marin au Canada, C & P, Environnement Canada.

Mudroch, A. and S. D. MacKnight. 1991. Handbook of techniques for aquatic sediments sampling. CRC Press, Boca Raton, FL.

Neff, J. M., D. J. Bean, B. W. Cornaby, R. M. Vaga, T. C. Gulbransen, and J. A. Scanlon. 1986. Sediment quality criteria methodology validation: calculation of screening level concentrations from filed data. Battelle Washington Environmental Program Office for U.S. EPA, 60 p.

Persaud, D., R. Jaagumagi, and A. Hayton, 1992. Guidelines for the protection and management of aquatic sediment quality in Ontario, Water Resources Branch, Ontario Ministry of the Environment.

Prairie, R. and J. Gagnon. 1990. Biological studies in the vicinity of F-group mine operation, May-September 1989. Ecology Group, Centre de Technologie Noranda, Pointe-Claire, QC.

Prairie, R., R. L. Levaque-Charron, and J. Gagnon. 1992. Biological studies in the vicinity of Mattabi mines operations, May-September 1989. Ecology Group, Centre de Technologie Noranda, Pointe-Claire, QC.

Prairie, R. 1993. Sediment quality assessment near some Noranda mine sites. Draft report, Centre de technologie Noranda, Pointe-Claire, QC.

Procéan Inc. 1991. Révision des critères d'évaluation de la qualité des sédiments du Saint-Laurent, final report for the Centre Saint-Laurent, Environment Canada.

Rapin, F., A. Tessier, P. G. C. Campbell, and R. Carignan. 1986. Potential artifacts in the determination of metal partitioning in sediments by a sequential extraction procedure. Environ. Sci. Technol. 20:836-840.

Tessier A., P. G. C. Campbell, and M. Bisson. 1979. Sequential extraction procedure for the speciation of particulate trace metals, Analytical Chem. 551:844-851.

Thomson, E. A., M. L. Uoma, D. J. Cain, and C. Johansson. 1980. The effect of sample storage on tile extraction of Cu, Zn, Fe, Mn and organic matter from oxidized estuarine sediments. Water, Air, Soil Pollut. 14:215-223.

APPLICATIONS OF GEOPHYSICAL METHODS FOR MONITORING ACID MINE DRAINAGE[1]

Alan R. King[2] and Tom Hynes[3]

Abstract: Following preliminary studies which indicated the potential for using geophysical methods for mapping acid mine drainage (AMD), the Mine Environmental Neutral Drainage or MEND committee, a Canadian industry-government forum for the development of new technology for the prevention, prediction and monitoring of AMD sponsored a study to demonstrate the applications of geophysical methods to the AMD problem.

High quality airborne, ground and borehole geophysical data were acquired over areas with well documented AMD problems, including tailings impoundments, waste rock piles and AMD ground water plumes. The geophysical data were correlated with hydrological and chemical data from ongoing ground water investigations to establish the utility of the methods.

The results confirmed that electromagnetic (EM) methods that remotely measure the conductivity of the subsurface are very useful for location and detailed three-dimensional mapping of AMD in ground water. Airborne surveys can provide rapid reconnaissance scale surveys, while ground surveys and borehole surveys provide progressively more detail.

In addition to the EM work, combined Induced Polarization (IP) and electrical resistivity surveys were tested on a large revegetated tailings area. Since the IP method detects disseminated sulphides, the combination of IP and resistivity surveys can be used for simultaneous three-dimensional mapping of sulphides and ground water quality in tailings.

All of these methods require measurement of the electrical properties of the subsurface and are adversely affected by electrical noise from power lines and surface and buried metal. The response of AMD may be masked by naturally conductive ground water, bedrock lithologies, or clay soils.

Additional Key Words: geophysics, electromagnetics, induced polarization.

Introduction

In 1991 INCO Limited proposed a program to investigate the applications of geophysical methods to Acid Mine Drainage (AMD) problems. This proposal was subsequently implemented with funding from the federal and provincial governments, through the Northern Ontario Development Agreement (NODA) program and INCO Limited under the technical sponsorship of the Canadian Mine Environmental Neutral Drainage (MEND) Committee. The proposal was based on evidence from work in related fields and tests on INCO properties that indicated that a number of the subsurface investigation techniques developed for geotechnical applications and mining exploration had direct application to AMD problems.

---

[1]Paper presented at the International Land Reclamation and Mine Drainage Conference and the Third International Conference on the Abatement of Acidic Drainage, Pittsburgh, PA, April 24-29, 1994.

[2]Alan R. King, Senior Geophysicist, INCO Exploration and Technical Services Inc., Copper Cliff, Ontario.

[3]Tom Hynes, Program Principal, CANMET, Natural Resources Canada.

In this work we have focused mainly on the electrical and electromagnetic methods since they had the potential for direct, low cost, non-intrusive, three-dimensional mapping of subsurface AMD problems. Airborne conductivity surveys were ground truthed with ground conductivity surveys which were in turn confirmed by borehole surveys and chemical analysis of water samples. The induced polarization method was also tested for direct mapping of sulphides in tailings.

Sudbury Basin

The Sudbury Igneous Complex (SIC), located 400 km north of Toronto in eastern Canada, hosts one of the largest concentrations of economic sulphide deposits in the world, with production of nickel, copper, cobalt and platinum group elements. The SIC is the result of a major meteor impact approximately 1.8 billion years ago. It is believed that the complex was originally circular in shape and subsequent tectonic events have deformed it to its present elliptical shape. It consists of basal crystalline intrusive rocks overlain successively by a tuff-like fallback breccia and an upper layer of carbonaceous sediments.

The major deposits and the associated mine facilities are all found at or near the contact between the basal crystalline intrusive rocks of the complex, which measures approximately 30 by 60 km, and surrounding metamorphosed volcanic, sedimentary and intrusive rocks. These host rocks are all electrically very resistive - an important factor in the application of electrical geophysical methods.

The first deposits were discovered in the 1890's and mining has been carried out continuously since then. There are currently 14 operating mines, and approximately 40 abandoned sites around the perimeter of the basin.

Mining has produced approximately one billion tons of reactive sulphide-bearing waste rock. Most of this is in tailings, with some in waste rock piles. The principal sulphide in the waste rock is pyrrhotite with concentrations in tailings ranging from less than one percent up to 60% sulphides in pyrrhotite storage areas. As is well known, on exposure to air the sulphides oxidize to produce dilute sulphuric acid plus metals, mainly Fe, but enough Ni and Cu to potentially affect drinking water quality.

The tailings are stored in large impoundments in topographically low areas and contained, where necessary, by large, semi-permeable dams. The two main INCO tailings are at Copper Cliff (6,000 acres) and Levack (150 acres). The Copper Cliff tailings are being expanded to handle future mine waste and are currently receiving about 40,000 tons per day of tailings. The Levack tailings are no longer active. Ongoing geotechnical and hydrogeological studies at both sites are gathering the detailed information required to design optimum containment, treatment and eventual closure plans.

The tailings areas are net recharge areas due to natural precipitation (0.2 m per year approximately, Coggans et al, 1991) and the addition of mine waters. The hydraulic gradients in the tailings areas are generally downward and outward, resulting in ground water flow through and below the dams. This results in plumes of tailings water which manifest themselves as low Ph, high sulphate, high iron, surface AMD seeps. All surface drainage is collected through an extensive network of interception ponds and pumping stations and is treated at a central facility.

Study Area

Originally, two sites, one at the INCO Copper Cliff tailings and the other at the INCO Levack tailings, were selected for geophysical tests. Subsequently, some excellent data provided by Falconbridge Ltd. at their Fault Lake tailings resulted in the inclusion of this site in the study as well.

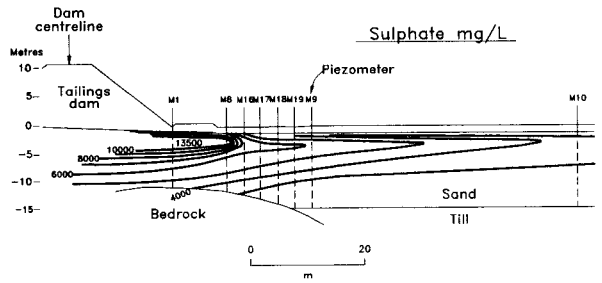

Figure 1. Nordic Mine - Sulphate in ground water.

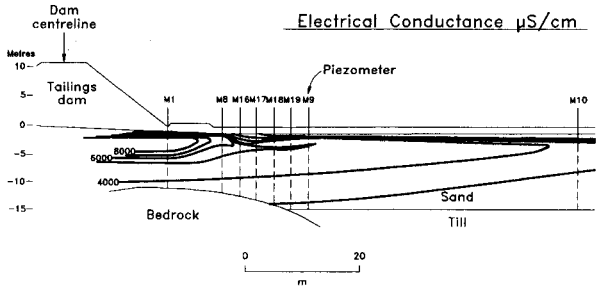

Figure 2. Nordic Mine - Ground water conductivity.

These areas were selected as known AMD sites where data from concurrent geotechnical and hydrological studies could be used to correlate with our geophysical work. This presentation focuses on selected results from the Copper Cliff and Levack tailings areas which are representative of the overall results of the study.

Basic Principles of Geophysical Methods

Geophysical methods rely on contrasts in bulk physical properties such as electrical conductivity, magnetic susceptibility, density, seismic velocity, etc. If there is a suitable physical property contrast, geophysical methods can be used to remotely map variations in physical properties in three dimensions. For these methods to be effective as direct detection methods for AMD, there has to be a correlation between ground water chemistry and a mappable physical property - in this case, electrical conductivity.

The correlation between AMD and conductivity is best demonstrated by work done by the University of Waterloo on sulphide-bearing uranium tailings at Elliot Lake, Ontario (Blair et al, 1980). As shown in figures 1 and 2, multilevel monitoring wells were used to measure the chemistry of a ground water AMD plume extending below one of the tailings dams. The measured data were plotted on a vertical section through the plume and contoured. Figure 1 shows the sulphate concentration in milligrams per litre and figure 2 shows the electrical conductivity in microsiemens per centimetre as measured on ground water samples. The correlation is excellent, and it is obvious that if the distribution of conductivity can be measured remotely using geophysical methods and there are no other sources of anomalous conductivity, then the location and concentration of AMD can be inferred.

Based on the work at Elliot Lake, particularly a pioneering ground conductivity survey by Pehme (1981), work in similar ground water investigations (King and Sartorelli, 1991), and ground conductivity tests at the Copper Cliff tailings, it was obvious that there was considerable potential for geophysical applications in AMD applications, and we proposed a project to the Canadian MEND (Mines Environmental Neutral Drainage) Committee to demonstrate and document the use of geophysics for AMD investigations.

In particular, we have tested airborne, ground and borehole electromagnetic (EM) conductivity surveying as well as ground and borehole electrical conductivity and induced polarization (IP) surveying. The principal use of the IP method in exploration has been the mapping of disseminated sulphides in bedrock. It was proposed at the start of this study that the method could be used to determine the distribution of sulphides in tailings. These methods and their applications to AMD mapping were described in more detail in King and Sartorelli (1991).

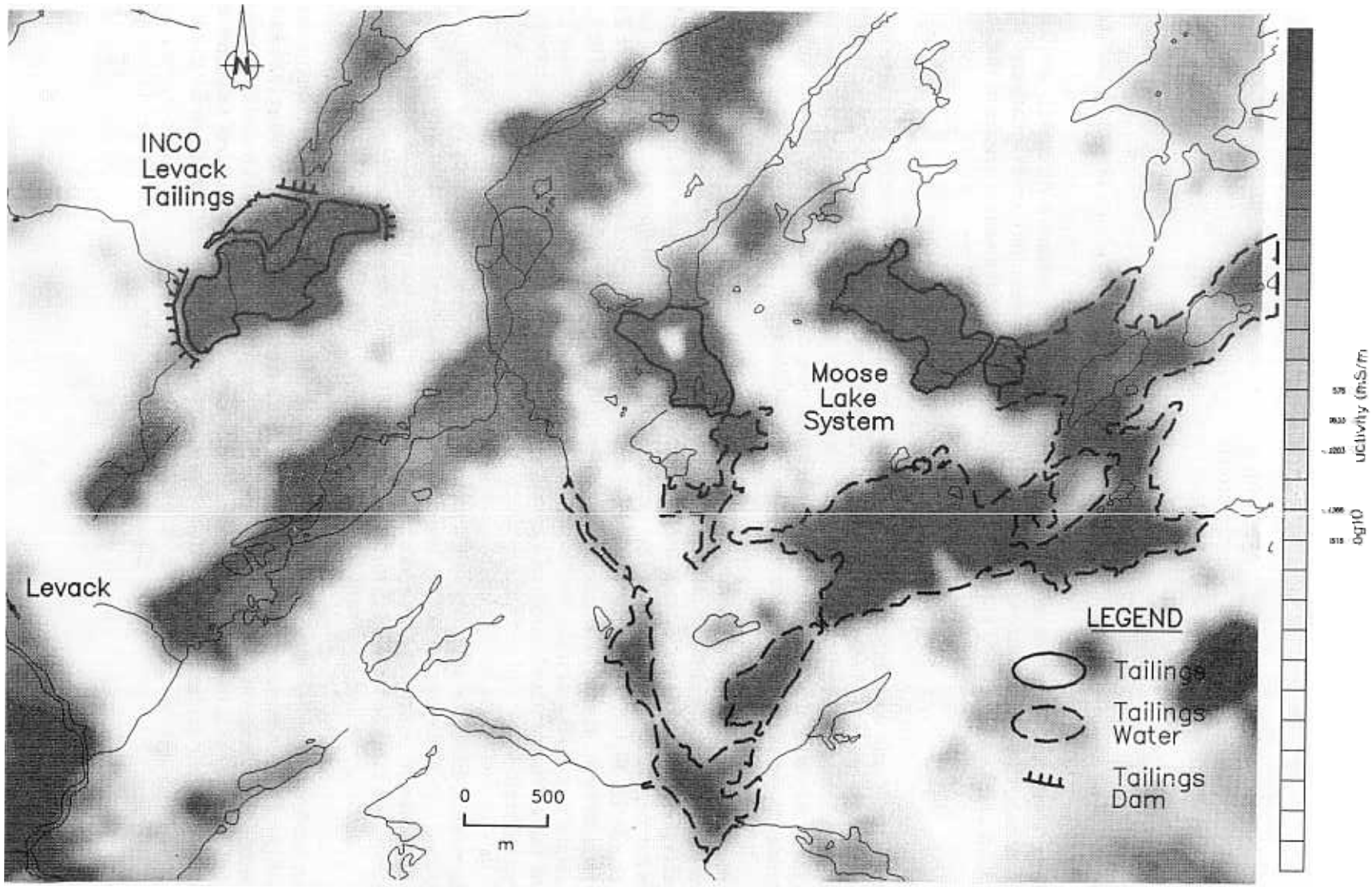

Figure 3. Levack Area Airborne conductivity data and surface drainage.

Description of Results

Helicopter EM Surveys

In 1987 most of the Sudbury Basin was flown with a multifrequency, multicoil, helicopter electromagnetic system as part of a regional minerals exploration program. It was immediately obvious from the responses over the tailings areas that the data would be useful for environmental applications as well as exploration.

The survey consisted of approximately 32,000 km of data acquisition at 100 m line spacing over a 40 km by 80 km area. The survey was navigated and the data positioned using a radio beacon triangulation system with an accuracy of better than 10 m. The data were sampled digitally at 5 m intervals along the survey lines and recorded. Following the calculation of conductivity values, the data were interpolated onto a 25 m by 25 m grid, contoured and presented in colour image form. The final gridded data file is a 15 megabyte digital data file suitable for input to image-processing or geographical information systems (GIS). This data set covers most of the existing and abandoned mine sites and provides an abundance of detailed conductivity information. A sample of these data over the Levack area was selected for ground truthing.

Figure 3 shows a grey scale version of the airborne electromagnetic (AEM) conductivity data superimposed on a topographic map of the Levack area showing surface drainage with the tailings areas highlighted. The grey scale is logarithmic with peak values over 30,000 mS/m.

The Falconbridge tailings and tailings water drainage are confined to rock-bounded lakes of the Moose Lake drainage system in the eastern part of the map area. The INCO Levack tailings are located to the north of the town of Levack in an elevated valley and are bounded by large dams to the north and south.

The outstanding features of the conductivity map are the strong conductivity highs (greater than 10,000 mS/m) over the tailings areas. The high conductivity over the tailings is due to high total dissolved solids in the tailings water. The water may be low pH, high sulphate, typical AMD where the tailings have been exposed to oxygen, or high pH, high sulphate, high calcium where the water is in its unoxidized state. Tailings are limed before discharge so unoxidized tailings are basic.

Background values over most of the survey area are very low (less than 5 mS/m) owing to the electrically resistive crystalline bedrock and freshwater-saturated, thin, sandy and gravelly overburden. This high contrast in electrical conductivity between background values and tailings water makes this an ideal environment for mapping ground water quality using geophysics.

The AEM data shows that the tailings in the Moose Lake system are confined to the rock-bounded lake and drainage system. There is no large scale migration of tailings water beyond the limits of the tailings themselves.

The AEM data over the INCO Levack tails clearly delimit the tailings area but also show moderate conductivity anomalies extending under the north dam into the lake to the north and beneath the south dam into the sand and gravel-filled valley to the south. These conductivity anomalies are due to AMD flowing in a sand and gravel aquifer which extends beneath the dams and the tailings. The AMD is apparent in a few iron-stained seeps in both areas. The airborne data show the essentially continuous nature of this conductive ground water in the valley. They also show that these are the only directions of leakage from the tailings and that the ground water flow is confined to the narrow valley. This information immediately focuses follow-up plans into well-defined areas, reducing sampling and monitoring costs as well as defining the approximate scope of future interception and treatment plans.

The low conductivity area over the town of Levack is an artifact of the data acquisition process. The helicopter is required to fly much higher than its normal survey altitude (aircraft 80 m; survey coils 30 m) over towns, so that the system is essentially measuring the conductivity of air.

Other areas of anomalous conductivity are due to cultural features such as mine buildings, power lines, railroads, etc., sulphides in bedrock (the original target of the survey), sulphides in waste rock piles, and other areas of ground water contamination in the vicinity of the mines. Most of these areas have yet to be followed up on the ground.

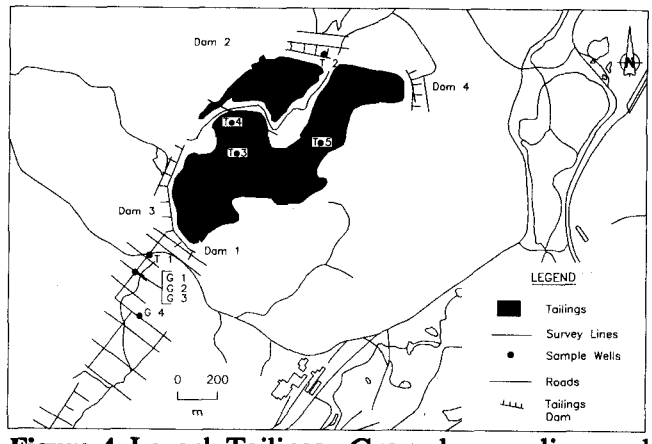

Figure 4. Levack Tailings - Ground survey lines and sampling well locations.

An alternative presentation of the airborne data provides more information on the variation of conductivity with depth. The helicopter system acquires data at three separate frequencies simultaneously (900 Hz, 4,000 Hz and 32,000 Hz.). Since depth penetration is inversely proportional to frequency, the multifrequency data can be used to create approximate sections or pseudosections of conductivity versus depth along the survey line. These are called Sengpiel sections after the developer of the method.

Sengpiel sections were calculated for all the lines over the INCO tailings and when stacked one above the other show the horizontal and vertical conductivity variations over the tailings and the north and south ground water plumes.

Ground EM Surveys

The airborne surveys in the vicinity of the INCO Levack tailings were followed up with detailed ground surveys using the EM31 (1-5 m depth penetration) and the EM34 (10-40 m depth penetration) ground conductivity systems. The larger scale topographic map shown in figure 4 shows the location of the survey lines as well as the location of the water sampling wells at the site. Most of these wells are multilevel, plastic-cased piezometers. Water samples were taken at regular intervals and analyzed for major ions and metals.

A sample of the EM31 data over the northern part of the tailings is shown plotted in profile form in figure 5. These data confirm the very high conductivities over the tailings themselves, the moderate but still highly anomalous conductivities over the northern ground water plume below the dam, and the very low background values. The rapid variations in values within the conductive areas are due largely to topographic variations or variations in the thickness of nonconductive fill. Because of the shallow depth penetration of the system, the readings are quite sensitive to the height of the instrument above the water table.

A sample of the EM34 data is shown in figure 6. These data were collected over the south ground water plume using vertical coplanar coils with a coil separation of 20 m and has an effective depth penetration of 10 m. The conductive area correlates well with airborne data in the area, but the conductivity values are somewhat lower. We believe that this is largely due to an improvement in water quality between the 1987 airborne survey and the 1991 ground survey due to flushing of the system with fresh water since the closure of the tailings.

At each station in the ground survey a total of five readings with different effective depths of penetration were taken with the EM31 and EM34. One-dimensional inversions were carried out on selected lines to produce approximate conductivity versus depth sections. One such section from the line along the base of the north dam

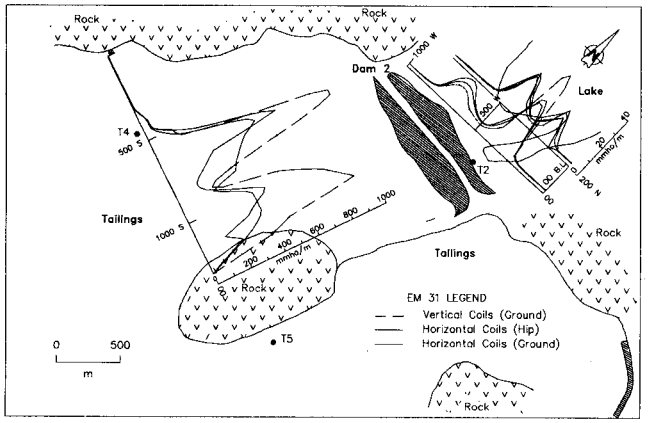

Figure 5. Levack Tailings North Dam - Shallow ground conductivity data (EM31).

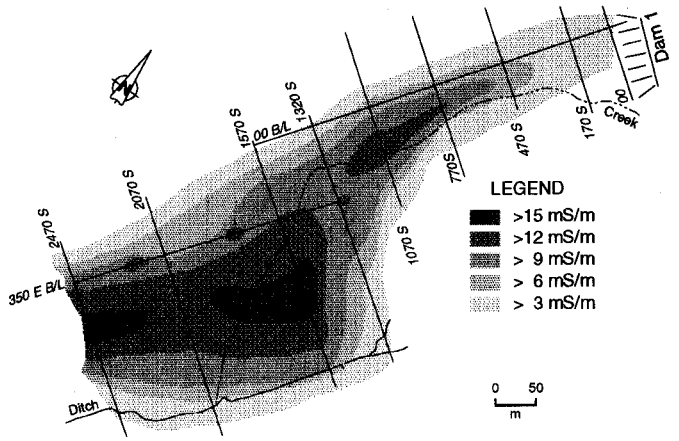

Figure 6. Levack Tailings South Dam - Deep ground conductivity (EM34, 20 metre coil separation, vertical coils).

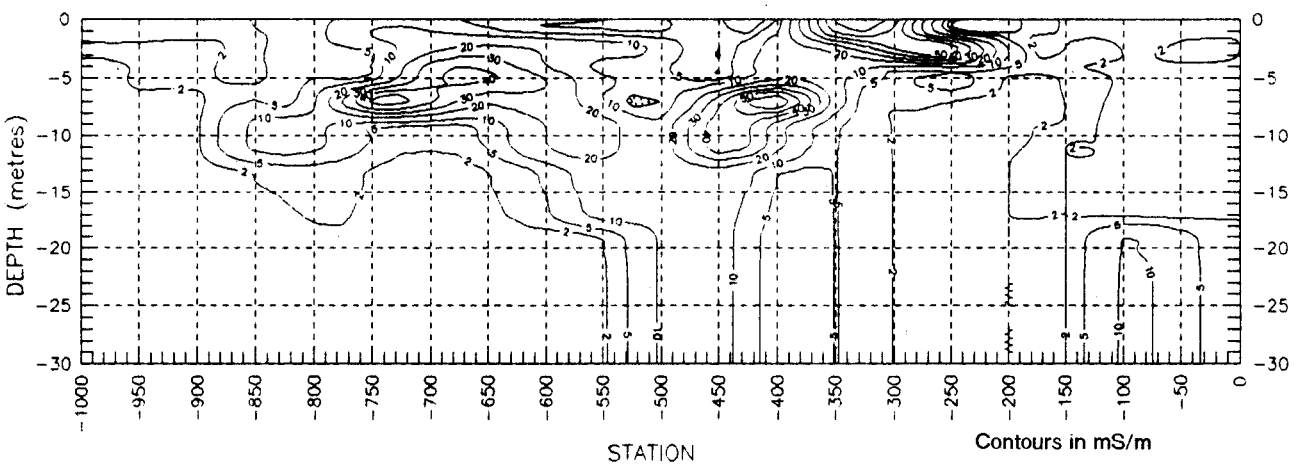

Figure 7. North Dam Line 00 - Vertical conductivity section.

is shown in figure 7. The general shape of the bedrock valley that contains the conductive ground water is apparent in the section. This shape has been confirmed by seismic refraction surveying and drilling.

Borehole EM Surveys

To establish a detailed correlation between bulk conductivity and ground water chemistry, downhole conductivity surveys were conducted in all available holes. Downhole natural gamma surveys were carried out at the same time to assist in mapping soil stratigraphy. The downhole electromagnetic conductivity tool measures the average electrical conductivity in the vicinity of the hole and can operate in plastic-cased boreholes. Readings are digitally recorded at 10 cm intervals, providing a very detailed conductivity profile.

Figure 8 shows a sample of logs from borehole T-2 located in the ground water plume just to the north of the north dam. Below the water table at 10 m, the conductivity log shows moderate bulk conductivity values throughout the sand and gravel aquifer associated with anomalous pore fluid conductivity values as measured on water samples. These values are consistent with measured airborne and ground conductivity values results.

The source of the conductivity is acidic ground water, as indicated by the low pH's.

Both the conductivity and gamma log show that the aquifer is not as uniform as indicated by the stratigraphic log. In general, the gamma values are inversely correlated with the conductivity. High gamma and low conductivity indicate areas of higher clay content and presumably lower permeability. Low gamma, high conductivity areas correspond to areas of lower clay content and higher permeability.

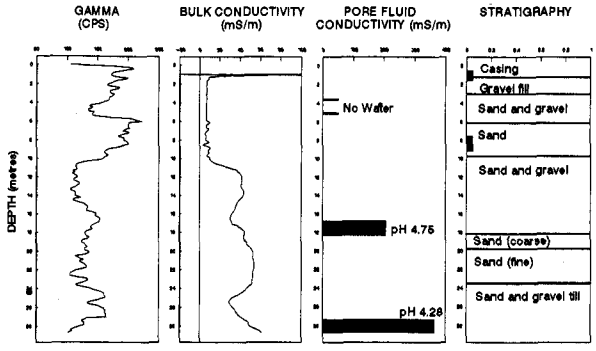

Figure 8. Downhole geophysical logs - Hole T2.

The relationship between chemistry and conductivity is illustrated in the next two figures. Figure 9 shows the concentration of all significant ionic species in a water sample from 28.9 m in depth in well T-2. This is a characteristic AMD chemical signature with sulphate as the dominant ionic species, followed by iron and calcium.

Figure 10 shows the contribution that each ionic species makes to the total conductivity as calculated from the chemical concentrations using the formulae given by McNeil (1980). It is apparent that the conductivity, like the concentration, is dominated by the sulphate, iron and calcium ions. At this moderately low pH (4.28) the H_3O+ ion makes a negligible contribution to the conductivity. However, due to the logarithmic nature of the pH measurement, the H_3O+ concentration and its contribution to the conductivity increase rapidly with decreasing pH.

Borehole conductivity measurements provide a detailed log of conductivity and can be used to locate precisely the source of anomalous conductivity, to interpolate water quality between water sample point and to locate suitable sampling points.

Induced Polarization and Resistivity

Combined induced polarization and electrical resistivity surveys were carried out along two lines on the Copper Cliff tailings. These two lines had been previously studied by the University of Waterloo, and a number of shallow stratigraphic holes together with ground water monitoring wells were available for correlation with the geophysics.

Different parts of the Copper Cliff tailings contain very different concentrations of sulphide with values ranging from over 50% in the pyrrhotite storage area to less than 1% in some of the low sulphide areas. The low sulphide tailings were deposited when an iron ore recovery plant was in operation and recovered iron and sulphuric acid from the rejected pyrrhotite. The lateral and vertical boundaries between different types of tailings are not always well known, particularly in older areas of the tailings. Since knowledge of the total volume of sulphide and the distribution of sulphides is important in predicting AMD production, it was hoped that the IP data could provide some information on sulphide distribution.

A sample of the data from one of the survey lines, shown in figure 11, extends from an area of known moderate pyrrhotite content (about 3% sulphides) around Station 0+00 into an area of lower pyrrhotite (less than 0.5% sulphides) around 340S. In this case the horizontal scale is in metres along the survey line and the vertical scale is measured in units of the electrode spacing. Since an increase in electrode spacing results in an increase in depth penetration this figure is an approximate vertical section through the earth to the maximum depth penetration of the system, which in this case is about 20 m. The IP results correlate well with the known sulphide distribution with values around 4 milliseconds (msec.) of chargeability at Station 0+00 and values

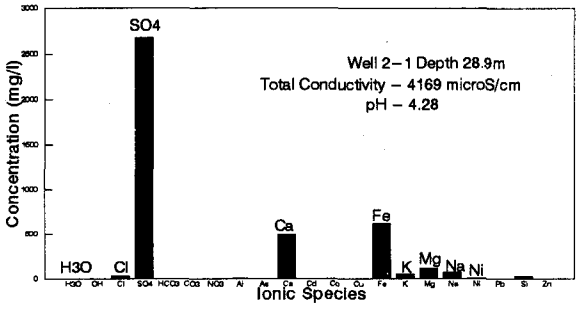

Figure 9. Groundwater chemistry - Hole T2.

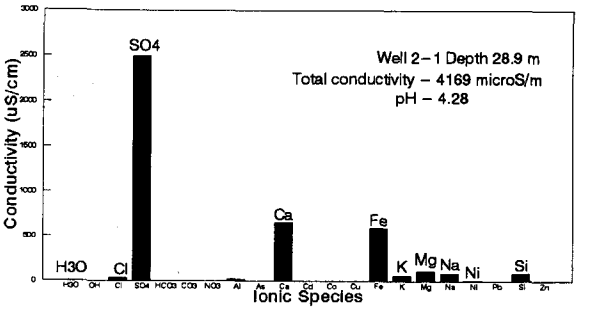

Figure 10. Conductivity per ion - Hole T2.

below 1 msec. south of 2+00S. The feature at 2+90S is due to a steel pipe. It appears from the data that the low sulphide area at the south end of the line onlaps the zone of higher sulphides as indicated by the higher chargeability values extending to depth to the south.

The conductivity values are higher over the higher chargeability area indicating higher concentrations of AMD associated with the sulphides. Based on the results of this work it appears that electrical IP and resistivity surveys are a useful tool for mapping the distribution of sulphides and AMD in tailings.

Conclusions

In the course of this work, we have demonstrated that, in suitable areas, electromagnetic and electrical geophysical methods can be used to map the three-dimensional distribution of sulphides in tailings and AMD in and around tailings. The airborne and surface methods are non-intrusive, fast and inexpensive when compared to reconnaissance drilling and sampling programs. The borehole methods provide detailed conductivity logs which can complement limited downhole water sampling.

It should be emphasized that geophysical methods should not be used in isolation. Because they do not uniquely identify the source of anomalies and the accuracy of interpretations is often limited by data density, signal noise, or the equivalent signatures of different sources, they should only be used as a guide to drilling and sampling, not as a replacement.

Bibliography

Blair, R. D., J. A. Cherry, T. P. Lim and A. J. Vivyurka. 1980. Ground water monitoring and contamination occurrence at an abandoned tailings area, Elliot Lake, Ont. In First International Conference on Uranium Waste Proposal, AIME.

Coggans, C., D. W. Blowes and W. Robertson. 1991. The Hydrogeology and Geochemistry of a Nickel Mine Tailings Impoundment, Copper Cliff, Ontario. In Proceedings of the Second International Conference on the Abatement of Acidic Drainage (Montreal, P.Q., September 16-18, 1991).

King, A. R. and A. N. Sartorelli. 1991. Mapping Acidified Ground Water using Surface Geophysical Methods. Second International Conference on the Abatement of Acidic Drainage, Montreal.

McNeill, J. D. 1980. Electrical Conductivity of Soils and Rocks. Geonics Limited Technical Note TN-S.

Pehme, P. E. 1981. Geophysical survey of the Nordic contamination plume. M.Sc. Thesis, University of Waterloo.

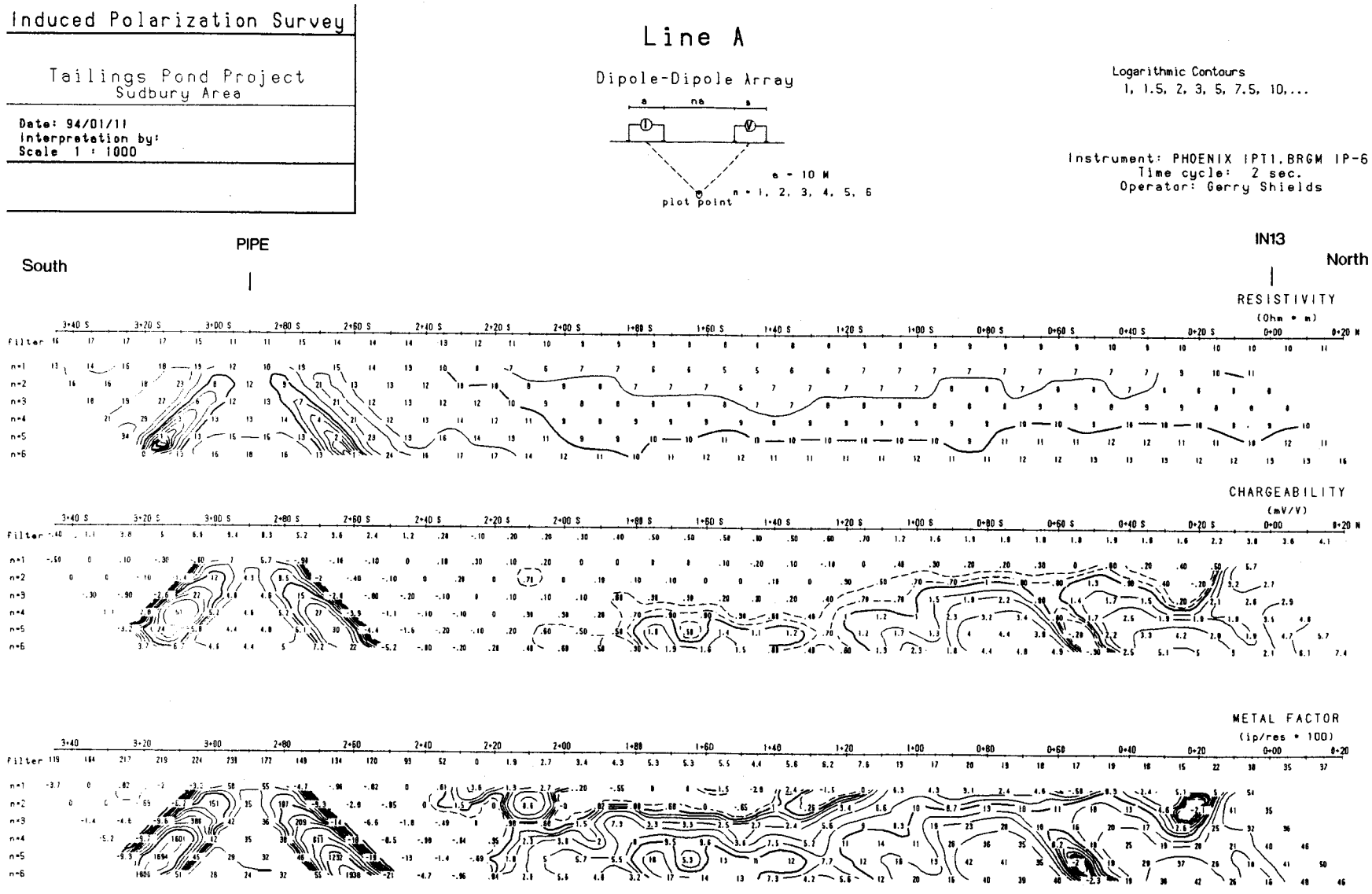

Figure 11. Induced polarization and resistivity data Copper Cliff Tailings.

METHODOLOGY FOR LOCATING AND QUANTIFYING ACID MINE DRAINAGE IN GROUND WATERS ENTERING SURFACE WATERS[1]

David R. Lee and Rob Dal Bianco[2]

Abstract: Subsurface migration of leachate from mining operations to rivers and lakes is now an issue at some sites, particularly where these operations adjoin public waters. Until now there has been no practical method for identifying and quantifying subsurface flows into surface waters. A new method for finding and measuring seepage into surface waters has been evaluated near a mining area in northern Ontario. A bottom-contacting probe was towed behind a slowly moving boat and used to locate areas of leachate discharge. The upward flux of high-dissolved solids ground water in these areas was confirmed (1) by measuring the pore water electrical conductivity 20 to 120 cm below the sediment-water interface, (2) by directly measuring flux using seepage meters or (3) by measuring gradient, hydraulic conductivity and solute chemistry. The discharges ranged from 12,820 to 43 uS/cm and from 6.9 to 4.8 pH. One discharge contributed 12 kg of nickel per annum to the receiving river. Combined with conventional methods, piezometers and seepage meters, the new method forms a methodology that starts with broad reconnaissance to identify potential discharge areas and ends with quantitative measurements in discharge areas.

Additional Key Words: monitoring, electrical conductivity, assessments, offsite migration, contaminant transport.

Introduction

In mining areas, water infiltrating the land surface may contact a large reservoir of noncarbonate, sulfide-bearing soil particles and rocks, become acidic and acquire elevated concentrations of iron and sulfate. These ground waters can also mobilize heavy metals, including radionuclides, and can transport them to points of discharge. There also may be significant attenuation or dilution between source areas and the entry of acid mine drainage (AMD) and metals into surface waters.

Because ground water moves to topographical lows, there is potential for transport of leachates, containing high metal concentrations and depressed pH levels, to aquatic environments. In some settings this may not be obvious because all seepage can move inconspicuously below the waterline to rivers, lakes or their contributing wetlands.

The conventional approach, using piezometers, can approximate the locations of ground water discharge zones, but, because of the heterogeneity of most geologic settings, this can require an enormous number of sampling locations, which are established and monitored at great cost. Data analysis of such point samples would also require a large degree of interpolation between sampling locations. The interpreter must decide whether samples are sufficient and representative. This has an important bearing on the validity of conclusions.

A technique for examining large areas of water-covered terrain was developed to help solve the problem of arbitrary point sampling. The technique involves the towing of a bottom-contacting probe behind a small, outboard-motor boat. This technique provides continuous recordings of electrical conductivity (EC) along bottom sediments while assigning a geographical coordinate to each measurement. This paper describes this technique, its first application to AMD, and shows collection of data and an estimatation of nickel flux to surface waters.

---

[1]Paper presented at the International Land Reclamation and Mine Drainage Conference and the Third International Conference on the Abatement of Acidic Drainage, Pittsburgh, PA, April 24-29, 1994.

[2]David R. Lee, Research Officer, Rob Dal Bianco, Technical Officer, AECL Research, Chalk River Laboratories, Chalk River, Ontario, K0J 1J0, Canada

Under good conditions, a sediment probe survey can cover 10 to 15 line-kilometers of lakebed or riverbed per day. This is intended to provide an accurate and inexpensive identification of locations where environmental impact has occurred or may occur in the future. Discharges, which have been identified with the probe, can then be characterized chemically and hydrogeologically to determine sources and transport times.

Methods

Mapping of Subaqueous Acid Mine Drainage

The presence of a subaqueous, ground water discharge zone was sensed as an increase in sediment EC above the local background using a probe (fig. 1) towed along the riverbed.

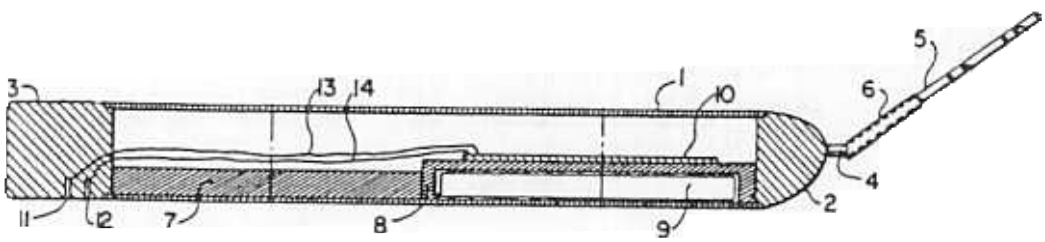

Figure 1. Sediment probe (after Lee and Beattie, 1991) consisting of a slim tubular body or shell **1** closed at one end with a nose cone **2** and at the other end with an end plug **3**. The nose cone has a rounded front which is provided with a waterproof connector **4** to which a towing cable is attached so that the probe can be towed along the bottom of a river or lake bed. A plastic abrasion guard **6** surrounds the lower portion of the cable **5**. One or more lead weights **7**, **8** are located in the bottom portion of the tubular body. A gamma radiation detector **9** may or may not be located in the probe. A ciruit board **10** is located above the lead weight. The end plug contains two or more electro-conductive pins which are flush with the lower surface of the plug and connected to the circuit board. The probe may contain other features (Lee and Beattie, 1991) not used in the present work.

The sediment-probe survey involved three people. The data acquisitions system had readouts for several data channels, so that the two people in the boat could observe data as collected, form mental images of results within the study area, and deploy anchored floats in areas of interest. A portable computer and a paper chart recorder provided visual displays and data logging. Custom software, prepared using LabWindows in C, was used to record input from both the probe and the positioning system.

The positioning system consisted of a shore-based tripod theodolite (for determination of angle and elevation), small computer, a radio telemetry unit and a laser range finder with a maximum range of 15 km. The accuracy was potentially better than plus or minus 0.5 m, but this was compromised to 3 m by the correction of probe position relative to the boat. The shore operator tracked a prism mounted on the boat through a telescope on the laser range finder. The shore-based part of this positioning system supplied the computer in the boat with x and y coordinates relative to the tripod reference point.

In most instances, a sufficient outline of the shoreline of a water body was recorded by tracking the boat as it moved along the edge of the water body as close to shore as possible. The system recorded probe readings every 0.2 to 0.4 s and the boat speed was 0.5 to 1 m/s.

The first step of data processing was conversion of the boat position, boat direction and cable length to the position of the sediment probe corresponding to each probe measurement. The probe was considered to follow the boat by a distance equal to the length of cable.

Data analysis employed software customized and developed by the Environmental Research Branch of AECL Research. Normally colors are used to define ranges of EC along a riverbed or lakebed, using a dot of color for each probe measurement on a map. However, in this paper a shaded gray version of the maps was used.

Confirmation of Sediment-Probe Survey Results

Ground water parameters were measured to quantify and evaluate sediment probe survey results. Harpoon piezometers (Lee and Welch 1989) were used to obtain ground water for EC and chemical analyses, measure hydraulic potentials and estimate hydraulic conductivity. To measure directly the flux of ground water entering surface waters, seepage meters were installed in appropriate locations, such as sandy bottoms in nonflowing waters (Lee and Cherry 1978).

Results and Discussion

Previous monitoring of surface waters had accounted for only 10% of the nickel exported by the Levack portion of the Onaping River (Wiseman, 1993) 40 km northwest of Sudbury, Ontario. In addition to testing the probe, we sought to locate additional sources of nickel loading and provide a basis for future work.

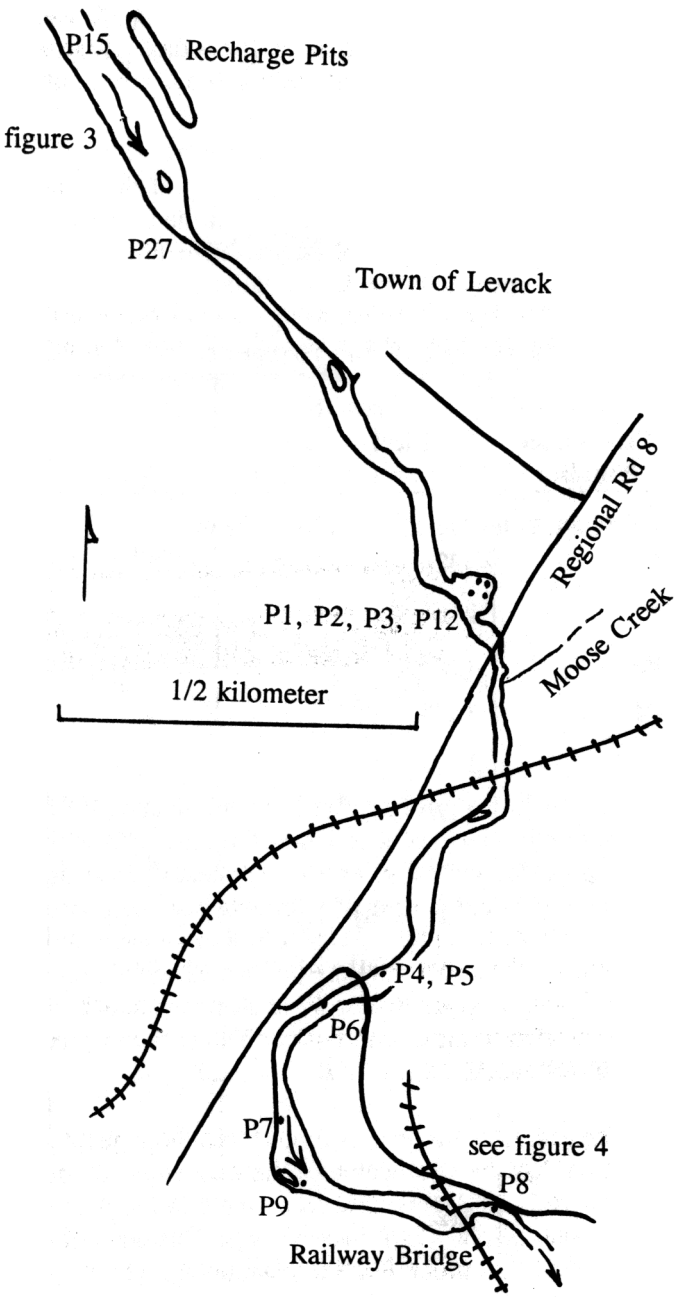

Figure 2. Study area near Levack, Ontario.

Initial survey

Initially the probe was towed up and down a 2 km-long section of river (fig.2). In areas of elevated EC, 12 harpoon piezometers were installed to determine whether high values of EC, identified with the sediment probe, coincided with locations of rapidly flowing, high dissolved solids seepage.

Further delineation of ground water discharge areas was conducted at four sites within this reach of river. Results at all four sites were similar and results at three sites are presented here. The fluxes of water and Ni were calculated from areas of discharge (based on probe survey results), measured seepage rate and pore water solute concentrations.

Samples of sediment pore water were withdrawn from the piezometers for laboratory measurement of EC and pH (table 1). The pore water EC in some of the samples was as much as 100 times greater than that of the river. River values of EC were 46.3 μS/cm at the highway bridge and 228 μS/cm at the rail bridge downstream (fig. 2). Measurements of hydraulic head, relative to the river surface, or measurements of artesian flow confirmed the existence of upward hydraulic potentials.

Table 1. Onaping Riverbed Piezometers

Piezometer Number	Porewater Elect. Cond. μS/cm @ 24-25°C	pH	Depth of Piezometer Screen Below Riverbed cm	Head of Water in Piezometer Above River cm
Piezometers northeast of highway bridge				
P1	1321 [Ni]=2.24	7.00	43	
P2	2160 [Ni]=1.00	6.81	30	
P3	1903	6.42	20	
P4	1075	5.96	75	
P5	1180	6.17	193	
P6	1570	6.55	111	
P7	961	4.91	41	
P8	3910 [Ni]=1.1	4.89	44	
P9	360 [Ni]=2.79	6.47	109	
P12	1869	6.18	30	
Piezometers near Recharge Pits, Fig. 3				
P13	43		108	75 (flowing)
P14			194	52
P15	123	6.49	75	~0
P16	72 [Ni]=≤0.02		79	20 flow=124mL/min
P17	326 [Ni]=2.8	6.05	94	~0
P27	1200	4.83	30	
Piezometers downstream of the RR Bridge, Fig. 4				
P8	1430 field			flow=0.8mL/min
P19	1800 field [Ni]=9.5	5.66	42	1
P20	12820 field	5.44	49	
P21	207			

There was generally excellent agreement of probe values (measured in situ) and the pore water values (collected from piezometers and measured in the laboratory); pH was occasionally depressed where EC was elevated (table 1).

Results at Three Sites

Northwest of the highway bridge (Fig. 2), probe results indicated a 350 m^2 area of elevated EC. While installing piezometers in a surficially sandy bottom, we encountered cobbles and boulders within 50 cm of the sediment-water interface. Due to the shallowness of these piezometers, gradients were too small to measure, except at P1, where the water level stood 0.5 cm above river level and the vertical gradient was 0.01. The piezometer samples (P1, P2, P23, P26) had EC values from 1530 to 2260 μS/cm. The river at this location had an EC of about 50 μS/cm. Nickel in P1 was 2.24 ppm, well above the river background concentration of 0.1 to 0.15 ppm.

Screened just 20 to 30 cm below the riverbed, P2 produced water with an EC of 2160 μS/cm and a nickel concentration of 1 ppm. This EC was 44 times greater than the river value at that location. Considering the proximity to the river and the permeability of the sediments, these water samples provided unequivocal evidence of solute discharge. AMD may enter the river at this site, based on the measured Ni values of 1 to 2.2 ppm in these very shallow piezometers. However, the relative contributions of AMD and road salt will have to be determined by further chemical analysis of water samples from riverbed piezometers.

Hydraulic heads in all the piezometers at P2 were within millimeters of the river level, and considering the currents of 20-30 cm/s, were not suitable for hydraulic potential measurement, except to indicate low or nonexistent gradients. Lack of measurable differences in water levels relative to river level was probably due to the shallow depth of penetration of all the piezometers and the highly permeable bottom materials.

Piezometers near P2 and P12 (fig. 2) also confirmed and quantified discharge of high EC ground waters at locations identified with the probe. Artesian flow of 0.1 mL/min at one peizometer proved upward hydraulic potentials, but the piezometric level could not be distinguished from river level. One piezometer contained 2.8 ppm Ni, which was intriguing, considering its relatively low EC of 360 μS/cm.

An anomaly was noted (fig. 3) in the middle of the river about 150 m below rapids. Here, in water 3.5 m deep, piezometer P15 was screened in gravel 75 cm below the riverbed. While sitting in the boat, we could not see a difference between the water level of this piezometer and the river, so we extended the piezometer tube to shore, 40 m away. The water level in this tube did not differ ($\pm$ 0.2 cm) from the level of the river at the shore, suggesting little or no hydraulic gradient, at least when measured at this location. Pore water pumped to shore from this piezometer had an EC of 123 μS/cm. Although this was three times greater than the river EC at that location, it was lower than expected based on the probe responses nearby. Based on probe response, we expected greater than 123 μS/cm in P15 (table 1). Perhaps the high-EC area was not sampled by P15, which was not installed exactly in the groove formed by the probe where river gravels were too coarse for our installation method. Later, when we visually inspected the bottom, we saw this groove in relation to our piezometer. We also noted a 0.5 to 1-m thick layer of 8°C bottom water, which, considering the overlying river currents, must have been supported by continuous discharge of ground water. The depressed temperature there would have depressed the probe readings by about 16%, not elevated the EC.

Table 2. Onaping River Seepage Meter Data

Seepage meter at piezometer number	*Seepage Flux, μm/s
16	0.8,0.5
8	0.8,0.8

*Seepage flux is equivalent to specific discharge. 1μm/s=31.5 m/yr

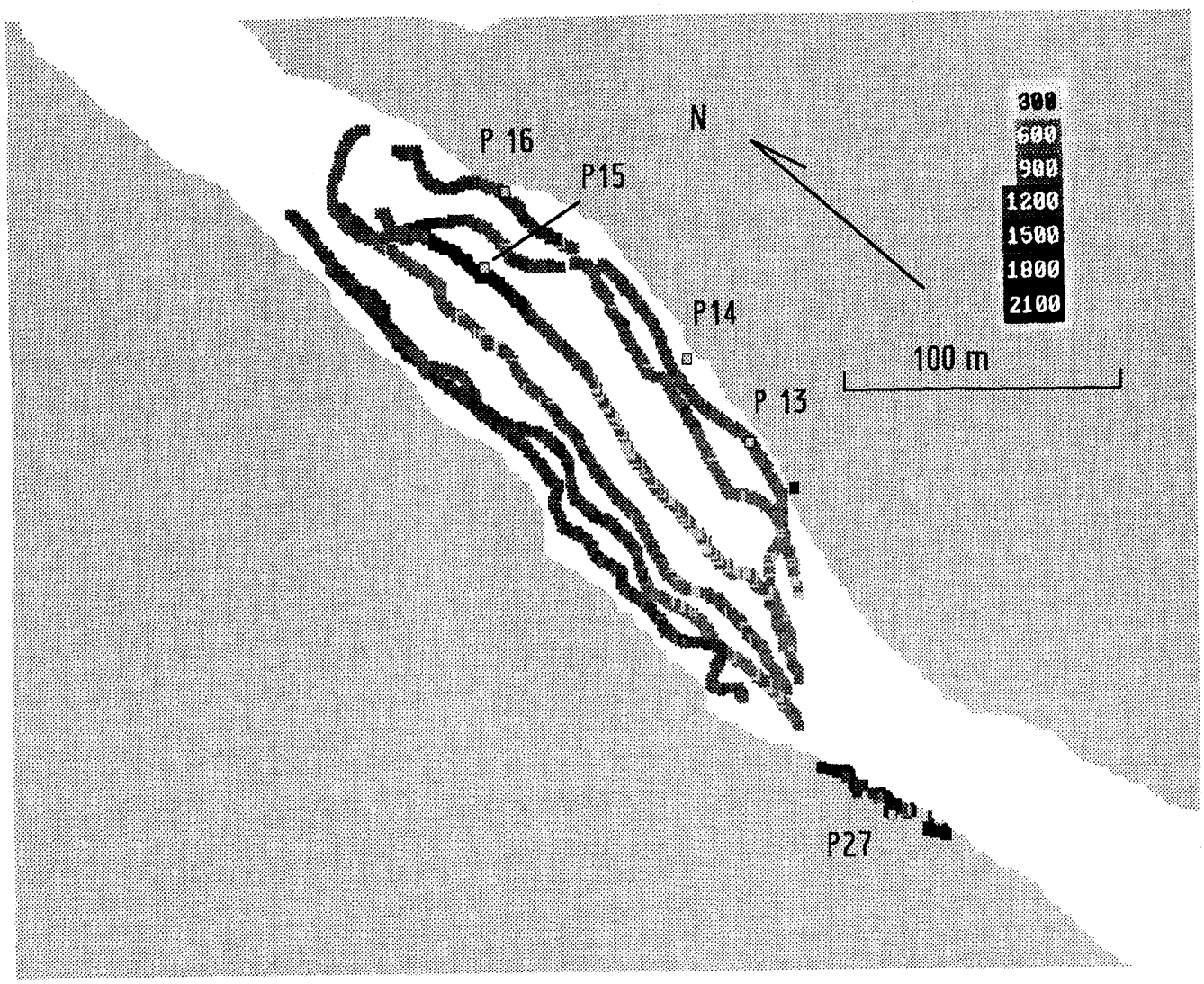

Figure 3. Sediment probe electrical conductivity of the Onaping Riverbed near the Levack, Ontario, municipal well recharge pits. Each dot represents one measurement location and value. The ranges of electrical conductivity from low to high are indicated with shades from white to black.

Where EC was predicted to be high based on the probe results (fig. 3), piezometer samples were correspondingly elevated in EC (table 1). However, along the shoreline adjacent to the recharge pits, the probe did not indicate seepage of high EC ground water. At that location, we observed the discharge of uncontaminated ground water using seepage meters (table 2) and by measuring head, artesian flow and EC in piezometers P13, P14, and P16 (Table 1). Discharge of low-EC water can be attributed to the adjacent pits, which were maintained above river level by pumping from the river with the intention of diverting AMD from municipal wells.

Another anomaly was found along the right bank of the river (P27, fig 4). A piezometer there (P27) yielded water with an EC of 1200 μS/cm, a nickel content of 2.8 ppm and a pH of 4.8 (table 1). Surface water levels in this area were slightly above the level of the adjacent river. The cold water ($< 9\,^{\circ}$C) discharging at this location was visibly pristine and not iron stained.

Two facts indicated that leachate from tailings is diverted from its natural course by a ground water mound produced by the pits, and discharges at locations farther upstream and downstream: a) a plume of tailings-contaminated ground water extends toward the river from tailings 2 to 3 km northeast of the pits (King, 1993), and b) two distinct areas of high EC were found on the river bottom, one above and one below the recharge pits (fig.3, near P15 and P27). To determine solute sources in these zones, it will be necessary to measure sulfate concentrations and environmental isotopes and possibly to install additional piezometers.

At another detailed study site below the railway bridge (fig. 4), the sediment-probe results focused work on an area that yielded pore water of 8,000 to 12,820 μS/cm, 9.5 ppm Ni (table 1) and ground water discharging at a rate of 0.8 μm/s (table 2). Judging by the probe results (fig. 4), the anomaly was 17 m in length. Its width was at least 3 m, based on the distance between piezometers P19 and P20, and seepage meter 8 (at P8). The nickel loading to the river was about 12 kg/yr assuming a rectangular discharge area of 3 m X 17 m, an average seepage rate of 25 m/yr and an average Ni value of 9.5 g/m^3.

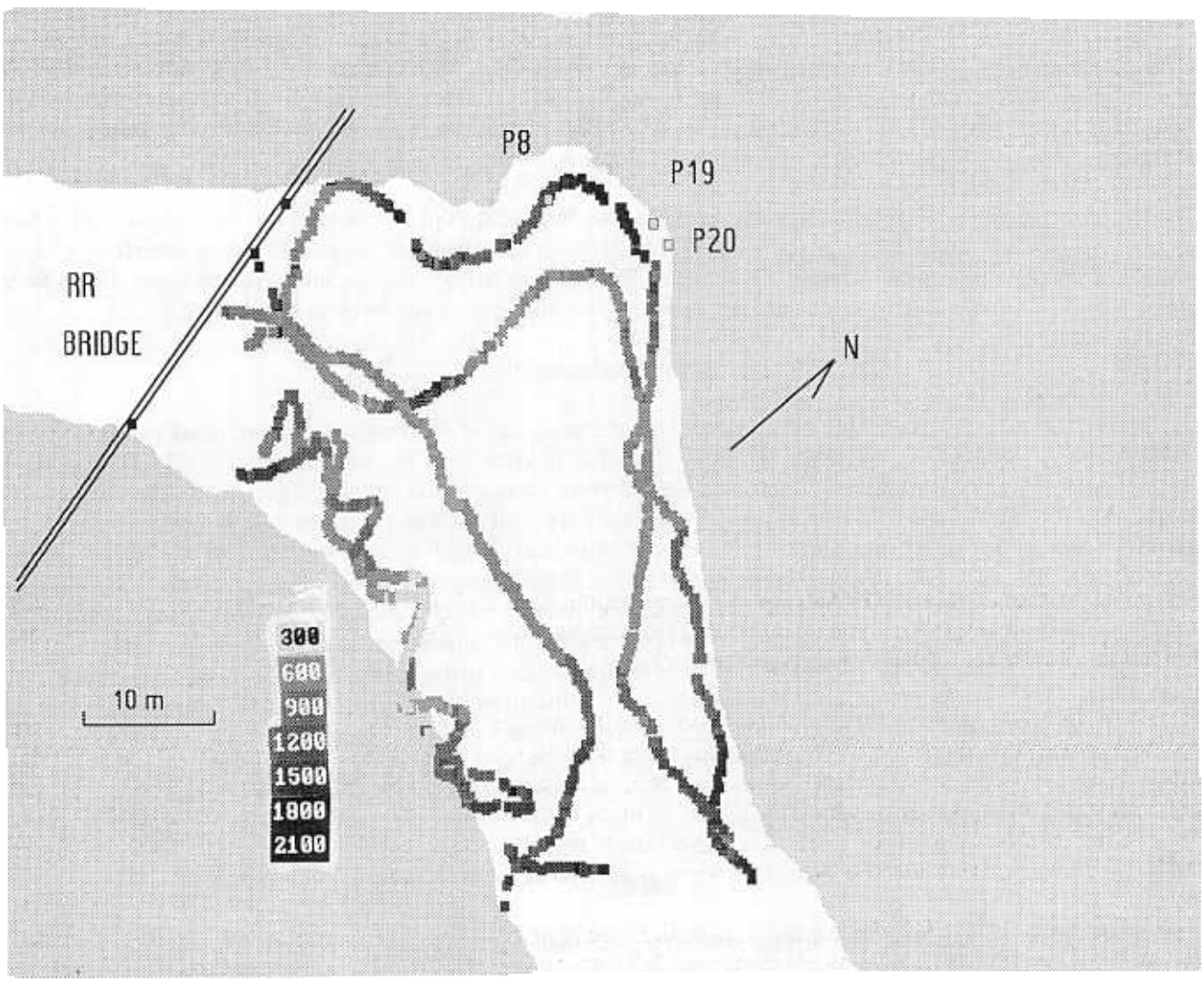

Figure 4. Sediment probe results on the Onaping River one kilometer below Levack near the Inco rail bridge.

Conclusions

1. Sediment probe surveys provided qualitative maps of areas of elevated EC ground water discharge. In every location of high EC identified with the sediment probe, pore water EC was elevated relative to the overlying water. Where the probe registered high values, there was also evidence of upward ground water flow. Pore water EC values were as high as 12,800 μS/cm. Therefore the sediment probe identified ground water discharge areas and these were found to contribute nickel to the Onaping River at concentrations ranging from 1 to 9.5 ppm. Sediment-probe results were used to estimate the size of the discharge area near three piezometers that had elevated EC and a nickel flux of 12 kg/yr was estimated in a 50 m^2 discharge area.

2. Probe performance was unaffected by overhead power lines and other materials that have hampered application of electromagnetic methods. Because the methodology includes quantitative analysis of discharge parameters as an essential part, it yields discharge information in areas of greatest potential contaminant flux. Experience on the Onaping River showed that even in whitewater this methodology can be effective.

3. Now that potential AMD areas have been identified and are known to occupy small areas of river, ground water and contaminant flux may be assessed efficiently. Samples may be collected at existing piezometers, so that additional chemical and isotopic analyses can help determine source areas. Helium-3/tritium analysis using mass spectrometry is recommended to determine ground water age (i.e., underground residence times) for water presently discharging. Some of the suspected AMD may turn out to be natural ground water.

4. In theory, sediment type affects probe response, but in practice did not prevent the identification of ground water discharge areas. Variation of sediment electrical properties was not large enough to interfere with the identification of discharge areas where the contrast in EC between surface and ground water is more than a factor of about 2 or 3. In more homogeneous environments, this contrast may not have to be so large.

Acknowledgements

Mark Wiseman (Falconbridge Ltd.) recognized the potential of this method and arranged partnerships for financial support: INCO Ltd., Falconbridge Ltd., the Mine Environment Neutral Drainage (MEND) program of the Department of Natural Resources Canada and the Northern Ontario Development Agreement. He also directed us to questions on the Onaping River and provided analysis for water samples. Bruce Mikila (Falconbridge Ltd.) suggested access points along the Onaping River and provided general familiarization with the area. Marcia Blanchette (MEND) set up the research contract within the MEND office and Department of Supply and Services Canada. Carl Weatherell (CANMET) gave us technical-contractual advice. Rick Janzen (AECL Research) looked after administrative details, especially those involved in amending the contract to allow work in the summer of 1993. Jeff Cheung (AECL Research) developed the software to compile data in the field, process it in the office and display it in the report. Mark Ungrin (Co-op student from the University of Waterloo) assisted in the field with the ground-truthing methods and with the laser positioning system. Ken Whitlock (AECL Research) helped design the sediment probe and manufactured harpoon piezometer drive tips. Mark St.Aubin (AECL Research) provided essential electronic support. Anonymous reviewers improved the manuscript. Janice Cochrane (AECL Research)adapted the writer's manuscript to meet editorial standards.

References

Lee, D.R. (in prep) Solute flux into surface waters via groundwater flow.

Lee, D.R. and J.A. Cherry. 1978. A field exercise on groundwater flow using seepage meters and mini-piezometers. J. Geol. Ed. 27:6-10.

Lee, D.R. and S.J. Welch. 1989. Methodology for locating and measuring submerged discharges: targeting tool, harpoon piezometer and more. In Proceedings Focus Conference on Eastern Regional Ground Water Issues. Co-sponsored by the Association of Ground Water Scientists and Engineers and Waterloo Centre for Groundwater Research (October 17-19, 1989).

Lee, D.R. and W.J. Beattie. 1991. Gamma survey probe for use on ocean, lake, estuary and river sediments. U.S. Pat. 5,050,525.

King, A. 1993. Pers. Comm. INCO Ltd., Copper Cliff, Ontario.

Wiseman, M. 1993. Pers. Comm. Falconbridge Ltd., Falconbridge, Ontario.

EFFECTS OF INCREASED IRON CONCENTRATIONS ON THE MOBILITY OF CADMIUM, COPPER AND ZINC IN LEACHATES AFTER REMEDIAL ACTIONS AT AN OLD SULPHIDIC MINE WASTE SITE[1]

K. Håkansson, S.Karlsson, and B. Allard[2]

Abstract: The covering of acidic mine waste occured from 1987 to 1989 at a former copper mine site in Bersbo, Sweden. The purpose of the cover was to reduce the weathering of the sulphidic ore residues (pyrite, sphalerite, chalcopyrite, galena).

Analysis of water quality data shows that in one of the two drainages from the covered area, comparatively minor decreases of cadmium, copper, and zinc (30% - 65%) have occurred after completion of the remedial actions. The concentration of sulphate on the other hand, has increased from 600 mg/L to 1 000 mg/L, and iron concentration from 6 mg/L to more than 200 mg/L.

The hypothesis is that these changes are caused by the reduction of iron(III)oxyhydroxides to iron(II) in the mine shafts and subsequent oxidation of sulphides. That is, a possible change from oxygen to iron as an oxidant for the sulphidic minerals.

The effects of the high iron(II) load on the recieving lake and the changes in hydrochemical conditions when this iron is oxidized anew is discussed. Water quality data before and after remedial action and effluent titrations at different (constant) pH have been combined to indicate the effects of metal sorption on iron oxyhydroxides and metal removal by sedimentation.

The amount of iron hydroxides deposited in the mine shafts and thus the potential capacity for weathering is estimated from analysis of the solid waste and concentrations in the leachates before and after restoration.

Additional Key Words: acid mine drainage, iron oxidation,

Introduction

Although the principal mechanisms of oxidation of pyrite are known (Stumm and Lee 1961; Stumm and Morgan 1981; Kelly and Tuovinen 1988), no uniform strategy of disposal of mine tailings has been developed. Thermodynamic calculations and laboratory tests are important tools to assess the impact of different parameters. Empirical studies of pilot- or full-scale projects are, however, a necessary complement to such investigations, since practical difficulties will influence the success of restoration projects.

The starting point of this study is the observed differences in the composition of the leachates, and water quality in adjacent surface waters, especially with regard to iron concentrations, of an old mine tailings deposit before and after a dry deposition covering project. The contrasting effects of iron on the adsorption of trace elements in scavenging of metals are discussed; 1 The formation of an important adsorbent for metals, 2 The lowered pH during oxidation of Fe(II).

---

[1]Paper presented at the International Land Reclamation and Mine Drainage Conference and the Third International Conference on the Abatement of Acidic Drainage, Pittsburgh, PA, USA, April 24 - 29, 1994.

[2] K. Håkansson, Ph.D., S. Karlsson, Ph.D., and B. Allard, Prof., Linköping University, S-581 83 Linköping, Sweden.

Field site

Bersbo is a former copper mine about 250 km south of Stockholm, Sweden. The bedrock is leptitic with younger granitic and amphibolic intrusions containing hornblende, augite, and calcium-rich plagioclase (Tegengren 1924; Allard et al. 1987). The ore veins contain pyrite, magnetic chalcopyrite, and sphalerite and, to some extent, galena. The same rock types constitute the primary fractions of the tailings on the site. A detailed description of the area is found in Allard et al. (1987).
The most intensive mining period in Bersbo started around 1760, with the highest production between 1850-70. Mining ceased around 1900, although minor extraction continued until 1930.

The waste material was piled near the shafts and covered before reclamation about 0.2 km^2. The leachates discussed in this work emanates from the western part of the tailings deposit (figure 1) and drains into the small lake (Gruvsjön). Since the ores were separated manually from the extraneous material, the mine waste consists of coarse material. Oxygen measurements in the dumps (Lundgren and Lindahl 1991) showed that the material was well ventilated, and oxidative weathering would proceed in the pile. It has been estimated that 700 000 m^3 of mine waste have been produced (Lundgren 1990).
A continued high weathering rate and the possibility to use Bersbo as a full-scale test site for other old sulphidic mine waste sites were some of the objectives for the reclamation project that took place from 1987 to 1989. The aim was to reduce the releases of Cd, Cu, Pb, and Zn associated with the pyrite with 90% [Länsstyresen 1986, (County board)].

Tailings were piled together in two heaps to minimize the area to be covered. To further minimize the area, 200 000 m^3 of tailings were dumped into the old shafts (Lundgren and Lindahl 1991). Areas where tailings had been removed were treated with lime. For a detailed description of the covering procedures and technical specifications, see Lundgren (1990) or Lundgren and Lindahl (1991).

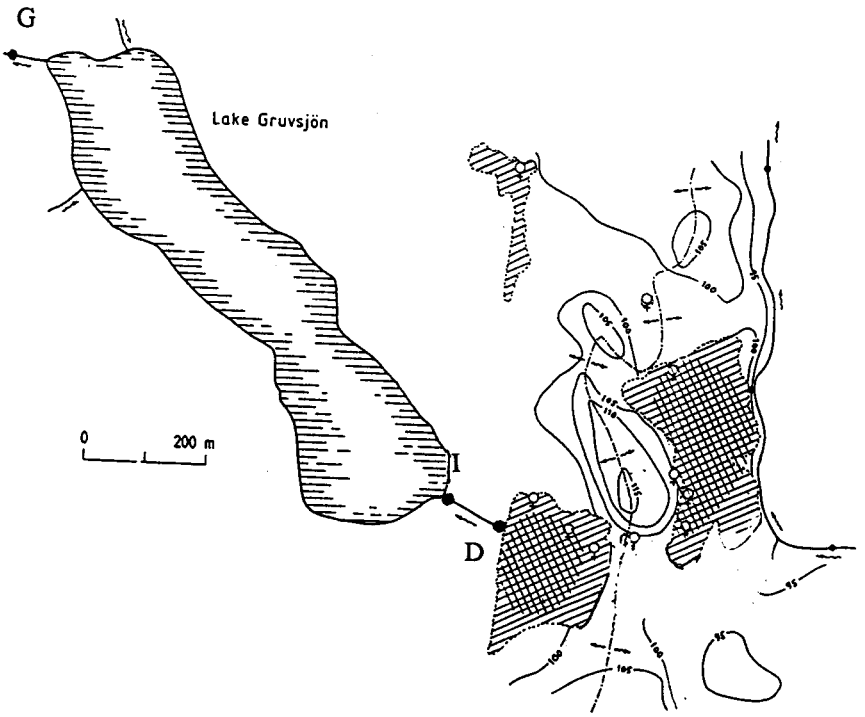

Figure 1. Map over the Bersbo area including sampling locations

Water quality monitoring

A program for water quality monitoring and hydrochemical studies in the area has been conducted since 1983 at up to 15 locations with sampling frequencies from twice daily to monthly. Detailed descriptions of sampling procedures and analytical methods are found in Allard et al. (1987) and Karlsson (1987). Results as well as the effects of hydrochemical and hydrological processes on transformation and redistribution of metals in the drainage system are discussed in Karlsson (1987) and Sandén (1988). The water quality in the drainage from the western part of the tailings is presented in figures 2 and 3 (time series of sulphate and iron) and median values in table 2 (pH, Fe, Cd, Cu, and Zn)

For several reasons, it is difficult to quantify differences in concentration or transport before and after restoration. First, the period after restoration has for some years been unusually dry. These conditions could affect the rate of weathering as well as metal retention in the lake, possibly leading to immobilization of elements. Second, waterflow data are incomplete and missing at locations D and I. Third, data are serially correlated and not normally distributed, indicating that conventional statistical testing is not applicable.

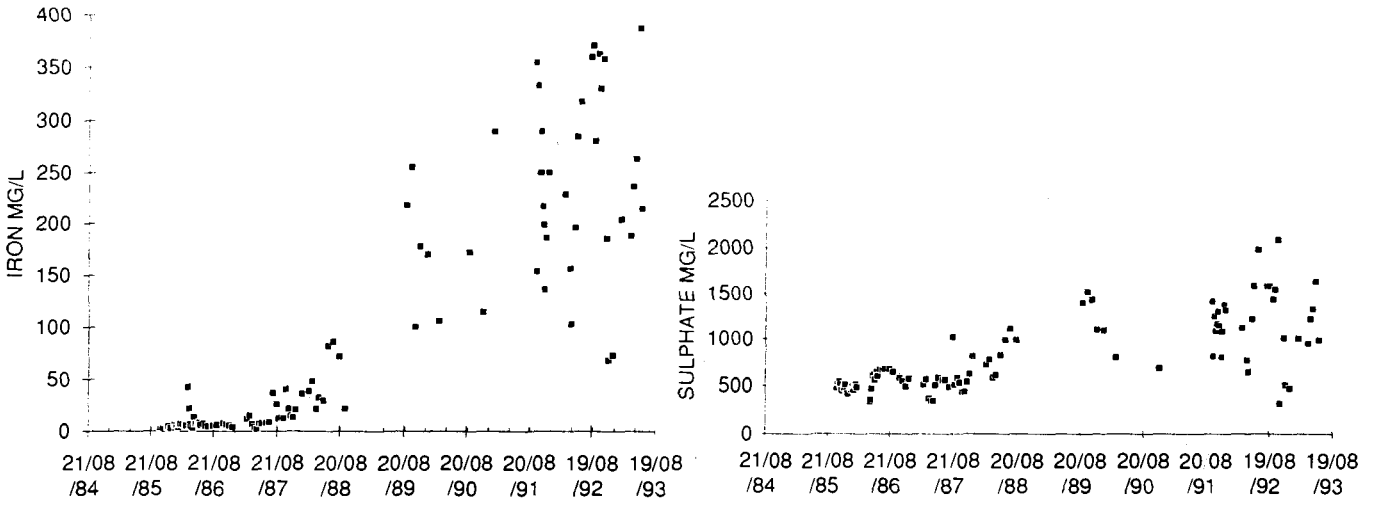

Figure 2. Time series of iron and sulphate at location I

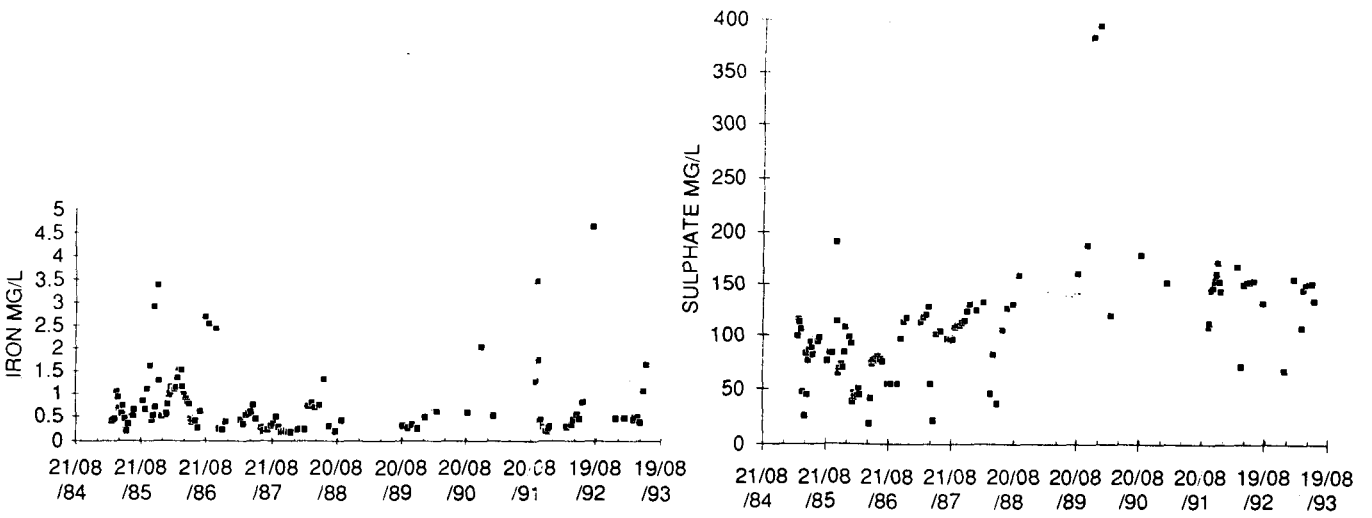

Figure 3. Time series of iron and sulphate at location G

However, the increase in iron concentrations after covering is most probably not only caused by reduced water volumes released from the engineered deposit as an effect of the protective cover (concentrated leachates). It is also observed that increases in concentrations of sulphate, calcium, and sodium at the inlet to the lake (location I) are correlated with increases of these constituents at the outlet (location G). The increases could partly be explained by the reduced precipitation (evaporation effect) 1991-92, but preliminary transport estimates, with simulated waterflow, (Sandén 1993) for these parameters support that the drainage from the mine still is an important source of metals to the lake.

Effects of iron

Principal reactions for the oxidation of pyrite are the following (Stumm and Morgan 1981)

$$FeS_2(s) + 7/2O_2 + H_2O = Fe^{2+} + 2SO_4^{2-} \quad (1)$$

$$Fe^{2+} + 1/4O_2 + H^+ = Fe^{3+} + 1/2H_2O \quad (2)$$

$$Fe^{3+} + 3H_2O = Fe(OH)_3(s) + 3H^+ \quad (3)$$

$$FeS_2(s) + 14Fe^{3+} + 8H_2O = 15Fe^{2+} + 2SO_4^{2-} + 16H^+ \quad (4)$$

Other sulphide minerals could also be oxidized by Fe^{3+} e.g.

$$ZnS(s) + 8Fe^{3+} + 4H_2O = Zn^{2+} + 8Fe^{2+} + SO_4^{2-} + 8H^+ \quad (5)$$

Ferrous forms are dominating in the effluent water from the tailings as well as in the lake (Karlsson et al. unpubl.). In contact with atmospheric oxygen it is oxidized, and precipitates of ferrous hydroxides are formed (especially noticable in the creek beween locations D and I). According to equations 2 and 3, this would lead to a net release of two protons, thereby increasing the acidity in the system. These conditions are in fact observed in the data series from locations D and I. As a result, increased loadings would decrease pH. It is noticed in several studies (for Zn e.g. Tessier et al., (1989)) that generally in natural waters and for many elements the solid/solution ratio decreases with decreasing pH. The same effect of pH is reported for Cd, Cu, Pb, and Zn in the Bersbo area (Karlsson et al. 1987). This general pattern is in some waters complicated by the tendency of humic and fulvic acids (HFA) to form complexes with metals (Pettersson et al. 1993) and adsorb onto fresh ferric hydroxides (Davis 1984). The maximum observed concentration of HFA is, however, only 0.3 mg/l in Lake Gruvsjön.
On the other hand, it is found that sorption-coprecipitation of trace elements on hydrous oxides of iron are important, and it is suggested that they regulate concentrations of trace elements in water and sediments (Singh and Subramanian 1984; Tessier et al. 1985; Johnson 1986).
To estimate the net effects on trace metal mobility of iron oxidation, ferrous iron was allowed to oxidize at different pH relevant for these acidic systems.

Material and methods

Water was sampled from location D on three occasions. The concentrations of Fe, Cd, Cu, and Zn is found in table 1.
The experiments were performed as titrations at constant pH (pH-stat) (4.1, 4.6, 5.0, and 5.4). Preliminary studies of kinetics of the oxidation were performed on one sample by the addition of copper (0, 2.65 and 5.30 mg/l) in the form of $CuSO_4$ (nine titrations). All titrations were performed in stirred vessels open to the atmosphere and at 25 °C.

Prior to titration, pH was adjusted on 100 ml of sample with NaOH (0.1 M). Phase separation was performed by centrifugation at 20 000 g in 15 min in an ultracentrifuge (Beckman J2 - 21M) to remove any precipitates formed during storage. The solution was carefully decanted into new vessels. A subsample of 30 ml was acidified for subsequent analysis of metals.
The additions of base to the 50 ml sample started immidiately after centrifugation. For the samples from 1992, the release of protons were monitored and pH kept constant with Radiometer PHM84. A combination electrode (GK2501C) was used. The rate of reaction was recorded by measuring the additions of NaOH with time. Base addition was stopped well before concentrations of Fe or Cu were limiting factors for the rate of reaction. The sample was then centrifugated and decanted into plastic vessels and acidified for metal analysis.
Titration of the sample collected 931019 was performed with Radiometer VIT 90 and measured by combination electrode GK2402B. This test was stopped after 2760 min for pH 4.1, respectively. Evaporation losses during titration was measured (weighing) and corrected for.
Fe, Cd, Cu, and Zn were analyzed on Perkin-Elmer 1100 with flame techniques. Humic material in the lake Gruvsjön was isolated according to Pettersson et al. (1989).

Calculation method

The weathering of Fe is calculated by comparisons of Zn and Fe in the leachates at location I (table 2), before and after remediation (I_{bZn}, I_{bFe} and I_{aZn}, I_{aFe}, respectively) and from data of the content in the waste material (Zn_s, Fe_s). The weathering rate of iron before remediation (Fe_{wb}) is expressed as $I_{bZn} * Fe_s/Zn_s$, and after remediation $Fe_{wa} = I_{aZn} * Fe_s/Zn_s$. Accumulation of iron in the tailings before and after remediation is calculated from the difference in the measured concentrations in the leachates ($Fe_{wb} - I_{bFe}$) and ($Fe_{wa} - I_{aFe}$). The difference in accumulated amounts is a measure of the total amount of iron available for oxidation by the mechanism described by equation 4.

Results

The concentrations of humic and fulvic acids in sample 920930 from the lake was 0.18 mg/l.
Results for metal concentrations in solutions are presented in table 1, together with total amount added NaOH and elapsed time for the titrations. It is found that 1.8 moles of NaOH corresponds to 1 mole of precipitated iron. This is a resonable number since there are also other species present. Dissolved Al probably exceeds saturation with respect to $Al(OH)_3(s)$

Kinetics for the overall reactions will be described elsewhere. The dependence of $[H^+]$ on the rate is, however, in accordance with findings from Millero (1985), who found that the dependence of rate on the hydrogen concentration was $[H^+]$ raised -2 for pH > 5 and -1 for pH < 4. In the present experiments it was found to be between -1.9 to -1.5.

Results for the metal concentrations (Cd, Cu, and Zn) in table 1 are plotted as quotients of the relative amount of sorbed/coprecipitated metal and the relative amount of precipitated iron as a function of pH (figure 4a). It is found for Cu that the efficiency for metal removal accounted for by the precipitation of iron decreases with pH. For Zn, however, this is not the case. By plotting the relative removal of metals from the solution, (figures 4d) with time in a logaritmic scale, a clear dependence is found, and it seems as if time could be an important parameter in the removal of zinc.

Table 1. Results from the pH-stat tests and metal analysis

		NaOH, ml	time, min	Fe, mg/L	Cd, ug/L	Cu, mg/L	Zn, mg/L
920318	start			538.3	261	4.47	121.4
pH 5.0	end	[1]1.25	286	326.2	246	2.31	99.2
920930	start			380.8	122	1.66	62.01
pH 4.6	end	3.20	1451	212.1	118	1.055	50.20
920930	start			380.8	122	4.308	62.01
pH 4.6	end	3.17	712	169.7	110	3.82	51.51
920930	start			380.8	122	6.956	62.01
pH 4.6	end	2.06	424	182.8	110	6.680	49.19
920930	start			375.7	123	1.67	61.61
pH 5.0	end	3.18	185	195.9	118	0.645	52.156
920930	start			375.7	123	4.318	61.61
pH 5.0	end	3.72	158	144.4	111	2.595	52.02
920930	start			375.7	123	6.966	61.61
pH 5.0	end	3.21	116	179.8	112	4.235	53.93
920930	start			330.3	116	1.190	57.47
pH 5.4	end			152.5	110	0.285	51.71
920930	start			330.3	116	3.838	57.47
pH 5.4	end	3.22	60	144.4	110	1.340	51.51
920930	start			330.3	116	6.486	57.47
pH 5.4	end	3.20	38	148.5	109	5.010	52.72
931018	start			188.87	327	11.135	124.53
pH 4.1	end	0.713	2760	157.56	320	9.95	115.14

[1]Sample volume 25 ml

Discussion

Will the increase in iron concentration affect the scavenging of metals? It is indicated that mobility from sediments are low, especially if the organic content of the sedimenting material is high (Håkansson et al. 1991; Pedersen et al. 1991 and Robertson 1991). (It is suggested that formation of sulphides by sulphate- reducing bacteria or binding of metals to surfaces coated with organic matter could be the explanation). Reactions that occur before sedimentation could thus be important regulators in the scavenging of metals.

The transport of iron to the lake under study was estimated with location I as the reference point (table 1). At this location, the specific effects of the cover will not influence waterflow (with the exception of a small decrease caused by the evaporation of water from an introduced but not vegetated soil layer). Ditches draining the surface layers of the deposit meet the main drainage near location D.
Through a comparison of the drainage areas of locations I and G a tentative estimate of the increase in transport of iron to the lake from the tailings can be done.

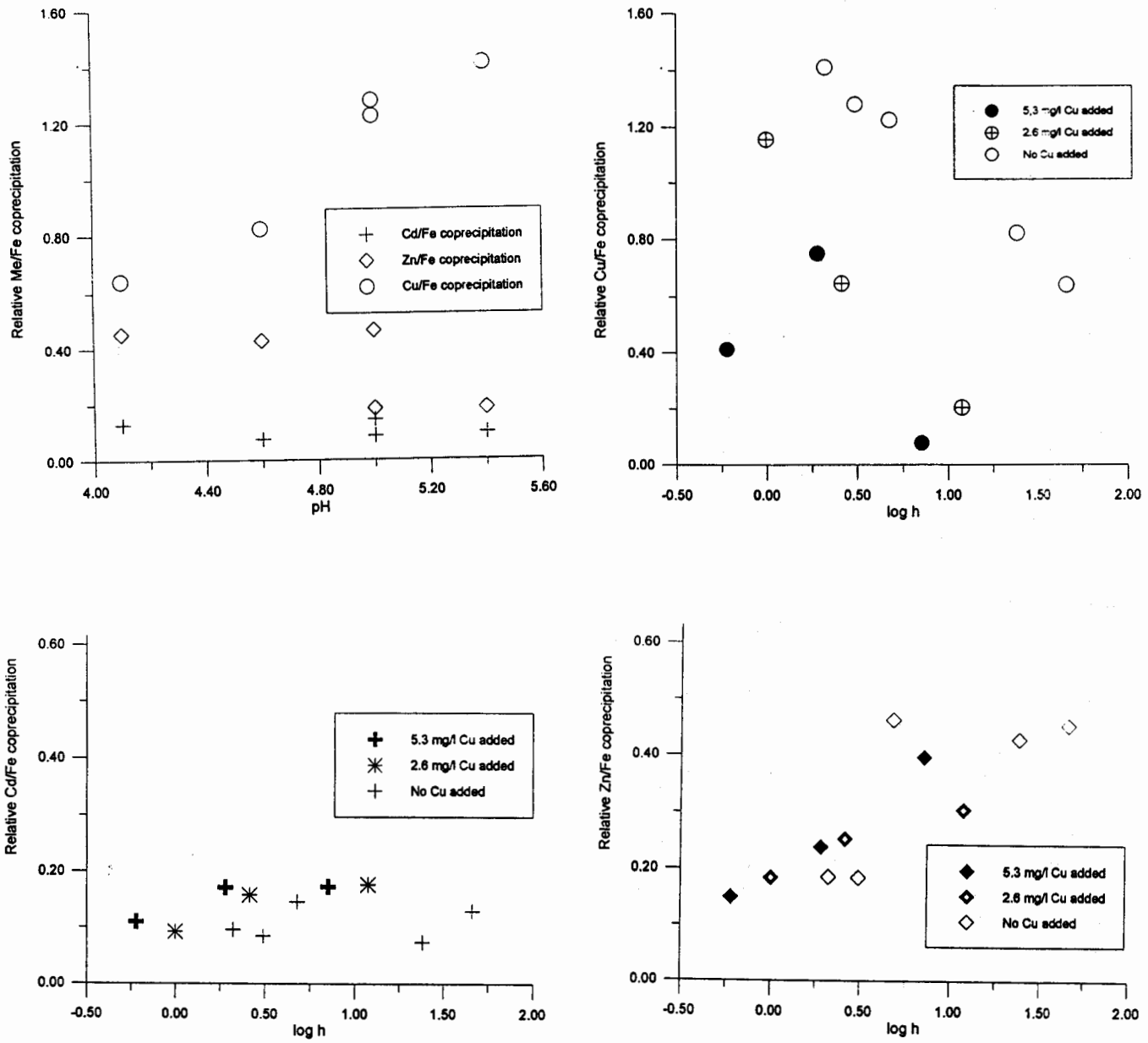

Figure 4. Sorption/coprecipitation of a) the metals Cd, Cu, and Zn as a function of pH $[Me_s/Me_{tot}]/[Fe_s/Fe_{tot}]$.
b) Cu as a function of time (log h) $[Cu_s/Cu_{tot}]/[Fe_s/Fe_{tot}]$,
c) Cd as a function of time (log h) $[Cd_s/Cd_{tot}]/[Fe_s/Fe_{tot}]$,
d) Zn as a function of time (log h) $[Zn_s/Zn_{tot}]/[Fe_s/Fe_{tot}]$

The estimated contribution of water from I based on drainage areas is estimated to be about 8% of the contribution at location G. Median values at location I and G for some constituents are given in table 2.

With a dilution in the lake, the increase in iron concentration in the lake water will be (223.6 - 6.68)*0.08 = 17.34 mg/l. This iron (Fe^{2+} is dominant both in the lake and at location I (Karlsson et al. unpubl.)) during oxidation will theoretically produce a water with a pH of 3.2 (equations 2 and 3). However, this pH is not (yet) obtained in the lake, as can be seen in table 2.

At pH 4.6, coprecipitation of Cd, Cu, and Zn is 0.0237 ug, 0.0036 mg, and 0.07mg, respectively, for each mg of precipitated Fe according to table 1. Additions of Fe in the order of 17 mg/l to the lake will thus cause additional amounts of 0.4 ug/L, 0.06 mg/L, and 1.19 mg/L for Cd, Cu, and Zn, respectively, to coprecipitate. However, according to figure 4a, about 50% less of Cu will coprecipitate with the solid phase as pH is lowered from 4.9 to 4.2. The net effect will thus be a decrease of the adsorption of Cu. For Zn an increase in adsorption is expected when pH is lowered, due to the long time needed for oxidation (figure 4d). The effects of the increased iron concentrations on the adsorption of Cd are not clear.

Table 2. Median values of metal concentrations at locations D,I, and G before (- 1987) and after (1989 -) remedial actions. The subscript b and a refers to the situation before and after remedial actions were taken. (n = 10 for most parameters at D_b, n for the other locations see figures 2 and 3).

	D_b	D_a	I_b	I_a	G_b	G_a
pH	4.90	4.57	3.95	3.73	4.93	4.29
Fe (mg/L)	17.71	403	6.68	223.6	0.55	0.44
Cd (ug/L)	204	161	198	145	16	9.4
Cu (mg/L)	8.79	3.50	10.62	4.09	0.533	0.238
Zn (mg/L)	46.5	74.8	81.6	59.4	7.56	5.76

The new hydrochemical conditions in the lake will increase the adsorption/coprecipitation of metals, on a solid phase, in the order Zn > Cd > Cu.

It is possible that oxidation of pyrite still proceeds despite the lowered oxygen content in the tailings (equation 4) This reaction means that weathering may continue with Fe(III) as a substrate for oxidation. The purpose of the calculations below are to give a rough estimate of the longevity of such a mechanism.
Assuming that all sulphides weather at the same rates and that no secondary minerals of Zn are formed, the quotient Fe/Zn in the solid phase could be taken as a measure of the weathering of iron. The covered solid phase have been analyzed by a prospecting company (Vieille Montagne): Fe 10.7%, Zn 0.7%, Cu 0.29%. The calculation method gives the amount of accumulated iron (556 mg/L). According to equation 5 it is required 406 mg/L of iron to oxidize the present amount of released Zn (59.4 mg/L). Available iron will be 1/3 of the accumulated, since that is the part dumped in the shafts and thus exposed to water. It is assumed that a more or less constant weathering and accumulation of iron has been going on for 150 years (Håkansson et al. 1991), indicating that a time scale for the continued weathering could be constructed. Weathering with this mechanism could thus continue for (556/406*1/3)*150 = 70 years.
This estimation is valid if no oxygen is present to regenerate the storage of Fe^{3+}.

Concluding remarks

The estimated maximum time for a continued weathering of pyrite with Fe^{3+} as a substrate for oxidation in the Bersbo area is 70 y.
Adsorption studies indicate that a lowered pH caused by Fe oxidation will decrease the retention of Cu in the receiving lake and increase the retention of Zn.
In relatively acid systems with a fast hydrological response, the net effect of high Fe concentration is likely to be an increased mobility of several elements.

References

Allard, B., S. Bergström, M. Brandt, S. Karlsson, U. Lohm and P. Sandén. 1987. Environmental impacts of an old mine tailings deposit - Hydrochemical and hydrological background. Nordic Hydrol. 18:279-290.

Davis, J. A. 1984. Complexation of trace metals by adsorbed natural organic matter. Geochim. Cosmochim. Acta 48:679-691.

Håkansson, K., S. Karlsson, L. Lundman and B. Allard. 1991. Redistribution of metals from a contaminated drainage system - Accumulation in sediments estimated from surface water quality and sediment analysis (submitted).

Johnson, C. A. 1986. The regulation of trace element concentration in river and estuarine waters contaminated with acid mine drainage: The adsorption of Cu and Zn on amorphous Fe oxyhydroxides. Geochim. Cosmochim. Acta 50:2433-2438.

Karlsson, S. 1987. Influence of hydrochemical parameters on the mobility and redistribution of metals from a mine waste deposit. (Diss.) Linköping Studies in Arts and Science 10. Linköping University.

Karlsson, S., P. Sandén and B. Allard. 1987. Environmental impacts of an old mine tailings deposit - Metal adsorption by particulate matter. Nordic Hydrol. 18:313-324.

Kelly, B. C. and O. H. Tuovinen. 1988. Microbiological oxidations of minerals in mine tailings. In Salomons, W. and U. Förstner, Chemistry and Biology of Solid Waste, Dredged Materials and Mine Tailings. pp. 33-53. Springer.

Länsstyrelsen, Östergötlands län, Planeringsavdelningen Beslut 1986-12-19. *County Board, Östergötland (in Swedish).*

Lundgren, T. 1990. The first full scale project in Sweden to abate acid mine drainage from old mining activities. In Proceedings of the International Conference of GAC-MAC. Vancouver.

Lundgren, T. and L-Å. Lindahl. 1991. The efficiency of covering the sulphidic waste rock in Bersbo, Sweden. In Proceedings of the Second International Conference on the Abatement of Acidic Drainage. Montreal.

Millero, F.J. 1985. The effect of ionic interactions on the oxidation of metals in natural waters. Geochim. Cosmochim. Acta 49:547-553.

Pedersen, T. F., B. Mueller, J. J. McNee and C. A. Pelletier. 1991. Diagenetic reactivity of mine tailings in mesotrophic and oligotrophic lakes in Manitoba and British Columbia. In Proceedings of the Second International Conference on the Abatement of Acidic Drainage. Montreal.

Pettersson, C., I. Arsenie, J. Ephraim, H. Borén and B. Allard. 1989. Properties of fulvic acids from deep groundwaters. Sci. Tot. Environ. 81/82:287-296.

Pettersson, C., K. Håkansson, S. Karlsson and B. Allard. 1993. Metal speciation in a humic surface water system polluted by acidic leachates from a mine deposit in Sweden. Wat. Res. 27:863-871.

Robertson, J. D. 1991. Subaqueous disposal of reactive mine waste: An overview of the practice with case studies. In Proceedings of the Second International Conference on the Abatement of Acidic Drainage. Montreal.

Sandén, P. 1988. Dynamics of metal concentrations and mass transport in an old mining area. (Diss.) Linköping Studies in Arts and Science 22. Linköping University.

Sandén, P. 1993. Övervakning av ytvattenkemi i Bersbo. Rapport från verksamheten 1992/1993. SMHI *Monitoring of surface water chemistry. Report. Swedish Meteorological and Hydrological Institute (in Swedish).*

Singh, S. K. and V. Subramanian. 1984. Hydrous Fe and Mn oxides - Scavengers of heavy metals in the aquatic environment. CRC, Critic. Rev. Environ. Control 14:33-90.

Stumm, W. and G. F. Lee. 1961. Oxygenation of ferrous iron. Industrial and Engineering Chemistry 53:143-146.

Stumm, W. and J. J. Morgan. 1991. Aquatic Chemistry. Wiley, New York, 2nd ed.

Tegengren, F. R. 1924. Sveriges ädlare malmer och bergverk. SGU. Ser Ca 7:313 329. Norstedt, Stockholm. *Swedish Geological Survey (in Swedish).*

Tessier, A., F. Rapin and R. Carignan. 1985. Trace metals in oxic lake sediments: possible adsorption onto iron oxyhydroxides. Geochim. Cosmochom. Acta 49: 183 - 194.

Tessier, A., R. Carignan, B. Dubreuil and F. Rapin. 1989. Partitioning of zinc between the water column and the oxic sediments in lakes. Geochim. Cosmochim. Acta 53: 1511-1522.

HIGH-FREQUENCY GEOCHEMICAL MONITORING OF TOE SEEPAGE FROM MINE-ROCK DUMPS, BHP MINERALS' ISLAND COPPER MINE, BRITISH COLUMBIA[1]

Kevin A. Morin[2], Ian A. Horne[3], and Derek Riehm[4]

Abstract: Recent studies of mine-rock dumps have shown that water can pass through a dump in hours to days. As this water initially flows downward and is focused into preferential channels within the dump, it collects dissolved metals from the rock. The water then either flows as surface seepage from the toe or enters the groundwater system beneath the dump. In the case of toe seepage, the water is often collected in ditches and diverted out of the area. Because of the variability in flow and chemistry expected in toe seepage, questions can arise as to the appropriate monitoring frequency.

This paper addresses monitoring frequency based on actual data from the Island Copper Mine in British Columbia. Data on flow and chemistry were repeatedly collected as frequently as every 15 minutes and every four hours, respectively, for six months in 1991-92 and again in 1992-93. The chemical parameters collected at 10 monitoring stations included pH, conductivity, alkalinity, acidity, sulfate, copper, zinc, cadmium, calcium, magnesium, and aluminum.

The combined database for this ongoing study currently contains tens of thousands of values and continues to grow. This paper presents some of the findings, correlations, and relationships noted to date. For example, distributions of the chemical data in 1991-92 and 1992-93 typically resemble lognormal or normal statistical distributions. The statistical analyses show that the results of hypothetical hourly sampling, for example, can be estimated from the actual results of weekly sampling. Based on this, a parallel is drawn with hydrology in which there is an annual peak chemical concentration of a particular duration. Also, relationships of chemical concentrations to both flow and time show the gradual depletion of reaction products that accumulated during summer months, as well as the later flushing of short-term accumulations that accrue between storm events. However, correlations of chemical parameters to flow alone are poor, reflecting the significant influence of other factors on chemistry. These factors are discussed further in other papers at this conference.

Additional Key Words: waste rock, mine rock, mine seepage, water chemistry, water quality, geochemistry.

Introduction and Objectives

Mine-rock dumps are recognized as physically and geochemically complex systems (e.g., Morin et al. 1991, Morin and Hutt 1994). In a general sense, precipitation and/or snowmelt initiates infiltration into a dump, the water is then focused into preferential channels as it collects metals and nonmetals from rock-particle surfaces, and the

---

[1]Paper presented at the International Land Reclamation and Mine Drainage Conference and the Third International Conference on the Abatement of Acidic Drainage, Pittsburgh, PA, USA, April 24-29, 1994.

[2]Kevin A Morin, Morwijk Enterprises Ltd, 47-115 Kamehameha Highway, Kaneohe, Hawaii, USA 96744 (address until 2/28/94).

[3]Ian A. Horne, Island Copper Mine, BHP Minerals Canada, P.O. Box 370, Port Hardy, Canada V0N 2P0

[4]Derek Riehm, Rescan Environmental Services, 6th Floor, 1111 West Hastings Street, Vancouver, British Columbia, Canada V6E 2J3

water with its chemical load exits into the underlying groundwater system or basal toe ditches. However, the specific details of this scenario of physical and chemical hydrogeology are difficult to monitor and define. As a result, there are currently two basic approaches for characterizing and predicting the effects of mine-rock dumps. The first is through internal studies of some dump processes that are thought to be most important (e.g., Gélinas et al. 1992, Morin et al. 1994a), which requires intensive long-term programs over several years. The second is seepage monitoring such as in basal toe ditches, which is more suited to short-term studies. The first approach describes a dump through internal monitoring of its behavior, whereas the second empirically describes a dump through monitoring of its cumulative effects at the base. This paper describes a study of the second type.

In the case of toe seepage, water leaving a dump is often collected in toe ditches and diverted from the area. Monitoring of toe ditches for chemistry and flow thus provides a detailed assessment of the cumulative effect of the dump and perhaps a suggestion of dominant processes operating within it. A major issue in this type of monitoring is the frequency at which the monitoring should be performed in order to obtain the necessary data for characterization and prediction. Frequency of monitoring has been addressed from theoretical and statistical viewpoints (e.g., Robertson 1990), but actual high-frequency data to test such theories are rare.

As part of closure studies at BHP Minerals' Island Copper Mine in British Columbia, the short-term peaks in flow and chemistry from the mine's dumps were identified as major issues for closure planning. Consequently, a high-frequency monitoring program was designed and initiated during the wet season from October 1991 to March 1992 (Rescan, 1992), with flow and chemistry measured as frequently as every 15 minutes and every four hours, respectively. This program was repeated from September 1992 to June 1993, and is again underway in 1993-94.

The first objective of this paper is to describe the results of the monitoring program. Due to the large number of analyses and values, results can only be presented through statistical summary parameters and distributions. As a second objective, the statistical distributions are used in predictive mode to estimate concentrations between and beyond monitoring events. This reflects the "hydrology-like" behavior of chemical concentrations at Island Copper, which means that there is an annual peak concentration, for example, of one hour duration. Another objective is to examine ditch flow over a selected period of time and to correlate flow with chemistry. All of these objectives provide a glimpse of the database and the interpretations that are leading to a closure plan in 1994.

Minesite Layout and Monitoring Program

Island Copper Mine is located on the northern end of Vancouver Island in British Columbia (fig. 1). This minesite contains several dumps from which toe drainage is carried by ditches to the Water Management Pond (fig. 2). For example, toe drainage from the Old North Dump is initially intercepted at Monitoring Station NDD, then carried along the upper rim of the pit past Station TED, and joins flow passing by Station EDT. This combined flow is carried past Station WME to the Water Management Pond.

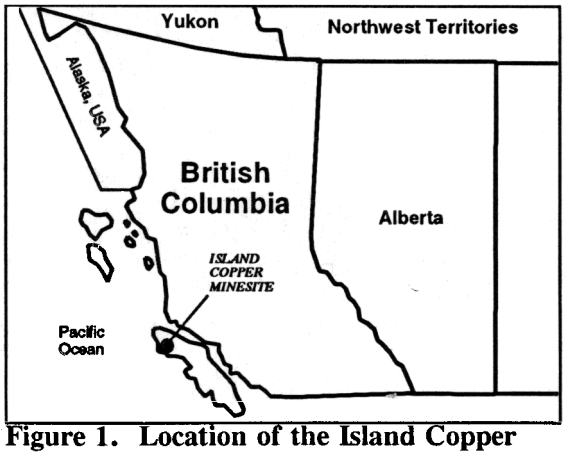

Figure 1. Location of the Island Copper Minesite in British Columbia.

The monitoring study involves eight stations: EDD, EDT, EMO, NDD, NWD, PDW, TED, and WME. Two new stations, TCR and TMP, have recently been added, but are not intensively monitored. During the 1991-92 hydrology study, ditch flows and water samples were obtained as frequently as every 15 minutes and every four hours, respectively, with automated equipment (Rescan 1992). Chemical analyses usually included pH, conductivity, alkalinity, acidity, sulfate, copper, zinc, cadmium, calcium, magnesium, and aluminum. However, sampling

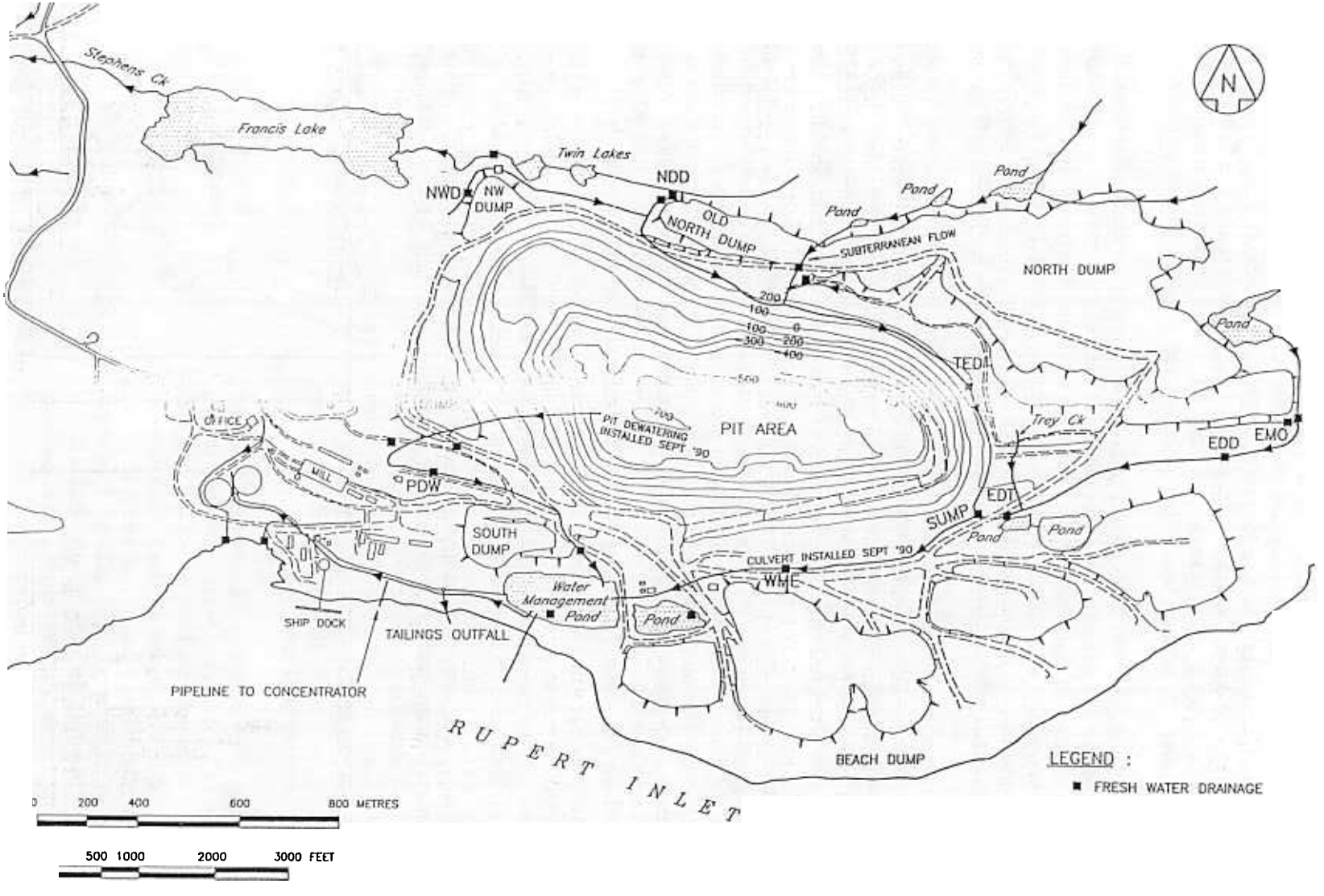

FIGURE 2. Map of Island Copper Minesite and Locations of Monitoring Stations

limitations, laboratory overload, and equipment breakdowns precluded extended periods of highest-frequency monitoring at most stations. Several stations were only monitored once a day through grab samples for chemistry and staff-gauge observations for flow.

As the final monitoring point before water treatment, WME is of greatest interest for closure studies and has the most extended period of highest-frequency monitoring. Consequently, this paper focuses on WME and only discusses other stations in a cursory manner.

Results for Water Chemistry

Statistical Distributions

Each year of intensive monitoring at Island Copper has generated thousands of values at each monitoring station for the chemical parameters mentioned above. The results can be presented graphically (e.g., fig. 9), but a more informative and concise presentation is through statistical summary parameters such as means and standard deviations.

The concept behind standard deviations is valid for statistically normal distributions. Therefore, we visually examined the frequency distributions of all parameters at all stations in all years. Normal and lognormal distributions (Morin et al., 1993) were often generally seen in the distributions (figs. 3 and 4), although bimodal distributions (fig. 5) and other types were also noted (fig. 6). The values of the means and standard deviations based on lognormal distributions were found to generally repeat yearly (table 1), suggesting that the internal processes within the dumps remain relatively consistent over a period of at least a few years. This annual repetition has also been noted at other sites (Morin et al. 1994a and 1994b).

Predictions Based On Statistical Results

The observations that valid means and standard deviations could be calculated for some parameters and that these values generally repeat on a yearly basis led to the realization that (1) concentrations between the frequent monitoring events could be estimated and (2) future concentrations should reflect the same statistical distributions at least in the short term unless independent variables such as pH change significantly (Morin et al. 1994b). For example, copper as μg/L at WME has a two-year-average mean and standard deviation as logarithmic values of 1.76 and 0.435, respectively (table 1). Based on the application of normal probability levels to a yearly period, the peak annual concentration of one-hour duration is +3.85 standard deviations above the mean (Morin et al. 1994a). For

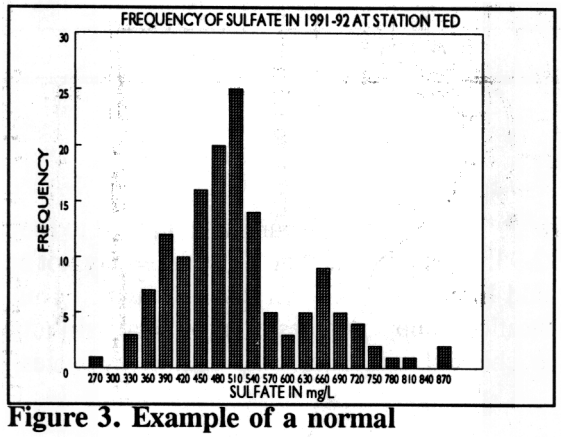

Figure 3. Example of a normal distribution.

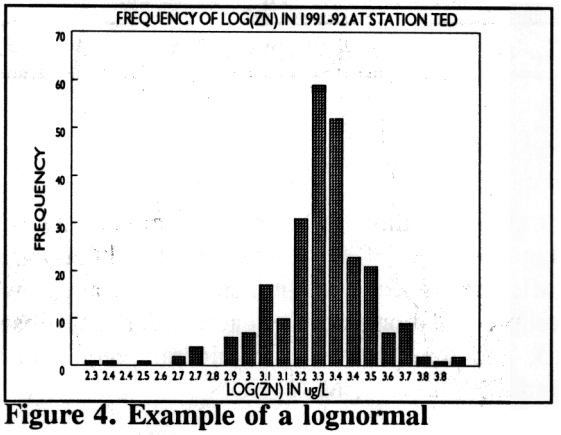

Figure 4. Example of a lognormal distribution.

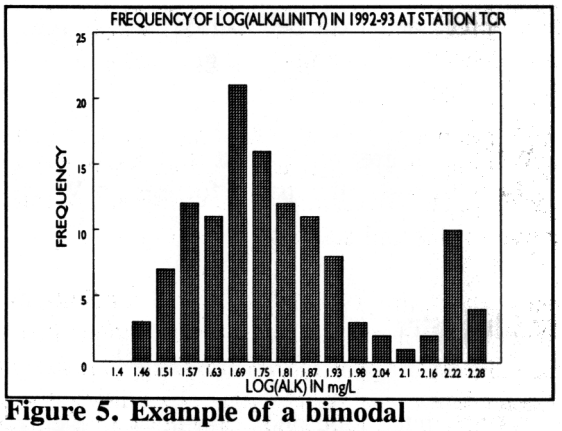

Figure 5. Example of a bimodal lognormal distribution.

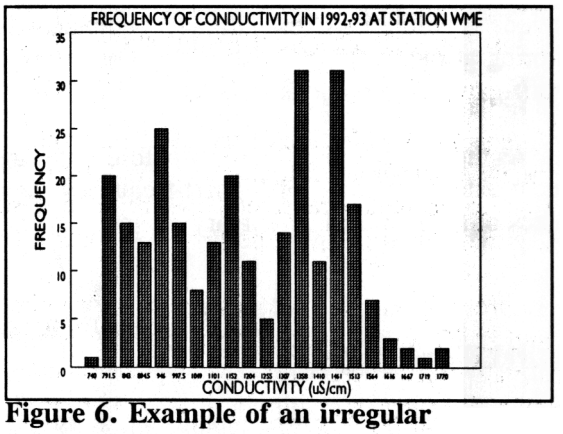

Figure 6. Example of an irregular distribution (step-like?).

Table 1. Logarithmic Means and Standard Deviations for Station WME.

Parameter	Log_{10} Mean		Log_{10} std dev	
	1991-92	1992-93	1991-92	1992-93
pH . . . . . pH units (n=401 & 265)	0.826	0.836	0.055	0.043
Conductivity . uS/cm (n=365 & 265)	3.058	3.056	0.075	0.098
Alkalinity mg $CaCO_3$/L (n=245 & 260)	1.795	1.575	0.666	0.314
Acidity . . mg $CaCO_3$/L (n=34 & 13)	1.438	1.513	0.303	0.239
Cu . . . . . μg/L (n=578 & 265)	1.906	1.609	0.445	0.424
Zn . . . . . μg/L (n=625 & 265)	3.373	3.432	0.305	0.231
Cd . . . . . μg/L (n=581 & 265)	1.217	1.268	0.234	0.228
Sulfate . . . . . mg/L (n=215 & 256)	2.875	2.889	0.089	0.067
Ca . . . . . mg/L (n=338 & 265)	2.334	2.413	0.057	0.050
Mg . . . . . mg/L (n=336 & 265)	1.427	1.553	0.146	0.046
Al . . . . . mg/L (n=313 & 265)	-0.676	-0.517	0.339	0.342

copper at WME, this one-hour peak would be 2720 μg/L ($10^{1.76 + 3.85*0.435}$), which can be compared to the measured four-hour peak of 580 μg/L in 1991-92 and 650 μg/L in 1992-93. It is possible that 2720 μg/L may not be possible at WME due to secondary-mineral precipitation, which would limit the maximum concentration. This effect of mineral precipitation also likely accounts for the observed truncation of upper values in some data distributions (e.g., fig. 5), and this potential for mineral precipitation will be checked at a later time against estimates from the geochemical program, MINTEQ.

Implications for Less-Frequent Monitoring

One primary objective of the 1991-92 monitoring at high frequency was to obtain sufficient information to determine the appropriate frequency for long-term monitoring. As explained above, the most important goals for monitoring are to obtain representative means and standard deviations. Thus, the basic question becomes "How frequently must monitoring be performed to obtain representative means and standard deviations?"

In order to answer the question on appropriate frequency, the entire 1991-92 databases for Stations WME, NDD, and EMO were used to calculate means and standard deviations for copper and zinc (for convenience called the "real values"). These values were then compared to those calculated under the assumptions that sampling had only occurred during the midpoint of each day, each week, each month, and each quarter. Additionally, the real values were compared with values obtained from a random-number generator that selected a random sample from each daily period for calculations of means and standard deviations, from each weekly period, etc. The random-number sampling was performed 25 times for each time-interval period (Morin et al. 1993) to determine statistically how accurately the various frequencies would have provided the "real" mean and standard deviation. For example, the mean values for copper in the 25 random runs using one sample from each quarter displayed a wide range from 20 to 600 μg/L, whereas the 25 runs with one sample from each day showed little variation and were within 25% of the "real" mean of the entire database (fig. 7). Similarly, the standard deviations for copper from the 25 runs converged to the "real" value as sampling frequency increased (fig. 8). Based on these results, sampling frequency at WME during 1992-93 was reduced from every four hours to daily. The frequency will be reduced further after 1993-94 data are similarly evaluated.

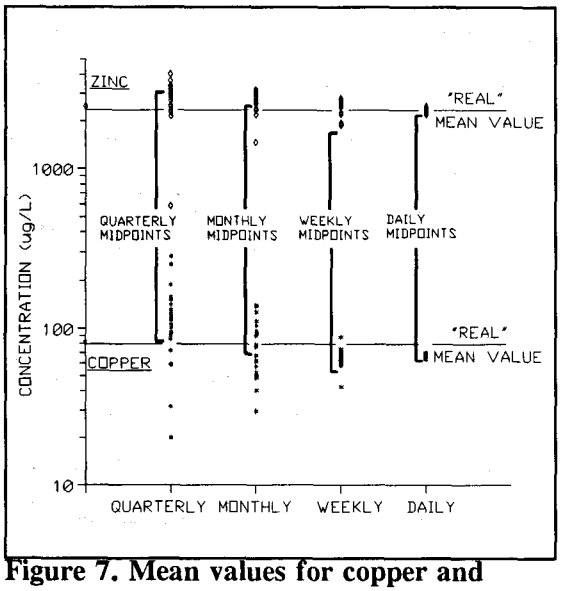

Figure 7. Mean values for copper and zinc at WME, including 25 random runs at each sampling frequency.

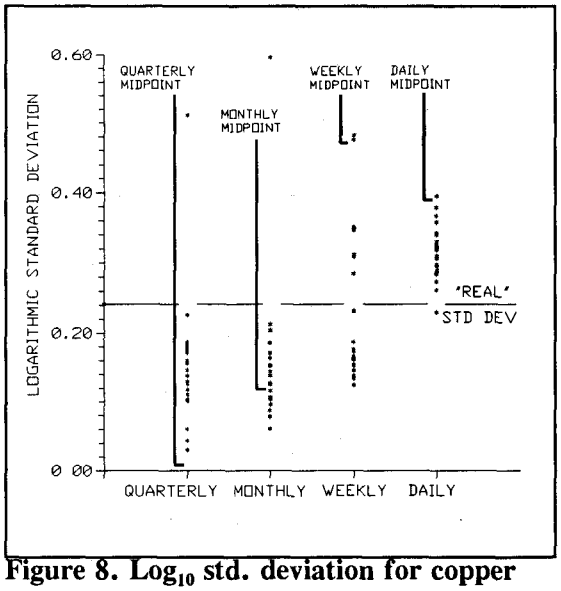

Figure 8. Log_{10} std. deviation for copper at WME, including 25 random runs at each sampling frequency.

Ditch Flow and Its Effect on Chemistry

Flows in the ditches at the various monitoring stations were measured with pressure transducers located at weirs and with staff gauges. Measurements with the transducers at frequencies up to every 15 minutes were

compared to flows occasionally calculated from the staff gauges to ensure accuracy and to allow recalibration of the transducers. Electronic drift in the transducers sometimes required significant corrections, and many of the transducer data are being carefully evaluated. Meanwhile, there is confidence in most WME readings, and these readings are available for a nearly continuous period extending from mid-December 1991.

The general trends in aqueous copper and zinc from October 1991 to March 1992 reveal initially sharp increases in concentrations, peaking by November, then decreasing over the next four months (fig. 9; alkaline samples caused by the addition of lime at WME have been filtered out). Copper particularly decreased in concentration and then generally stabilized by late December, which would be consistent with the depletion of reaction products that accumulated during summer months. These trends in chemistry before mid-December cannot be closely correlated with trends in flow because high-frequency flow measurements are not available until mid-December. The more frequent data after this date then account for the appearance of frequent peaks in flow in fig. 9 (enlarged in fig. 10).

WME provides an opportunity to inspect the high-frequency temporal trends in copper (fig. 11) and zinc (fig. 12) with flow during the period from 10 December 1991 to 10 February 1992. For example, copper concentrations show "background" values of 20 to 80 μg/L, but reach peak values of several hundred μg/L before late December and peaks usually below 200 μg/L after late December. Since the source of most copper and zinc to late December is thought to be the depletions of summer accumulations, storm events could cause a dilution in concentration as the removal progresses. This effect can be seen in the first two storm events in figs. 11 and 12. After the accumulated products are removed and the rock is only generating new products, storm events could cause an increase in concentration as the water removes products accumulated over the short time intervals between the storms. Such increases can be seen in storm events on figs. 11 and 12 after the first two events.

Despite the aforementioned relationships between flow and chemistry, scatterplots of flow against copper (fig. 13) and zinc (fig. 14) do not reveal good correlations. This lack of correlation holds for both the entire 1991-92 dataset (figs. 13 and 14) and the data between 10 December 1991 and 10 February 1992 (not shown). Initially, this may be surprising in view of the previous temporal relationships; however, there is more than the one variable of flow that determines chemistry. Other variables are discussed by Morin and Hutt (1994) and Morin et al. (1994b).

Conclusion

This paper has presented the results of high-frequency measurements of dump-drainage flow and aqueous chemistry at the Island Copper Mine in British Columbia. Flow and chemistry were measured as frequently as every 15 minutes and every four hours, respectively. The chemical results allow several useful assessments including that of (1) statistical distributions and summary parameters, (2) the estimation of concentrations between and beyond the monitoring events, and (3) the decreased frequency of monitoring that would still provide representative values of the required statistical parameters. The flow results showed the influence of storm events which cause short-term peaks in flow. These peak flows were accompanied by either a decrease or an increase in aqueous concentrations of copper and zinc. The decreases in concentration were attributed to the depletion of accumulated reaction products during summer months and the later increases were attributed to flushing of short-term accumulations between storm events. These findings are applicable to other minesites as discussed in Morin et al (1994a and 1994b).

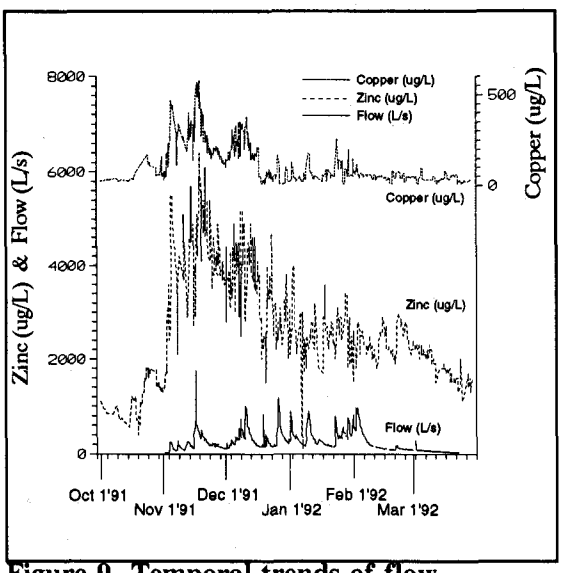

Figure 9. Temporal trends of flow, copper, and zinc at WME from 01 October 1991 to 31 March 1992.

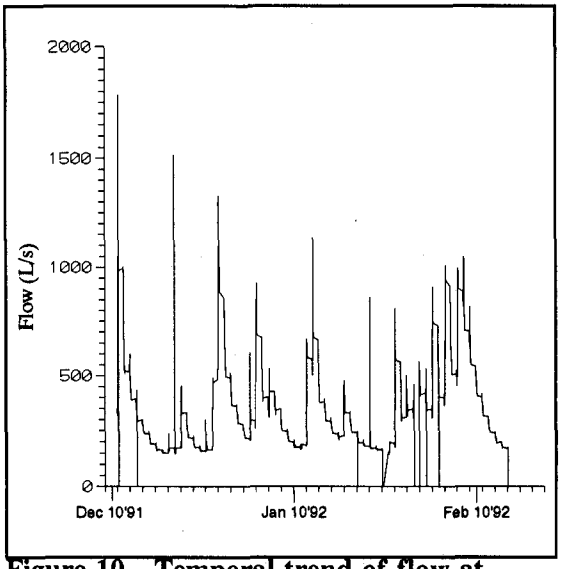

Figure 10. Temporal trend of flow at WME from 10 December 1991 to 10 February 1992.

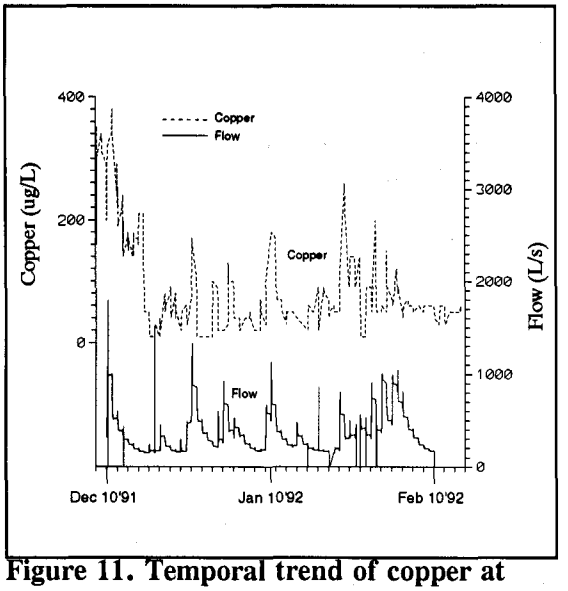

Figure 11. Temporal trend of copper at WME From 10 December 1991 to 10 February 1992.

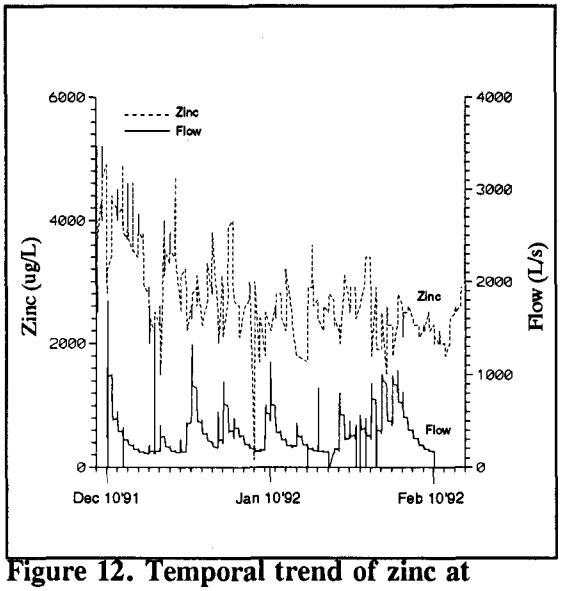

Figure 12. Temporal trend of zinc at WME From 10 December 1991 to 10 February 1992.

Acknowledgements

Obviously a study of this magnitude required contributions from many people. We would particularly like to thank Maged Said and the staff of Island Copper's laboratory who were deluged with samples and data, staff at Rescan including Clem Pelletier, David Flather, and Diane Howe who designed and initiated the hydrology study, and Nora Hutt of Normar Enterprises who assisted in data management and graphics. We also thank the three anonymous reviewers who helped to improve the quality and clarity of this paper and the coordinators of this conference who carefully managed manuscript submission and printing.

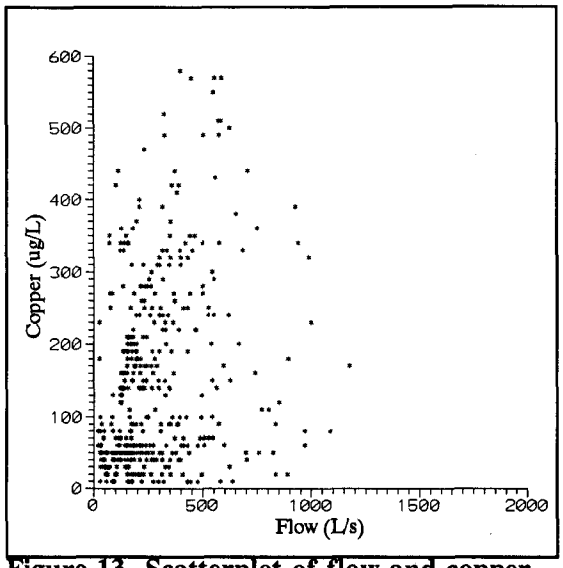

Figure 13. Scatterplot of flow and copper at WME for the 1991-1992 dataset.

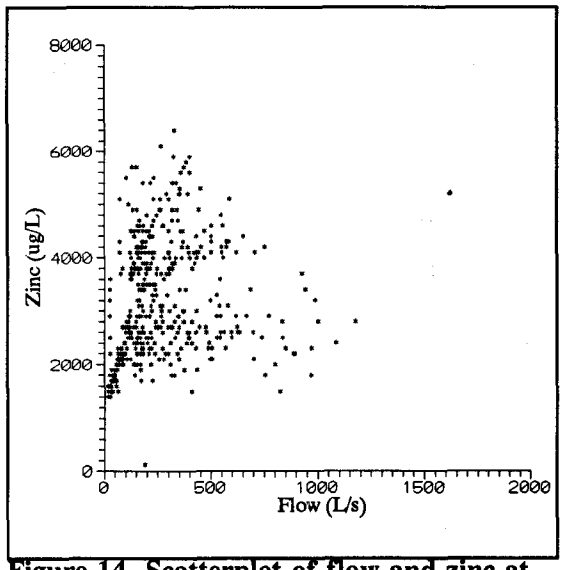

Figure 14. Scatterplot of flow and zinc at WME for the 1991-1992 dataset.

References

Gélinas, P.J., R. Lefebvre, and M. Choquette. 1992. Monitoring of acid mine drainage in a waste rock dump [Mine Doyon]. p.747-756. In Proceedings of the Second International Conference on Environmental Issues and Management of Waste in Energy and Mineral Production. (Calgary, Alberta).

Morin, K.A., and N.M. Hutt. 1994. An empirical technique for predicting the chemistry of water seeping from mine-rock piles. In Third International Conference on the Abatement of Acidic Drainage (these proceedings).

Morin, K.A., C.E. Jones, and R.P. van Dyk. 1994a. Internal hydrogeologic monitoring of an acidic waste-rock dump at Westmin Resources' Myra Falls Operations, British Columbia. In Third International Conference on the Abatement of Acidic Drainage (these proceedings).

Morin, K.A., N.M. Hutt, and R. McArthur. 1994b. Prediction of minewater chemistry from available monitoring data, Noranda Minerals' Bell Mine, British Columbia. In Third International Conference on the Abatement of Acidic Drainage (these proceedings).

Morin, K.A., I.A. Horne, and D. Flather. 1993. The appropriate geochemical monitoring of toe seepage from a mine-rock dump. p.149-129. In Proceedings of the Seventeenth Annual British Columbia Mine Reclamation Symposium. (Port Hardy, British Columbia, May 4-7, 1993).

Morin,K.A., E. Gerencher, C.E. Jones, and D.E. Konasewich. 1991. Critical literature review of acid drainage from waste rock. Report for the Mine Environment Neutral Drainage (MEND) Program.

Rescan Consultants Inc. 1992. Hydrological and metal loadings study, Phase 1 Report. Mine Report for Island Copper Mine, BHP Minerals Canada Limited.

Robertson, E. 1990. Monitoring acid mine drainage. Report for the British Columbia AMD Task Force and the Federal MEND Program.

INTERNAL HYDROGEOLOGIC MONITORING OF AN ACIDIC WASTE-ROCK DUMP AT WESTMIN RESOURCES' MYRA FALLS OPERATIONS, BRITISH COLUMBIA[1]

Kevin A. Morin[2], Carol E. Jones[3], and Rudy P. van Dyk[4]

Abstract: Planning for closure at Westmin's Myra Falls Operations (British Columbia) began indirectly in the early 1980's with hydrogeologic and water-chemistry studies downstream of the primary waste-rock dump and mine workings. The hydrogeologic investigation was expanded significantly in 1988 and again in 1990, culminating in a Decommissioning Plan submitted in 1992. The Plan and its supporting technical documentation defined strategies to minimize acidic drainage and metal leaching in waste rock, underground workings, and pit walls. A primary target for decommissioning was Waste-Rock Dump #1.

Dump #1 contains approximately 10 million metric tonnes (mt) of coarse-to-fine pyritic waste rock. This dump was built against a valley wall and is approximately 800 m long parallel to the wall by approximately 300 m wide at the base. It reaches a maximum measured height of 42 meters. Sixty-five boreholes have been drilled into the dump since 1988. Over 230 rock samples have been submitted for acid-base accounting, providing stratigraphic data on sulfide and neutralization potential.

Five boreholes contain multilevel gas ports for a total of 25 ports to monitor internal levels of oxygen and carbon dioxide. One year of monitoring data showed that oxygen could vary from essentially zero to full atmospheric level at any particular depth and lateral location within the dump. Overall, sulfide-mineral oxidation within the dump was not oxygen limited.

Four boreholes contain thermistor strings for a total of 20 thermistors. These thermistors have transmitted temperature data to dataloggers every 12 h for the last three years. The temperature data show a maximum value of 51.6°C at intermediate depths. During precipitation and subsequent infiltration events, the upper and intermediate temperatures are cooled by the infiltration, but the deeper temperatures are raised by the infiltration because it has warmed to a maximum of 52°C.

A total of fifty-one 0.75-inch-diameter and five 2-inch-diameter piezometers have been installed within and below the dump. Four of the 2-inch wells contain pressure transducers which have transmitted groundwater levels to dataloggers every 12 h for the past three years. Fluctuations of up to 4 m have been recorded during intense storm events of approximately 10 cm of rain in 12 h.

Infiltration events from individual storms were tracked downward through the dump by their effects on internal temperature and basal water-table levels. This tracking shows that infiltration can pass through up to 45 m of waste rock within 12 h, based on initial temperature responses, to 36 h, based on midpoints of water-table responses.

Additional Key Words: waste rock, hydrogeology, groundwater, subsurface temperature, poregas composition

---

[1]Paper presented at the International Land Reclamation and Mine Drainage Conference and the Third International Conference on the Abatement of Acidic Drainage, Pittsburgh, PA, USA, April 24-29, 1994.

[2]Kevin A Morin, Morwijk Enterprises Ltd, 47-115 Kamehameha Highway, Kaneohe, Hawaii, USA 96744 (address until 2/28/94).

[3]Carol E. Jones, CE Jones & Associates Ltd., Suite 204, 26 Bastion Square, Victoria, British Columbia, Canada V8W 1H9

[4]Rudy P. van Dyk, Westmin Resources Limited, Myra Falls Operations, P.O. Box 8000, Campbell River, British Columbia, Canada V9W 5E2

Introduction and Objectives

Westmin Resources' Myra Falls Operations are located in Strathcona Provincial Park, near the geographic center of Vancouver Island in British Columbia (fig. 1). The minesite contains several base-metal ore zones, which are mined and processed on-site primarily for zinc and lead with minor amounts of other metals including gold. Mining is currently conducted from underground workings, but initial mining was in an open pit excavated into a valley wall.

Myra Falls Operations recently celebrated their 25th anniversary of mining, and some estimates have extended the mine life to another 25 yr. Nevertheless, closure and decommissioning are inevitable, and thus several years ago Westmin Resources initiated detailed monitoring of several mine components. These components included several levels of underground workings, the former pit area, and the primary waste-rock dump known as Dump #1. All results to the end of 1991 were used in the design of the initial Decommissioning Plan (C.E. Jones and Associates 1992, Northwest Geochem 1992); however, results up to mid-1993 are now available.

Figure 1. Location of Westmin Resources' Myra Falls Operations in British Columbia.

The primary objective of this paper is to describe the monitoring network for Dump #1 and some of the monitoring results, which probably form one of the largest hydrogeologic databases currently available for a waste-rock dump (Morin et al. 1991). Monitoring has included solid, gas, and water phases as well as internal temperatures and water chemistry below the water table, but length restrictions preclude presentation and justification of much of the database here. A second, more focused objective of this paper is to track the infiltration of water during two storm events from the top of the dump to the water table, over a distance of up to 45 m and a time period of several days. Another, indirect objective is to show (1) the sporadic damage to monitoring equipment that can occur on a dump that continues to undergo active disposal and contouring and (2) the compromises that must be made to data collection in order to accommodate active mining.

Layout of the Myra Falls Operations and Dump #1

The Myra Falls Operations lie in a narrow valley where Myra Creek flows over floodplain and colluvium sediments consisting predominantly of sand and gravel. The valley walls are composed of intact fractured rock, covered in places by talus or debris-avalanche deposits, and rise up to mountain peaks that are capped by snow throughout most of the year. The minesite consists of several components including a tailings impoundment built on the floodplain, a mill, the Lynx Pit excavated laterally into the north valley wall, and waste-rock dumps.

Dump #1 is the primary, active dump at the minesite, containing an estimated 10 million (10^7) mt, and is located along the north valley wall (fig. 2). Dumps #2, #3, and #4 are relatively minor and are not discussed here. The Lower Lift of Dump #1 is located laterally adjacent to the tailings impoundment and in fact is mostly buried by tailings. Within a year, the tailings are expected to cover the Lower Lift entirely. The Middle Lift extends laterally from the south end of the dump half-way to the northern end. This lift has been partly covered by recent waste-rock dumping. The Upper Lift is comprised of rock slopes rising tens of meters above the other lifts. The top of the Upper Lift is used for storage and disposal of mine equipment, rock core, and waste oil. A diversion ditch along the northwest perimeter of this lift carries water from the slopes above the dump to Myra Creek below the dump. This ditch is lined in places above the dump and is shotcreted adjacent to the dump.

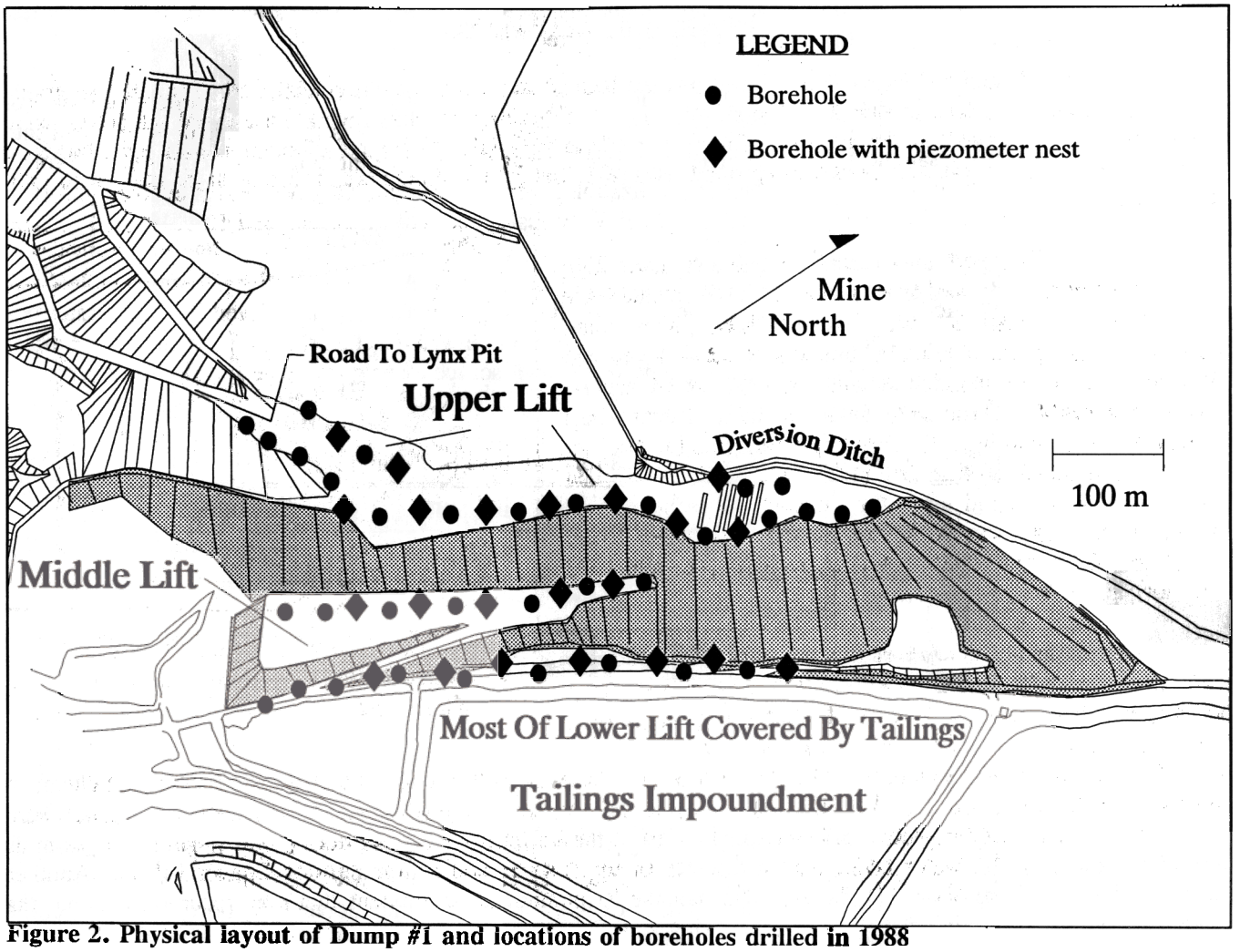

Figure 2. Physical layout of Dump #1 and locations of boreholes drilled in 1988

Stratigraphy and Acid-Base Accounting of Dump #1

In 1988, 57 boreholes were drilled into the three lifts of Dump #1 (fig. 2), using tricone and downhole-hammer techniques (Northwest Geochem 1990). A total of 1,642 m were drilled and sampled for acid-base accounting (ABA) analysis and the delineation of stratigraphy. During this drilling program, up to three 0.75-inch-diameter piezometers were installed in 22 boreholes to monitor groundwater levels and water chemistry below the water table.

The upper and middle portions of the dump were found to vary from coarse boulders to fine-grained rock. The fine-grained layers may reflect surfaces across which heavy equipment moved during delivery and dumping of the rock, and have implications for perched water tables (Morin et al. 1991). The lowest portions of the dump consist of fine-grained waste rock mixed with other materials including wood and brown-colored "sludge". The underlying bedrock could not often be differentiated from the deepest waste rock through the drilling techniques, and thus the presence of peat, soil, or timber was often the indicator used for top of bedrock.

Based on contour interpolation of waste-rock thickness, the Upper Lift rises 26 to 32 m above the original land surface, reaching a maximum of 42 m near the center of the dump and a minimum of a few meters where it

drapes onto the valley wall. The Middle Lift is approximately 20 to 30 m thick. The Lower Lift is generally less than 16 m thick, but much of this thickness at the toe is covered by tailings.

ABA is a common static test used in the prediction of acidic drainage. In its basic form, it consists of measurements of paste pH, Neutralization Potential (NP), and total sulfur, which is mathematically converted into an Acid Potential (AP). A sample's ability to generate acidic drainage at some point in time is then assessed through the evaluation of NP:AP ratios or values of Net Neutralization Potential (NNP = NP - AP). This evaluation should be performed on a site-specific basis, rather than through universal criteria (e.g., Morin and Hutt 1994a).

During the 1988 drilling program, 236 samples were collected for ABA of waste rock (179 samples), bedrock (40 samples), basal organic layer (11 samples), and alluvium (6 samples). The results showed that the waste rock on average was considered a potential acid generator, and paste pH confirmed net acid generation in some samples (table 1). This was not unexpected as Dump #1 has been a known source of acid drainage for almost 20 yr.

Table 1. Summary statistics of waste-rock ABA analyses for Dump #1 (179 samples)

Parameter	Mean	Minimum	Maximum
Paste pH	7.23	4.00	8.16
AP . . t $CaCO_3$/1000 t	108	0.63	438
NP . . t $CaCO_3$/1000 t	23.2	1.74	50.4
NNP . t $CaCO_3$/1000 t	-84.8	-424	25.7
NP/AP	0.99	0.01	42.1

The ABA results for individual boreholes revealed stratification of ABA parameters with depth. For example, values of paste pH showed that the entire thickness of waste rock can be acidic where the thickness is smallest: at the toe and in the Upper Lift against the valley wall. For the remainder of the Upper Lift, boreholes were either (1) essentially pH-neutral, but generally capable of generating net acidity at a later time, (2) acidic from the top down to depths of roughly 8 to 15 m, or (3) acidic only within distinct zones at depth. Values of other ABA parameters in individual boreholes revealed other trends, such as pyrite-rich and NP-rich layers at distinct depths.

Internal Gas Monitoring

Following the 1988 drilling program, a second drilling program in 1990 involved nine boreholes with 235 m of rock drilled with a downhole hammer. Various combinations of 2-inch-diameter monitor wells, thermistor strings, and gas ports were installed in these boreholes (fig. 3). For monitoring of internal gas composition, two gas-port stations were installed in the Lower Lift (G1 and G2), one in the Middle Lift (G3), and two in the Upper Lift (G4 and G5). Each gas port at a station consisted of a continuous, individual length of flexible polyethylene tubing, which terminated at a specific depth to a maximum of 30 m.

Over a period of nearly a year, gas concentrations of oxygen and carbon dioxide were measured on four occasions with an in-line pump and gas analyzer. Results of oxygen measurements depicted a transient system with oxygen concentrations often ranging from nearly atmospheric to nearly zero at most depths throughout the year (e.g., fig. 4). Based on these results, the dump was found to be open to sufficient oxygen at all depths to allow sulfide-mineral oxidation, although occasional periods of oxygen limitation occurred. No further monitoring of gas concentrations was conducted.

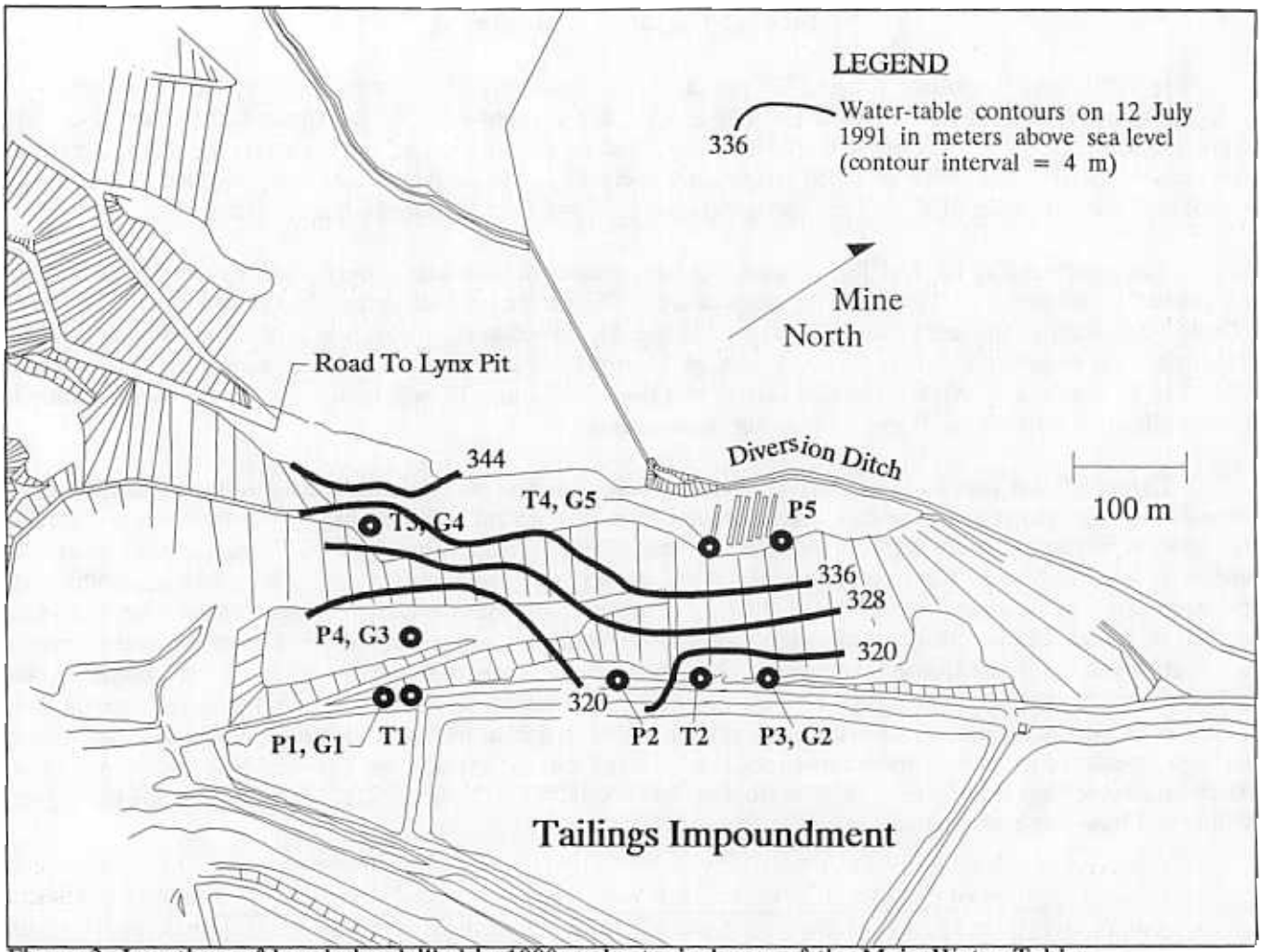

Figure 3. Locations of boreholes drilled in 1990 and a typical map of the Main Water Table.

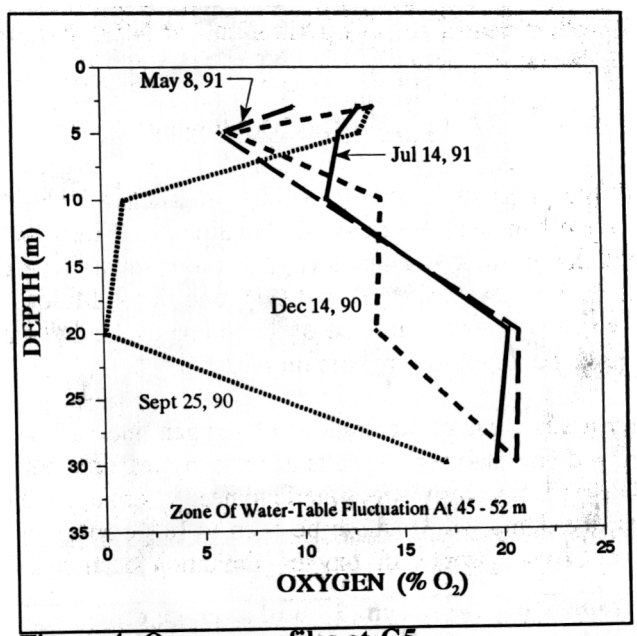

Figure 4. Oxygen profiles at G5.

Internal Temperature Monitoring

In 1990, four thermistor strings ("T" prefix, fig. 3) consisting of commercially supplied thermistors were installed in two boreholes on the Lower Lift (T1 and T2) and two boreholes on the Upper Lift (T3 and T4). The number and depth of the individual thermistors depended on the location of the borehole; all thermistors were connected to dataloggers which recorded temperature every 12 h. These thermistors were installed to identify the lateral and vertical extent of significant heat generation resulting from sulfide-mineral oxidation.

The results at T1, T2, and T3 indicated that temperatures at most depths only slightly exceeded the average annual surface temperature. However, the temperature at T4 near the northern end of the Upper Lift (fig. 3) showed elevated temperatures above the average annual value (fig. 5), reflecting significant heat production and transmission. The maximum measured temperature was 51.6°C at T4 at a depth of 10 m. This is consistent with an acidic zone identified in this area by ABA (discussed above) to a depth of 26 m. T4 will be used in the following section to track infiltration through the Upper Lift during storm events.

The significant gaps in data caused by datalogger failures have plagued interpretations due to the incomplete records (fig. 5). However, these data gaps were not caused by internal failures, but by external events. Because Dump #1 is still active, there is traffic movement across all lifts on most days. This traffic carries fresh waste rock and used equipment from the mines and mill. Also, there is road maintenance and, during winter months, road plowing. Such activity has resulted in the crushing or covering of instrumentation and piezometer nests and in the cutting of cables attached to the dataloggers. All of this work is part of normal mine operation and cannot be eliminated without great expense. As a result, the gaps in the data cannot be easily eliminated and controlled, and must be taken as part of the normal problems encountered at an active mine. In turn, interpretations based on these data must recognize the limitations that an active dump places on data availability. In any case, Dump #1 is evolving through time as old rock weathers and new rock is added, and thus the physical and chemical hydrogeology of Dump #1 could change significantly through time from current conditions. The intermittent records from the dataloggers will reveal how this evolution occurs.

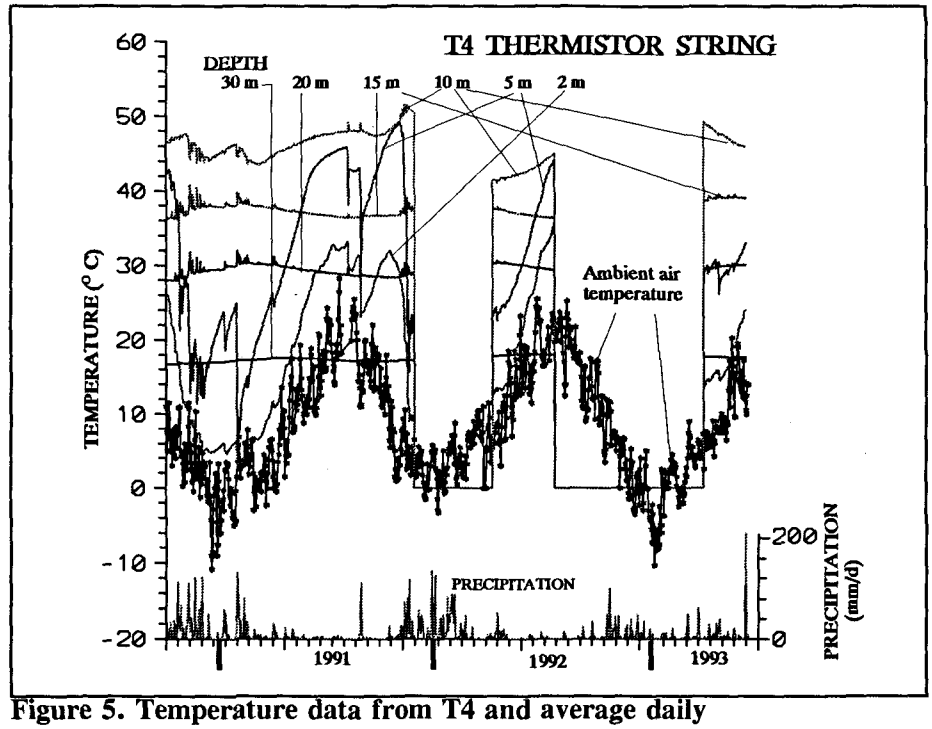

Figure 5. Temperature data from T4 and average daily temperature at Myra Falls.

Water-Table Fluctuations in Dump #1

Five 2-inch-diameter monitor wells were installed in the lifts of Dump #1 ("P" prefix, fig. 3) All except P2 contain pressure transducers, which have transmitted water levels every 12 h to dataloggers.

All P-series monitor wells are installed in the "main" or "basal" water table near the base of the dump. This water table passes through waste rock or bedrock, depending on location, as it extends from the valley wall to the floodplain and tailings impoundment (fig. 3). In addition to the main water table, there are other, perched water tables within the dump. These perched tables affect the movement, chemistry, and timing of infiltrating water in a dump (Morin and Hutt 1994b, Morin et al. 1991).

The hydraulic gradient of the main water table is approximately 0.2 to 0.3 towards the east, and the groundwater thus flows towards the tailings where it is intercepted at the toe (now buried with tailings) by the Inner Drain (van Dyk 1987). This subsurface drain was specially designed to intercept dump seepage and to carry it to the treatment plant.

Based on single-well-response tests, the hydraulic conductivity of the bedrock and basal waste rock ranges from 10^{-5} to 10^{-8} m/s. With a porosity of 5% from the relative fluctuations of precipitation and groundwater level, groundwater beneath the main water table requires at least a few weeks to travel from the top end of the dump to the Inner Drain.

Mass-balance calculations have shown that approximately 10% of total annual groundwater flow beneath the main water table is derived from infiltration directly through waste rock, while the remainder is background groundwater from behind the valley wall (Northwest Geochem, 1992). Despite its relative unimportance on an annual basis, most infiltration through the dump occurs during the wet season from October to March and periodic storm events carry acid-generation products downward through the dump to the water table, affecting the chemistry of the Inner Drain water (Northwest Geochem 1990, Northwest Geochem 1992). Concepts behind such flushing of waste-rock dumps are discussed in Morin and Hutt (1994b) and Morin et al. (1994).

The results of 12-h measurements along the south-end flowpath from P4 to P1 (fig. 3) show a relationship in which water levels rise roughly 2 m during storm events. This response is more dramatic along the north-end flowpath (P5 to P3) in which P3 has fluctuations up to 4 m during storm events (fig. 6). These fluctuations can carry major implications for oxygen pumping within the dump (discussed above). When a storm event of roughly 10 cm causes a water table response of 2 to 4 m, mass-balance relationships indicate porosity of the rock would be around 2 to 5%, which is used above in groundwater-velocity calculations.

Instead of examining the entire database of water levels, a detailed examination of water-level responses to individual storm events is more informative. For this paper, the storm events that occurred around February 1, 1991 and August 29, 1991, and their resulting effects at T4/P5 in the Upper Lift (fig. 3) and at T2/P3 in the Lower Lift, will be highlighted. During the 12-h period centered around 00:00 on January 31, 1991, precipitation began falling and increased to roughly 7 cm in 12 h by 00:00 on February 1, 1991 (fig. 7). Within 12 h, this storm event caused a rapid decrease in temperature at T4 to depths of 10 m. Since the highest measured temperatures occur at 10 m, the corresponding responses at greater depths occurred as increases in temperature as the warmed infiltration passed through within the 12 h. There was no temperature response at the 30 m depth.

The water table at this location with a depth of approximately 45 m, however, did not respond to the storm event for nearly 24 h, with the midpoint of the response at 36 h (table 2). The discrepancy between this delayed response of 36 h and the temperature responses in less than 12 h to depths of 20 m suggests either (1) there is a perched zone between 20 and 45 m which slows infiltration or (2) the temperature responds to an initial, minimal amount of initial infiltration, whereas the water table reflects the response to volume. A storm event three days later produced similar results.

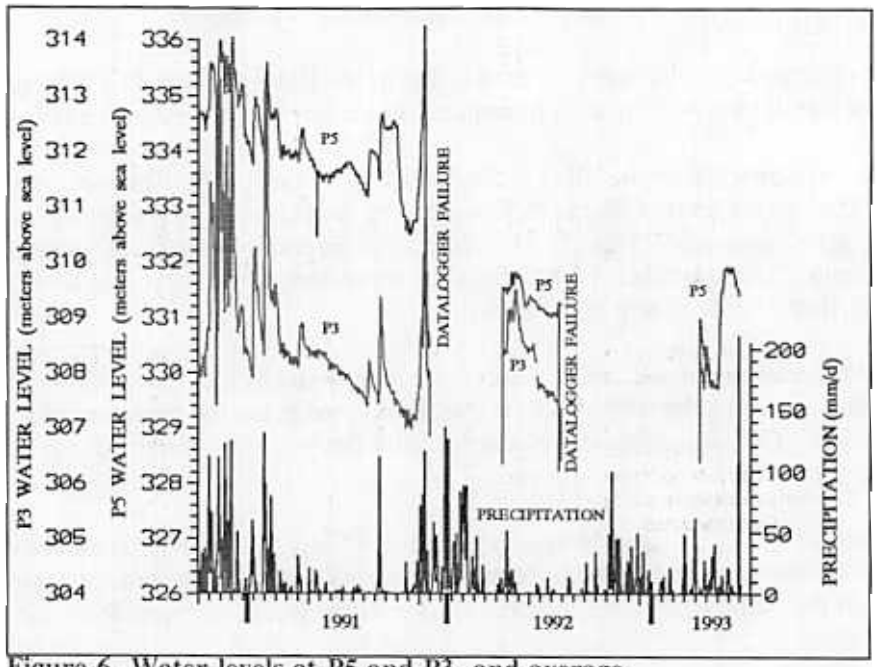

Figure 6. Water levels at P5 and P3, and average daily precipitation.

At T2 and P3 (fig. 8), temperature responses could only be clearly seen at depths of 5 m (in 12 h) and at 12 m (in 24 h). The water-table response at a depth of approximately 16 m had a midpoint response at 36 h (table 2). Because of the greater thickness at T4/P5, the similar time lags at the water table indicate infiltration passes through a unit depth at T2/P3 more slowly.

The storm event during the 12-h period centered at 12:00 on August 29, 1991 generated similar, but generally more rapid, responses at both locations (figs. 9 and 10; table 2). The more rapid responses could be the result of the precipitation that occurred during the prior 36-h period. In any case, a significant storm event at Myra Falls is capable of initiating infiltration through the dump to depths of 45 m within 12 h to 36 h based on temperature and water-table response, respectively.

Table 2. Time delay between the start of a storm event and the midpoint response of temperature and water level.

Station AND DEPTH	STORM EVENT		STATION AND DEPTH	STORM EVENT	
	1 FEB 91	29 AUG 91		1 FEB 91	29 AUG 91
T4 - 2 m	<12 h	<12 h	T2 - 2 m	?	?
T4 - 5 m	<12 h	<12 h	T2 - 5 m	12 h	<12 h
T4 - 10 m	<12 h	none	T2 - 8 m	?	<12 h
T4 - 15 m	<12 h	none	T2 - 12 m	24 h	<12 h
T4 - 20 m	<12 h	none	P3 (16 m)	36 h	12 h
T4 - 30 m	none	none			
P5 (45 m)	36 h	24 h			

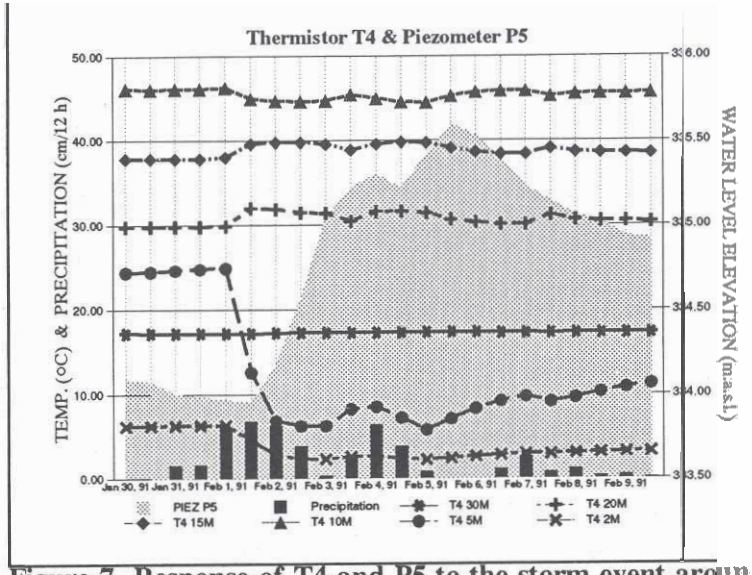

Figure 7. Response of T4 and P5 to the storm event around February 1, 1991.

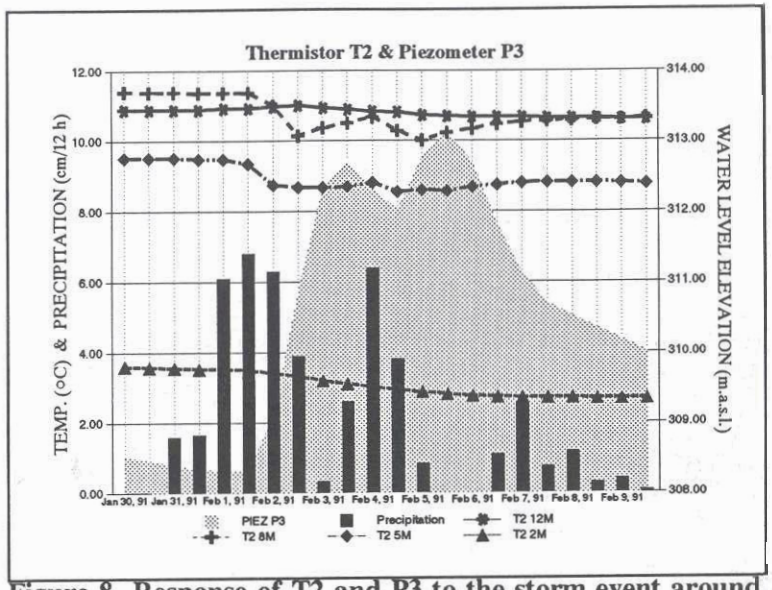

Figure 8. Response of T2 and P3 to the storm event around February 1, 1991.

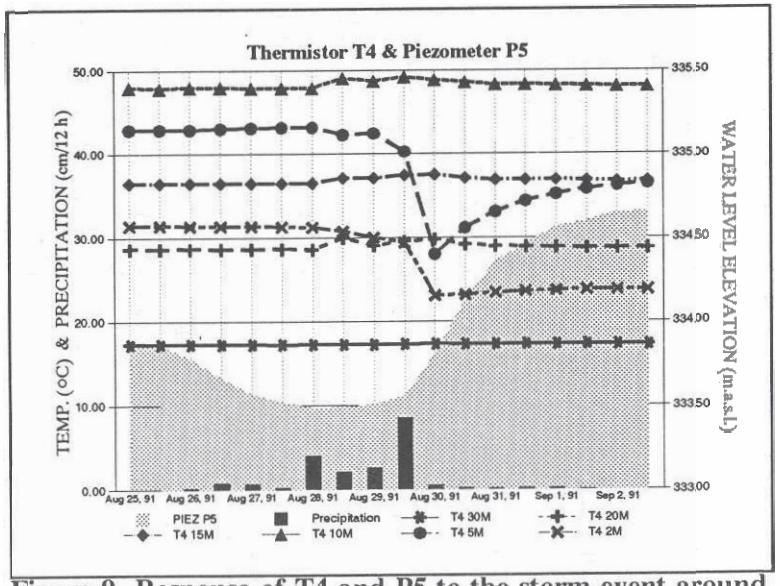

Figure 9. Response of T4 and P5 to the storm event around August 29, 1991.

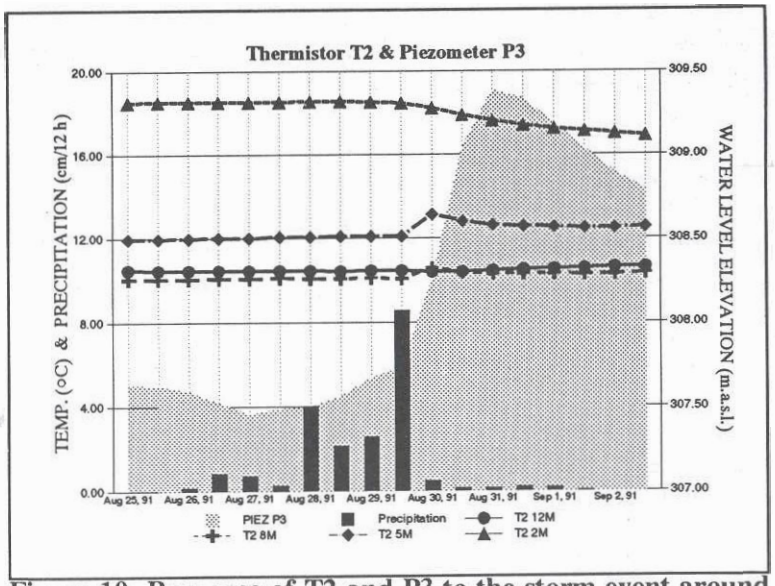

Figure 10. Response of T2 and P3 to the storm event around August 29, 1991.

Conclusion

This paper has presented the monitoring program for Dump #1 at Westmin Resources' Myra Falls Operations in British Columbia. The database consists of data on solid, gas, and water phases as well as internal temperatures and water chemistry below the water table.

The monitoring of Dump #1 is providing valuable information from which to select decommissioning options (Northwest Geochem 1992). For example, shotcreting of the dump surface appears viable (Wong et al. 1993). However, in a more general sense, the monitoring database also provides valuable information from which to draw empirical correlations and to test theoretical relationships on waste-rock dumps.

Acknowledgements

We thank Nora Hutt of Normar Enterprises for preparing figures. We also express our gratitude to the three anonymous reviewers who improved the clarity and quality of this paper. Unfortunately, all their suggestions could not be implemented due to length restrictions. We also thank the conference coordinators, particularly Ms. Lowanse who managed manuscript submissions.

References

C.E. Jones and Associates. 1992. Decommissioning plan. Report for Westmin Resources Limited.

Morin, K.A., and N.M. Hutt. 1994a. Observed preferential depletion of neutralization potential over sulfide minerals in kinetic tests: Site-specific criteria for safe NP/AP ratios. In Third International Conference on the Abatement of Acidic Drainage (these proceedings).

Morin, K.A., and N.M. Hutt. 1994b. An empirical technique for predicting the chemistry of water seeping from mine-rock piles. In Third International Conference on the Abatement of Acidic Drainage (these proceedings).

Morin, K.A., I.A. Horne, and C. Pelletier. 1994. High-frequency geochemical monitoring of toe seepage from mine-rock dumps, BHP Minerals' Island Copper Mine, British Columbia. In Third International Conference on the Abatement of Acidic Drainage (these proceedings).

Morin, K.A., E. Gerencher, C.E. Jones, and D.E. Konasewich. 1991. Critical literature review of acid drainage from waste rock. Report for the Mine Environment Neutral Drainage (MEND) Program.

Northwest Geochem. 1992. Physical and chemical hydrogeology of the Lynx Area of the Myra Falls Operations. Report for Westmin Resources.

Northwest Geochem. 1990. Hydrogeological assessment and development of AMD control technology for Myra Falls waste rock. Report for Westmin Resources.

van Dyk, R.P. 1987. Environmental control and reclamation at Westmin Myra Falls Operations. p.227-234. In Proceedings of the Eleventh Annual British Columbia Mine Reclamation Symposium. (Campbell River, British Columbia, April 8-10).

Wong, J.Y., C.E. Jones, and R.P van Dyk. 1993. Use of shotcrete to control acid mine drainage in waste rock piles. p.65-74. In Proceedings of the Seventeenth Annual British Columbia Mine Reclamation Symposium. (Port Hardy, British Columbia, May 4-7).

EFFECTS OF SELECTIVE HANDLING OF PYRITIC, ACID-FORMING MATERIALS ON THE CHEMISTRY OF PORE GAS AND GROUND WATER AT A RECLAIMED SURFACE COAL MINE, CLARION COUNTY, PA, USA[1]

Charles A. Cravotta III[2], Diana L. Dugas[2], Keith B. C. Brady[3], and Thomas E. Kovalchuk[3]

Abstract: A change from dragline to "selective handling" mining methods at a reclaimed surface coal mine in western Pennsylvania did not significantly affect concentrations of metals in ground water because oxidation of pyrite and dissolution of siderite were not abated. Throughout the mine, placement of pyritic material near the land surface facilitated the oxidation of pyrite, causing the consumption of oxygen (O_2) and release of acid, iron, and sulfate ions. Locally in the unsaturated zone, water sampled within or near pyritic zones was acidic, with concentrations of sulfate exceeding 3,000 milligrams per liter (mg/L). However, acidic conditions generally did not persist below the water table because of neutralization by carbonate minerals. Dissolution of calcite, dolomite, and siderite in unsaturated and saturated zones produced elevated concentrations of carbon dioxide (CO_2), alkalinity, calcium, magnesium, iron, and manganese. Alkalinity concentrations of 600 to 800 mg/L as $CaCO_3$ were common in water samples from the unsaturated zone in spoil, and alkalinities of 100 to 400 mg/L as $CaCO_3$ were common in ground-water samples from the underlying saturated zone in spoil and bedrock. Saturation indices indicated that siderite could dissolve in water throughout the spoil, but that calcite dissolution or precipitation could occur locally. Calcite dissolution could be promoted as a result of pyrite oxidation, gypsum precipitation, and calcium ion exchange for sodium. Calcite precipitation could be promoted by evapotranspiration and siderite dissolution, and corresponding increases in concentrations of alkalinity and other solutes. Partial pressures of O_2 (Po_2) and CO_2 (Pco_2) in spoil pore gas indicated that oxidation of pyrite and precipitation of ferric hydroxide, coupled with dissolution of calcite, dolomite, and siderite were the primary reactions affecting water quality. Highest vertical gradients in Po_2, particularly in the near-surface zone (0-1 m), did not correlate with concentrations of total sulfur in spoil. This lack of correlation could indicate that total sulfur concentrations in spoil do not reflect the amount of reactive pyrite or that oxidation rates can be controlled more by rates of O_2 diffusion than the amount of pyrite. Hence, if placed in O_2-rich zones near the land surface, even small amounts of disseminated pyritic material can be relatively significant sources of acid and mineralized water.

Introduction

Acidification and mineralization of ground water commonly result from the accelerated oxidation of pyrite (FeS_2) and the consequent dissolution of other minerals exposed during surface coal mining. Innovative mining and reclamation techniques, such as "selective handling," have potential to reduce water-quality degradation by minimizing these processes. Selective handling involves the segregation of pyritic, high-sulfur overburden during mining and the subsequent burial of this material in compacted pods in the backfill. In the Appalachian Coalfield of the Eastern United States, the pyritic pods commonly are encapsulated with alkaline materials and are placed below the plant-root zone but above the projected, postreclamation ground-water table within the backfill (Pionke and Rowgowski 1982; Phelps and Saperstein 1982; Geidel and Caruccio 1984). The objectives of selective handling are to (1) minimize transport of acid by preventing contact between ground water and pyritic materials or minimize oxidation of pyrite by limiting its exposure to oxygen, and (2) add alkalinity to infiltrating water, which can slow acid production, neutralize acid, and reduce the mobility of metals (Williams et al. 1982). If the objectives can be realized, mining with selective-handling techniques may be permitted in areas and on coal seams where traditional mining methods produced acidic ground water and mine drainage.

This paper evaluates the effects of selective handling of pyritic overburden materials on the chemistry of pore gas and ground water, and the mechanisms of producing alkalinity, at a reclaimed surface coal mine in western Pennsylvania. In a companion paper, Cravotta et al. (1994) give details of the geochemical and geohydrological characteristics of bedrock and spoil at the study area.

---

[1]Paper presented at the International Land Reclamation and Mine Drainage Conference and the Third International Conference on the Abatement of Acidic Drainage, Pittsburgh, PA, April 24-29, 1994.
[2]Hydrologist, U.S. Geological Survey, 840 Market Street, Lemoyne, PA 17043.
[3]Hydrogeologist, Pennsylvania Department of Environmental Resources, Harrisburg, PA 17105.

The study area is a reclaimed surface coal mine on two hilltops in southern Clarion County, PA (fig. 1). During 1980-86, the middle and lower Kittanning coals were mined (Glover 1987). The mined coalbeds were less than 1 m thick, dipped gently west-northwest, and were separated by about 18 to 20 m of medium- to dark-gray shale which graded upward to siltstone and claystone (Cravotta et al. 1994). The lower Kittanning coal and a 1.2-m-thick stratum of carbonaceous shale overlying the coal were pyritic, had total sulfur (S) concentrations greater than 2.5 weight percent (wt %), and were laterally continuous across the mine. Calcareous shale and siltstone above these strata had neutralization potential (NP) values as high as 125 grams as calcium carbonate per kilogram (g/kg $CaCO_3$) and generally thinned northward across the mine. Most of the overburden had total S concentrations less than 1 wt % and NP values less than 25 g/kg $CaCO_3$. Mass-weighted averages of net-neutralization potential (NNP) for spoil were negative and decreased northward (Cravotta et al. 1994).

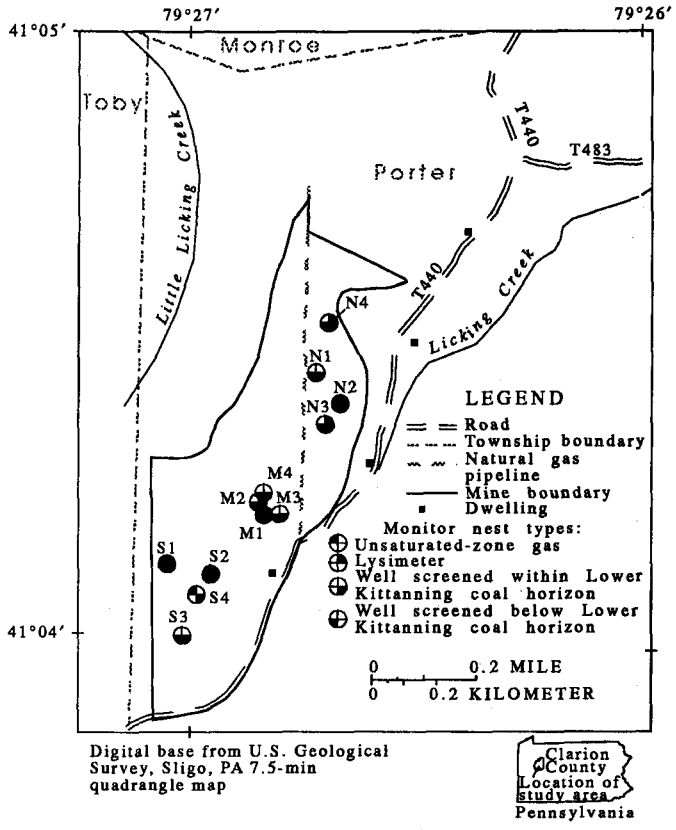

Figure 1. Location of monitoring sites at reclaimed surface coal mine in southern Clarion County, PA.

Different methods were used to handle overburden and spoil at the mine (Cravotta et al. 1994). In the northern area, bulldozers and front-end loaders were used to selectively handle the pyritic shale overlying the lower Kittanning coal and to add crushed limestone (56 Mg/ha) to the pit floor and spoil. The selectively handled material was layered on benches of low-S (<0.2 wt %) material in the unsaturated zone. Disposal of the pyritic material below the water table would not have been practical because of the locally thin saturated zone in the backfill (Cravotta et al. 1994). In the southern area, a dragline was used. High-S (≥0.5 wt %) material was placed above intermediate-S material in the unsaturated zone. In the middle area, where mining methods used are uncertain, high-S material was placed near the surface and on the pit floor, within the zone of water-table fluctuation.

Experimental Design and Methods

Different mining methods can have different effects on ground-water quality by altering the distribution of acid-forming and alkaline-producing materials, spoil permeability and pore-gas-exchange rates, and ground-water recharge and flow paths, because these factors determine the sequence and extent of water-rock interactions. Hence, a nested monitoring network was designed and installed to measure chemical variations in the unsaturated and saturated zones in areas mined by different methods.

Monitoring Network

In each of the northern, middle, and southern areas, a minimum of four clusters of two or more boreholes were drilled in spoil and underlying bedrock by air-rotary methods during November 1991. At least one cluster, or monitoring nest, in each area included boreholes for ground-water (saturated-zone) sampling, pore-water (unsaturated-zone) sampling, and pore-gas sampling (fig. 1). Figure 2 shows construction details for monitoring nest components. At all monitoring nests, except at nest S4, where only one well was installed, two ground-water wells were installed in adjacent boreholes approximately 1.5 m apart; one well was screened in the horizon of the lower Kittanning coal to depths from 13.4 to 32.6 m, and the other well was screened in the unmined underlying bedrock at a 4.6-m greater depth (Cravotta et al. 1994). Each well was constructed of 5.1-cm-diameter, polyvinyl chloride (PVC) pipe with a slotted screen at least 3-m long. At many nests, PVC pressure-vacuum lysimeters with ceramic tips (Parizek and Lane 1970) and polyethylene gas-sampling tubes were installed in unsaturated mine spoil. Lysimeter tips and gas-sampling ports were placed at depths of 1 to 1.5 m, 4 to 4.6 m, 7 to 7.6 m, and 10.7 to 11 m below the spoil surface to enable comparison of chemical concentrations in pore-water and pore-gas samples, respectively, at comparable depths.

Sampling and Analytical Methods

Rock samples from each borehole were collected as composites of drill cuttings over 1.5-m intervals and were logged for lithology. Rock samples from selected holes also were analyzed for mineralogical and chemical content, including total S, total C, and NP, as described by Cravotta et al. (1994).

During February-December 1992, samples of gas and water were collected monthly. Pore-gas and ambient air samples were collected directly into 1-L Tedlar bags within an airtight chamber that was evacuated with a hand-operated pressure-vacuum pump. Pore water from the unsaturated zone was collected into evacuated lysimeters, and samples were retrieved by applying pressure with a hand pump (Parizek and Lane 1970). Ground-water samples from spoil and bedrock were collected after purging water from each monitoring well with PVC bailers.

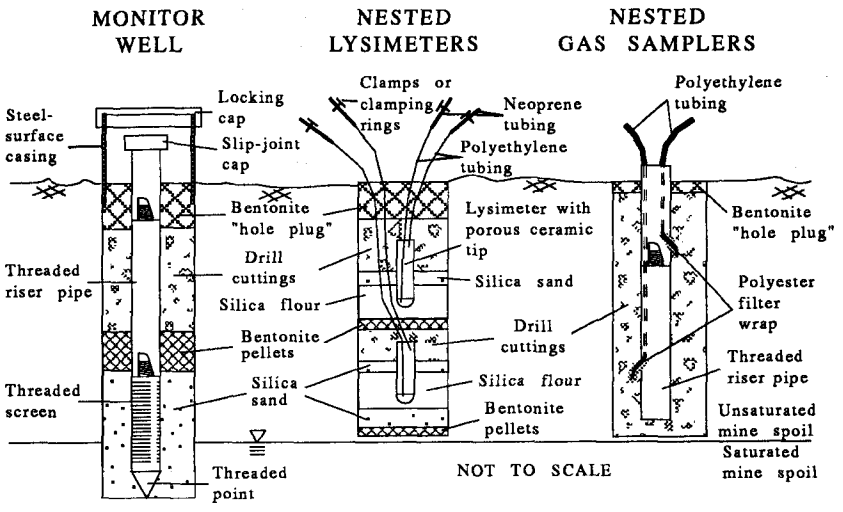

Figure 2. Schematic diagram showing nested monitoring design.

Field measurements and sample processing were conducted by use of methods of Wood (1976) and Claassen (1982). Before purging wells, ground-water levels, temperature, and dissolved oxygen were measured with downhole probes. After purging, specific conductance and redox potential (Eh) were measured by draining water from the bailer into a glass flow cell. Water samples were stored in polyethylene bottles on ice until laboratory analysis. One subsample for analysis of pH, acidity, alkalinity, sulfate, chloride, and nutrients was capped without head space. The second subsample for analysis of dissolved metals and silica was filtered through a 0.45-µm-pore nitrocellulose filter, transferred to an acid-rinsed bottle, and preserved with nitric acid.

Chemical analyses were conducted at the Pennsylvania Department of Environmental Resources (PaDER) Bureau of Laboratories facility in Harrisburg, PA. Concentrations of O_2 and CO_2 in gas samples were measured by gas chromatography according to methods of Bremner and Blackmer (1982). Laboratory pH and concentrations of alkalinity, acidity, calcium, magnesium, sodium, potassium, nitrate, ammonia, phosphate, chloride, fluoride, sulfate, iron, manganese, aluminum, silica, and selected trace metals in water samples were analyzed by methods of Skougstad et al. (1979). Alkalinity and acidity were estimated by use of pH 3.9 and 8.2 titration endpoints, respectively. Chemical data for gas and water samples were reported by Lescinsky et al. (1993).

Data-Analysis Methods

Computerized graphical, statistical, and geochemical modeling methods were used to evaluate the pore-gas and water-chemical data. Statistical tests for differences among data subsets were conducted by use of notched boxplots (Velleman and Hoaglin 1981) generated by the P-Stat EDA procedure (P-Stat 1989). If the notches on either side of medians in a pair of boxplots do not overlap, the medians for the two subsets are significantly different at the 95-percent confidence level (Velleman and Hoaglin 1981). Aqueous speciation and mineral saturation indices for selected water samples were computed by use of WATEQF (Plummer et al. 1976).

Effects of Selective Handling of Pyritic, Acid-Forming Material

Segregation of pyritic, high-sulfur materials in pods surrounded by calcareous material and placed above the water table hypothetically can reduce the production of acidic ground water and increase the neutralization of acid and production of alkaline ground water. Oxidation of pyrite, the principal sulfur-bearing mineral at the mine (Cravotta et al. 1994), consumes O_2 and releases acid, iron, and sulfate. Dissolution of carbonate minerals, predominantly calcite ($CaCO_3$), dolomite [$CaMg(CO_3)_2$], siderite ($FeCO_3$), and manganosiderite [$(Fe,Mn)CO_3$], which were present in noncoal horizons at the mine (Cravotta et al. 1994), can neutralize acid and produce CO_2, alkalinity, and dissolved calcium, magnesium, iron, and manganese.

Gas Chemistry

Partial pressures of O_2 and CO_2 in spoil are expected to vary depending on the predominant reactions involving the gases, relative rates of the reactions, and rates of gas exchange with surrounding zones (Jaynes et al. 1984a,b; Lusardi and Erickson 1985). In general, where pyrite-oxidation and carbonate-dissolution reactions are active, Po_2 will decrease and Pco_2 will increase. Data on pore-gas compositions at the mine (tables 1-2, fig. 3) indicate that Po_2 decreases from about 21 volume percent (vol %) at the land surface to less than 2 vol % at 10.7 m below the surface, with corresponding increases in Pco_2 with increasing depth in all three areas. Dissolution of carbonate minerals and production of alkalinity are favored by conditions characterized by elevated Pco_2 (Stumm and Morgan 1981; Bruno et al. 1992a,b). Because the pore water in spoil is extremely mineralized and dissolved solutes result primarily from mineral decomposition or weathering, oxidation of organic matter is not considered to be an important control of Po_2 and Pco_2.

Table 1. Mean concentration of oxygen and carbon dioxide[1] in pore gas samples collected February-December 1992. [Values in volume percent, unless noted; <, less than; --, no data]

Depth (m)	Oxygen for gas well nest--					Carbon dioxide for gas well nest--				
	N2	M1	S1	S2	S4	N2	M1	S1	S2	S4
0	21.66	21.66	21.66	21.66	21.66	<0.50	<0.50	<0.50	<0.50	<0.50
1	14.62	17.79	14.59	12.55	16.26	5.82	3.27	6.17	6.31	5.72
4	10.37	10.70	3.39	11.08	14.29	8.70	9.20	12.66	8.36	7.69
7	6.80	4.32	4.56	6.79	12.98	11.87	16.61	14.17	13.02	8.57
11	3.18	5.00	4.28	3.34	--	13.63	15.78	15.72	16.44	--

[1]To compute mean, CO_2 concentration was assumed to be 0.2 if below detection (<0.5).

Table 2. Vertical gradient[1] of mean concentration of oxygen and carbon dioxide in pore gas samples collected February-December 1992. [Values in volume percent per meter, unless noted; --, no data]

Depth range (m)	Oxygen for gas well nest--					Carbon dioxide for gas well nest--				
	N2	M1	S1	S2	S4	N2	M1	S1	S2	S4
0-1	-7.70	-4.23	-7.73	-9.96	-5.90	6.15	3.35	6.53	6.68	6.04
1-4	-1.39	-2.33	-3.67	-.48	-.65	.94	1.95	2.13	.67	.65
4-7	-1.17	-2.10	.38	-1.41	-.43	1.04	2.43	.49	1.53	.29
7-11	-.91	.17	-.07	-.87	--	.44	-.21	.39	.86	--

[1]Gradient = (concentration at depth 2 - concentration at depth 1)÷(depth 2 - depth 1). Negative value for gradient indicates decreasing concentration with increasing depth.

The observed changes in Po_2 proportional to Pco_2 in spoil (fig. 3) generally can be explained on the basis of theoretical stoichiometry of reactions involving pyrite, calcite, dolomite, and siderite. Two summary reactions can be written for the complete oxidation of pyrite combined with calcite dissolution (Cravotta et al. 1990):

$$FeS_2 + 2CaCO_3 + 3.75O_2 + 1.5H_2O \rightarrow Fe(OH)_3 + 2SO_4^{2-} + 2Ca^{2+} + 2CO_2 \quad (1)$$

$$FeS_2 + 4CaCO_3 + 3.75O_2 + 3.5H_2O \rightarrow Fe(OH)_3 + 2SO_4^{2-} + 4Ca^{2+} + 4HCO_3^-. \quad (2)$$

Reactions 1 and 2 represent end-member reactions with respect to the quantity of calcite dissolved and its products. In both reactions, iron is presumed to oxidize and hydrolyze forming solid iron hydroxide [$Fe(OH)_3$]. In reaction 1, CO_2 is a product, and the stoichiometric ratio of O_2 consumed relative to CO_2 produced (ΔPo_2:ΔPco_2) is 1.875. In reaction 2, bicarbonate (HCO_3^-) is a product, not CO_2. If ferrous iron (Fe^{2+}) is produced instead of $Fe(OH)_3$, ΔPo_2:ΔPco_2 is 3.5 or larger. Similar reactions can be written with dolomite as a reactant instead of calcite that yield identical values of ΔPo_2:ΔPco_2. Hence, if predominant reactions involve oxidation of pyrite and neutralization by calcite or dolomite then values of ΔPo_2:ΔPco_2 will be a minimum of 1.875.

Alkalinity and CO_2 also can be produced by the dissolution of siderite and manganoan siderite. Several reactions can be written for siderite dissolution with respect to the consumption of O_2 and the production of CO_2. Under anoxic conditions, siderite dissolution can neutralize acid and produce alkalinity:

$$FeCO_3 + H^+ \rightarrow Fe^{2+} + HCO_3^-. \quad (3)$$

Neither O_2 nor CO_2 is involved in reaction 3. However, under acidic or oxic conditions, CO_2 can be a product:

$$FeCO_3 + 2H^+ \rightarrow Fe^{2+} + CO_2 + H_2O \quad (4)$$

$$FeCO_3 + 0.25O_2 + 1.5H_2O \rightarrow Fe(OH)_3 + CO_2. \quad (5)$$

In reaction 4, O_2 is not involved. In reaction 5, $\Delta Po_2:\Delta Pco_2$ is 0.25. Hence, if siderite is the predominant reactant, $\Delta Po_2:\Delta Pco_2$ will be a maximum of 0.25.

Absolute values of the slopes of the linear trends of O_2 relative to CO_2 in a gas nest (fig. 3) correspond to values of $\Delta Po_2:\Delta Pco_2$ and range from 1.1 to 1.4. If reactions 1-2 predominated, $\Delta Po_2:\Delta Pco_2$ values greater than 1.875 would be expected, whereas if reactions 3-5 predominated, $\Delta Po_2:\Delta Pco_2$ values less than 0.25 would be expected. Hence, the gas data are consistent with the occurrence of some combination of reactions 1-5.

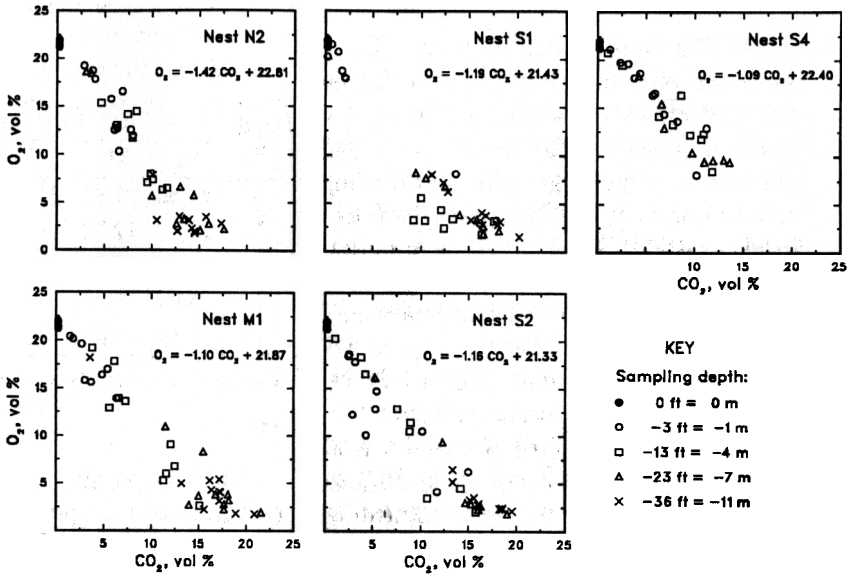

Figure 3. Concentration of oxygen (O_2) relative to that of carbon dioxide (CO_2) in pore-gas samples collected February-December 1992 from unsaturated spoil in Clarion County, PA (fig. 1). Regression equation calculated assuming O_2 is independent variable.

In general, the rapid decrease in Po_2 and the corresponding increase in Pco_2 at shallow depths (fig. 3, table 2), indicate that oxidation of pyrite and dissolution of carbonate minerals are most active in the unsaturated zone near the land surface. In all five gas-monitoring nests, the steepest O_2 and CO_2 gradients are indicated in the 0- to 1-m depth interval (table 2). Steep gradients are not restricted to the shallowest zone, however. For example, in nests M1 and S2, substantial O_2 and CO_2 gradients are indicated in the 4- to 7-m depth interval. Similar gradients were measured during nonrecharge periods in all seasons, which suggests biological respiration and decomposition are subordinate influences. Hence, mineral weathering is more extensive near the surface but can be active locally to depths of 7 m or more.

Zones exhibiting steep gradients in gas composition do not coincide with zones having highest acid-producing potentials in the mine spoil. For example, the total S concentration in rock sampled from the 0- to 1.5-m depth interval at gas-sampling nest S4 is <0.05 wt % and that at nest M1 is 1.16 wt % (Cravotta et al. 1994). Because high vertical gradients may be independent of relative quantities of high-S material, pyrite oxidation rates could be controlled by rates of O_2 diffusion, or total S concentrations in spoil may not reflect the amount of reactive pyrite. Hence, even small amounts of disseminated pyritic material can be relatively significant sources of acid and mineralized water.

Water Chemistry

Ground water in spoil produced by the selective-handling method was neither less acidic nor more alkaline than ground water in spoil produced by the dragline method. Throughout the mine, overall ground-water quality was alkaline (figs. 4 and 5) despite overburden chemical data for spoil that indicated potential for development of acidic conditions (Cravotta et al. 1994). Median values of pH and concentrations of net alkalinity (= alkalinity - acidity) and alkalinity are significantly higher in ground water from mine spoil in the southern area relative to the middle and northern areas (fig. 4). This difference probably reflects an effect of decreasing concentration of NP in overburden from south to north across the mine (Cravotta et al. 1994). However, median concentrations of dissolved sulfate, iron, and manganese in the ground-water samples are not significantly different between the northern and southern areas, where selective-handling and dragline methods, respectively, were used.

Water samples from spoil throughout the northern, middle, and southern areas of the mine are highly mineralized, with concentrations of sulfate that typically exceed 400 mg/L (fig. 4), presumably as a product of pyrite oxidation. Despite high sulfate concentrations, water samples from most intervals in the unsaturated and saturated zones of spoil are alkaline. Alkalinity concentrations of 100 to 400 mg/L as $CaCO_3$ are common in ground-water samples from spoil, and alkalinities of 600 to 800 mg/L as $CaCO_3$ are common in water samples from the overlying unsaturated zone (fig. 5). Locally in the unsaturated zone of the northern area, however, shallow pore water sampled

within or near pyritic pods is acidic and has concentrations of sulfate exceeding 3,000 mg/L (fig. 5). For example, pore waters sampled in December 1992 (table 3) at nests N2 and N4 from a depth of 4.6 m have pH values less than 4 and sulfate concentrations greater than 5,000 mg/L. Despite substantial pyritic material within and below the 4.6-m depth interval, such as at nest N2 (see Cravotta et al. 1994), acidic conditions and high sulfate concentrations were only locally significant (table 3), and alkaline conditions prevail below the water table.

Dissolution of calcite and dolomite can produce alkalinity, calcium, and magnesium, and dissolution of siderite also can add these constituents plus iron and manganese. High concentrations of sodium relative to calcium and magnesium in pore waters and ground waters (table 3) can result from cation-exchange reactions (Foster 1950; Chapelle and Knobel 1985). Sodium bentonite, which was added to all boreholes containing lysimeters and wells (fig. 2), probably is not an important reactant because all water samples do not have elevated concentrations of sodium.

In general, pore-water samples have higher concentrations of alkalinity, sulfate, and base cations than in underlying ground-water samples (fig. 5, table 3). The trend of decreasing mineralization of pore waters with increasing depth probably results from intensive mineral weathering combined with evapotranspiration or freezing within shallow unsaturated mine spoil followed by dilution within the saturated zone. Evapotranspiration or freezing could produce elevated concentrations of solutes such as chloride (table 3). Dilution can result by mixing of waters with different residence times in chemically active zones and by mixing of waters from zones with different minerals or activities of reactions. Residence times and flow paths of percolating water can differ during recharge and nonrecharge periods (Diodato and Parizek 1988; Hawkins and Aljoe 1991).

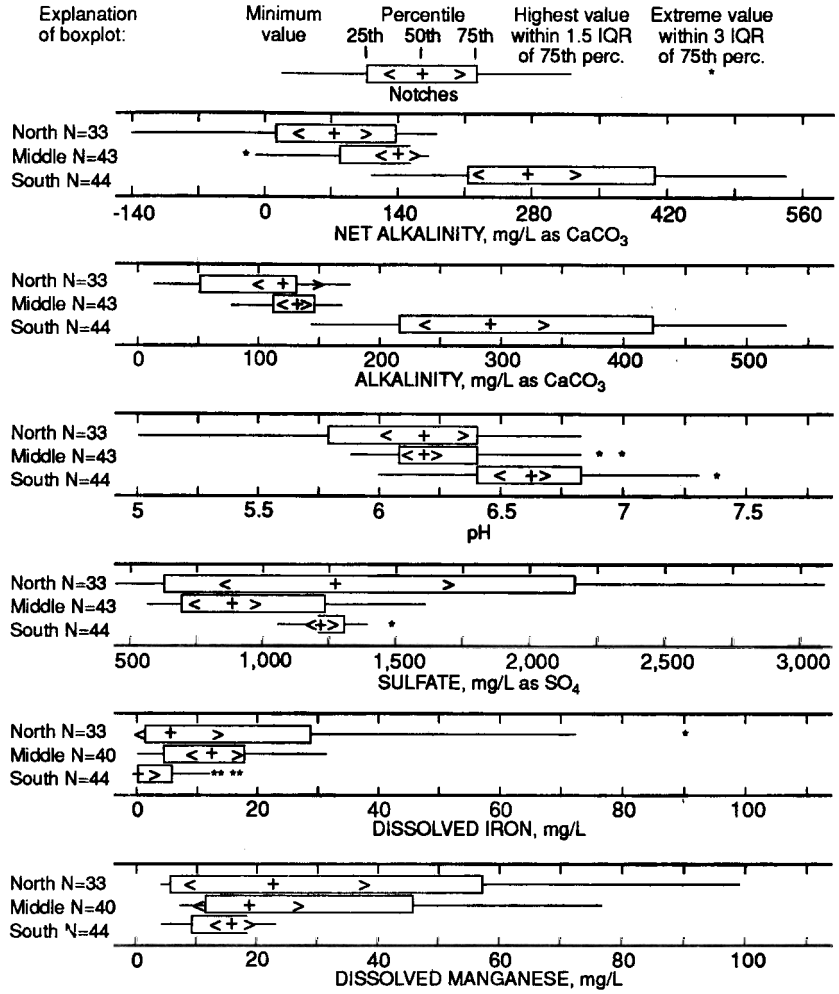

Figure 4. pH and concentrations of net alkalinity, alkalinity, sulfate, iron, and manganese in ground water from spoil. Data for monthly samples collected February-December 1992 from northern area wells N2-1, N3-1, and N4-1, middle area wells M1-1, M2-1, M3-1, and M4-1, and southern area wells S1-1, S2-1, S3-1, and S4-1 (fig. 1). IQR=75th-25th percentile.

Pyrite oxidation is a disequilibrium process that can occur as long as O_2 is available, whereas calcite dissolution and precipitation can achieve equilibrium (Geidel 1979). At this equilibrium condition, alkalinity accumulation will cease or be retarded. The potential for dissolution or precipitation of a solid phase by a pore-water or ground-water solution can be evaluated by use of water-quality data and thermodynamic data to compute a saturation index [SI = log (Q/K), where K is the solubility product constant and Q is the corresponding observed activity product] (Plummer et al. 1976; Stumm and Morgan 1981). Values of SI that are negative (<-0.1), zero (±0.1), or positive (>0.1) indicate the water is undersaturated, saturated, or supersaturated, respectively, with the solid phase. If undersaturated, the water can dissolve the solid phase. If supersaturated, the water cannot dissolve the solid phase, but can potentially precipitate it. Table 3 shows values of SI for calcite, siderite, amorphous $Fe(OH)_3$, and gypsum ($CaSO_4 \cdot 2H_2O$) plus corresponding values of measured pH and major solute concentrations in water samples collected during December 1992.

Table 3. Measured composition and calculated saturation indices for water samples collected during December 1992. [Water-quality constituents in milligrams per liter, except for pH; saturation index, unitless; --, no data; <, less than]

Sample site name[1]	Measured water-quality constituent									Saturation index[2]			
	pH	Ca	Mg	Na	Fe	Mn	Cl	SO_4	Alkalinity, $CaCO_3$	Calcite	Siderite	Fe $(OH)_3$	Gypsum
Well N1-0	6.5	200	78	2.9	7.8	5.6	3	630	150	-0.8	-2.1	2.7	-0.6
Well N1-1	6.7	170	74	2.7	.6	5.9	3	570	130	-.7	-2.3	2.0	-.7
Lys N2-05	6.8	470	270	170.0	<.1	7.4	3	2,300	260	-.1	-2.3	-.7	-.0
Lys N2-15	4.0	490	1200	190.0	1.3	260.0	3	7,600	7	-4.8	-5.5	-5.3	.1
Lys N2-25	6.8	260	200	490.0	1.0	37.0	5	2,100	290	-.3	-.9	.3	-.3
Lys N2-35	6.8	210	120	460.0	.4	33.0	4	1,800	310	-.4	-1.3	-.0	-.4
Well N2-0	6.2	270	140	2.8	10.0	6.8	4	1,100	94	-1.3	-1.2	2.5	-.4
Well N2-1	6.1	320	240	6.4	30.0	59.0	4	2,200	120	-1.3	-.6	2.5	-.2
Lys N3-05	6.6	300	100	140.0	<.1	.3	3	1,300	130	-.7	-3.7	-2.1	-.3
Lys N3-15	6.8	460	400	620.0	<.1	20.0	13	3,500	430	-.0	-3.2	-2.0	.0
Lys N3-25	6.9	410	350	970.0	<.1	62.0	19	3,900	420	-.0	-3.1	-1.9	-.0
Well N3-0	6.8	170	35	3.9	1.5	.3	4	540	310	-.2	-1.5	2.5	-.7
Well N3-1	6.1	180	94	3.5	2.0	3.6	4	680	170	-1.2	-1.6	1.7	-.6
Lys N4-05	5.1	140	55	6.7	<.1	14.0	<1	580	12	-3.4	-5.2	-4.1	-.7
Lys N4-15	3.4	460	630	110.0	14.0	160.0	<1	5,000	0	--	--	-5.4	.1
Lys N4-25	6.7	470	290	98.0	<.1	20.0	6	2,300	230	-.3	-2.8	-1.5	-.0
Well N4-0	6.5	400	180	3.5	32.0	7.9	3	1,200	170	-.6	.0	3.0	-.2
Well N4-1	5.5	205	145	4.7	3.3	18.5	4	1,150	51	-2.4	-2.5	1.1	-.4
Lys M1-05	7.3	160	58	600.0	<.1	4.5	3	1,300	610	.3	-1.9	-.3	-.6
Lys M1-15	6.6	470	340	28.0	<.1	35.0	6	2,600	250	-.4	-2.7	-1.4	.0
Lys M1-25	6.5	510	310	31.0	1.8	14.0	4	2,300	390	-.2	-.8	.2	.0
Well M1-0	7.1	170	35	3.9	1.5	.3	3	270	220	-.0	-2.7	2.8	-.9
Well M1-1	5.9	260	240	25.0	21.0	58.0	5	1,600	130	-1.5	-.9	2.3	-.3
Lys M2-05	6.8	160	50	3.6	<.1	.4	3	520	70	-.9	-2.9	-.8	-.7
Lys M2-15	7.3	530	290	970.0	<.1	3.6	15	3,600	750	.7	-2.4	-.8	.1
Lys M2-25	6.9	55	38	300.0	2.3	10.0	9	670	230	-.8	-.4	1.2	-1.1
Well M2-0	7.5	100	27	6.8	1.0	.2	4	160	240	.2	-2.8	3.0	-1.3
Well M2-1	6.2	200	130	7.0	11.0	15.0	4	950	140	-1.2	-.9	2.5	-.5
Well M3-0	7.1	120	48	6.7	1.9	1.0	3	380	220	-.2	-1.6	2.9	-.9
Well M3-1	6.1	140	70	19.0	.5	7.2	4	750	84	-1.7	-3.5	1.4	-.7
Well M4-0	7.3	150	39	11.0	.9	.7	4	220	270	.2	-2.1	2.8	-1.0
Well M4-1	6.3	160	77	3.7	5.5	12.0	3	770	150	-1.2	-1.2	2.4	-.6
Lys S1-05	6.9	660	240	240.0	<.1	13.0	10	2,100	560	.4	-1.6	-.5	.1
Lys S1-15	6.9	610	220	230.0	1.8	19.0	14	1,600	600	.5	-.2	.9	-.0
Well S1-1	6.7	380	130	11.0	.8	5.1	8	1,300	500	.1	-2.1	2.2	-.2
Lys S2-05	7.0	560	210	550.0	<.1	6.6	39	2,300	750	.6	-1.7	-.4	.0
Lys S2-15	6.9	650	230	260.0	5.7	7.5	110	1,900	730	.5	.3	1.4	.0
Well S2-0	6.8	300	110	28.0	.2	1.7	4	1,300	220	-.3	-4.9	1.6	-.3
Well S2-1	6.3	290	140	7.5	8.2	17.0	4	1,200	230	-.8	-1.7	2.8	-.3
Well S3-0	7.3	110	40	57.0	<.1	.3	4	410	210	-.1	-4.7	1.7	-.9
Well S3-1	6.0	340	120	13.0	.6	16.0	8	1,300	150	-1.2	-2.9	1.4	-.2
Well S4-1	6.3	410	180	9.7	.7	16.0	4	1,400	360	-.5	-2.4	1.7	-.2

[1]Sample site name indicates sample type (well or lysimeter) and location (fig. 1). Well numbers with suffix "-1", screened within horizon of mined coal; "-0", screened below horizon of mined coal. Lysimeter number suffix indicates sample depth, in feet; metric equivalents are "-05" = 1.5 m, "-15" = 4.6 m, "-25" = 7.6 m, and "-35" = 10.7 m.
[2]Saturation index [SI=log (Q/K)] calculated with WATEQF (Plummer et al. 1976) and reported measured data (above), less abundant constituents (including fluoride, nitrate, ammonia, orthophosphate, aluminum, silica, strontium, and zinc), temperature, and measured Eh or computed Eh from Po_2.

Most pore-water samples from shallow depths of 1.5 and 4.6 m, except those from or near pyritic pods (N2-15, N4-15), are saturated or supersaturated with calcite and gypsum and are undersaturated with siderite and $Fe(OH)_3$ (table 3). Underlying ground-water samples from the spoil generally are undersaturated with calcite, siderite, and gypsum, and are supersaturated with $Fe(OH)_3$. These trends indicate that siderite can dissolve throughout the spoil; dissolution of siderite can add alkalinity and promote supersaturation with calcite. In systems at equilibrium with calcite, loss of calcium by ion-exchange for sodium and by precipitation of gypsum can promote calcite dissolution and the production of alkalinity. However, gypsum can precipitate on calcite and reduce its reactive surface area. Because shallow pore waters generally are undersaturated with $Fe(OH)_3$, iron armoring of carbonate minerals is not likely. In deeper zones, where hydrolysis of iron and precipitation of $Fe(OH)_3$ may be active, additional acid and CO_2 can be produced, which can promote the dissolution of carbonate minerals, hence buffering the ground water to be near neutral with median pH values of 6.2-6.6 (fig. 4).

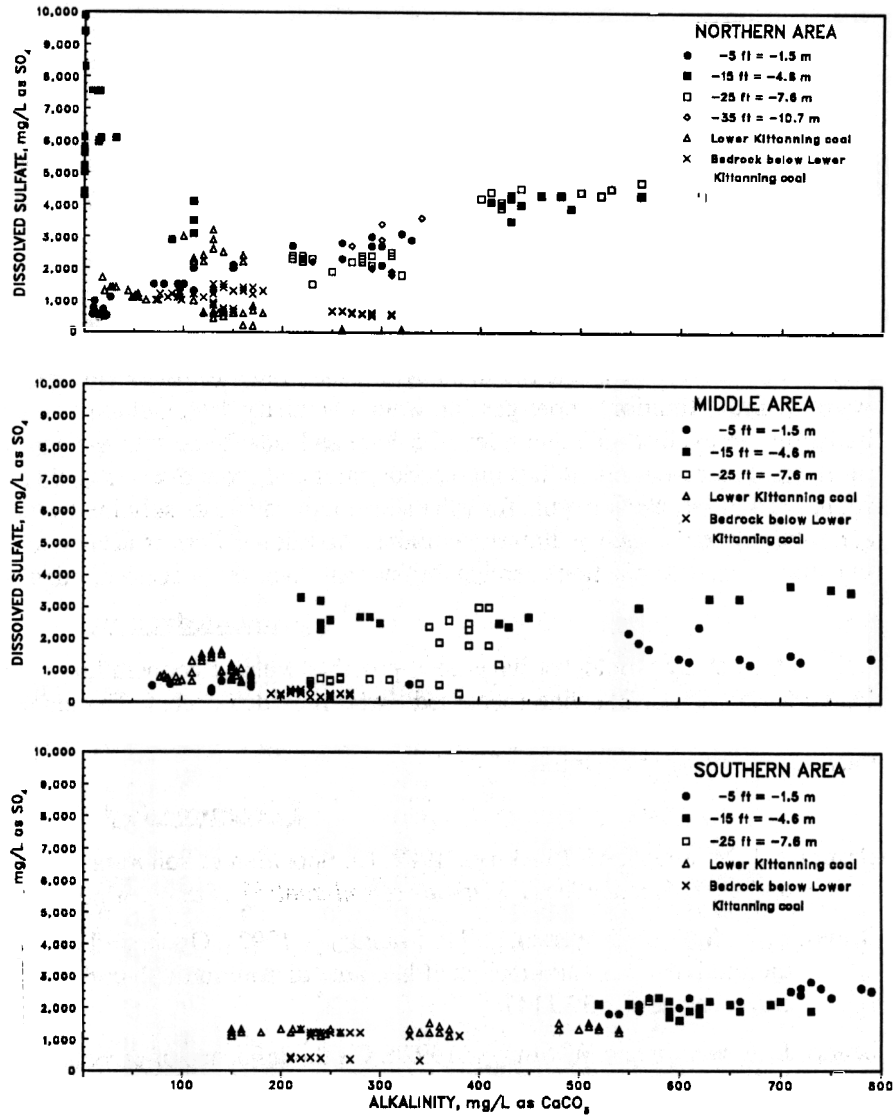

Figure 5. Concentration of sulfate relative to that of alkalinity in pore-water and ground-water samples from spoil and bedrock at a reclaimed coal mine in Clarion County, PA (fig. 1). Data for monthly samples collected February-December 1992 from lysimeters and wells.

Conclusions

A change from dragline to selective-handling mining methods at a surface coal mine in Clarion County, PA, did not have a significant effect on concentrations of sulfate and metals in the ground water because oxidation of pyrite and dissolution of siderite were not abated. Throughout the mine, ground water was extremely mineralized, but it was more alkaline than expected on the basis of overburden chemical data. High concentrations of alkalinity in ground water from spoil indicate that both dragline and selective-handling mining methods may have promoted active dissolution of carbonate minerals. Dissolution of calcite and dolomite can result after pyrite oxidation, as a consequence of acid neutralization, and can be perpetuated by removal of dissolved calcium by ion exchange for sodium and precipitation of gypsum. Even at conditions of calcite supersaturation, increases in concentrations of alkalinity and other solutes can result as a consequence of evapotranspiration and freezing in shallow zones or dissolution of siderite. In addition, dissolved iron and manganese can be produced by dissolution of siderite. However, because calcareous minerals are not abundant in the spoil, the permanence of alkaline conditions at the mine is uncertain.

Although placement of pyritic material above the water table within mine spoil may be an effective means of isolating toxic material from ground water, its placement near the surface contributes to weathering and the consequent mineralization of ground water. Chemical data for pore-gas and water samples from mine spoil indicate that acid production and neutralization reactions are active in localized zones above the water table, particularly in the near-surface zone (0-1.5 m), regardless of the mining method used. High vertical gradients of pore-gas Po_2 in the near-surface zone are independent of relative quantities of pyritic, high-S material in the shallow spoil. This indicates that pyrite oxidation rates may be controlled by rates of O_2 diffusion, or total S concentrations in spoil may not reflect the amount of reactive pyrite. Hence, despite efforts to isolate spoil containing substantial amounts of pyrite, even small amounts of pyritic material may be significant sources of acid if placed in O_2-rich zones near the land surface.

Long-term monitoring, coupled with periodic determinations of quantities and identities of mineral sources of acidity and alkalinity, would aid in an evaluation of the persistence of alkaline conditions and potential for changes in water quality. Additional pore-gas and water-chemistry data, including unsaturated-zone temperature gradients, would be helpful to evaluate relative roles of calcite and siderite dissolution and the relative effect of depth of placement of pyritic and calcareous materials on reaction rates and ground-water quality. Enhanced production of alkalinity in mine spoil, particularly the potential for enhancement of calcite dissolution by cation exchange, can be important in aquifers and other systems, such as limestone drains. Additional work is needed to determine the nature of the minerals active in cation-exchange reactions and conditions that favor the process in mine spoil.

Acknowledgments

This study would not have been possible without cooperation of the property owners, Allan and Mary Jane Yingling and Grace Bashline (deceased), who provided access. The authors wish to thank James Fagley and James Kindell of C&K Coal Company for providing information on mining activities, and staff of the PaDER for conducting monthly sampling at the mine.

Literature Cited

Bremner, J. M. and A. M. Blackmer. 1982. Composition of soil atmospheres. p. 873-901. In Page A. L., R. H. Miller, and D. R. Keeney (eds), *Methods of soil analysis, Part 2*. American Society of Agronomy, Madison, WI.

Bruno, J., W. Stumm, P. Wersin, and F. Brandberg. 1992a. On the influence of carbonate in mineral dissolution--I. The thermodynamics and kinetics of hematite dissolution in bicarbonate solutions at T = 25°C. Geochim. Cosmochim. Acta 56:1139-1147.

Bruno, J., P. Wersin and W. Stumm. 1992b. On the influence of carbonate in mineral dissolution--II. The solubility of $FeCO_3$ (s) at 25°C and 1 atm total pressure. Geochim. Cosmochim. Acta 56:1149-1155.

Chapelle, F. C. and L. L. Knobel. 1985. Stable carbon isotopes of HCO_3^- in the Aquia aquifer, Maryland: Evidence for an isotopically heavy source of CO_2. Ground Water 23(5)592-599.

Claassen, H. C. 1982. Guidelines and techniques for obtaining water samples that accurately represent the water chemistry of an aquifer. U.S. Geol. Surv. Open-File Rep. 82-1024. 49 p.

Cravotta, C. A., III, K. B. C. Brady, M. W. Smith and R. L. Beam. 1990. Effectiveness of the addition of alkaline materials at surface coal mines in preventing or abating acid mine drainage--Part 1. Geochemical considerations. p. 221-225. *In* Proceedings of the 1990 Mining and Reclamation Conference and Exhibition, v. 1. (Charleston, WV, April 23-26, 1990).

Cravotta C. A. III, K. B. C. Brady, L. C. Gustafson-Minnich and M. R. DiMatteo. 1994. Geochemical and geohydrological characteristics of bedrock and spoil from two methods of mining at a reclaimed surface coal mine, Clarion County, PA, USA. Bur. Mines IC (this Proceedings).

Diodato, D. M. and R. R. Parizek. 1988. Unsaturated fluid flow in mine spoil--Investigative methods leading to a quantitative characterization. Bur. Mines IC 9183. p. 104-108.

Foster, M. D. 1950. The origin of high sodium bicarbonate waters in the Atlantic and Gulf Coastal Plains. Geochim. Cosmochim. Acta 1:33-48.

Geidel, G. 1979. Alkaline and acid production potentials of overburden materials--the rate of release. Reclam. Rev. 2:101-107.

Geidel, G. and F. T. Caruccio. 1984. A field evaluation of the selective placement of acidic material within the backfill of a reclaimed coal mine. p. 127-131. *In* 1984 Symposium on Surface Mining Hydrology, Sedimentology and Reclamation. (Univ. KY, Lexington, KY).

Glover, A. D. 1987. Coal resources of Clarion County, Pennsylvania--Part 1. Coal crop lines, mined out areas, and structure contours. PA Geol. Surv. Min. Res. Rep. 92.

Hawkins, J. W. and W. W. Aljoe. 1991. Hydrologic characteristics of a surface mine spoil aquifer. p. 47-58. *In* Proceedings 2nd International Conference on the Abatement of Acidic Drainage. (Montreal, PQ, September 16-18, 1991).

Jaynes, D. B., H. B. Pionke and A. S. Rogowski. 1984a. Acid mine drainage from reclaimed coal strip mines--2. Simulation results of model. Water Resour. Res. 20(2):243-250.

Jaynes, D. B., A. S. Rogowski and H. B. Pionke. 1984b. Acid mine drainage from reclaimed coal strip mines--1. Model description. Water Resour. Res. 20(2):233-242.

Lescinsky, J. B., M. B. Coll, Jr. and R. W. Siwicki. 1993. Water resources data Pennsylvania, water year 1992, volume 3. Ohio River and St. Lawrence River Basins. U.S. Geol. Surv. Water-Data Rep. PA-92-3.

Lusardi, P. J. and P. M. Erickson. 1985. Assessment and reclamation of an abandoned acid-producing strip mine in northern Clarion County, Pennsylvania. p. 313-321. *In* 1985 Symposium on Surface Mining Hydrology, Sedimentology and Reclamation. (Univ. KY, Lexington, KY).

P-Stat. 1989. P-Stat user's manual. 2 vols. P-Stat, Inc., Princeton, NJ.

Parizek, R. R. and B. E. Lane. 1970. Soil-water sampling using pan and deep pressure-vacuum lysimeters. J. Hydrol. 11:1-21.

Phelps, L. B. and L. W. Saperstein. 1982. Spoil modification to minimize the mobilization of formed toxic fluids. p. 593-599. *In* 1982 Symposium on Surface Mining Hydrology, Sedimentology and Reclamation. (Univ. KY, Lexington, KY).

Pionke, H. B. and A. S. Rogowski. 1982. Placement of acid spoil materials. Reclam. Reveg. Res. 1:3-11.

Plummer, L. N., B. L. Jones and A. H. Truesdell. 1976. WATEQF--a FORTRAN IV version of WATEQ, a computer program for calculating chemical equilibrium of natural waters. U.S. Geol. Surv. Water Resour. Inv. 76-13. 70 p.

Skougstad, M. W., M. J. Fishman, L. C. Friedman, D. E. Erdmann and S. S. Duncan (eds.). 1979. Methods for the determination of inorganic substances in water and fluvial sediments. U.S. Geol. Surv. Techniques of Water-Resour. Inv., book 5, ch. A1. 626 p.

Stumm, W. and J. J. Morgan. 1981. *Aquatic chemistry.* Wiley-Interscience, New York. 780 p.

Velleman, P. F. and D. Hoaglin. 1981. *Applications, basics, and computing of exploratory data analysis.* Duxbury Press, Boston, MA. 354 p.

Williams, E. G., A. W. Rose, R. R. Parizek and S. A. Waters. 1982. Factors controlling the generation of acid mine drainage: PA State Univ., University Park, PA, Final Report on Research Grant G5105086. 256 p.

Wood, W. W. 1976. Guidelines for collection and field analysis of ground-water samples for selected unstable constituents. U.S. Geol. Surv. Techniques of Water-Resour. Inv., book 1, ch. D2. 24 p.

ALKALINE OVERBURDEN ADDITION TO ACID-PRODUCING MATERIALS TO PREVENT ACID MINE DRAINAGE[1]

Jeff Skousen and Glenn Larew[2]

Abstract: Alkaline addition to acid-producing overburdens during surface mining and reclamation has shown variable results in improving postmining water quality. This paper describes a mining operation where acid mine drainage from an abandoned deep mine was eliminated by surface remining the deep mine workings and adding alkaline material during reclamation. About 15,000 mt/ha (6,600 st/ac) of alkaline shale were hauled to the remined site and placed on the pit floor and also on top of toxic material placed "high and dry" in the backfill. No acid mine drainage has come from the site during the past 2 yrs since reclamation. The cost of hauling the alkaline material to the site was about $9,880/ha ($4,000/ac). Chemical treatment costs of acid mine drainage previously coming from the site before remining were projected to be $8,000 to $15,000/yr depending on the chemical reagent.

Additional Key Words: acid-base account, coal spoil, overburden analysis, remining, special handling.

Introduction

Accurate prediction of acid mine drainage (AMD) before surface mining requires a complete understanding of many components at a mine site. Three of the most important factors are 1) overburden geochemistry, 2) the postmining hydrology of the site, and 3) method and precision of overburden handling and placement in the backfill during reclamation.

Overburden Geochemistry

Premining analyses of soils, overburden, and the coal pavement are required by law to ascertain the physical and chemical characteristics of the strata above and immediately below the coal bed. Overburden analysis and characterization provides important information about overburden layers that are acid toxic, potentially acid-producing, neutral, potentially alkaline-producing, or alkaline. Overburden analysis for surface mining begins with acid-base accounting. This analytical technique provides a simple, relatively inexpensive, and consistent procedure to evaluate overburdens. It balances potential acidity (based on sulfur content) against total neutralizers (mostly carbonates, measured by reaction with hydrochloric acid) in an overburden sample. Samples containing more acid potential than alkaline material for neutralization result in values in the "max needed" column, while the reverse causes "excess" values (Skousen et al. 1990). On rock layers where low values in max needed or excess columns give little information relative to the chemical production potential of the rock, it may be helpful to subject the overburden sample to leaching/weathering analyses. These additional analyses provide more information than that given by the acid-base account and often help designate how that particular rock may react in a backfill. Identification of the chemical production potential of overburden layers aids in developing overburden handling and placement plans. It is then critical for each operator to carefully follow the overburden handling and placement prescription based on overburden characterization for the particular site.

---

[1]Paper presented at the International Land Reclamation and Mine Drainage Conference and the Third International Conference on the Abatement of Acidic Drainage, Pittsburgh, PA, April 24-29, 1994.

[2]Jeff Skousen, Associate Professor and Extension Reclamation Specialist, West Virginia University, Morgantown, WV, USA; Glenn Larew, President, Coaltrain Corporation, Reedsville, WV, USA.

Spoil Hydrology

The hydrology of a backfill and its effect on AMD are very complex, and research on the movement of water into and through a mine backfill has provided little information on how to control AMD. The movement of water over the surface and into and through the backfill is not well understood, but it is a significant factor in preventing and controlling AMD. Generally, the porosity and hydraulic conductivity of the materials in a backfill are greater than those of the consolidated rock overburden that existed before mining, and changes in flow patterns and rates should be expected after mining (Caruccio and Geidel 1989). Often, the fine-grained topsoil placed over the backfill conducts water more slowly than the underlying coarser material, and thus the topsoil may determine the amount and rate of water movement into the backfill (Guebert and Gardner 1992). As water moves into the coarse material in the backfill, it follows the path of least resistance, flowing through the more permeable acid sandstones and around the calcareous shales, and continues downward until it encounters a barrier, the pavement, or other compacted or slowly permeable layer. Water does not move uniformly through the backfill by a consistent wetting front. The chemistry of the water emanating from the backfill will reflect only the rock types encountered in the water flow path and will not be related to the geochemistry of the total overburden (Ziemkiewicz and Skousen 1992).

Overburden Handling and Placement

The prevailing approach to control AMD in the Appalachian Coal Region of the U.S. is to keep water away from pyritic material. Recommendations have focused on segregating and placing acid-producing materials on top of a 1- to 2-m (4- to 6-ft) layer of nontoxic material on the pavement, placing the toxic material above the water table, and then treating, compacting, and covering it with a clay cap or other type of sealant material to reduce surface water infiltration into this material (Skousen et al. 1987). Diverting surface water above the site to decrease the amount of water entering the backfill is also recommended.

In areas where limestone or other alkaline layers occur in the overburden, blending of overburden materials may be used where the alkaline materials are capable of neutralizing the acidic materials. The topsoil should be limed to neutralize any residual acidity and to raise the pH for vegetation establishment. Water courses above the mined areas with low mineral acidity can also be limed to improve water quality.

Alkaline Addition

Importing alkaline materials to mine sites to offset the acid-producing potential of overburdens has shown variable success (Brady et al. 1990, Hamric 1993, Ziemkiewicz and Skousen 1993). On some sites where this practice has been implemented, AMD has been reduced (Brady et al. 1990). For example, Meek (1991) documented that selective placement of overburden with alkaline addition reduced AMD production 40 to 50%. However, none of the AMD prevention techniques employed on Meek's sites were completely successful in eliminating the production of AMD. In fact, the greatest reduction of AMD (70%) was achieved on his sites with selective placement of overburden and covering the acid-producing material with a PVC liner.

The objective of this study was to evaluate the effectiveness of importing and adding alkaline shale overburden as an amendment to acid-producing materials to prevent AMD. The costs of treating AMD were compared to the costs of adding alkaline material to assess the economic feasibility of alkaline addition during surface mining and reclamation.

Site Descriptions and Methods

Coaltrain Corp. mines coal from the Upper Freeport, Bakerstown, and Pittsburgh beds (Pennsylvanian System, Allegheny and Conemaugh Groups) in northern West Virginia. The company is a small, family-run operation employing 12 to 18 men. Coaltrain operations have worked at two locations concurrently. The first operation has generally mined in the Bakerstown coal bed, while the other was either a Pittsburgh or Upper Freeport coal remining

operation. Because of the alkaline nature of Bakerstown coal overburden, the most alkaline portions of this overburden have been used as an alkaline amendment to the potentially acid-producing Pittsburgh and Freeport coal overburdens.

Bakerstown Operation

In 1986, Coaltrain received a permit to mine 28 ha (70 ac) of land underlain by the Bakerstown coal near Masontown, WV. The premining land use was pasture, and the surrounding land use was predominately pasture and hayland for cattle. The overburden was characterized by 9 m (30 ft) of gray shale, 7.6 m (25 ft) of alkaline red shale and limestone, and 4.5 m (15 ft) of fractured sandstone (table 1). The alkaline red shale on the site correlates to the Pittsburgh Red Shale described by Hennen and Reger (1913), and contains nuggets of impure limestone and is generally red or purple in color. Due to this red shale in the overburden, no AMD has been documented with surface mining of the Bakerstown coal in this area. In fact, disturbance of this overburden material has often improved the water quality of surrounding streams to pH values greater than 7.5.

Contour haulback mining methods were used on the site. The overburden was blasted by the use of an emulsion explosive because of the high water content of the overburden. A Clark 475C loader (12-cu-yd bucket) was employed for overburden removal into two International 350 Pay Haulers, each carrying approximately 50 st of rock. A Fiat Allis HD 31 bulldozer was used for regrading and backfilling the site. The Bakerstown coal was extracted using a 7-cu-yd front end loader and hauled by truck to a nearby coal stockpile facility where it was mixed with other coals. Annual coal production at the site between 1988 and 1991 averaged 55,000 mt/yr (60,000 st/yr). No water quality problems were experienced during surface mining. Approximately one-fourth of the alkaline red shale in the overburden was separately loaded and hauled to the nearby Upper Freeport operation.

Upper Freeport Operation

The Upper Freeport job was located about 1.6 km (1 mile) northwest of the Bakerstown site. The site was a surface remining operation which daylighted abandoned deep mines. Little topsoil was available on the site; however, the small amount found on the site was saved and stockpiled. The overburden was characteristic of the Upper Freeport coal with respect to rock type. Approximately 18 m (60 ft) of massive and fractured sandstones along with 3 m (10 ft) of gray shale were present. According to data from the acid-base account, the overburden on this site had more neutralization potential (NP) than many other Upper Freeport overburdens in this area (table 2). However, AMD from an old deep mine on this site and other surrounding abandoned deep mines had contaminated the receiving stream, Mountain Run, for decades and verified the acid-producing potential of the coal and overburden in this area (table 3). Knowing of the extreme alkaline material nearby on the Bakerstown job, Coaltrain decided to remove the old stumps of Upper Freeport coal by remining and eliminate acid mine drainage by importing alkaline material from the Bakerstown job to this Freeport site.

Selective handling and placement of acid-producing materials along with importation and placement of alkaline material on the pavement was deemed an essential element of the mining and reclamation plan. Compaction of the acid-producing material would reduce water infiltration and oxygen diffusion into the material, and covering the acid material with alkaline material should reduce the potential of AMD production. With proper identification, handling, and placement of the acid-producing materials, Coaltrain expected that AMD would not be a problem and the old deep mine discharges would be eliminated.

The permit was received in March 1990. One overburden cut averaging 46 m (150 ft) back into the deep mine was taken. Slope at the site was steep; therefore, only one cut was taken before the overburden became more than 21 m (70 ft) thick. The overburden was blasted on 4- to 5-m (16- to 18-ft) centers with ANFO. Blasting was conducted to fracture the rock and shale to facilitate removal with dozers and loaders. However, blasting was controlled so that the acid-producing material was not pulverized. This process was important because large chunks of acid material expose less surface area for weathering and acid generation. The large chunks of acid material also

Table 1. Partial acid-base account of the Bakerstown overburden showing the alkaline nature of the red shale separately loaded and hauled to the Upper Freeport site for alkaline addition.

Sample	Depth m	Strata Thick m	Rock Type	Fizz	S %	Max %S g/kg	NP g/kg	Max Needed g/kg	Excess g/kg	Paste pH
1	0-1.5	1.5	SH	5	0.001	0.1	150.0	---	149.1	7.9
2	1.5-3	1.5	SH	5	0.002	0.1	213.1	---	213.0	8.1
3	3-4.5	1.5	SH	5	<0.001	0.1	569.2	---	569.1	8.3
4	4.5-6	1.5	SH	5	<0.001	0.1	335.9	---	335.8	8.3
5	6-7.5	1.5	SH	5	0.010	0.3	119.8	---	119.5	8.2

Table 2. Acid-base account of the Upper Freeport overburden.

Sample	Depth m	Strata Thick m	Rock Type	Fizz	S %	Max %S g/kg	NP g/kg	Max Needed g/kg	Excess g/kg	Paste pH
1	0-1.5	1.5	Soil	0	0.007	0.2	1.6	---	1.4	4.4
2	1.5-3	1.5	SS	0	0.013	0.4	1.9	---	1.5	4.9
3	3-4.5	1.5	SS	0	0.008	0.2	2.1	---	1.9	5.7
4	4.5-6	1.5	SS	0	<0.001	0.1	2.6	---	2.5	6.4
5	6-7.5	1.5	SS	2	<0.001	0.1	10.6	---	10.5	8.0
6	7.5-9	1.5	SS	0	<0.001	0.1	3.8	---	3.7	7.2
7	9-10.5	1.5	SS	0	0.042	1.3	3.0	---	1.7	6.8
8	10.5-12	1.5	SS	0	0.280	8.7	2.6	6.1	---	6.6
9	12-13.5	1.5	SH	3	0.001	0.1	63.3	---	63.2	7.7
10	13.5-15	1.5	SS-SH	0	0.393	12.3	21.4	---	9.1	7.3
11	15-16.5	1.5	SH	0	0.277	8.7	9.7	---	1.0	7.7
12	16.5-18	1.5	SS-SH	0	0.103	3.2	27.6	---	24.4	7.7
13	18-19.5	1.5	SH-SS	0	1.050	32.8	30.3	2.5	---	7.2
14	19.5-22	2.5	COAL	0	2.160	67.5	1.6	65.9	---	4.6
15	22-23.5	1.5	SH	0	0.173	5.4	6.3	---	0.9	7.0

required less alkaline material for neutralization. The alkaline material was a friable shale that weathered very rapidly, reacted quickly, thereby releasing nearly all of its neutralizing capability.

The overburden was removed with an International 400 loader and two International 50-st trucks. The acid material was compacted and covered within a day or two of its excavation to prevent oxidation and leaching. Coal was mined by a 7-cu-yd loader in two lifts, loaded into trucks, and taken to the coal stockpile. A black shale binder of 7- to 15-cm (3- to 6-in) thick in the coal was removed and handled separately. Once the bottom coal was loaded from the Upper Freeport bed, about 1 m (3 ft) of alkaline red shale from the Bakerstown job was placed on the Upper Freeport coal pavement and covered with overburden. As trucks hauled coal out, alkaline shale was backhauled in. The pit floor was covered with alkaline shale the same day coal was removed.

The black shale binder between the breast and bottom coal in the Upper Freeport coal bed was placed about 6 m (20 ft) above the pavement and compacted. It was then covered with 0.3 m (1 ft) of alkaline red shale from the Bakerstown job. These layers were then compacted by bulldozers and trucks. Backfilling continued until approximate original contour (AOC) was reached, and topsoil was replaced on the surface. Several inches of alkaline shale were also spread on the surface and mixed with the topsoil.

Results and Discussion

The amount of alkaline material imported to the Upper Freeport site from the Bakerstown job was about 15,000 mt/ha (6,600 st/ac). This amount represented about 1 m (3 ft) of alkaline material if it was spread evenly over 0.4 ha (1 ac) of mined area. Using the data from the acid-base account, the alkaline material from the Bakerstown job had NP values greater than 300 mt $CaCO_3$ equivalent per 1000 mt material (or g/kg). The shale binder in the Upper Freeport coal bed showed a deficiency (or max needed) of about 60 g/kg to neutralize the acid created from pyrite oxidation. Theoretically, 0.3 m (1 ft) of Bakerstown alkaline material (300 g/kg excess) should neutralize the acidity generated from 1.5 m (5 ft) of Upper Freeport toxic material (60 g/kg max needed) if the particle size of the two materials is similar.

In reality, the Upper Freeport overburden contained only 15 cm (6 in) of toxic material (60 g/kg max needed) and 6 m (20 ft) of potentially acid-producing material (ranging from 6 g/kg max needed to 5 g/kg excess). Based on the blasting technique, the particle size of the materials favored the alkaline material. When these items are all considered together, a large safety factor was built in by importing 1 to 1.3 m (3 to 4 ft) of alkaline material from the Bakerstown job when only about 0.3 m (1 ft) was theoretically needed.

The quantity of alkaline material transported to the Upper Freeport job represented a cost of about $0.55/mt ($0.50/st) of coal removed. An average of about 18,000 mt/ha coal (8,000 st/ac) was removed, making the cost of hauling the alkaline material to the site around $10,000/ha ($4,000/ac). This cost only included hauling the material from the Bakerstown job to the Upper Freeport site. Handling and compaction costs were integrated into the method of mining and done in concurrence with normal mining. Therefore with a little advance planning and coordination, these costs were minimal.

Water quality from the deep mine before remining averaged about pH 3.7 and 75 mg/L total acidity (table 3). After the site was remined and reclaimed, water collected in a pond located immediately below the previous old deep mine discharge averaged a pH above 7.0 (table 3). No acidity has been measured in water samples, and iron and manganese in the water have always been within the U.S. Environmental Protection Agency's National Pollutant Discharge Elimination System (U.S. EPA NPDES) effluent limits over a 2-yr period. Chemical treatment of the water is unnessary.

Unfortunately, the flow and low acidity (95 L/min and 75 mg/L) of the AMD from the deep mine was not a significant contributor to the total acidity in Mountain Run (table 4). The quantity of water in the stream was 20 to 50 times greater than the flow from the deep mine and improving the quality of the water coming from the remined

Table 3. Water quality of the deep mine discharge before mining (data before 4/91) and from ponds after mining on the Upper Freeport operation.

Date	pH	Total Acidity mg/L	Iron mg/L	Manganese mg/L	Suspended Solids mg/L
11/89	3.7	73.5	2.65	0.40	<1
12/89	3.8	88.2	3.54	0.60	4
1/90	3.7	68.0	3.00	1.00	14
4/91	6.7	<1	<.05	0.02	
11/91	7.3	<1	.31	0.40	2
3/92	7.5	<1	<.05	0.24	<1
6/92	7.8	<1	<.05	0.03	<1
9/92	7.4	<1	<.05	0.04	3
12/92	7.5	<1	<.05	0.02	3
3/93	7.7	<1	<.05	<0.01	9
4/93	7.5	<1	.10	0.48	4
6/93	7.4	<1	<.05	0.07	1

Table 4 Water quality of Mountain Run, the stream that receives acid mine drainage from abandoned deep mines before remining (data before Mar 90) and after remining (data after 1/90).

Date	Flow L/m	pH	Total Acidity mg/L	Iron mg/L	Manganese mg/L	Suspended Solids mg/L
11/89	1,064	3.5	92.0	0.36	0.34	<1
12/89	1,216	3.4	78.0	2.67	0.41	<1
1/90	1,349	3.5	48.0	1.26	0.28	<1
9/93	552	3.6	77.0	0.30	0.88	4
12/93	608	3.5	64.0	2.89	0.41	13

Table 5 Annual and 20-yr water treatment costs with various chemicals of a 95-L/m (25-gpm) flow and 75-mg/l acidity.

Chemical	Annual cost	20-yr cost
Caustic Soda	8,489	169,780
Soda Ash Briquettes	15,278	305,560
Ammonia	9,712	194,240
Hydrated Lime	14,545	290,900

site showed no overall improvement in the quality of Mountain Run. In fact between January 1990 and September 1993, the flow in Mountain Run appears to have decreased by half (roughly 500 L/min), and reducing the flow from the remined site (averaging around 25 L/min) would not have decreased the stream flow by that much. No other active mining jobs are operating in the watershed above the Coaltrain Operation, so it is not clear why the flow has decreased. Other remining permits are being sought by Coaltrain to continue to daylight surrounding abandoned deep mines. Only when more of the deep mines with acid discharges are remined and reclaimed will a significant improvement in Mountain Run's water quality be realized.

Based on average premining water flows and analyses of the deep mine discharge on the site, the chemical cost for treating AMD on this site would be expected to range from $8,000 to $15,000/yr (table 5). These costs were calculated from interviews with mine operators and costs associated with chemical reagent, electricity, labor, and equipment installation, repair, and salvage costs (Skousen et al. 1993). Without eliminating AMD through alkaline addition (and not accounting for the other attending liabilities associated with water treatment and permitting problems), the cost of treatment would range from $169,000 to $300,000 over a 20-yr period.

Literature Cited

Brady, K., M. Smith, R. Beam, and C. Cravotta. 1990. Effectiveness of the addition of alkaline materials at surface coal mines in preventing or abating acid mine drainage: part 2. mine site case studies. p. 227-241. In: Proceedings of the Mining and Reclamation Conference. (Charleston, WV, April 23-26, 1990).

Caruccio, F., and G. Geidel. 1989. Water management strategies in abating acid mine drainage - Is water diversion really beneficial? In: 1989 Multinational Conference on Mine Planning and Design. (Lexington, KY, May 23-26, 1989).

Guebert, M., and T. Gardner. 1992. Macropore flow effect on infiltration, throughflow, and surface runoff on a reclaimed surface-mined watershed. p. 91-100. In: Proceedings of the International Symposium: Land Reclamation. (Nashville, TN, December 12-15, 1992).

Hamric, R. 1993. Utilization of CFB ash in reclamation to prevent post-mining AMD. In: Proceedings of the 14th West Virginia Surface Mine Drainage Task Force Symposium. (Morgantown, WV, April 27-28, 1993).

Hennen, R., and D. Reger. 1913. Geological report for Marion, Monongalia, and Taylor Counties, West Virginia. West Virginia Geological Survey, Morgantown, WV.

Meek, A. 1991. Evaluation of acid preventative techniques used in surface mining. p. 167-172. In: Environmental Management for the 1990's. p. 167-172. In: Environmental Management for the 1990's. AIME. (Denver, CO, February 25-28, 1991).

Skousen, J., R. Lilly, and T. Hilton. 1993. Special chemicals for treating acid mine drainage. Green Lands 23(3): 34-41.

Skousen, J., J. Sencindiver, and R. Smith. 1987. A review of procedures for surface mining and reclamation in areas with acid-producing materials. Publ. EWRC871, West Virginia University, Morgantown, WV.

Skousen, J., R. Smith, and J. Sencindiver. 1990. The development of the acid-base account. Green Lands 20(1): 32-37.

Ziemkiewicz, P., and J. Skousen. 1992. Prevention of acid mine drainage by alkaline addition. In: Proceedings of the 13th West Virginia Surface Mine Drainage Task Force Symposium. (Morgantown, WV, April 8-9, 1992).

CONCENTRATED ALKALINE RECHARGE POOLS FOR ACID SEEP ABATEMENT: PRINCIPLES, DESIGN,CONSTRUCTION AND PERFORMANCE[1]

Jack R. Nawrot[2], Pat S. Conley[2], and James E. Sandusky[3]

Abstract: Concentrated alkaline recharge pools have been constructed above previously soil covered acid gob at the Peabody Will Scarlet Mine to abate acid seeps. Preliminary monitoring results (1989-1994) from a concentrated alkaline recharge pool demonstration project in the Pit 4 area have documented a 45 to 90% reduction in acidity in the principal recharge pool groundwater zone. A 23% reduction in acidity has occurred in the primary seep located downslope from the alkaline recharge pools. The initial improvements in water quality are seen as a positive indication that groundwater acidity will decrease further and amelioration of the acid seep will continue.

Additional Key Words: acid seeps, mine refuse, acid mine drainage, alkaline recharge.

Introduction

Covering acid producing coal refuse with 4-ft of soil cover does not preclude pyrite oxidation under the soil cover. When pyrite oxidation does occur overlying soil covers may become acidified and acid seeps may be generated following several seasons of rainfall infiltration and flushing cycles. Burial of potentially acid producing coal waste in a zone of fluctuating groundwater elevations is conducive to chronic acid seep generation when the upslope groundwater chemistry has insufficient alkalinity to neutralize downslope acid groundwater pools generated by the buried refuse. Soil covering after limestone is applied in sufficient quantities to overcome the potential acidity of refuse, or limestone amendment and direct seeding are effective reclamation techniques that enhance long-term vegetation success and establish a favorable acid-base balance (Warburton et al. 1987, Nawrot et al. 1991). These reclamation techniques can prevent the formation of acid seeps and preclude the need for acid mine drainage treatment.

However, after more than three decades of research, treatment of symptoms rather than elimination of the cause has been the focus of much acid mine drainage research (Nawrot et al 1988, Caruccio 1988). In-situ abatement technology (Caruccio et al. 1984, Snyder and Caruccio 1988) can minimize or eliminate acid seeps through an alkaline-loading process, effectively altering the geochemistry of upslope groundwater recharge zones (Caruccio 1968, Geidel 1979). Alkaline groundwater loading is similar to reclamation practices designed to restore (replace depleted neutralization potential) and enhance (establish excess alkaline surface soil zones) alkalinity in surface zones of coarse refuse (Nawrot et al. 1986, Warburton et al. 1987, Sandusky and Nawrot 1992), slurry (Nawrot and Warburton 1987), and pre-law acid spoils (Nawrot et al. 1988). However, constructing zones of excess alkalinity to recharge groundwater increases the potential effectiveness of the reclamation process by directly addressing key physical (topography), geochemical (recharge zone alkalinity), and hydrologic (groundwater quantity and quality) factors.

---

[1]Paper presented at the International Land Reclamation and Mine Drainage Conference and the Third International Conference on the Abatement of Acidic Drainage, Pittsburgh, PA, April 24-29, 1994.

[2]Jack R. Nawrot, Associate Scientist, and Pat S. Conley, Researcher II, Cooperative Wildlife Research Laboratory, Southern Illinois University, Carbondale, IL, USA.

[3]James E. Sandusky, Reclamation Manager, Peabody Coal Company, Stonefort, IL, USA

When chronic acid seeps occur it is generally too late and too expensive to remove or reposition the acid-producing materials. An acid seep is an "after-the-fact" verification of an imbalance in the acid-base equilibrium of the groundwater and/or overburden (Figure 1). Establishment of net alkalinity must be accomplished below the surface zone (0-23 cm) of mechanical neutralization amendment. When measures to prevent acid seeps are unsuccessful, abatement techniques must be implemented. Acid seep treatment is undesirable due to high costs and the need for a perpetual neutralization facility. Alkaline groundwater recharge may be the only practical reclamation technique for acid seep abatement (Figure 2). Although instant success cannot be expected, alkaline recharge strategies may be the only long-term and cost-effective approach to reverse those geochemical processes (i.e., subsurface acidification) that have taken 20-25 years to generate acid seeps. Abatement techniques using an in-situ neutralization approach can be beneficial if site-specific conditions permit alkaline loading of upslope groundwater recharge zones.

Construction of concentrated alkaline recharge pools is a reclamation approach (previously demonstrated by Caruccio et al. 1984) being implemented and monitored at the Peabody Will Scarlet Mine located in Williamson County, Illinois. The Will Scarlet Mine "Old Works" (pre-law) area encompasses approximately 970 ha of acid gob and slurry. The Pit 4 recharge pool demonstration area includes more than 8 ha of pre-law gob that had been disposed of in a final cut and its associated inclines. Following disposal, groundwater recharge eventually (~25 years) increased water elevations to within 0.5 to 1 m of the surface of the buried refuse. Seasonally fluctuating ground water levels produced ideal conditions for pyrite oxidation and downslope acid seep generation. Without some form of acid seep abatement, the seeps in the Pit 4 area would require perpetual treatment. The primary objective of the Will Scarlet Concentrated Alkaline Recharge Pool (CARP) project was to implement a full-scale field demonstration of the alkaline groundwater recharge approach to ameliorate the effects of a chronic acid seep. CARP is based on the principle of alkaline enhancement of groundwater recharge zones located directly above and upslope of buried refuse (Figures 1 and 2). Maximization of alkaline groundwater recharge zones generates upslope alkaline environments that alter the groundwater chemistry and geochemical acid generating mechanism within the buried refuse zone.

The Will Scarlet CARP project evaluated recharge pool construction techniques and monitored the effects of alkaline surface loading on a shallow groundwater recharge area using seasonally inundated alkaline recharge zones constructed upslope of the subsurface acid generation zone (Figure 2). This field demonstration was supported by the U.S. Bureau of Mines-National Mined Land Reclamation Center, the Illinois Abandoned Mine Lands Reclamation Council, and Peabody Coal Company.

Research Methods

The Pit 4 area of the Peabody Will Scarlet Mine was selected as a reclamation demonstration site due to the presence of chronic acid seeps (Figure 3). Pre-project (January 1989) sampling was conducted to identify acid concentration and flow rates. Aerial photo sequences (i.e., 1958 through 1988), topographic maps, and mine operation maps were used to identify coal waste backfill areas contributing to the acid groundwater seeps.

Construction of the Pit 4 concentrated alkaline recharge pools began July 1989. Berms were constructed to impede surface runoff and promote groundwater infiltration within recharge zones (0.6 to 1.2 ha). Alkaline amendments for neutralization loading consisted of a hydrated lime sludge by-product of acetylene gas production (Table 1). The highly reactive (saturated solution pH of 10.4) hydrated lime sludge contained 30-35% moisture prior to drying. To promote maximum alkaline concentrations within the recharge pools, and enhance infiltration, the hydrated lime sludge (applied @ 618 t/ha in September 1989) was rough-disked in the upper 15-23 cm of the spoil terraces. When lime sludge became limited during late summer 1989, Code H (Mississippi Lime Co., Alton, IL) was used to complete all recharge pools.

Table 1. Neutralization treatment potential of selected alkaline waste materials evaluated[1] for alkaline recharge pool amendment.

Waste Product	AMD Treatment Potential (lbs/100 gal/1000 ppm)	Calcium Carbonate Equivalent (% $CaCO_3$)
Acetylene gas sludge	1.04 lbs/100 gal/1000 ppm	121.0
Cement kiln dust (Joppa)	6.25 lbs/100 gal/1000 ppm	79.3
Code H	2.08 lbs/100 gal/1000 ppm	130.0
Hydrated Lime[2]	1.00 lbs/100 gal/1000 ppm	135.0

[1]Determinations were made by direct addition of pulverized solid (0.05-0.1g increments) to 100 ml of a known-acidity solution. The pH of the solution was monitored to an endpoint of 7.0 and total additions recorded (grams). The total weight of each alkaline material required to neutralize 100 gallons of 1,000 ppm $CaCO_3$ (Acidity) solution was then calculated.

[2]The hydrated lime treatment potential reflects the AMD treatment "standard" and was not determined by above methods.

Recharge pools constructed during 1990 consisted of a series of five checkdams perpendicular to the surface drainage pattern of a soil covered refuse area. Checkdams were constructed of existing soil/spoil cover materials from above the buried refuse as well as adjacent spoil materials. Excavation of soil materials for the checkdam construction decreased cover thickness above the shallow buried refuse, thereby decreasing the distance (5-8 cm) and time required for alkaline recharge pool water to infiltrate and intercept the acid groundwater zone within the buried refuse. Downslope perimeters of recharge pools were purposely excavated to the surface of, or within 8 to 13 cm of the acid groundwater pool to maximize mixing of alkaline and acid groundwater. Three checkdams were constructed to impound a maximum of 1.5 to 1.8 m of water at the toe of the deepest recharge pool checkdam; other recharge pools supported temporary inundation ranging in depth from 15 to 56 cm.

Code H was delivered in pneumatic tank trucks and applied upslope of checkdams within each recharge pool at a rate of 618 t/ha. Two additional recharge pools constructed during 1992 incorporated a design change to increase surface water infiltration and groundwater recharge. Rip-rap filled infiltration "chimneys" (1-m wide x 1.5-m long x 1.8-m deep) that extended into the buried refuse were installed at the inside toe of each embankment. Three to five chimneys were installed within each recharge pool. Maximizing the surface acreage for collection and infiltration of watershed runoff was considered an important design consideration to more effectively stabilize and moderate seasonal extremes (volume and alkaline concentration) of alkaline recharge events and groundwater response.

Groundwater/Seep Monitoring

Groundwater was monitored monthly from a network of 11 piezometers installed in the Pit 4 recharge area (Figure 3). Groundwater wells were constructed of 5.1 cm Brainard-Kilman Triloc® slotted (0.25 cm slot size) PVC threaded wellpipe. Wellpipes were installed in backfilled overburden pits to a depth of 1.8 to 2.4 m below the surface. Wells were bailed prior to monthly monitoring. Laboratory analyses included pH, acidity, alkalinity, total iron, conductivity, and sulfates.

Results and Discussion

Seep and Overburden Characterization

Preconstruction (January 1989) sampling of the primary Pit 4 acid seep (Seep 1) identified low pH (pH $\leq$3.6), high sulfates (5170 mg/L), and total iron (820 mg/L). Flow exceeded 280 L/min. Seasonal increases in excess of 450 L/min. have been recorded following early spring (1990, 1991, 1992, and 1993) rains. Seasonal

decreases in groundwater elevation and associated seep flows were recorded during mid- to late-summer throughout the four year monitoring program. Seasonal low flow values of < 150 L/min. were recorded for Seep 1 during July 1991. Extremely heterogenous composition of graded and backfilled overburden materials further contributed to the "pseudo-karst" conditions in the Pit 4 seep generating area. Large sandstone boulders, weathered shales, and clay lenses associated with graded and ungraded spoilbanks produced an overburden matrix conducive to fracture flow zones of high groundwater velocities [$2x10^{-2}$ cm/sec (40 ft/day)] and isolated zones of compacted, less permeable strata with significantly lower groundwater velocities [$4x10^{-3}$ cm/sec (2 in/day)]. Extremes of groundwater flow as well as seasonal fluctuations in recharge events and seep flow response were factors that were considered when locating, designing and constructing recharge pools.

The 6 ha coarse refuse area located in the final cut and incline above seep 1 consisted of extremely acid (pH $\leq$3.1) black shales characterized by pyritic sulfur values of 3.2 to 9 percent. Refuse was covered by less than 1m of sparsely vegetated (<60% cover) clay, shale, and sandstone spoil materials. Water table elevations within the buried refuse area fluctuated seasonally and ranged from 50 to 200 cm from the soil cover surface.

Seep Monitoring

Water quality monitoring included pre-construction baseline characterization of acid seeps and groundwater in the Pit 4 alkaline recharge demonstration area. Initial monitoring (January-September 1989) of Seep 1 water quality documented baseline acid conditions prior to neutralization amendment. Seep 1 was characterized by chronically low pH (<4.0) and high acidity (>2,500 mg/L $CaCO_3$). High concentrations of iron and sulfates also typified pre-treatment (before August 1989) acid groundwater and seeps.

Seep 1 water quality reflected groundwater chemistry in the well-established acid generating system of the upslope Pit 4 buried refuse area. Although Seep 1 exhibits seasonal fluctuations in water quality (Figure 4), the consistent trend of decreasing acidity from June 1990 through January 1994 suggests that upslope alkaline amelioration of the Pit 4 recharge area is beginning to be effective. A reduction in total acidity of more than 800 ppm (23% reduction in acid load) was recorded for Seep 1 flow quality between 1989 to January 1994 (Table 2). Although a 800 ppm reduction in total acidity would represent a very significant decrease in acid load for almost any chronic acid seep, this four year reduction represents only a partial, and presumably initial, amelioration of the Pit 4 Seep 1 water quality problem. It is anticipated that decreases in acidity will continue as additional recharge pools have been constructed and the cumulative effects of alkaline loading and seasonal flushing in the Pit 4 area combine to establish a more favorable groundwater acid-base equilibrium. Expectations of continued Seep 1 water quality improvement are based on the dramatic acidity decreases being documented in upslope groundwater wells (No. 3, 4, 5) of the Pit 4 final cut refuse system (Figure 4).

At this point in the monitoring of Seep 1, the 800 ppm (23%) reduction in acidity is encouraging. Recognizing that acid seep amelioration is a long term task requiring reversal of geochemical processes that were initiated 20 years earlier, any initial improvement should be viewed as a positive sign that more improvement can be obtained if patience and perseverance are part of the reclamation plan.

Groundwater Monitoring

Groundwater quality has continually improved in the Pit 4 recharge area (wells 3, 4, and 5) that is directly associated with the buried refuse acid groundwater pool. Two wells (4 and 5) are located in the final cut refuse disposal area approximately 230 m upslope of the main seep (No. 1). These wells are affected by approximately 1.4 to 1.8 ha of alkaline recharge pools, which extend more than 305 m upslope of the sampling wells. Well 3 is approximately 107 m upslope of Seep 1, but is located 4.5 to 7.6 m within the spoil side of the Pit 4 refuse disposal area.

Wells 3, 4, and 5 water quality has consistently improved (Figure 4). Average annual (1989 to 1994) acidity has decreased from 80% to more than 90% for wells 4 and 5, respectively (Table 2). These continued annual decreases in acidity are particularly significant and encouraging as occasional seasonal increases in acidity have consistently been ameliorated by subsequent alkaline recharge pool flushing cycles. More frequent alkaline flushing should lead to greater reductions in acid generation as an alkaline environment temporarily replaces a portion of the acid refuse groundwater pool. Eventual cessation, or at best a significant reduction, of the chronic cycle of ferric iron oxidation of pyrite can be expected when either the frequency or duration of alkaline flushing is capable of sustaining a prolonged alkaline groundwater front within the buried refuse system.

Monitoring data through January 1994 for wells 4 and 5 indicate that the initial stage of acid seep abatement has begun. Reductions in acidity included concomitant reductions in total iron and sulfate, indicating that the by-products of pyrite oxidation are decreasing as the acid generating mechanism is being partially abated by alkaline flushing cycles. Reductions of 70 to 95% in total iron and sulfate values between August 1989 to January 1994 in Wells 4 and 5 correlate well with the 83 and 94% reductions in total acidity that occurred during the same period. Further decreases in acidity in the Pit 4 recharge area wells can be expected as two additional concentrated alkaline recharge pools were recently installed in the Middle Incline of Pit 4.

Summary and Conclusion

This ongoing research demonstration evaluated upslope alkaline recharge pools for the purpose of abating an acid seep. During 1989 to 1994 groundwater and seep quality improved within the Pit 4 buried acid refuse zone. Significant decreases were recorded for sulfates, iron, acidity, and conductivity in recharge basin wells, indicating the ameliorative effect of increased recharge pool alkalinity on the acid generating mechanism in the Pit 4 buried acid refuse zone. Continued improvement in groundwater quality within the alkaline recharge zone is expected.

Improvement in the Pit 4 recharge area water quality suggests that annual cycles of alkaline flushing are responsible for a reversal of the chronic acid generation mechanism that had existed for 20 years in the buried refuse areas. Complete elimination of pyrite oxidation in Pit 4 buried refuse areas may not be feasible, due to such variables as fracture flow patterns and inaccessible alkaline loading areas. However, the extremely encouraging results of this reclamation demonstration prompted the installation of additional recharge pools to accelerate the rate of acid seep amelioration in previously untreated areas above Pit 4 refuse zones. Effectiveness of the recharge pool technique is based on a relatively simple principle: acid seep abatement requires upslope enhancement of groundwater alkalinity. Basic considerations for the alkaline recharge pool approach include:

1. use highly soluble alkaline materials (e.g., calcium oxide, or calcium hydroxide waste products) for recharge pool loading sites.
2. maximize the alkaline groundwater flow volume;
3. decrease surface runoff and maximize alkaline infiltration above buried refuse recharge areas;
4. use multiple upslope alkaline recharge pools to increase probability of intercepting groundwater flow paths entering the refuse zone;
5. construct infiltration drains to reduce time required for alkaline diffusion and flushing; and,
6. allow sufficient time (possibly 3 to 5 annual cycles) for alkaline diffusion and transport to the recharge pool and buried acid refuse site.

Time is an important design factor in acid seep abatement. Several seasons of alkaline flushing will be required to reverse the acidification process that may have originally taken 20 to 25 years to generate an acid seep. Alkaline enhancement of the upslope groundwater recharge zone offers an alternative to perpetual treatment by addressing the geochemical process that controls subsurface acid seep generation. As with any reclamation process that directly affects acid-base equilibrium, reclamation success can only be judged by long-term results. The alkaline recharge pool alternative will require long term monitoring, as has been initiated in this research demonstration.

References

Caruccio, F.T. 1988. Acid mine drainage research: hydrology's critical role and unifying theme. p. 228-231. In Proceedings of the Mine Drainage and Surface Mine Reclamation Conference, Vol. I: Mine Water and Mine Waste. USDI, BOM IC 9183. (Pittsburgh, PA, April 17-22).

Caruccio, F. T. 1968. An evaluation of factors affecting acid mine drainage production and the groundwater interactions in selected areas of western Pennsylvania. p. 107-151. In Proceedings of the Second Symposium on Coal Mine Drainage Research. (Mellon Inst., Pittsburgh, PA).

Caruccio, F. T., G. Geidel, and R. Williams. 1984. Induced alkaline recharge zones to mitigate acid seeps. p. 43-47 In Proceedings of National Symposium on Surface Mining, Hydrology, Sedimentology, and Reclamation, (University of Kentucky, Lexington, KY, December 2-7).

Geidel, G. 1979. Alkaline and acid production potentials of overburden materials: the rate of release. Reclamation Review 2:101-107.

Nawrot, J.R., J. Sandusky, and W.B. Klimstra. 1988. Acid soils reclamation: applying the principles. p. 99-103. In Proceedings of the Mine Drainage and Surface Mine Reclamation Conference. Vol. II: Mine Reclamation Abandoned Mine Lands and Policy Issues. USDI, BOM IC 9184. (Pittsburgh, PA, April 17-22).

Nawrot, J. R., G. Smout, and D. Brenningmeyer. 1991. Soil cover and alkaline amendment alternatives for coal slurry impoundments. Wendall R. Oaks and Joe Bowden (eds.). p. 311-322. In Proceedings of 1991 National Meeting of American Society for Surface Mining and Reclamation. (Durango, CO, May 14-17).

Nawrot, J. R., and D. B. Warburton. 1987. Guidelines for slurry reclamation alternatives. p. 277-283. In Proceedings of National Symposium on Surface Mining, Hydrology, Sedimentology, and Reclamation, (University of Kentucky, Lexington, KY, December 7-11).

Nawrot, J. R., D.B. Warburton, and W.B. Klimstra. 1986. Coarse refuse reclamation: alkaline enhancement for direct vegetation establishment. C. Carlson and J. Swisher (eds.). p. 613-636. In Proceedings of The National Mined Land Reclamation Conference Innovative Approaches to Mined Land Reclamation. (Southern Illinois University Press, Carbondale, IL. October 28-29).

Sandusky, J. E. and J. R. Nawrot. 1992. Peabody Will Scarlet Mine acid drainage reclamation. p. 123-144. In Proceedings of the 14th Annual Abandoned Mined Land Conference New Trends - Utilization of Recycled Materials and Waste Products in Mine Reclamation. (Chicago, IL, August 23-27).

Snyder, D.T. and F.T. Caruccio. 1988. The partitioning of flow components of acidic seeps from surface coal mines and the identification of acid-producing horizons within the backfill. p. 59-66. In Proceedings of the Mine Drainage and Surface Mine Reclamation Conference, Vol. I: Mine Water and Mine Waste. USDI, BOM IC 9183. (Pittsburgh, PA, April 17-22).

Warburton, D.B., J.R. Nawrot, and W.B. Klimstra. 1987. Coarse refuse: alkaline enhancement and reduced soil cover - an effective reclamation alternative. p. 91-98. In Proceedings of National Symposium on Surface Mining, Hydrology, Sedimentology, and Reclamation. (University of Kentucky, Lexington, KY, December 7-11).

Table 2. Peabody Will Scarlet Old Works seep abatement project. Seep 1 and Well 3, 4, and 5 mean annual water quality data. Collected monthly August 1989 through January 1994.

		pH	Conductivity (mmhos/cm)	Acidity (ppm$CaCO_3$)	Total Iron (ppm)	Sulfates (ppm)
Seep 1						
	1989–1990	3.4	4.3	3764	753	5240
	1990–1991	3.5	4.2	3165	672	4605
	1991–1992	3.7	3.9	2940	683	4637
	1992–1993	3.4	3.2	3010	681	4329
	1993–1994	3.2	3.2	2893	640	4295
	Percent Decrease[1]		27	23	12	18
Well 3						
	1989–1990	2.5	5.2	6738	1128	7722
	1990–1991	2.8	4.1	3292	616	4211
	1991–1992	3.0	4.3	4101	707	5185
	1992–1993	2.5	3.5	4007	714	5062
	1993–1994	2.6	3.1	3595	622	5013
	Percent Decrease[1]		42	47	40	34
Well 4						
	1989–1990	2.5	5.4	7725	1476	8684
	1990–1991	2.7	5.2	5359	1452	7610
	1991–1992	2.9	4.4	3990	993	4843
	1992–1993	2.7	3.2	2393	559	3279
	1993–1994	2.7	2.3	1318	269	2385
	Percent Decrease[1]		57	83	81	72
Well 5						
	1989–1990	2.6	13.4	11859	6366	19380
	1990–1991	3.4	4.0	2953	960	4081
	1991–1992	3.6	3.5	2224	739	3395
	1992–1993	3.5	2.3	1009	336	1948
	1993–1994	3.4	1.8	749	280	1744
	Percent Decrease[1]		87	94	95	91

[1] 1989–1990 compared to current (1993–1994) annual mean value.

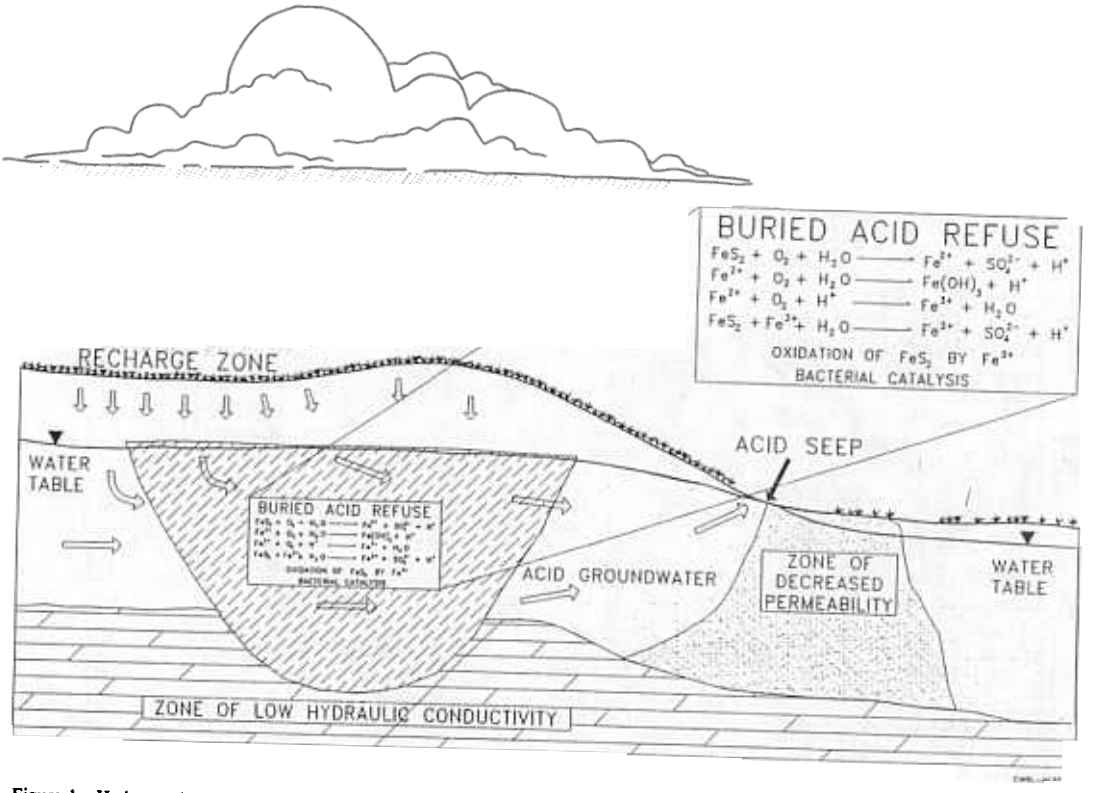

Figure 1. Hydrogeochemical factors affecting acid seep generation in buried refuse areas.

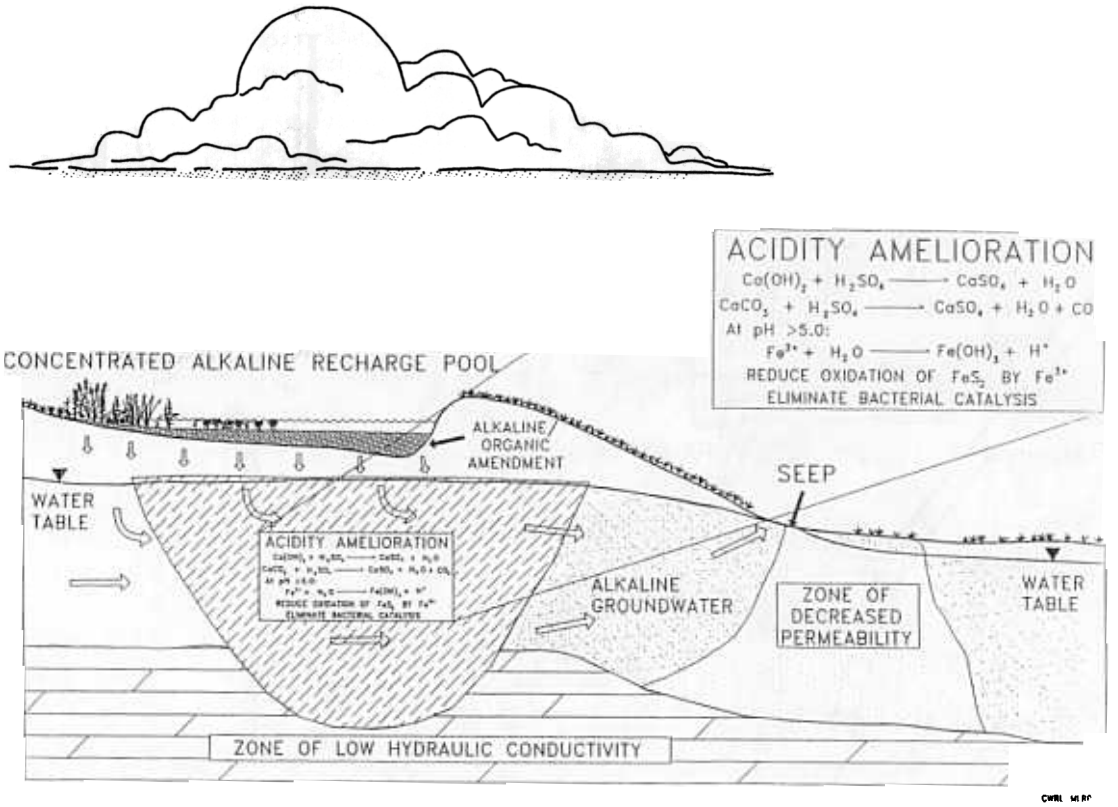

Figure 2. Concentrated alkaline recharge pool approach for abatement of acid seeps generated by buried refuse areas.

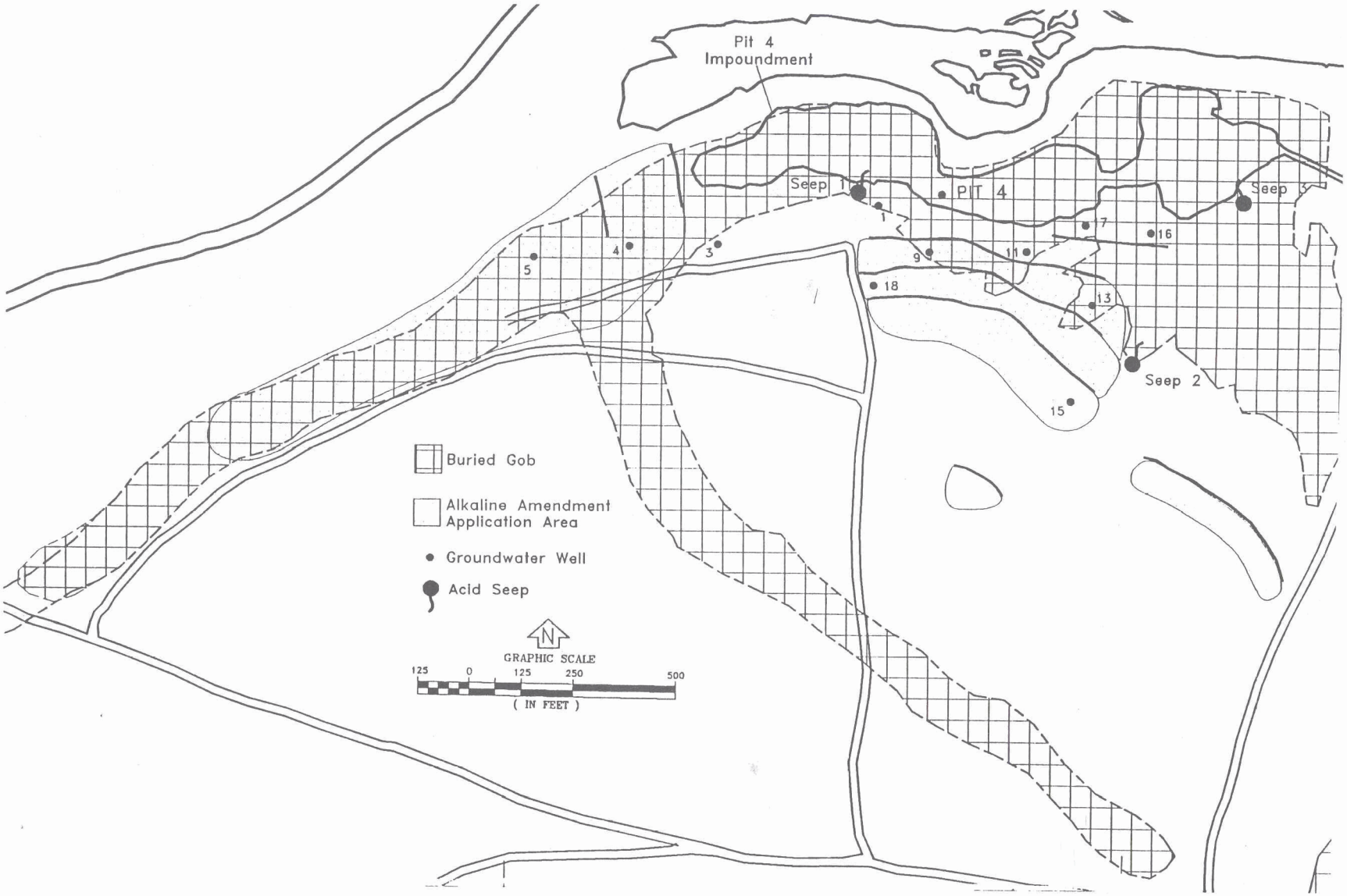

Figure 3. Peabody Will Scarlet Mine Pit 4 acid seep abatement demonstration area.

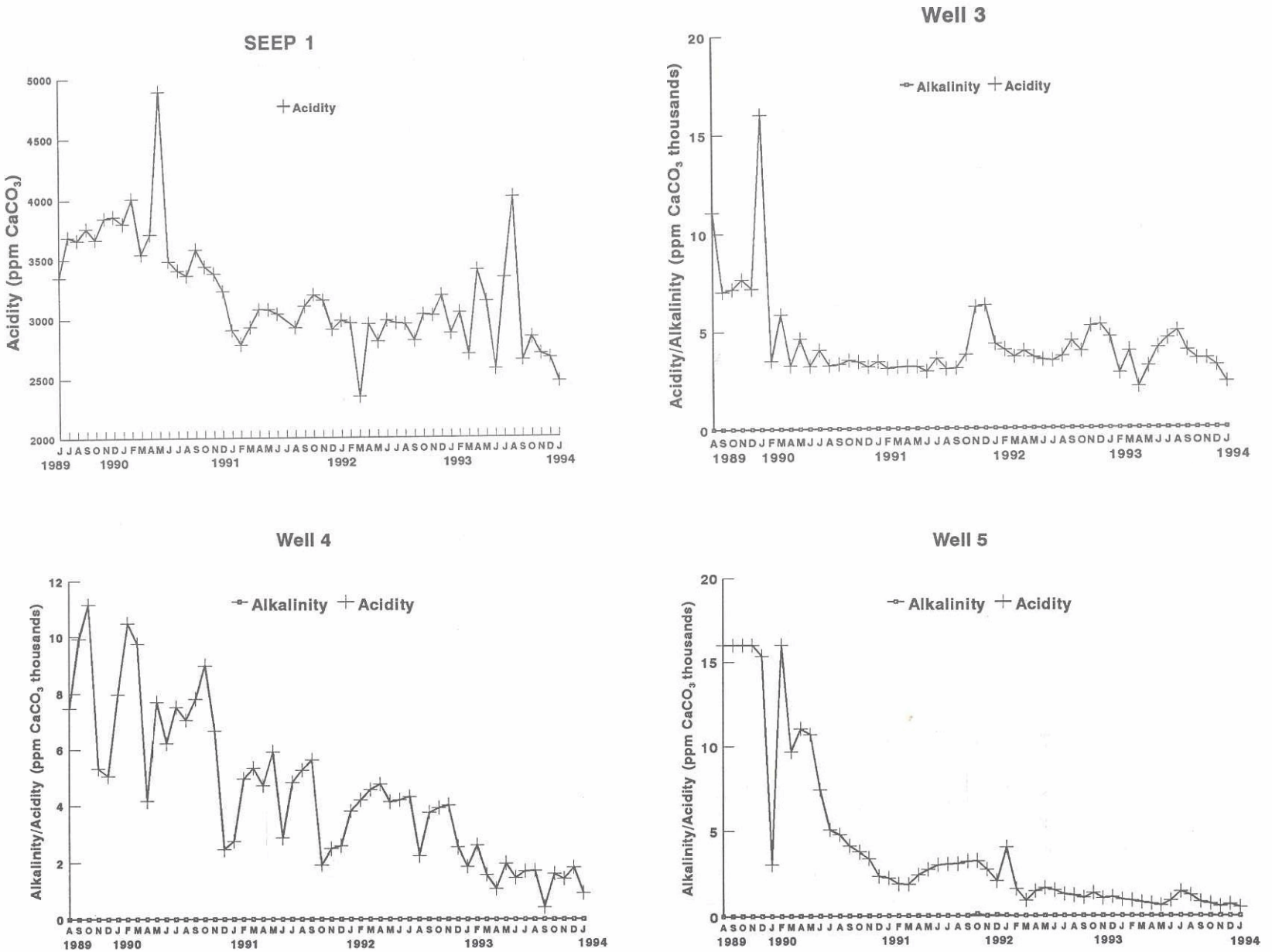

Figure 4. Peabody Will Scarlet Old Works Pit 4 alkaline (alkaline amendment initiated fall 1989) recharge area. Acidity trends for recharge zone wells (3, 4, 5) and primary seep (Seep 1).

COAL REFUSE DISPOSAL USING ENGINEERING DESIGN AND LIME CHEMISTRY[1]

Douglas H. Rich[2] and Kenneth R. Hutchison[3]

Abstract: High Power Mountain is a large surface mine located in central West Virginia. The majority of production is by mountaintop removal; however, contour combined with highwall mining occurs in a lower seam. Maximum annual production is 3 million raw tonnes.

Refuse varies between 600,000 to 900,000 thousand tonnes annually. Combined (coarse and fine) refuse disposal is planned as part of the mining reclamation process by use of "refuse cells". These engineered structures are designed to encapsulate and isoloate the refuse from the environment.

In addition, lime chemistry (lime kiln dust) is used to control acid mine drainage and stabilize the combined refuse. The benefits of the lime kiln dust amendment include increased pH and alkalinity, elimination of bacterial growth, limiting the formation of acid water, decreasing metal mobilization, increasing the workability of combined refuse, and stabilizing the refuse.

By using engineering design concepts combined with lime chemistry, it has been demonstrated (both from a theoretical standpoint and practical experience) that acid mine drainage is controllable and that refuse can be disposed of in an environmentally sound manner. The key is to treat the problem (refuse), not the symptom (AMD) of the problem.

Additional Key Words: lime kiln dust, combined coal refuse, engineered refuse cells, acid mine drainage.

Introduction

High Power Mountain (HPM) is a large surface mine located in the central portion of West Virginia. The mine began production in 1985 and has produced over 16 million raw tonnes of coal by the mountaintop removal, contour and highwall mining methods. Annual maximum production is 3.0 million raw tonnes.

The coal seams are in the upper portion of the Pottsville Series

---

[1]Paper presented at the International Land Reclamation and Mine Drainage Conference and the Third International Conference on the Abatement of Acid Drainage, Pittsburgh, PA, April 24-29, 1994.

[2]Douglas H. Rich, Supervison Planning and Development, HPM Corporation, Drennen, WV, USA.

[3]Kenneth R. Hutchison, Senior Sales Representative, APG Lime Corporation, Charleston, WV, USA.

and lower portion of the Allegheny Series of the Pennsylvania Era. The seams are: the Upper Kittanning, Middle Kittanning, Lower Kittanning (Five Block), Clarion, Stockton "A", Stockton, Coalburg, and Winifrede.

Each of the seams have multiple splits, with each split having varying coal quality. Typically, twenty to twenty five (20-25) different splits of coal are mined from the eight seams. As a result, to meet customer specifications the splits must be blended.

Coal preparation occurs in a 700 tonne per hour heavy media plant. The plant circuitry consists of three heavy media cyclones to process the coarse size fraction (5.08cm x 0.5mm). Hydrocyclones and classifying cyclones are used to process the 0.5mm x 0mm. material. The minus 0.5mm material, being higher in ash and moisture, is not recovered.

The minus 0.5mm material is combined with flocculant in the static thickener to enhance settling. The slurry material is pumped to belt filter presses and is de-watered. The end product of this process is filter cake, a high clay content material having a moisture of approximately 28% to 30%.

The filter cake is carried by conveyor to the main refuse belt where it is combined with the coarse refuse. The combined refuse, having a moisture of 15% to 20%, is conveyed to a 500 tonne refuse bin. Transportation from the bin to the disposal site is by 85 tonne capacity haul trucks.

Refuse Disposal

The production of refuse varies between 600,000 to 900,000 tons annually, thus refuse at HPM is a major part of the total material handling system. In the initial design of the mine, refuse disposal was planned as part of the reclamation process. To this end the concept of the "refuse cell" was developed.

As initially conceived, the refuse cell was to be an integral part of the mine development/reclamation process. Figure 1 illustrates the original design of the cell.

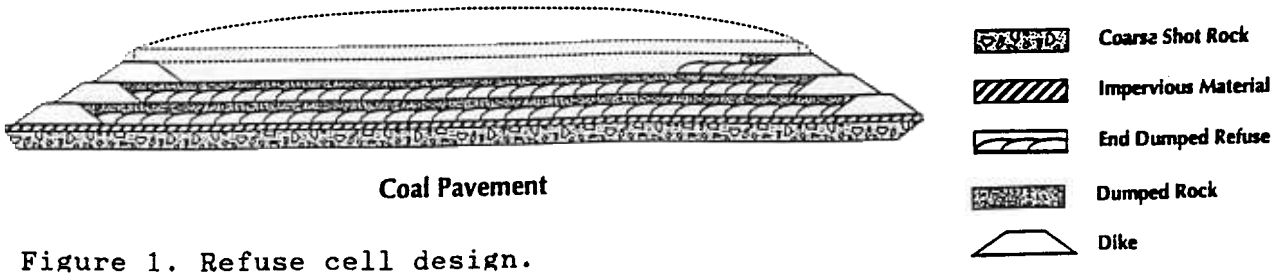

Figure 1. Refuse cell design.

The first phase of construction begins after the lowest coal seam is removed by mountaintop removal methods. The coal pavement is thoroughly cleaned to remove any potential acid producing material. Next, a 2.25 - 3.0 meter layer of large shot rock (sandstone) is placed on the pavement, forming the base. In practice, this layer acts as a french drain and an under drain. As a benefit, the upward capillary action of groundwater is broken by the large interstitial space between rock fragments.

Construction continues with the placement of the outer dike structure. This berm consists of compacted soil and shale material. Water from the refuse cell is contained by this dike system and directed to the refuse cell sediment control structure. If needed, water can be treated at this point prior to release.

Once the outer dike is complete, approximately a 1 meter layer of soil and shale is used to form an "impervious" barrier. The first level of the inner dike system is now ready to be constructed. This dike also consists of compacted soil and shale. Once a layer of refuse is placed, the next higher inner dike is constructed. Prior to the use of lime kiln dust, it was necessary to "bridge over" the combine refuse with a layer of rock in order to facilitate the placement of the next layer of refuse. This presented multiple operational problems and added cost. This process of alternating layers of refuse and rock continues until the design height is obtained. At this point, the cell is capped in a dome shape using soil and shale and revegetated.

The refuse is largely isolated from the environment since groundwater cannot enter by capillary action and the dome shape diverts rainfall to the outside dike system, thereby reducing infiltration. Thus, after interstitial water is squeezed out by weight of compaction, the long term environmental impact is minimized. If water quality does not meet standards, the outer dike system diverts the water to a central sediment control structure where it can be treated prior to release.

Refuse Quality

The sulfur content of the coal seams vary and therefore the acid producing potential of the refuse also varies. Table 1 illustrates the sulfur content of the seams at different float/sink gravities.

TABLE 1. Percent Sulfur by Seam

Seam	Raw	Float 1.60	Float 1.45
Upper Kittanning	1.32	0.98	0.92
Middle Kittanning	0.95	0.85	0.85
Lower Kittanning	0.66	0.68	0.69
Clarion	0.83	0.84	0.83
Stockton "A"	0.71	0.71	0.76
Stockton	4.97	3.53	3.13
Coalburg	1.11	0.93	0.93
Winifrede	0.65	0.68	0.68

Overall the sulfur content is generally less than 1%. However, the Stockton seam is the notable exception. The sulfur in the run of mine Stockton coal varies from 4% to 6% and remains high (3%) even after the coal is cleaned. The Stockton refuse also contains an elevated level of pyritic sulfur.

Initial laboratory testing of the HPM refuse consisted of acid base accounting and column leaching. These tests indicated that the refuse has a $CaCO_3$ equivalent deficiency of 26 to 53 tonnes for every 1,000 tons of material.

After plant start-up, field tests were conducted on the refuse by placing low sulfur (0.9 %), medium sulfur (1.1 %) and high sulfur (2.5 %) refuse in three separate test sites. These sites were exposed to rainfall and weathering. Water samples were collected on a regular basis. Figure 2 delineates the change in pH over time. As shown, the water acidified very quickly.

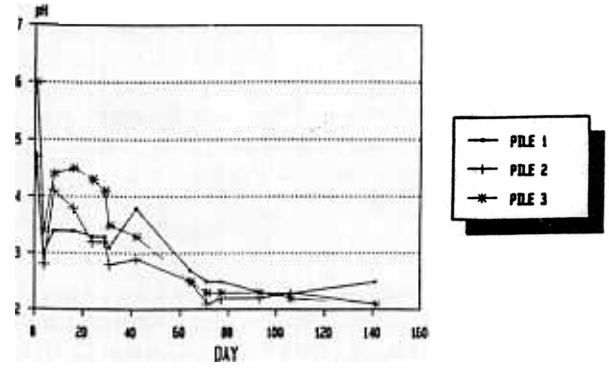

Figure 2. Water Quality Leachate Data (Sturm, 1987).

From laboratory and field testing, it was clear that the refuse generates acidic waters. If this problem was not addressed these waters would be a continuing source of environmental problems.

Neutralization

Acid generation is the result of the oxidation of pyrite. In the presence of water this reaction generates iron hydroxide ($Fe(OH)_3$) and sulfuric acid (H_2SO_4). Studies have shown that, in the presence of iron consuming bacteria (Ferrobacillus and Thiobacillus), the oxidation rate of pyrite and the generation of sulfuric acid is greatly enhanced. In the absence of bacteria, the natural oxidation of pyrite and thus generation of sulfuric acid occurs at a reduced level.

It was evident from the testing that neutralization of the refuse was required. Five neutralizing agent were applied to bulk samples of 25-30 tons. These agents were: Agricultural lime, Spent lime, Limestone rock dust, Phosphate, and Lime kiln dust. With the exception of the phosphate, all agents neutralized the refuse, but to varying degrees.

The method first used by HPM to treat refuse consisted of slurrying limestone rock dust and spraying it over the top of the refuse piles after the combined refuse was back-dumped into the cell. The intent was to add alkalinity. It was anticipated that rainfall, buffered by the limestone, would permeate through the back-dumped pile and neutralize the acidic waters. In practice however, the low reactivity of limestone rock dust did not allow for a sufficient increase in alkalinity and the rainfall did not permeate uniformly throughout the piles. Thus, acidic waters continued to be generated. These waters were treated in the refuse sediment control structure prior to release.

Concurrently, operational problems were encountered in the refuse cell. In order to place the next layer of combined refuse into the cell, a rock bridge was required on top of the back-dumped piles. This rock bridge, overlying the non-stable combined refuse, needed to be thick enough to support the fully loaded refuse trucks. This situation required over fifty percent of the refuse cell being filled with rock bridge material, thereby dramatically reducing the active life of the cell.

Therefore, two problems needed to be addressed. A more efficient method of neutralization was required and a way to stabilize the combined refuse was needed.

Application of Lime Chemistry

The initial neutralization data suggested that the use of calcium oxide provided greater neutralization potential than the use of limestone rock dust. Also, lime has been used for soil stabilization of clayey material in the construction industry for years. It was decided to modify the operating procedure and use lime kiln dust as the neutralizing agent instead of limestone rock dust.

Lime kiln dust is a by-product of the lime industry, being generated during the calcining process. Crushed limestone is heated in a rotary kiln, driving off the carbon dioxide and producing calcium oxide. In the process of calcining, the heated air stream picks up dust consisting of calcium oxide and uncalcined calcium carbonate. In addition, the coal fly ash is also carried in the stream. The air is passed through a baghouse to remove particulate matter prior to being released to the atmosphere. The baghouse dust purchased by HPM contains approximately 15% calcium oxide, 75% calcium carbonate, and the remaining 10% is fly ash which is high in silica and alumina.

Lime kiln dust is alkaline, producing a pH of 12.4 in a saturated solution. In addition to its obvious neutralization potential, it also acts as a drying agent forming calcium hydroxide when the calcium oxide comes in contact with water.

The mechanism for the soil stabilization process is facilitated in a high pH environment and occurs during the ionic substitution of calcium into the clay mineral lattice crystal structure. The soil-lime reactions are complex and not completely understood. According to Chou (1987), an oversimplified qualitative view of some typical soil-lime reactions are:

- o $Ca(OH)_2 > Ca^{++} + 2(OH)^-$
- o $Ca^{++} + 2(OH)^- + SiO_2 >$ Calcium Silicate Hydrate (CSH)
- o $Ca^{++} + 2(OH)^- + Al_2O_3 >$ Calcium Alumina Hydrate (CAH)

J.L. Eades (1962) suggested that the high pH causes silica from the clay minerals to dissolve and, in combination with Ca^{++}, form calcium silicate. Diamond, et al. (1964) theorized that lime molecules are absorbed by clay surfaces and react with other clay surfaces to

precipitate reaction products. These studies suggest that the clay lattice components are dissolved from the clay structure and are precipitated as CSH and CAH. Stocker (1972) proposed the diffuse cementation theory, in which lime reacts directly with clay crystal edges, generating accumulations of cementatious material.

Discussion

Regardless of the theoretical reactions, application of lime kiln dust at HPM appeared to offer the solution to the operational problems of combined refuse disposal in the refuse cells.

In 1989, a bin was erected directly over the preparation plant refuse belt and the lime kiln dust application process begun. This placement increased the contact of the kiln dust with the refuse, thereby providing greater mixing potential. The refuse moisture, combining with the calcium oxide component to form calcium hydroxide, reacts to generate an alkaline environment while at the same time decreasing free moisture. This is immediately noticeable in that the refuse is able to maintain a sharp angle of repose.

The generation of calcium hydroxide is the key chemical reaction to the treatment of the refuse. The high pH environment facilitates the elimination of iron oxidizing bacteria and provides the pH environment required for soil stabilization.

By eliminating the bacteria the rate of pyrite oxidation is substantially lowered. Without the availability of the sulfate radical, the formation of sulfuric acid is curtailed. The acid generation is now dependant on the slow, abiotic oxidation of pyrite. The long term control of acid generation is controlled by the calcium carbonate component of the lime kiln dust. With its lower reactivity rate, the dissociation of calcium carbonate neutralizes the slow abiotic oxidation products of pyrite.

Ziemkiewicz, et al.,(1992) tested HPM refuse using the ten week soxhlet leach process. Figure 3 represents the non-treated control sample of Coalburg refuse. Note the decrease in pH and the increase in sulfate. Figure 4 shows the effect of the lime kiln dust additive on the Coalburg refuse. Again note the pH and sulfate levels. Based on this work and observations in the field, an alkaline environment is maintained in the refuse cell and acid generation is controlled.

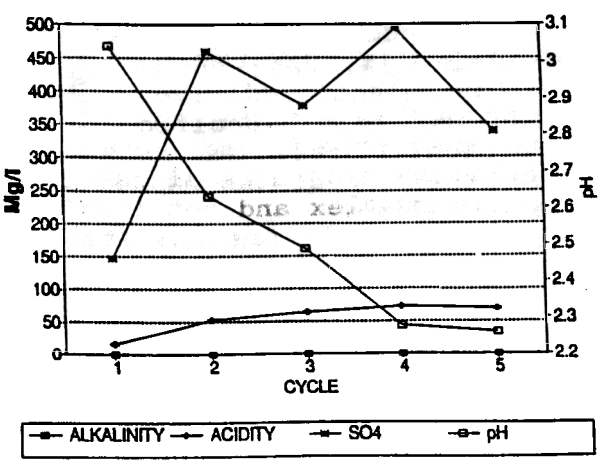

Figure 3. Untreated refuse (control).

Another benefit to the process is the control of metal mobilization. The solubility and thus mobilization potential of metals is, among other parameters, dependant on pH. Metals such as iron and manganese become mobilized in environments which are less than pH 7. However, the solubility of iron and manganese is greatly decreased in alkaline environments. Based on this concept, if refuse is kept alkaline, not only is acid generation eliminated but also iron and manganese levels are maintained within acceptable limits.

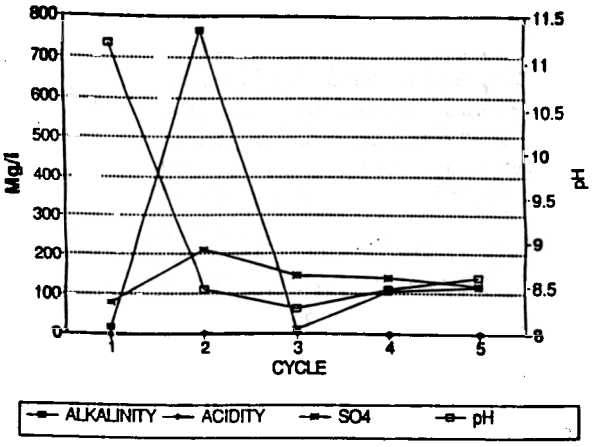

Figure 4. Refuse treated with 2% lime kiln dust.

The high pH environment, again derived from the formation of calcium hydroxide, drives the complex soil-lime stabilization reactions. These reactions, noticeable in the refuse cell three to five days after refuse placement, stabilizes the refuse. By allowing the refuse to stabilize, the rock bridge construction technique is not required. Fully loaded refuse trucks (85 tonne back-dump trucks) are able to drive directly on top of the stabilized combined refuse for lift placement.

Proprietary studies have shown strength is gained over time. Samples of refuse mixed with varying percentages of kiln dust were tested. Figure 5 shows the unconfined compressive strength obtained over time using 1%, 2%, and 3% kiln dust (by weight) additive. These data are site specific and are presented only as an example of the effect of the soil-lime stabilization reactions.

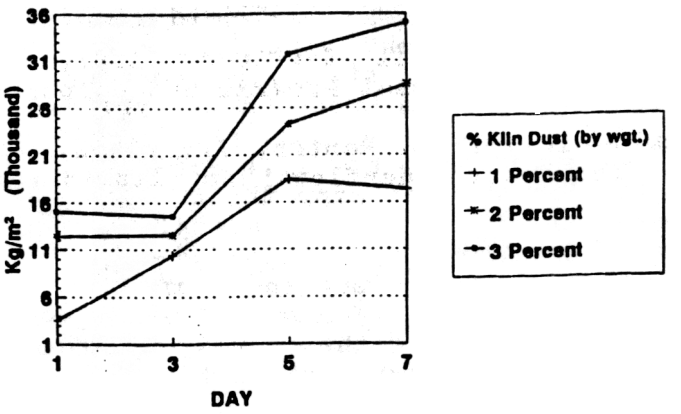

Figure 5. Unconfined compressive strength of treated combined coal refuse.

Conclusions

The refuse cell concept is a leading edge technology for the handling of coal refuse in an environmentally safe manner. Since 1989 HPM has been using lime kiln dust as an additive to its combined

refuse. From the experience which has been gained, a successful long term method of treating acid mine drainage has been developed. Treatment of water associated with the refuse disposal system has not been required since the application of lime kiln dust began. Water quality, both pH and metals, has remained within NDPES limits for the last four years and indications are that the refuse will not become an environmental problem in the future. By use of the refuse cell concept, including treatment with lime kiln dust, the long term environmental liability appears to be minimized.

Literature Cited

Chou, L. (Ed.), 1987, Lime Stabilization, Reactions, Properties, Design, and Construction. State of the Art Report 5, Transportation Research Board, National Research Council, Washington, D.C.

Diamond, S., White, J.L., and Dolch, W.L. 1964, Transformation of Clay Minerals by Calcium Hydroxide Attack. p. 359-379. In Proceedings of the 12th National Conference on Clays and Clay Minerals, Pergamon Press, New York, N.Y.

Eades, J.L. 1962, Reactions of Ca(OH) with Clay Minerals in Soil Stabilization. PhD thesis, University of Illinois

Stocker, P.T. 1972, Diffusion and Diffuse Cementation in Lime and Cement Stabilized Clayey Soils. Special Report 8, Australian Road Research Board, Victoria, Australia

Sturm Environmental Services. 1985, Refuse Disposal Criterion for High Power Energy. Unpublished report.

Sturm Environmental Services. 1987, Field and Laboratory Studies: Refuse Disposal Program HPM Corporation. Unpublished report.

Ziemkiewicz, P.F., Renton, J.J. 1992, WV51 Kiln Dust to Control AMD in Thickener Underflow. Unpublished report

OXIDATION RATES AND POLLUTION LOADS IN DRAINAGE; CORRELATION OF MEASUREMENTS IN A PYRITIC WASTE ROCK DUMP[1]

J.W. Bennett,[2] D.K. Gibson,[2] A.I.M. Ritchie,[2] Y. Tan,[2] P.G. Broman,[3] and H. Jönsson[3]

Abstract: There are several methods by which the oxidation rate in a pyritic waste rock dump may be inferred. Pore gas oxygen concentration profiles, temperature profiles, and drainage-monitoring data have been analysed to quantify the oxidation processes occurring in a waste rock dump at the Aitik Mine in northern Sweden. Analysis of oxygen concentration profiles showed that material in some regions of the portion of the dump investigated had an intrinsic oxidation rate (IOR) of about 10^{-8} kg m^{-3} s^{-1} which was some 60 times greater than that of material in other regions. A comparison with pollution loads from measurements in the cutoff drain indicates that if 14% of the dump has an IOR of 10^{-8} kg m^{-3} s^{-1} then 86% has an IOR that contributes little to the total pollution load from the dump. The higher IOR found for the Aitik waste rock dump material is about eight times lower than the highest value found for waste rock at Rum Jungle in northern Australia. It is stressed, however, that the comparatively low IOR of the Aitik waste rock dump material still generates significant pollution loads in drainage. The case study presented emphasizes the utility of using temperature and oxygen profile measurements together with flow and concentration measurements to characterize pollution generation and drainage from a dump.

Additional Key Words: acid mine drainage, oxygen concentration, temperature, gas diffusion, sulfate.

Introduction

The primary process that leads to pollution generation in a pyritic waste rock dump is the oxidation of the pyrite. For this reason it is important to have data on the rate at which this reaction proceeds in a dump. The overall dump oxidation rate, which is the space integral of the oxidation rate over the dump at any one time, is a direct measure of the primary pollution generation rate in the waste rock dump and a major determinant of pollution loads in drainage from the dump. The intrinsic oxidation rate (IOR), for any one particular type of waste rock, is a function that relates the oxidation rate to any parameters that might be considered relevant, such as the oxygen and pyrite concentrations, the dump temperature, local pH, and so forth. An approximation to this function is required in most modeling of dump behavior.

There are several methods by which the oxidation rate in a pyritic waste rock dump may be inferred. One is the analysis of oxygen concentration profiles within the dump. Analysis is straightforward if diffusion is the dominant oxygen transport process. The IOR, in units of kilograms of oxygen consumed per cubic meter of rock per second, is readily inferred from the pore gas oxygen concentration profiles and the diffusion coefficient for oxygen in the waste rock.

Another approach is to measure the temperature rise brought about by the exothermic oxidation process. Interpretation of temperature measurements may be made difficult by the effects of seasonal variations in solar radiation and uncertainties about the boundary conditions at the base of the dump. Despite this, reasonable estimates of oxidation rates have been derived by this means (Harries and Ritchie 1981).

---

[1] Paper presented at the International Land Reclamation and Acid Mine Drainage Conference and the Third International Conference on the Abatement of Acidic Drainage, Pittsburgh, PA, April 24-29, 1994.

[2] John Bennett, Senior Research Scientist, David Gibson, Principal Research Scientist, Ian Ritchie, Senior Principal Research Scientist, and Yunhu Tan, Research Scientist, Australian Nuclear Science and Technology Organisation, Lucas Heights, NSW, Australia.

[3] Per Broman, Vice President Environment, and Hans Jönsson, Project Manager, Boliden Mineral AB, Boliden, Sweden.

The third approach is to measure the rate of output of chemical species in drainage water and infer the oxidation rate in the dump (for example, Galbraith 1991). Sulfate makes a good tracer for the oxidation of pyrite because it is a direct product of the reaction and is abundant, reaching concentrations of a few grams per liter. Care must be taken however to ensure that it is conservative through the system. The average sulfate load, in units of tonnes per year can be measured relatively easily if good measurements of sulfate concentration and flow rate of drainage from the dump are available.

The application of these techniques to a waste rock dump at the Aitik copper mine in northern Sweden is discussed in this paper.

Background and Field Measurements

Aitik Waste Dumps

The Aitik Mine is located near the town of Gällivare in the north of Sweden, about 100 km north of the Arctic Circle. Aitik is operated by Boliden Mineral AB and is Europe's largest copper mine. The opencut operation which was begun around 1960 now produces approximately 14 million tonnes of waste rock per year and about the same quantity of mill tailings. The waste rock from the pit has been disposed of by end-dumping from trucks in dumps which currently average about 25 m in height and cover an area of about 400 ha.

The ore deposit at Aitik consists principally of biotite gneiss, and the waste rock also contains muscovite schist and skarn-banded gneiss. Chalcopyrite and pyrite are the dominant sulfides, with the pyrite content in the waste rock varying from 0 to 5 wt%, and averaging about 1%. The oxidation of pyrite can be taken then as the sole oxygen-consuming reaction in the Aitik dumps.

The average annual temperature at the site is just above 0°C, ranging from an average of 13.2°C in July to -13.5°C in January. The average precipitation is 680 mm/yr and the net infiltration rate into the waste rock dumps is about 500 mm/yr (Axelsson et al. 1992). From the middle of October to the middle of April the precipitation falls as snow, which then melts over a period of about 6 weeks to the end of May.

Site Selection

The waste rock dump at the southwestern corner of the opencut pit was known to be a source of pollution and was chosen for detailed study. This dump was started around 1975 and had been left undisturbed since about 1989. The area met the criteria that the site be accessible to machinery, contain relatively old waste rock material, have had no rehabilitation works, and would be left undisturbed for the 2-yr timescale of the project. A further advantage of the site was that there was a cutoff drain that collected the drainage from the dump and provided an effective means of monitoring pollutant loads and waterflows. The site tailings dam was upstream of this dump.

Temperature and Oxygen Measurements

Probe holes were drilled in the dump in April and August 1991 using rotary percussion airblast, with steel casing and a 140-mm eccentric bit. Once the casing was removed, the holes were lined with PVC plumbing pipe, 50 mm in external diameter, and capped at the bottom to exclude moisture and so prevent any possible perturbation of the temperature profile in the liner by vapor transport.

Nylon pressure tubing, 3/16-in internal diameter, was attached with adhesive glass filament tape to the outside of the PVC pipe. A tube ran the full length of the liner, from the bottom cap to the top of the pipe, and then one tube ran from each successive meter up to the top. These nylon tubes were to enable pore gas samples to be removed from the dump for determination of the oxygen concentration. The top of the tubes were attached to schrader valves and mounted on a brass plate.

The gap between the drilled hole and the inserted liner was backfilled using builders' sand, with the aim of limiting gas transmission between the ports since the gas diffusion coefficient of sand is not less than that of the dump material. A plug of concrete was put in the top 30 cm of the hole to prevent preferential flow of rainwater along the liner. The suitability of this liner design for temperature profile measurements has been established by Harries and Ritchie (1981).

Figure 1 shows the section of the 130 hectare dump under study and indicates the locations of the 11 probe holes. It can be seen that six holes penetrate the base of the dump.

Pore gas oxygen concentrations were determined by passing gas samples across a commercially available oxygen fuel cell. This enabled oxygen concentrations to be measured from 0% to 20.95%, with an accuracy of better than 0.05%. Temperatures were measured at meter intervals with a precision of ±0.02°C using a calibrated thermistor which was lowered down the PVC pipe. Temperature and oxygen profiles were measured at roughly monthly intervals throughout the project.

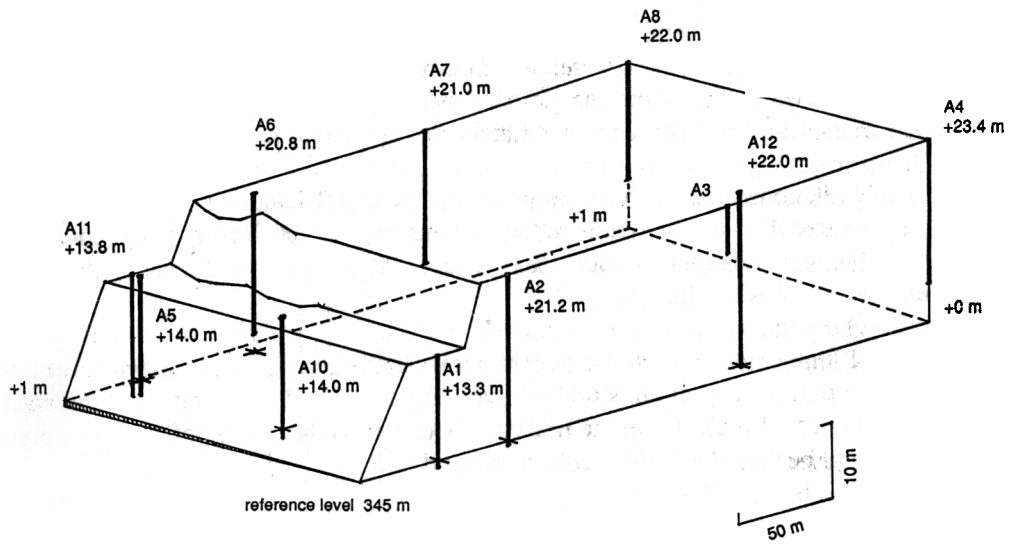

Figure 1. The relative location of the probe holes on the dump used for temperature and oxygen measurements.

Drain and Weir Measurements

To deduce the overall oxidation rate in any given waste rock dump from drainage measurements, it is necessary to know the total load of a relevant pollutant from the dump. This can be obtained by measuring the total water flow through the dump and the concentration of pollutant in the drainage water. Care must be taken that losses of infiltrating water, e.g., to deep ground water, are small. One must also know that the drainage does not contain pollutants from another source. In practice, if either of these complications arise, it may be accounted for if the extent of the loss or gain of pollutant can be estimated. As the flows, concentrations, and loads may vary greatly owing to seasonal factors, regular measurements must be taken at least over a 12-month period.

The glacial till below the Aitik dumps has such a low hydraulic conductivity (Axelsson et al. 1992) that essentially all the water infiltrating them appears at the toe of the dumps and may be collected in cutoff drains. All the flow from the 130 ha dump under study was collected in one drain which had been installed with several flow weirs. Flow rates were measured at various times, the frequency of measurement depending on the season; when flow rates changed quickly during the spring snowmelt measurements were made every few days. Water samples were taken at the time of flow determination and sent to a laboratory for chemical analysis.

Sulfate concentrations were measured to determine the dump oxidation rate for the reasons given above. This

approach requires the sulphate to be conserved in the system. The most common reason for the removal of sulphate from solution flow in dumps is the precipitation of gypsum when the calcium concentration is above the gypsum solubility limit. Ion analysis of the Aitik drainage waters showed the calcium concentrations to be well below this limit.

Analysis of Oxygen Profiles

The rate of pollutant production from the oxidation of pyrite in a waste rock dump can be deduced from estimates of the rate of oxygen consumption in the dump, which in turn is derived from an analysis of measured pore gas oxygen concentration profiles.

Where oxygen diffusion is the sole supply mechanism, oxygen is transported from regions of higher pore gas oxygen concentration to regions of lower concentration. A section of measured profile with constant gradient indicates that oxygen is being transmitted without consumption, whereas a curved profile denotes a region where oxygen is being consumed.

Oxygen profiles can be interpreted qualitatively to infer the dominant gas transport mechanism in a dump and the relative magnitude of pyritic oxidation rates in different regions. Vertical profiles in which the oxygen concentration decreases monotonically with depth are consistent with oxygen being supplied from the top surface by diffusion, higher gradients implying higher oxygen consumption rates in the dump. This is discussed more completely below. Zones of relatively higher oxygen concentrations at depth suggest that either advective transport processes are dominant or there is significant diffusion from the sides. Advection will be accompanied by elevated temperatures resulting from the heat generated by higher oxidation rates.

If it can be assumed that the gas diffusion coefficient does not vary greatly with location, as is most usually the case in waste rock dumps, then it follows that different gradients in the oxygen concentration profiles are due to different oxidation rates.

In the absence of advection (including convection), one-dimensional oxygen transport into the dump by diffusion from the surface can be described as

$$\varepsilon_g \frac{\partial C}{\partial t} = D\frac{\partial^2 C}{\partial x^2} - S(x, t) \tag{1}$$

where C is the pore gas oxygen concentration, t is time, x is distance, D is the oxygen diffusion coefficient, ε_g is the gas-filled pore space, and S is the volume oxygen absorption rate.

The analytical approach requires a knowledge of the diffusion coefficient of the dump material but this does not present such a big problem as it might seem. The primary requirement in characterizing an oxidising dump is to establish oxidation rates to within an order of magnitude so a variation in D by some factors is of little consequence. In practice, the values of D fall within a narrow range because the diffusion coefficient is largely governed by a fixed parameter, the coefficient for diffusion of oxygen in air (under the narrow range of temperature and pressure encountered), and one that has a narrow range of variation, the gas-filled porosity of the dump. The gas diffusion coefficient is not expected to show much spatial variation in any given dump either because of the relative uniformity of porosity and moisture content found in typical waste rock dumps.

In most waste rock dumps the timescale for oxidation of pyrite is much longer than the timescales for gas transport. The oxygen profiles are then pseudo steady state and equation 1 can be simplified to

$$D\frac{\partial^2 C}{\partial x^2} - S(x) = 0. \tag{2}$$

So, if an analytic function can be found to represent a particular oxygen concentration profile well, and the assumptions on which equation 2 is based are satisfied, then the volume oxygen absorption rates or oxidation rates (S) can be easily found by calculating the second derivative or curvature of the function at a given depth.

Results

Oxygen Results

Typical results from the pore gas oxygen concentration measurement program are presented in figures 2 and 3. In general, the oxygen concentration fell monotonically from the surface of the dump, indicating that the oxygen supply mechanism to the sites of pyritic oxidation was dominated by diffusion.

The measured profiles fell into two groups. There was a region near the edge of the dump (probe holes A1, A2, A5, A10, and A11; see figure 2 for example) where there were high gradients in the oxygen concentration profiles and in the central part of the dump the gradients were low (A3, A4, A6, A7, A8, and A12; see figure 3 for example). In the absence of any significant heating in the dump (see below) and making the assumption that the diffusion coefficient of the waste rock does not vary greatly with location, then it is reasonable to conclude that pyritic oxidation rates are relatively high in the region where the gradients are high, and are relatively low where the gradients are low.

The oxygen profiles in the material oxidizing at the higher rate indicate that oxygen was supplied by diffusion and that the rate was not limited by the oxygen supply rate. This means then that the rate is not dependent on the geometry of the dump or the location of the material in the dump, but is a property of the material itself. Clearly, such material may occur anywhere in the dump.

The oxygen profiles in the region with low oxidation rate settled down in a few weeks after installation of the holes. In the regions of high oxidation rate, however, the profiles were variable with time, as shown in figure 2. Whilst the changes were significant with respect to the accuracy with which the oxygen concentrations were measured, they were still relatively small. As a consequence, it was possible to use the region with the greatest gradient to establish a reasonable upper bound on the oxidation rate within the dump.

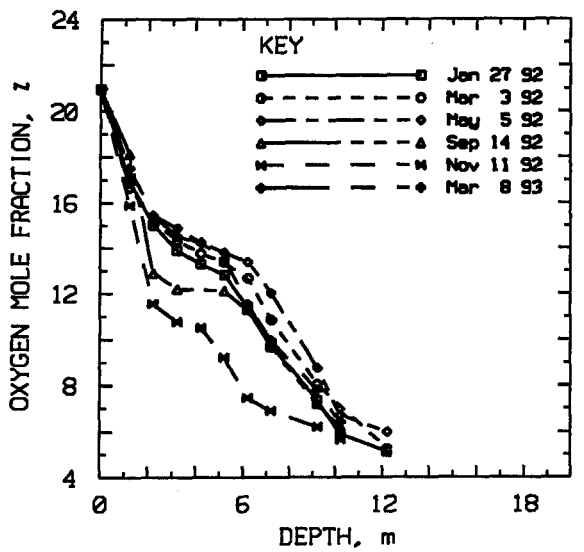

Figure 2. Pore gas oxygen concentrations measured in probe hole A1.

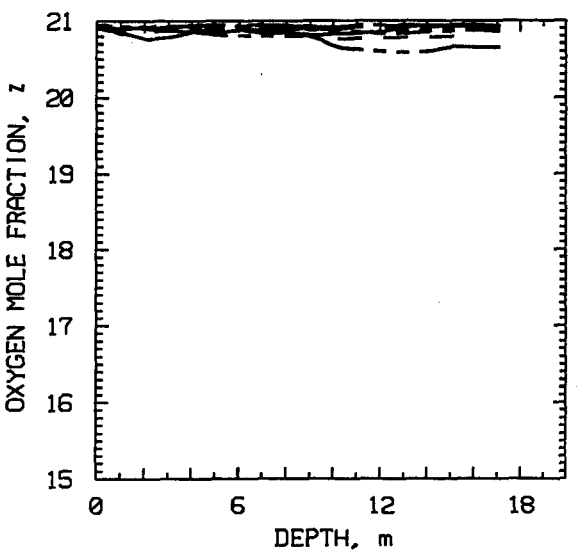

Figure 3. Oxygen concentrations measured in probe hole A7 between April 1991 and January 1992.

So, if an analytic function can be found to represent a particular oxygen concentration profile well, and the assumptions on which equation 2 is based are satisfied, then the volume oxygen absorption rates or oxidation rates (S) can be easily found by calculating the second derivative or curvature of the function at a given depth.

Results

Oxygen Results

Typical results from the pore gas oxygen concentration measurement program are presented in figures 2 and 3. In general, the oxygen concentration fell monotonically from the surface of the dump, indicating that the oxygen supply mechanism to the sites of pyritic oxidation was dominated by diffusion.

The measured profiles fell into two groups. There was a region near the edge of the dump (probe holes A1, A2, A5, A10, and A11; see figure 2 for example) where there were high gradients in the oxygen concentration profiles and in the central part of the dump the gradients were low (A3, A4, A6, A7, A8, and A12; see figure 3 for example). In the absence of any significant heating in the dump (see below) and making the assumption that the diffusion coefficient of the waste rock does not vary greatly with location, then it is reasonable to conclude that pyritic oxidation rates are relatively high in the region where the gradients are high, and are relatively low where the gradients are low.

The oxygen profiles in the material oxidizing at the higher rate indicate that oxygen was supplied by diffusion and that the rate was not limited by the oxygen supply rate. This means then that the rate is not dependent on the geometry of the dump or the location of the material in the dump, but is a property of the material itself. Clearly, such material may occur anywhere in the dump.

The oxygen profiles in the region with low oxidation rate settled down in a few weeks after installation of the holes. In the regions of high oxidation rate, however, the profiles were variable with time, as shown in figure 2. Whilst the changes were significant with respect to the accuracy with which the oxygen concentrations were measured, they were still relatively small. As a consequence, it was possible to use the region with the greatest gradient to establish a reasonable upper bound on the oxidation rate within the dump.

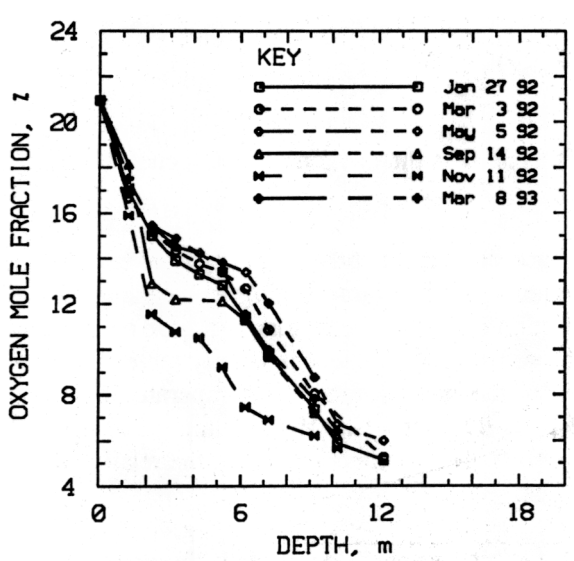

Figure 2. Pore gas oxygen concentrations measured in probe hole A1.

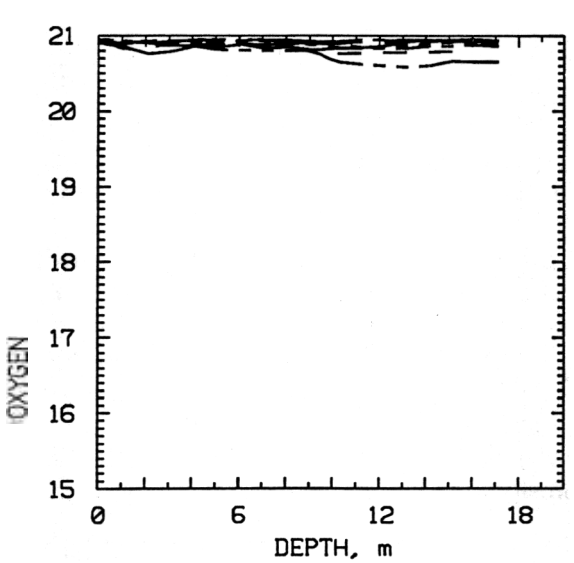

Figure 3. Oxygen concentrations measured in probe hole A7 between April 1991 and January 1992.

Following the method described above, functions of a suitable form were constructed and fitted using a least-squares method to the data points of the oxygen profiles measured in hole A1 over a 2-yr period, from April 1991 to April 1993. Since the oxygen concentration (mole fraction) at the surface of the dump is fixed at 20.95% (atmospheric), the fitted curves were constrained to pass through this point.

Figure 4 presents an example of the graphical results of the best fit of the predetermined function to data measured in the top 6.2 m of hole A1 in May 1992. (The measured profile indicates no oxygen consumption in the waste rock below this depth.) In the figure the axes have been normalized so that the atmospheric oxygen concentration (20.95%) = 1 and the depth of 11.22 m = 1. The normalized data and error estimates are also shown. The function clearly describes the measured pore gas oxygen concentration profiles very well. The second derivative or curvature of the fitted curve at a chosen depth was determined and converted to the volume absorption rate or oxidation rate. The oxygen diffusion coefficient in the dump, D, was taken as 4.1×10^{-6} m^2 s^{-1}, taking the gas-filled porosity as 0.28 and using the curve of Papendick and Runkles (1965). This procedure produced a set of oxidation rates at a series of depths and time.

The oxidation rates thus determined from the hole A1 profiles ranged from $(3.1 \pm 0.2) \times 10^{-9}$ kg m^{-3} s^{-1} to $(4.3 \pm 0.3) \times 10^{-8}$ kg m^{-3} s^{-1}, with an average volume absorption rate for the high oxidation region of the dump of close to 1×10^{-8} kg m^{-3} s^{-1}.

Another method for quantifying oxidation rates in the dump from the measured pore gas oxygen concentration profiles involved obtaining the oxygen fluxes into the top surface of the dump. The gradient of the pore gas oxygen concentration at the surface for each measured profile was determined graphically, and the surface oxygen fluxes were estimated using the oxygen diffusion coefficient given above. The surface oxygen fluxes varied with location, with two distinct classes of surface oxygen fluxes being seen in the test area. In keeping with the earlier analysis, higher fluxes were found at the edge of the dump, with lower fluxes in the central region. The average values of surface oxygen flux into the dump were found to be $(15 \pm 9) \times 10^{-8}$ kg m^{-2} s^{-1} at A1, A2, A5, A10, and A11 and $(0.25 \pm 0.25) \times 10^{-8}$ kg m^{-2} s^{-1} at A3, A4, A6, A7, A8, and A12. The standard deviation on the averages represents flux variations with location and time, although a clear seasonal pattern was not seen.

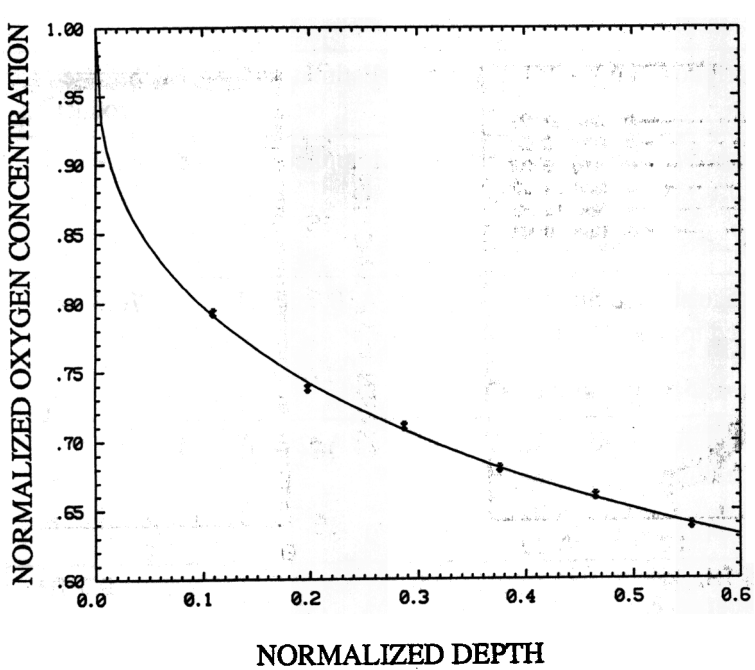

Figure 4. Function fitted to the pore gas oxygen concentration data measured in probe hole A1 in May 1992.

The shape of the oxygen profiles at the bottom of A1 implies a flux through the base of the dump. The average value of this flux was estimated to be 2×10^{-8} kg m^{-2} s^{-1}. The net oxygen flux (oxygen consumed in the dump) is then simply the difference between the surface and bottom oxygen fluxes, which was found to be 13×10^{-8} kg m^{-2} s^{-1}. The flux through the base of the dump in the central region of the dump was taken to be negligibly small, because the gradients at the bottom of the profiles show no indication of such a flux, and because neglecting any flux through the base leads to an overestimate rather than an underestimate of pollution generation in the dump.

The total amount of oxygen consumed in the whole dump can be estimated by using either the surface flux values or the volume oxygen absorption rates. Assuming that all the oxygen diffusing into the dump surface was consumed by pyritic oxidation, then oxygen consumption can be converted into sulfate production using the overall stoichiometry of the reaction of oxygen with pyrite (1 kg oxygen → 1.714 kg sulfate).

Three estimates of the pollution generation rate from the 130 ha dump which drains into the cutoff drain have been made, which effectively put upper and lower bounds on the rate:

1. The average volume absorption rate of 1×10^{-8} kg m^{-3} s^{-1} obtained from hole A1 was applied to the whole dump. At this rate of absorption, diffusion will limit oxidation to the top 15 m of the dump, so the effective thickness of the 130-ha dump is taken to be 15 m. This gives an annual sulfate production rate of 10,500 t/yr.

2. An estimate of 10,000 t/yr of sulfate was obtained by applying the average surface flux at A1, A2, A5, A10, and A11 (15×10^{-8} kg m^{-2} s^{-1}) to the whole dump.

3. A lower bound was estimated by using the average of the six lowest oxygen fluxes (A3, A4, A6, A7, A8, and A12). The average of these fluxes, 0.25×10^{-8} kg m^{-2} s^{-1}, was applied to the whole dump and yielded a rate of 180 t/yr of sulfate.

The results are summarized in table 1, expressed in units of tonnes per hectare per year.

Table 1. Annual Sulfate Production from the 130-ha Dump (t ha^{-1} yr^{-1}).

Description of Method Used for the Estimate	Sulfate production
Oxygen volume absorption rate at A1 applied to whole dump. Rate = 1×10^{-8} kg m^{-3} s^{-1}	80.9
Average surface flux at A1, A2, A5, A10, and A11 applied to whole dump. Flux = 15×10^{-8} kg m^{-2} s^{-1}	76.9
Average flux at A3, A4,A6,A7,A8, and A12 applied to whole dump. Flux = 0.25×10^{-8} kg m^{-2} s^{-1}	1.4

Oxidation Rates From Temperature

Whilst oxidation rates can in principle be obtained from measured temperature profiles, where heat is generated by the pyritic oxidation reaction, this has been found to be too difficult with the Aitik data owing to a number of factors as outlined below.

The ambient average monthly temperatures at the Aitik site range from -13.5°C in January to 13.2°C in July. The near-surface temperatures in the dump follow the ambient ones closely when they are positive, but once the surface freezes the dump temperatures do not drop below -5°C. During the months when the dump surface is warming up, the temperature in the dump is highest at the surface, but as the surface cools down, the temperature peak travels deeper into the dump. The attenuation and phase shift of the Fourier components of the temperature signal at the surface depend on the thermal properties of the dump.

Figure 5 shows the temperature profiles measured in hole A1 over a 10-month period and illustrates how the large seasonal swing in surface temperatures affects the temperature of the dump to a depth of at least 10 m. Because the average ambient temperature at the site is close to 0°C, the temperature of about 2.5°C which is seen in the lower part of the dump can be attributed to heating due to pyritic oxidation. This is a relatively small signal, especially when compared with the temperature fluctuations due to insolation in the top half of hole A1, where the oxidation has been found to be occurring.

A further difficulty with any analysis of the temperature data is that the boundary condition at the base of the dump is unknown. Water is flowing close to the interface between the dump and the original ground surface and will have affect measured temperature distributions, but not enough is known about the system to be able to quantify this reliably.

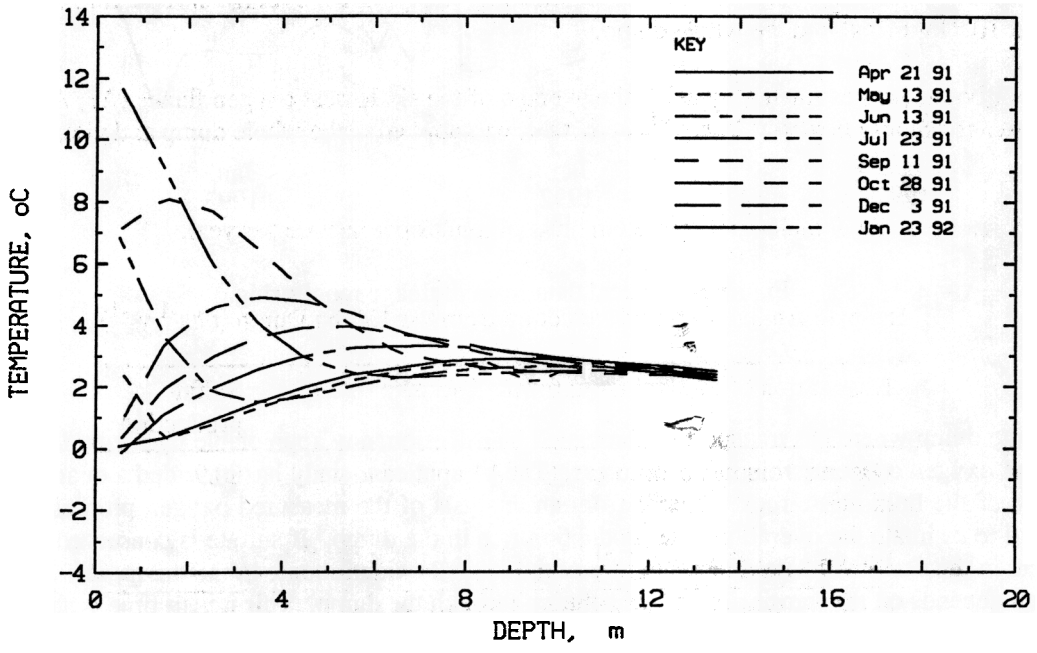

Figure 5. Temperature profiles measured in probe hole A1.

Flows, Concentrations and Loads

Figure 6 shows a typical result for the monitoring in the cutoff drain of drainage flow rates and sulfate concentrations. The instantaneous load is the product of the flow and concentration. The average annual load was obtained by integrating the load over the period. A careful analysis of the water balance and drainage data showed that a constant sulfate load was coming from the tailings dam, underflowing the waste rock dump and entering the cutoff drain. This load was subtracted from the total load in the drain to give a value of 12.1 t ha^{-1} yr^{-1} for the annual sulfate

production of the waste rock dump. As presented in table 1, the annual sulphate production rate from the high and low IOR material in the dump has been estimated to be 80.9 t ha^{-1} yr^{-1} and 1.4 t ha^{-1} yr^{-1}, respectively. The drain data implies, then, that 14% of the dump is composed of the high IOR material and the rest has the low IOR.

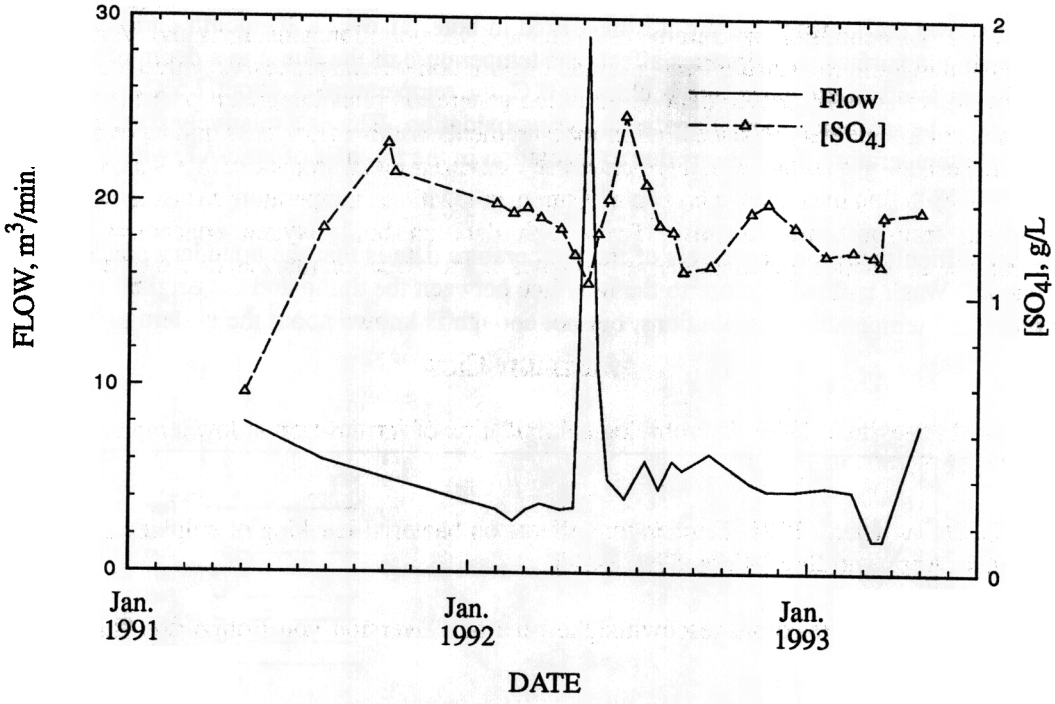

Figure 6. Typical data from drainage monitoring.

Discussion and Conclusions

In a large dump where gas transport is dominated by diffusion, any appreciable pyrite oxidation rate leads to a reduction in the oxygen concentration in the pore gas. The present case study has provided a quantitative estimate of oxidation rates of the bulk waste rock material from an analysis of the measured oxygen profiles. These oxidation rates were used to estimate the overall sulfate production rate in the dump. If sulfate is conserved in the system then the sulfate load in the drain will be a direct measure of the overall oxidation rate in the dump, shifted in time by some function which depends on the transit time of the solution through the dump. This transit time is short, of the order of a few years in typical dumps, compared with the time to oxidize the whole dump.

Analysis of oxygen concentration profiles showed that material in some regions of the dump investigated had an IOR of about 10^{-8} kg m^{-3} s^{-1} which was some 60 times greater than that of material in other regions. A comparison with pollution loads from measurements in the cutoff drain indicates that if 14% of the dump has an IOR of 10^{-8} kg m^{-3} s^{-1} then 86% has an IOR that contributes little to the total pollution load from the dump.

The temperature rise in the dump from heat produced in the pyritic oxidation reaction was too small to extract the oxidation rate from the temperature profiles, particularly in the top 6 m of the dump, where the changes caused by seasonal temperature changes were large. Hence, although in principle the oxidation rate can be extracted from both the temperature and oxygen concentration profiles in the dump, in practice it was possible to use only one of these methods.

It is important to note that the "high" IOR found for the Aitik waste rock dump material is about eight times lower than the highest value found for waste rock at Rum Jungle in northern Australia (Harries and Ritchie 1981). It should be stressed, however, that a comparatively low IOR such as that found for the Aitik waste rock dump material still generates significant pollution loads in drainage. The main reason is that in the early history of the dump, which may last for many years, a low IOR means that a large region of dump is involved in oxidation.

The case study presented here has emphasized the utility of using pore gas oxygen profile measurements together with flow and concentration measurements to characterize pollution generation and drainage from a dump. In general, oxygen and temperature measurements provide information on rate processes within the dump, while the flow and concentration measurements provide data on pollution generation rates integrated over the whole dump. The set of measurements is complementary. Concentration measurements without flow rates and an overall water balance for the dump lead, at best, to a qualitative assessment of the environmental impact of the waste rock dump or of the effectiveness of rehabilitation measures. Oxygen measurements without temperature measurements can lead to wrong conclusions on gas transport mechanisms. Even with data on both oxygen concentrations and temperature distributions it may be in practice that quantitative estimates of the oxidation rate can be extracted from only one set of data.

Literature Cited

Ahonen, L. and O. H. Tuovinen. 1989. Microbiological oxidation of ferrous iron at low temperatures. Appl. and Env. Micro. 55:312-316.

Ahonen, L. and O. H. Tuovinen. 1991. Temperature effects on bacterial leaching of sulphide minerals in shake flask experiments. Appl. and Env. Micro. 57:138-145.

Arrhenius, S. 1889. Uber die Reaktionsgeschwindigkeit bei der Inversion von Rohrzucker durch Sauren. Z. Phys. Chem. 4:226-248.

Axelsson, C.L., J. Byström, J. Holmén, and T. Jansson. 1992. Efterbehandling av sandmagasin och gråbergsupplag i Aitik, Hydrogeologiska förutsättningar för åtgärdsplan. Report 927-1801 (in Swedish), Golder Geosystem AB.

Ferroni, G. D., L. G. Leduc, and M. Toddm. 1986. Isolation and temperature characterization of psychrotrophic strains of *Thiobacillus ferrooxidans* from the environment of a uranium mine. J. Gen. Appl. Micro. 32:169-175.

Galbraith, D.M. 1991. The Mount Washington acid mine drainage reclamation project. p. 145-161. In Proceedings of Second International Conference on the Abatement of Acidic Drainage, v. 2. (Montreal, PQ, September 16-18, 1991).

Harries, J.R. and A.I.M. Ritchie. 1981. The use of temperature profiles to estimate the pyritic oxidation rate in a waste rock dump from an open-cut mine. Water, Air, Soil Pollution 15:405-423.

Okerke, A, and S. E. Stevens. 1991. Kinetics of iron oxidation by *Thiobacillus ferrooxidans*. Appl. and Env. Micro. 57:1052-1056.

Papendick, R. I. and J. R. Runkles. 1965. Transient-state oxygen diffusion in soil: I. The case when rate of oxygen consumption is constant. Soil Science 100(4):251-261.

MONITORING GASEOUS AND LIQUID FLUX IN SULFIDE WASTE ROCK[1]

William M. Schafer[2], Steven Smith[2], Chris Luckay[2] and Troy Smith[3]

ABSTRACT: A monitoring program was used to compare water migration, oxygen concentration, temperature, and solution chemistry in paired reclaimed and unreclaimed sulfide waste rock dumps in southwestern Montana. Slope regrading to a 2:1 gradient, addition of cover-soil, and revegetation appear to limit infiltration. In most locations, pyrite oxidation is only present in the upper 30 ft of the dump the region most affected by the wetting front to date. Waste rock in the lower 100 ft of the dump may be too dry to support microbial oxidation of pyrite.

Additional Key Words: acid mine drainage, hard-rock mining, waste rock, acid drainage abatement, environmental monitoring.

Introduction

Acid mine drainage (AMD) from waste rock disposal facilities is a prevalent concern at a number of Western U.S. hard rock mining sites. Relationships between waste rock geochemistry, internal water movement, and oxygen supply and their effect on surface and groundwater quality and on overall reclamation success are concerns of regulatory agencies. The dynamics of the sulfide oxidation reaction are closely related to waste rock mineralogy and hydrology. Infiltrating water may promote the migration of acidic and metal enriched pore water. While gaseous oxygen is usually abundant within a dump owing to the abundant porosity, heat produced during microbial pyrite oxidation may create a thermally driven advective circuit, in effect pumping oxygen to the reactive core of unreclaimed waste rock dumps (Harries and Ritchie 1987)(Fig. 1).

A number of facility engineering and reclamation practices may be used to minimize the risk of AMD for mine waste facilities in semi-arid areas (Schafer 1992). Regrading of the angle-of-repose dump slope may seal off the permeable "rubble zone" that forms at the base of end-dumped waste. In so doing, the advective oxygen supply may be limited. More importantly, placement of cover-soil and establishment of vegetation may promote surface runoff and increase evaporative consumption of water. In this way off-site AMD can be alleviated by reducing the rate of seepage through the facility. Other engineering practices such as dump construction in thin compacted lifts, and construction of waste cells within clay layers (Krauss 1990) have also been used.

The Golden Sunlight Mine is a large scale open-pit gold producer located in southwestern Montana. Gold is hosted in a breccia pipe system which is superimposed in a thick argillite sequence and quartz latite intrusives. Unoxidized waste rock typically contains 2% to 5% pyritic S and has negligible neutralization capacity. Over 100 million mt of waste rock have been placed in single stage dumps around the perimeter of the pit. Owing to the steep terrain, dump height exceeds 600 ft in some locations.

Reclamation techniques utilized at the Golden Sunlight Mine (Fig. 2) are designed to limit acid production and migration by (1) reducing infiltration of water and (2) reducing the supply of oxygen. Regrading of slopes from all angle of repose of 1.4:1 to 2:1 is designed both to reduce the slope steepness and to seal off rubble zones at the original dump toe, thus reducing the potential for advective air movement into the dump. Application of rock

---

[1]Paper presented at the International Land Reclamation and Mine Drainage Conference and the Third International Conference on the Abatement of Acidic Drainage, Pittsburgh, PA, April 24-29, 1994.

[2]William M. Schafer, Principal, Steven Smith, Senior Scientist, and Chris Luckay, Staff Engineer, Schafer and Associates, Bozeman, MT, USA.

[3]Troy Smith, Reclamation Scientist, Golden Sunlight Mine, Whitehall, MT, USA.

capping material and cover-soil limits water infiltration, increases runoff, and further reduces oxygen movement into the dump. As vegetation becomes established in the applied cover-soil, plant water use and evaporative water loss will increase. Information acquired in this study will enable the long-term effectiveness of waste rock reclamation to be evaluated at the Golden Sunlight Mine.

The objective of this on going investigation is to concurrently monitor the hydrologic conditions in a large unreclaimed angle-of-repose waste rock dump and a paired reclaimed dump. A combination of downhole monitoring techniques was used to measure differences in gaseous oxygen concentrations, temperature, water content, and pore water chemistry.

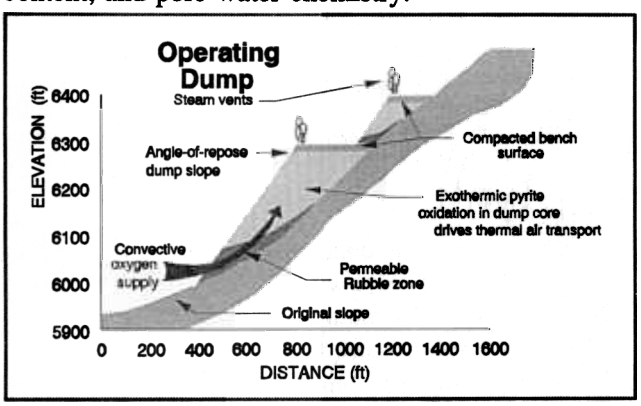

Figure 1. Characteristics of an operating high sulfide dump.

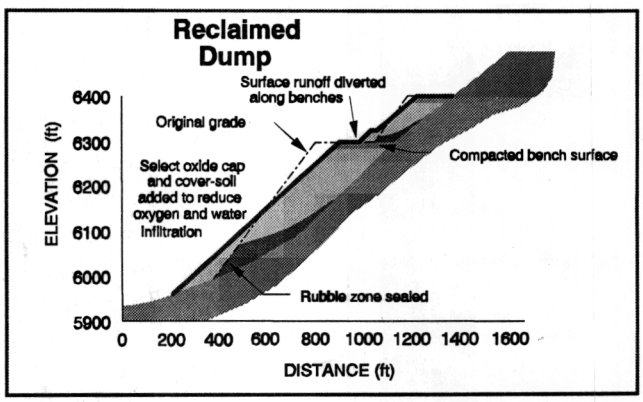

Figure 2. Reclaimed waste rock dump showing placement of soil cover and sealing of the rubble zone.

Methods

A large portion of the northwest dump complex at the Golden Sunlight Mine was regraded in 1991. Approximately 60 cm of oxidized waste rock and 50 cm of cover-soil were placed over the 2:1 regraded slopes. A mixture of dryland grasses and forbs were seeded in spring 1992. Monitoring installations were placed near the crest (site 1) and toe (site 3) of the reclaimed slope (section A-A' in Figs. 3 and 4). In addition, monitoring devices were installed on a prominent reclaimed bench (site 2) designed to direct runoff off the regraded slope. Similar monitoring devices were installed on the bench (site 6) and toe (site 7) of an unreclaimed angle-of-repose dump (section C-C', Figs. 3 and 4).

A climate station was installed at site 2 to provide daily rainfall and temperature data. Downhole devices included thermistors, heat dissipation units, neutron probe access tubes, gas sampling ports, and pore water samplers. Due to the cost of drilling in waste rock, most installations involved multiple-depth completion in the same hole. Neutron probe access tubes consisted of core steel augered into the waste rock. This installation technique maintained close contact with waste material to facilitate water content measurement. Gas-sampling ports were staggered throughout the depth of waste rock (Figs. 5 and 6) which varied from 40 to 170 feet. Shallow pore water samplers installed at depth of 3, 5 and 10 ft consisted of Soil Moisture model 1920 ceramic tip pressure-vacuum lysimeters. Lysimeters installed near the base of the dump (at over 100 ft) were BAT lysimeters which are more suitable for sample recovery from greater depths.

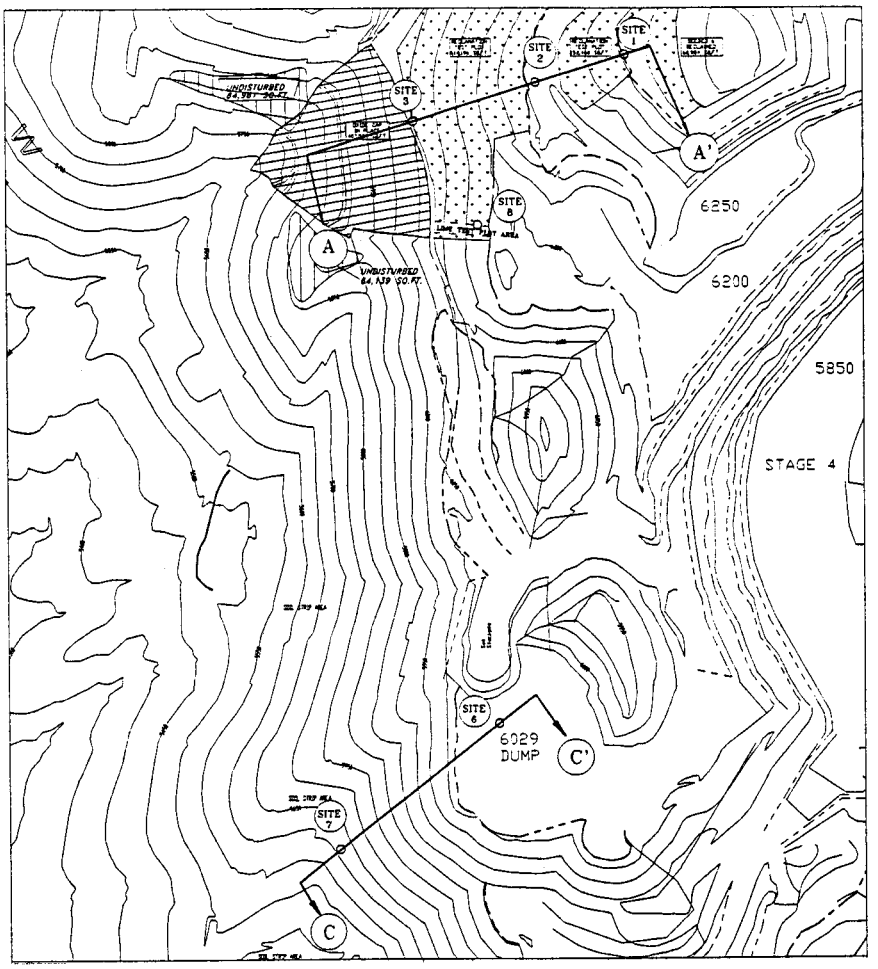

Figure 3. Plan view of Golden Sunlight Mine northwest dump showing reclaimed (north) and unreclaimed (south) test dumps.

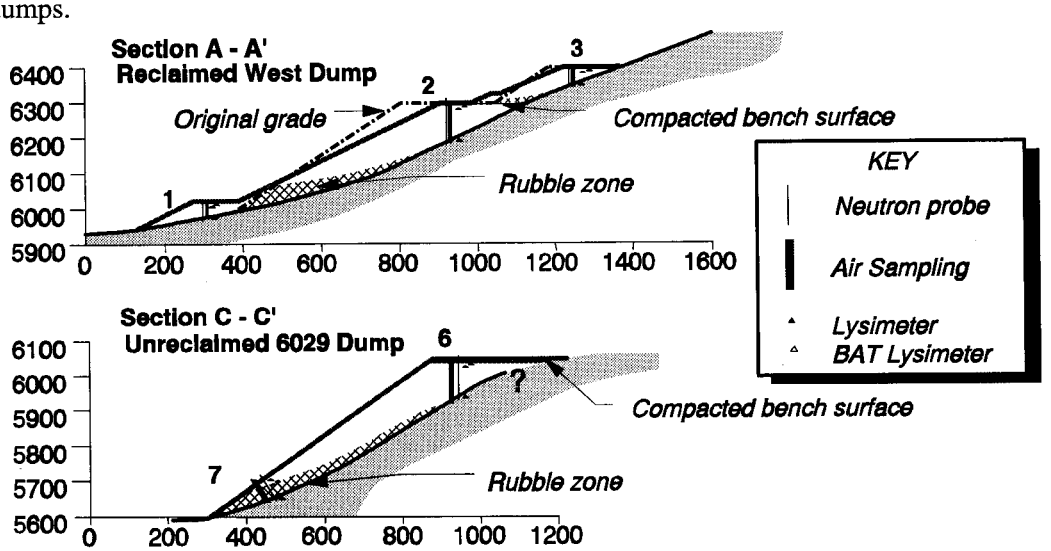

Figure 4. Cross-section view of monitoring devices installed in the northwest dump.

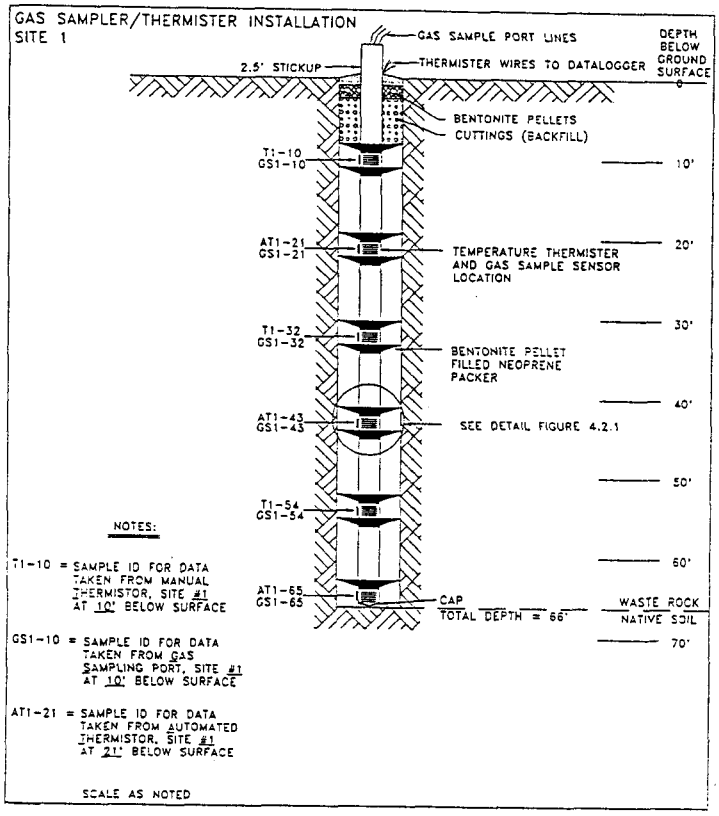

Figure 5. Typical multiple completion gas port assembly for site 1 in the reclaimed section of the Golden Sunlight Northwest Dump.

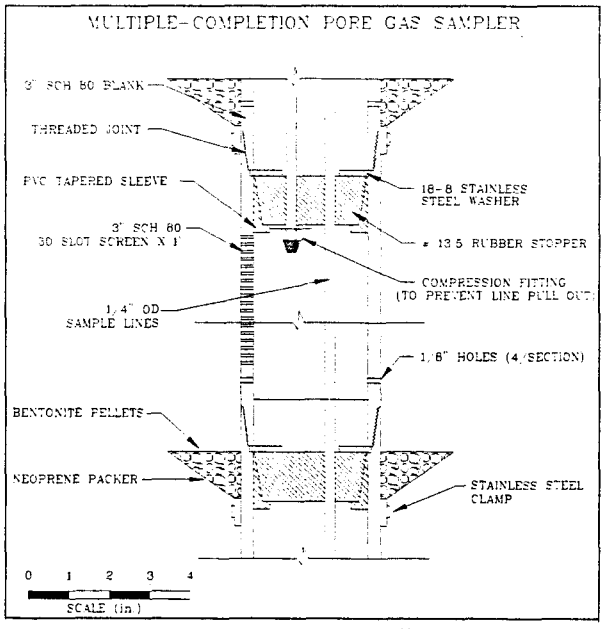

Figure 6. Detail of gas sampling port.

Routine monitoring of temperature, water content, oxygen levels, soil suction levels, and pore water chemistry began in mid-1992. The purpose of the hydrologic monitoring program was to identify differences in oxygen supply, water flux, and pore water chemistry in reclaimed and unreclaimed dumps.

Results

Water Content and Water Balance

Water content in waste rock at the Golden Sunlight Mine is a function of the average rock particle size, and prior saturation by rainfall infiltration. During placement, freshly shot waste rock typically has a volumetric water content of less than 6 percent. The rock particle size gradually increases with depth due to gravity sorting in the end-dumping sequence. As a consequence, residual saturation varies between 8 and 12 percent within the dump with residual saturation generally lower near the base of the dump where larger particles are deposited. Overall, the waste rock has a volumetric "wetting requirement" of 3 to 5 percent. Infiltration gradually wets the waste rock from its initial water content to residual saturation or field capacity. The upper 6 to 10 ft of each waste rock bench differs from the remaining waste rock due to vehicle compaction which pulverizes the material. The fines generated cause residual saturation levels to reach 15 to 20 percent. A 100 ft column of waste rock would retain 3 to 5 ft of solution before seepage could migrate out of the pile.

The overall water balance for each monitoring point is presented in Fig. 8. The cumulative precipitation from July 1992 to October 1993 is compared to the cumulative change in water within the vertical extent of the

dump. Essentially all of the incident precipitation appeared to infiltrate into the toe of the unreclaimed waste rock pile (site 7). The wetting front appears to have nearly reached the base of the dump at site 7. Both the reclaimed dump bench (site 2) and the crest of the unreclaimed dump (site 6) gained far more water than the cumulative rainfall. This apparent anomaly is probably due to run-on from natural hillslopes upgradient of the dump and lateral seepage along the dump foundation. The reclaimed 6300 bench (site 2) was located in a depression which collected a significant amount of runoff water from the 6400 slope in both 1992 and 1993. The control crest location appeared to decrease in water content between spring and late summer of 1993. This change in water content may represent flux of water below the base of the dump.

Both site 1 and site 3, the crest and toe of the reclaimed dump, exhibited a greatly reduced intake of water, averaging about 30 to 40 percent of the incident precipitation. As vegetation becomes better established, the performance of the revegetated soil cap in reducing infiltration is expected to improve. Rainfall received during 1993 was approximately double the long-term average rainfall at the site.

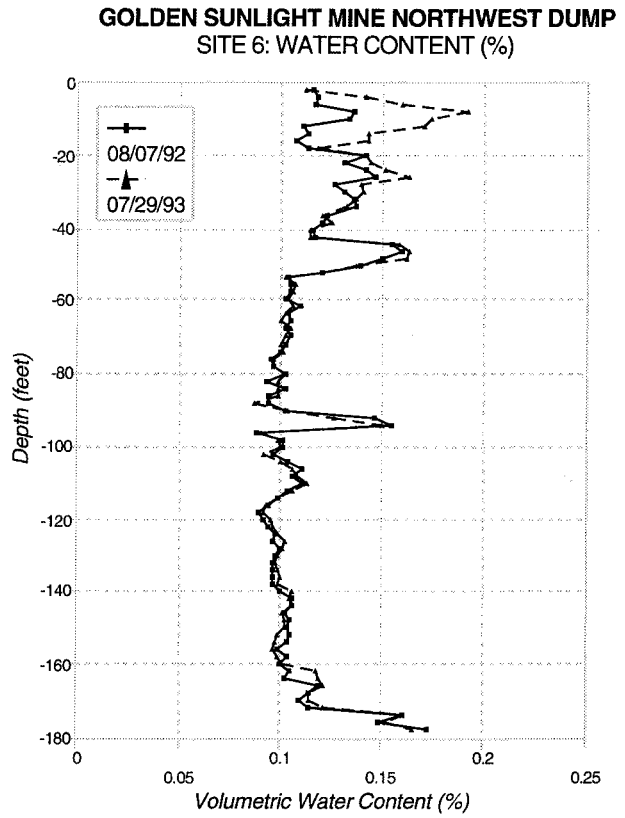

Figure 7. Water content variation with depth in the untreated dump crest. Natural soils were encountered at 175 feet.

Suction Levels

Heat dissipation units are automated devices used to measure soil water potential in soils. A data-logger is used to measure soil suction levels hourly. Long-term trends in suction at site 1 (Fig. 9) corroborated the soil water content data. The base of the dump remained extremely dry at the end of 1993 (water potential <-10 bars) because the wetting front had not reached this level. Soil water potential at 3, 5 and 10 feet generally ranged from -0.6 to -0.3 bars indicating that materials are at residual saturation at these depths. Minor increases in water potential occurred in response to rainfall events.

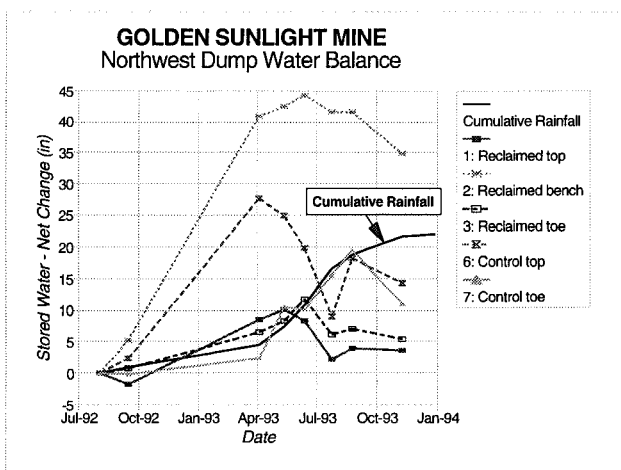

Figure 8. Site water balance for the reclaimed and unreclaimed Northwest Dumps.

Temperature

Temperature is particularly important in this investigation because pyrite oxidation is strongly exothermic. Hence, elevated temperatures provide a direct indication of the spatial extent of microbial pyrite oxidation. Temperature trends for numerous measurement depths at each site are presented in Fig. 10. Site 1 does not indicate significant pyrite oxidation. Temperatures average 8°C, the average annual air temperature. Seasonal temperature fluctuation is only pronounced at the three foot depth. Pyrite oxidation has been triggered between 40 and 75 feet at site 2, the reclaimed 6300 bench. Interestingly, heating is confined to the wetting front which has moved from 40 to 80 feet during the two years of monitoring. It appears that dry waste rock placed at water content below residual saturation (less than about 10%) may be too dry to support *Thiobacillus ferrooxidans* activity. Similarly, the upper 10 feet of the unreclaimed crest is just beginning to heat, and the 33 foot depth which was wetted in mid 1993 may be beginning to heat. The toe of the angle of repose dump had extremely cold temperatures indicative of cold air drainage within the pile. Water content measurements indicated that a large mass of ice developed at this location and melted in late summer.

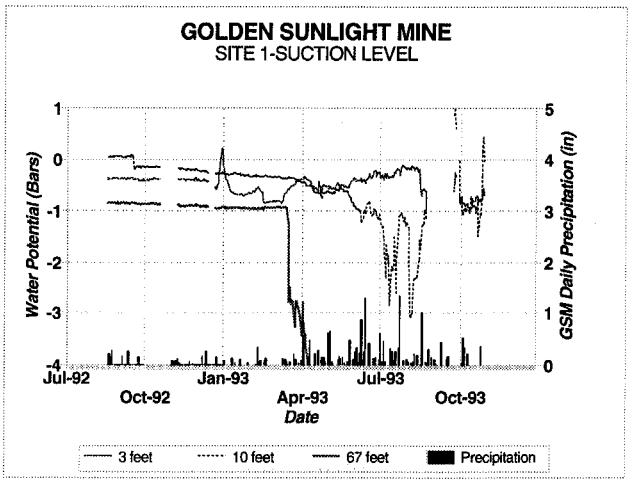

Figure 9. Seasonal variation in soil suction beneath the crest of the reclaimed dump.

Oxygen Levels in Waste Rock Pore Space

Oxygen concentrations were highly elevated at all depths in the reclaimed and unreclaimed waste rock at Golden Sunlight (Fig. 11). Minor decreases in O_2 were noted near the surface of reclaimed sites during the 1993 growing season. The applied cover-soil layer did not serve as an effective oxygen diffusion barrier, however. Reduced oxygen levels were only noted at 33 feet at site 2, the depth at which extreme heating was also noted. The high oxygen levels throughout most of the dump could be either attributed to rapid oxygen advection or diffusion rate or to a lack of oxygen consumption. For the drier, lower half of the dump, oxygen demand appears to be slight due to the apparent minor microbial pyrite respiration.

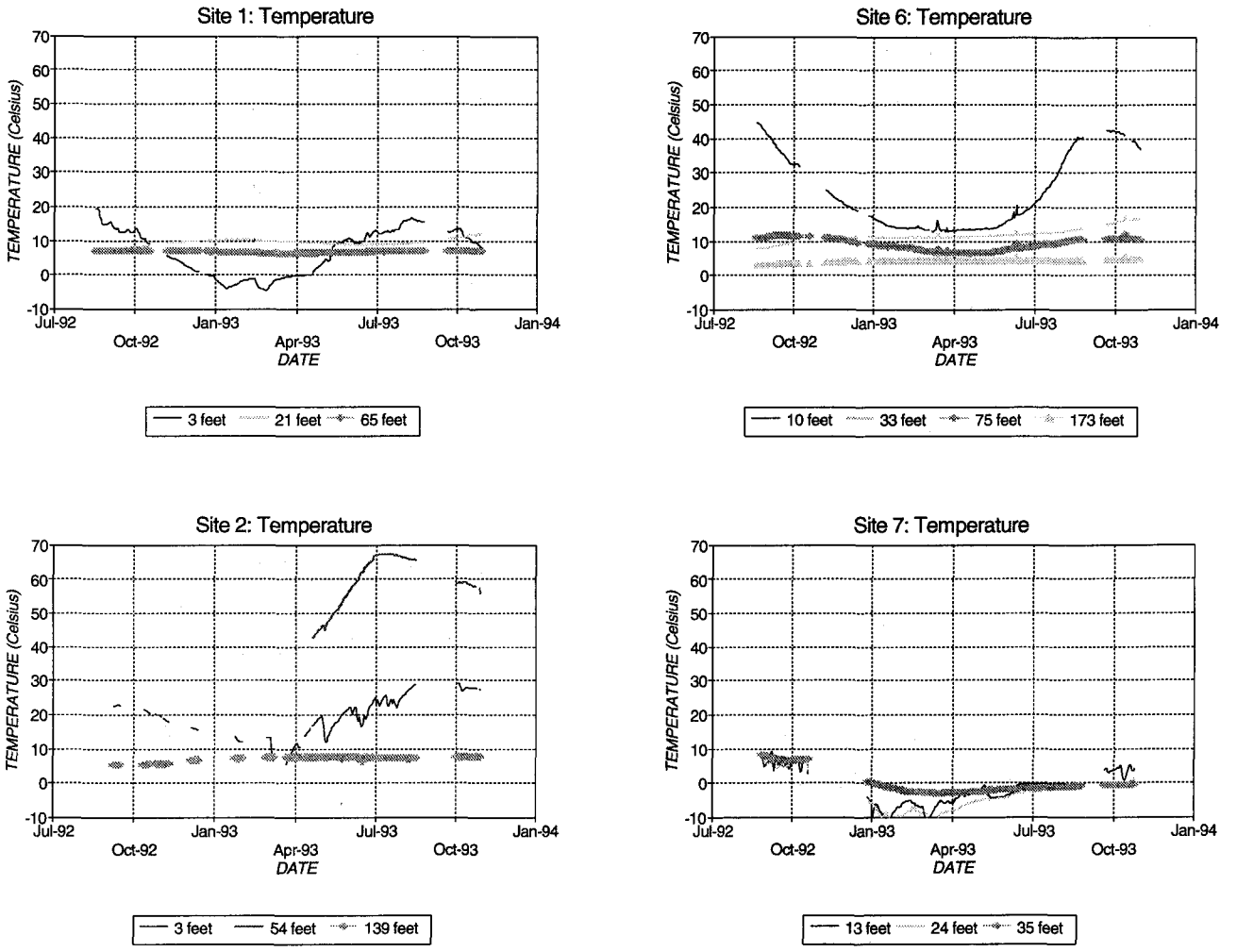

Figure 10. Soil temperatures at reclaimed and unreclaimed monitoring sites.

Pore Water Chemistry

Pore water samples were obtained from 3, 5 and 10 feet in depth at most sites. Samples of pore water could not be obtained from deeper lysimeters placed at the foundation of the dump either due to mechanical damage of the access tube from consolidation or due to very low soil suction levels. In general, pH of pore water ranged from 1.5 to 3 in sulfide waste rock and was from 4 to 7 in oxide waste rock and cover-soil layers.

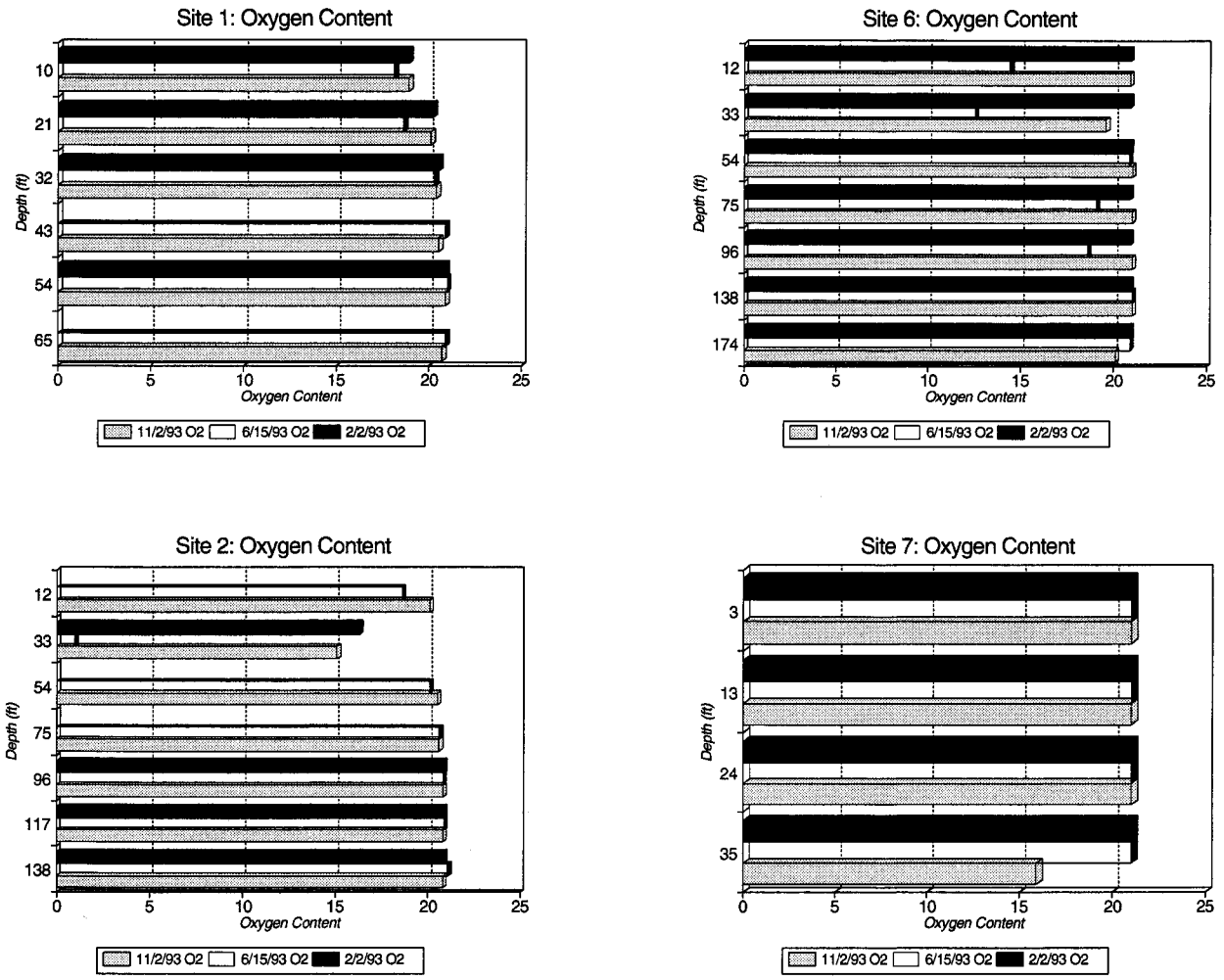

Figure 11. Oxygen levels in pore space at reclaimed and unreclaimed monitoring sites.

Conclusions

Regrading and addition of cover-soil to sulfide waste rock dumps appears to be effective in reducing infiltration of water into the dump. As vegetation becomes established, infiltration may decrease to the point that the rate of migration of the wetting front will be diminished.

Oxidation of pyrite is accompanied by evolution of heat. Although thermally-driven advection was thought to maintain an ample oxygen supply to reactive zones within the dump, the advective cells may be surficial rather than being fed from the coarse-textured dump foundation as originally hypothesized.

Migration of the wetting front, which is currently at around 30 feet through most of the dump, appears to trigger sulfide oxidation. Deeper materials that are relatively dry do not appear to be reacting at present. Pronounced hillslope effects also affect water movement within the dump. Run-on from upgradient areas, and ponding of water on erosion control benches has stimulated deeper water movement in few portions of the Northwest Dump at Golden Sunlight. The practice of concurrent reclamation, that is progressive regrading and revegetation during mining, may be particularly important for sulfide waste rock facilities in semi-arid climates.

Literature Cited

Harries, J.R. and A.I.M. Ritchie. 1987. The effect of rehabilitation on the rate of oxidation of pyrite in a mine waste rock dump. Environ. Geochem Health 9:27-36.

Krauss, Raymond E., 1990. Reclamation Practices at Homestake's McLaughlin Mine. Mining Engineering Nov. 1990(1239-1241).

Schafer, W.M. 1992. Acid-Forming Mining Waste: Prediction, Control and Treatment. pg 345-353 In Randol Gold Forum, Vancouver, B.C., Canada. March, 1992.

COMPARISON OF DULUTH COMPLEX ROCK DISSOLUTION IN THE LABORATORY AND FIELD[1]

Kim A. Lapakko[2]

Abstract: The quality of drainage and the release of sulfate, calcium, and magnesium from five field test piles of Duluth Complex rock with sulfur contents of 0.63% (three piles), 0.79%, and 1.41% were determined for periods of 12 to 14 yr. The pH of drainage from the piles decreased over time and with increasing solid-phase sulfur content. The ultimate drainage pH values for the 0.63% S piles ranged from 4.8 to 5, similar to values observed in the laboratory. Ultimate drainage pH values for sulfur contents of 0.79% (pH 4) and 1.41% (pH 3.5) were about one unit lower than the corresponding laboratory values for these sulfur contents. Over the entire period of record, average rates of sulfate release (2.1 to 10.5 mmol/mt/d) and magnesium release (0.55 to 3.7 mmol/mt/d) increased as the solid-phase sulfur content of the pile increased, while those of calcium release (1.2 to 2.4 mmol/mt/d) were relatively constant with respect to solid-phase sulfur content. Annual release rates for sulfate and calcium were relatively constant over time, while those for magnesium tended to increase over time. Annual release rates for all three parameters increased with increased annual drainage volume, a variable not examined in the laboratory. Release rates in the field were typically 10% to 30% (and in one case, nearly 40%) of those observed in the laboratory. Empirical neutralization potentials in the field decreased as solid-phase sulfur content decreased and were typically 10% to 50% of the corresponding average laboratory values. The empirical neutralization potentials to maintain drainage pH above 6.0 were approximately 0.5% to 8% of ABA NP values for Duluth Complex rock.

Additional key words: acid mine drainage, sulfide mineral oxidation, pyrrhotite, field test, rates.

Introduction

In the mid-1970's AMAX Exploration Inc. was evaluating the potential for developing copper-nickel resources of the Duluth Complex in northeastern Minnesota. At this time little information existed on the potential drainage problems associated with copper-nickel development in Minnesota. The State and AMAX agreed to commence field leaching tests on Duluth Complex rock. AMAX began excavation of a shaft in 1975 and in 1977 constructed six test stockpiles containing lean ore material. Water quality samples were collected periodically from each pile in 1977, and the data were compiled by AMAX Environmental Services Inc. (1978). The test pile studies were conducted from 1978 through the present by the Minnesota Department of Natural Resources (MNDNR), Division of Minerals (Eger and Lapakko 1981, 1985). As part of a cooperative research project with the U. S. Bureau of Mines, the compilation and analysis of data from the test piles were updated through 1991 to aid in development of a dissolution model by the Salt Lake City Research Center. This paper presents data on the quality and quantity of drainage from five of the test piles and the rates of mineral dissolution observed from 1978 through 1991. The period of record for pile 4 was only 5 yr, and these data are not presented. The data are compared with those previously presented on laboratory studies on the dissolution of Duluth Complex rock.

Objectives

The objectives of this paper on the quality of drainage from Duluth Complex rock field test piles are to

1. Describe the variation of drainage quality with respect to solid-phase sulfur content, time, and flow.
2. Determine the rates of sulfate, calcium, and magnesium release.
3. Describe the variation of drainage quality and mass release with respect to sulfur content, time, and flow.

---

[1]Paper presented at the International Land Reclamation and Mine Drainage Conference and the Third International Conference on the Abatement of Acidic Drainage, Pittsburgh, PA, April 24-29, 1994.
[2]Kim A. Lapakko, Principal Engineer, Minnesota Department of Natural Resources, Division of Minerals, St. Paul, MN, USA.

4. Determine the empirical acid neutralization potentials of the Duluth Complex rock samples examined.
5. Compare field results with those generated in the laboratory.

Methods

Climate

Annual precipitation in the study area averages 72.1 cm (Hickok and Associates 1977), and the average watershed runoff is 26.2 cm/yr (Siegel and Ericson 1980). Temperatures are extreme, averaging -14° C in January and 19.1° C in July, with an annual mean of 3.6° C; the ground is covered with snow for an average of 140 days per year (Hickok and Associates 1977).

Test Pile Construction

Materials. Six test stockpiles containing 820 to 1300 metric tons (mt) of low-grade copper-nickel material were constructed in 1977. The piles were approximately 4 m high and 15 m by 25 m at the base. Stockpiles 1 to 4 were constructed of rock mined during the shaft-sinking operation, while piles 5 and 6 contain material from underground drifts. The chemical compositional ranges for the piles are 0.63% to 1.41% S, 0.30% to 0.35% Cu, and 0.083% to 0.085% Ni (table 1). A grab sample was taken from test pile 1 for more extensive chemical and mineralogical analyses (Eger and Lapakko 1981). The major sulfide minerals identified and their volume percentages were pyrrhotite (0.844%), chalcopyrite-cubanite (0.769%), and pentlandite (0.037%). The major silicate minerals and their approximate volume percentages were plagioclase (59%), clinopyroxene (11%), olivine (11%), orthopyroxene (3.7%), and monocrystalline amphibole (3.6%).

Approximately 40% of test pile 4 was removed in 1982 for use in another study of stockpile reclamation techniques (Eger et al. 1984, Lapakko et al. 1986). At this time a representative sample weighing over 3 mt was collected for analysis of particle size distribution, specific surface area, chemistry, and mineralogy. The methods and detailed results of this characterization are presented in Lapakko et al. (1986). The particle size analysis revealed that 11% of the grains were larger than boulder/cobble size classification ($d > 305$mm), 6.8% were boulder/cobble ($76.2 < d \leq 305$ mm), 63% were gravel ($2 < d \leq 76.2$ mm), 15.8% were sand ($0.074 < d \leq 2$ mm), and 4.7% were silt/clay ($0.053 < d \leq 0.105$ mm). The sand, silt, and clay fractions were analyzed for specific surface area, chemistry, and mineralogy. The specific surface area of the fine fractions was roughly inversely proportional to the particle size diameter (table 2). The pH decreased and the sulfide and trace metal content increased with decreasing particle size of the rock. The finer sand, silt, and clay fractions had S, Cu, and Ni contents above the 0.634% S, 0.348% Cu, and 0.083% Ni levels estimated for pile 4 as a whole.

Table 1 Summary of chemical and physical characteristics of test piles

		Pile 1	Pile 2	Pile 3	Pile 6	Pile 5
Date completed				4/20/77		9/10/77
S	%			0.63		1.41
Cu	%			.35		.30
Ni	%			.083		.085
Mass	mt			830		815
Volume	m^3			400		400
Collecting area	m^2			300		340
Surface area .	m^2			430		370
Cover material				Glacial till (coarse sand)		Sandy till over coarse sand
Ave. cover depth	cm	0	23	34	0	54
Vegetated		No	Yes	Yes	No	Yes

Table 2. Characterization of fine fractions from test pile 4.

Size fraction, mm	pH	Total sulfur, %	Sulfide, %	Cu, %	Ni, %	Co, %	Zn, %	Specific surface area, m^2/g
Sand								
0.50 -2.00	6.56	0.67	0.65	0.337	0.062	0.012	0.015	0.60
.177- .50	6.37	.80	.75	.381	.078	.013	.015	.78
.149- .177	6.18	.88	.80	.391	.103	.015	.015	1.1
.105- .149	NA	1.12	1.05	.495	.147	.019	.017	1.6
.075- .105	5.95	1.37	1.30	.585	.221	.022	.019	1.7
Silt and clay								
.053- .075	5.78	1.65	1.57	.647	.253	.024	.019	2.6
<.053	5.77	1.94	1.86	.814	.295	.027	.023	4.7

NA Not available.

X-ray diffraction (XRD) analyses were conducted on the 0.053- to 0.075-mm, the 0.075- to 0.105-mm, and the 0.105- to 0.149-mm size fractions of the rock. Approximately half of this material was plagioclase (with a Na:Ca ratio of about 2:3), and half was a mixture of olivine (with a Fe:Mg ratio of 1:4 to 1:9), pyroxene, and biotite. Lesser amounts of magnetite, amphibole, chlorite, and possibly smectite and/or vermiculite were also identified. The phyllosilicate minerals (biotite, chlorite, smectite, vermiculite) were more common in the finer size fractions.

Piles 1, 3, and 6 were partly covered by plastic at the end of the 1989 field season, for the practical purpose of reducing the volume of drainage the MNDNR is required to treat. The plastic covers were shredded during 1990 by exposure to the elements. A more robust Hypalon cover was placed onto pile 3, thereby terminating flow from this pile at the end of the 1989 field season.

Reclamation Treatments. Three of the piles were left uncovered, as controls, and the remaining three piles were covered (May 1978) with 18 to 29 cm of soil obtained from a nearby borrow pit. Pile 2 was covered with fertile topsoil obtained from the top 30 cm of the borrow pit, while piles 3 and 5 were covered by infertile coarse sand. In 1980 an additional 30 cm of sandy till was added to pile 5. Additional details on vegetation, fertilization, and the application of lime-stabilized sludge to pile 3 (1980, 1982) and a sodium-lauryl-based bactericide to pile 5 (1982) are available in Eger and Lapakko (1981, 1985).

Water Sampling and Analysis. For drainage collection, each pile is underlain by an impervious Hypalon liner (30 mil) which is sloped toward a 15.2-cm perforated plastic pipe. The drainage collected from the piles flows to a common sump. A limited number of water quality samples were collected in 1977, but no flow measurements were made. Since methods in this year deviated from those over the remainder of the study and the data were sparse, the results are not addressed in the text. During 1978, each pile was fitted with a cumulative flow meter and a flow-weighted composite sampler (Eger and Lapakko 1981). For each pump discharge, a fixed volume of sample was placed into the compositing container.

The composite samples were analyzed weekly through 1990 and biweekly subsequently. Samples were filtered through 0.45-μm filters to remove suspended materials prior to analysis. Routine analyses included pH, alkalinity, specific conductance, sulfate, copper, nickel, cobalt, zinc, calcium, and magnesium, although calcium and magnesium were not analyzed in 1983. (Some samples were also analyzed for sodium, potassium, chloride, and dissolved organic carbon.) Specific conductance was analyzed using a Myron L conductivity meter. pH was determined using a Radiometer 29 pH meter from 1978 to 1988, and subsequently using an Orion SA 720 with a

Ross combination electrode (8165). Sulfate was analyzed using the barium sulfate turbidimetric technique (APHA et al. 1992). Metals were analyzed with a Perkin Elmer 603 atomic absorption spectrophotometer.

Calculations

For each period over which composite samples were collected, the mass release was calculated as the product of the concentration in the composite sample and the volume of flow during the period over which the composite was collected. Annual mass release was calculated as the sum of the mass release values for the individual periods for each year. Annual flow-weighted mean concentrations were calculated by dividing the annual mass release by the annual flow. The annual rates of release were calculated as the annual mass release divided by the product of the number of days of flow and the mass of the pile (mt). Average rates of release for the entire period of record were calculated by dividing the total mass release by the number of days of flow.

Empirical neutralization potentials (ENP) were calculated to determine the amount of acid neutralized by the solids prior to the drainage pH decreasing and, for the duration of the period of record, remaining below pH values of 7, 6, 5, 4.5, and 4. The acid neutralized was calculated as the cumulative calcium and magnesium release (expressed as kilograms of $CaCO_3$ per metric ton of rock, or kg/mt $CaCO_3$) prior to the drainage pH decreasing and remaining below the specified pH value. If the drainage pH from a given solid never decreased permanently below a specified value, the ENP was reported as "greater than" the total calcium plus magnesium release for the period of record. Sulfate release was not used for the ENP calculation since some of the sulfate was the product of trace metal sulfide oxidation. The sulfate released from oxidation of copper and nickel sulfides, which comprised 15% to 35% of the sulfide mineral content of the test piles, does not necessarily result in acid production.

Results

Drainage Quality

The test piles typically produced drainage between the middle of March and the middle of November, with an average flow season of 245 days. The pH of drainage from the test piles generally decreased over time, and decreased as the solid-phase sulfur content increased (fig. 1). At the beginning of 1978, the pH of drainage from all piles was between 7 and 8. For the three piles containing 0.63% sulfur, drainage pH decreased gradually from circumneutral to the range of 4.8 to 5.3. The pH of drainage from the piles containing 0.79% and 1.4% sulfur decreased and plateaued within a range of about 0.2 to 0.3 pH unit. The pH of drainage from the 0.79%-sulfur pile decreased until 1982 and subsequently oscillated in the typical range of 4.0 to 4.3. The pH of drainage from the 1.41%-sulfur pile decreased to a lower level, from a median value of 5.5 in 1978 to a typical range of 3.4 to 3.6 from 1979 to 1991. The annual median values actually increased from 1982 (3.40) to 1991 (3.60).

Annual flow-weighted mean sulfate concentrations for the individual piles tended to increase during the first 3 to 4 yr and then oscillated within a fairly constant range, increased as the solid-phase sulfur content increased, and were independent of the annual flow volume. Some deviations from the general trends were observed. Most notably, sulfate concentrations in drainage from the 1.41%-sulfur pile increased to peak levels between 1981 and 1985 and then decreased. From 1987 to 1991 the flow-weighted mean sulfate concentrations from this pile were comparable to, or lower than, those from the 0.79%-sulfur pile. Sulfate concentrations from the 0.79%-sulfur pile increased over time. However, these temporal variations from 1981 through 1991 were relatively small. In general the maximum annual flow-weighted mean sulfate concentrations were typically within a factor of 2 of the minimum value observed during this period.

Annual flow-weighted mean magnesium concentration variations over time were generally parallel to those observed for sulfate and were independent of annual flow volume. Magnesium concentrations were lowest in drainage from the 0.63%-sulfur piles, typically ranging from 2 to 6 mmol/L. The corresponding range for the two piles of higher sulfur content was 7 to 15 mmol/L. For the individual piles, annual flow-weighted mean magnesium

concentrations tended to increase as the annual median pH decreased.

Annual flow-weighted mean calcium concentrations were typically fairly constant, ranging from about 4 to 7 mmol/L. As implied by the constant range, there was little dependence of annual flow-weighted mean calcium concentrations on time of dissolution, sulfur content, or annual flow. The values for the 1.41%-sulfur pile appeared to parallel the decreasing trend observed for sulfate concentrations from 1985 to 1991.

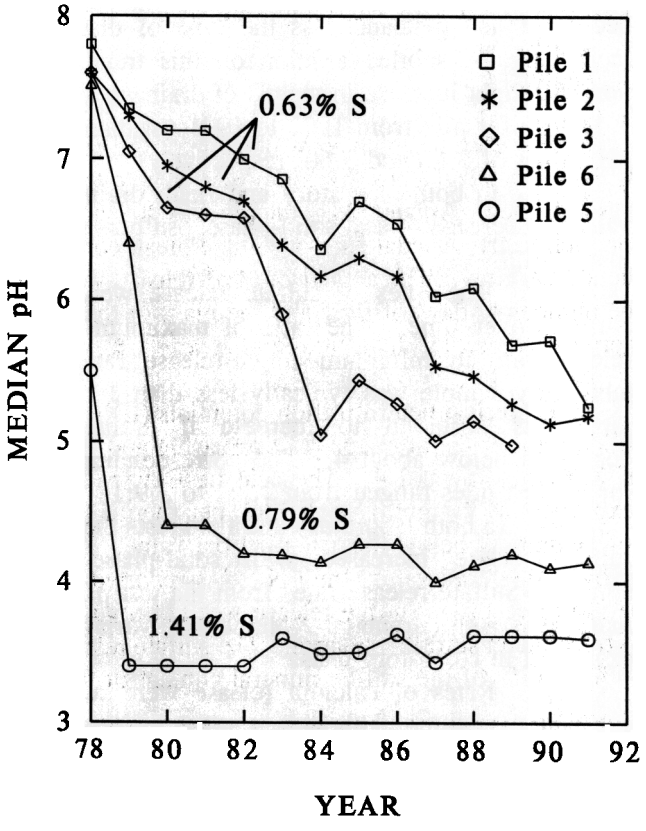

Figure 1. Annual median pH from 1978 to 1991. Drainage pH decreased over time and as solid-phase sulfur content increased.

Annual Rates of Release

The annual rate of sulfate release from each pile oscillated within a fairly constant range (fig. 2). In general, annual sulfate release increased with the solid-phase sulfur content of the pile, although the rates for the 0.79%-sulfur pile were comparable to or exceeded those for the 1.41%-sulfur pile from 1984 to 1991. Sulfate release also increased with annual flow, and temporal variations in the annual rate were largely due to variations in annual flow volume. A graphic example of the flow dependence is the low sulfate-release rate from the 0.79%-sulfur pile in 1990, while the pile was partly covered with plastic. The drainage volume and sulfate mass release were consequently low.

Variations in magnesium release followed similar trends. Similar to the sulfate-release rates from 1984 through 1991, magnesium release from the 0.79%-sulfur pile was usually higher than that from the 1.41%-sulfur pile. In contrast, the annual rates of calcium release typically fell into the range of 1 to 3 mol/mt/d. They did not vary with time or solid-phase sulfur content, but did increase linearly with annual flow.

Empirical Neutralization Potential (ENP)

The pH of drainages from the 0.63%-sulfur rock did not decrease permanently below 5.0. The approximate ranges of ENP values determined for endpoint pH values of 7.0 and 6.0 (ENP_{pH7} and ENP_{pH6}, respectively) were 0.2 to 0.4 and 0.4 to 1.3 kg/mt $CaCO_3$, respectively. The pH of drainage from pile 3 approached 5 at the end of 1989. The 1.3 kg/mt $CaCO_3$ ENP value determined for this pile is assumed to be near the ENP_{pH5} for this pile. The lowest ENP endpoint pH values for the piles with sulfur contents of 0.79% and 1.41% were pH 4.5 and pH 4.0, respectively. The ENP values for any pH value tended to decrease as sulfur content increased.

Comparison of Field and Laboratory Data

Certain qualitative similarities were apparent between the field data and laboratory data (Lapakko 1988, Lapakko and Antonson 1993).

1. Drainage pH generally decreased, or decreased and plateaued, as the time of dissolution increased. A subtle variation on this trend was a possible slight increase in the pH of drainage from the 1.41%-sulfur pile from 1982 to 1991 (median annual pH values of 3.40 and 3.60, respectively).

2. In both laboratory and field, drainage pH values decreased as solid-phase sulfur content increased.

3. The rates of sulfate release were fairly constant over time. The ratio of maximum-sulfate-release rate to minimum-sulfate-release rate for a laboratory sample was typically less than 3:1. This ratio was observed to increase if drainage pH decreased below about 4. The corresponding ratios for the test piles ranged from 2.7:1 to 3.9:1.

4. In both laboratory and field tests the rate of sulfate release increased with solid-phase sulfur content. Sulfate release rates from the test piles also increased with drainage volume, a variable not examined in laboratory tests.

5. Rates of calcium release were relatively constant over time, although it must be noted that laboratory data on calcium release are limited.

6. Rates of calcium release were relatively constant with respect to sulfur content. The rates of calcium release from the test piles also increased with drainage volume, a variable not examined in laboratory tests.

7. Rates of magnesium release increased as time increased, although it must be noted that laboratory data on magnesium release are limited.

8. Rates of magnesium release increased as solid-phase sulfur content increased. The rates of magnesium release from the test piles also increased with drainage volume, a variable not examined in laboratory tests.

9. Neutralization potential values were low and decreased with increasing sulfur content.

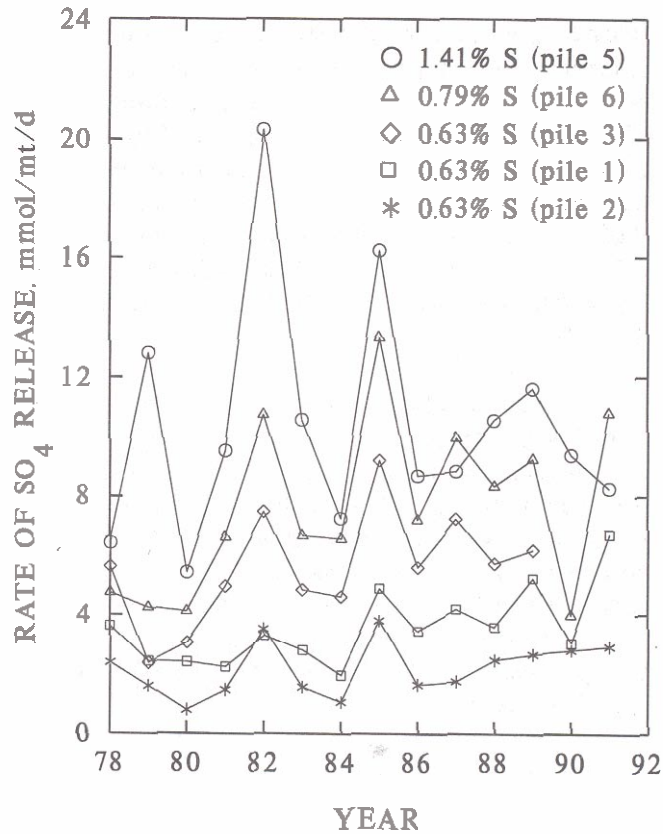

Figure 2. Annual sulfate release rate from 1978 to 1991. Sulfate concentrations generally increased with solid-phase sulfur content and were within a constant range over time.

Field and laboratory data were also quantitatively compared based on drainage pH, neutralization potentials, and rates of release. The minimum drainage pH values observed for the 0.63%-sulfur rock in the field ranged from 4.71 to 4.96 and were reasonably consistent with the laboratory relationship between drainage pH and solid-phase sulfur content. However, the minimum pH values for drainages from the test piles with sulfur contents of 0.79% and 1.41% were about one unit lower than expected based on laboratory data (fig. 3). The minimum pH values observed were typically occasional excursions, and recurrent low pH values were typically 0.1 to 0.2 unit higher.

For the entire period of record, average rates of sulfate release ranged from 2.0 to 10 mmol/mt/d, and increased as sulfur content and drainage volume increased. The average rates of calcium release ranged from 2.1 to 2.4 mmol/mt/d and were fairly constant with respect to sulfur content. Average rates of magnesium release ranged from 0.55 to 3.7 mmol/mt/d and were lowest for the low-sulfur solids and highest for the solids containing 0.79% sulfur.

The rates of sulfate, calcium, and magnesium release observed for the test piles were compared to laboratory rates for the Duluth Complex samples of similar sulfur content (Lapakko and Antonson 1993). The laboratory rates were from the last 15 to 36 weeks of the period of record. The ratios of field rates to laboratory rates, or retardation factors, ranged from 0.053 to 0.46, with most values in the range of about 0.1 to 0.36 (table 3). This indicates that the laboratory rates were roughly 3 to 10 times those in the field.

The neutralization potentials of the test piles were lower than those for laboratory samples, which is consistent with the lower drainage pH levels observed in the field. The ENP values for the 0.63%-sulfur rock were roughly 25% to 50% of those observed for laboratory samples of similar sulfur content (table 4). Although the ENP_{pH6} and ENP_{pH7} values from pile 3 were higher than this range, the ENP_{pH5} value was 46% of the corresponding value for laboratory samples.

The field ENP values for the 0.79%-sulfur rock were 13% to 54% of the corresponding values for laboratory samples of similar sulfur content. The ratios of field to laboratory ENP were lowest for the 1.41%-sulfur rock, typically 5% or less than those determined in the laboratory.

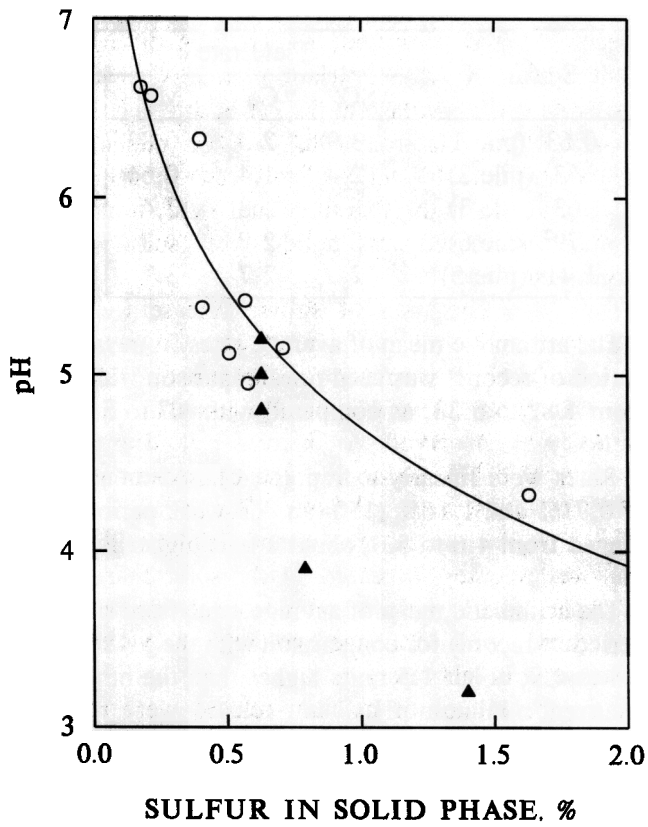

Figure 3. Comparison of recurrent minimum drainage pH in field (▲) and laboratory (○). Laboratory data represents drainage pH after 150 weeks of dissolution of Duluth Complex samples (Lapakko and Antonson 1993).

Discussion

There were several differences between the conditions in the laboratory dissolution experiment and those in the field study. Laboratory particles were smaller than the average particle in the field, ranging from 0.053 mm to 0.149 mm in diameter, and therefore had a higher specific surface area. Due to the relatively uniform particle size, the available mineral surface area was roughly proportional to the amount of the mineral present. In contrast, the fraction of the rock surface area comprised of iron sulfide minerals in the field was most likely higher than that indicated by the sulfur content of 0.63%. Sulfide minerals comprised a disproportionately large fraction of the fine material the field, as indicated by the elevated sulfur content of this fraction (table 2). This material also had the highest specific surface area of the field rock. Therefore, iron sulfide minerals comprised a larger fraction of the field rock surface area than indicated by the sulfur content alone.

Hydrologic differences also existed. The volume of rinse water per unit mass rock yielded approximately 300 L per ton of rock per day of drainage in the laboratory, roughly three orders of magnitude greater than the yields of 0.27 to 0.38 L per ton of rock per day in the field. Furthermore, the flow of the laboratory rinse water through the solids was fairly uniform, whereas preferential flow was probable in the field setting.

Despite these differences there were numerous similarities between the field and laboratory results. As cited earlier, the variations of drainage pH and chemical mass release were qualitatively comparable in the two settings.

Table 3. Comparison of field and laboratory release rates. Rates in moles per gram rock per second x 10^{-14}.

Sulfur, %	Field rate			Lab rates			Retardation factor			
	SO_4	Ca	Mg	SO_4	Ca	Mg	SO_4	Ca	Mg	Ave.
0.63[1] (pile 1)	3.9	2.5	0.86	[1]25	[1]6.7	[1]12	0.16	0.37	0.072	0.20
.63[1] (pile 2)	2.4	1.4	0.64	25	6.7	12	0.096	0.21	0.053	0.12
.63[1] (pile 3)	6.4	2.8	2.4	25	6.7	12	0.26	0.42	0.20	0.29
.79[2] (pile 6)	8.5	2.8	4.3	[2]26	[2]6.1	[2]12	0.33	0.46	0.36	0.38
1.41[3] (pile 5)	12	2.7	3.7	[3]66	[3]19	[3]21	0.18	0.14	0.18	0.17

[1] The arithmetic mean of average rates from samples with sulfur contents of 0.57%, 0.58%, and 0.71% (150 week period of record) was used for comparison with 0.63%-sulfur rock. Minimum pH values for these samples ranged from 4.82 to 5.38, as compared with 4.7 to 5.0 in the field.

[2] Rates were linearly extrapolated based on sulfur content using average rates from samples with sulfur contents of 0.71% and 1.16% (150- and 69-week periods of record, respectively). Minimum pH values for these samples ranged from 4.6 to 5.0, about 1 unit higher than the pH 3.7 minimum value for the field pile.

[3] The arithmetic mean of average rates from samples with sulfur contents of 1.40% and 1.44% was used (69-week period of record) for comparison with the 1.41%-sulfur pile. Minimum drainage pH for these samples ranged from 4.4 to 4.9, about 1.5 units higher than the minimum drainage pH for the field pile and and 1 unit higher than its recurrent minimum pH.

Table 4. Comparison of field and laboratory neutralization potentials.

S, %	pH 7	pH 6	pH 5	pH 4.5	pH 4	pH 3.5
FIELD NEUTRALIZATION POTENTIAL[1]						
0.63 (pile 1)	0.346	0.781	>1.059	>1.059	>1.059	>1.059
.63 (pile 2)	.179	.393	>.642	>.642	>.642	>.642
.63 (pile 3)	.442	1.254	>1.340	>1.340	>1.340	>1.340
.79 (pile 6)	.157	.172	.226	1.702	>2.074	>2.074
1.41 (pile 5)	.044	.044	.096	.130	.136	>1.889
RATIO OF FIELD ENP TO LABORATORY ENP						
0.63 (pile 1)	0.52	0.52	NAp	NAp	NAp	NAp
.63 (pile 2)	.27	.26	NAp	NAp	NAp	NAp
.63 (pile 3)	.66	.84	NAp	NAp	NAp	NAp
.79 (pile 6)	.54	.23	0.13	NAp	NAp	NAp
1.41 (pile 5)	.17	.056	<.056	<0.045	<0.044	NAp

[1] kg/mt $CaCO_3$
NAp Not applicable.

Quantitatively, the drainage from 0.63-percent sulfur rock in the laboratory approximated that in the field. However, pH of field drainages from the 0.79%- and 1.4%-sulfur rock were about 1 and 1.5 units, respectively, lower than the corresponding laboratory values. These field drainage pH values may have been lower due to a higher iron sulfide surface area than indicated by the sulfur content alone. The low rinse water to rock ratio in the field would also lend to increased H^+ concentrations.

Both the rates of mineral dissolution and subsequent reaction product transport probably contributed to the lower sulfate, calcium, and magnesium release rates (per unit mass) observed in the field. First, the larger field particles have a lower specific surface area (surface area per unit mass) than the smaller particles used in the laboratory. The lower surface area in the field would retard the sulfate, calcium, and magnesium release per unit mass rock, since both sulfide mineral oxidation and silicate mineral dissolution are surface reactions. The reaction environment in the field, where temperatures are colder, may also retard reaction rates. Limitation of sulfide oxidation by oxygen transport seems unlikely due to the small test pile size.

Limited transport of reaction products in the field also may have reduced rates of release. Hydrologic variables, which were not influential in the laboratory, could have contributed to this transport limitation. The relatively low flow in the field may have limited transport. This is supported by the observation that release rates in the field increased with flow. Preferential flow would limit the transport of reaction products from some rock surfaces. This would essentially reduce the amount of rock in the test piles that was actually contributing to the observed chemical release. The degree of transport in the field may also be limited by chemical precipitation of dissolution reaction products. In particular, the formation of gypsum might limit the rates of sulfate and calcium release. Gypsum formation was not a problem in the laboratory since the high rinse-water-to-solid ratio produced relatively low concentrations of sulfate and calcium in the drainages.

In addition to the larger particle size in the field, the low field ENP values may have been influenced by factors similar to those discussed regarding drainage pH. First, preferential flow in the field piles would reduce the amount of silicate minerals, which could contribute to acid neutralization. For example, if flow through the pile contacted only half the silicate minerals, the observed neutralization potential of the rock would be half the actual value for the entire pile. Second, if the fraction of rock surface area comprised of silicate minerals in the laboratory samples exceeded that in the test piles, the laboratory solids would be expected to neutralize acid more efficiently. Third, the ratio of available reactive surface area of sulfide minerals to that of silicate minerals present in the test pile rock may have been greater than that in the laboratory. This would be equivalent to increasing the sulfur content of rock in the laboratory. As was observed in the laboratory, neutralization potential tended to decrease as sulfur content increased.

More rigorous analysis of the recently compiled laboratory and field data is presently in progress at the Minnesota Department of Natural Resources. The data are also being used to aid development of a geochemical predictive model for acid mine drainage at the US Bureau of Mines Salt Lake City Research Center.

Acknowledgments

The test piles were constructed by AMAX Exploration Inc. Sulfate was analyzed by Jean Matthew, while calcium and magnesium were analyzed by Albert Klaysmat at the Hibbing office of the Minnesota Department of Natural Resources. Since 1978 sampling and sampling maintenance have been the responsibility of several people: Bruce Johnson, Anne Jagunich, and, most recently, Cal Jokela and David Antonson. Paul Eger has supervised these activities. Jon Wagner provided much of the data input and Jim Porter was responsible for the most recent data management, as well as tabular and graphical output. The U. S. Bureau of Mines provided funding to support data compilation and analysis as part of Cooperative Agreement C0219003.

References

AMAX Environmental Services Inc. 1978. The field leaching summary report, 1977, Minnamax project. AMAX Exploration Inc. Denver CO.

American Public Health Association, American Water Works Association, Water Environment Federation. 1992. Standard methods for the examination of water and wastewater, 18th Edition, American Public Health Association, Washington, DC.

Eger, P. and K. A. Lapakko. 1981. The leaching and reclamation of low-grade mineralized stockpiles. p. 157-166. In Proceedings 1981 Symposium on Surface Mining Hydrology, Sedimentology and Reclamation. (Lexington, KY, December 7-11, 1981).

Eger, P. and K. A. Lapakko. 1985. Heavy metals study: Progress report on the field leaching and reclamation program: 1977-1983. MN Dept. Nat. Resour., Division of Minerals, St. Paul, MN. 53 p.

Eger, P., K. A. Lapakko, and P. G. Chamberlain. 1984. Mixed disposal of waste rock and tailings to reduce trace metal release from waste rock. p. 49-56. In Proceedings 1984 Symposium on Surface Mining Hydrology, Sedimentology, and Reclamation. OES Publications, College of Engineering, Univ. KY, Lexington, KY.

Hickok and Associates. 1977. Water resources investigation for the possible MINNAMAX mining facility Minneapolis, MN. 96 p.

Lapakko, K. A. 1988. Prediction of acid mine drainage from Duluth Complex mining wastes in northeastern Minnesota. p. 180-190. In Mine Drainage and Surface Mine Reclamation. v. 1. Mine Water and Mine Waste. Proceedings 1988 Mine Drainage and Surface Mine Reclamation Conference. BuMines IC 9183.

Lapakko, K. A. and D. A. Antonson. 1993. Oxidation of sulfide minerals present in Duluth Complex rock: A laboratory study. p. 593-607. In Environmental geochemistry of sulfide oxidation. ACS Symposium Series No. 550, American Chemical Society, Washington, DC.

Lapakko, K. A., P. Eger, and J. D. Strudell. 1986. Low-cost removal of trace metals from copper-nickel mine drainage. Final report, BuMines Contract J0205047, NTIS#PB 87-186136. 103 p.

Siegel, D. I. and D. W. Ericson. 1980. Hydrology and water quality of the copper-nickel study region, northeastern Minnesota. U.S. Geol. Surv., Water Resour. Inv. 80-739, Open file report.

ACID-NEUTRALIZATION REACTIONS IN INACTIVE MINE TAILINGS IMPOUNDMENTS AND THEIR EFFECT ON THE TRANSPORT OF DISSOLVED METALS[1]

David W. Blowes[2], Carol J. Ptacek[3], Emil O. Frind[2],
Raymond H. Johnson[2], William D. Robertson[2], and John W. Molson[2]

Abstract: The H^+ generated by sulfide oxidation in inactive mine wastes is consumed by a series of mineral-dissolution reactions. Previous studies conducted at the Nordic uranium tailings impoundment near Elliot Lake, ON, indicated these H^+-consuming reactions occur in a stepwise sequence: calcite dissolution, siderite dissolution, $Al(OH)_3$ dissolution and $Fe(OH)_3$ dissolution. Similar series of acid neutralization reactions have been observed at tailings impoundments at the Heath Steele Zn-Pb mine, NB, the Waite Amulet Cu-Zn mine, Noranda, QC, the Delnite Au mine, Timmins, ON, and the Copper Cliff and Nickel Rim Ni-mines, Sudbury, ON. At all of these locations, near-equilibrium conditions, as indicated by geochemical modelling conducted using MINTEQA2 or PHRQPITZ, are attained with respect to similar sequences of pH-buffering phases. These acid-neutralization reactions have a strong effect on the transport of dissolved metals. Calculations conducted using the 2-D coupled solute-transport/geochemical mass-transfer model MINTRAN predict pH buffering sequences and metal attenuation mechanisms that are similar to those observed at the field sites. Model simulations suggest that some pH-sensitive metals should be retained within the tailings or underlying aquifers.

Additional Key Words: acid-neutralization, tailings, metals, solute-transport modelling, groundwater, aquifers

Introduction

Acid-neutralization processes are fundamental in controlling the environmental effects of wastes from base- and precious-metal mines. In mine tailings impoundments, the balance between H^+-generating sulfide-oxidation reactions and H^+-consuming mineral-dissolution reactions controls the pH at the location of sulfide oxidation and at locations downgradient along the groundwater flow path. Buffering reactions that control the pH near the location of sulfide oxidation affect the rate of sulfide oxidation and the release of dissolved Fe^{2+} and other metals to the tailings pore water. Buffering reactions that occur along the groundwater flow path affect the mobility of dissolved metals as they are transported through the mine wastes and through underlying geologic materials. Tailings impoundments are characterized by a large number of dissolved constituents and a large quantity of tailings solids, all contributing to the chemical evolution of the tailings pore water. The extent of pH buffering depends on the mass of acid-consuming minerals and on the mineralogy of these materials.

The importance of acid-neutralization reactions in mine wastes has been recognized for several decades, as has the benefit of attaining a balance between acid generation and acid neutralization. In response to the need to predict the potential for release of acid drainage from mine wastes, a series of predictive tests and acid-base accounting procedures has been developed (e.g. Ferguson and Erickson 1987). The objective of acid-base accounting procedures and acid-generation predictive tests is to assess the potential for a given mine waste to generate acid.

---

[1]Paper presented at the International Land Reclamation and Mine Drainage Conference and the Third International Conference on the Abatement of Acidic Drainage, Pittsburgh, PA, April 24-29, 1994.

[2]David W. Blowes, Assistant Professor, Emil O. Frind, Professor, Raymond H. Johnson, M.Sc. Graduate, William D. Robertson, Research Assistant Professor, and John W. Molson, Research Associate, Waterloo Centre for Groundwater Research, University of Waterloo, Waterloo, ON, Canada.

[3]Carol J. Ptacek, Research Scientist, Environment Canada, Burlington, ON, Canada.

The results of field studies indicate that acid neutralization in mine wastes and underlying aquifers occurs through a complex series of reactions (Smyth 1981; Morin 1983; Dubrovsky 1986; Morin et al. 1988). It is necessary to investigate the benefits and effects of these pH-buffering reactions because of the variety of metal-bearing sulfide minerals present in base- and precious-metal tailings impoundments and because the mobilities of many of the metals derived from oxidation of these sulfide minerals varies with changing pH.

Acid Generation in Mine Wastes

The principal reactions that generate H^+ are the oxidation of sulfide minerals, the oxidation of Fe^{2+} and hydrolysis of Fe^{3+}, and the precipitation of metal hydroxide and hydroxysulfate phases. The most common sulfide minerals in base- and precious-metal mine tailings are pyrite (FeS_2) and pyrrhotite ($Fe_{(1-x)}S$). The oxidation of pyrite produces two moles of H^+ for each mole of pyrite oxidized through the reaction:

$$FeS_2 + \frac{7}{2}O_2 + H_2O \rightarrow Fe^{2+} + 2SO_4^{2-} + 2H^+ \tag{1}$$

Subsequent oxidation of Fe^{2+} and hydrolysis and precipitation of $Fe(OH)_3$ produces an additional two moles of H^+ resulting in the overall reaction:

$$FeS_2 + \frac{15}{4}O_2 + \frac{7}{2}H_2O \rightarrow Fe(OH)_3 + 2SO_4^{2-} + 4H^+ \tag{2}$$

The precipitation of other Fe(III)-bearing phases, such as goethite (α-FeOOH) or schwertmannite ($Fe_8O_8(OH)_6SO_4$) (Bigham et al. 1990), may occur, releasing differing amounts of H^+. Alternatively, Fe^{3+} may be consumed through further oxidation of sulfide minerals, e.g.

$$FeS_2 + 14Fe^{3+} + 8H_2O \rightarrow 15Fe^{2+} + 2SO_4^{2-} + 16H^+ \tag{3}$$

In many tailings impoundments, particularly those resulting from the concentration and recovery of nickel, pyrrhotite is the most abundant sulfide mineral. Oxidation of pyrrhotite may proceed to completion through the reaction:

$$Fe_{(1-x)}S + (2-\frac{x}{2})O_2 + xH_2O \rightarrow (1-x)Fe^{2+} + SO_4^{2-} + 2xH^+ \tag{4}$$

or may proceed to partial completion, generating Fe^{2+} and elemental S^0 through the reaction:

$$Fe_{(1-x)}S + (2-2x)Fe^{3+} \rightarrow (3-3x)Fe^{2+} + S^0 \tag{5}$$

This elemental S^0 may be subsequently oxidized to SO_4^{2-}. Partial oxidation of pyrrhotite, resulting in accumulation of S^0, has been observed at two Ni mine-tailings impoundments (Coggans et al. 1994; Jambor and Owens 1993), and at an inactive Cu-Zn mine-tailings impoundment (Jambor 1987; Blowes and Jambor 1990).

The zone of active sulfide oxidation in most tailings impoundments is limited to the vadose zone, near the tailings surface, where oxygen transport by gas-phase diffusion is rapid. In this zone, the weathering of sulfide minerals may be complete (reaction 2), resulting in the formation of stable secondary precipitates such as goethite, or incomplete, with some of the Fe derived from the initial sulfide remaining in solution as dissolved Fe^{2+} (reaction

1). Ferrous iron-bearing sulfate and hydroxide minerals are relatively soluble. As a result, dissolved Fe^{2+} concentrations contained in tailings pore waters may be high (up to 70 g/L; Blowes et al. 1991). This dissolved Fe^{2+} is displaced along groundwater flow paths and ultimately discharged to the surface water flow system where oxidation to Fe^{3+} and precipitation of ferric oxyhydroxide phases result in the generation of H^+ in the surface-water flow system (Dubrovsky et al. 1984a; Coggans et al. 1994).

Table 1. Principal pH-buffering phases in mine tailings impoundments.

Mineral	Formula
Calcite	$CaCO_3$
Dolomite	$CaMg(CO_3)_2$
Siderite	$FeCO_3$
Mixed carbonates	$(Ca,Mg,Fe,Mn)CO_3$
Gibbsite[1]	$Al(OH)_3$
Ferrihydrite[1]	$Fe(OH)_3$
Goethite	α-FeOOH
K-Jarosite	$KFe_3(SO_4)_2(OH)_6$
Aluminosilicates	

[1]or equivalent amorphous phase

Acid Neutralization in Mine Wastes

The principal acid-neutralization mechanisms in inactive mine tailings impoundments are carbonate mineral dissolution, hydroxide mineral dissolution, and aluminosilicate mineral dissolution (table 1). Unlike sulfide-oxidation reactions, many acid-neutralization reactions are independent of gas-phase O_2 concentration. Acid-neutralization reactions can occur along the groundwater flow path throughout the tailings impoundment and in underlying aquifers, limited only by the availability of acid-consuming mineral phases. These H^+-consuming reactions result in the general increase in pH with increasing depth that is observed at many tailings impoundments (fig. 1; Dubrovsky et al. 1984a; Morin et al. 1988; Blowes and Jambor 1990; Blowes et al. 1991; Coggans et al. 1994). Consequently, the water present near the base of tailings impoundments, or present in aquifers underlying the tailings impoundment, is usually near-neutral in pH, but may contain high concentrations of acid-generating Fe^{2+}.

Acid-consuming reactions affect both the rate of sulfide oxidation and the distribution of sulfide-oxidation products between the tailings pore water and solid-phase precipitates. Numerous studies have concluded that the rate of sulfide oxidation in mine waste piles and heap-leach systems is controlled by the supply of oxidant to the mineral surface (Cathles 1979; Davis and Ritchie 1986; Nicholson et al. 1990). Processes limiting the supply of oxidant are transport through the mine waste pile to the depth of active oxidation and diffusion of oxidants (O_2 or Fe^{3+}) through oxide coatings that surround unaltered sulfide cores (Davis and Ritchie 1986). Nicholson et al. (1990) concluded that transport of oxygen through alteration rims surrounding pyrite grains controlled the rate of pyrite oxidation in an experimental study conducted under near-neutral pH conditions. In the field, Blowes and Jambor (1990) and Coggans et al. (1994) observed well-developed alteration rims, composed of goethite and jarosite, surrounding sulfide grains under low pH (3.5<pH<4.5) conditions. No alteration rims were observed by Blowes et al. (1994) on sulfide grains present under very low pH conditions (pH<1.5). This pattern suggests that the formation of secondary alteration rims may be a primary control on the rate of sulfide oxidation in all but the most extreme low pH settings.

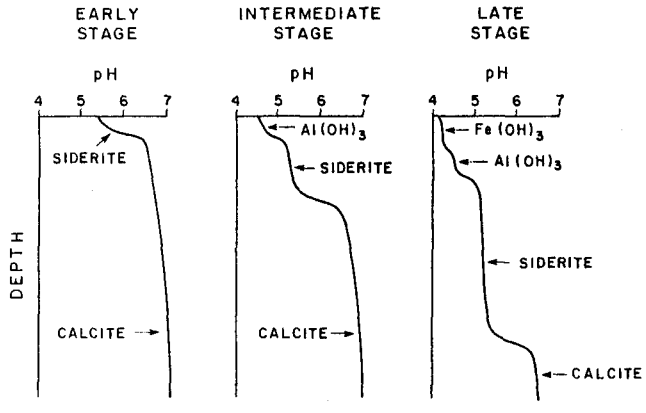

Figure 1. Development of pH-buffering zones during early, intermediate and late stages of sulfide oxidation.

Field observations made at tailings impoundments with similar sulfide contents but varying

carbonate mineral contents suggest that the location of H^+ consumption is important in determining the potential for future acid production. The Nordic U tailings impoundment near Elliot Lake, Ontario, and the Delnite Au tailings impoundment at Timmins, Ontario both contain approximately 5 wt% sulfide minerals, primarily as pyrite. The carbonate content of the Nordic tailings is generally <0.1 wt% as $CaCO_3$, whereas the carbonate content of the Delnite tailings is >20 wt%. At the Nordic site, the pH in the vadose zone is low (1<pH<4) and much of the Fe^{2+} released through pyrite oxidation remains in solution, resulting in pore-water Fe concentrations that exceed 20,000 mg/L at some locations (Dubrovsky et al. 1984b). This water is being displaced down through the tailings and laterally through an underlying aquifer where it is neutralized along the groundwater flow path. Concentrations of dissolved Fe^{2+}, however, remain high along the groundwater flow path. Acidic conditions are generated as this ferrous-rich water discharges to the surface-water flow system downgradient from the tailings impoundment. At the Delnite site, the pH in the vadose zone has remained high (6<pH<8), favoring precipitation of Fe oxyhydroxide minerals, dominantly goethite (Jambor and Blowes 1991). As a result of goethite precipitation, Fe concentrations are generally < 50 mg/L (Blowes 1990). These Fe concentrations represent an acid-generating potential that is less than the acid-consuming potential of the pore-water alkalinity, therefore no acidity is generated as this water is discharged to the surface-water flow system. The importance of maintaining high carbonate contents in the vadose zone of the tailings impoundments is thus illustrated. At both sites, acid-neutralization reactions have produced pore waters near the base of the impoundments that are near neutral in pH, but the high concentrations of dissolved Fe^{2+} in the Nordic pore water represent a high acid-generating potential in contrast to the low acid-generating potential at Delnite.

Sequential pH Buffering Reactions

Field studies conducted in a number of tailings impoundments indicate series of equilibrium pH-buffering reactions controlling the pH of the tailings pore water (Smyth 1981; Dubrovsky et al. 1984a; Blowes and Jambor 1990; Johnson 1993). These series are similar to those which Morin et al. (1988) observed in a plume of tailings-derived water moving outward from beneath the Nordic Main uranium tailings impoundment near Elliot Lake, Ontario, where the sequence follows the order: calcite dissolution, siderite dissolution, $Al(OH)_3$ dissolution and $Fe(OH)_3$ dissolution.

The following example is based on results of a field study conducted at the old and new Heath Steele Zn-Pb tailings impoundments, New Brunswick (Blowes 1990; Blowes et al. 1991). As H^+ is released by sulfide oxidation reactions, the tailings pore water becomes undersaturated with respect to calcite and dolomite, leading to calcite and dolomite dissolution buffering the pore-water pH between 6.5 and 7.5.

$$CaCO_3 + H^+ \rightleftharpoons Ca^{2+} + HCO_3^- \tag{6}$$

$$CaMg(CO_3)_2 + 2H^+ \rightleftharpoons Ca^{2+} + Mg^{2+} + 2HCO_3^- \tag{7}$$

Geochemical equilibrium calculations suggest that the precipitation of siderite, $Al(OH)_3$ and $Fe(OH)_3$ is favored as calcite and dolomite dissolve. Ferrous iron generated from sulfide oxidation can react with calcite to form siderite through:

$$CaCO_3 + Fe^{2+} \rightleftharpoons FeCO_3 + Ca^{2+} \tag{8}$$

or can react directly with HCO_3^- released from dissolution of calcite or dolomite to form secondary siderite (Morin and Cherry 1986, Ptacek and Blowes 1993). When calcite is completely consumed, the pore water pH abruptly declines, favoring dissolution of primary siderite originally present in gangue materials or secondary siderite. In the siderite-buffered zone the precipitation of $Al(OH)_3$ and $Fe(OH)_3$ is favored. As siderite dissolves, the pH is buffered to between pH 4.8 and pH 6.3. After siderite is completely consumed, the pH again declines abruptly until the dissolution of the next pH buffer in the series, $Al(OH)_3$, is favored. Dissolution of $Al(OH)_3$ buffers the pH to values

between approximately 4.0 to 4.3. When $Al(OH)_3$ is completely consumed, the pH declines, favoring the dissolution of $FeOH_3$ and resulting in pH values that fall below pH 3.5.

Sequences of similar pH-buffering zones have been observed at a number of tailings impoundments, including the Nordic Main U tailings impoundment (Dubrovsky et al. 1984a), the Waite Amulet Cu-Zn tailings impoundment (Blowes and Jambor 1990), the Copper Cliff Ni tailings impoundment (Coggans et al. 1994) and the Nickel Rim Ni tailings impoundment (Johnson 1993). At these sites, the amount of time required to deplete a given mineral phase and the relative thicknesses of the zones developed varied, depending on the original mass of solid-phase buffers contained in the gangue materials and on the initial mass of sulfide minerals. At other sites, where the H^+ generated by sulfide oxidation is less than the acid consumed by carbonate-mineral dissolution, such as at the Delnite site (Blowes 1990; Jambor and Blowes, 1991), the pore-water pH is controlled completely by carbonate-mineral dissolution, limiting the development of the remaining pH buffering zones.

The Effect of pH-Buffering Reactions on Trace Metal Mobility

Complete development of the pH-buffering sequence and its effect on the mobility of dissolved metals are illustrated by observations made at the Nickel Rim Ni tailings impoundment near Sudbury, Ontario (Johnson 1993). At the Nickel Rim site, sulfide oxidation in the vadose zone has released H^+ to the tailings water, resulting in low-pH ($2.1<pH<3.5$) conditions near the tailings surface. Interaction with H^+-consuming minerals has resulted in the progressive increase in pH with increasing depth observed in figure 2. Geochemical calculations conducted using MINTEQA2 (Allison et al. 1990) indicate that the pore waters approach or attain equilibrium with respect to $Fe(OH)_3$, $Al(OH)_3$, siderite and calcite, forming a series of pH-buffering zones moving downward from the tailings surface. The pH-buffering zones in figure 2 are labelled according to the dominant pH buffering process. Irregularities in the shapes of these pH-buffer zones are likely due to variations in the pore-water velocity, composition of the tailings solids and rates of acid generation.

At the Nickel Rim site, the pH of the tailings pore water has a strong effect on the movement of dissolved Al and Ni in the impoundment (fig. 2). At the interface between the Al-mineral pH-buffering zone and the siderite pH-buffering zone the concentration of dissolved Al decreases sharply. For example, at location NR2, located in the central portion of the tailings impoundment, the dissolved Al concentration decreases from > 1,150 mg/L to < 10 mg/L within a one meter interval (fig. 2). In this interval the pH increases from ~4 to ~5.8. Geochemical calculations conducted using MINTEQA2 indicate that the water samples from this location are saturated or slightly undersaturated with respect to amorphous $Al(OH)_3$ and supersaturated with respect to the crystalline aluminum hydroxide mineral gibbsite. These observations suggest that Al is removed from solution through the precipitation of an aluminum hydroxide or hydroxysulfate phase.

The concentration of dissolved Ni is also strongly dependent on the pore-water pH, showing a sharp decrease from > 250 mg/L to < 10 mg/L as the pH increases to above 5.8 within the siderite pH-buffering zone. Geochemical calculations conducted using MINTEQA2 suggest that the water at this depth is consistently undersaturated with respect to all of the secondary nickel-bearing hydroxide and hydroxysulfate phases included in the MINTEQA2 database. It is inferred therefore that Ni is removed from solution through adsorption or coprecipitation with the secondary ferric oxyhydroxide precipitates. Mineralogical study of the tailings solids indicated that the goethite contained near the surface of the tailings impoundment is Ni bearing (Jambor and Owens 1993), further suggesting that Ni is removed from the tailings pore water through adsorption or coprecipitation reactions.

Modelling Acid Neutralization and Trace-Metal Attenuation

The complexity of the interactions between the large number of dissolved constituents in the tailings pore waters and the large quantity of tailings solids make it difficult to determine *a priori* the changes in pH and metal ion mobility that are likely to occur as sulfide oxidation proceeds. Geochemical modelling of tailings pore water and mineralogical analysis of tailings solids can be used to delineate the principal reactions contributing to pH buffering

and metal attenuation (Dubrovsky 1986; Blowes 1990). Incorporation of the observed pH-buffering and metal-controlling reactions into a solute transport model allows calculations to be made to estimate the rate of dissolved metal migration. Using the multicomponent reactive solute transport model MINTRAN (Walter et al. 1994; Frind et al. 1994), simulations were conducted to estimate the migration of low-pH conditions through an underlying aquifer affected by acidic tailings water and their effect on the transport of dissolved metals. MINTRAN couples the geochemical speciation mass transfer model MINTEQA2 (Allison et al. 1990) with an efficient two-dimensional solute transport model (Frind et al. 1990). The model, as applied in this study, includes only equilibrium reactions and is limited, therefore, to conditions where the local equilibrium conditions apply.

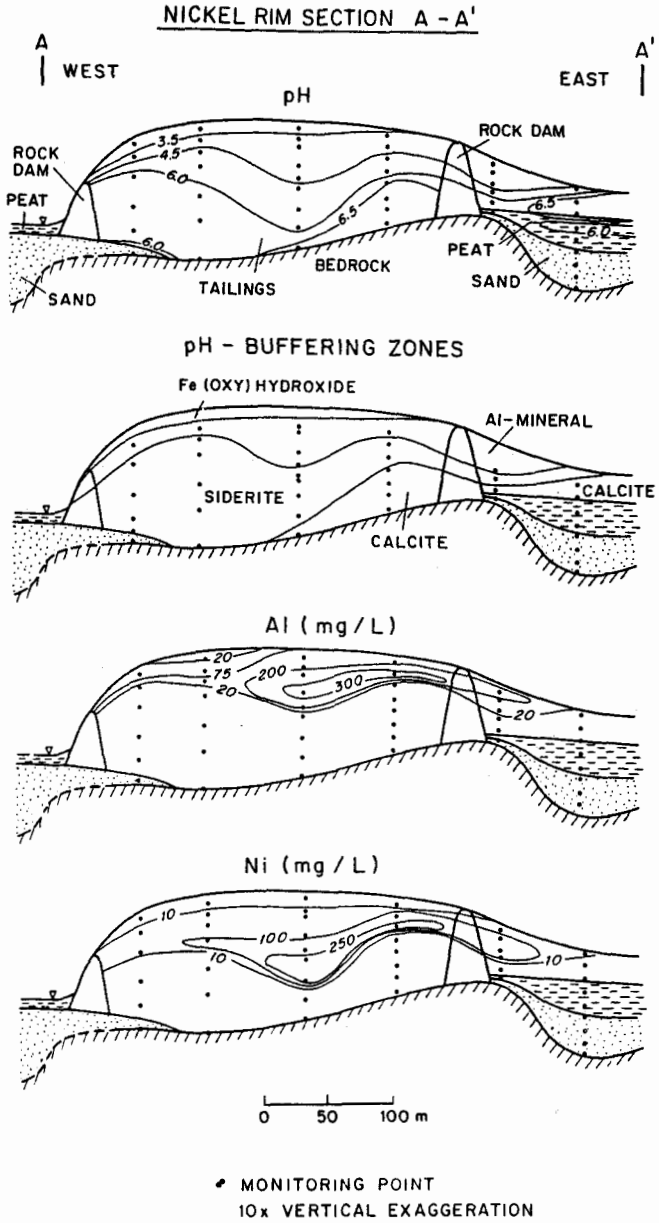

Figure 2. Values of pH, pH-buffering zones, and pore-water concentrations of Al and Ni in the Nickel Rim tailings impoundment near Sudbury, ON.

The simulations were based loosely on the description of the plume of tailings-derived water moving through an unconfined aquifer underlying the Nordic Main uranium tailings impoundment (Morin et al. 1988). The aquifer characteristics and tailings water compositions and background water compositions were selected to be similar to those at the field site. The aqueous components and initial mineral reserves included in the simulation are similar to those observed by Morin and Cherry (1988). The dissolved metals observed at the Nordic site include Al, Fe(II) and Fe(III). Important mineral phases include calcite, siderite, gibbsite, gypsum, amorphous silica and ferrihydrite. To enhance the generality of our simulation, we added higher concentrations of Pb, Cr and Mn and the associated mineral phases anglesite, cerussite, amorphous chromium hydroxide and rhodochrosite. This selection of phases was based on observations we have made at other field sites. In the model simulation, low-pH tailings water infiltrated into the source area of the aquifer for 24 years. The source area covers 10 m < x < 30 m at the watertable. The watertable boundary receives a flux of 0.142 m/yr., the downgradient boundary has a constant head of 13.6 m, and the left and lower boundaries are impermeable. The hydraulic conductivity is 2.5 x 10^{-6} m/s, the porosity is 0.3, the longitudinal dispersivity is 3.00 m, and the transverse dispersivity is 0.03 m.

The results of the simulations (figs. 3 and 4) show the development of a low-pH plume moving outward from the source area. Figure 3 shows contours and vertical profiles at x = 25 m for pH and dissolved Al, Cr and Pb and figure 4 shows solid-phase distributions for the associated mineral phases. The pH plume contains a series of pH plateaus similar to those observed in field studies (fig. 3). Far from the source, the pH ranges from 7.0 to 6.5 and is near equilibrium with respect to calcite, siderite and gibbsite. In this region of the aquifer, calcite is dissolving and siderite and gibbsite are accumulating. Closer to the source, the pH decreases sharply as the calcite initially

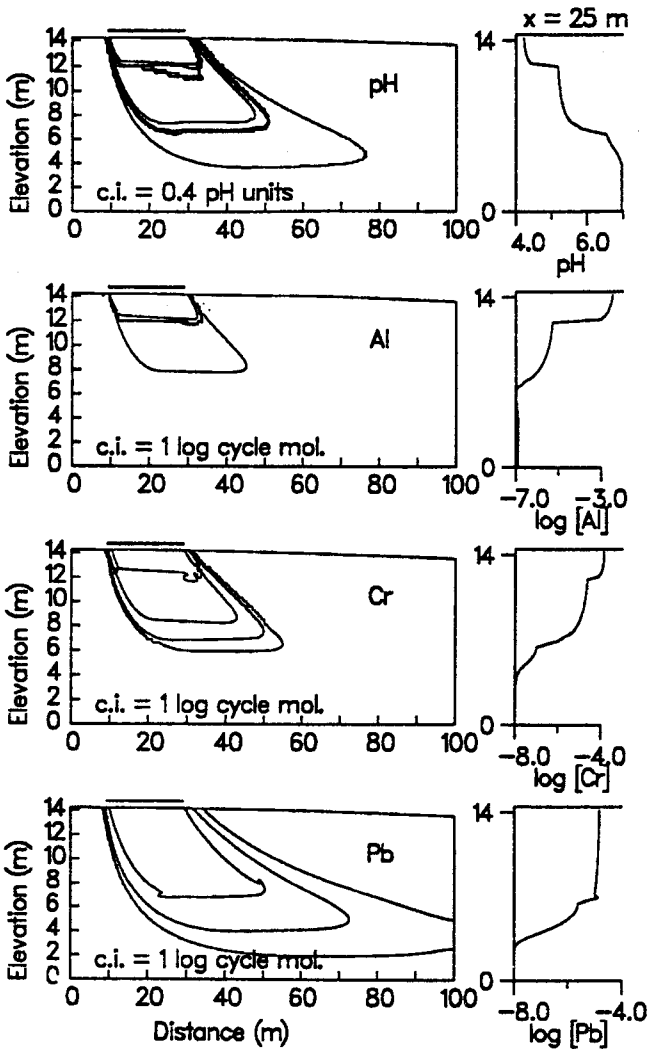

Figure 3. Simulated distributions of pH and concentrations of dissolved Al, Cr and Pb in aquifer receiving acidic drainage from a tailings impoundment at 24 years.

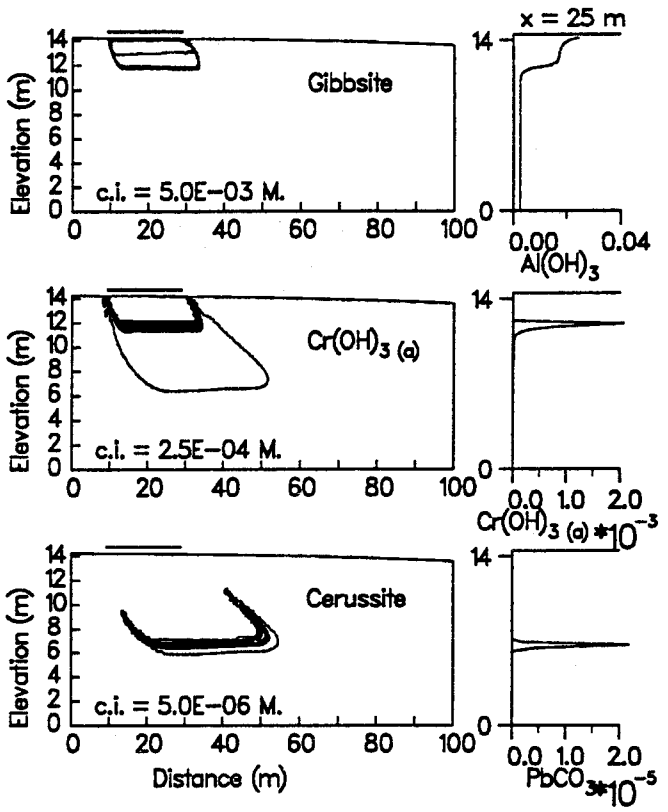

Figure 4. Simulated distributions of solid masses of gibbsite, amorphous $Cr(OH)_3$, and cerussite in aquifer receiving acidic drainage at 24 years.

present in the aquifer is depleted. At this front, the water becomes undersaturated with respect to calcite and the pH decreases from 6.5 to 5.5 (fig. 3) until equilibrium with respect to the second pH-buffering mineral siderite is attained. As siderite dissolves the mass of gibbsite continues to increase. Near the source, the pH decreases again as the primary and secondary siderite present in the aquifer is depleted. At this front, the pH decreases from 5.2 to 4.3 (fig. 3) and equilibrium with respect to gibbsite controls the pH from this point to the source. In this final region, the pH varies from 4.3 to 4.1.

The pH of the plume water affects the concentrations of the dissolved metals Al, Cr, and Pb assumed to be present in the plume. The secondary phases allowed to precipitate and dissolve include gibbsite, amorphous chromium hydroxide ($Cr(OH)_3$), and cerussite ($PbCO_3$). The mobilities of Al and Cr are dependent directly on the pH of the plume water, whereas the mobility of Pb is dependent on the activity of CO_3^{2-} , and therefore, indirectly dependent on the plume-water pH. The dissolved concentrations of Al and Cr show sharp decreases (fig. 3) that

correspond with the changes in pH accompanying the siderite and calcite dissolution fronts. These decreases are sufficient to lower the concentration of Cr to below the recommended concentration for drinking water (< 0.05 mg/L; OMOE 1983) and the Al concentration to below the recommended maximum concentration for the protection of freshwater aquatic life. The decreases in dissolved Cr and Al are accompanied by increases in the masses of gibbsite and $Cr(OH)_3$ retained in the aquifer (figs. 3 and 4). The total mass of $Cr(OH)_3$ is much less than the mass of gibbsite; the greatest accumulation of $Cr(OH)_3$ occurs at the siderite dissolution front. Lead is removed from the plume water through the precipitation of cerussite at the calcite dissolution front. Lead concentrations, however, remain above the recommended drinking water limit (< 0.01 mg/L, OMOE 1983) downstream of the cerussite precipitation front. Frind et al. (1994) conducted simulations describing the conditions in the aquifer following the period of sulfide oxidation, representing conditions where sulfide minerals have been depleted or an effective sulfide oxidation control put in place. These simulations show that the low solubilities of the metal-bearing precipitates are sufficient to maintain low concentrations of dissolved metals. The aqueous concentrations of all the metals considered, except Pb, decrease to below current regulatory guidelines shortly after the source of acidic drainage is terminated. These results suggest that metals precipitated in the aquifer are effectively immobilized under these conditions.

Summary and Conclusions

A series of acid-neutralization reactions controls the pore-water pH at four inactive mine tailings impoundments: the Waite Amulet Cu-Zn tailings impoundment (Blowes and Jambor 1990), the Heath Steele Pb-Zn tailings impoundment (Blowes et al. 1991), the Copper Cliff Ni tailings impoundment (Coggans et al. 1994) and the Nickel Rim Ni tailings impoundment (Johnson 1993). The sequence, calcite/dolomite dissolution, siderite dissolution, $Al(OH)_3$ dissolution, and $Fe(OH)_3$ dissolution, is the same as the pH-buffering sequence observed in the Nordic U tailings impoundment near Elliot Lake, Ontario (Dubrovsky 1986) and in a plume of tailings derived water adjacent to the Nordic tailings impoundment (Morin et al. 1988). The sequence of pH-buffering reactions observed at these inactive mine tailings impoundments results in the development of a series of pH regions that controls the mobility of several dissolved trace metals, including Al, Cr, Ni and Pb. The zones of pH buffering and metal attenuation are described well by a model which couples solute transport mechanisms with equilibrium geochemical reactions. Simulations conducted using this model suggest that in tailings impoundments with large masses of acid-consuming materials some of these metals may be retained in the tailings or underlying aquifers throughout the duration of acid release.

Literature Cited

Allison, J.D., D.S. Brown and K.J. Nova-Gradac. 1990. MINTEQA2/PRODEFA2, a geochemical assessment model for environmental systems: user's manual. Environmental Research Laboratory, Office of Research and Development, US EPA, Athens GA.

Bigham, J.M., U. Schwertmann, L. Carlson and E. Murad. 1990. A poorly crystallized oxyhydroxysulfate of iron formed by bacterial oxidation of Fe(II) in acid mine waters. Geochimica Cosmochimica Acta 54:2743-2758.

Blowes, D.W. 1990. The geochemistry, hydrogeology and mineralogy of decommissioned sulfide tailings: a comparative study. Ph.D. Thesis, University of Waterloo, Waterloo, ON, Canada, 637 pp.

Blowes, D.W. and J. L. Jambor. 1990. The pore-water geochemistry and the mineralogy of the vadose zone of sulfide tailings, Waite Amulet, Quebec, Canada. Applied Geochemistry 5:327-346.

Blowes, D.W., J.L. Jambor, E.J. Reardon and J.A. Cherry. 1994. The geochemical evolution of a high-sulfide mine tailings impoundment. Applied Geochemistry. In press.

Blowes, D.W., E.J. Reardon, J.L. Jambor and J.A. Cherry. 1991. The formation and potential importance of cemented layers in inactive sulfide mine tailings. Geochimica Cosmochimica Acta 55:965-978.

Cathles, L.M. 1979. Predictive capabilities of a finite difference model of copper leaching in low grade sulfide waste dumps. Mathematical Geology 11: 175-191.

Coggans, C.J., D.W. Blowes, W.D. Robertson and J.L. Jambor. 1994. The hydrogeochemical evolution of a nickel mine tailings impoundment, Copper Cliff, Ontario. Reviews in Economic Geology, In press.

Davis, G.B. and A.I.M. Ritchie. 1986. A model of oxidation in pyritic mine wastes. I. Equations and approximate solution. Applied Mathematical Modelling 10: 314-322.

Dubrovsky, N.M. 1986. Geochemical evolution of inactive pyritic tailings in the Elliot Lake uranium district, Ph.D. Thesis, University of Waterloo, Waterloo, ON, Canada.

Dubrovsky, N.M., J.A. Cherry, E.J. Reardon and A.J. Vivyurka. 1984a. Geochemical evolution of inactive pyritic tailings in the Elliot Lake Uranium district: 1. The groundwater zone. Canadian Geotechnical Journal 22:110-128.

Dubrovsky, N.M., K.A. Morin, J.A. Cherry, D.J.A. Smyth. 1984b. Uranium tailings acidification and subsurface contaminant migration in a sand aquifer. Water Pollution Research Journal of Canada 19:55-89.

Ferguson, K.D. and P.M. Erickson. 1987. Will it generate AMD? An overview of methods to predict acid mine drainage. p. 215-244. In Proceedings Acid Mine Drainage Seminar/Workshop (Halifax, Nova Scotia, March 23-26, 1987).

Frind, E.O., D.W. Blowes, J.W. Molson and C.J. Ptacek. 1994. Simulation of multicomponent reactive transport in groundwater. Submitted to the International Symposium on Transport and Reactive Processes in Aquifers, ETH, Zurich, Switzerland, April 11-15, 1994.

Frind, E.O., W.H.M. Duynisveld, O. Strebel and J. Boettcher. 1990. Modeling of multicomponent transport with microbial transformation in groundwater: The Fuhrberg case. Water Resources Research 26:1707-1719.

Jambor, J.L. 1987. Mineralogical and chemical investigation of cores from piezometric sites in Waite Amulet tailings, Noranda, Quebec. Division Report MSL 87-32(IR), CANMET, Energy, Mines and Resources, Canada.

Jambor, J.L. and D.W. Blowes. 1991. Mineralogical study of low-sulphide, high-carbonate, arsenic-bearing tailings from the Delnite minesite, Timmins, Ontario. In Proceedings of the Second International Conference on the Abatement of Acidic Drainage. (Montreal, Quebec, September 16-18, 1991).

Jambor, J.L. and D.R. Owens. 1993. Mineralogy of the tailings impoundment at the former Cu-Ni deposit of Nickel Rim Mine Ltd., eastern edge of the Sudbury structure, Ontario. Division Report MSL 93-4 (CF), CANMET, Energy, Mines and Resources, Canada, 92 p.

Johnson, R.H. 1993. The physical and chemical hydrogeology of the Nickel Rim Mine tailings, Sudbury, Ontario. M.Sc. Thesis, University of Waterloo, Waterloo, Ontario, Canada, 108 p.

Morin, K.A. 1983. Prediction of subsurface contaminant transport in acidic seepage from uranium tailings impoundments. Ph.D. Thesis, University of Waterloo, Waterloo, Ontario, Canada.

Morin, K.A. and J.A. Cherry. 1986. Trace amounts of siderite near a tailings impoundment, Elliot Lake, Ontario, and its implication in controlling contaminant migration in a sand aquifer. Chemical Geology 56:117-134.

Morin, K.A. and J.A. Cherry. 1988. Migration of acidic groundwater seepage from uranium-tailings impoundments. 3. Simulation of the conceptual model with application to seepage area A. Journal of Contaminant Hydrology 2:323-342.

Morin, K.A., J.A. Cherry, N.K. Dave, T.P. Lim, A.J. Vivyurka. 1988. Migration of acidic groundwater seepage from uranium-tailings impoundments. 1. Field study and conceptual hydrogeochemical model. Journal of Contaminant Hydrology 2:271-303.

Nicholson, R.N., R.W. Gillham amd E.J. Reardon. 1990. Pyrite oxidation in carbonate-buffered solution. 2. Rate control by oxide coatings. Geochimica Cosmochima Acta 54: 395-402.

Ontario Ministry of the Environment (OMOE) 1983. Ontario drinking water objectives. Ontario Ministry of the Environment, Toronto, Ontario, Technical Report, 56 pp.

Ptacek, C.J. and Blowes, D.W. 1993. Influence of siderite on the geochemistry of inactive mine tailings impoundment. p. 172-189. In Environmental Geochemistry of Sulfide Oxidation, C.N. Alpers and D.W. Blowes (Eds.), American Chemical Society Symposium Series, Vol. 550.

Smyth, D.J.A. 1981. Hydrogeological and geochemical studies above the water table in an inactive uranium tailings impoundment near Elliot Lake, Ontario. M.Sc. Project, University of Waterloo, Waterloo, Ontario.

Walter, A.L., E.O. Frind, D.W. Blowes, C.J. Ptacek and J.W. Molson. 1994. Modelling of multicomponent reactive transport in aquifers impacted by mine tailings effluents. Water Resources Research, in press.

Adrian, L. W. 109
Allard, B. 336
Beam, R. L. 138
Bender, J. 99
Bennett, J. W. 400
Bensley, J. G. 241
Bisko, D. C. 138
Blowes, D. W. 429
Brady, K. B. C. 138, 365
Britt, C. 99
Broman, P. G. 400
Chambers, D. B. 30
Conley, P. S. 382
Cravotta III, C. A. 365
Dal Bianco, R. 327
Davé, N. K. 297
Destouni, G. 50
Dietz, J. M. 70
Domvile, S. J. 167
Donohue, T. A. 177
Donovan, J. J. 119
Dugas, D. L. 365
Dvorak, D. H. 214
Eddy, D. P. 89
Edenborn, H. M. 214
Eger, P. 80
Eriksson, N. 50
Ferguson K. D. 2
Finch, J. A. 223
Flather, D. H. 288
Fox, J. R. W. 241
Fraser, W. W. 250
Frind, E. O. 429
Fyson, A. 109
Gardner, M. D. 138
Gibson, D. K. 400
Giovannitti, E. F. 60
Goering, J. G. 40
Grady, T. R. 40
Håkansson K. 336
Hammack, R. W. 214
Hawkins, J. W. 20
Hedin, R. S. 185
Hellier, W. W. 60
Horne, I. A. 346
Hustwit, C. C. 233
Hutchinson, K. R. 392
Hutt, N. M. 12, 148
Hynes, T. 317
Jeffery, J. J. 177
Johnson, R. H. 429
Jones, C. E. 355
Jönsson, H. 400
Kalin, M. 109
Karlsson, S. 336
Kassa, Z. 80
Kepler, D. A. 195
King, A. R. 317
Kovalchuk, T. E. 365
Kuyucak, N. 223
Kwong, E. C. 30
Lapakko, K. A. 129, 270, 419
Larew, G. 375
Lee, D. R. 327
Leroux, M. 223
Li, M. G. 167
Lin, C. 157
Luckay, C. 410
Maynard, A. W. 260
McCleary, E. C. 195
McKee, P. 307
McNee, J. J. 288
Melchert, G. D. 80
Miller, S. D. 177
Molson, J. W. 429
Morin, K. A. 12, 148, 346, 355
Mueller, B. 288
Murdock, D. J. 241
Nawrot, J. R. 382
Nesbitt, W. 167
Neuman, D. R. 40
Pedersen, T. F. 288
Pelletier, C. A. 288
Perry, E. F. 138
Pettit, C. M. 30
Phillips, P. 99
Piroshco, B. M. 205
Prairie, R. 307
Ptacek, C. J. 429
Rao, S. R. 223
Rich, D. H. 392
Riehm, D. 346
Ritchie, A. I. M. 400
Robertson, J. D. 2, 250
Robertson, W. D. 429
Rodriguez-Eaton, S. 99

Rowley, M. V. 205
Sandusky, J. E. 382
Schafer, W. M. 40, 410
Scharer, J. M. 30
Sheremata, T. 223
Simms, R. 99
Skousen, J. 375
Slack, P. T. 60
Smith, S. 410
Smith, T. 410
Sollner, D. D. 167
Spotts, E. 40
St-Arnaud, L. C. 279
Stark, L. R. 89
Stevens, Jr., S. E. 89
Stidinger, D. M. 70
Sykes, R. G. 233
Tan, Y. 400
Tarantino, J. M. 138
Thomas, K. B. 260
Trujillo, E. M. 157
van Dyk, R. P. 355
Vivyurka, A. J. 297
Wagner, J. R.. 80
Warkentin, D. D. 205
Watts, R. G. 70
Watzlaf, G. R. 185
Wheeland, K. G. 223
White, III, W. W. 157
Williams, F. M. 89
Yan, V. T. 205
Ziemkiewicz, P. F. 119

* U.S. GOVERNMENT PRINTING OFFICE: 1994-509-021/05002